IAEA-TECDOC-1285

Reference neutron activation library

INTERNATIONAL ATOMIC ENERGY AGENCY IAEA

April 2002

The originating Section of this publication in the IAEA was:

Nuclear Data Section
International Atomic Energy Agency
Wagramer Strasse 5
P.O. Box 100
A-1400 Vienna, Austria

REFERENCE NEUTRON ACTIVATION LIBRARY
IAEA, VIENNA, 2002
IAEA-TECDOC-1285
ISSN 1011–4289

Printed by the IAEA in Austria
April 2002

FOREWORD

A major objective of the IAEA nuclear data programme is to promote improvement of the quality of nuclear data used in science and technology and to provide users with high quality and easily available libraries. For many years various national projects around the world have engaged in the compilation and evaluation of neutron activation cross-sections. Generally these evaluation efforts were carried out independently and arrived at different values for the same quantities. Therefore, a user in need of evaluated data has to search through the national libraries for the necessary evaluations and decide which one of those available is the best. While interrogating various libraries is time consuming (and not always possible) the selection of the most suitable data set presents a major challenge. It requires understanding of the evaluation procedures, comparisons against experimental data and results of the systematics and judicious use of various nuclear models. In practice, it can only be done by a professional evaluator.

To facilitate users' access to the high quality activation data, the IAEA established in 1994 a Co-ordinated Research Project (CRP) with the objective of providing a universal, internationally recognized library of neutron activation cross-sections for the reactions which are most important for practical applications. The CRP accomplished this task, producing the Reference Neutron Activation Library (RNAL), containing cross-sections for the 255 neutron induced reactions relevant to a wide range of applications. This report describes the contents of the RNAL library. It also includes graphical comparison of recommended cross-sections against available experimental data.

The RNAL library can be conveniently accessed using the Web interface
(**http://www-nds.iaea.org/ndspub/rnal/www/**):
or via anonymous FTP at:
(**iaeand.iaea.org/**)
in the directory **rnal**. In addition, the library is available cost-free from the IAEA Nuclear Data Section on a CD-ROM upon request.

The IAEA wishes to thank all the participants of the CRP for their contribution to the library development. Particular recognition goes to J. Kopecky and S. Hlavac for the assessment of the library. The IAEA staff member responsible for this report was M. Herman of the Division of Physical and Chemical Sciences.

Contents

INTRODUCTION

Many scientific endeavors require accurate nuclear data. Examples include studies of environmental protection connected with the running of a nuclear installation, the conceptual designs of fusion energy producing devices, astrophysics and the production of medical isotopes. In response to this need, many national and international data libraries have evolved over the years. Initially nuclear data work concentrated on materials relevant to the commercial power industry which is based on the fission of actinides, but recently the topic of activation has become of increasing importance. Activation of materials occurs in fission devices, but is generally overshadowed by the primary fission process. In fusion devices, high energy (14 MeV) neutrons produced in the D-T fusion reaction cause activation of the structure, and (with the exception of the tritium fuel) is the dominant source of activity. Astrophysics requires cross-sections (generally describing neutron capture) for its studies of nucleosynthesis. Many analytical techniques require activation analysis. For example, borehole logging uses the detection of gamma rays from irradiated materials to determine the various components of rocks.

To provide data for these applications, various specialized data libraries have been produced. The most comprehensive of these have been developed for fusion studies, since it has been appreciated that impurities are of the greatest importance in determining the overall activity, and thus data on all elements are required. These libraries contain information on a wide range of reactions: (n,γ), (n,2n), (n,α), (n,p), (n,d), (n,t), (n,^{3}He) and (n,n') over the energy range from 10^{-5} eV to 15 or 20 MeV. It should be noted that the production of various isomeric states have to be treated in detail in these libraries, and that the range of targets must include long-lived radioactive nuclides in addition to stable nuclides. These comprehensive libraries thus contain almost all the reactions of interest to the other applications mentioned above. However, because these fusion activation libraries are so large (more than 10,000 reactions are common), there are cases where specialized libraries contain or require more accurate information. For this reason the IAEA felt that research in these areas could be helped by developing a library of particularly important activation reactions which would be of benefit to a broad range of applications, some of which are mentioned above.

1. Description of the Reference Neutron Activation Library

1.1. Progression of the Co-ordinated Research Project

The initial aims of the Co-ordinated Research Project (CRP) were to provide a universal database of neutron and charged particle activation cross-sections that would satisfy the following requirements:

- be of use to many applications.
- contain data on a set of reactions judged to be of the highest importance.

- cover the energy range up to 20 MeV, with possible extension to higher energies later.
- include cross-section uncertainty estimates if possible.
- tested against experiments.

At the first Research Co-ordination Meeting (RCM) at Debrecen in October 1994, the aims were revised. The main points agreed were:

1. The range of applications that should be covered by the library should contain:
    - Magnetic confinement fusion
    - Inertial confinement fusion
    - Fission reactors
    - Geophysical and borehole logging
    - Dosimetry
    - Astrophysics
2. For the neutron induced library it was agreed to produce a master list of reactions appropriate for all selected applications, and to produce plots of the various evaluated files with the available experimental data. From such plots a choice from the candidate evaluations could be made and a starter file in an agreed format could be produced. A full covariance description of uncertainties is required only for the dosimetry reactions. Any less complete uncertainty data available for other reactions will be included in the starter file.
3. For the charged particle library it was agreed to consider a very restricted set of reactions most commonly used for production of medical radioisotopes.

The second RCM held in Madrid in May 1996 modified some of the aims of the library. It was recognised that a new IAEA CRP on charged particle data was a more appropriate place to consider the development of a charged particle library. Therefore all work on charged particles was transferred to the new CRP. The second meeting concentrated on the questions of changes to the master list of reactions, the choice of candidate for each reaction and the format of the starter file.

Later sections of this report describe assembling of the library and contain a detailed description and plot for each of the reactions. Readers can judge from these the quality of the data contained in the **R**eference **N**eutron **A**ctivation **L**ibrary (RNAL), and appreciate the benefit in having such data available in the concise format used here.

1.2. Selected reactions and their applications

Reactions selected for the RNAL are listed below. For each reaction one or more applications which justify the selection are given. In most cases applications are followed by a more specific description of the reaction usage.

^{1}H(n,γ)^{2}H	Borehole logging
^{10}B(n,α)^{7}Li	Borehole logging
^{12}C(n,2n)^{11}C	Dosimetry - high energies
^{12}C(n,γ)^{13}C	Borehole logging
^{13}C(n,γ)^{14}C	Fission Reactors - decommissioning
^{14}N(n,p)^{14}C	Inertial Fusion - waste, Magnetic Fusion - waste
^{16}O(n,n'α)^{12}C	Borehole logging - interfering
^{16}O(n,p)^{16}N	Borehole logging
^{19}F(n,2n)^{18}F	Dosimetry, Magnetic Fusion - safety/maintenance
^{23}Na(n,2n)^{22}Na	Magnetic Fusion - safety/maintenance, Borehole logging
^{23}Na(n,γ)^{24}Na	Geophysical - detector, Magnetic Fusion - safety/maintenance, Dosimetry
^{24}Mg(n,p)^{24}Na	Geophysical - interfering, Magnetic Fusion - safety/maintenance, Dosimetry
^{26}Mg(n,γ)^{27}Mg	Geophysical - detector, Astrophysics
^{27}Al(n,2n)^{26}Al	Magnetic Fusion - waste, Inertial Fusion - waste
^{27}Al(n,nα)^{23}Na	Magnetic Fusion - safety/maintenance
^{27}Al(n,γ)^{28}Al	Geophysical - detector
^{27}Al(n,p)^{27}Mg	Dosimetry, Magnetic Fusion - safety, Geophysical - interfering
^{27}Al(n,α)^{24}Na	Geophysical - interfering, Magnetic Fusion - safety/maintenance, Inertial Fusion - safety (Na-22 from Si)
^{28}Si(n,p)^{28}Al	Dosimetry - fusion, Borehole logging
^{28}Si(n,d+np)^{27}Al	Magnetic Fusion - waste, Inertial Fusion - safety (Na-22 from Si)
^{29}Si(n,p)^{29}Al	Borehole logging
^{29}Si(n,t)^{27}Al	Magnetic Fusion - tritium from SiC
^{29}Si(n,d+np)^{28}Al	Geophysical -interfering
^{30}Si(n,α)^{27}Mg	Geophysical - interfering
^{30}Si(n,γ)^{31}Si	Inertial Fusion - safety, Magnetic Fusion - safety, Borehole logging, Astrophysics
^{31}P(n,γ)^{32}P	Inertial Fusion - safety, Magnetic Fusion - safety, Astrophysics - s-process
^{31}P(n,p)^{31}Si	Dosimetry
^{31}P(n,α)^{28}Al	Geophysical - interfering
^{32}S(n,p)^{32}P	Dosimetry
^{34}S(n,γ)^{35}S	Astrophysics s-process, origin of
^{34}S(n,p)^{34}P	Borehole logging
^{36}S(n,γ)^{37}S	Borehole logging
^{35}Cl(n,2n)^{34m}Cl	Borehole logging
^{35}Cl(n,γ)^{36}Cl	Fission Reactors - decommissioning
^{37}Cl(n,γ)^{38}Cl	Borehole logging, Astrophysics - s-process (origin of S-36)

^{37}Cl(n,p)^{37}S	Borehole logging - interfering
^{37}Cl(n,α)^{34}P	Borehole logging - interfering
^{36}Ar(n,γ)^{37}Ar	Astrophysics - s-process (origin of S-36)
^{38}Ar(n,γ)^{39}Ar	Astrophysics - s-process (origin of S-36)
^{40}Ar(n,γ)^{41}Ar	Magnetic Fusion - safety/maintenance
^{39}K(n,p)^{39}Ar	Magnetic Fusion - waste
^{41}K(n,γ)^{42}K	Astrophysics - s-process (Ca isotopes)
^{41}K(n,α)^{38}Cl	Borehole logging - interfering
^{40}Ca(n,γ)^{41}Ca	Fission Reactors - decommissioning
^{44}Ca(n,p)^{44}K	Borehole logging
^{45}Ca(n,α)^{42}Ar	Magnetic Fusion - waste
^{48}Ca(n,γ)^{49}Ca	Borehole logging
^{45}Sc(n,γ)^{46}Sc	Dosimetry, Astrophysics - s-process (Ti isotopes)
^{46}Ti(n,2n)^{45}Ti	Dosimetry
^{46}Ti(n,p)^{46}Sc	Dosimetry - PWR, Magnetic Fusion - safety/maintenance, Inertial Fusion - safety
^{47}Ti(n,p)^{47}Sc	Magnetic Fusion - safety/maintenance
^{47}Ti(n,d+np)^{46}Sc	Dosimetry
^{48}Ti(n,p)^{48}Sc	Magnetic Fusion - safety/maintenance
^{48}Ti(n,d+np)^{47}Sc	Dosimetry
^{48}Ti(n,α)^{45}Ca	Magnetic Fusion - waste, Inertial Fusion - waste
^{50}Ti(n,α)^{47}Ca	Magnetic Fusion - safety
^{50}Ti(n,γ)^{51}Ti	Borehole logging Interfering
^{50}V(n,2n)^{49}V	Magnetic Fusion - waste
^{51}V(n,γ)^{52}V	Geophysical - detector, Magnetic Fusion -safety, Astrophysics - s-process (Cr isotopes)
^{51}V(n,p)^{51}Ti	Borehole logging - interfering
^{51}V(n,α)^{48}Sc	Magnetic Fusion - safety/maintenance, Dosimetry
^{50}Cr(n,γ)^{51}Cr	Magnetic Fusion - safety/maintenance, Inertial Fusion - safety, Borehole logging, Astrophysics - s-process (Cr isotopes)
^{52}Cr(n,2n)^{51}Cr	Dosimetry, Magnetic Fusion - safety/maintenance
^{52}Cr(n,p)^{52}V	Geophysical - interfering
^{53}Cr(n,d+np)^{52}V	Geophysical - interfering
^{54}Cr(n,γ^{55})Cr	Astrophysics - s-process (Cr isotopes)
^{54}Cr(n,α)^{51}Ti	Borehole logging - interfering
^{53}Mn(n,γ)^{54}Mn	Geophysical - detector
^{55}Mn(n,2n)^{54}Mn	Magnetic Fusion- safety/maintenance, Fission Reactors - decommissioning, Borehole logging, Dosimetry
^{55}Mn(n,γ)^{56}Mn	Magnetic Fusion - safety/maintenance, Inertial Fusion - safety, Astrophysics - s-process, Borehole logging - interfering, Dosimetry
^{55}Mn(n,α)^{52}V	Geophysical - interfering
^{54}Fe(n,2n)^{53}Fe	Dosimetry - fusion
^{54}Fe(n,γ)^{55}Fe	Fission Reactors - decommissioning
^{54}Fe(n,p)^{54}Mn	Magnetic Fusion - safety/maintenance, Fission Reactors - decommissioning, Dosimetry
^{56}Fe(n,2n)^{55}Fe	Magnetic Fusion - safety, Inertial Fusion - safety, Fission Reactors - decommissioning

$^{56}Fe(n,\gamma)^{57}Fe$	Inertial Fusion - safety/maintenance (Co-60 from Fe), Magnetic Fusion - safety/maintenance (Co-60 from Fe)
$^{56}Fe(n,p)^{56}Mn$	Geophysical - interfering, Magnetic Fusion - safety/maintenance, Dosimetry
$^{57}Fe(n,\gamma)^{58}Fe$	Inertial Fusion - safety/maintenance (Co-60 from Fe), Magnetic Fusion - safety/maintenance (Co-60 from Fe)
$^{58}Fe(n,\gamma)^{59}Fe$	Inertial Fusion - safety/maintenance (Co-60 from Fe), Magnetic Fusion - safety/maintenance (Co-60 from Fe), Astrophysics - s-process (anomalies), Dosimetry
$^{60}Fe(n,\gamma)^{61}Fe$	Astrophysics - s-process (anomalies)
$^{59}Co(n,2n)^{58}Co$	Dosimetry
$^{59}Co(n,\gamma)^{60}Co$	Magnetic Fusion - safety/maintenance, Inertial Fusion - safety/maintenance, Astrophysics - s-process, Fission Reactors - decommissioning, Dosimetry
$^{59}Co(n,\alpha)^{56}Mn$	Geophysical - interfering, Dosimetry
$^{60}Co(n,\gamma)^{61}Co$	Magnetic Fusion - waste (Ni-63 from Co), Inertial Fusion - waste (Ni-63 from Co)
$^{60}Co(n,p)^{60}Fe$	Inertial Fusion - waste, Magnetic Fusion - waste
$^{58}Ni(n,2n)^{57}Ni$	Dosimetry
$^{58}Ni(n,\gamma)^{59}Ni$	Magnetic Fusion - waste, Inertial Fusion - waste, Fission Reactors - decommissioning
$^{58}Ni(n,p)^{58}Co$	Dosimetry, Magnetic Fusion - safety/maintenance, Fission Reactors - decommissioning
$^{58}Ni(n,d+np)^{57}Co$	Magnetic Fusion - safety/maintenance, Fission Reactors - decommissioning
$^{60}Ni(n,2n)^{59}Ni$	Magnetic Fusion - waste
$^{60}Ni(n,p)^{60}Co$	Magnetic Fusion - safety/maintenance, Inertial Fusion - safety/maintenance, Fission Reactors - decommissioning, Dosimetry
$^{61}Ni(n,\gamma)^{62}Ni$	Magnetic Fusion - waste (Ni-63 from Ni & Co), Inertial Fusion - waste (Ni-63 from Co)
$^{62}Ni(n,\gamma)^{63}Ni$	Magnetic Fusion - waste, Inertial Fusion - waste, Fission Reactors - decommissioning
$^{64}Ni(n,2n)^{63}Ni$	Magnetic Fusion - waste
$^{64}Ni(n,\gamma)^{65}Ni$	Astrophysics - s-process
$^{63}Cu(n,2n)^{62}Cu$	Dosimetry
$^{63}Cu(n,\gamma)^{64}Cu$	Magnetic Fusion - safety, Astrophysics - s-process (branching to Zn-64), Dosimetry
$^{63}Cu(n,p)^{63}Ni$	Magnetic Fusion - waste
$^{63}Cu(n,\alpha)^{60}Co$	Magnetic Fusion - safety/maintenance, Inertial Fusion - safety/maintenance, Dosimetry
$^{65}Cu(n,2n)^{64}Cu$	Magnetic Fusion - safety, Dosimetry
$^{65}Cu(n,\gamma)^{66}Cu$	Geophysical - detector, Magnetic Fusion - safety, Astrophysics - s-process (branching)
$^{64}Zn(n,\gamma)^{65}Zn$	Fission Reactors - decommissioning, Astrophysics - s-process (branching to Zn-64)
$^{64}Zn(n,p)^{64}Cu$	Dosimetry

^{66}Zn(n,p)^{66}Cu	Geophysical - interfering
^{68}Zn(n,γ)^{69}Zn	Astrophysics - s-process
^{70}Zn(n,γ)^{71}Zn	Astrophysics - s-process
^{69}Ga(n,γ)^{70}Ga	Astrophysics - s-process
^{69}Ga(n,α)^{66}Cu	Geophysical - interfering
^{71}Ga(n,γ)^{71}Ga	Astrophysics
^{74}Se(n,γ)^{75}Se	Astrophysics - p-process
^{78}Se(n,γ)^{79}Se	Inertial Fusion - waste
^{79}Se(n,γ)^{80}Se	Fission Reactors
^{80}Se(n,γ)^{81}Se	Astrophysics - s-process (branching)
^{82}Se(n,γ)^{83}Se	Astrophysics - s-process (branching)
^{80}Kr(n,γ)^{81}Kr	Astrophysics
^{84}Kr(n,γ)^{85}Kr	Astrophysics
^{86}Kr(n,γ)^{87}Kr	Astrophysics
^{85}Rb(n,γ)^{85}Rb	Astrophysics
^{84}Sr(n,γ)^{85}Sr	Astrophysics - p-process
^{89}Sr(n,γ)^{90}Sr	Fission Reactors - decommissioning
^{90}Sr(n,γ)^{91}Sr	Fission Reactors
^{90}Zr(n,2n)^{89}Zr	Magnetic Fusion -safety/maintenance, Dosimetry
^{93}Zr(n,γ)^{94}Zr	Fission Reactors
^{94}Zr(n,γ)^{95}Zr	Magnetic Fusion - safety/maintenance
^{96}Zr(n,2n)^{95}Zr	Magnetic Fusion - safety/maintenance
^{93}Nb(n,n')^{93m}Nb	Dosimetry - fission reactors, Magnetic Fusion - safety/maintenance, Fission Reactors - decommissioning
^{93}Nb(n,2n)^{92}Nb	Magnetic Fusion - waste
^{93}Nb(n,γ)^{94}Nb	Magnetic Fusion - waste, Inertial Fusion - waste, Fission Reactors - decommissioning
^{92}Mo(n,γ)^{93}Mo	Magnetic Fusion - waste
^{92}Mo(n,p)^{92}Nb	Magnetic Fusion - waste
^{92}Mo(n,d+np)^{91}Nb	Magnetic Fusion - waste, Inertial Fusion - waste
^{93}Mo(n,d+np)^{92}Nb	Magnetic Fusion - waste
^{94}Mo(n,2n)^{93}Mo	Magnetic Fusion - waste
^{94}Mo(n,p)^{94}Nb	Magnetic Fusion - waste, Inertial Fusion - waste
^{94}Mo(n,d+np)^{93m}Nb	Magnetic Fusion - safety/maintenance, Inertial Fusion - safety/maintenance
^{95}Mo(n,p)^{95}Nb	Magnetic Fusion - safety/maintenance
^{95}Mo(n,d+np)^{94}Nb	Magnetic Fusion - waste, Inertial Fusion - waste
^{98}Mo(n,γ)^{99}Mo	Magnetic Fusion - safety/waste (Tc-99 from Mo), Inertial Fusion - safety/waste (Tc-99 from Mo), Astrophysics, Fission Reactors - decommissioning (Tc-99 from Mo)
^{100}Mo(n,2n)^{99}Mo	Magnetic Fusion - safety/waste (Tc-99 from Mo)
^{100}Mo(n,γ)^{101}Mo	Astrophysics - cross-section systematics in Mo
^{99}Tc(n,2n)^{98}Tc	Magnetic Fusion - waste
^{96}Ru(n,γ)^{97}Ru	Astrophysics - p-process
^{102}Ru(n,γ)^{103}Ru	Astrophysics
^{104}Ru(n,γ)^{105}Ru	Astrophysics
^{103}Rh(n,n')^{103m}Rh	Dosimetry

$^{103}Rh(n,\gamma)^{104}Rh$	Astrophysics - comparison with differential data
$^{102}Pd(n,\gamma)^{103}Pd$	Astrophysics - p-process
$^{108}Pd(n,\gamma)^{109}Pd$	Astrophysics - s-process (Pd isotopes)
$^{110}Pd(n,\gamma)^{111}Pd$	Astrophysics - s-process (Pd isotopes)
$^{107}Ag(n,\gamma)^{108m}Ag$	Magnetic Fusion - waste, Inertial Fusion - waste, Fission Reactors - decommissioning
$^{108m}Ag(n,\gamma)^{109}Ag$	Magnetic Fusion - waste, Inertial Fusion - waste
$^{109}Ag(n,2n)^{108m}Ag$	Magnetic Fusion - waste, Fission Reactors - decommissioning, Inertial Fusion - waste
$^{109}Ag(n,\gamma)^{110m}Ag$	Fission Reactors - decommissioning, Dosimetry
$^{106}Cd(n,\gamma)^{107}Cd$	Astrophysics - p-process
$^{108}Cd(n,\gamma)^{109}Cd$	Astrophysics - p-process
$^{114}Cd(n,\gamma)^{115}Cd$	Astrophysics
$^{113}In(n,\gamma)^{114}In$	Astrophysics - s-process branchings at A=113, 115
$^{115}In(n,n')^{115m}In$	Dosimetry - D-D diagnostics, Inertial Fusion
$^{115}In(n,\gamma)^{116m}In$	Dosimetry, Astrophysics - s-process branchings at A=113, 115
$^{120}Sn(n,\gamma)^{121m}Sn$	Magnetic Fusion - waste
$^{121}Sn(n,\gamma)^{122}Sn$	Astrophysics
$^{122}Sn(n,2n)^{121m}Sn$	Magnetic Fusion - waste
$^{125}Sn(n,\gamma)^{126}Sn$	Magnetic Fusion - waste
$^{126}Sn(n,\gamma)^{127}Sn$	Fission Reactors
$^{123}Sb(n,\gamma)^{124}Sb$	Astrophysics, Fission Reactors - decommissioning (production of Sb-125)
$^{124}Sb(n,\gamma)^{125}Sb$	Fission Reactors - decommissioning
$^{120}Te(n,\gamma)^{121}Te$	Astrophysics - p-process
$^{128}Te(n,\gamma)^{129}Te$	Astrophysics
$^{130}Te(n,\gamma)^{131}Te$	Astrophysics
$^{127}I(n,2n)^{126}I$	Dosimetry
$^{127}I(n,\gamma)^{128}I$	Astrophysics
$^{128}I(n,\gamma)^{129}I$	Fission Reactors - decommissioning
$^{134}Xe(n,\gamma)^{135}Xe$	Astrophysics
$^{136}Xe(n,\gamma)^{137}Xe$	Astrophysics
$^{133}Cs(n,\gamma)^{134}Cs$	Astrophysics, Fission Reactors - decommissioning
$^{135}Cs(n,\gamma)^{136}Cs$	Fission Reactors
$^{136}Cs(n,\gamma)^{137}Cs$	Fission Reactors Decommissioning
$^{137}Cs(n,\gamma)^{138}Cs$	Fission Reactors
$^{130}Ba(n,\gamma)^{131}Ba$	Astrophysics
$^{132}Ba(n,\gamma)^{133}Ba$	Fission Reactors -decommissioning, Astrophysics - p-process
$^{137}Ba(n,p)^{137}Cs$	Magnetic Fusion - waste
$^{138}Ba(n,\alpha)^{135}Xe$	Magnetic Fusion - waste (Cs-135 from Ba), Astrophysics
$^{138}La(n,\gamma)^{139}La$	Astrophysics - s-process
$^{139}La(n,\gamma)^{140}La$	Astrophysics, Dosimetry
$^{143}Ce(n,\gamma)^{144}Ce$	Fission Reactors - decommissioning
$^{146}Nd(n,\gamma)^{147}Nd$	Astrophysics
$^{148}Nd(n,\gamma)^{149}Nd$	Astrophysics
$^{150}Nd(n,\gamma)^{151}Nd$	Astrophysics
$^{144}Sm(n,\gamma)^{145}Sm$	Astrophysics - p-process

^{152}Sm(n,γ)^{153}Sm	Astrophysics
^{154}Sm(n,γ)^{155}Sm	Astrophysics
^{151}Eu(n,2n)^{150}Eu	Magnetic Fusion - waste
^{151}Eu(n,γ)^{152}Eu	Astrophysics, Fission Reactors - decommissioning
^{153}Eu(n,2n)^{152}Eu	Magnetic Fusion - waste
^{153}Eu(n,γ)^{154}Eu	Fission Reactors - decommissioning
^{154}Eu(n,γ)^{155}Eu	Fission Reactors - decommissioning
^{159}Tb(n,2n)^{158}Tb	Magnetic Fusion - waste
^{159}Tb(n,γ)^{160}Tb	Astrophysics - s-process (lanthanides)
^{158}Dy(n,γ)^{159}Dy	Astrophysics - p-process
^{158}Dy(n,p)^{158}Tb	Magnetic Fusion - waste
^{164}Dy(n,γ)^{165}Dy	Astrophysics - s-process (lanthanides)
^{165}Ho(n,γ)^{166}Ho	Astrophysics, Magnetic Fusion - waste
^{162}Er(n,γ)^{163}Er	Astrophysics
^{164}Er(n,γ)^{165}Er	Astrophysics
^{168}Er(n,γ)^{169}Er	Astrophysics s-process (lanthanides)
^{170}Er(n,γ)^{171}Er	Astrophysics
^{169}Tm(n,γ)^{170}Tm	Astrophysics - s-process (lanthanides)
^{168}Yb(n,γ)^{169}Yb	Astrophysics - p-process
^{174}Yb(n,γ)^{175}Yb	Astrophysics - s-process (lanthanides)
^{176}Yb(n,γ)^{177}Yb	Astrophysics
^{175}Lu(n,γ)^{176}Lu	Astrophysics
^{176}Lu(n,γ)^{177}Lu	Astrophysics
^{174}Hf(n,γ)^{175}Hf	Astrophysics - p-process
^{179}Hf(n,2n)^{178n}Hf	Magnetic Fusion - waste
^{181}Ta(n,3n)^{179}Ta	Magnetic Fusion -safety (Hf-178^{n} from Ta)
^{181}Ta(n,γ)^{182}Ta	Magnetic Fusion - safety
^{182}W(n,2n)^{181}W	Magnetic Fusion - safety/maintenance
^{182}W(n,nα)^{178n}Hf	Magnetic Fusion - waste
^{183}W(n,γ)^{184}W	Inertial Fusion - waste (Re-186m from W), Magnetic Fusion - waste (Re-186m from W)
^{184}W(n,γ)^{185}W	Magnetic Fusion - safety, Inertial Fusion - waste, Astrophysics - s-process
^{186}W(n,2n)^{185}W	Magnetic Fusion - safety
^{186}W(n,nα)^{182}Hf	Magnetic Fusion - waste
^{186}W(n,γ)^{187}W	Geophysical - detector, Magnetic Fusion - safety, Inertial Fusion - safety, Dosimetry
^{185}Re(n,2n)^{184}Re	Magnetic Fusion - maintenance
^{185}Re(n,γ)^{186m}Re	Magnetic Fusion - waste, Inertial Fusion - waste
^{187}Re(n,2n)^{186m}Re	Magnetic Fusion - waste
^{187}Re(n,γ)^{188}Re	Inertial Fusion -safety, Magnetic Fusion - safety
^{187}Re(n,p)^{187}W	Geophysical - interfering, Magnetic Fusion - maintenance
^{184}Os(n,γ)^{185}Os	Astrophysics - p-process
^{188}Os(n,γ)^{189}Os	Inertial Fusion - waste, Magnetic Fusion - waste
^{190}Os(n,γ)^{191}Os	Inertial Fusion - safety, Magnetic Fusion - safety, Astrophysics - s-process (branchings at A=191, 192)
^{190}Os(n,α)^{187}W	Geophysical - interfering

$^{192}Os(n,\gamma)^{193}Os$	Astrophysics - s-process (branchings at A=191, 192)
$^{191}Ir(n,\gamma)^{192n}Ir$	Inertial Fusion - waste, Magnetic Fusion - waste
$^{192}Ir(n,n')^{192n}Ir$	Inertial Fusion - waste, Magnetic Fusion - waste
$^{192n}Ir(n,\gamma)^{193}Ir$	Inertial Fusion - waste
$^{193}Ir(n,2n)^{192n}Ir$	Magnetic Fusion - waste, Inertial Fusion - waste
$^{190}Pt(n,\gamma)^{191}Pt$	Astrophysics - p-process
$^{192}Pt(n,\gamma)^{193}Pt$	Inertial Fusion - waste, Magnetic Fusion - waste, Astrophysics - s-process (branchings)
$^{194}Pt(n,\gamma)^{195}Pt$	Astrophysics
$^{196}Pt(n,\gamma)^{197}Pt$	Astrophysics
$^{198}Pt(n,\gamma)^{198}Pt$	Astrophysics
$^{197}Au(n,2n)^{196}Au$	Dosimetry
$^{197}Au(n,\gamma)^{198}Au$	Astrophysics, Borehole logging, Dosimetry
$^{196}Hg(n,\gamma)^{197}Hg$	Astrophysics - p-process
$^{202}Hg(n,\gamma)^{203}Hg$	Astrophysics - s-process (branchings at A=203, 204)
$^{204}Hg(n,\gamma)^{205}Hg$	Astrophysics - s-process (branchings at A=203, 204)
$^{203}Tl(n,\gamma)^{204}Tl$	Astrophysics - s-process (branchings at A=203, 204)
$^{205}Tl(n,\gamma)^{206}Tl$	Astrophysics - s-process (branchings at A=203, 204)
$^{204}Pb(n,2n)^{203}Pb$	Magnetic Fusion - safety/maintenance
$^{206}Pb(n,2n)^{205}Pb$	Magnetic Fusion - waste
$^{206}Pb(n,\alpha)^{203}Hg$	Magnetic Fusion - safety/maintenance
$^{208}Pb(n,\gamma)^{209}Pb$	Magnetic Fusion - safety
$^{209}Bi(n,2n)^{208}Bi$	Magnetic Fusion - waste, Inertial Fusion - waste
$^{209}Bi(n,\gamma)^{210m}Bi$	Magnetic Fusion - waste, Inertial Fusion -waste

1.3. Development of the library

This section describes how the data for the RNAL library have been selected. As potential data candidates the following activation libraries have been considered: EAF-4.1, FENDL/A-1, FENDL/A-2.0, JENDL-Act96 and ADL-3. Among these libraries, only two libraries (JENDL-Act96 [1] and ADL-3 [2]) are exclusively based on their original evaluations. The EAF-4.1 library [3] is a combination of adopted data from other libraries with the original evaluations (primarily of the (n,γ) reactions). Both FENDL activation libraries are based purely on data adopted from other libraries. FENDL/A-1 is a combination of EAF-3, as a basic data library, with about 250 important reactions adopted from other sources (for details see Ref. [4]). FENDL/A-2.0 [5], the follow-up of FENDL/A-1, used EAF-4.1 as the basic library together with 398 reactions important for fusion applications.

A special procedure for the selection of the best available data for these reactions in FENDL has been applied. An international panel of 8 members used graphical intercomparisons of all recently available evaluations for these reactions against the EXFOR experimental data base (for details see Ref. [5]) to choose the best evaluation. The selected data represent the state of the art evaluations for these reactions and therefore these selections have also been almost in all cases adopted in the RNAL library

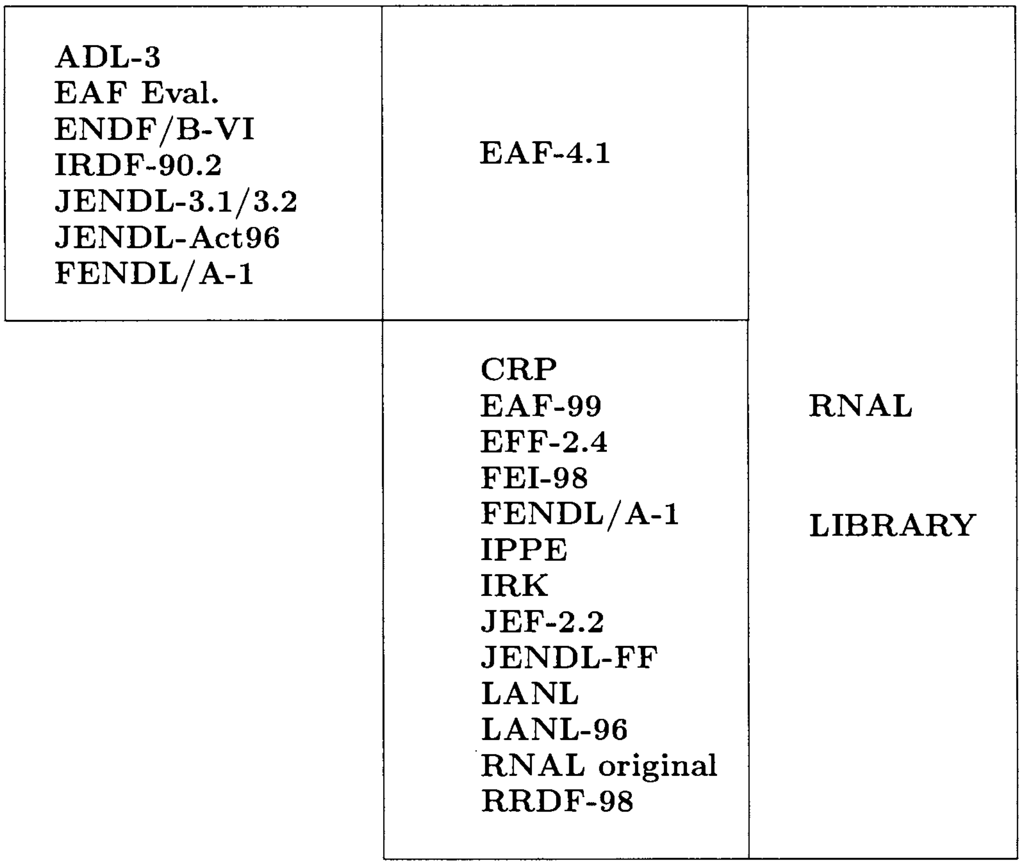

FIG. 1. The chronological development of the RNAL library

The data selection for the RNAL library has been done in parallel with the FENDL/A-2.0 assembling taking advantage of the FENDL important reaction choices. However, in some cases, some new (and better) data have been adopted within this CRP. In two cases original RNAL evaluations were developed. The flow of the selection steps of the RNAL library is shown in Fig.1.

The master list of the RNAL reference reactions with their data sources is given in Table 1. The column 'Reaction' defines the reaction. All selected (n,d) reactions are activation reactions and they represent the sum of (n,d) and (n,np) reaction channels. For all reactions, the initial state (IS) is the ground state, except reactions Ag-108(n,γ) and Ir-192(n, γ) with the initial states being the first and the second metastable states, respectively. Further, the status of the data to different final states, as stored in the RNAL data base, is given in the column FS employing symbols 99 (for total cross-section), 0 (for ground state), 1 (for the first metastable state) and 2 (for the second metastable state). The metastable states are in the reaction nomenclature described by 'm' and 'n' for the FS=1 or 2. Note, that FS flags are only used in the text of the present document and not in the files. The latter conform to the ENDF-6 standard and use MF=10 to describe partial cross-sections.

In the column 'Data source' the library or evaluation is given, at the assembling level of the FENDL/A-2.0 library. In other words, the data source is given as chosen for the FENDL/A-2.0 library, except a number of new selections made within this CRP (see Ref. [6] and this report) selection procedure and recommendations. Remaining data are automatically based on EAF-4.1. The original data, as adopted in EAF-4.1 and FENDL/A-1 libraries, are given in brackets. The original EAF evaluations are denoted with EAF-4.1 without any data source in brackets. The references to the national/regional projects that contributed to RNAL are given in Table 2. A total of 255 reactions have been included in the Master list (see Table 1).

Table 1. List of RNAL reactions with their data sources.

#	Reaction	FS	Data
1	H-1(n,γ) H-2	99	EAF-4.1(JEF-2.2)
2	B-10(n,α) Li-7	99	EAF-4.1(IRDF-90.2)
3	C-12(n,2n) C-11	99	RRDF-98
4	C-12(n,γ) C-13	99	JENDL-FF
5	C-13(n,γ) C-14	99	EAF-4.1
6	N-14(n,p) C-14	99	ENDF/B-VI
7	O-16(n,n'α)C-12	99	JENDL-Act96
8	O-16(n,p) N-16	99	FENDL/A-1 (ENDF/B-VI)
9	F-19(n,2n) F-18	99	FENDL/A-1 (IRDF-90.2)
10	Na-23 (n,2n) Na-22	99	ADL-3
11	Na-23 (n,γ) Na-24	0,1	EAF-4.1 (JEF-2.2)
12	Mg-24 (n,p) Na-24	0,1	IRDF-90.2
13	Mg-26 (n,γ) Mg-27	99	EAF-4.1 (JENDL-3.1)
14	Al-27 (n,2n) Al-26	0,1	ADL-3
15	Al-27 (n,nα) Na-23	99	ADL-3
16	Al-27 (n,γ) Al-28	99	EAF-4.1 (JEF-2.2)
17	Al-27 (n,p) Mg-27	99	RRDF-98
18	Al-27 (n,α) Na-24	0,1	IRDF-90.2
19	Si-28 (n,p) Al-28	99	JENDL-Act96
20	Si-28 (n,d+np) Al-27	99	JENDL-Act96
21	Si-29 (n,p) Al-29	99	JENDL-Act96
22	Si-29 (n,d+np) Al-28	99	JENDL-3.1 [(n,np)], ADL-3 [(n,d)]
23	Si-29 (n,t) Al-27	99	ADL-3
24	Si-30 (n,α) Mg-27	99	JENDL-3.1
25	Si-30 (n,γ) Si-31	99	EAF-4.1 (JENDL-3.1)
26	P-31 (n,γ) P-32	99	EAF-4.1 (JEF-2.2)
27	P-31 (n,p) Si-31	99	EAF-4.1 (IRDF-90.2)
28	P-31 (n,α) Al-28	99	JENDL-Act96
29	S-32 (n,p) P-32	99	IRDF-90.2
30	S-34 (n,γ) S-35	99	EAF-4.1 (JEF-2.2)
31	S-34 (n,p) P-34	99	ADL-3
32	S-36 (n,γ) S-37	99	EAF-4.1 (JEF-2.2)
33	Cl-35 (n,2n) Cl-34m	0,1	EAF-4.1
34	Cl-35 (n,γ) Cl-36	99	EAF-4.1
35	Cl-37 (n,γ) Cl-38	0,1	JENDL-3.2
36	Cl-37 (n,p) S-37	99	JENDL-Act96
37	Cl-37 (n,α) P-34	99	ADL-3
38	Ar-36 (n,γ) Ar-37	99	EAF-4.1 (JEF-2.2)
39	Ar-38 (n,γ) Ar-39	99	EAF-4.1 (JEF-2.2)
40	Ar-40 (n,γ) Ar-41	99	EAF-4.1 (JEF-2.2)
41	K-39 (n,p) Ar-39	99	ADL-3
42	K-41 (n,γ) K-42	99	EAF-4.1 (JENDL-3.1)
43	K-41 (n,α) Cl-38	0,1	ADL-3

Table 1. Cont.

#	Reaction	FS	Data
44	Ca-40 (n,γ) Ca-41	99	EAF-4.1 (JENDL-3.1)
45	Ca-44 (n,p) K-44	99	ADL-3
46	Ca-45 (n,α) Ar-42	99	ADL-3
47	Ca-48 (n,γ) Ca-49	99	EAF-4.1 (JENDL-3.1)
48	Sc-45 (n,γ) Sc-46	0,1	EAF-4.1 (ENDF/B-VI)
49	Ti-46 (n,2n) Ti-45	99	RRDF-98
50	Ti-46 (n,p) Sc-46	0,1	ADL-3
51	Ti-47 (n,p) Sc-47	99	JENDL-Act96
52	Ti-47 (n,d+np) Sc-46	99	RNAL
53	Ti-48 (n,p) Sc-48	99	IRK
54	Ti-48 (n,d+np) Sc-47	99	FENDL/A-1 [(n,d)], IRDF-90.2 [(n,np)]
55	Ti-48 (n,α) Ca-45	99	IPPE
56	Ti-50 (n,α) Ca-47	99	JENDL-Act96
57	Ti-50 (n,γ) Ti-51	99	EAF-4.1 (JENDL-3.1)
58	V-50 (n,2n) V-49	99	JENDL-Act96
59	V-51 (n,γ) V-52	99	EAF-4.1 (JENDL-3.1)
60	V-51 (n,p) Ti-51	99	JENDL-Act96
61	V-51 (n,α) Sc-48	99	EAF-4.1 (IRDF-90.2)
62	Cr-50 (n,γ) Cr-51	99	EAF-4.1 (EFF-2.4)
63	Cr-52 (n,2n) Cr-51	99	IRDF-90.2
64	Cr-52 (n,p) V-52	99	ADL-3
65	Cr-53 (n,d+np) V-52	99	EFF-2.4
66	Cr-54 (n,γ) Cr-55	99	EAF-4.1 (EFF-2.4)
67	Cr-54 (n,α) Ti-51	99	IPPE
68	Mn-53 (n,γ) Mn-54	99	EAF-4.1
69	Mn-55 (n,2n) Mn-54	99	ADL-3
70	Mn-55 (n,γ) Mn-56	99	EAF-4.1 (JEF-2.2)
71	Mn-55 (n,α) V-52	99	IPPE
72	Fe-54 (n,2n) Fe-53	0,1	RRDF-98
73	Fe-54 (n,γ) Fe-55	99	EAF-4.1 (ENDF/B-VI)
74	Fe-54 (n,p) Mn-54	99	JENDL-Act96
75	Fe-56 (n,2n) Fe-55	99	ADL-3
76	Fe-56 (n,γ) Fe-57	99	EAF-4.1 (ENDF/B-VI)
77	Fe-56 (n,p) Mn-56	99	EAF-4.1 (IRDF-90.2)
78	Fe-57 (n,γ) Fe-58	99	EAF-4.1 (ENDF/B-VI)
79	Fe-58 (n,γ) Fe-59	99	EAF-4.1 (ENDF/B-VI)
80	Fe-60 (n,γ) Fe-61	99	EAF-4.1
81	Co-59 (n,2n) Co-58	99	IRDF-90.2
82	Co-59 (n,γ) Co-60	0,1	EAF-4.1 (JEF-2.2)
83	Co-59 (n,α) Mn-56	99	EAF-4.1 (IRDF-90.2)
84	Co-60 (n,γ) Co-61	99	EAF-4.1
85	Co-60 (n,p) Fe-60	99	ADL-3
86	Ni-58 (n,2n) Ni-57	99	EAF-4.1 (IRDF-90.2)
87	Ni-58 (n,γ) Ni-59	99	EAF-4.1 (EFF-2.4)

Table 1. Cont.

#	Reaction	FS	Data
88	Ni-58 (n,p) Co-58	99	IPPE
89	Ni-58 (n,d+np) Co-57	99	EAF-4.1 (JEF-2.2)
90	Ni-60 (n,2n) Ni-59	99	ADL-3
91	Ni-60 (n,p) Co-60	0,1	ADL-3
92	Ni-61 (n,γ) Ni-62	99	EAF-4.1 (EFF-2.4)
93	Ni-62 (n,γ) Ni-63	99	EAF-4.1 (EFF-2.4)
94	Ni-64 (n,2n) Ni-63	99	ADL-3
95	Ni-64 (n,γ) Ni-65	99	EAF-4.1 (EFF-2.4)
96	Cu-63 (n,2n) Cu-62	99	EAF-4.1 (IRDF-90.2)
97	Cu-63 (n,γ) Cu-64	99	EAF-4.1 (ENDF/B-VI)
98	Cu-63 (n,p) Ni-63	99	ADL-3
99	Cu-63 (n,α) Co-60	99	RRDF-98
100	Cu-65 (n,2n) Cu-64	99	JENDL-Act96
101	Cu-65 (n,γ) Cu-66	99	EAF-4.1 (ENDF/B-VI)
102	Zn-64 (n,γ) Zn-65	99	EAF-4.1 (JEF-2.2)
103	Zn-64 (n,p) Cu-64	99	JENDL-Act96
104	Zn-66 (n,p) Cu-66	99	JENDL-Act96
105	Zn-68 (n,γ) Zn-69	0,1	EAF-4.1
106	Zn-70 (n,γ) Zn-71	0,1	EAF-4.1
107	Ga-69 (n,γ) Ga-70	99	EAF-4.1
108	Ga-69 (n,α) Cu-66	99	JENDL-Act96
109	Ga-71 (n,γ) Ga-72	99	EAF-4.1
110	Se-74 (n,γ) Se-75	99	EAF-4.1 (JEF-2.2)
111	Se-78 (n,γ) Se-79	0,1	EAF-4.1 (JEF-2.2)
112	Se-79 (n,γ) Se-80	99	EAF-4.1
113	Se-80 (n,γ) Se-81	0,1	EAF-4.1 (JEF-2.2)
114	Se-82 (n,γ) Se-83	0,1	EAF-4.1 (JEF-2.2)
115	Kr-80 (n,γ) Kr-81	0,1	EAF-4.1 (JEF-2.2)
116	Kr-84 (n,γ) Kr-85	0,1	EAF-4.1 (JEF-2.2)
117	Kr-86 (n,γ) Kr-87	99	EAF-4.1 (JEF-2.2)
118	Rb-85 (n,γ) Rb-86	0,1	EAF-4.1 (JEF-2.2)
119	Sr-84 (n,γ) Sr-85	0,1	EAF-4.1
120	Sr-89 (n,γ) Sr-90	99	EAF-4.1 (JEF-2.2)
121	Sr-90 (n,γ) Sr-91	99	EAF-4.1 (JEF-2.2)
122	Zr-90 (n,2n) Zr-89	0,1	ADL-3
123	Zr-93 (n,γ) Zr-94	99	EAF-4.1 (JEF-2.2)
124	Zr-94 (n,γ) Zr-95	99	EAF-4.1 (JEF-2.2)
125	Zr-96 (n,2n) Zr-95	99	JENDL-Act96
126	Nb-93 (n,n') Nb-93m	1	RRDF-98
127	Nb-93 (n,2n) Nb-92	0,1	JENDL-Act96
128	Nb-93 (n,γ) Nb-94	0,1	EAF-4.1 (JEF-2.2)
129	Mo-92 (n,γ) Mo-93	0,1	EAF-4.1 (JEF-2.2)
130	Mo-92 (n,p) Nb-92	0,1	ADL-3

Table 1. Cont.

#	Reaction	FS	Data
131	Mo-92 (n,d+np) Nb-91	1	RNAL
132	Mo-93 (n,d+np) Nb-92	0,1	ADL-3
133	Mo-94 (n,2n) Mo-93	0,1	ADL-3
134	Mo-94 (n,p) Nb-94	0,1	CRP
135	Mo-94 (n,d+np)Nb-93m	1	ADL-3
136	Mo-95 (n,p) Nb-95	0,1	ADL-3
137	Mo-95 (n,d+np) Nb-94	0,1	ADL-3
138	Mo-98 (n,γ) Mo-99	99	EAF-4.1 (JEF-2.2)
139	Mo-100(n,2n) Mo-99	99	JENDL-Act96
140	Mo-100(n,γ) Mo-101	99	EAF-4.1 (JEF-2.2)
141	Tc-99 (n,2n) Tc-98	99	ADL-3
142	Ru-96 (n,γ) Ru-97	99	EAF-4.1 (JEF-2.2)
143	Ru-102(n,γ) Ru-103	99	EAF-4.1 (JEF-2.2)
144	Ru-104(n,γ) Ru-105	99	EAF-4.1 (JEF-2.2)
145	Rh-103(n,n') Rh-103m	1	IRK
146	Rh-103(n,γ) Rh-104	0,1	EAF-4.1 (JEF-2.2)
147	Pd-102(n,γ) Pd-103	99	EAF-4.1 (JEF-2.2)
148	Pd-108(n,γ) Pd-109	0,1	EAF-4.1 (JEF-2.2)
149	Pd-110(n,γ) Pd-111	0,1	EAF-4.1 (JEF-2.2)
150	Ag-107(n,γ) Ag-108m	1	EAF-4.1 (JEF-2.2)
151	Ag-108m(n,γ) Ag-109	0,1	EAF-4.1
152	Ag-109(n,2n) Ag-108m	1	CRP
153	Ag-109(n,γ) Ag-110m	1	EAF-4.1 (JEF-2.2)
154	Cd-106(n,γ) Cd-107	99	EAF-4.1 (JEF-2.2)
155	Cd-108(n,γ) Cd-109	99	EAF-4.1 (JENDL-3.1)
156	Cd-114(n,γ) Cd-115	0,1	EAF-4.1 (JEF-2.2)
157	In-113(n,γ) In-114	0,1	EAF-4.1 (JEF-2.2)
158	In-115(n,n') In-115m	1	ENDF/B-VI
159	In-115(n,γ) In-116	0,1	ENDF/B-VI [FS=0], JEF-2.2 [FS=1]
160	Sn-120(n,γ) Sn-121m	1	EAF-4.1 (JEF-2.2)
161	Sn-121(n,γ) Sn-122	99	EAF-4.1
162	Sn-122(n,2n) Sn-121m	1	EAF-4.1 (JEF-2.2)
163	Sn-125(n,γ) Sn-126	99	EAF-4.1 (JEF-2.2)
164	Sn-126(n,γ) Sn-127	99	EAF-4.1 (JEF-2.2)
165	Sb-123(n,γ) Sb-124	0,1,2	EAF-4.1 (JEF-2.2)
166	Sb-124(n,γ) Sb-125	99	EAF-4.1 (JEF-2.2)
167	Te-120(n,γ) Te-121	0,1	EAF-4.1 (JEF-2.2)
168	Te-128(n,γ) Te-129	0,1	EAF-4.1 (JEF-2.2)
169	Te-130(n,γ) Te-131	0,1	EAF-4.1 (JEF-2.2)
170	I-127(n,2n) I-126	99	EAF-4.1 (IRDF-90.2)
171	I-127(n,γ) I-128	99	EAF-4.1 (JEF-2.2)
172	I-128(n,γ) I-129	99	EAF-4.1
173	Xe-134(n,γ) Xe-135	0,1	EAF-4.1 (JEF-2.2)
174	Xe-136(n,γ) Xe-137	99	EAF-4.1 (JEF-2.2)

Table 1. Cont.

#	Reaction	FS	Data
175	Cs-133(n,γ) Cs-134	0,1	EAF-4.1 (JEF-2.2)
176	Cs-135(n,γ) Cs-136	0,1	EAF-4.1 (JEF-2.2)
177	Cs-136(n,γ) Cs-137	99	EAF-4.1 (JEF-2.2)
178	Cs-137(n,γ) Cs-138	0,1	EAF-4.1 (JEF-2.2)
179	Ba-130(n,γ) Ba-131	0,1	EAF-4.1
180	Ba-132(n,γ) Ba-133	0,1	EAF-4.1 (JENDL-3.1)
181	Ba-137(n,p) Cs-137	99	ADL-3
182	Ba-138(n,α) Xe-135	0,1	ADL-3
183	La-138(n,γ) La-139	99	EAF-4.1 (JENDL-3.1)
184	La-139(n,γ) La-140	99	EAF-4.1 (JEF-2.2)
185	Ce-143(n,γ) Ce-144	99	EAF-4.1 (JEF-2.2)
186	Nd-146(n,γ) Nd-147	99	EAF-4.1 (JEF-2.2)
187	Nd-148(n,γ) Nd-149	99	EAF-4.1 (JEF-2.2)
188	Nd-150(n,γ) Nd-151	99	EAF-4.1 (JEF-2.2)
189	Sm-144(n,γ) Sm-145	99	EAF-99
190	Sm-152(n,γ) Sm-153	99	EAF-4.1 (JEF-2.2)
191	Sm-154(n,γ) Sm-155	99	EAF-4.1 (JEF-2.2)
192	Eu-151(n,2n) Eu-150	0,1	CRP [FS=0], ADL-3 [FS=1]
193	Eu-151(n,γ) Eu-152	0,1,2	EAF-4.1 (JEF-2.2)
194	Eu-153(n,2n) Eu-152	0,1,2	CRP [FS=0], EAF-4.1 [FS=1,2]
195	Eu-153(n,γ) Eu-154	0,1	EAF-4.1 (JEF-2.2)
196	Eu-154(n,γ) Eu-155	99	EAF-4.1 (JEF-2.2)
197	Tb-159(n,2n) Tb-158	0,1	CRP [FS=0], ADL-3 [FS=1]
198	Tb-159(n,γ) Tb-160	99	EAF-4.1 (JEF-2.2)
199	Dy-158(n,γ) Dy-159	99	EAF-4.1
200	Dy-158(n,p) Tb-158	0,1	EAF-4.1 (ADL-3)
201	Dy-164(n,γ) Dy-165	0,1	EAF-4.1 (JEF-2.2)
202	Ho-165(n,γ) Ho-166	0,1	EAF-4.1 (JEF-2.2)
203	Er-162(n,γ) Er-163	99	EAF-4.1
204	Er-164(n,γ) Er-165	99	EAF-4.1
205	Er-168(n,γ) Er-169	99	EAF-4.1
206	Er-170(n,γ) Er-171	99	EAF-4.1
207	Tm-169(n,γ) Tm-170	99	EAF-4.1
208	Yb-168(n,γ) Yb-169	0,1	EAF-4.1
209	Yb-174(n,γ) Yb-175	99	EAF-4.1
210	Yb-176(n,γ) Yb-177	0,1	EAF-4.1
211	Lu-175(n,γ) Lu-176	0,1	EAF-4.1 (JEF-2.2)
212	Lu-176(n,γ) Lu-177	0,1	EAF-4.1 (JEF-2.2)
213	Hf-174(n,γ) Hf-175	99	EAF-4.1 (JEF-2.2)
214	Hf-179(n,2n) Hf-178n	2	CRP
215	Ta-181(n,3n) Ta-179	99	ADL-3
216	Ta-181(n,γ) Ta-182	0,1,2	EAF-4.1 (JEF-2.2)
217	W-182(n,2n) W-181	99	ADL-3
218	W-182(n,nα) Hf-178n	2	ADL-3

Table 1. Cont.

#	Reaction	FS	Data
219	W-183(n,γ) W-184	99	EAF-4.1 (JEF-2.2)
220	W-184(n,γ) W-185	99	EAF-4.1 (LANL)
221	W-186(n,2n) W-185	0,1	JENDL-Act96
222	W-186(n,nα) Hf-182	0,1	ADL-3
223	W-186(n,γ) W-187	99	EAF-4.1 (JEF-2.2)
224	Re-185(n,2n) Re-184	0,1	EAF-4.1 (ENDF/B-VI)
225	Re-185(n,γ) Re-186m	1	EAF-4.1 (LANL)
226	Re-187(n,2n) Re-186m	1	CRP
227	Re-187(n,γ) Re-188	0,1	EAF-4.1 (JEF-2.2)
228	Re-187(n,p) W-187	99	ADL-3
229	Os-184(n,γ) Os-185	99	EAF-4.1
230	Os-188(n,γ) Os-189	0,1	EAF-4.1
231	Os-190(n,γ) Os-191	0,1	EAF-4.1
232	Os-190(n,α) W-187	99	EAF-99
233	Os-192(n,γ) Os-193	99	EAF-4.1
234	Ir-191(n,γ) Ir-192n	2	EAF-4.1
235	Ir-192(n,n') Ir-192n	2	EAF-4.1 (ADL-3)
236	Ir-192n(n,γ) Ir-193	0,1	EAF-4.1
237	Ir-193(n,2n) Ir-192n	2	EAF-4.1 (ADL-3)
238	Pt-190(n,γ) Pt-191	99	EAF-4.1
239	Pt-192(n,γ) Pt-193	0,1	EAF-4.1
240	Pt-194(n,γ) Pt-195	99	LANL-96
241	Pt-196(n,γ) Pt-197	99	LANL-96
242	Pt-198(n,γ) Pt-198	99	LANL-96
243	Au-197(n,2n) Au-196	99	EAF-4.1 (IRDF-90.2)
244	Au-197(n,γ) Au-198	0,1	EAF-4.1 (JEF-2.2)
245	Hg-196(n,γ) Hg-197	0,1	EAF-4.1
246	Hg-202(n,γ) Hg-203	99	EAF-4.1
247	Hg-204(n,γ) Hg-205	99	EAF-4.1
248	Tl-203(n,γ) Tl-204	99	EAF-4.1
249	Tl-205(n,γ) Tl-206	0,1	EAF-4.1
250	Pb-204(n,2n) Pb-203	0,1	ADL-3
251	Pb-206(n,2n) Pb-205	99	FENDL/A-1 (ENDF/B-VI)
252	Pb-206(n,α) Hg-203	99	ADL-3
253	Pb-208(n,γ) Pb-209	99	EAF-4.1 (ENDF/B-VI)
254	Bi-209(n,2n) Bi-208	99	IPPE
255	Bi-209(n,γ) Bi-210m	1	EAF-4.1 (JEF-2.2)

Table 2. Sources of adopted evaluations.

Data source	Number
ADL-3 [2]	42
CRP [7]	7
EAF-4.1 [3]	39
EAF-99 [8]	2
EFF-2.4 [9]	7
ENDF/B-VI [10]	14
FENDL/A-1 [4]	1
IPPE [11–13]	5
IRDF-90.2 [14]	16
IRK [15]	2
JEF-2.2 [16]	79
JENDL-3.1 [17]	12
JENDL-3.2 [18]	1
JENDL-Act96 [1]	19
JENDL-FF [19, 20]	1
LANL [21]	2
LANL-96 [22]	3
RNAL	2
RRDF-98 [23]	6
Total	260

Statistics of the evaluation origins and related references are displayed in Table 2. In most cases, all channels (FS=0,1 or (n,np) and (n,d)) contributing to a reaction were taken from the same source. However, for 5 reactions evaluations from two different libraries were accepted for separate channels. This brings the sum in Table 2 to 260.

1.4. Library format and structure

The strict ENDF-6 format has been adopted without any modifications. The total cross-sections are stored in file MF=3. The partial cross-sections, leading to the ground state or metastable states of the residual nucleus are coded in file MF=10. Within MF=10 the identifiers LIS and LFS are used to indicate states (isomers) of the target and final nuclei, respectively. According to standard ENDF-6 convention LFS is 0 for the ground state, 1 for the first metastable state and 2 for the second metastable state.

The RNAL library is stored in separate files for each reaction and final state (g.s., first metastable and second metastable states if appropriate), unless reaction to the metastable state is the reference reaction. If no metastable state exists in the final nucleus the total cross-sections are given. The total cross-sections are also given for some reactions leading to the nuclei with metastable states if partial cross-sections were not available in the recommended evaluation. In addition, separate evaluations are generally given for the (n,np) and (n,d) reaction channels. Only in the two original RNAL evaluations (^{47}Ti and

^{92}Mo calculated with EMPIRE-2.13) the data represent a sum of (n,np) and (n,d) reaction channels. Thus, RNAL contains 342 evaluations which are listed in Table 3. The names of the files consist of 'za' characters followed by Z and A numbers, dot, and MT of the reaction. In the case of a partial cross-section the standard ENDF-6 MT number (in the file name only!) is increased by 300 for the reaction leaving a residue in the first metastable state and by 600 for the second metastable state.

For the convenience of the user a single ENDF-6 file containing all RNAL evaluations is also provided (compressed with GNU gzip, size 6 Mb).

Table 3. List of RNAL files.

#	Reaction	total	g.s.	meta-1	meta-2
1	H- 1(n,γ)	za01001.102			
2	B-10(n,α)	za05010.107			
3	C-12(n,2n)	za06012.016			
4	C-12(n,γ)	za06012.102			
5	C-13(n,γ)	za06013.102			
6	N-14(n,p)	za07014.103			
7	O-16(n,nα)	za08016.022			
8	O-16(n,p)	za08016.103			
9	F-19(n,2n)	za09019.016			
10	Na-23(n,2n)	za11023.016			
11	Na-23(n,γ)		za11023.102	za11023.402	
12	Mg-24(n,p)		za12024.103	za12024.403	
13	Mg-26(n,γ)	za12026.102			
14	Al-27(n,2n)		za13027.016	za13027.316	
15	Al-27(n,nα)	za13027.022			
16	Al-27(n,γ)	za13027.102			
17	Al-27(n,p)	za13027.103			
18	Al-27(n,α)		za13027.107	za13027.407	
19	Si-28(n,p)	za14028.103			
20	Si-28(n,np)	za14028.028			
	Si-28(n,d)	za14028.104			
21	Si-29(n,p)	za14029.103			
22	Si-29(n,np)	za14029.028			
	Si-29(n,d)	za14029.104			
23	Si-29(n,t)	za14029.105			
24	Si-30(n,α)	za14030.107			
25	Si-30(n,γ)	za14030.102			
26	P-31(n,γ)	za15031.102			
27	P-31(n,p)	za15031.103			
28	P-31(n,α)	za15031.107			
29	S-32(n,p)	za16032.103			
30	S-34(n,γ)	za16034.102			
31	S-34(n,p)	za16034.103			
32	S-36(n,γ)	za16036.102			
33	Cl-35(n,2n)		za17035.016	za17035.316	
34	Cl-35(n,γ)	za17035.102			
35	Cl-37(n,γ)		za17037.102	za17037.402	
36	Cl-37(n,p)	za17037.103			
37	Cl-37(n,α)	za17037.107			
38	Ar-36(n,γ)	za18036.102			
39	Ar-38(n,γ)	za18038.102			
40	Ar-40(n,γ)	za18040.102			
41	K-39(n,p)	za19039.103			
42	K-41(n,γ)	za19041.102			

Table 3. Cont.

#	Reaction	total	g.s.	meta-1	meta-2
43	K-41(n,α)		za19041.107	za19041.407	
44	Ca-40(n,γ)	za20040.102			
45	Ca-44(n,p)	za20044.103			
46	Ca-45(n,α)	za20045.107			
47	Ca-48(n,γ)	za20048.102			
48	Sc-45(n,γ)		za21045.102	za21045.402	
49	Ti-46(n,2n)	za22046.016			
50	Ti-46(n,p)		za22046.103	za22046.403	
51	Ti-47(n,p)	za22047.103			
52	Ti-47(n,np+d)	za22047.104			
53	Ti-48(n,p)	za22048.103			
54	Ti-48(n,np)	za22048.028			
	Ti-48(n,d)	za22048.104			
55	Ti-48(n,α)	za22048.107			
56	Ti-50(n,α)	za22050.107			
57	Ti-50(n,γ)	za22050.102			
58	V-50(n,2n)	za23050.016			
59	V-51(n,γ)	za23051.102			
60	V-51(n,p)	za23051.103			
61	V-51(n,α)	za23051.107			
62	Cr-50(n,γ)	za24050.102			
63	Cr-52(n,2n)	za24052.016			
64	Cr-52(n,p)	za24052.103			
65	Cr-53(n,np)	za24053.028			
	Cr-53(n,d)	za24053.104			
66	Cr-54(n,γ)	za24054.102			
67	Cr-54(n,α)	za24054.107			
68	Mn-53(n,γ)	za25053.102			
69	Mn-55(n,2n)	za25055.016			
70	Mn-55(n,γ)	za25055.102			
71	Mn-55(n,α)	za25055.107			
72	Fe-54(n,2n)		za26054.016	za26054.316	
73	Fe-54(n,γ)	za26054.102			
74	Fe-54(n,p)	za26054.103			
75	Fe-56(n,2n)	za26056.016			
76	Fe-56(n,γ)	za26056.102			
77	Fe-56(n,p)	za26056.103			
78	Fe-57(n,γ)	za26057.102			
79	Fe-58(n,γ)	za26058.102			
80	Fe-60(n,γ)	za26060.102			
81	Co-59(n,2n)	za27059.016			
82	Co-59(n,γ)		za27059.102	za27059.402	
83	Co-59(n,α)	za27059.107			
84	Co-60(n,γ)	za27060.102			

Table 3. Cont.

#	Reaction	total	g.s.	meta-1	meta-2
85	Co-60(n,p)	za27060.103			
86	Ni-58(n,2n)	za28058.016			
87	Ni-58(n,γ)	za28058.102			
88	Ni-58(n,p)	za28058.103			
89	Ni-58(n,np)	za28058.028			
	Ni-58(n,d)	za28058.104			
90	Ni-60(n,2n)	za28060.016			
91	Ni-60(n,p)		za28060.103	za28060.403	
92	Ni-61(n,γ)	za28061.102			
93	Ni-62(n,γ)	za28062.102			
94	Ni-64(n,2n)	za28064.016			
95	Ni-64(n,γ)	za28064.102			
96	Cu-63(n,2n)	za29063.016			
97	Cu-63(n,γ)	za29063.102			
98	Cu-63(n,p)	za29063.103			
99	Cu-63(n,α)	za29063.107			
100	Cu-65(n,2n)	za29065.016			
101	Cu-65(n,γ)	za29065.102			
102	Zn-64(n,γ)	za30064.102			
103	Zn-64(n,p)	za30064.103			
104	Zn-66(n,p)	za30066.103			
105	Zn-68(n,γ)		za30068.102	za30068.402	
106	Zn-70(n,γ)		za30070.102	za30070.402	
107	Ga-69(n,γ)	za31069.102			
108	Ga-69(n,α)	za31069.107			
109	Ga-71(n,γ)	za31071.102			
110	Se-74(n,γ)	za34074.102			
111	Se-78(n,γ)		za34078.102	za34078.402	
112	Se-79(n,γ)	za34079.102			
113	Se-80(n,γ)		za34080.102	za34080.402	
114	Se-82(n,γ)		za34082.102	za34082.402	
115	Kr-80(n,γ)		za36080.102	za36080.402	
116	Kr-84(n,γ)		za36084.102	za36084.402	
117	Kr-86(n,γ)	za36086.102			
118	Rb-85(n,γ)		za37085.102	za37085.402	
119	Sr-84(n,γ)		za38084.102	za38084.402	
120	Sr-89(n,γ)	za38089.102			
121	Sr-90(n,γ)	za38090.102			
122	Zr-90(n,2n)		za40090.016	za40090.316	
123	Zr-93(n,γ)	za40093.102			
124	Zr-94(n,γ)	za40094.102			
125	Zr-96(n,2n)	za40096.016			
126	Nb-93(n,n')			za41093.051	
127	Nb-93(n,2n)		za41093.016	za41093.316	

Table 3. Cont.

#	Reaction	total	g.s.	meta-1	meta-2
128	Nb-93(n,γ)		za41093.102	za41093.402	
129	Mo-92(n,γ)		za42092.102	za42092.402	
130	Mo-92(n,p)			za42092.403	
131	Mo-92(n,d+np)			za42092.404	
132	Mo-93(n,np)		za42093.028	za42093.328	
	Mo-93(n,d)		za42093.104	za42093.404	
133	Mo-94(n,2n)		za42094.016	za42094.316	
134	Mo-94(n,p)		za42094.103	za42094.403	
135	Mo-94(n,np)			za42094.328	
	Mo-94(n,d)			za42094.404	
136	Mo-95(n,p)		za42095.103	za42095.403	
137	Mo-95(n,np)		za42095.028	za42095.328	
	Mo-95(n,d)		za42095.104	za42095.404	
138	Mo-98(n,γ)	za42098.102			
139	Mo-100(n,2n)	za42100.016			
140	Mo-100(n,γ)	za42100.102			
141	Tc-99(n,2n)	za43099.016			
142	Ru-96(n,γ)	za44096.102			
143	Ru-102(n,γ)	za44102.102			
144	Ru-104(n,γ)	za44104.102			
145	Rh-103(n,n')			za45103.304	
146	Rh-103(n,γ)		za45103.102	za45103.402	
147	Pd-102(n,γ)	za46102.102			
148	Pd-108(n,γ)		za46108.102	za46108.402	
149	Pd-110(n,γ)		za46110.102	za46110.402	
150	Ag-107(n,γ)			za47107.402	
151	Ag-108m(n,γ)		za47108.102	za47108.402	
152	Ag-109(n,2n)			za47109.316	
153	Ag-109(n,γ)			za47109.402	
154	Cd-106(n,γ)	za48106.102			
155	Cd-108(n,γ)	za48108.102			
156	Cd-114(n,γ)		za48114.102	za48114.402	
157	In-113(n,γ)		za49113.102	za49113.402	
158	In-115(n,n')			za49115.051	
159	In-115(n,γ)		za49115.102	za49115.402	
160	Sn-120(n,γ)			za50120.402	
161	Sn-121(n,γ)	za50121.102			
162	Sn-122(n,2n)			za50122.316	
163	Sn-125(n,γ)	za50125.102			
164	Sn-126(n,γ)	za50126.102			
165	Sb-123(n,γ)		za51123.102	za51123.402	za51123.702
166	Sb-124(n,γ)	za51124.102			
167	Te-120(n,γ)		za52120.102	za52120.402	

Table 3. Cont.

#	Reaction	total	g.s.	meta-1	meta-2
168	Te-128(n,γ)		za52128.102	za52128.402	
169	Te-130(n,γ)		za52130.102	za52130.402	
170	I-127(n,2n)	za53127.016			
171	I-127(n,γ)	za53127.102			
172	I-128(n,γ)	za53128.102			
173	Xe-134(n,γ)		za54134.102	za54134.402	
174	Xe-136(n,γ)	za54136.102			
175	Cs-133(n,γ)		za55133.102	za55133.402	
176	Cs-135(n,γ)		za55135.102	za55135.402	
177	Cs-136(n,γ)	za55136.102			
178	Cs-137(n,γ)		za55137.102	za55137.402	
179	Ba-130(n,γ)		za56130.102	za56130.402	
170	Ba-132(n,γ)		za56132.102	za56132.402	
181	Ba-137(n,p)	za56137.103			
182	Ba-138(n,α)		za56138.107	za56138.407	
183	La-138(n,γ)	za57138.102			
184	La-139(n,γ)	za57139.102			
185	Ce-143(n,γ)	za58143.102			
186	Nd-146(n,γ)	za60146.102			
187	Nd-148(n,γ)	za60148.102			
188	Nd-150(n,γ)	za60150.102			
189	Sm-144(n,γ)	za62144.102			
190	Sm-152(n,γ)	za62152.102			
191	Sm-154(n,γ)	za62154.102			
192	Eu-151(n,2n)		za63151.016	za63151.316	
193	Eu-151(n,γ)		za63151.102	za63151.402	za63151.702
194	Eu-153(n,2n)		za63153.016	za63153.316	za63153.616
195	Eu-153(n,γ)		za63153.102	za63153.402	
196	Eu-154(n,γ)	za63154.102			
197	Tb-159(n,2n)		za65159.016	za65159.316	
198	Tb-159(n,γ)	za65159.102			
199	Dy-158(n,γ)	za66158.102			
200	Dy-158(n,p)		za66158.103	za66158.403	
201	Dy-164(n,γ)		za66164.102	za66164.402	
202	Ho-165(n,γ)		za67165.102	za67165.402	
203	Er-162(n,γ)	za68162.102			
204	Er-164(n,γ)	za68164.102			
205	Er-168(n,γ)	za68168.102			
206	Er-170(n,γ)	za68170.102			
207	Tm-169(n,γ)	za69169.102			
208	Yb-168(n,γ)		za70168.102	za70168.402	
209	Yb-174(n,γ)	za70174.102			
210	Yb-176(n,γ)		za70176.102	za70176.402	
211	Lu-175(n,γ)		za71175.102	za71175.402	

Table 3. Cont.

#	Reaction	total	g.s.	meta-1	meta-2
212	Lu-176(n,γ)		za71176.102	za71176.402	
213	Hf-174(n,γ)	za72174.102			
214	Hf-179(n,2n)				za72179.616
215	Ta-181(n,3n)	za73181.017			
216	Ta-181(n,γ)		za73181.102	za73181.402	za73181.702
217	W-182(n,2n)	za74182.016			
218	W-182(n,nα)				za74182.622
219	W-183(n,γ)	za74183.102			
220	W-184(n,γ)	za74184.102			
221	W-186(n,2n)		za74186.016	za74186.316	
222	W-186(n,nα)		za74186.022	za74186.322	
223	W-186(n,γ)	za74186.102			
224	Re-185(n,2n)		za75185.016	za75185.316	
225	Re-185(n,γ)			za75185.402	
226	Re-187(n,2n)			za75187.316	
227	Re-187(n,γ)		za75187.102	za75187.402	
228	Re-187(n,p)	za75187.103			
229	Os-184(n,γ)	za76184.102			
230	Os-188(n,γ)		za76188.102	za76188.402	
231	Os-190(n,γ)		za76190.102	za76190.402	
232	Os-190(n,α)	za76190.107			
233	Os-192(n,γ)	za76192.102			
234	Ir-191(n,γ)				za77191.702
235	Ir-192n(n,n')				za77192.604
236	Ir-192(n,γ)		za77192.102	za77192.402	
237	Ir-193(n,2n)				za77193.616
238	Pt-190(n,γ)	za78190.102			
239	Pt-192(n,γ)		za78192.102	za78192.402	
240	Pt-194(n,γ)	za78194.102			
241	Pt-196(n,γ)	za78196.102			
242	Pt-198(n,γ)	za78198.102			
243	Au-197(n,2n)	za79197.016			
244	Au-197(n,γ)		za79197.102	za79197.402	
245	Hg-196(n,γ)		za80196.102	za80196.402	
246	Hg-202(n,γ)	za80202.102			
247	Hg-204(n,γ)	za80204.102			
248	Tl-203(n,γ)	za81203.102			
249	Tl-205(n,γ)		za81205.102	za81205.402	
250	Pb-204(n,2n)		za82204.016	za82204.316	
251	Pb-206(n,2n)	za82206.016			
252	Pb-206(n,α)	za82206.107			
253	Pb-208(n,γ)	za82208.102			
254	Bi-209(n,2n)	za83209.016			
255	Bi-209(n,γ)			za83209.402	

1.5. Final remarks

From the description given above it can be seen how the work of the CRP aiming towards the production of the RNAL has developed. Such work is necessarily of a long term nature and in addition to the production of the deliverable — in this case the RNAL library in electronic form and the present report — there is the very valuable by-product of increased international cooperation and information exchange between the relatively small number of groups working on these problems. The overriding initial considerations in the setting up of the CRP were to focus on the encouragement of new relevant experimental measurements that could be used to validate activation libraries, and on innovative work on data uncertainties, intermediate energy data and sequential charged particle interactions. Valuable contributions on these topics were presented at the two meetings, and although some are not directly present in the final library, the results of these studies will be incorporated in the various national and international programmes. This illustrates the IAEA's important role in stimulating and coordinating scientific work as well as making the results available to all in the form of data libraries. Another strand of the IAEA nuclear data programme over the last ten years has led to the production of the FENDL library. This library is targeted at the fusion community and includes many parts, one of which is an activation library. The exchange of information between RNAL and the FENDL activation library has been in both directions and the two libraries have consequently been improved. But the main reason for the production of RNAL in addition to FENDL has been the possibility of concentrating on activation reactions for applications other than fusion, and by providing data in a format appropriate for users of data in many applications. The production of an international library such as RNAL exposes it to wider scrutiny than a regional library and therefore the quality of the data can be significantly improved.

2. Assessment of the library

The RNAL library has been assembled and checked at the IAEA Nuclear Data Section. All individual evaluations were reformatted to conform to the ENDF-6 standard. A number of deviations form the ENDF-6 format were removed. All Q-values and thresholds were consistently recalculated using recent recommended masses [24] and isomer energies taken from NUDAT [25]. Finally, the library was checked using CHECKR, FIZCON and PSYCHE codes, which produced no serious diagnostics.

In the following every reaction will be shortly commented. These comments give information on the following items:

1. The original source of the data (the library) is quoted. This may help the user to look for more details on the data evaluation, if needed, in the corresponding library documentation. If EAF-4.1 is the original source (only for (n,γ) data), the code used in the evaluation is quoted.

2. The basic information on the determination of the branching ratio for the partial cross-sections to the ground state (FS=0), first and second isomeric state (FS=1,2). For reactions with partial cross-sections the redundant total cross-section is not included in the RNAL database.
3. The agreement of the adopted excitation curve with the experimental data, retrieved from the EXFOR data base, is commented on and discussed.
4. In many capture reactions additional experimental information exists (not included in EXFOR), in particular 30 keV and 14.5 MeV cross-sections, as compiled in Refs. [26] and [27]. These data are also used in the discussion of the evaluation agreements with the experimental data. The graphical presentation of many of these data can also be found in Ref. [28].
5. Finally, in cases when the agreement is not satisfactory and a revision or improvement of data is needed, this recommendation is included as a comment.

In the following, comments are given on all evaluations together with their graphical comparison with the experimental data base. This graphical validation section includes 260 figures (in 5 cases, due to the large number of experimental points, two plots are provided for a single reaction).

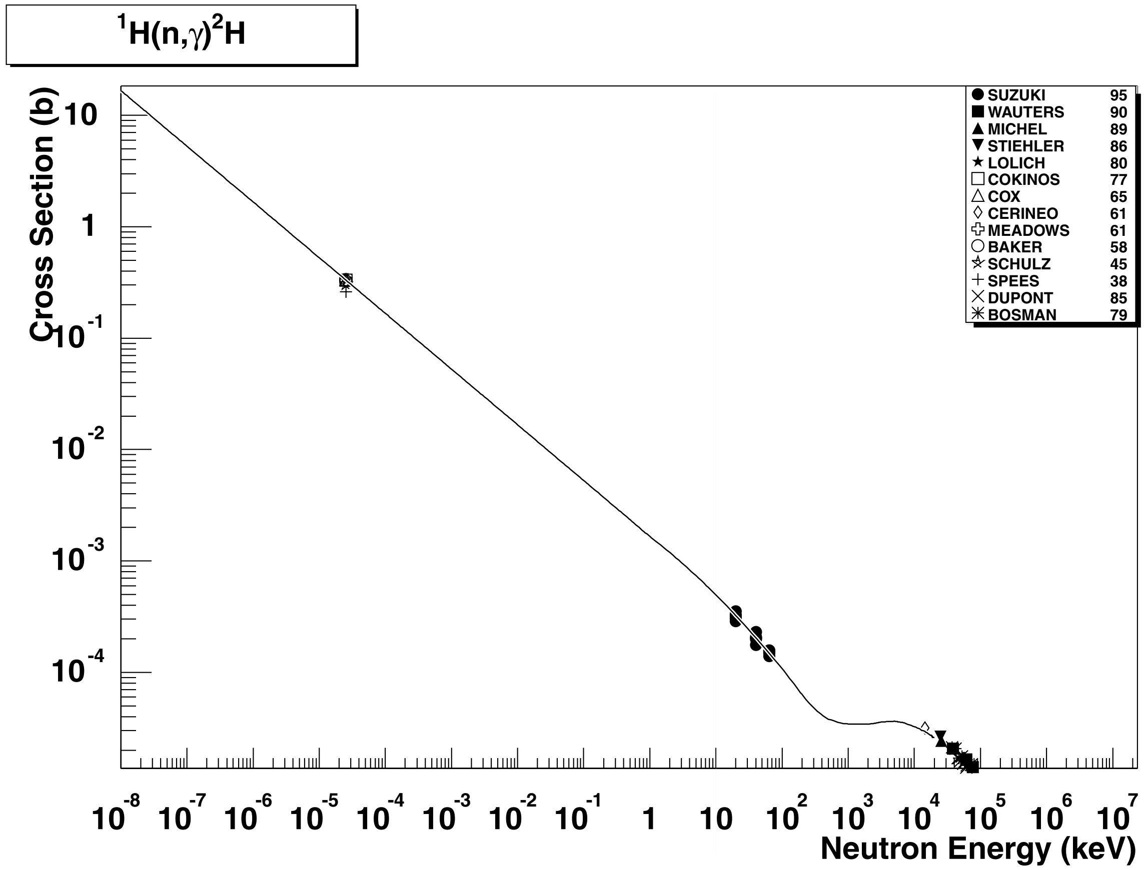

2.1. ^{1}H (n,γ) ^{2}H

final state: total
source: EAF-4.1 (JEF-2.2)

The adopted evaluation, which originates from ENDF/B-VI, reproduces well all experimental data points. There are recent experimental data obtained by Igashira et al. (private communication) between 1-100 keV, which nicely confirm the adopted ENDF/B-VI in the 1/v region.

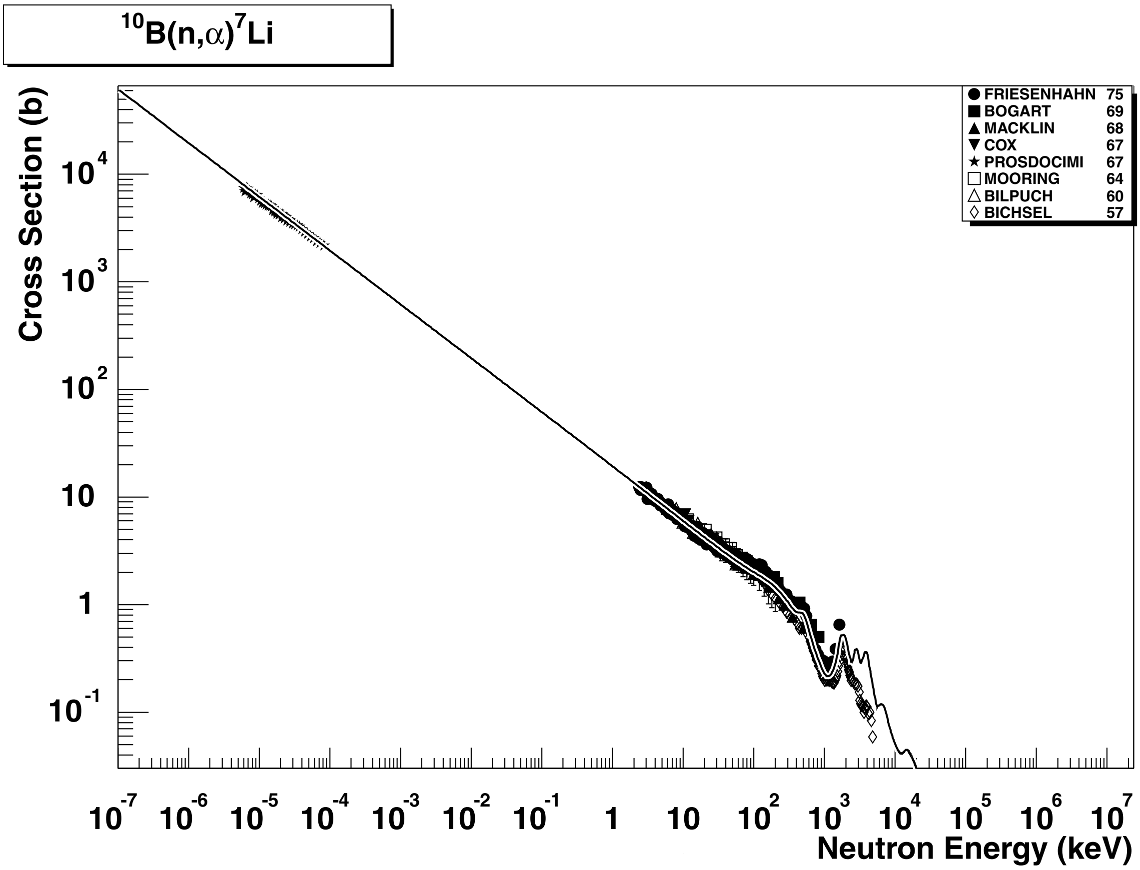

2.2. ^{10}B (n,α) ^{7}Li

final state: total
source: EAF-4.1 (IRDF-90.2)

The recommended evaluation provides for a very good reproduction of the experimental data up to the energy of 2 MeV. Above this energy several d-resonances have been included in the evaluation, which are missing in the EXFOR data.

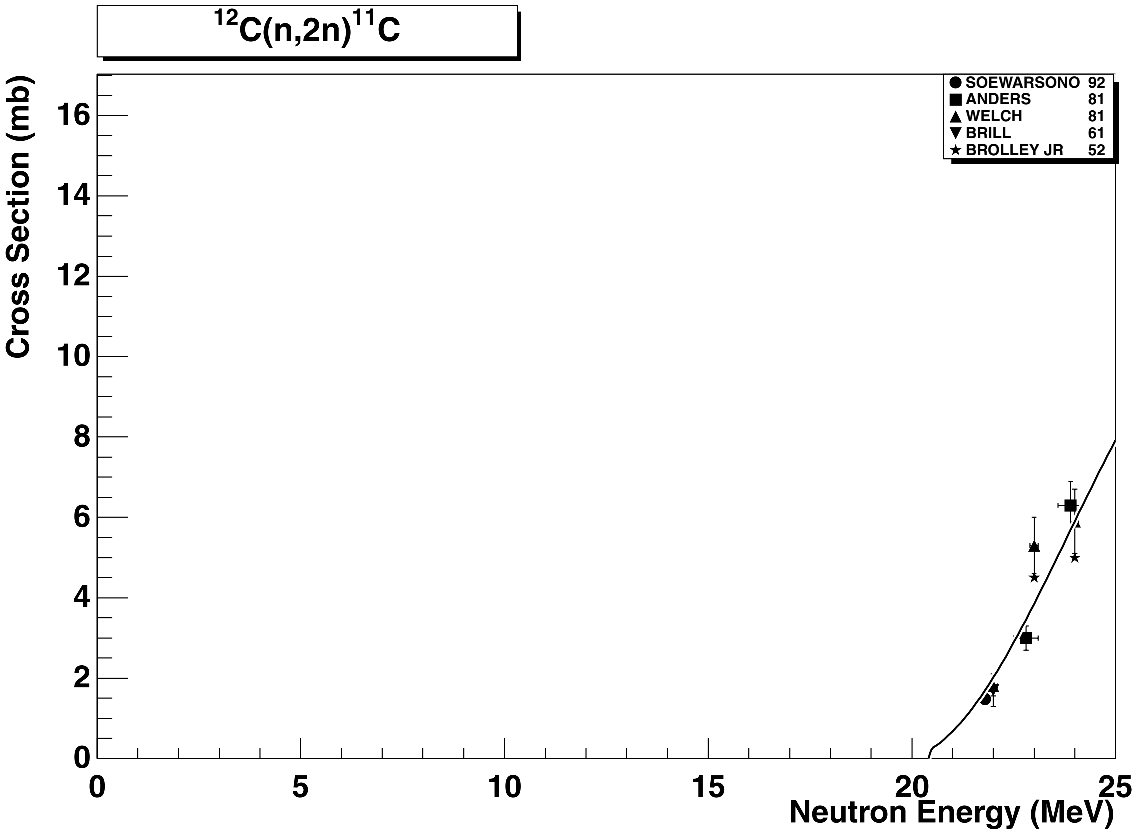

2.3. ^{12}C (n,2n) ^{11}C

final state: total
source: RRDF-98

RRDF-98 evaluation runs satisfactorily through all the experimental data.

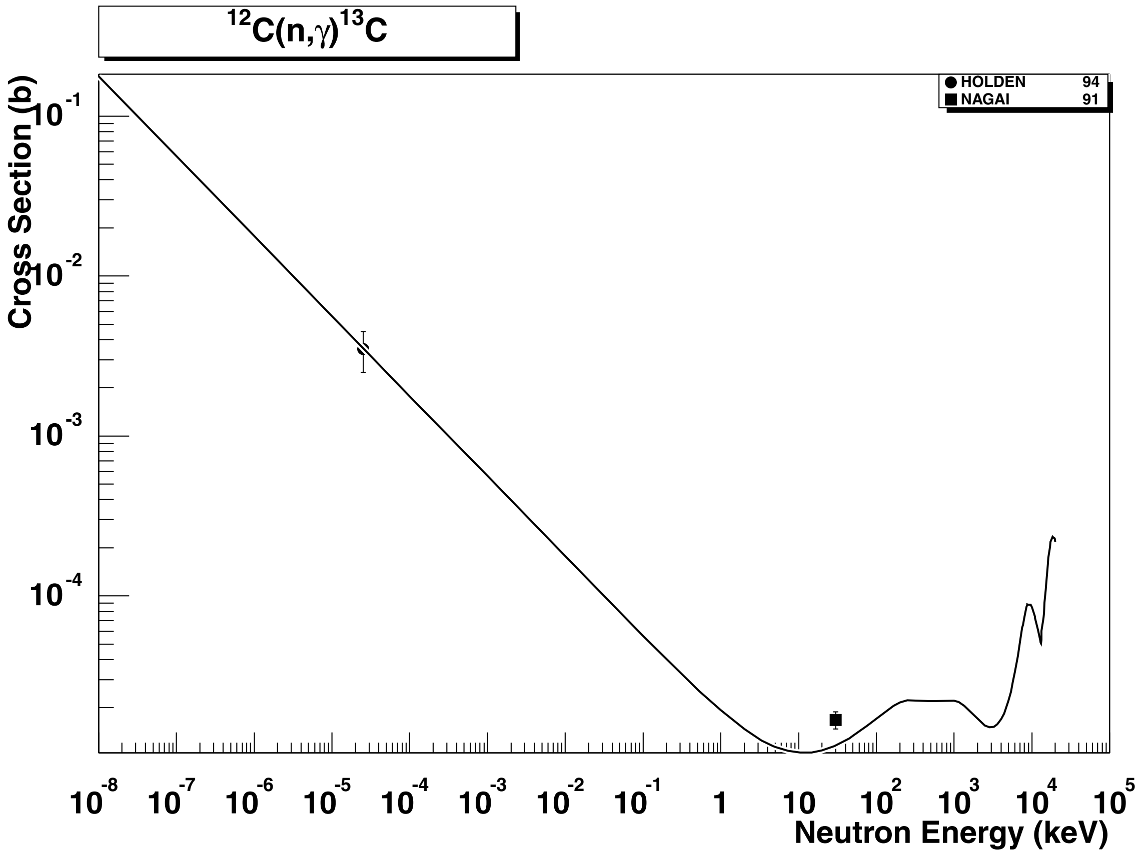

2.4. ^{12}C (n,γ) ^{13}C

final state: total
source: JENDL-FF

A new evaluation, prepared for JENDL-FF, which includes the recent direct radiation capture calculations by Mengoni [29] has been adopted. It reproduces the experimental data of Holden94, Nagai91 and recent data of Oshaki et al. [30] rather well.

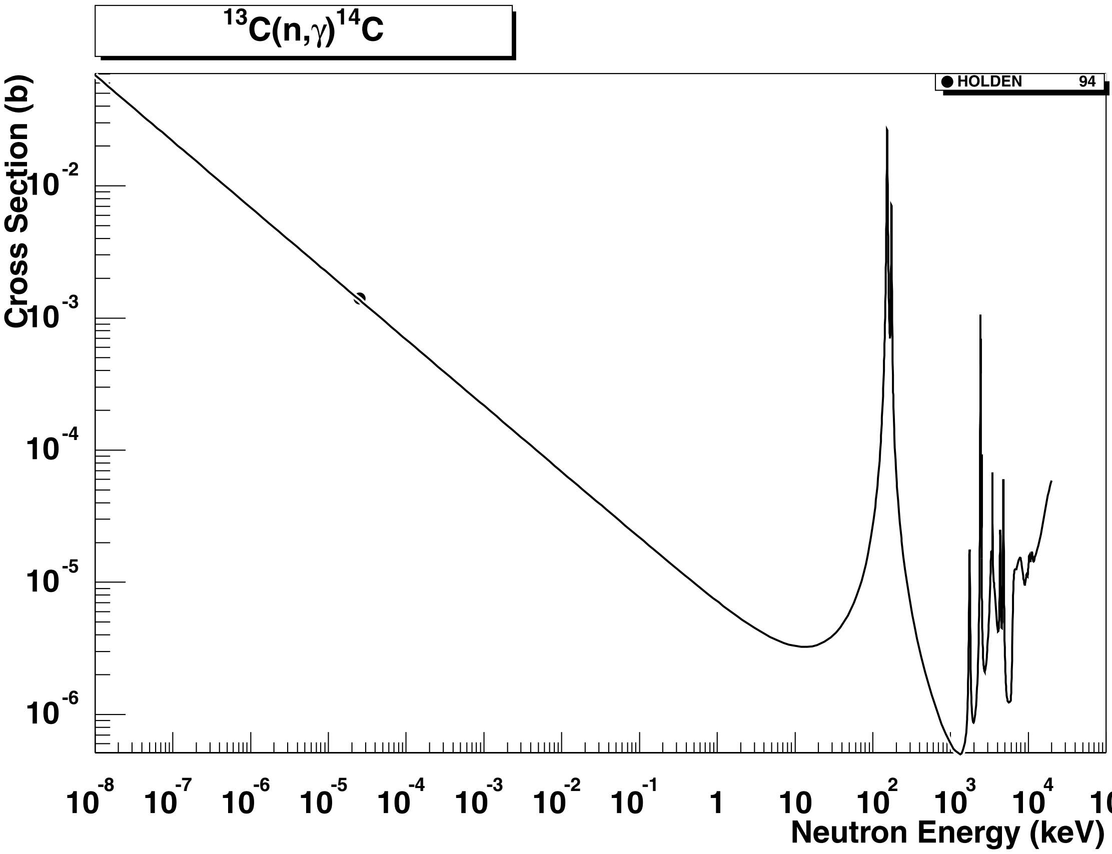

2.5. ^{13}C (n,γ) ^{14}C

final state: total
source: EAF-4.1

No experimental data are included in EXFOR. The EAF-4.1 evaluation generated cross-sections up to 7 MeV from the resolved resonance parameters of Ref. [31] (MLBW option in NJOY). These were joined smoothly with the high energy component taken over from the ACTL library. The evaluation reproduces well the thermal cross-section of Holden94 [32] (C/E=1.00) but misses the contribution of the p-wave DRC. This contribution may result in a slight increase of the cross-section in the high energy region. However, strong resolved resonance contributions make the p-wave DRC less dominant. No revision is needed at this moment, DRC calculations by Mengoni are in progress.

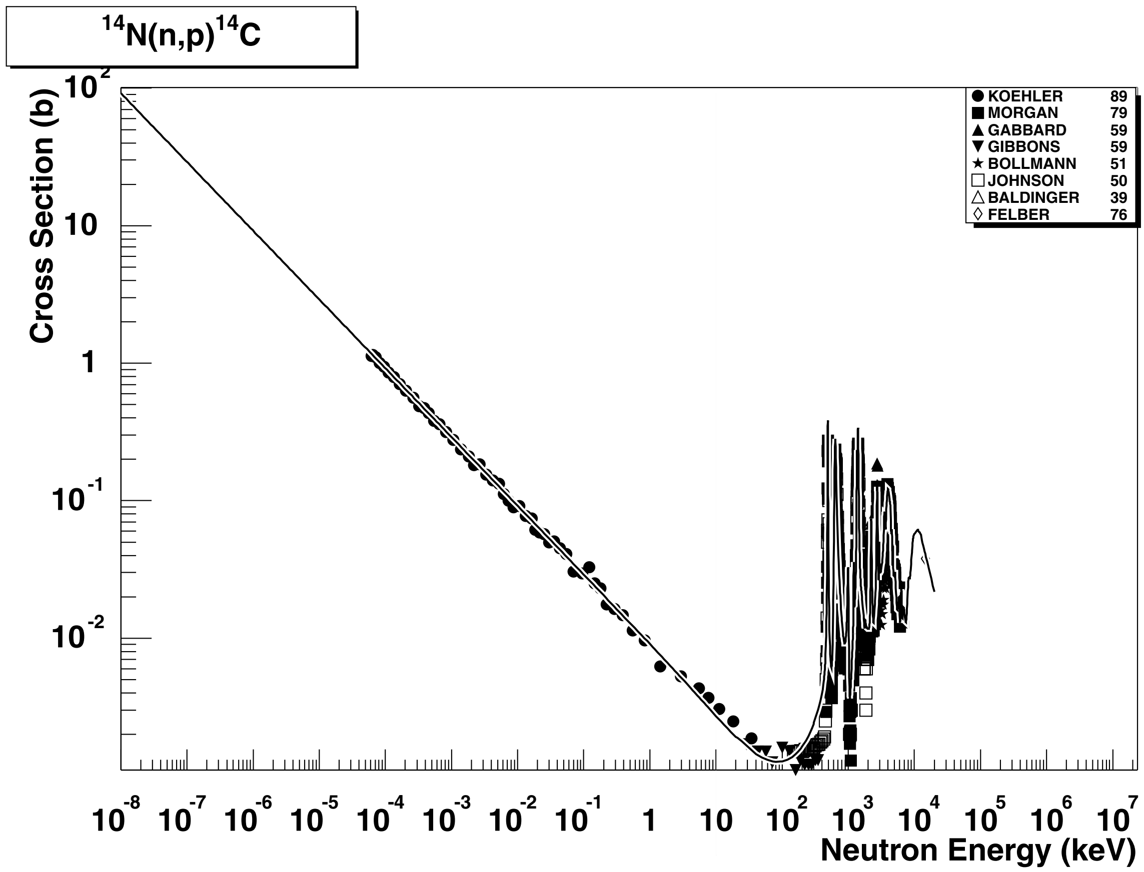

2.6. ^{14}N (n,p) ^{14}C

final state: total
source: ENDF/B-VI

The ENDF/B-VI evaluation is in excellent agreement with all experimental data in the whole energy range. The resolved resonance region is fully included.

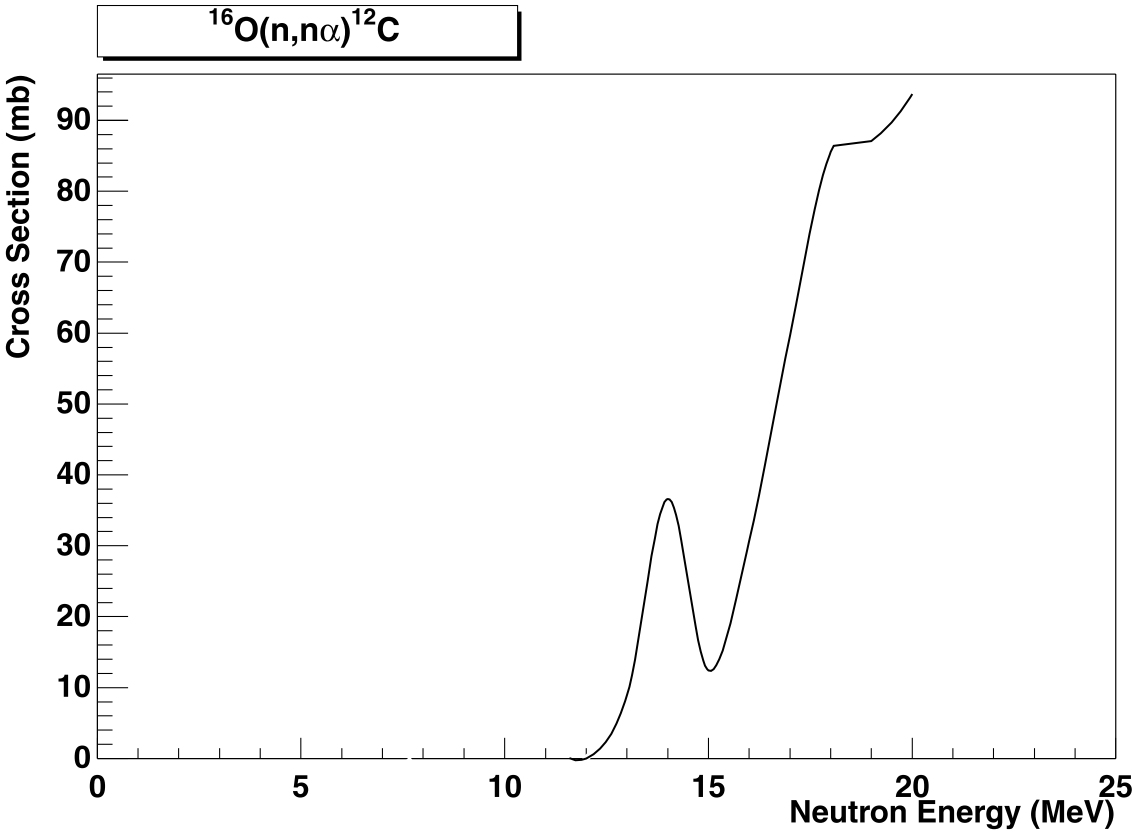

2.7. ^{16}O (n,n'α)^{12}C

final state: total
source: JENDL-Act96

No EXFOR data are available. The evaluation results from the calculation with the SINCROSII code, results of which are usually reliable.

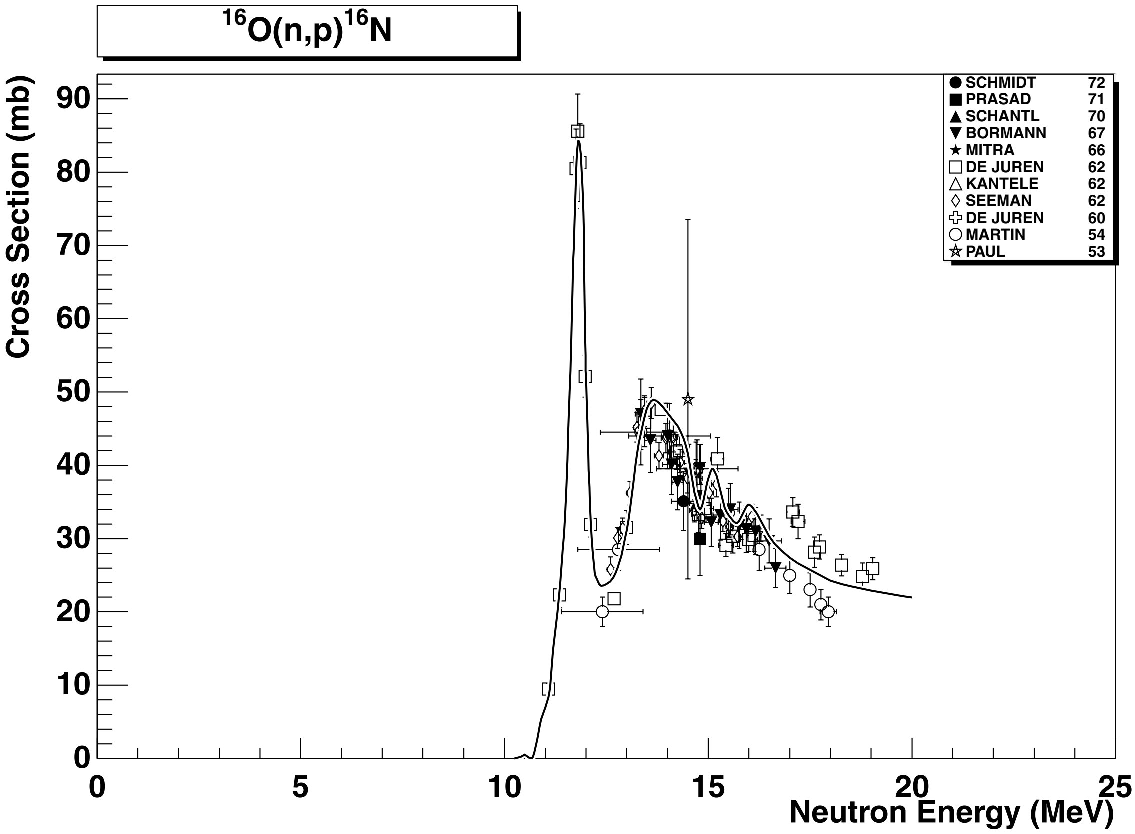

2.8. ^{16}O (n,p) ^{16}N

final state: total
source: FENDL/A-1 (ENDF/B-VI)

ENDF-B-VI reproduces all experimental data including several strong overlapping resonances above 12 MeV.

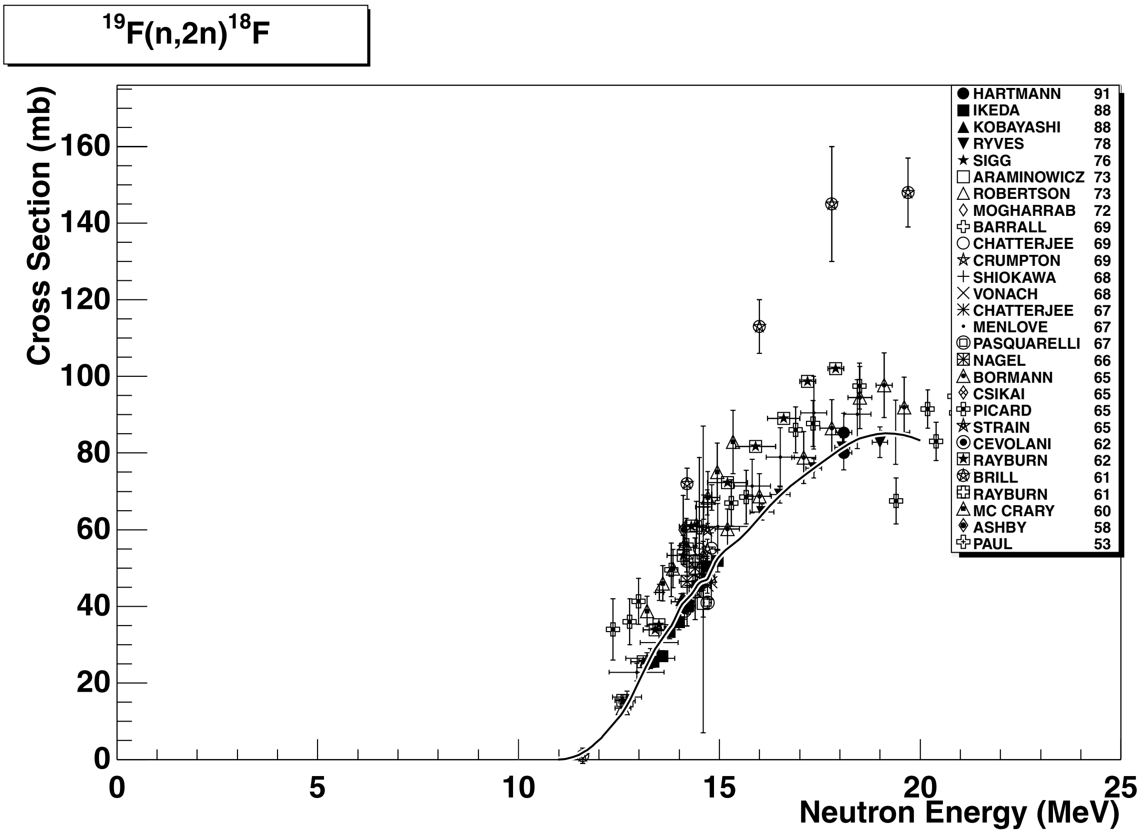

2.9. ^{19}F (n,2n) ^{18}F

final state: total
source: FENDL/A-1 (IRDF-90.2)

IRDF-90.2 evaluation lies at the lower part of the experimental data band, however, it reproduces well the latest and reliable data of Ryves78, Kobayashi88, Ikeda88 and Hartmann91. This may suggest that older data are systematically too large (Brill61 should be definitely disregarded).

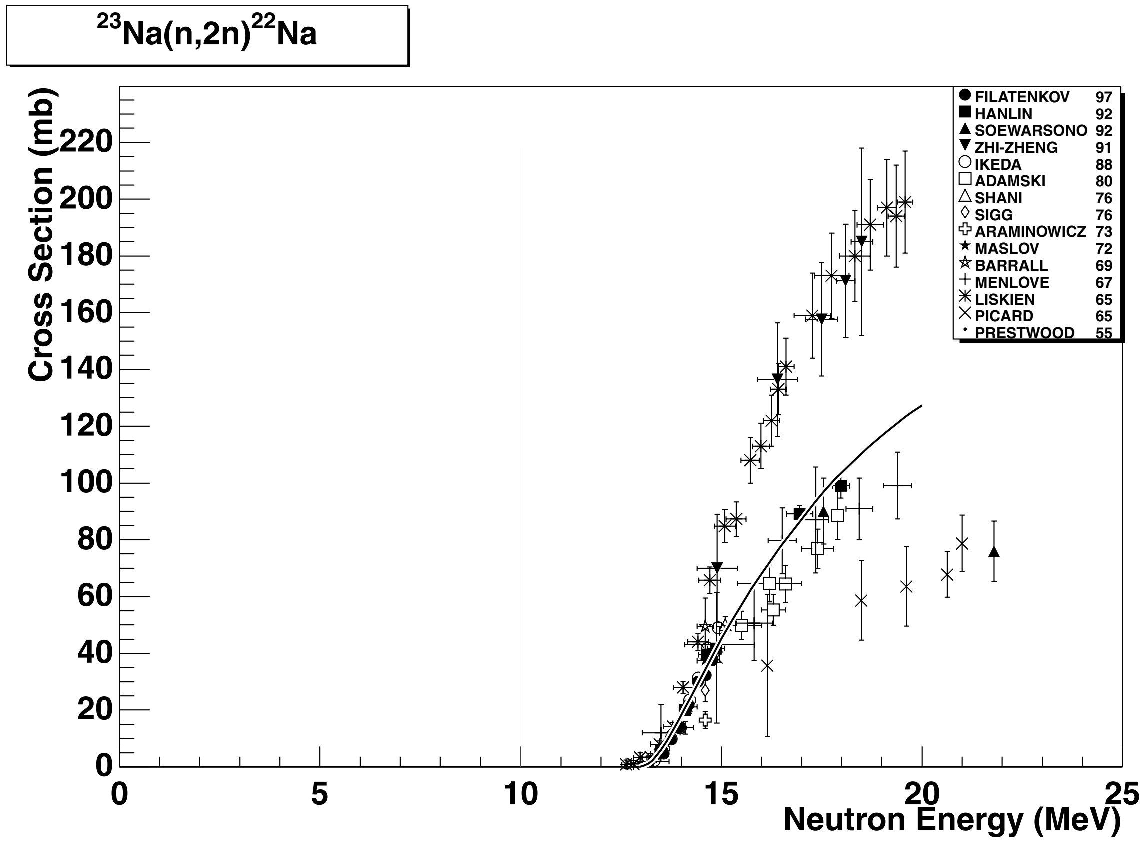

2.10. ^{23}Na (n,2n) ^{22}Na

final state: total
source: ADL-3

ADL-3 reproduces the experimental data below 15 MeV rather well. However, the experimental situation above 15 MeV is inconsistent and the data show three different trends. ADL-3 follows reasonably the intermediate trend, which includes the most recent data, such as Hanlin92, Filatenkov97 and Soerwarsono92. This is also supported by recent measurement of Wagner [33], which gives 115 mb at 19.6 MeV. The higher data set consists of Liskien65 and Zhi-zheng91, while the lower one is due to Picard65. Both these outer trends can be disregarded.

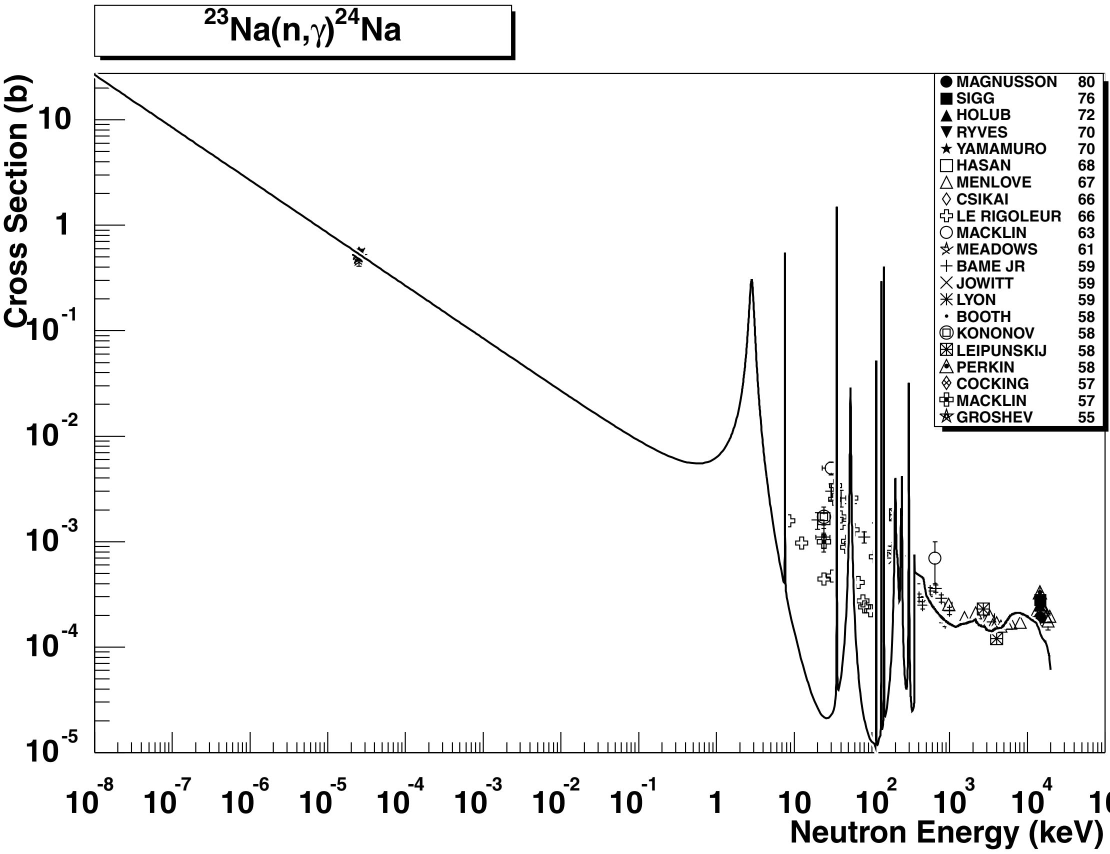

2.11. ^{23}Na (n,γ) ^{24}Na

final states: g.s., meta
source: EAF-4.1 (JEF-2.2)

The JEF-2.2 evaluation has adopted the JENDL-3.2 data. The splitting into g.s. and meta-1 cross-sections is based on the experimental data from Ref. [26] and applied up to the end of the resolved resonance region. The energy dependent branching ratio systematics [2] is applied for the high energy region. The total cross-section reasonably reproduces experimental points at the thermal energy and also the smooth component above 400 keV. The pre-equilibrium region around 15 MeV slightly underestimates the experimental data, probably due to the application of a simplified D-SD model in the calculation.

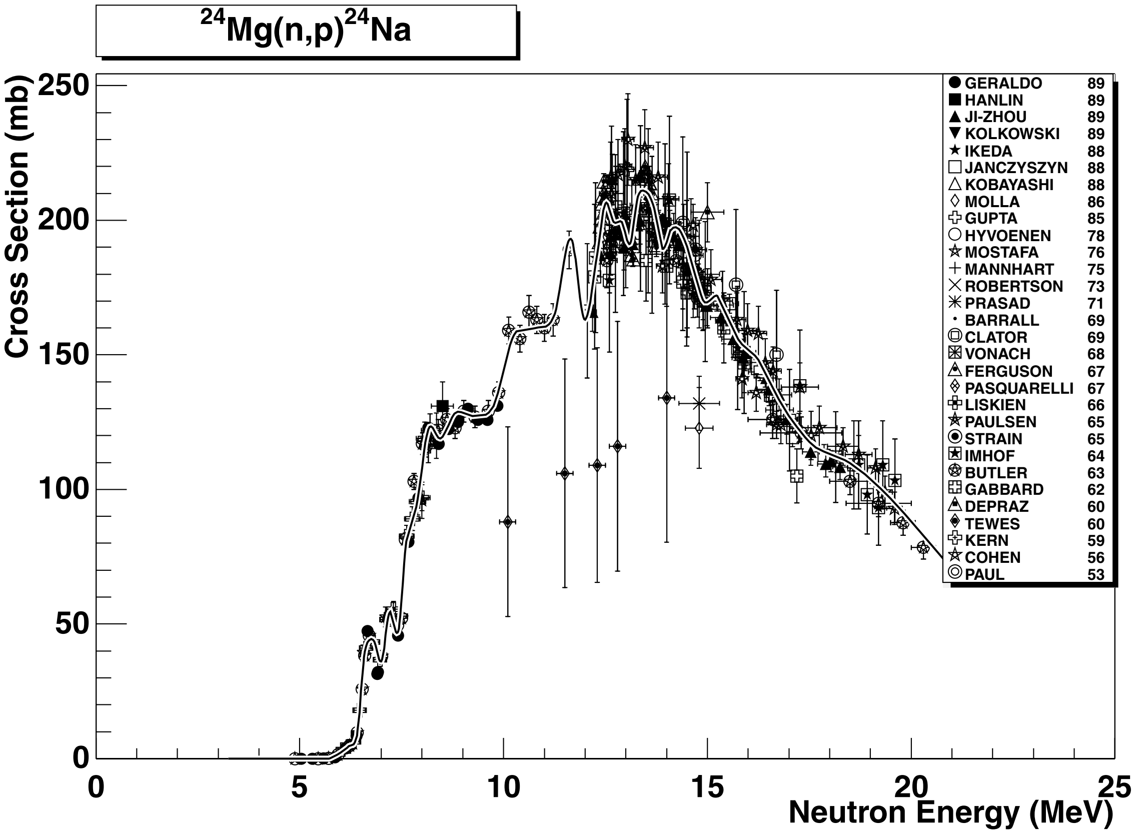

2.12. ^{24}Mg (n,p) ^{24}Na

final states: g.s., meta
source: IRDF-90.2

The evaluation from the dosimetry library IRDF-90.2 has been adopted and the branching ratio systematics of Ref. [2] has been applied to generate cross-sections to the ground state and to the metastable state. The total cross-section agrees very well with the experimental data in the whole energy range.

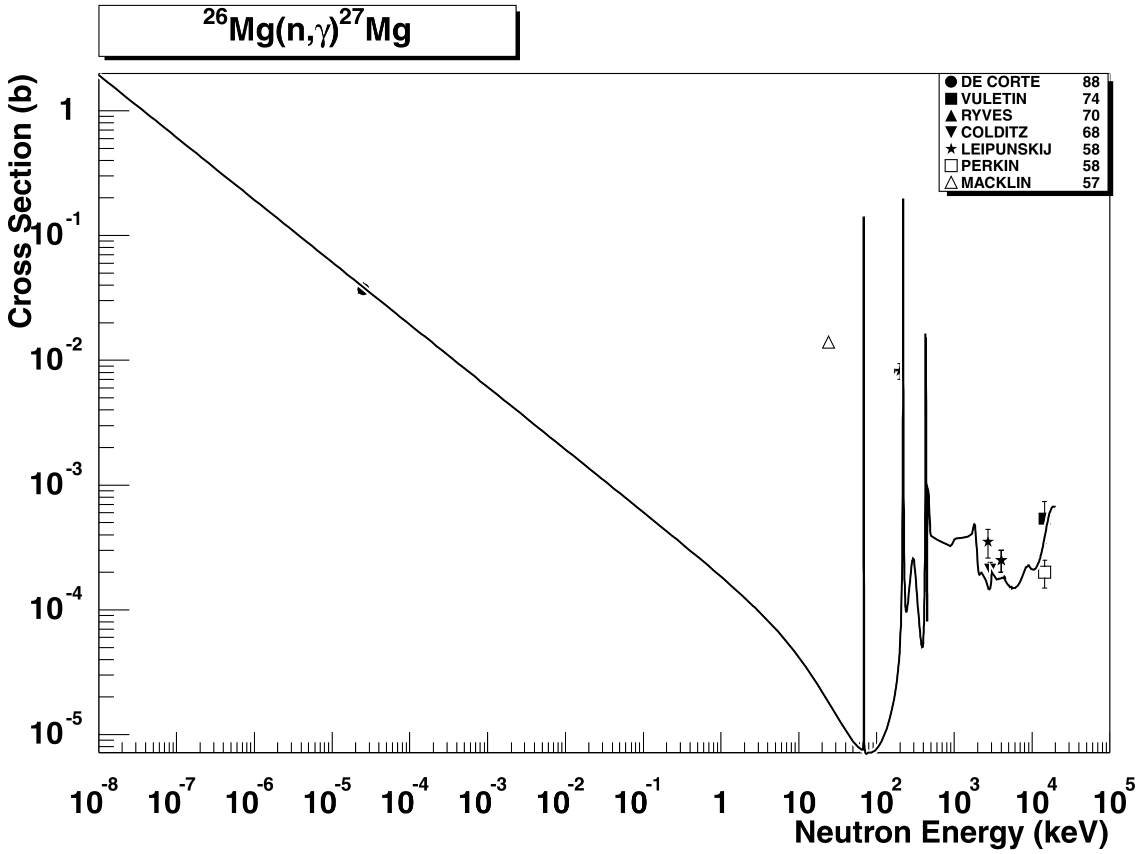

2.13. ^{26}Mg (n,γ) ^{27}Mg

final state: total
source: EAF-4.1 (JENDL-3.1)

The experimental data base is rather small. The JENDL-3.1 evaluation agrees well with the thermal point of De Corte88 and reasonably well with other experimental data except Macklin57 at about 30 keV. The latter one is an averaged value and should not be considered.

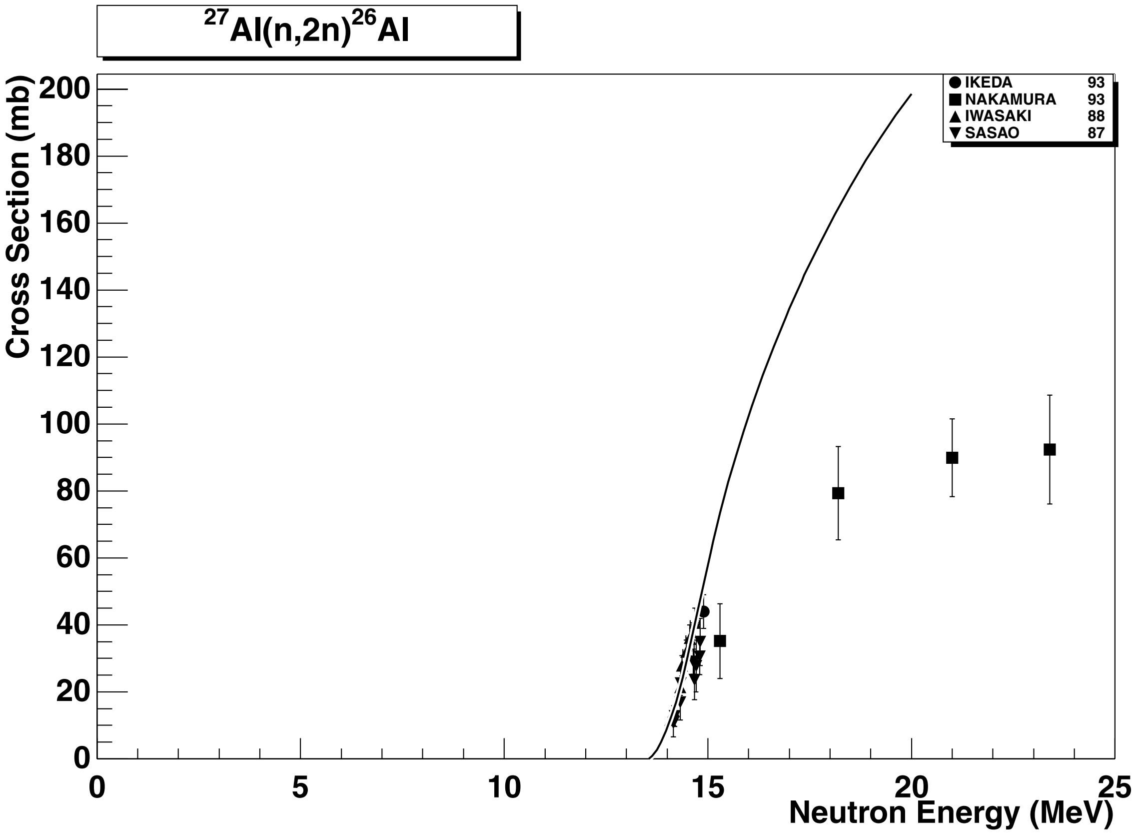

2.14. ^{27}Al (n,2n) ^{26}Al

final states: g.s., meta
source: ADL-3

ADL-3 evaluation follows nicely the experimental points below 15 MeV. The total cross-section is measured by Iwasaki88 only. Sudbrock99, Ikeda93, Nakamura93 and Sasao87 report cross-sections to the g.s.. However, population of the meta state below 15 MeV incident energy is so small that they have been plotted as total. Nakamura93 is by a factor 2 lower than the recommended evaluation. The recent data by Wallner97 [34] (not plotted due to lack of numerical data) partially confirm this trend being 30 to 40% lower than the ADL-3 evaluation. There are indications that the recommended evaluation is too high also above 15 MeV. The sum of the meta state contribution (˜40 mb at 18 MeV according to Arnold65) and the ground state cross-section (˜80 and 90 mb according to Nakamura93 and Wallner97) is well below the recommended value of about 160 mb. The g.s. and metastable cross sections result from model calculations.

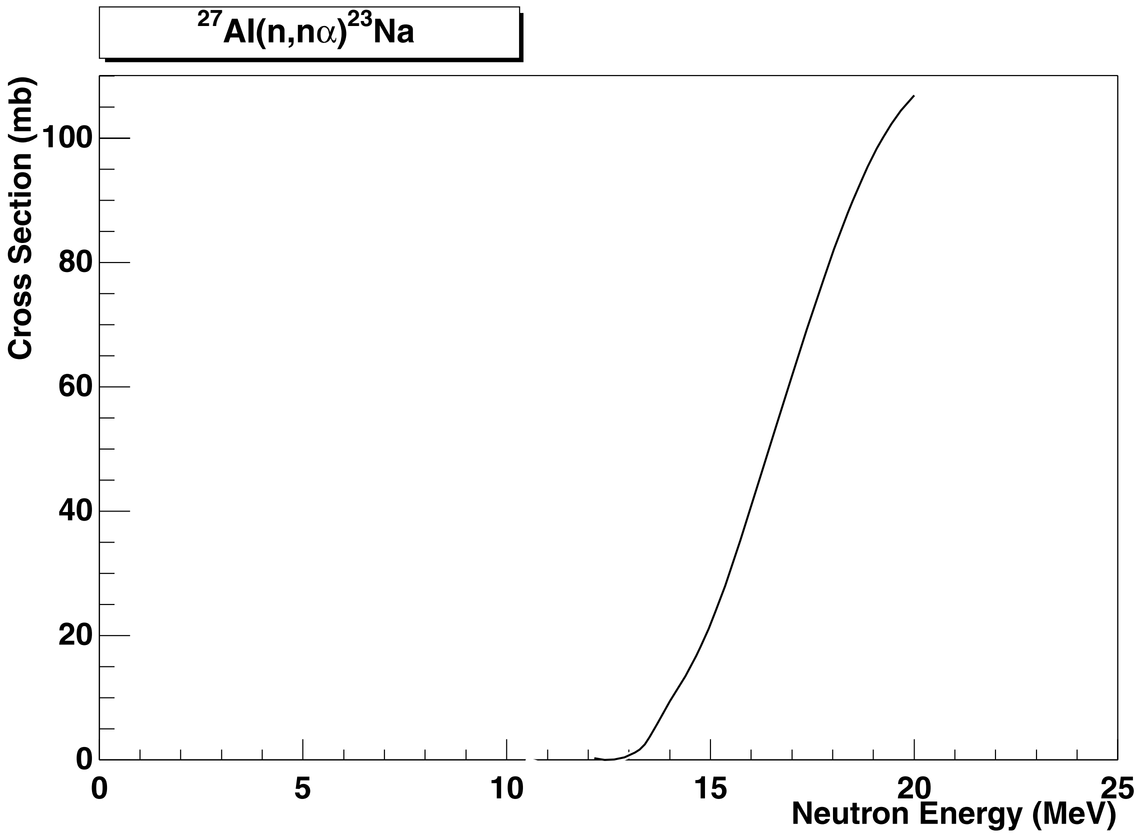

2.15. ^{27}Al (n,nα) ^{23}Na

final state: total
source: ADL-3

No EXFOR data are available. The evaluation results from the calculation with the STAPRE code, results of which are usually reliable.

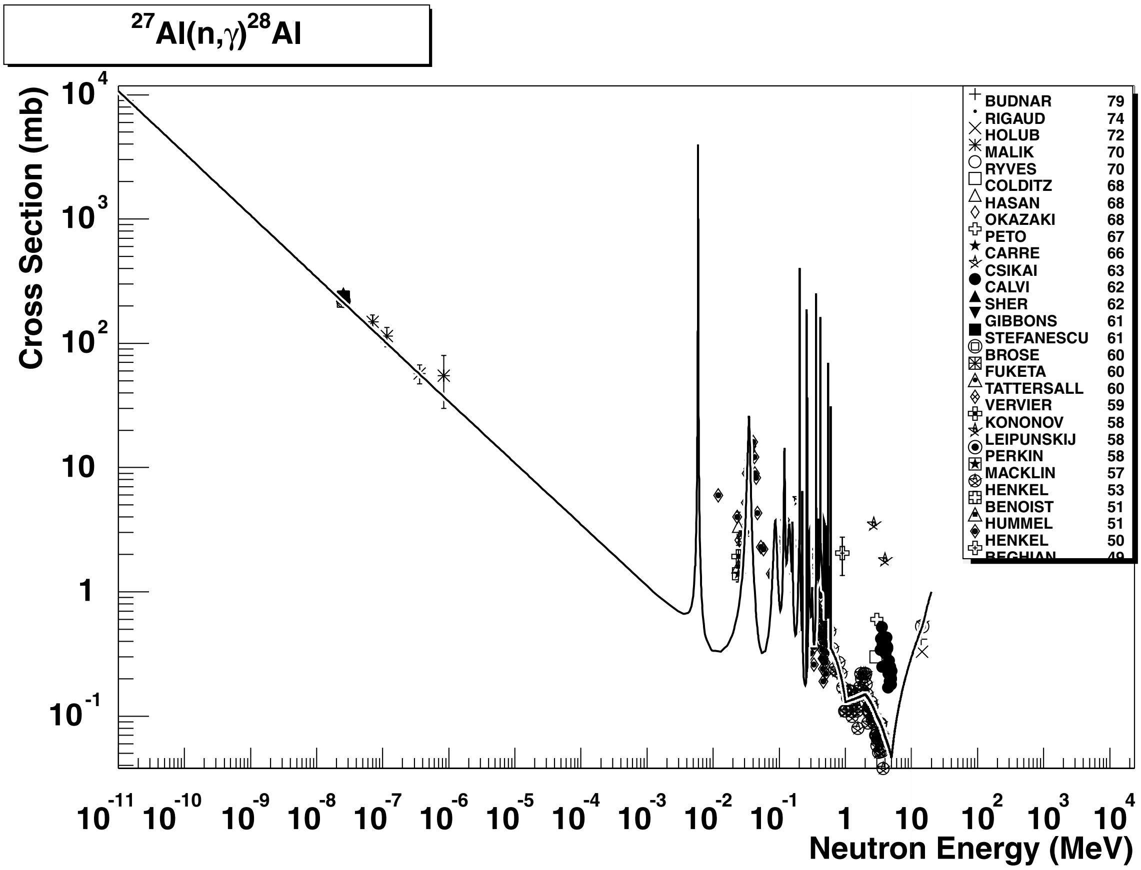

2.16. ^{27}Al (n,γ) ^{28}Al

final state: total
source: EAF-4.1 (JEF-2.2)

ENDF/B-V evaluation was adopted in JEF-2.2 and reproduces reasonably the majority of experimental information. Several old measurements (Beghian49, Leipunskij58, Calvi62 and Peto67) between 1-4 MeV seem to be too large, compared to the trend of other data.

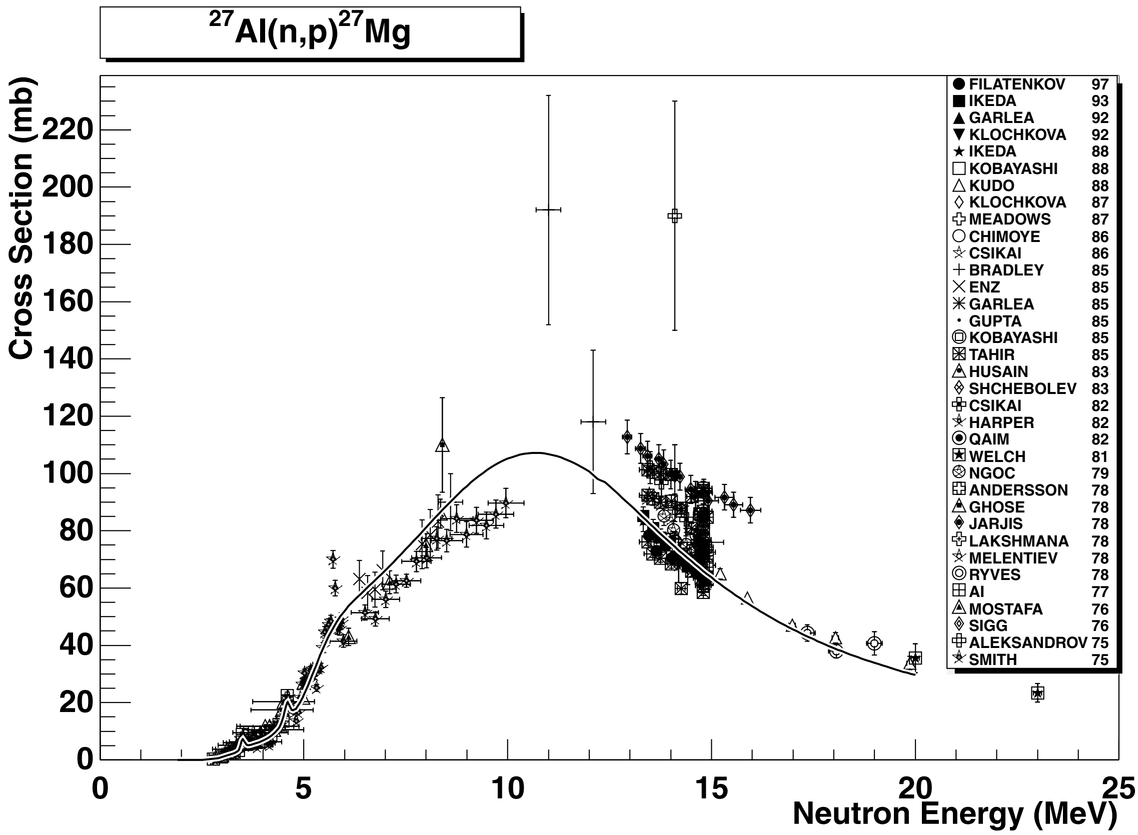

27Al(n,p)27Mg
Cross Section (mb)
Neutron Energy (MeV)
FILATENKOV 97
IKEDA 93
GARLEA 92
KLOCHKOVA 92
IKEDA 88
KOBAYASHI 88
KUDO 88
KLOCHKOVA 87
MEADOWS 87
CHIMOYE 86
CSIKAI 86
BRADLEY 85
ENZ 85
GARLEA 85
GUPTA 85
KOBAYASHI 85
TAHIR 85
HUSAIN 83
SHCHEBOLEV 83
CSIKAI 82
HARPER 82
QAIM 82
WELCH 81
NGOC 79
ANDERSSON 78
GHOSE 78
JARJIS 78
LAKSHMANA 78
MELENTIEV 78
RYVES 78
AI 77
MOSTAFA 76
SIGG 76
ALEKSANDROV 75
SMITH 75

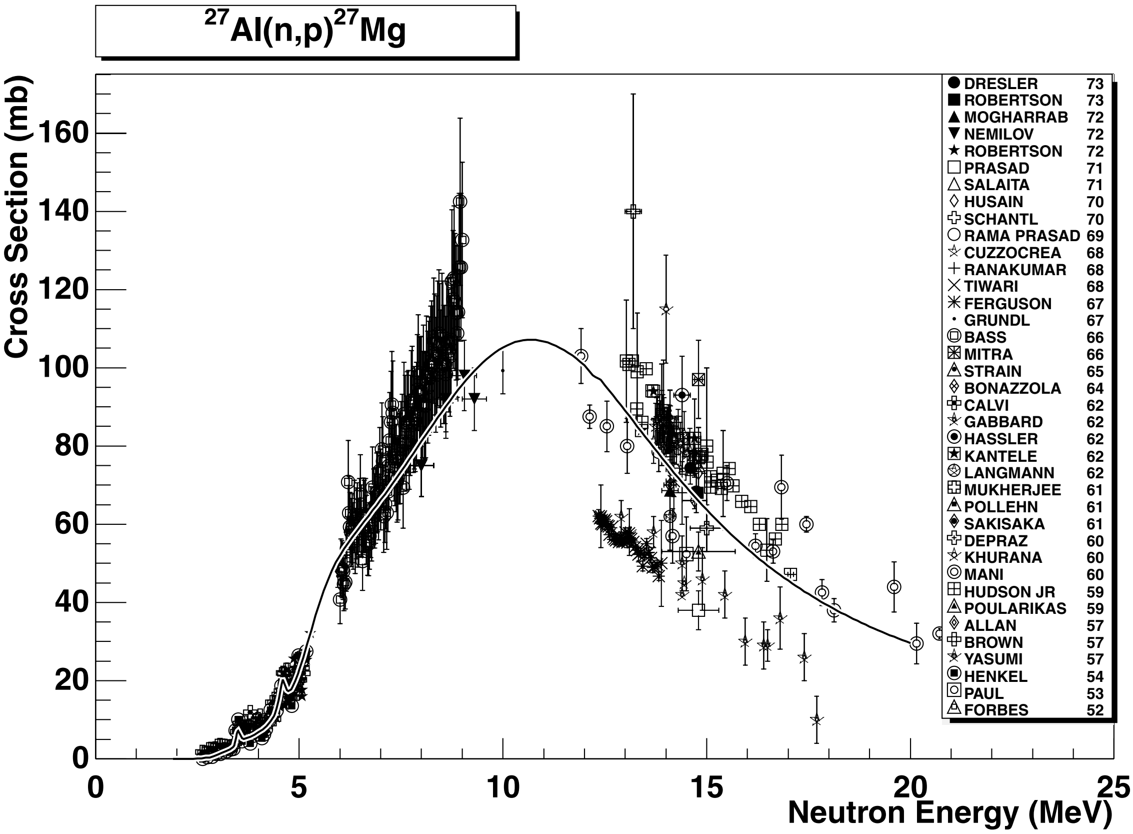

2.17. ^{27}Al (n,p) ^{27}Mg

final state: total
source: RRDF-98

A very extensive data base is available, covering the period from 1952 to 1997, which shows a large data scatter in particular above 12 MeV. RRDF-98 evaluation runs intermediate to the scatter of data and around 13-15 MeV fits nicely the latest reliable data of Ikeda93 and Filatenkov97.

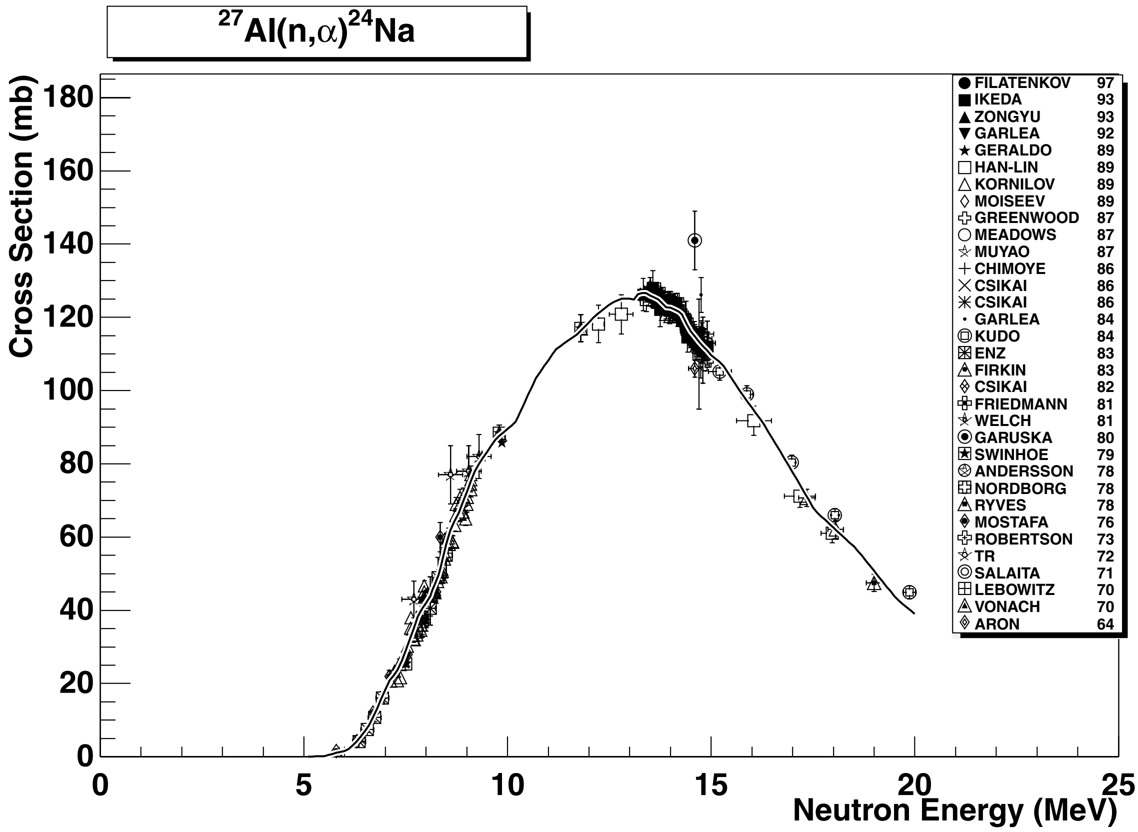

^{27}Al(n,α)^{24}Na
Cross Section (mb)
Neutron Energy (MeV)
0
20
40
60
80
100
120
140
160
180
0
5
10
15
20
25
FILATENKOV 97
IKEDA 93
ZONGYU 93
GARLEA 92
GERALDO 89
HAN-LIN 89
KORNILOV 89
MOISEEV 89
GREENWOOD 87
MEADOWS 87
MUYAO 87
CHIMOYE 86
CSIKAI 86
CSIKAI 86
GARLEA 84
KUDO 84
ENZ 83
FIRKIN 83
CSIKAI 82
FRIEDMANN 81
WELCH 81
GARUSKA 80
SWINHOE 79
ANDERSSON 78
NORDBORG 78
RYVES 78
MOSTAFA 76
ROBERTSON 73
TR 72
SALAITA 71
LEBOWITZ 70
VONACH 70
ARON 64

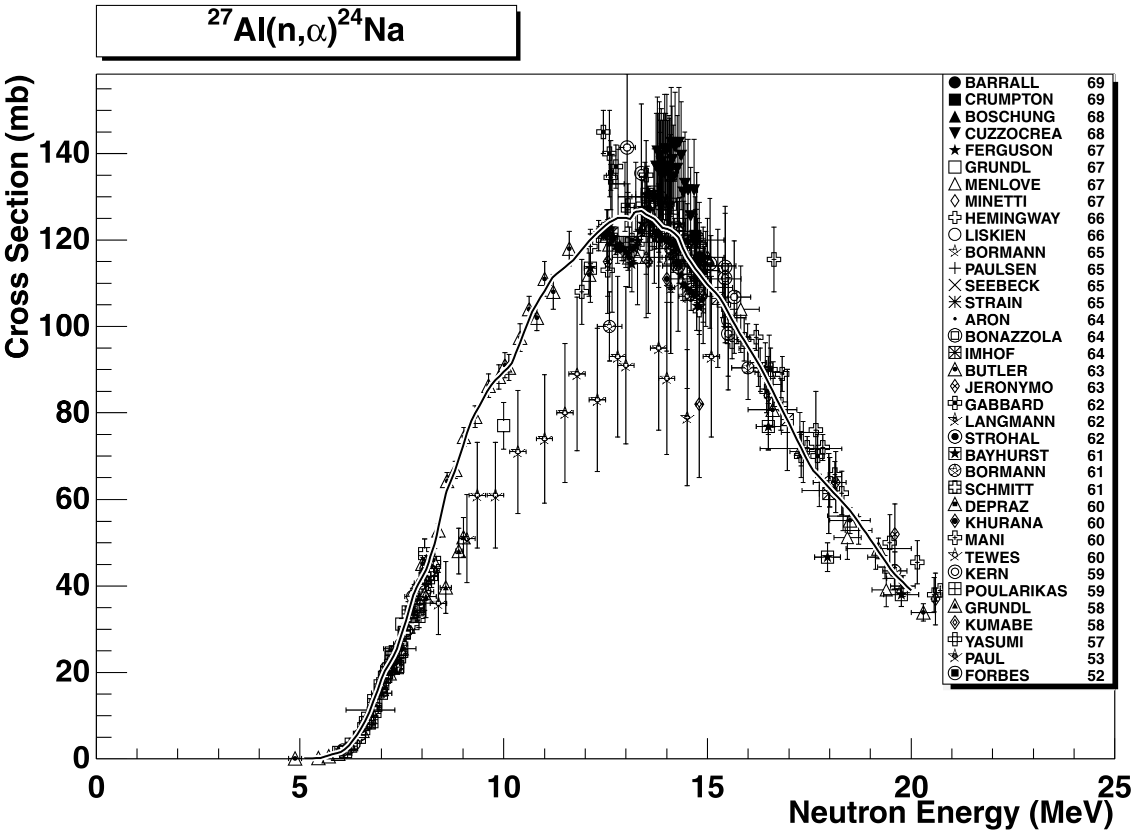

2.18. ^{27}Al (n,α) ^{24}Na

final states: g.s., meta
source: IRDF-90.2

The IRDF-90.2 evaluation of the total cross-section correctly describes all recent experimental data. Some of the older data (e.g. Tewes60) may be disregarded, they are in significant disagreement with the latest experiments. The branching ratio systematics has been applied to obtain the g.s. and metastable cross sections.

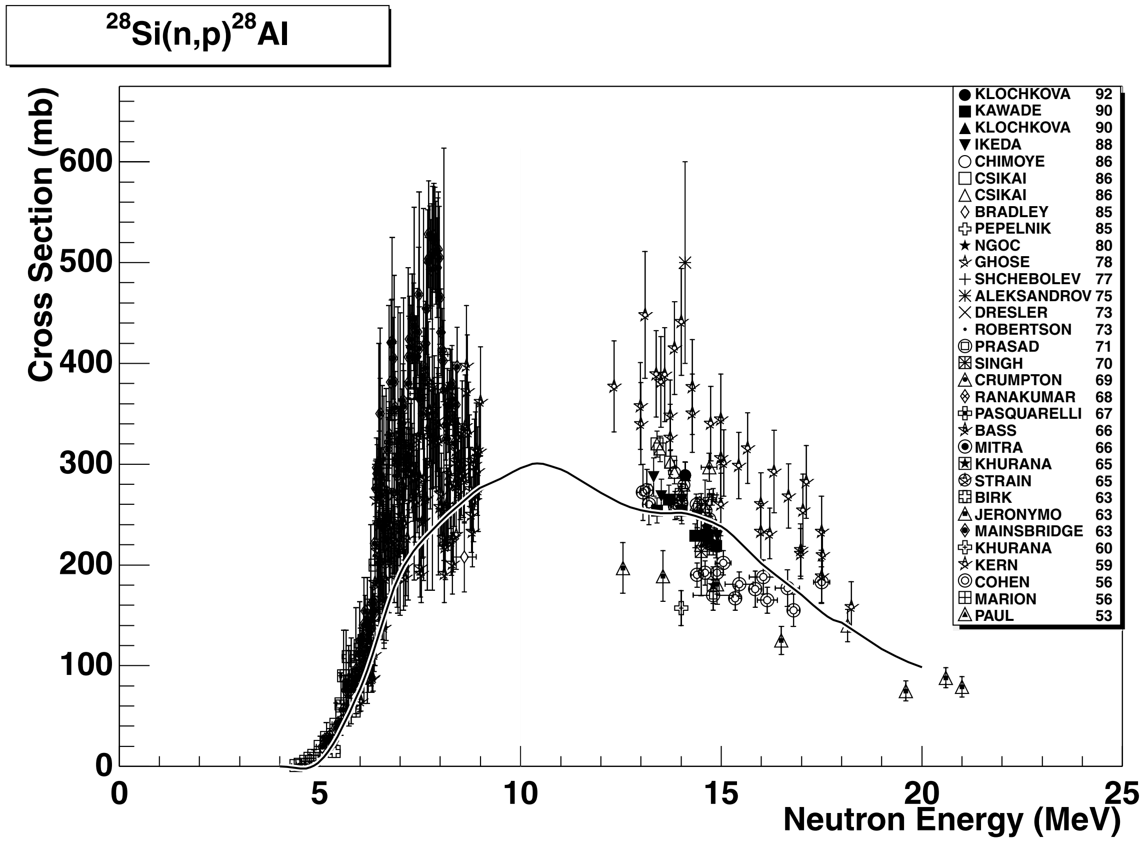

2.19. ^{28}Si (n,p) ^{28}Al

final state: total
source: JENDL-Act96

Experimental data, existing in two energy regions (4-9 MeV and 13-20 MeV), have a very broad distribution due to a large number of old data with inferior quality. The adopted JENDL-Act96 evaluation fits the recent experimental data of Klochkova92,90, Kawade90 and Ikeda88 between 13-15 MeV very well. The low energy part of the excitation curve (below 10 MeV) lies at the lower part of the experimental data band, however, this is still probably a good representation.

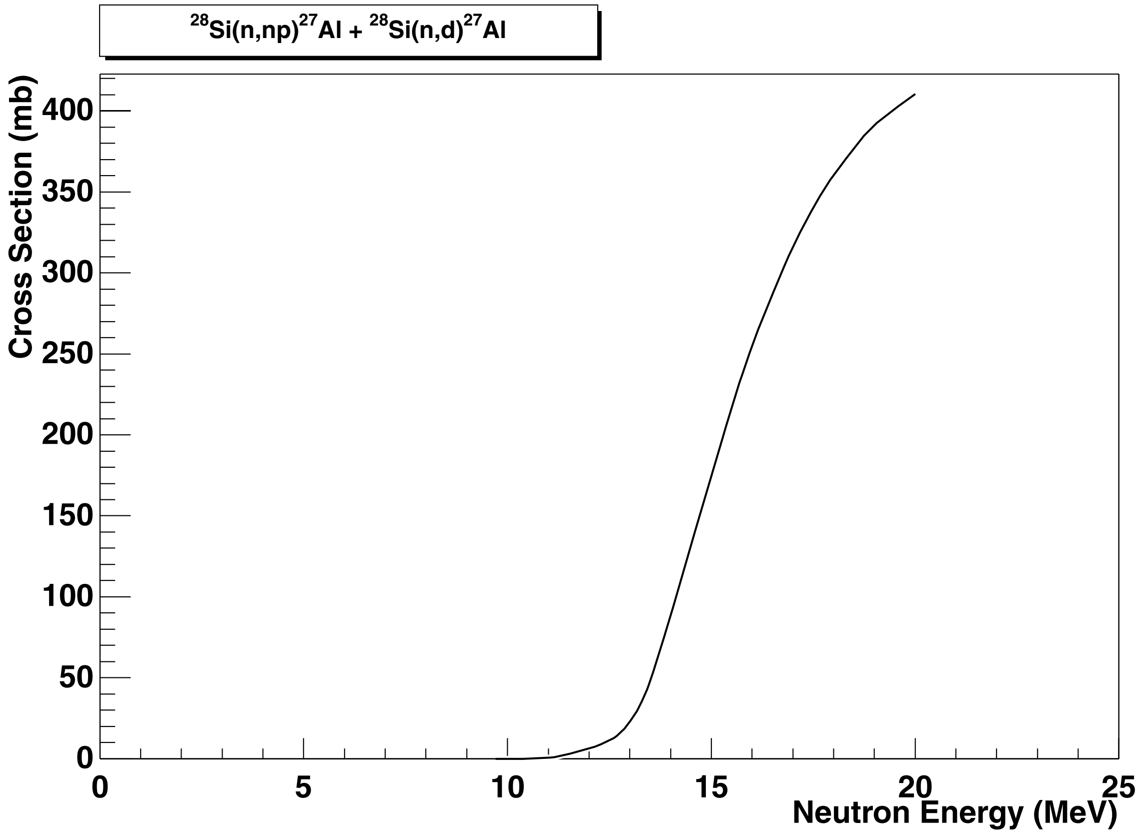

2.20. ^{28}Si (n,d+np) ^{27}Al

final state: total
source: JENDL-Act96

No experimental results are available. The data are stored separately for (n,d) and (n,np) reaction channels.

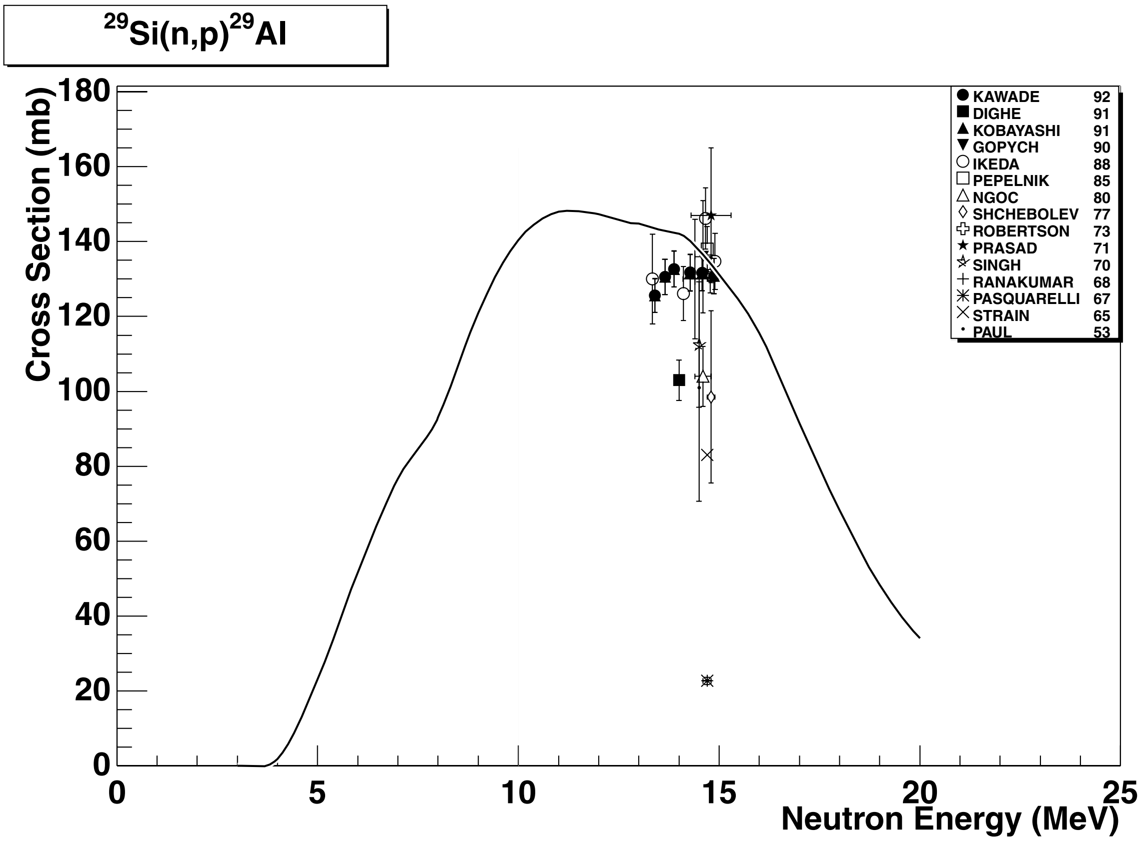

2.21. ^{29}Si (n,p) ^{29}Al

final state: total
source: JENDL-Act96

JENDL-Act96 evaluation slightly overestimates experimental data of Kawade96 but agrees with data of Gopycs90 and lies between the data of Ikeda88. As for the remaining (older) data around 14-15 MeV, the excitation curve runs in the middle of them. A slight decrease (10-15%) of the flat part of the excitation curve may be considered.

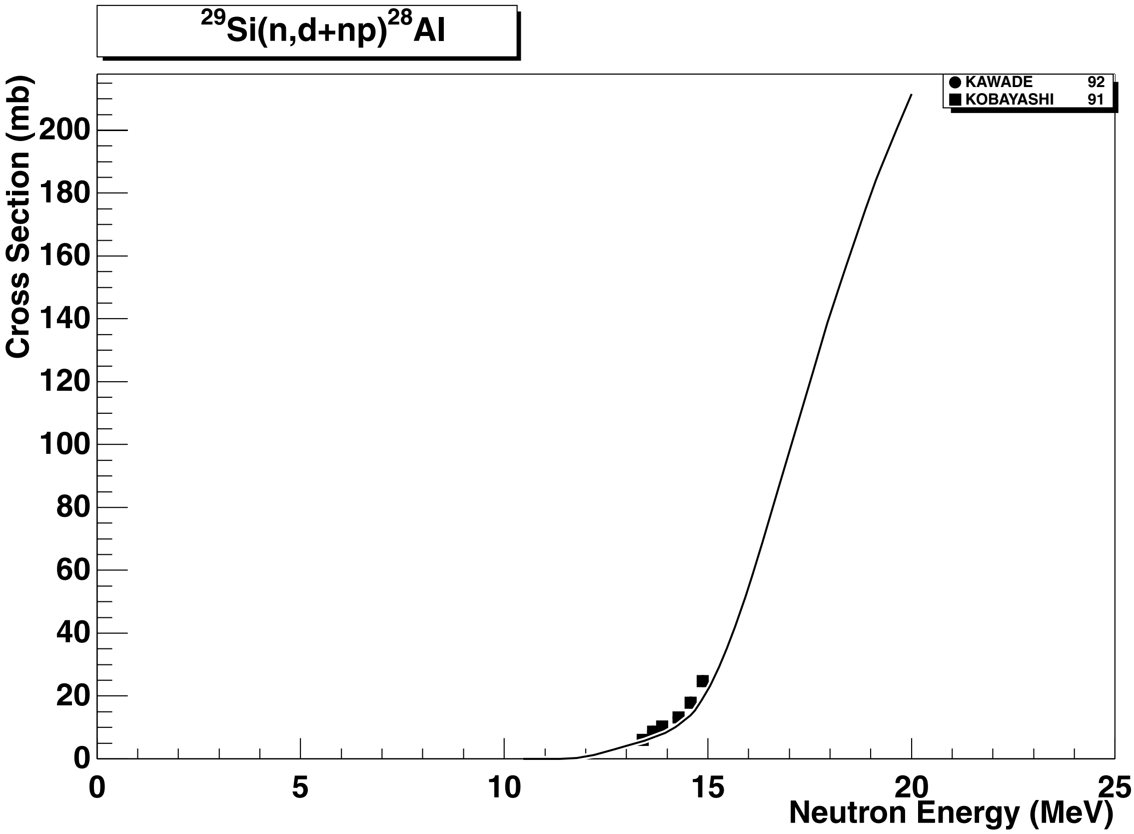

2.22. ^{29}Si (n,d+np) ^{28}Al

final state: total
source: JENDL-3.1 [(n,np)], ADL-3 [(n,d)]

Two measurements, up to 15 MeV only, are reported in EXFOR. The evaluated cross-sections reproduce these experiments very well. The data are stored separately for (n,d) and (n,np) reaction channels.

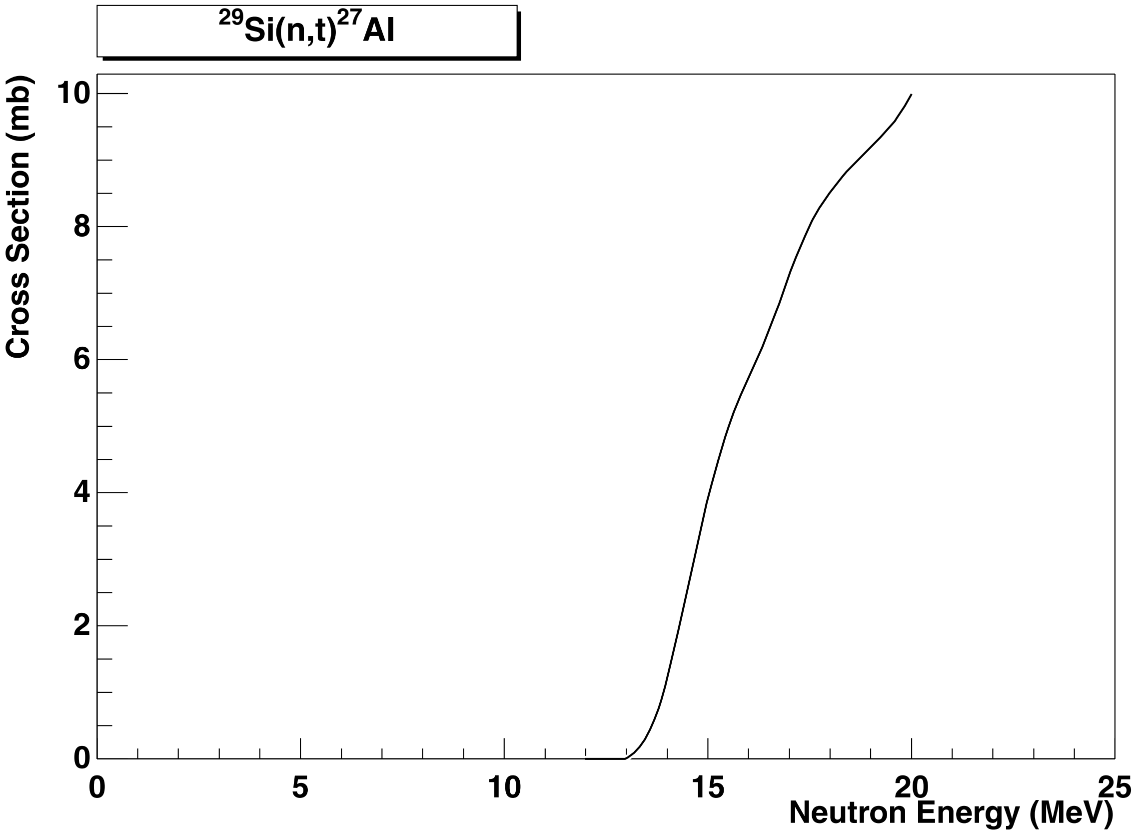

2.23. ^{29}Si (n,t) ^{27}Al

final state: total
source: ADL-3

No EXFOR data are available. The evaluation results from the calculation with the STAPRE code. The evaluation is supported by a reasonable value (C/S= 1.18) against the systematics (see Ref. [2]).

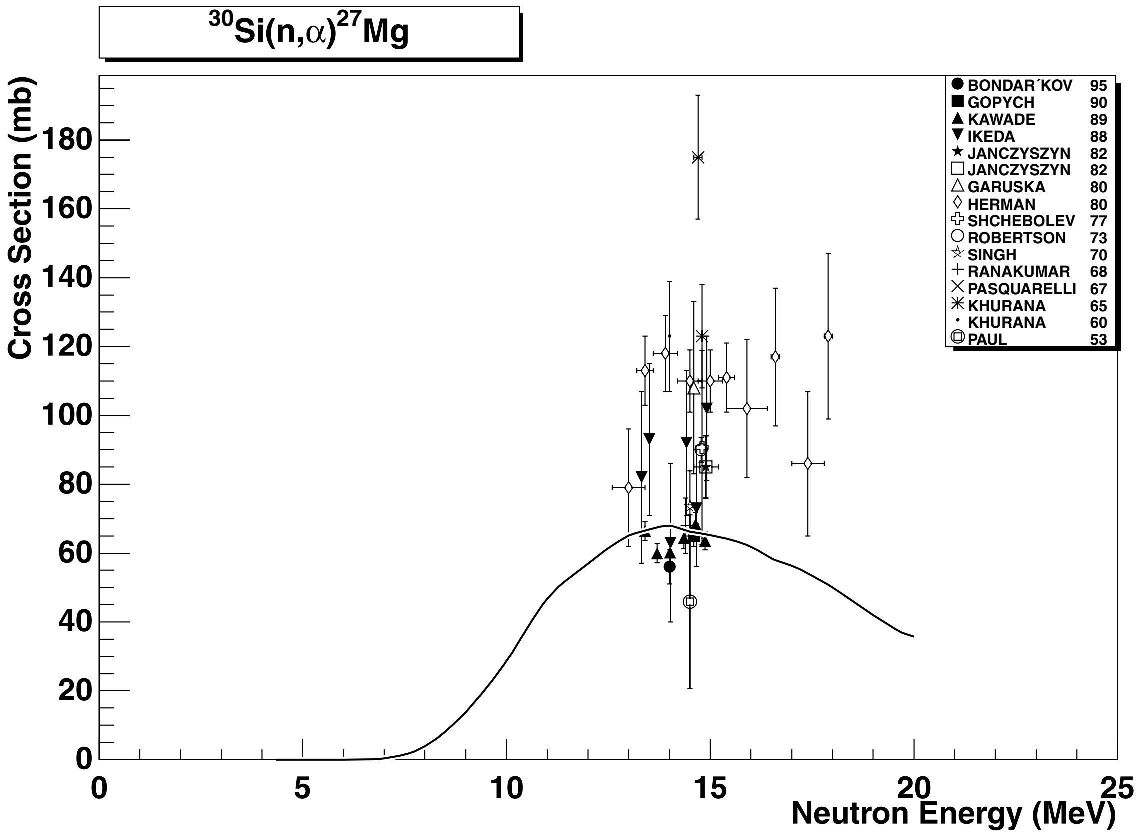

2.24. ^{30}Si (n, α) ^{27}Mg

final state: total
source: JENDL-3.1

The JENDL-3.1 evaluation fits the latest experimental data (Bondarkov95, Gopych90, Kawade89 and Ikeda88) at about 14 MeV. The older data (too large compared to the recent ones) can be disregarded.

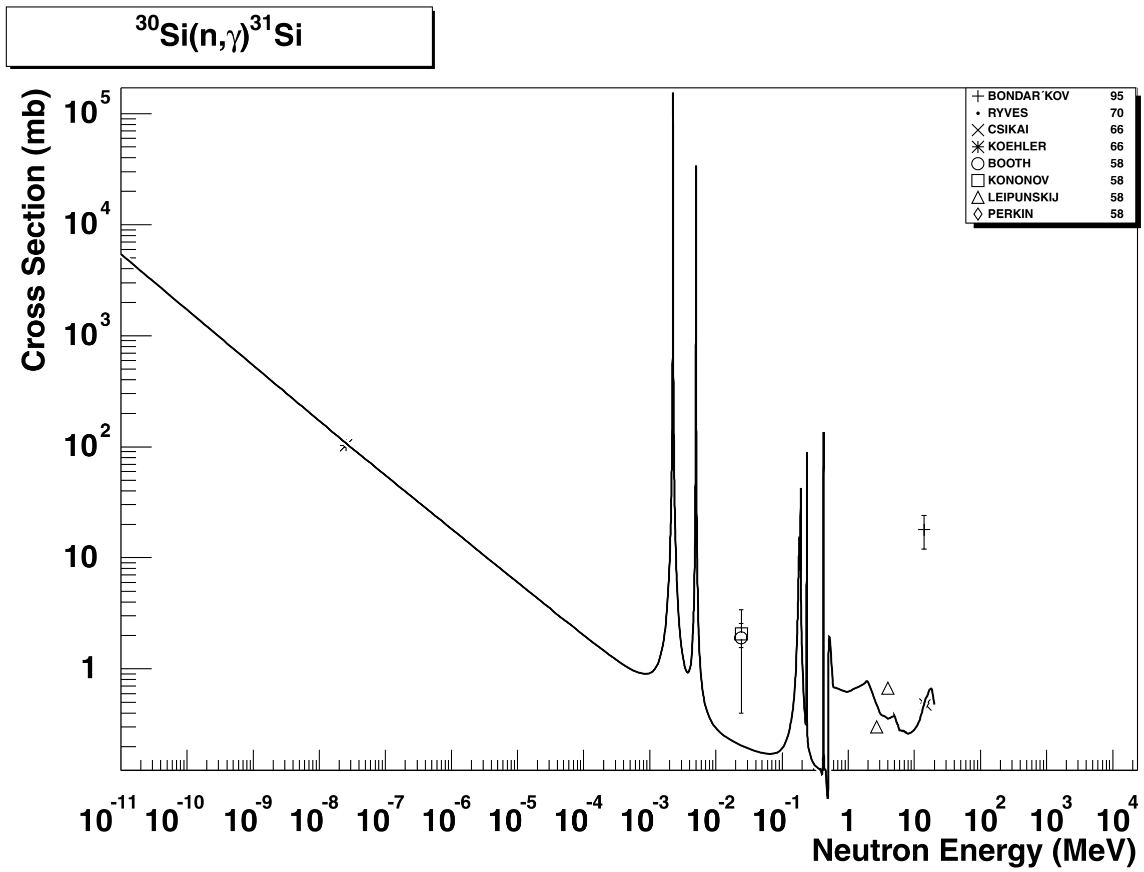

2.25. ^{30}Si (n,γ) ^{31}Si

final state: total
source: EAF-4.1 (JENDL-3.1)

The JENDL-3.1 evaluation fits the thermal cross-section value and reasonably reproduces the few experimental points above 1 MeV. Booth58 and Kononov58 at 30 keV are averaged values, the 14 MeV experimental point of Bondarkov95 is ignored. A value of about 20 mb at this energy is excluded. The pre-equilibrium component was missing in the original JENDL-3.1 evaluation and was added during the EAF-4.1 revision and is based on the PEQ- systematics (for details see Refs. [3] and [35].

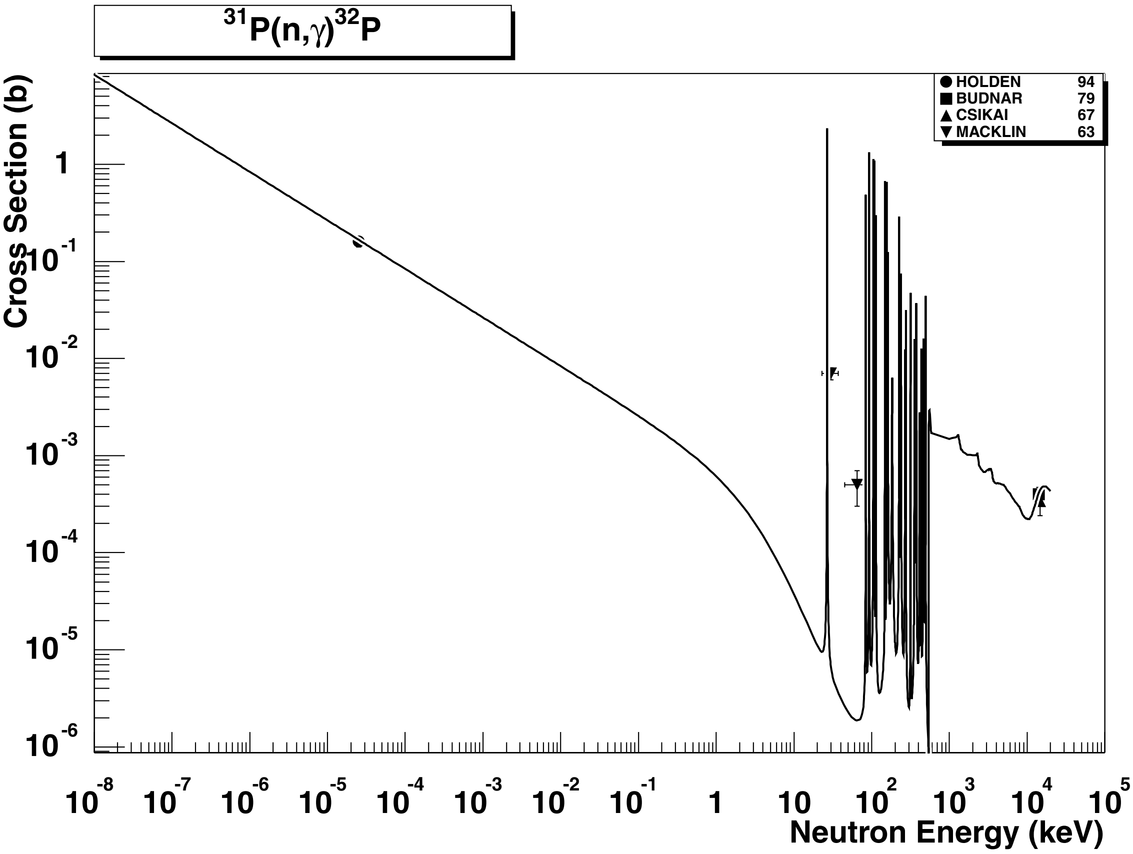

2.26. ^{31}P (n,γ) ^{32}P

final state: total
source: EAF-4.1 (JEF-2.2)

JENDL-3.1 evaluation has been adopted in JEF-2.2 and reproduces well two experimental values at about 15 MeV. The excitation curve nicely reproduces the thermal cross section value of Holden94 [32] with C/E=1.04.

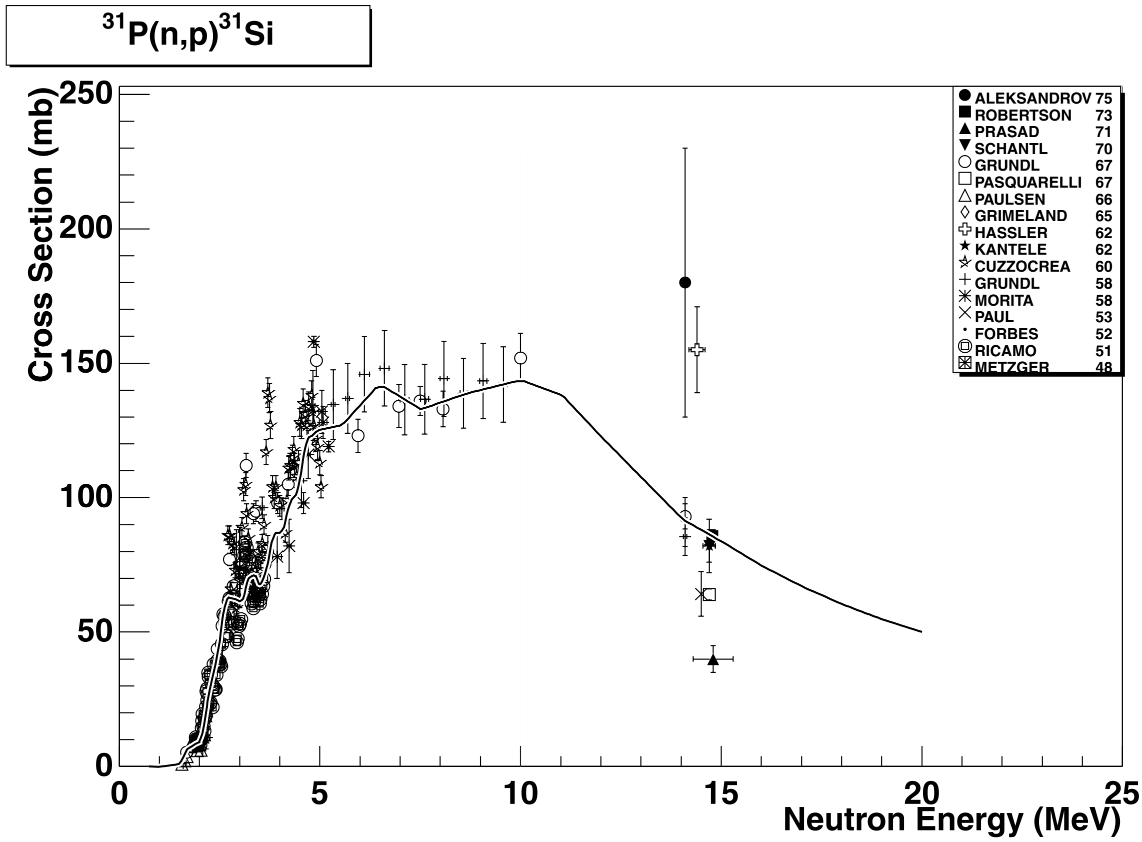

2.27. ^{31}P (n,p) ^{31}Si

final state: total
source: EAF-4.1 (IRDF-90.2)

IRDF-90.2 is in a good agreement with the experimental information in the whole energy range covered by the evaluation. Experimental data of Hassler62, Pasquarelli67 and Prasad71 at 14-15 MeV have been disregarded, they are very different from the recent values and also from the value based on the systematics.

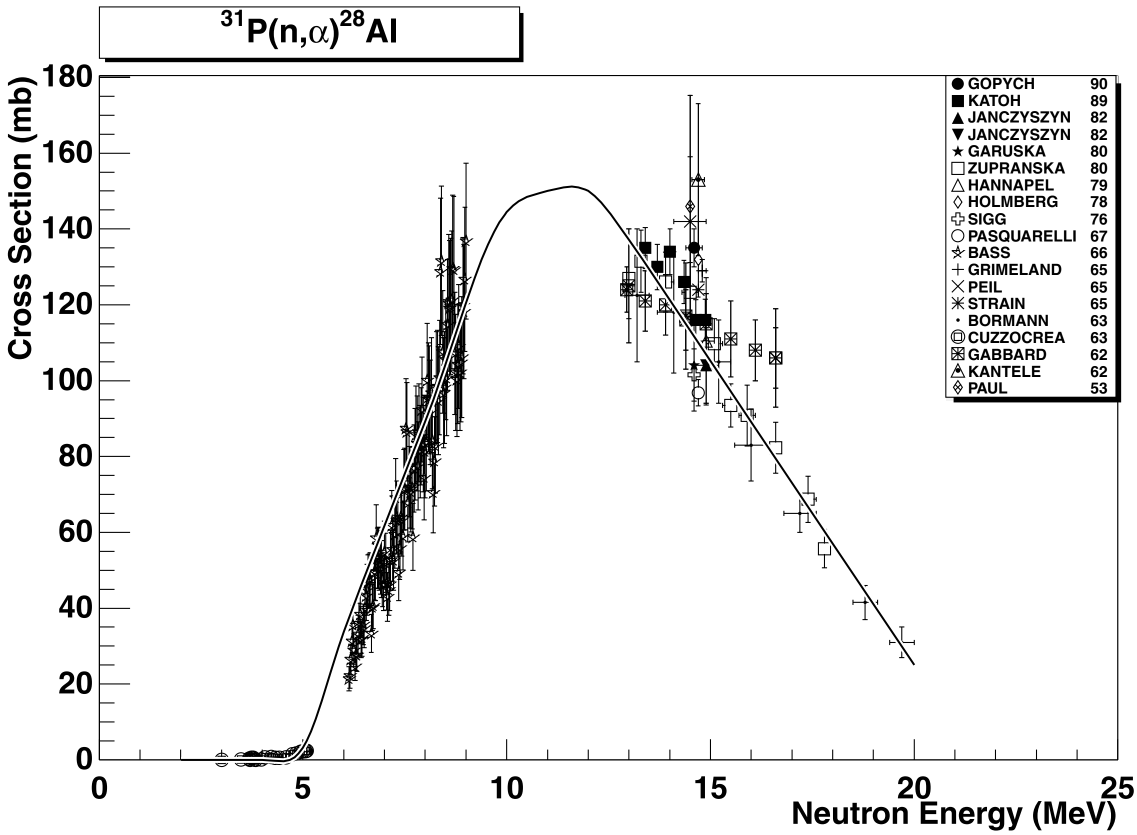

2.28. ^{31}P (n,α) ^{28}Al

final state: total
source: JENDL-Act96

A very good agreement of the JENDL-Act96 evaluation against the large set of experimental data in the whole energy range.

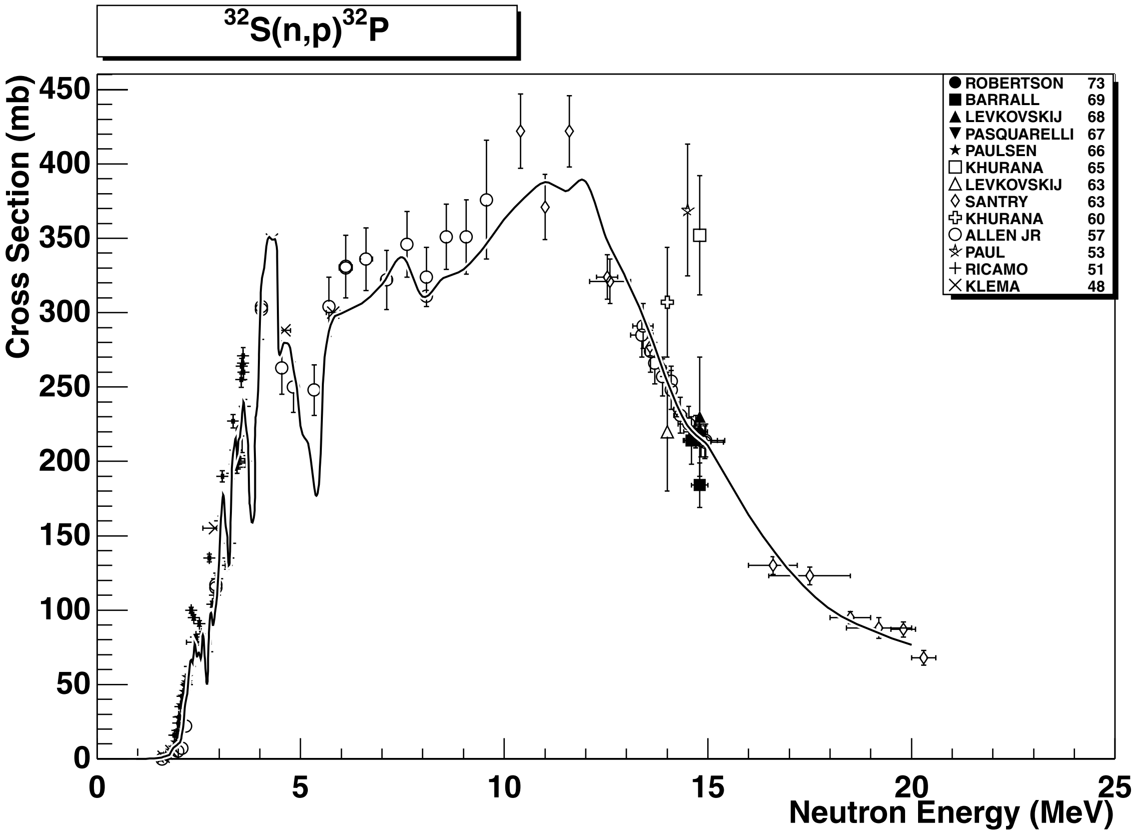

2.29. ^{32}S (n,p) ^{32}P

final state: total
source: IRDF-90.2

A good reproduction of the experimental information in the whole energy range by the IRDF-90.2 evaluation.

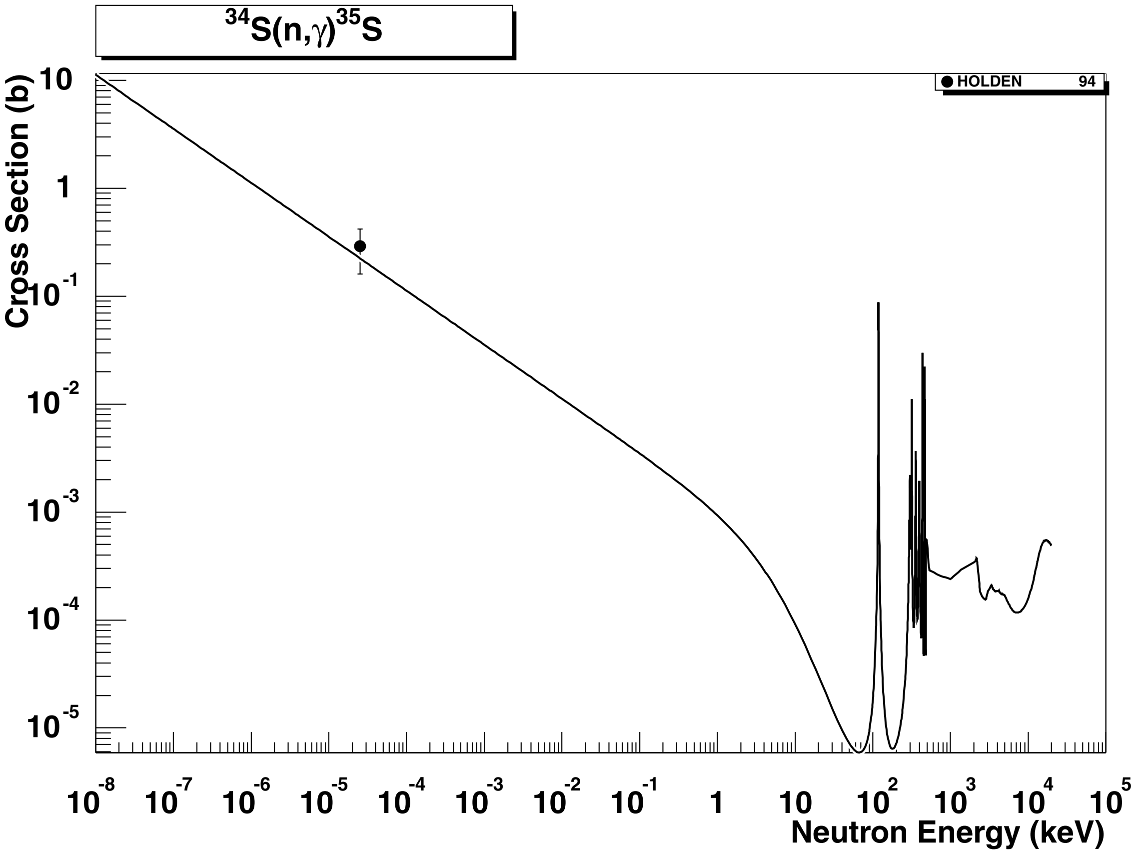

2.30. ^{34}S (n,γ) ^{35}S

final state: total
source: EAF-4.1 (JEF-2.2)

JENDL-3.2 data have been chosen for JEF-2.2. No experimental data outside resonance region are included in EXFOR, however, the value of thermal cross-section of Holden94 [32] is reproduced with C/E=0.77. The missing pre-equilibrium component was added based on the PEQ-systematics (for details see Refs. [3] and [35]).

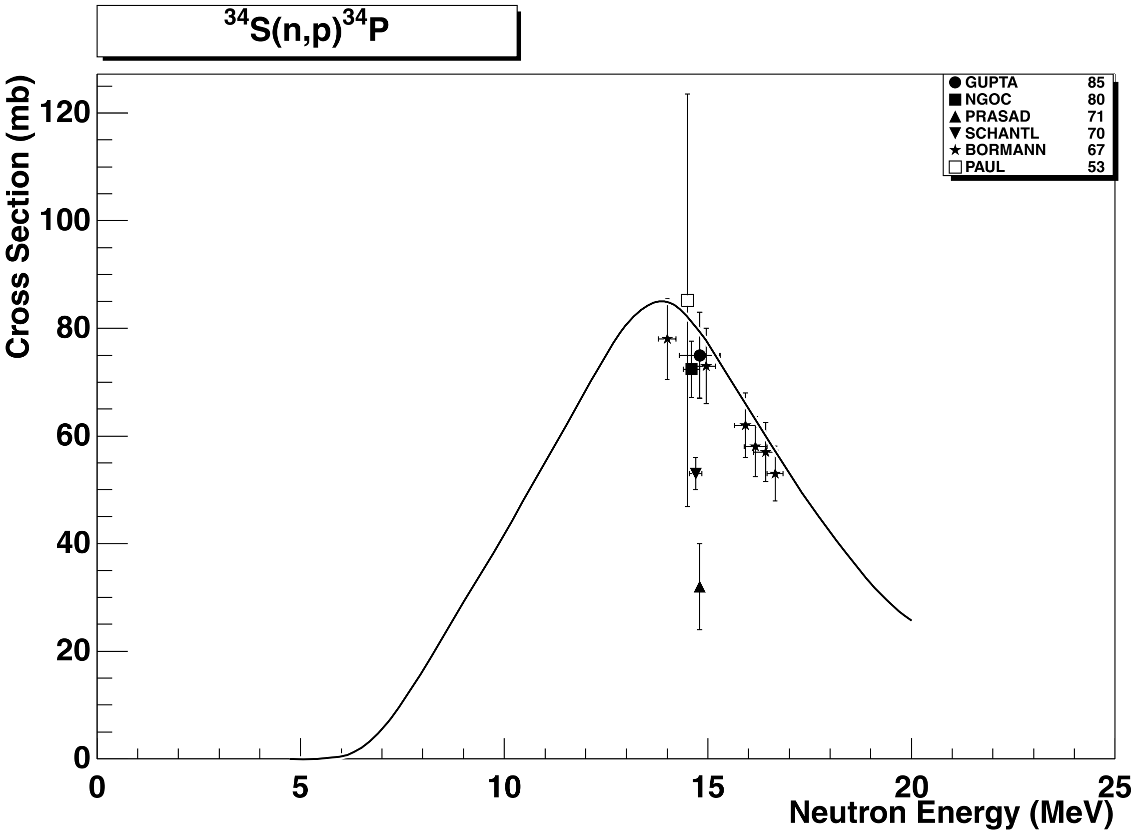

2.31. ^{34}S (n,p) ^{34}P

final state: total
source: ADL-3

ADL-3 evaluation slightly overestimates the experimental data. The renormalization of the whole excitation curve by a decrease of about 5% is recommended.

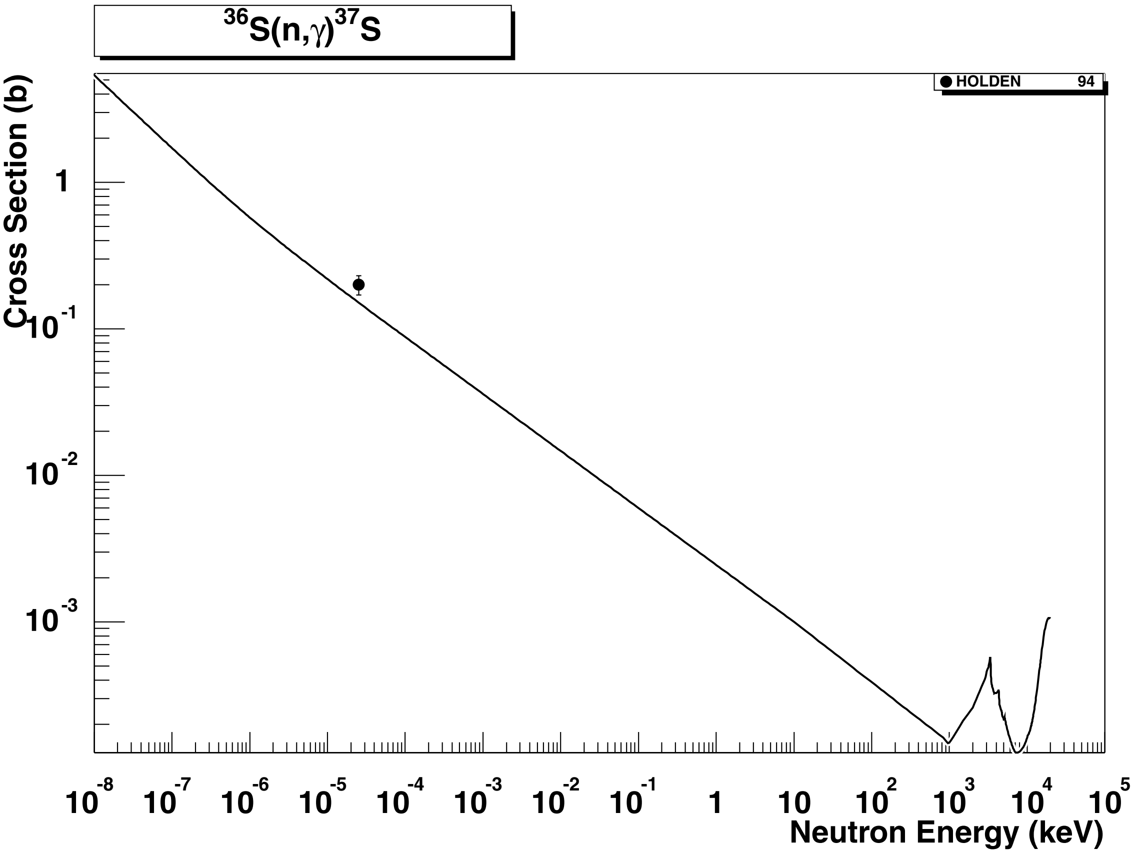

2.32. ^{36}S (n,γ) ^{37}S

final state: total
source: EAF-4.1 (JEF-2.2)

JENDL-3.2 evaluation was adopted as a basis in JEF-2.2. For the adoption in EAF-4.1, the missing pre-equilibrium component was added based on the PEQ-systematics (for details see Refs. [3] and [35]). No experimental data have been found in the EXFOR data base. The thermal cross-section of Holden94 from Ref. [32] is slightly underestimated with C/E=0.76.

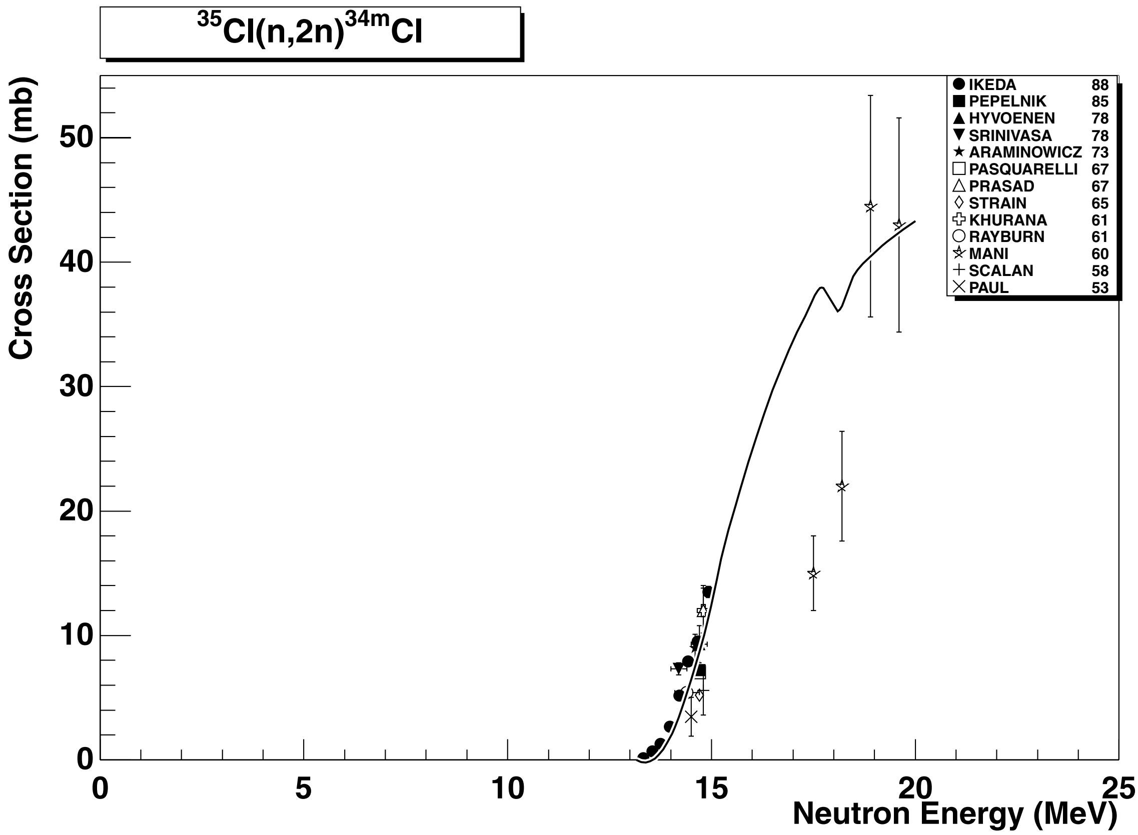

2.33. ^{35}Cl (n,2n) ^{34m}Cl

final states: g.s., meta
source: EAF-4.1

The reaction leading to the first isomeric state is the reference reaction. Branching ratio for cross-sections to the g.s. and meta state result from model calculations. The calculated excitation curve to metastable state is in good agreement with the experimental data. First two data points of Mani60 are wrong.

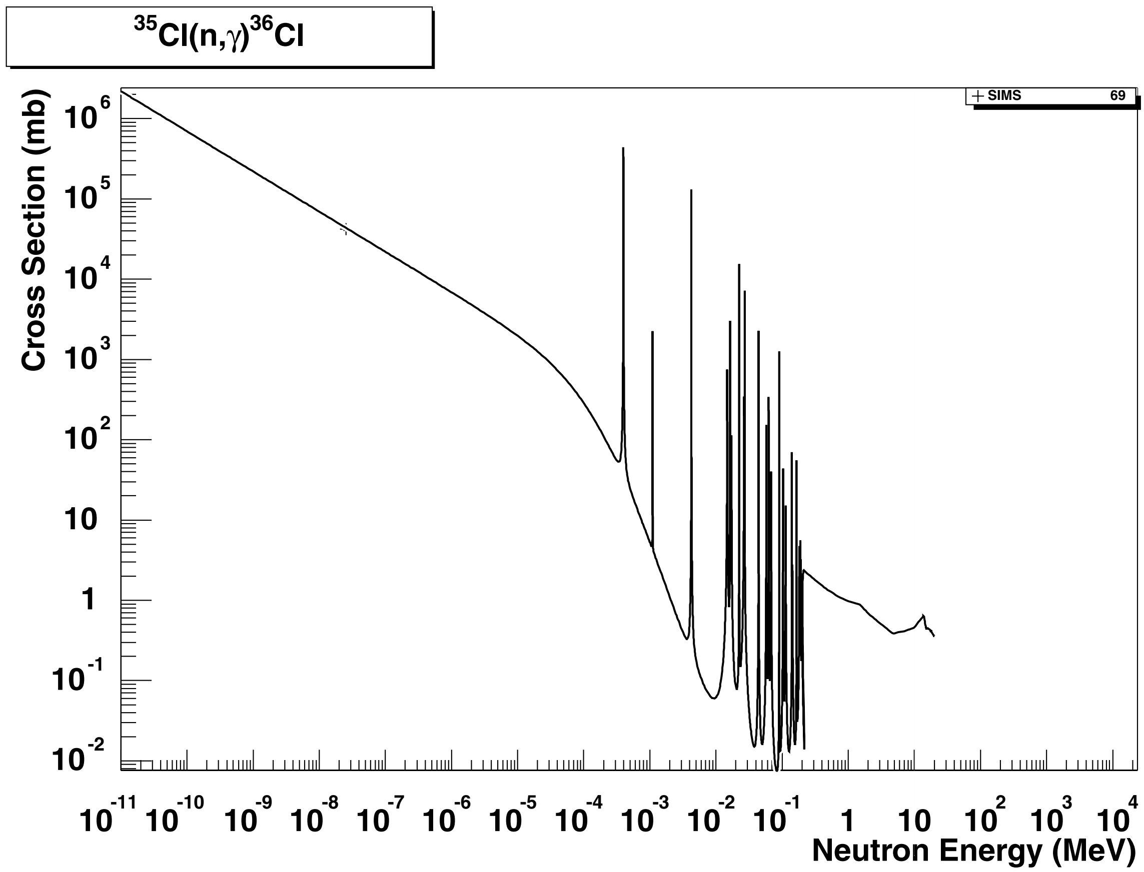

2.34. ^{35}Cl (n,γ) ^{36}Cl

final state: total
source: EAF-4.1

This is the EAF-4.1 evaluation calculated with the code SIGECN-MASGAM. Full MLBW resonance treatment is included. MASGAM is a statistical (Hauser-Feshbach) code with the pre-equilibrium component based on the D-SD model (for details see Ref. [35]). The global parameters are applied for optical model, level densities and gamma-ray strength functions. The thermal cross-section of Sims69 is well reproduced.

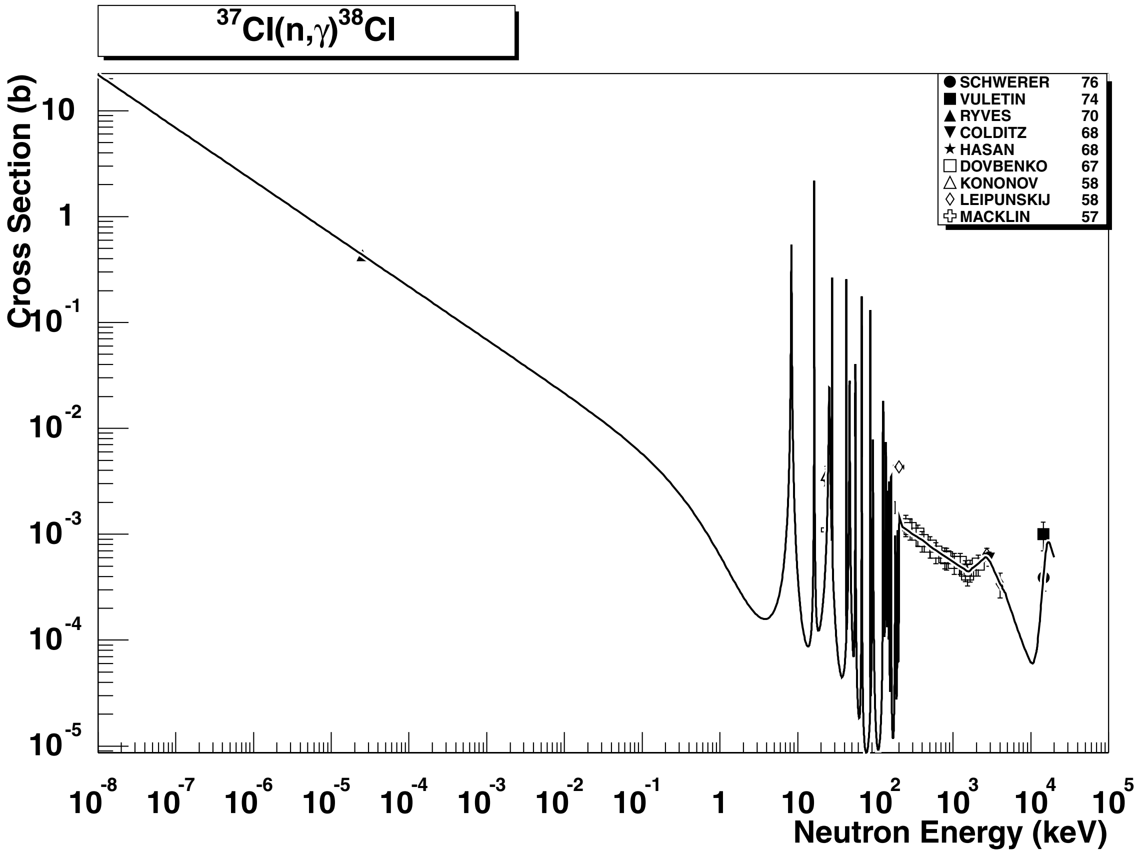

2.35. ^{37}Cl (n,γ) ^{38}Cl

final states: g.s., meta
source: JENDL-3.2

JENDL-3.2 agrees very well with the experimental data, especially in the thermal and high energy regions.

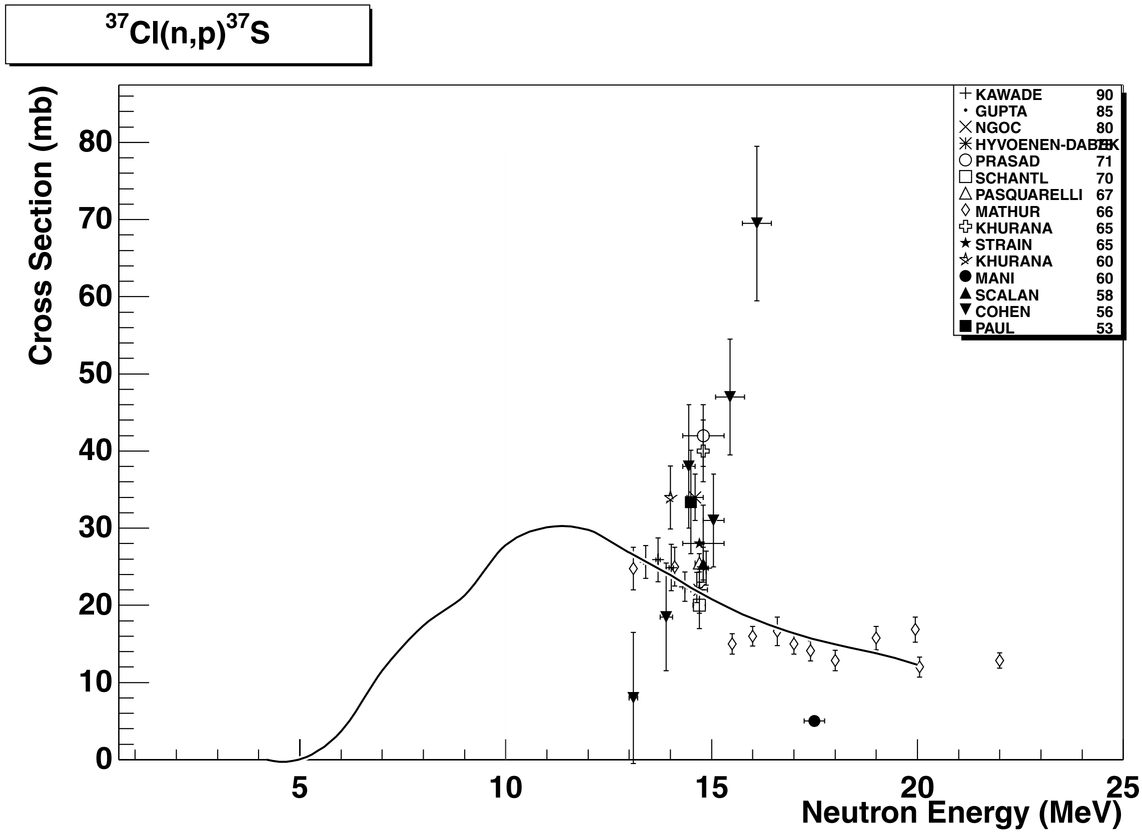

2.36. ^{37}Cl (n,p) ^{37}S

final state: total
source: JENDL-Act96

JENDL-Act96 evaluation reproduces the recent data of Kawade 90 between 13-15 MeV and fits nicely also data of Mathur66 up to 20 MeV. The large scatter of data around 14 MeV is primarily due to very old data (Cohen56, Scalan58) and they seem to be unreliable. They also deviate strongly from the value based on the 14.5 MeV systematics.

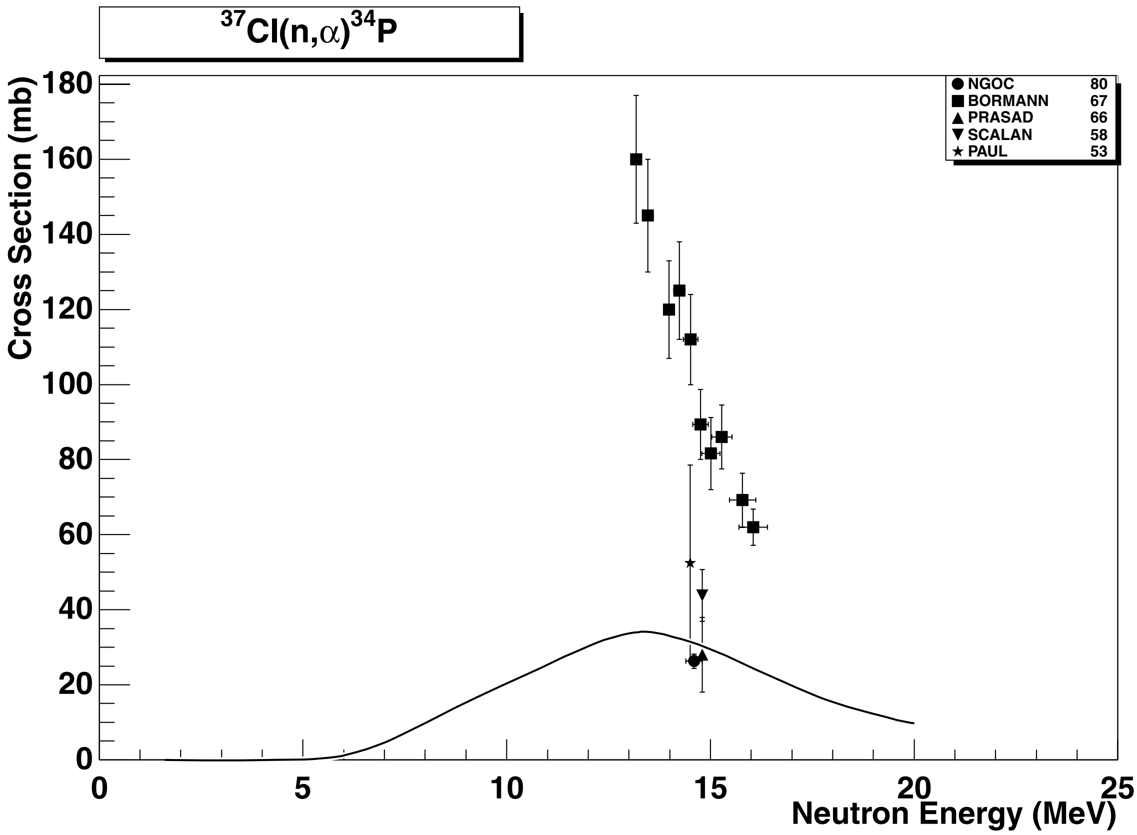

2.37. ^{37}Cl (n,α) ^{34}P

final state: total
source: ADL-3

ADL-3 evaluation fits reasonably four data points around 15 MeV except the data of Botmann67, which are probably wrong (shape as well as values above 120 mb) and can be disregarded.

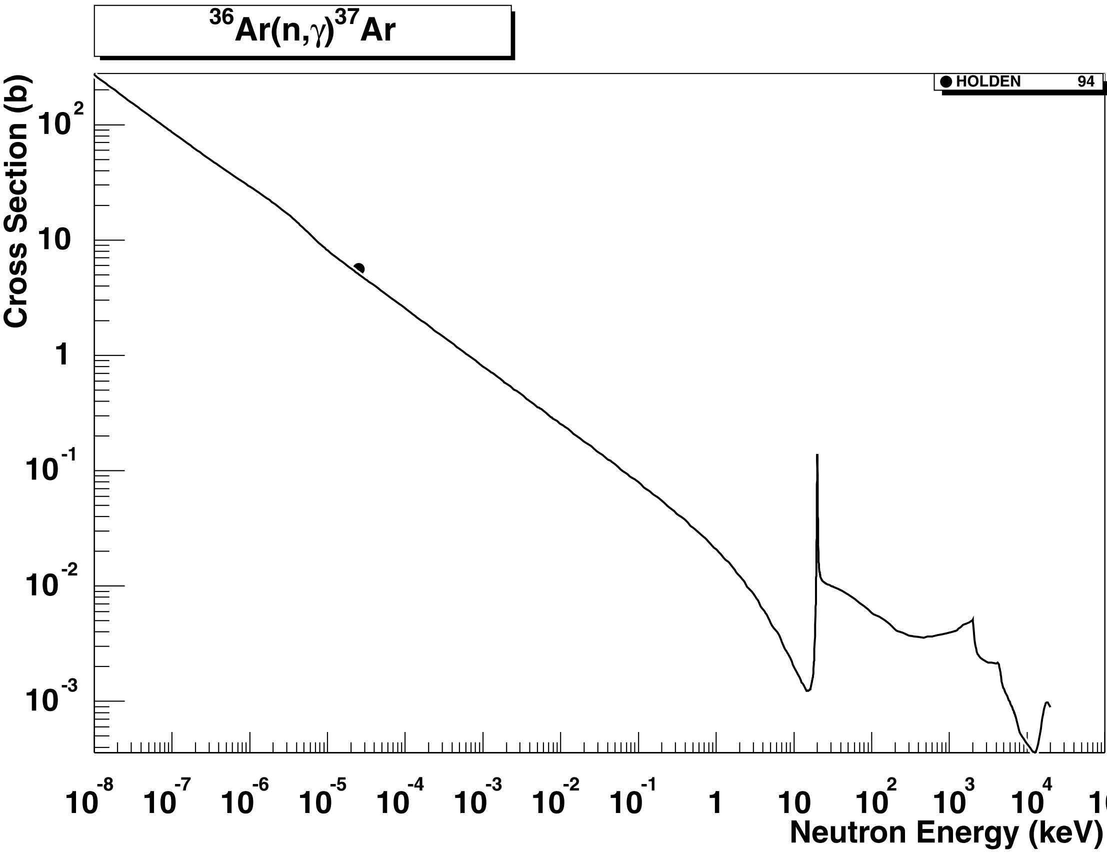

2.38. ^{36}Ar (n,γ) ^{37}Ar

final state: total
source: EAF-4.1 (JEF-2.2)

Original JEF-2.2 evaluation with no resonance parameters is available. No EXFOR data has been found. The thermal cross-section of Holden94 [32] is well reproduced (C/E=0.97). The resonance-like shape at 20 keV is not real and is generated due to an incorrect interpolation law during the linearization procedure in NJOY.

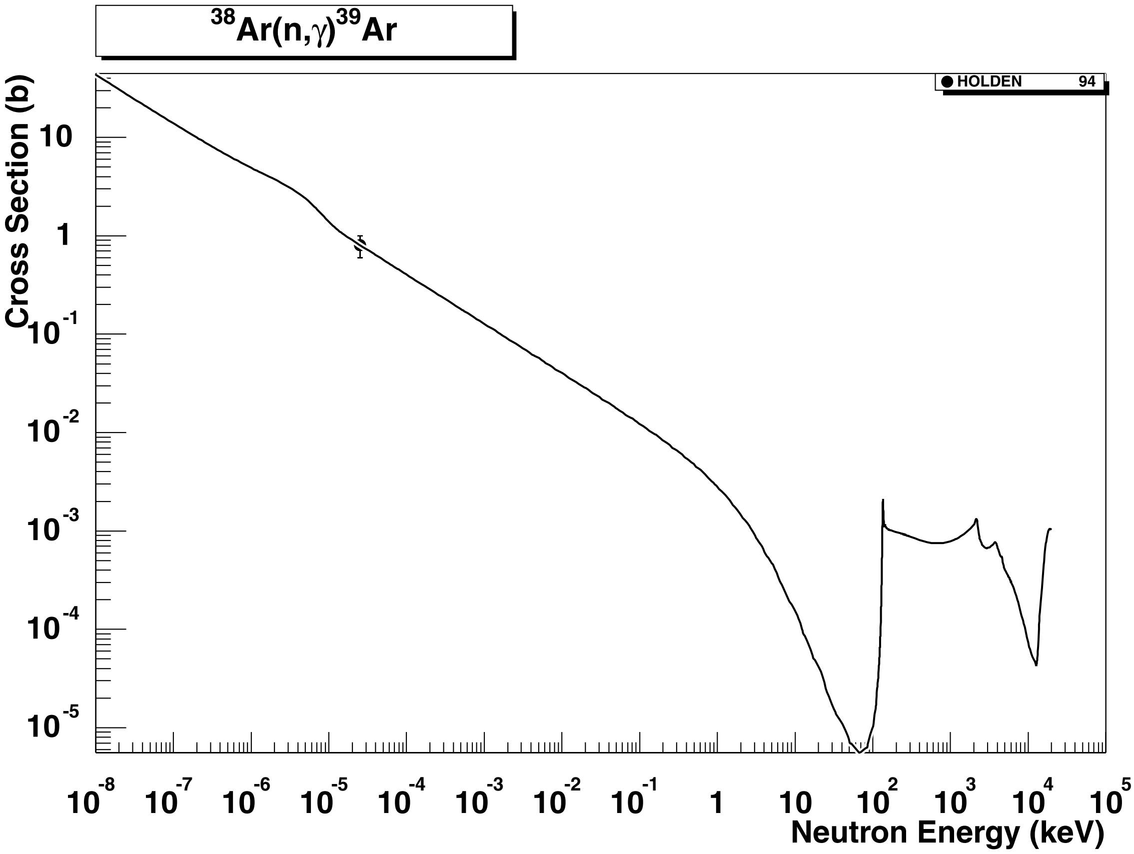

2.39. ^{38}Ar (n,γ) ^{39}Ar

final state: total
source: EAF-4.1 (JEF-2.2)

Original JEF-2.2 evaluation with no resonance parameters is available. The thermal cross-section of Holden94 [32] is well reproduced (C/E=1.00).

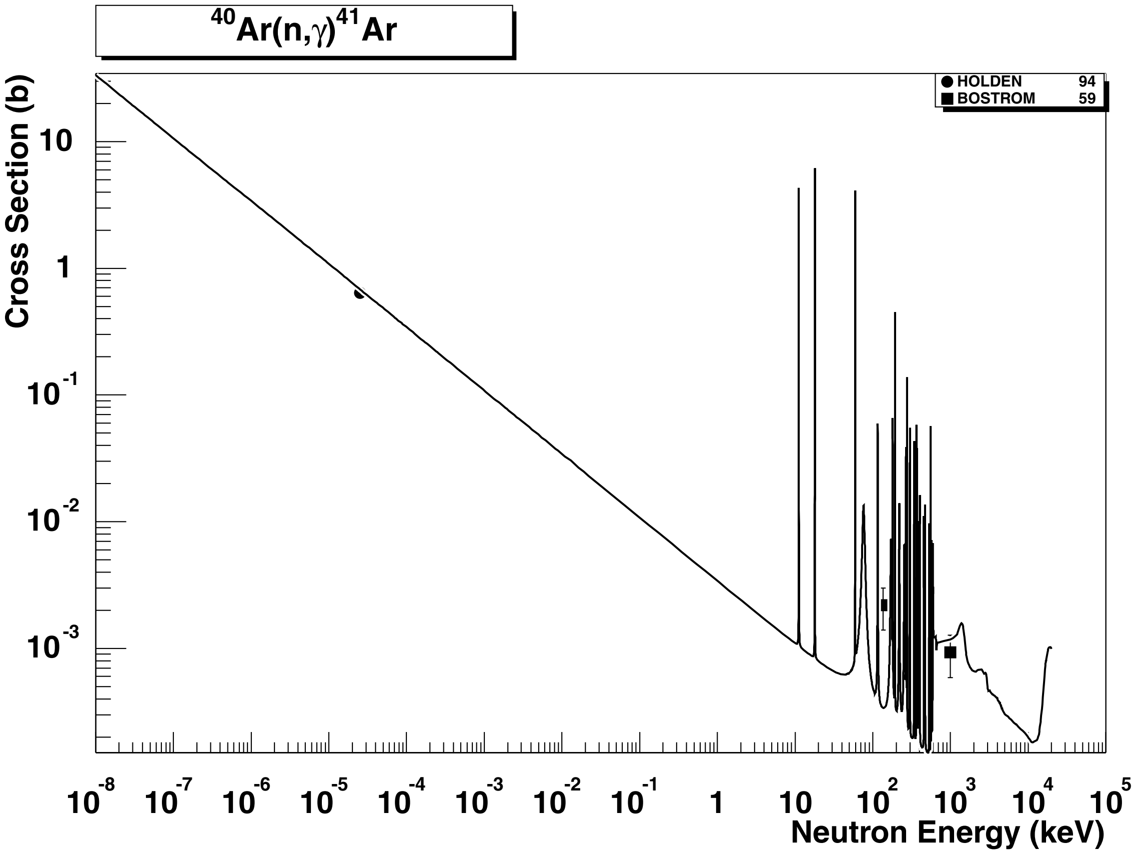

2.40. ^{40}Ar (n,γ) ^{41}Ar

final state: total
source: EAF-4.1 (JEF-2.2)

The original JEF-2.2 evaluation includes the MLBW treatment of resonance parameters. Only two single experimental cross-sections are available in EXFOR. The thermal cross section of Holden94 [32] is well reproduced with C/E=1.03.

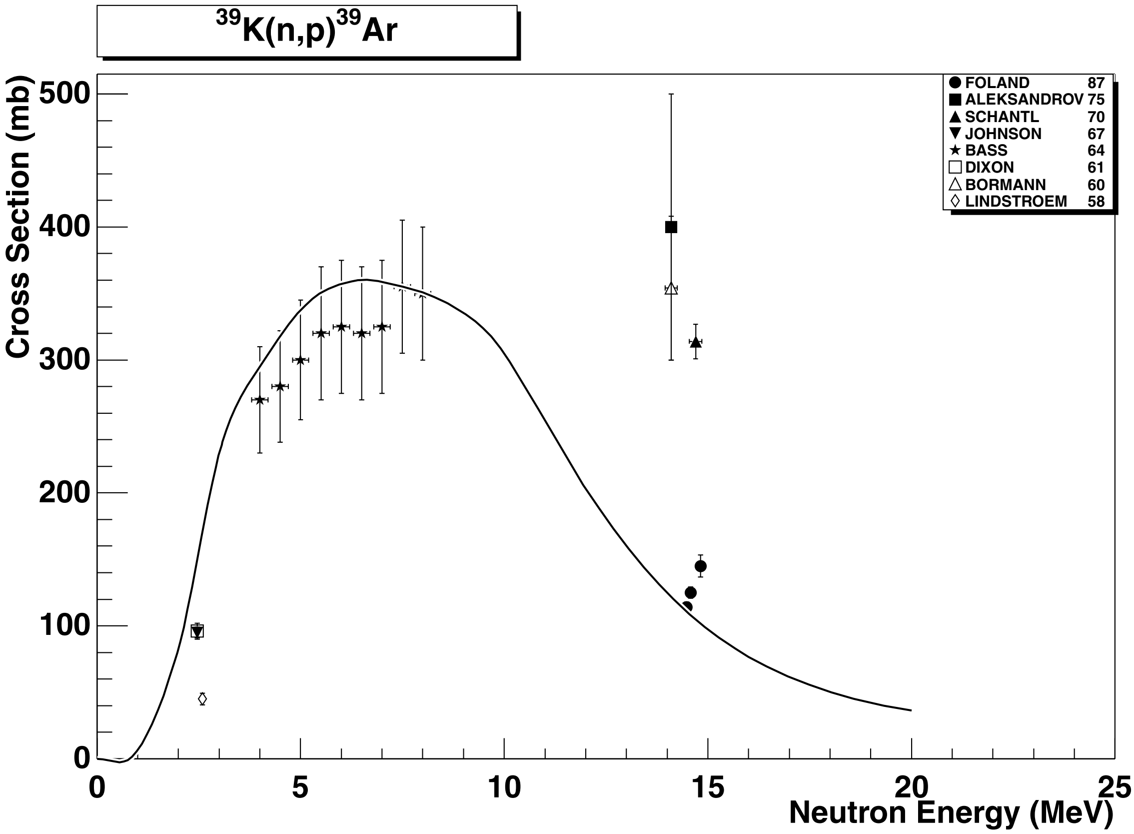

2.41. ^{39}K (n,p) ^{39}Ar

final state: total
source: ADL-3

The available data are reasonably reproduced by the ADL-3 evaluation. Three data points around 15 MeV with values between 300-400 mb are too large (also compared to systematics) and can be disregarded.

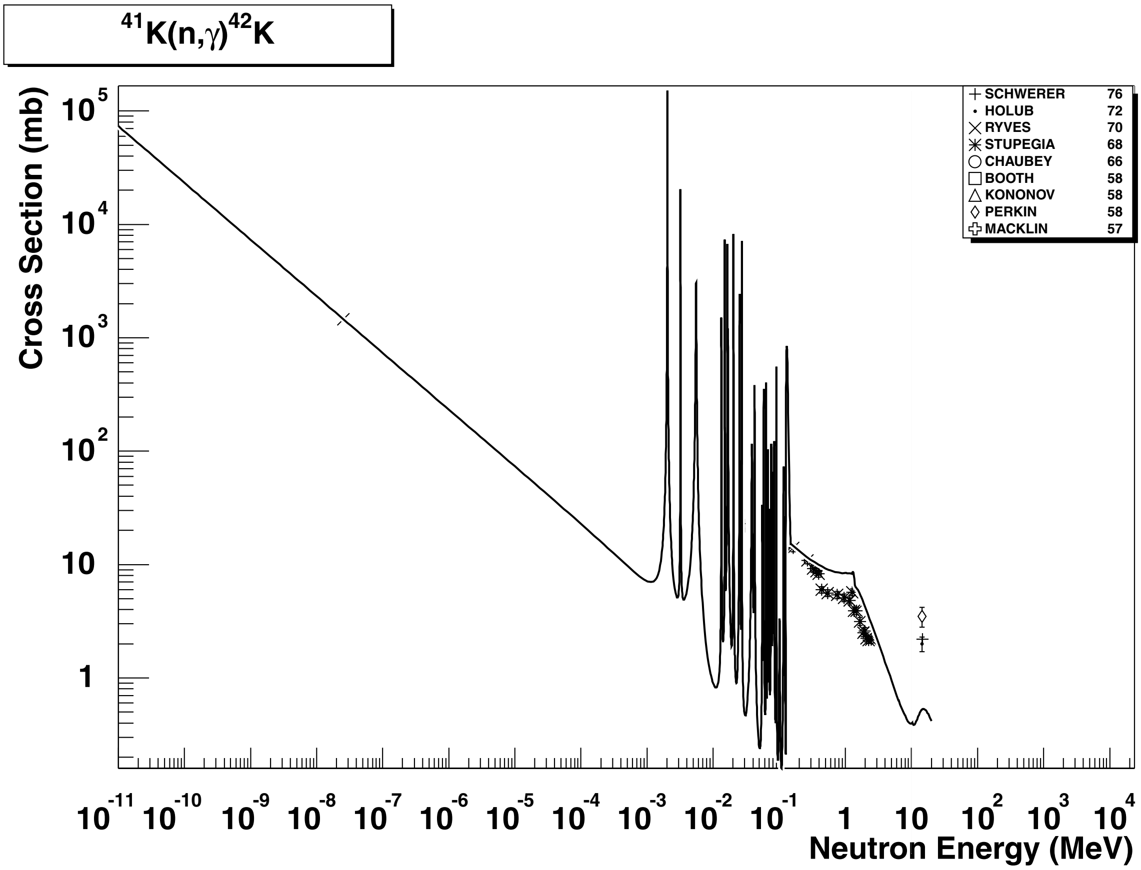

2.42. ^{41}K (n,γ) ^{42}K

final state: total
source: EAF-4.1 (JENDL-3.1)

JENDL-3.1 agrees with the thermal cross-section experimental value of Ryves70 and follows the shape but slightly overestimates data between 400 keV and 2 MeV. The 14 MeV data of Perkin58, Holub72 and Schwerer76 with values above 20 mb are wrong (much too large) and can be disregarded. The pre-equilibrium component was missing in the original JENDL-3.1 evaluation and was added during the EAF-4.1 revision based on the PEQ-systematics [3] and [35].

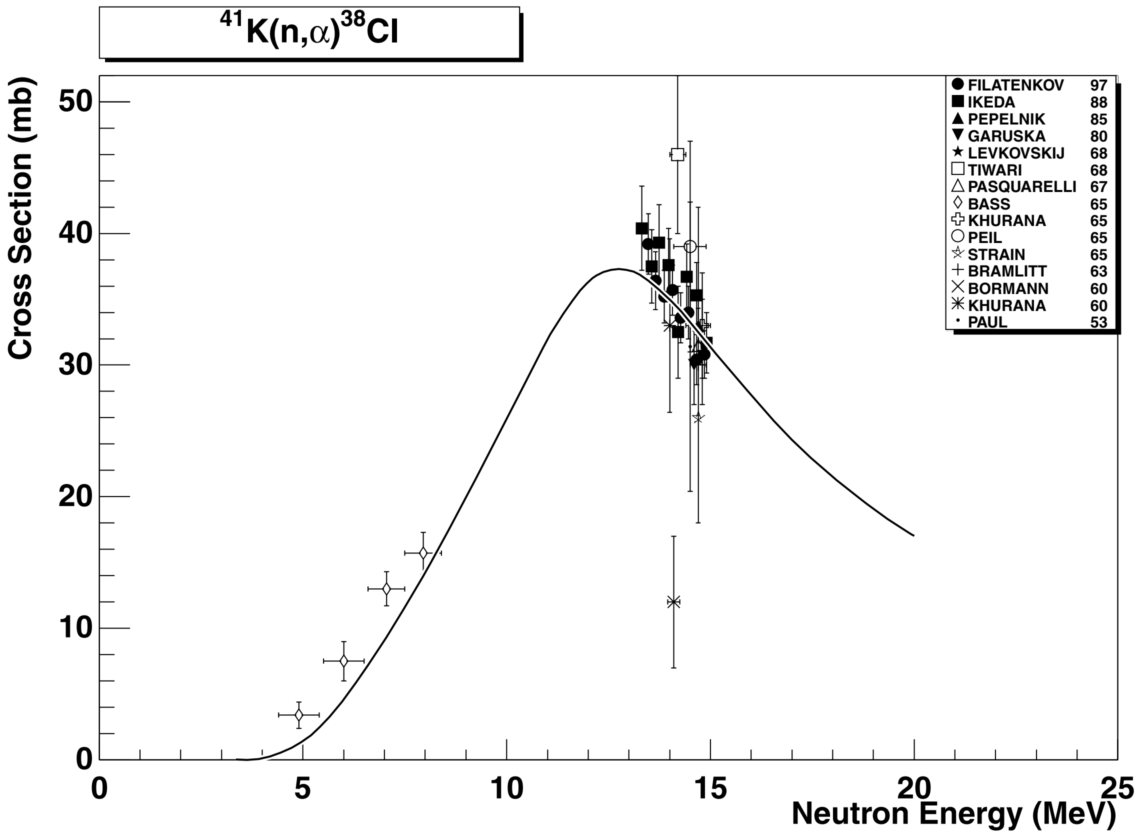

2.43. ^{41}K (n,α) ^{38}Cl

final states: g.s., meta
source: ADL-3

A slight increase of ADL-3 evaluation (by about 5%) may still improve a reasonable agreement with all experimental data. Partial cross-sections to the g.s. and meta state result from model calculations.

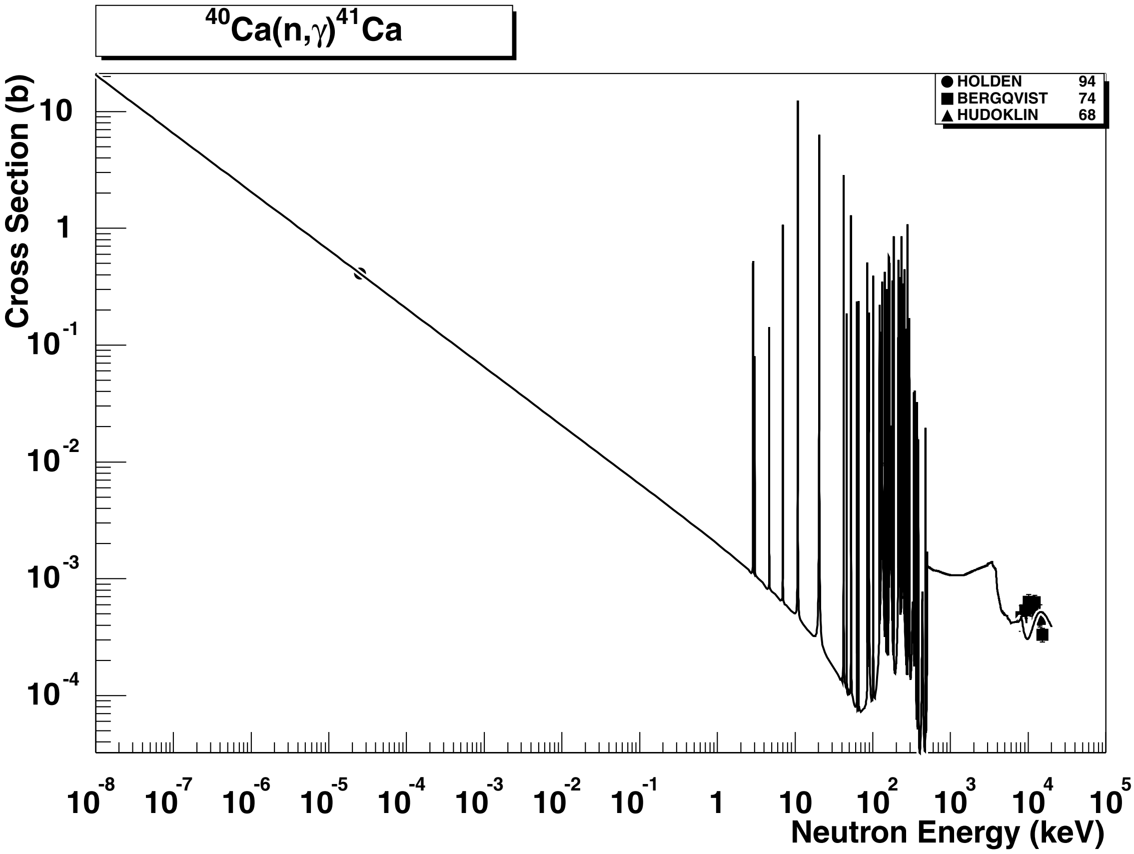

2.44. ^{40}Ca (n,γ) ^{41}Ca

final state: total
source: EAF-4.1 (JENDL-3.1)

JENDL-3.1 evaluation reasonably agrees with the EXFOR data above 10 MeV. The thermal cross-section of Holden94 from Ref. [32] is well reproduced (C/E=1.00). The pre-equilibrium component was missing in the original JENDL-3.1 evaluation and was added during the EAF-4.1 revision based on the PEQ-systematics [3] and [35].

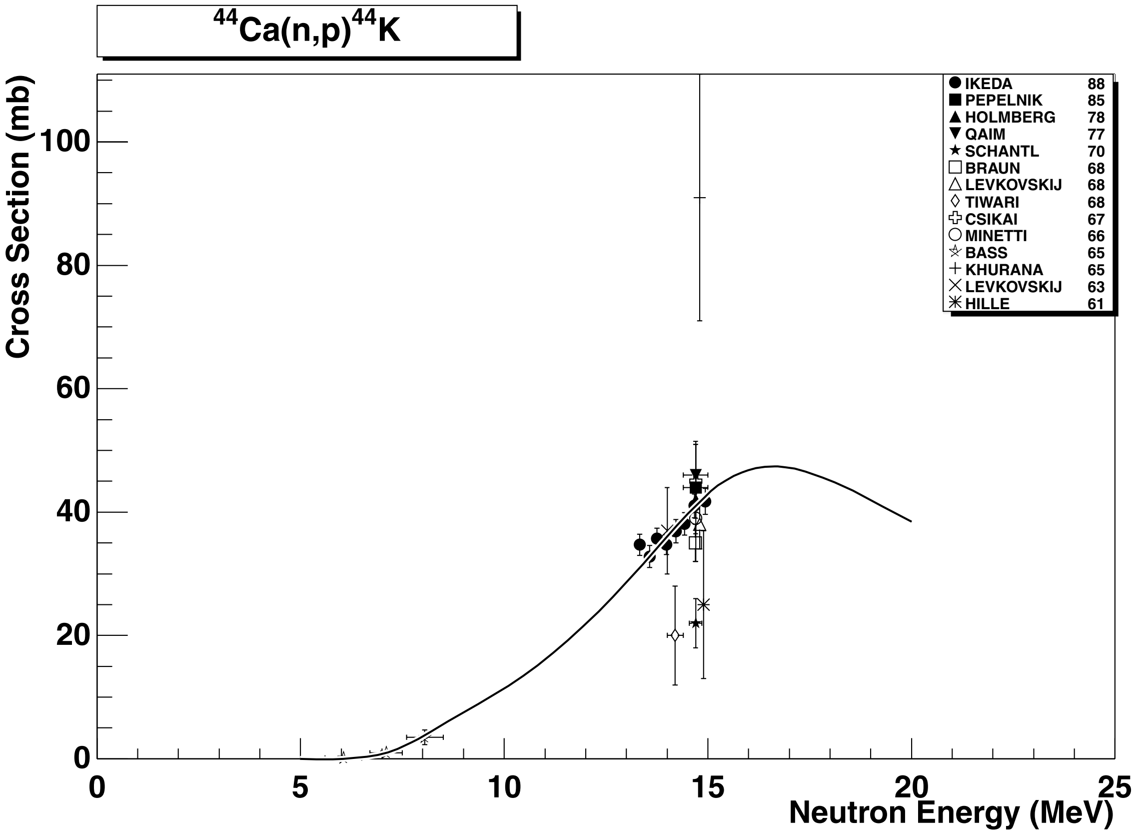

2.45. ^{44}Ca (n,p) ^{44}K

final state: total
source: ADL-3

The shape and absolute values of the ADL-3 evaluation are supported by a number of recent data around 6-8 MeV and 13-15 MeV. Some deviating experimental points can be excluded (in particular Khuvana65 and probably also Hille61, Tivari68, Schantel70).

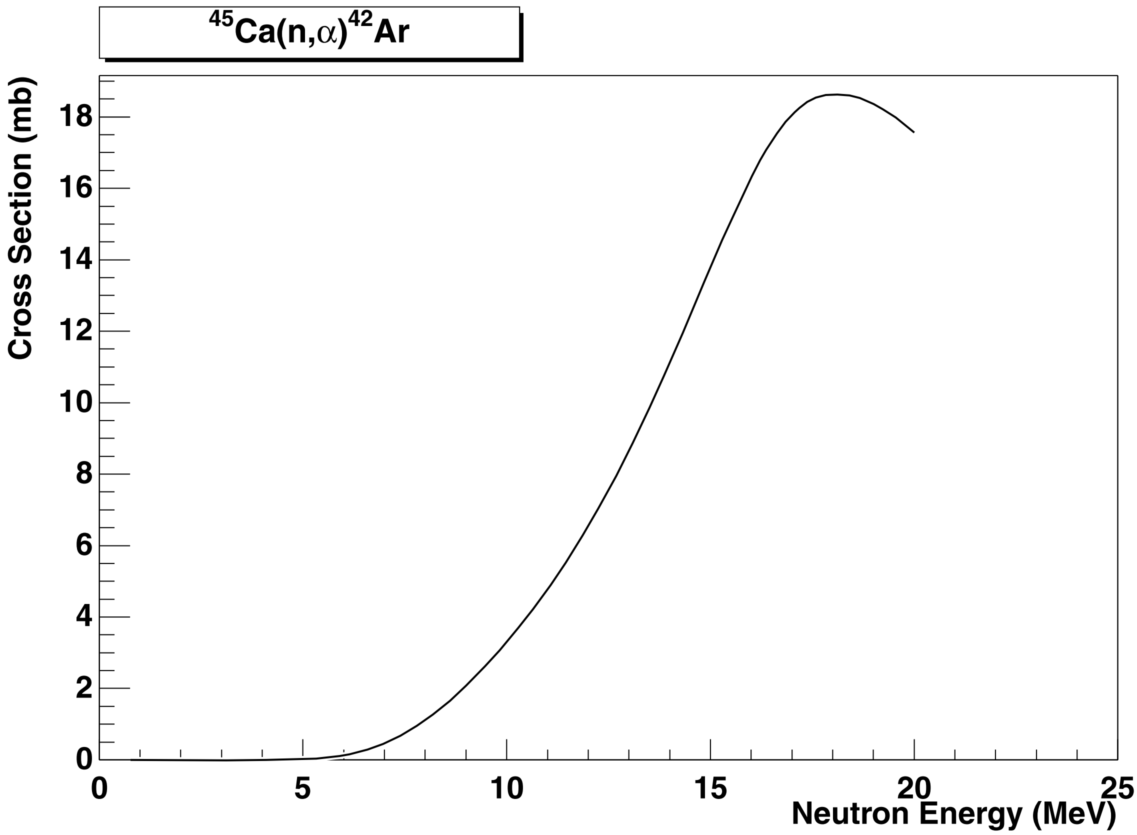

2.46. ^{45}Ca (n,α) ^{42}Ar

final state: total
source: ADL-3

This is a STAPRE calculation for the ADL-3 evaluation. No EXFOR data are available.

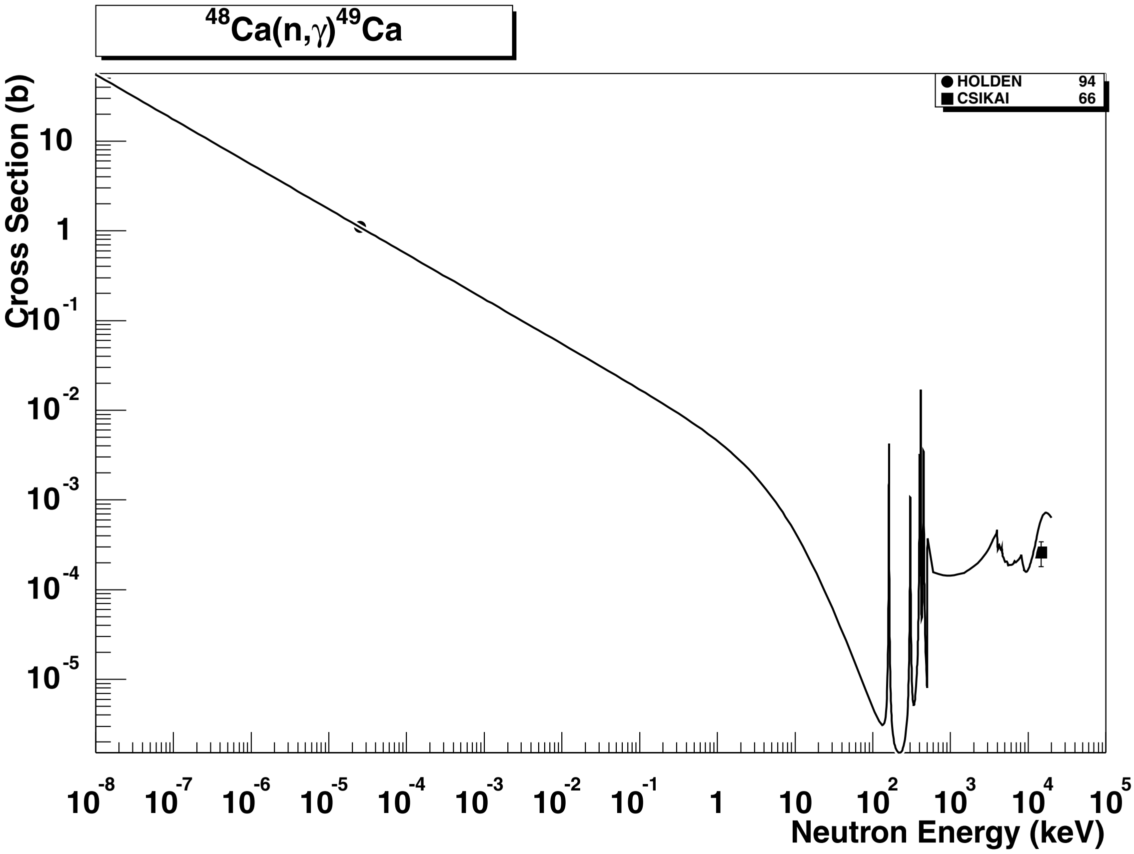

2.47. ^{48}Ca (n,γ) ^{49}Ca

final state: total
source: EAF-4.1 (JENDL-3.1)

JENDL-3.1 evaluation is in acceptable agreement with the single point of Csikai66 at 14.5 MeV. The pre-equilibrium component was missing in the original JENDL-3.1 evaluation and was added during the EAF-4.1 revision based on the PEQ-systematics [3] and [35]. The thermal cross-section of Holden94 [32] is well reproduced (C/E = 1.0).

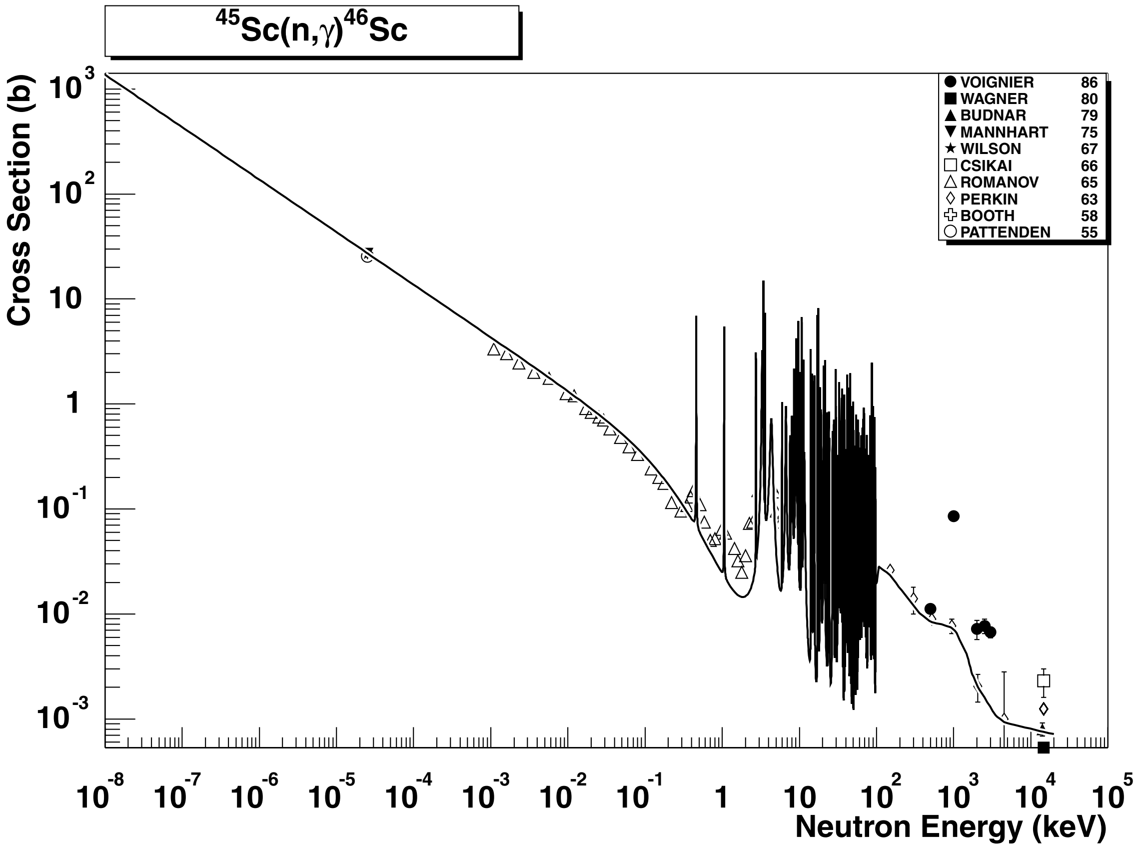

2.48. ^{45}Sc (n,γ) ^{46}Sc

final states: g.s., meta
source: EAF-4.1 (ENDF/B-VI)

The ENDF/B-VI excitation curve agrees well with the experimental data in the whole energy range. The distribution of Voignier86 data is strange, in particular the experimental point at 1 MeV. The 14.5 MeV value is correct, Csikai66 and Perkin63 are too large. Branching ratio between the g.s. and meta state is based on the thermal cross-sections [26] applied up to the end of resolved resonance region, and on the energy dependent systematics [2] for the high energy region. The partial thermal cross-sections are reproduced with C/E=1.0.

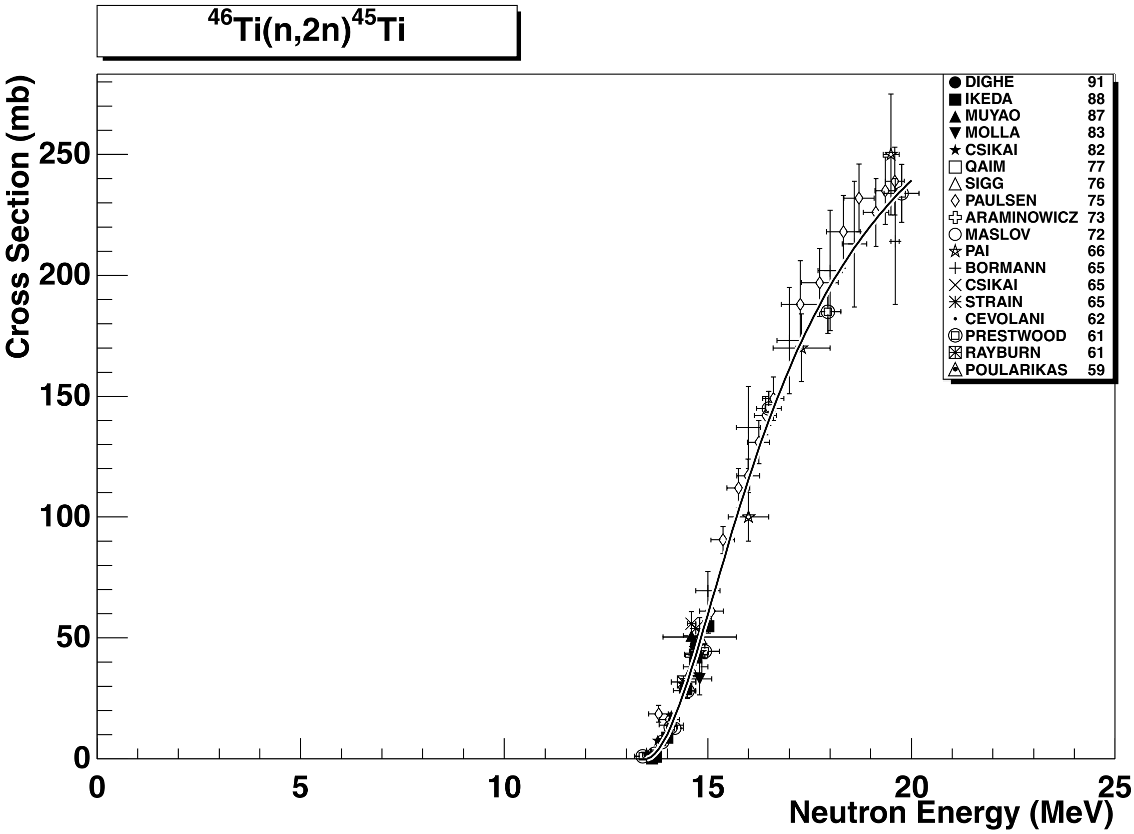

2.49. ^{46}Ti (n,2n) ^{45}Ti

final state: total
source: RRDF-98

A consistent set of experimental data is perfectly reproduced by the recent RRDF-98 evaluation.

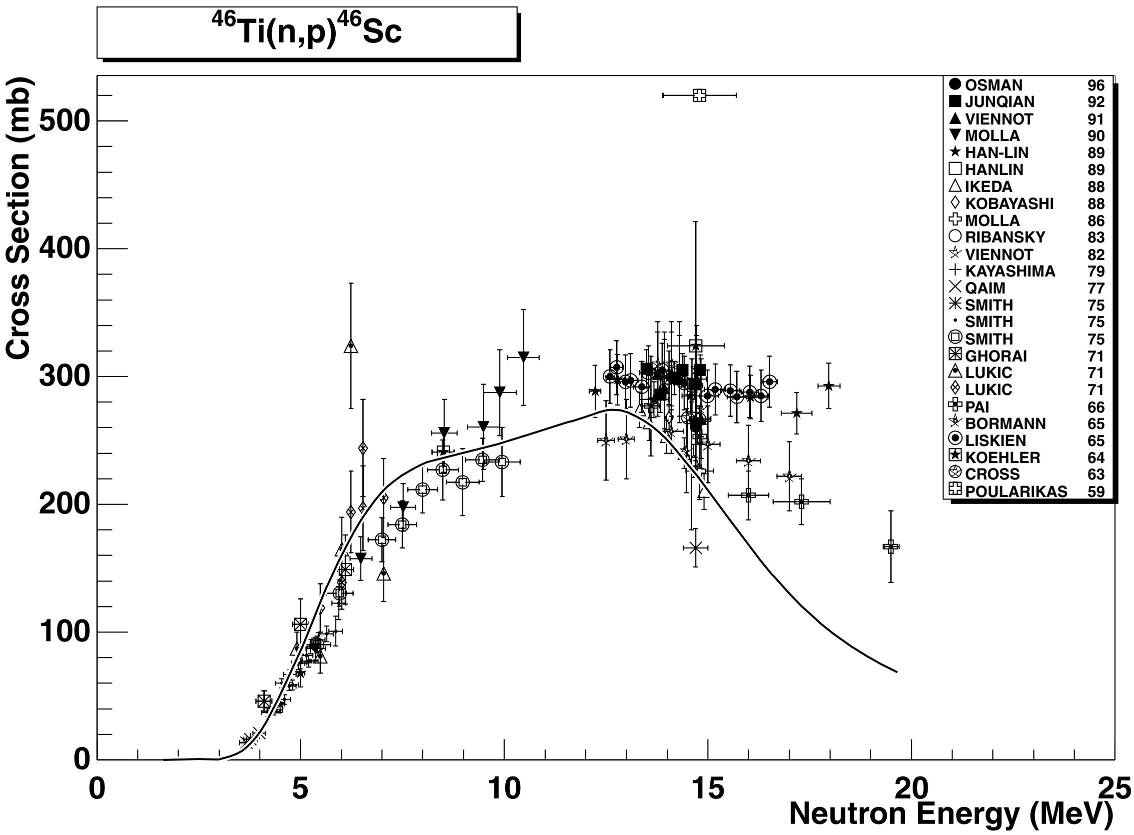

2.50. ^{46}Ti (n,p) ^{46}Sc

final states: g.s., meta
source: ADL-3

ADL-3 evaluation reproduces the experimental data well, however, the maximum of the excitation curve around 15 MeV is slightly below the very recent data.

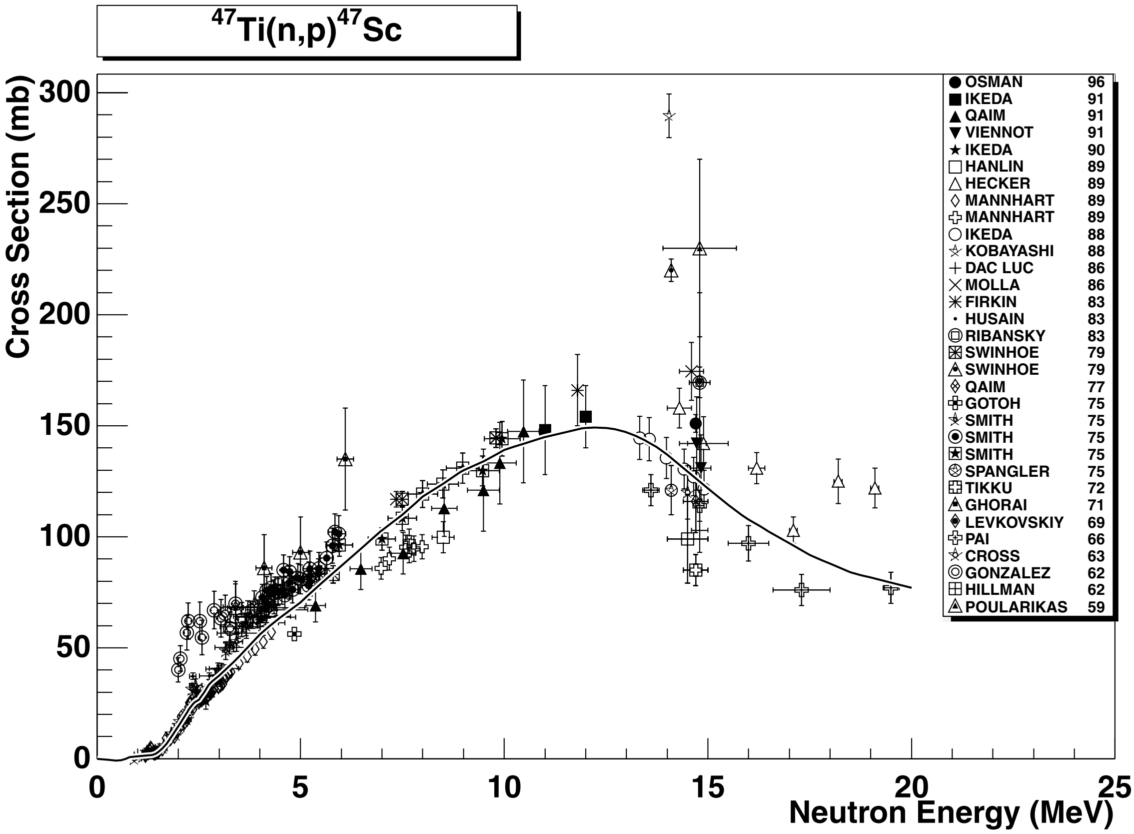

2.51. ^{47}Ti (n,p) ^{47}Sc

final states: total
source: JENDL-Act96

An excellent agreement with all relevant data, some data around 15 MeV can be disregarded (e.g. Kobayashi88).

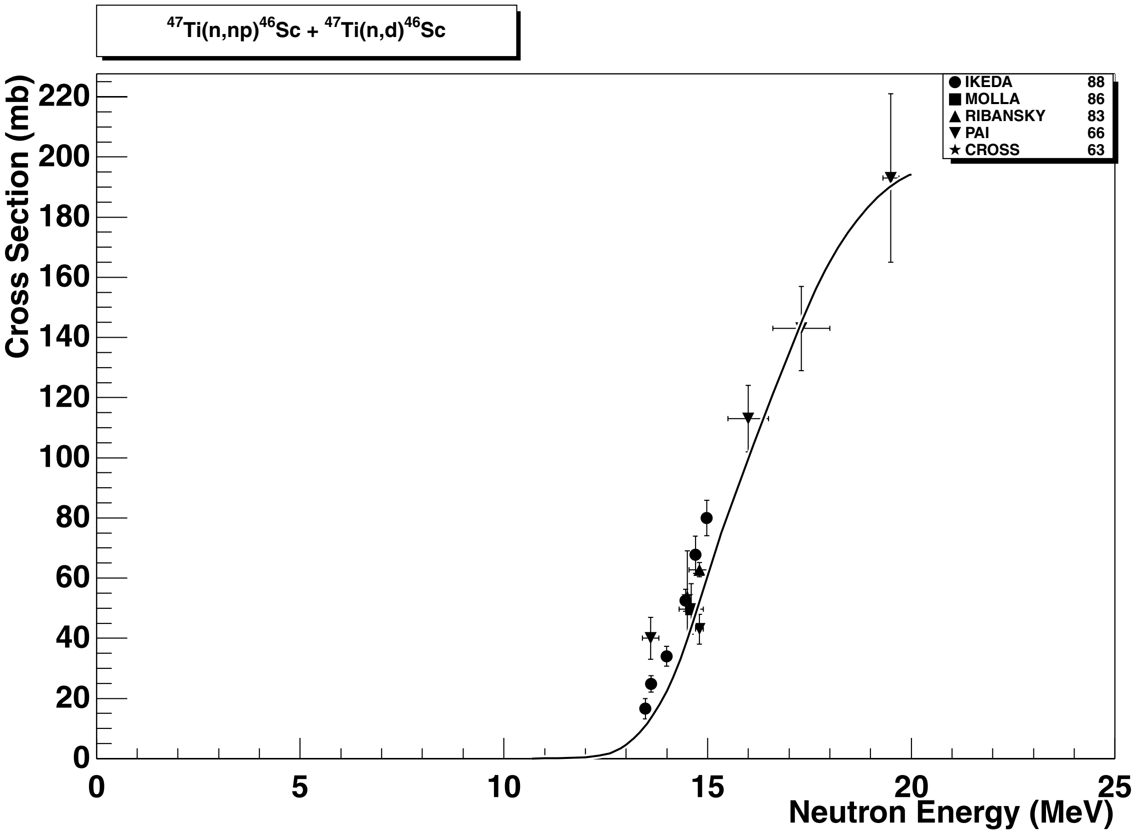

2.52. ^{47}Ti (n,d+np) ^{46}Sc

final states: total
source: RNAL

The evaluation is based on the theoretical calculations with EMPIRE-2.13[36] code. The agreement with experimental data is very good above 15 MeV. Below this energy the recommended cross-sections might be slightly underestimated. The evaluated data are stored in a single file and represent a sum of cross-sections to the g.s. and metastable state resulting from both ((n,d) and (n,np)) reactions.

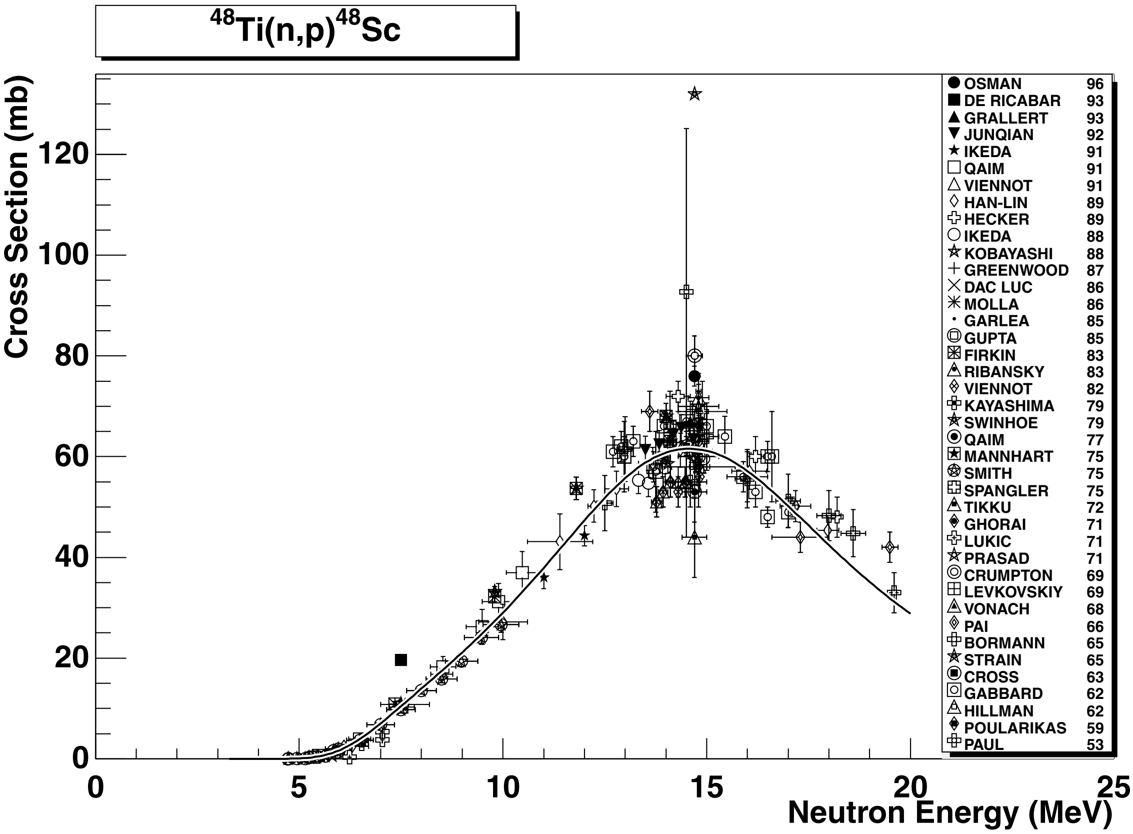

2.53. ^{48}Ti (n,p) ^{48}Sc

final state: total
source: IRK

An excellent agreement with all relevant data (Strain65 has been disregarded).

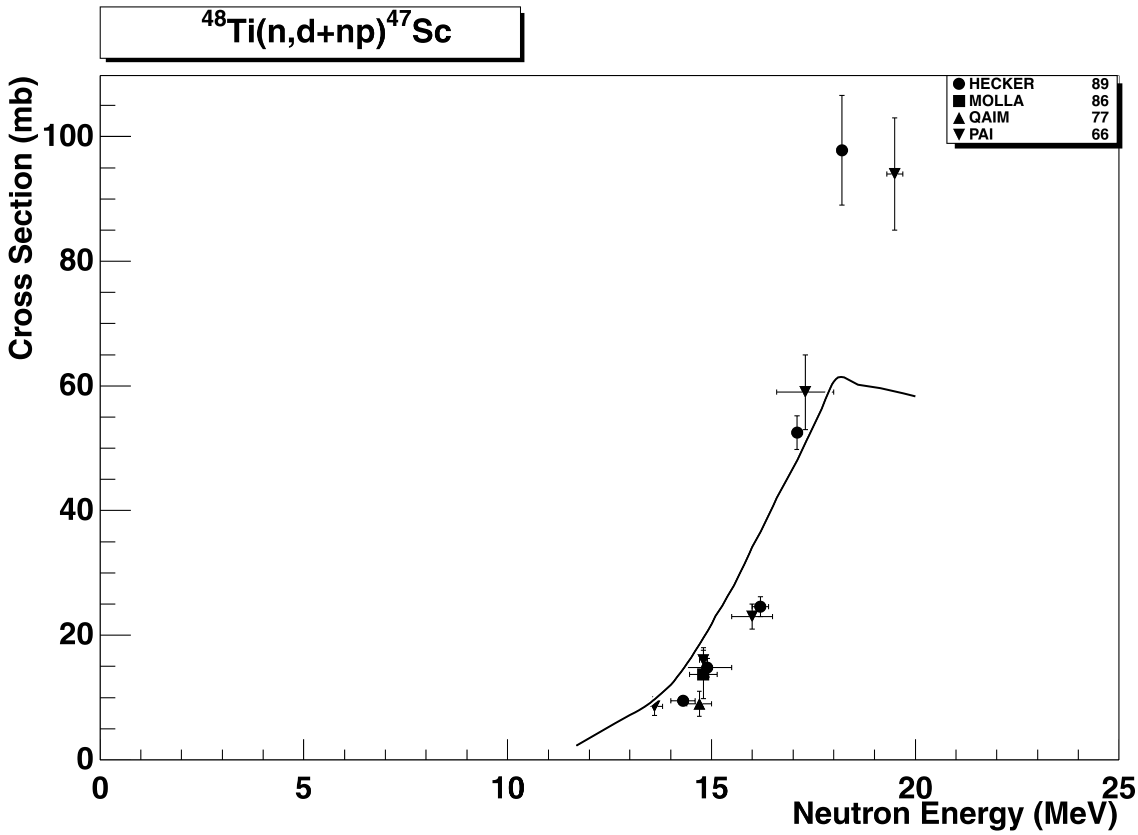

2.54. ^{48}Ti (n,d+np) ^{47}Sc

final state: total
source: FENDL/A-1 [(n,d)], IRDF-90.2 [(n,np)]

The sum of the evaluations reasonably agrees with the (n,d+np) data up to 17 MeV. Two data points above 18 MeV (Heckler89 and Pai60) may indicate, that the shape of the excitation curve above 18 MeV should be revised. The data are stored separately as (n,d) and (n,np) reaction channels.

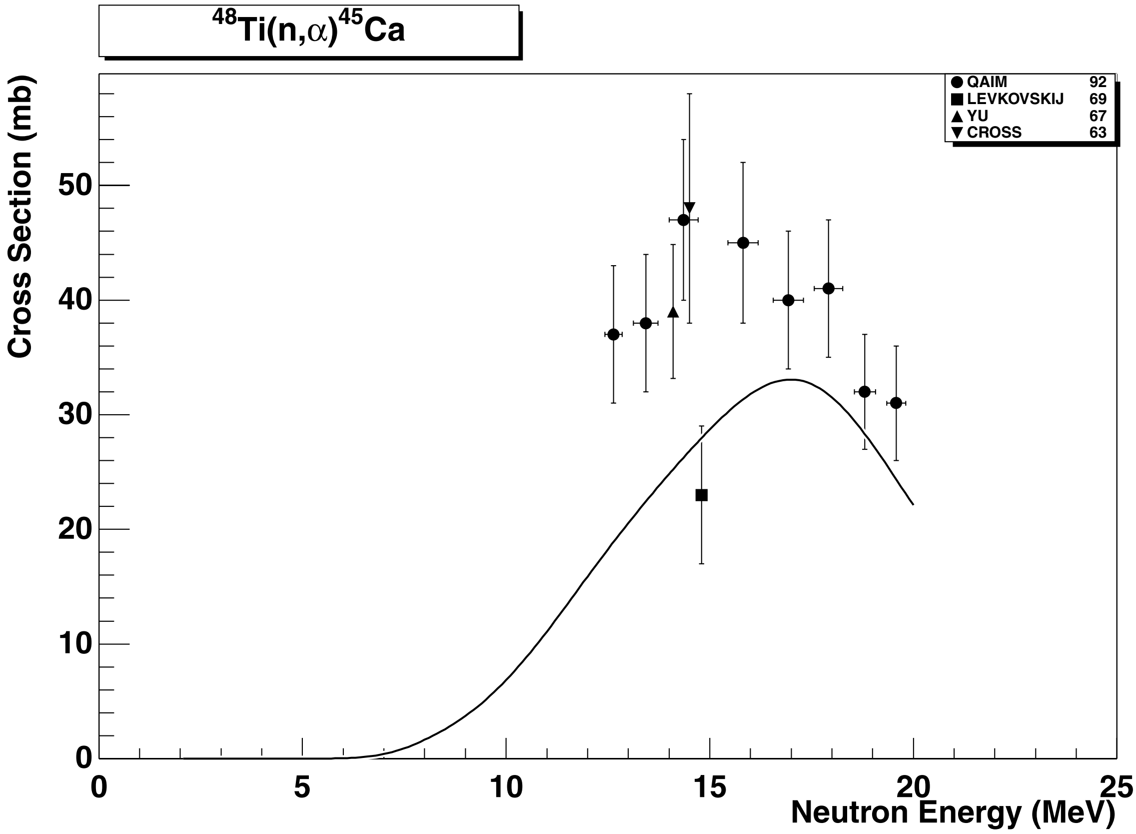

2.55. ^{48}Ti (n,α) ^{45}Ca

final state: total
source: IPPE

The IPPE evaluation [11] underestimates (by about 15%) the experimental data in the energy range between 13-20 MeV. A renormalization of the excitation curve is recommended.

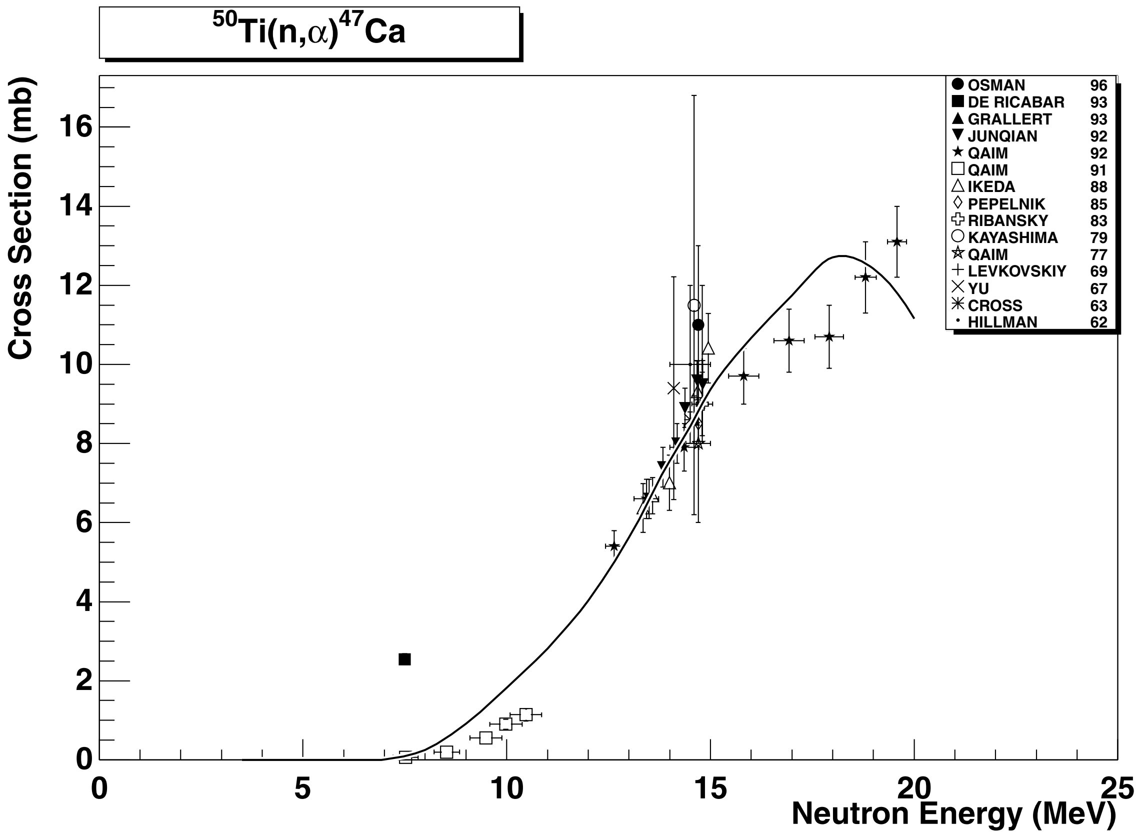

2.56. ^{50}Ti (n,α) ^{47}Ca

final state: total
source: JENDL-Act96

JENDL-Act96 reproduces the data very well, the single point of De Ricabar93 can be certainly disregarded. There is a small shape discrepancy with Qaim92 data above 15 MeV.

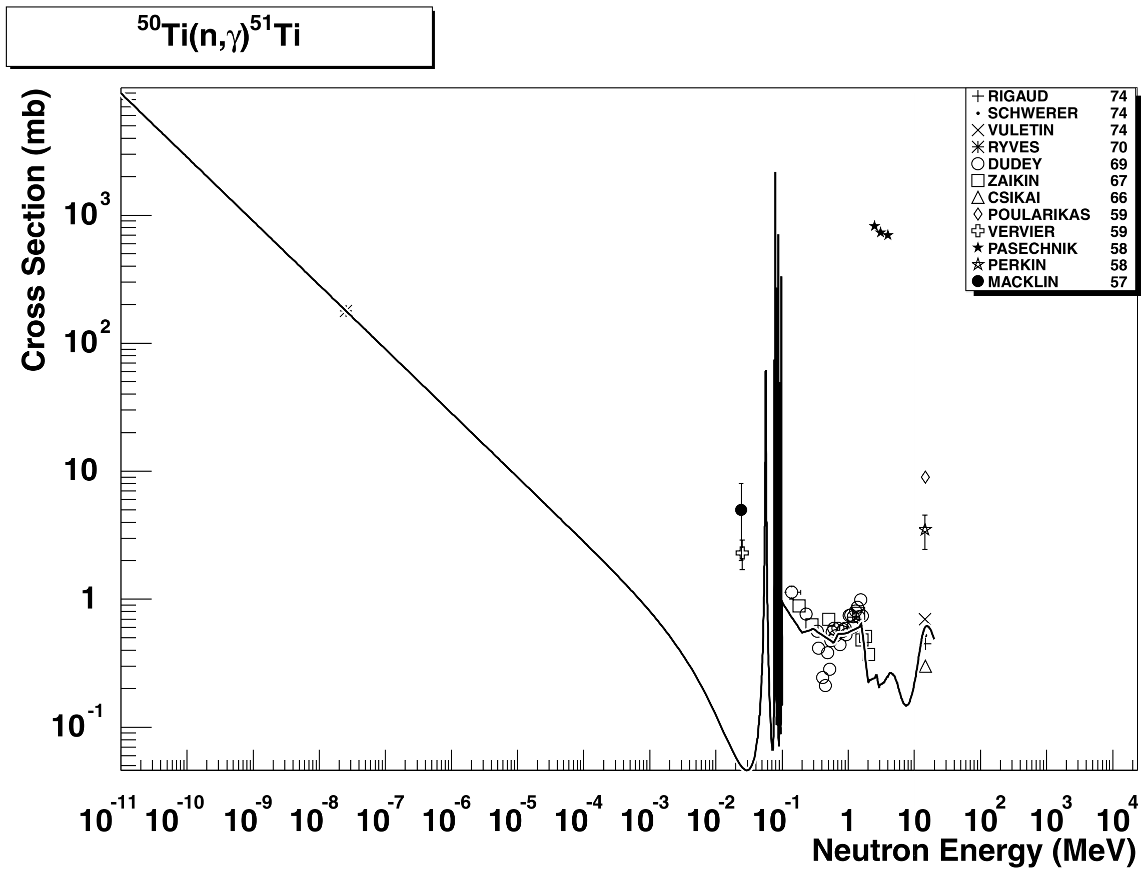

2.57. ^{50}Ti (n,γ) ^{51}Ti

final state: total
source: EAF-4.1 (JENDL-3.1)

JENDL-3.1 evaluation agrees in general with the majority of experimental data. The data of Pasechnik58 at about 3 MeV and of Perkin58 and Poulakiras59 (at 14 MeV) are definitely too large and can be disregarded. The pre-equilibrium component was missing in the original JENDL-3.1 evaluation and was added during the EAF-4.1 revision based on the PEQ-systematics [3] and [35] and agrees with experimental data.

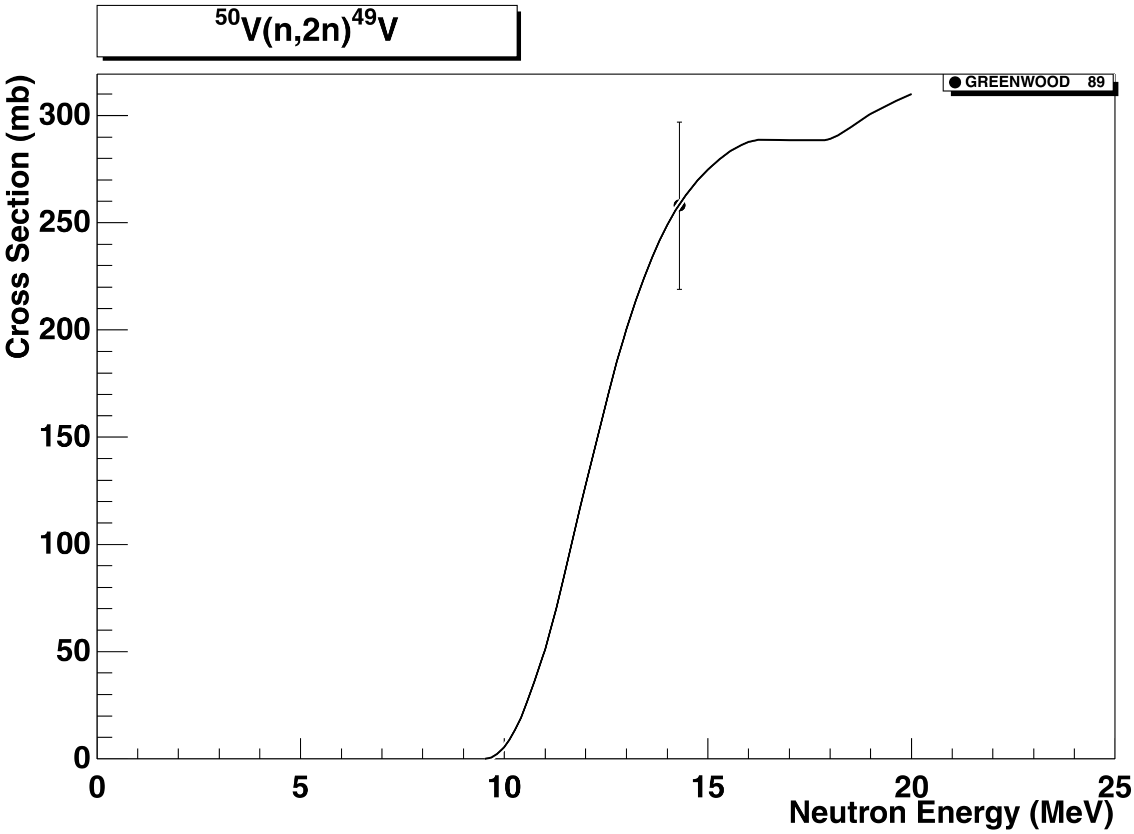

2.58. ^{50}V (n,2n) ^{49}V

final state: total
source: JENDL-Act96

The single experimental point at 14 MeV is in agreement with the JENDL-Act96 evaluation.

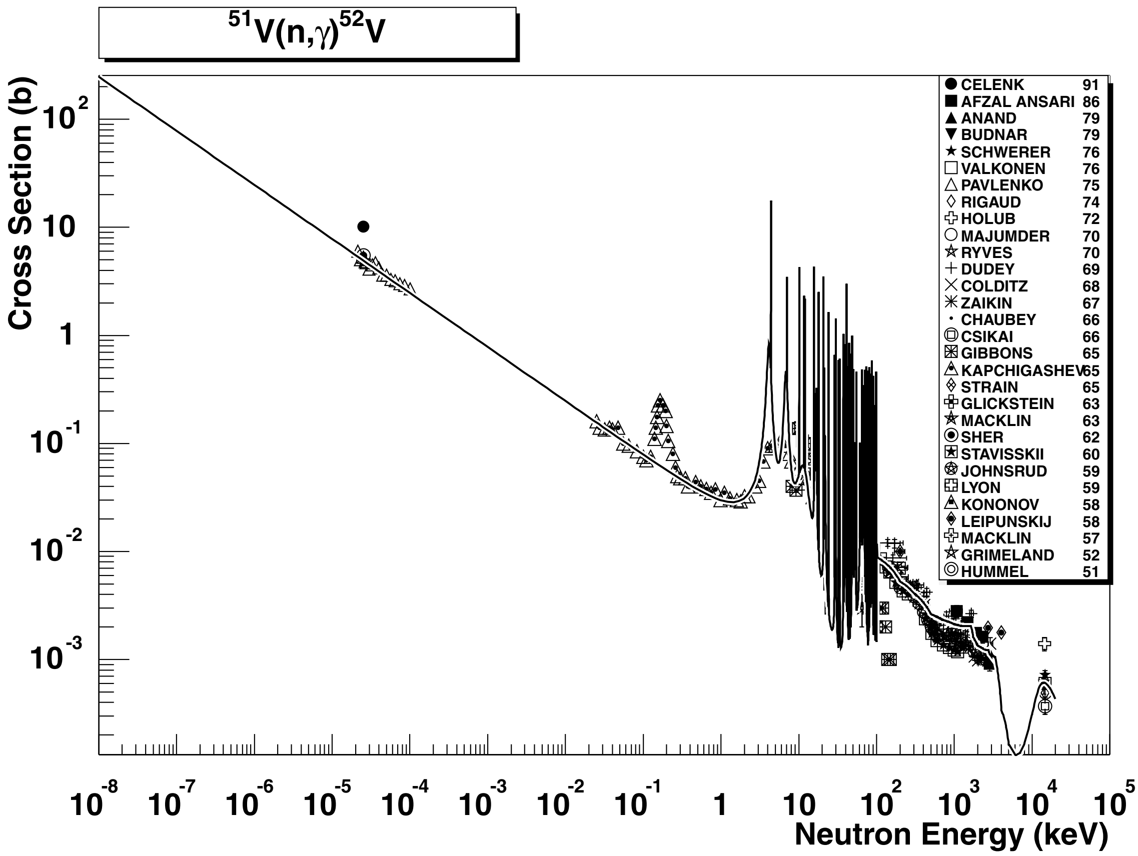

2.59. ^{51}V (n,γ) ^{52}V

final state: total
source: EAF-4.1 (JENDL-3.1)

There is a good agreement with the experimental information in the whole energy range. A broad resonance like structure in the experimental data at about 200 eV does not belong to the V-51(n,γ) reaction.

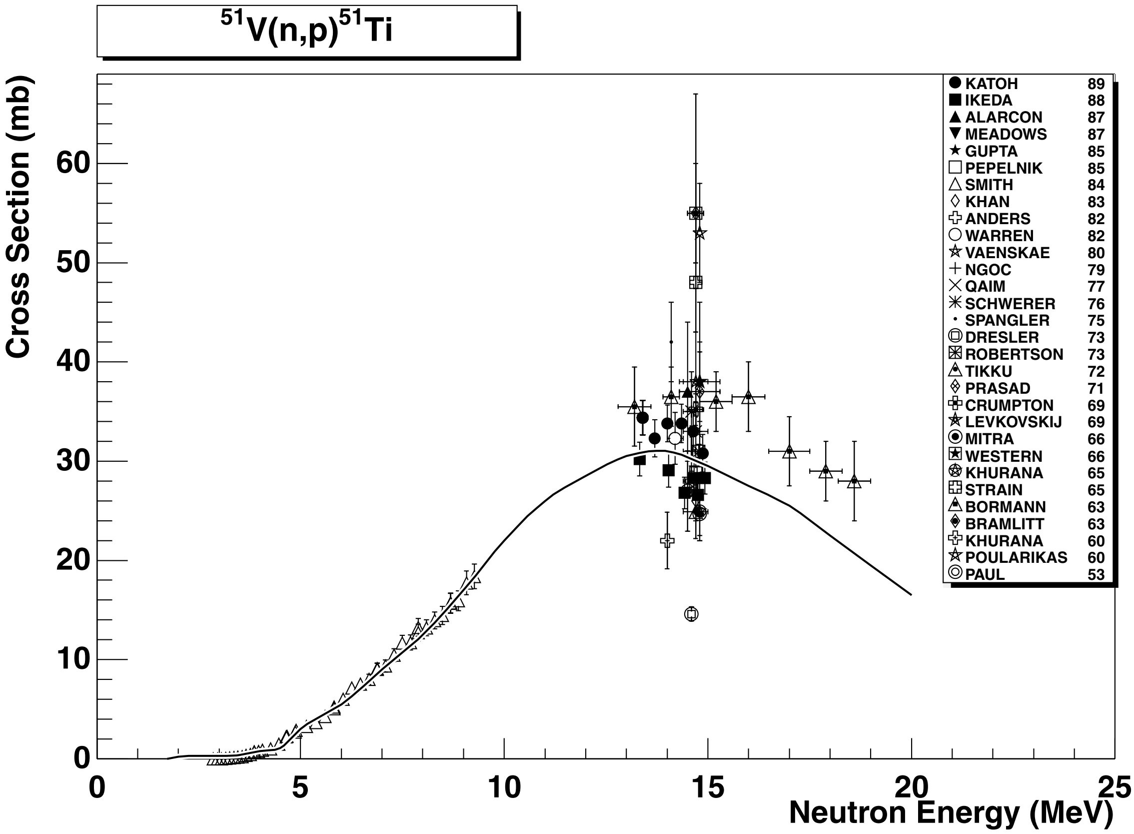

2.60. ^{51}V (n,p) ^{51}Ti

final state: total
source: JENDL-Act96

JENDL-Act96 agrees very well with the data below 10 MeV. The recent data of Katoh89 and Ikeda88 around 14 MeV agree nicely with each other and are assumed to be superior to the rest. The excitation curve runs in the middle between the above mentioned two experiments.

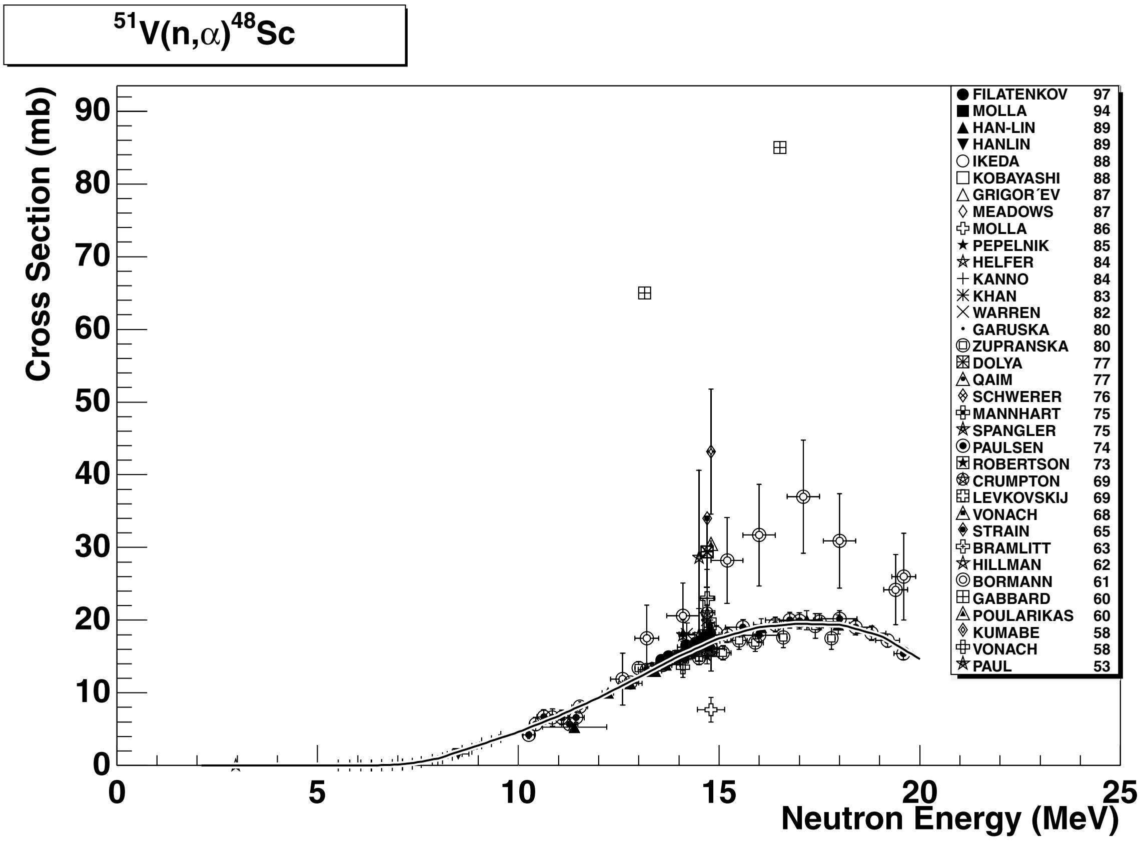

2.61. ^{51}V (n,α) ^{48}Sc

final state: total
source: EAF-4.1 (IRDF-90.2)

IRDF-90.2 shows a good agreement with all major recent data (around 14 MeV). Data of Borman61 and Gabbard60 proved to be wrong during the FENDL selection panel and were disregarded.

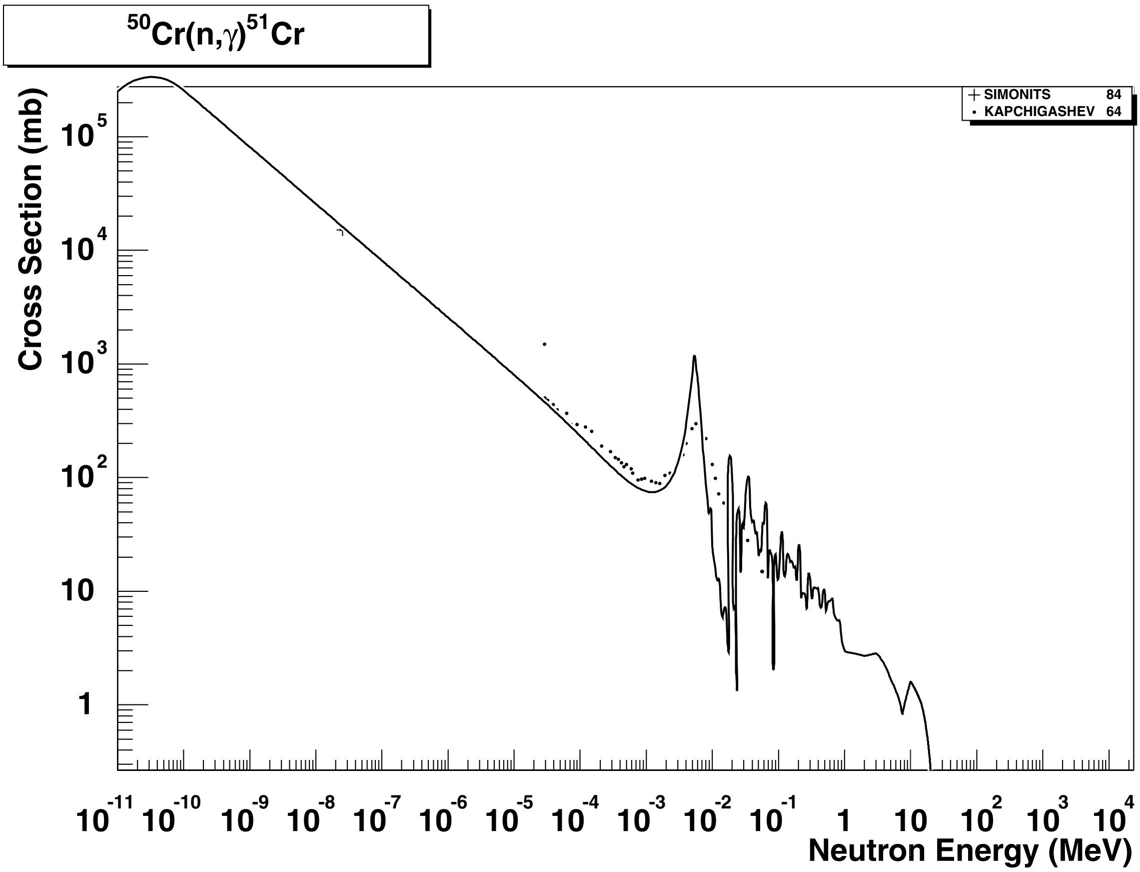

2.62. ^{50}Cr (n,γ) ^{51}Cr

final state: total
source: EAF-4.1(EFF-2.4)

ENEA evaluation (EFF-2.4) is reasonably close to the experimental data at low energies, however, the high energy part of the excitation curve looks strange. A replacement of this data by ENDF/B-VI may be considered. Data are stored in SANDII group structure, the original EFF-2.4 point-wise data include 9519 energy points.

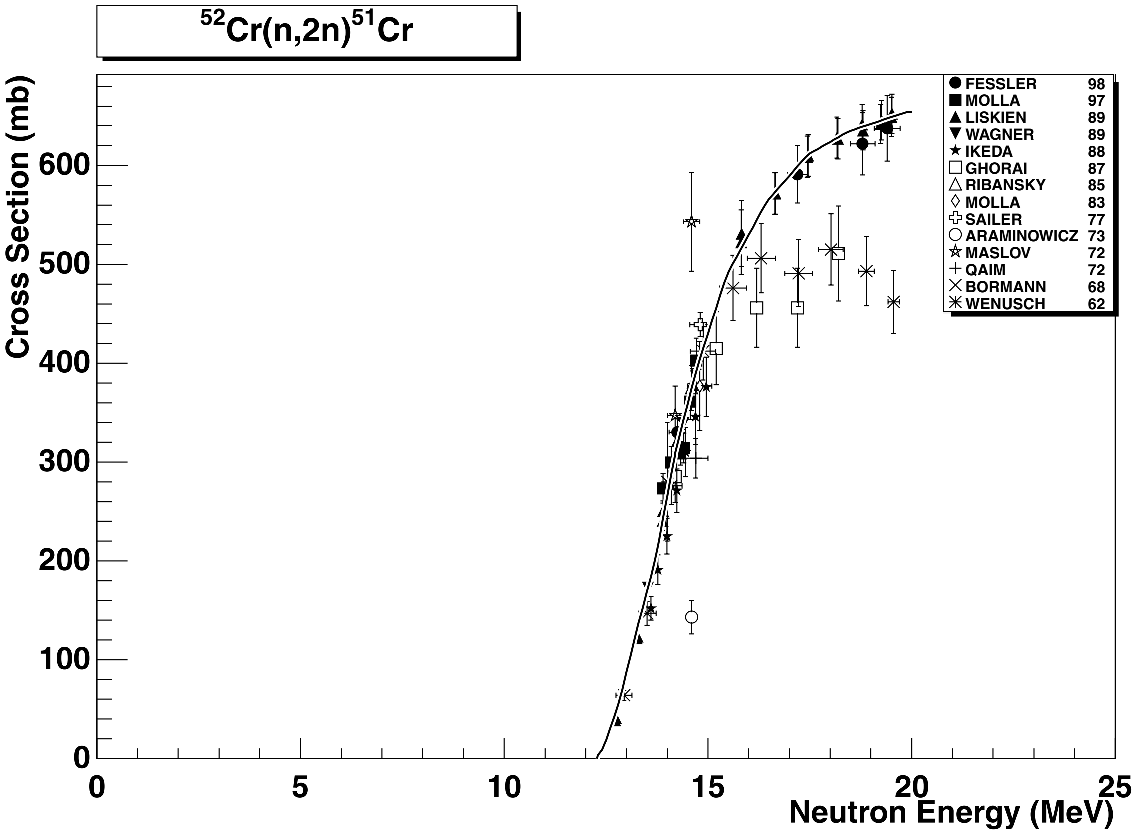

2.63. ^{52}Cr (n,2n) ^{51}Cr

final state: total
source: IRDF-90.2

IRDF-90.2 reproduces the experimental data very well. The experiment of Liskien89 was decisive for the shape above 15 MeV and overruled the previously measured data.

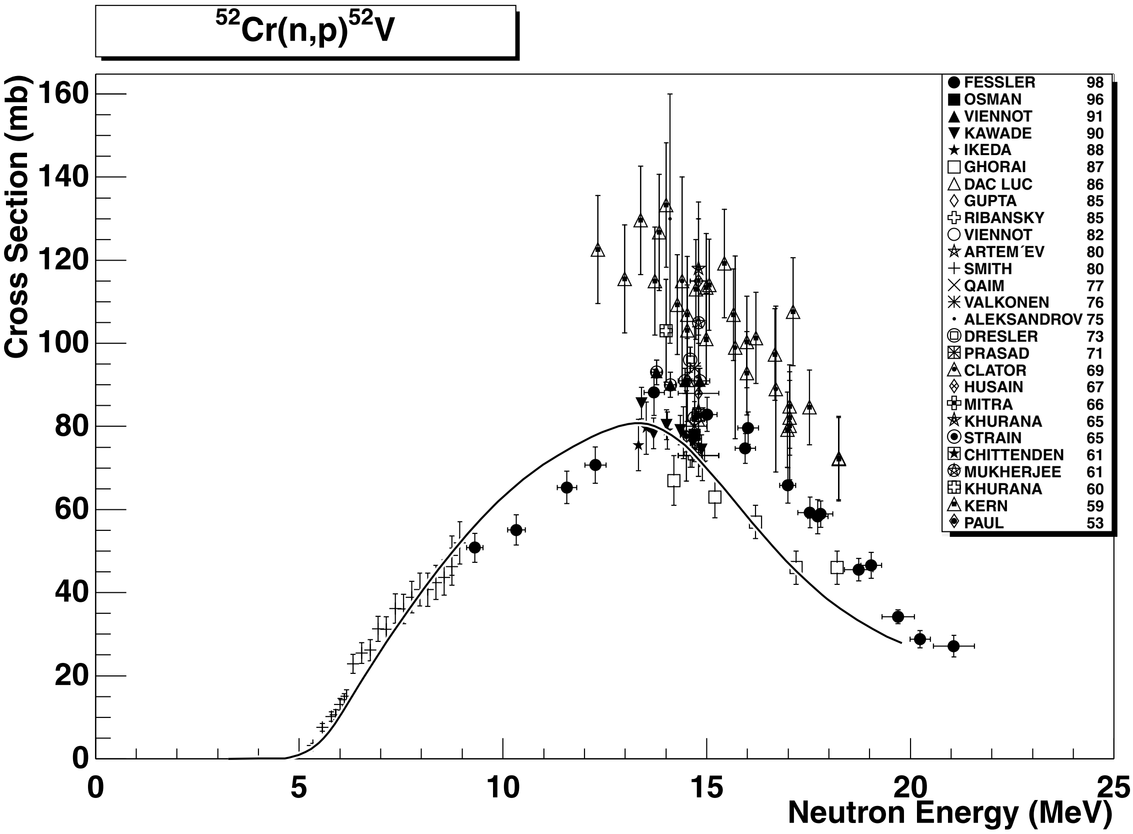

2.64. ^{52}Cr (n,p) ^{52}V

final state: total
source: ADL-3

ADL-3 evaluation agrees nicely with Smith80 below 10 MeV. Around 14 MeV the evaluation runs between the data of Ikeda88 and Kawade90. The slightly larger data of Viennot91 have been shown too large by the very recent measurement of Osman96, which support values of Ikeda88 and Kawade90. Data of Kern59 may be disregarded.

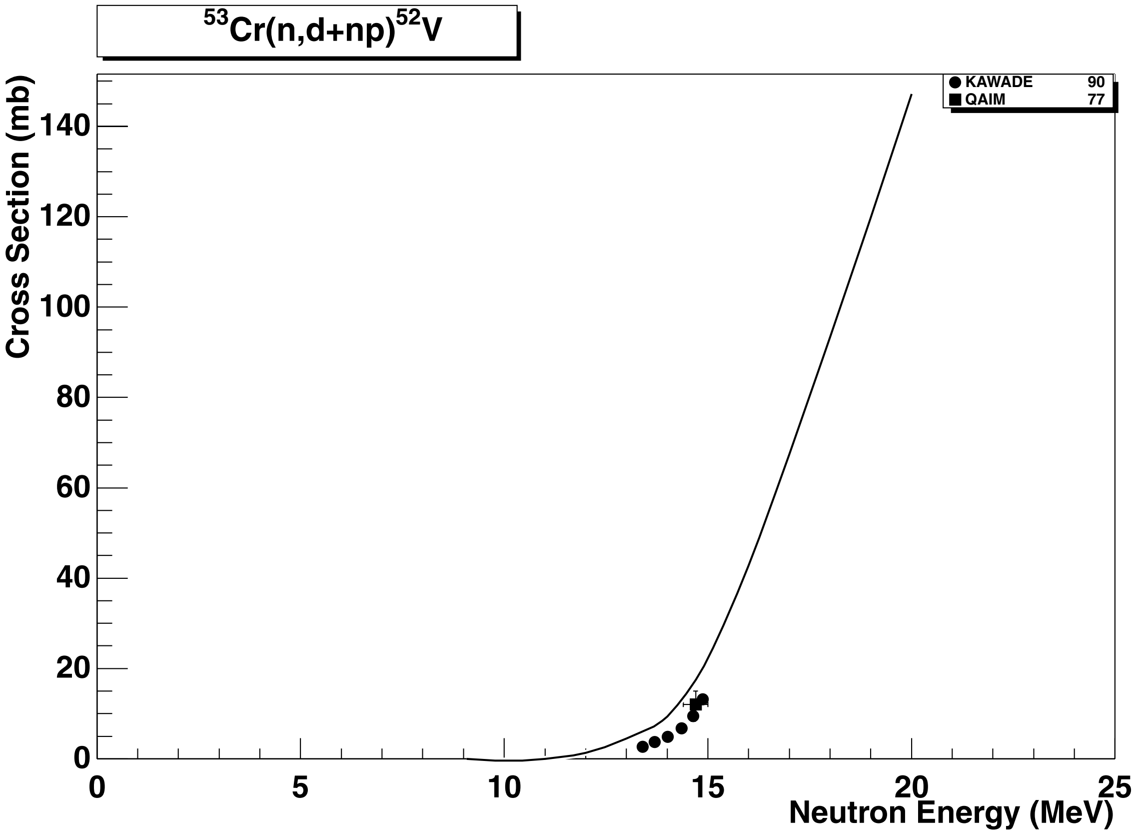

2.65. ^{53}Cr (n,d+np) ^{52}V

final state: total
source: EFF-2.4

EFF-2.4 evaluation is plotted against (n,d+np) data. The 14-15 MeV cross section value lies reasonably close to the experimental data of Qaim77 and Kawade90. The data are stored separately as (n,d) and (n,np) reaction channels.

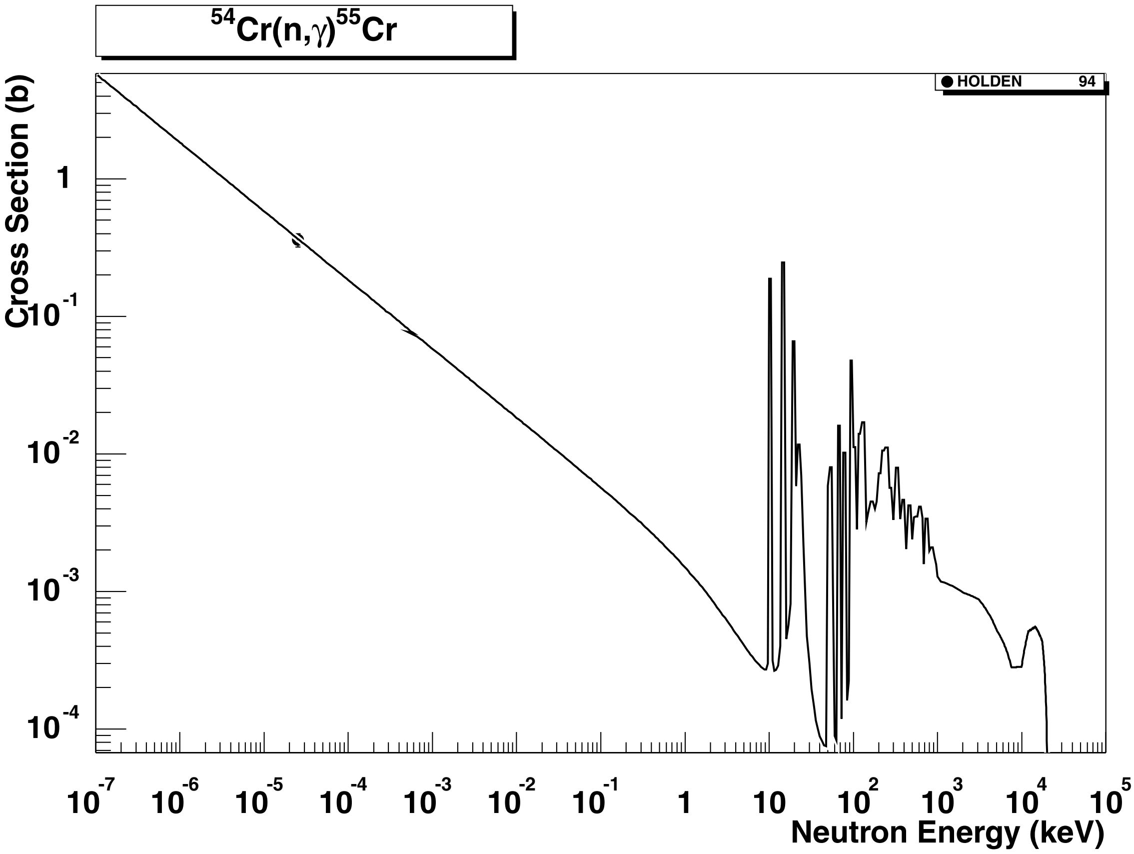

2.66. ^{54}Cr (n,γ) ^{55}Cr

final state: total
source: EAF-4.1 (EFF-2.4)

EFF-2.4 evaluation includes the resolved resonance data. No high energy data is available. The thermal cross-section of Holden [32] is nicely reproduced with C/E=1.01. Data are plotted in the multigroup SANDII structure.

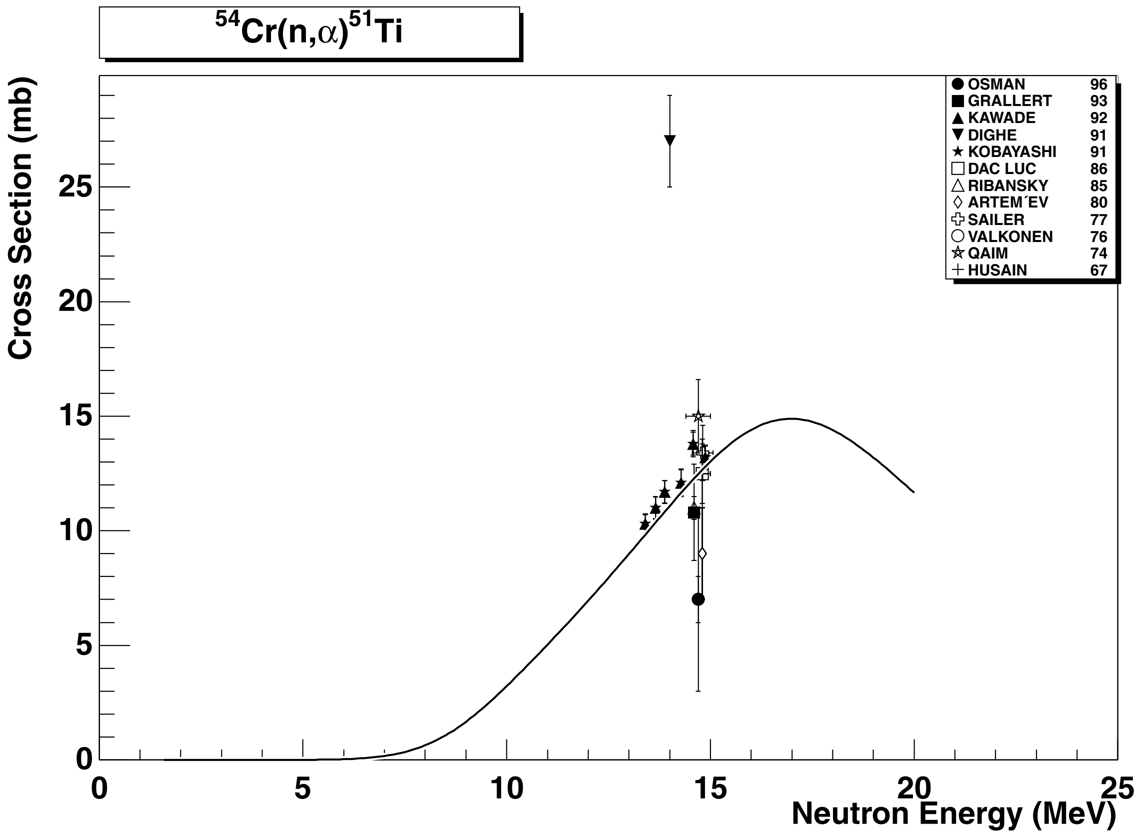

2.67. ^{54}Cr (n,α) ^{51}Ti

final state: total
source: IPPE

Recent IPPE evaluation [11] is close to the Kawade92 data around 14 MeV. Dighe91 is too large and can be disregarded.

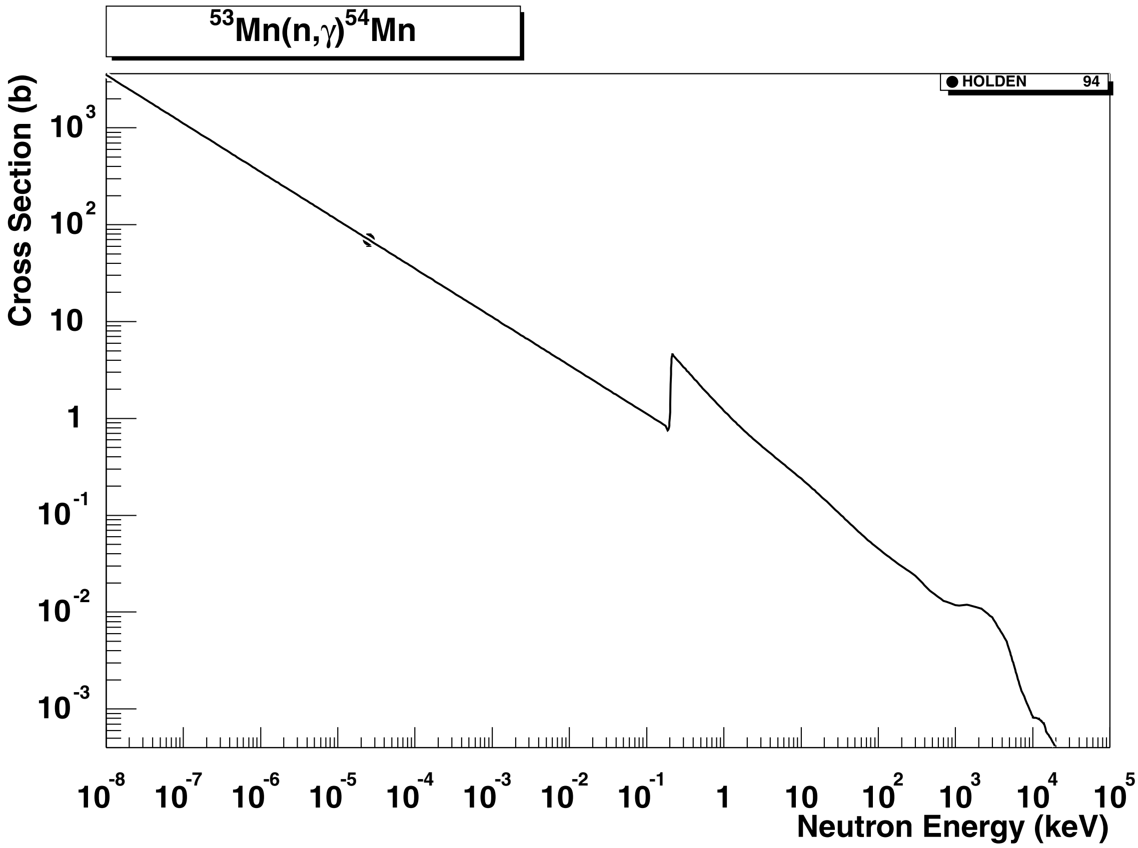

2.68. ^{53}Mn (n,γ) ^{54}Mn

final state: total
source: EAF-4.1

This EAF-4.1 evaluation is based on calculations with the MASGAM code. MASGAM is a statistical (Hauser-Feshbach) code with the pre-equilibrium component based on the D-SD model (for details see Ref. [35]). The global parameters are applied for optical model, level densities and gamma-ray strength functions. The thermal cross-section of Holden94 [32] is well reproduced with C/E=1.0.

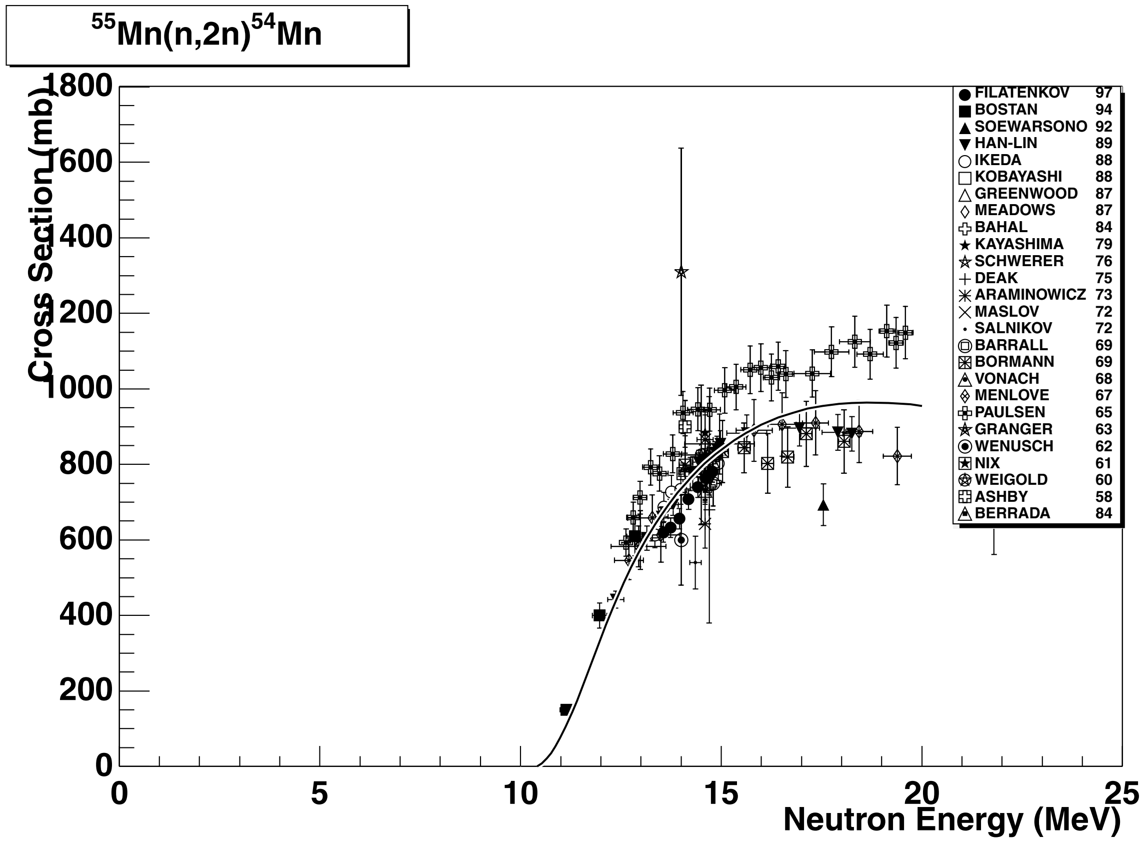

2.69. ^{55}Mn (n,2n) ^{54}Mn

final state: total
source: ADL-3

ADL-3 excitation curve fits the data well up to 15 MeV, in particular the recent data of Filatenkov97 and Bostan94. The shape above 15 MeV is closer to the lower data of Han-Lin89, but in principle lies between the data sets. The excitation curve around 18 MeV starts to be uncertain.

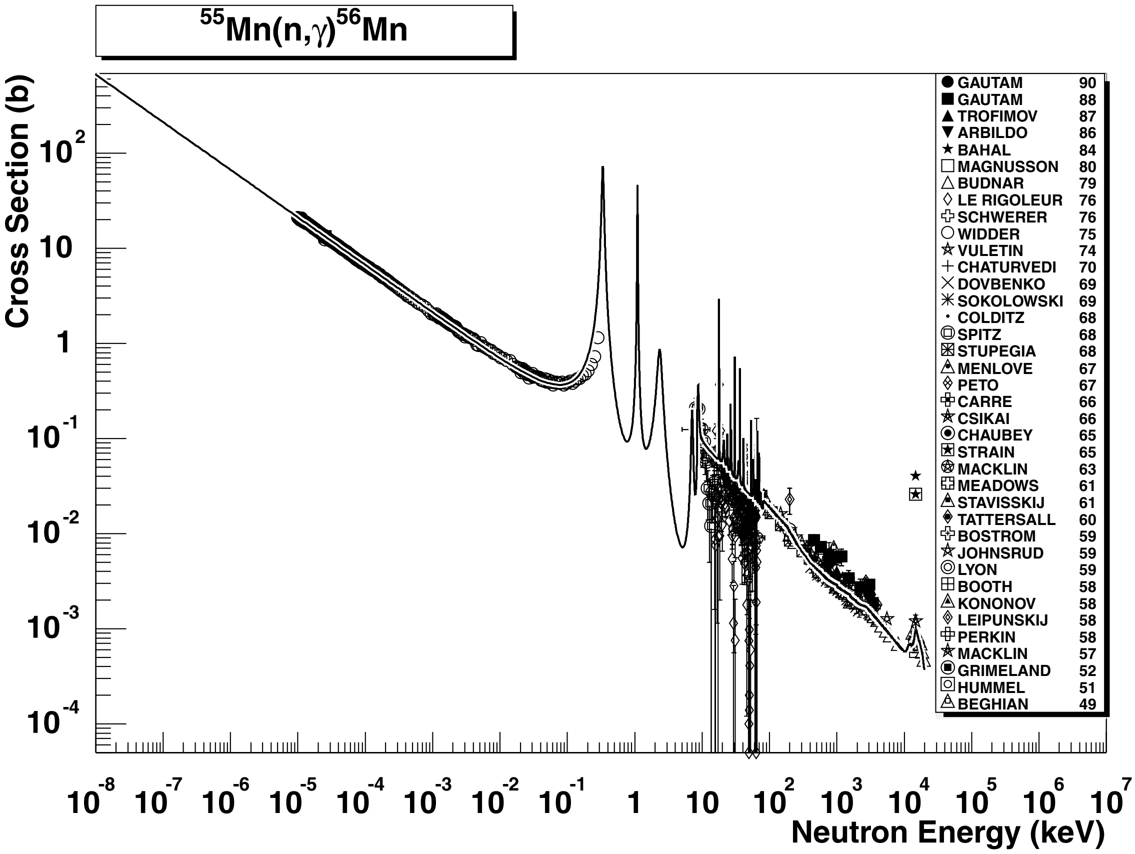

2.70. ^{55}Mn (n,γ) ^{56}Mn

final state: total
source: EAF-4.1 (JEF-2.2)

The evaluation originates from ENDF/B-VI and runs well through the experimental data in the whole energy range. Two large data points at 14 MeV (Strain65 and Bahal84) are ignored.

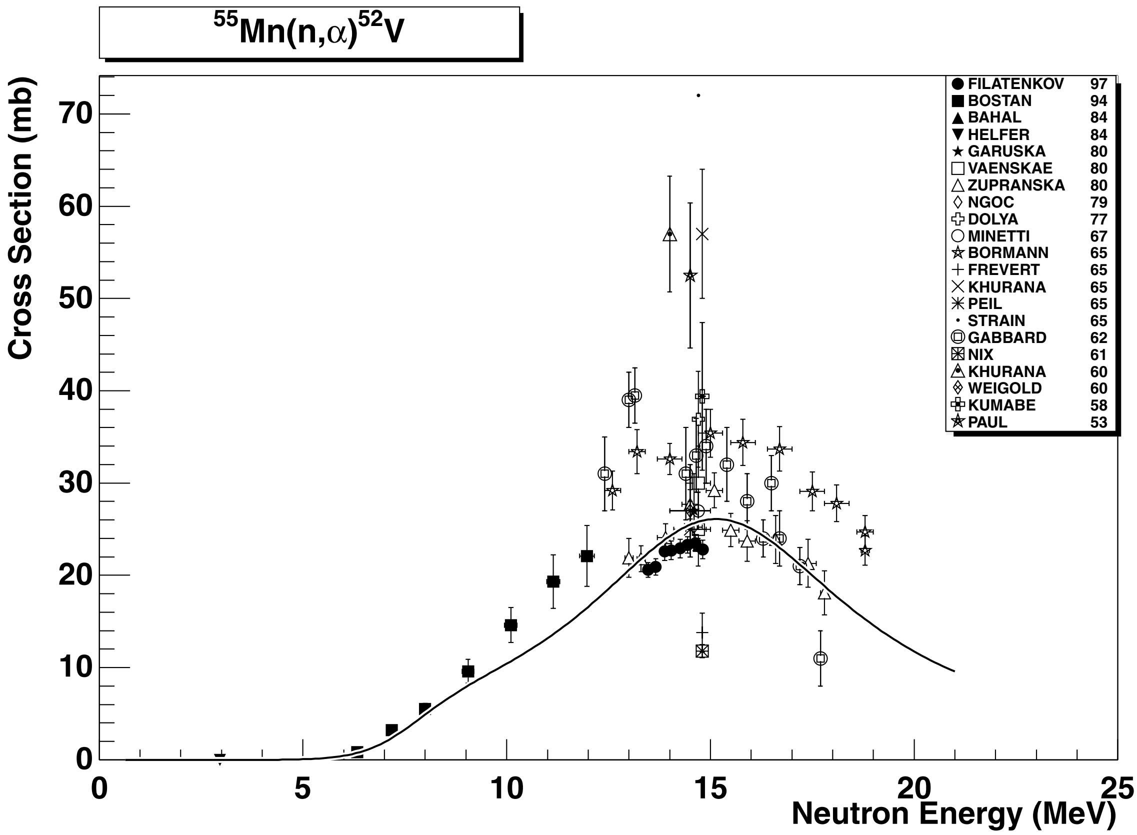

2.71. ^{55}Mn (n,α) ^{52}V

final state: total
source: IPPE

Recent IPPE evaluation[11] runs between the two latest experimental data sets of Bostan94 (below 12 MeV) and Filatenkov97 (between 13-15 MeV). There are a number of the old data (Paul53, Khurana60,65, Gabbard62 and Borman65) which were found too large and not considered in the IPPE evaluation adjustment.

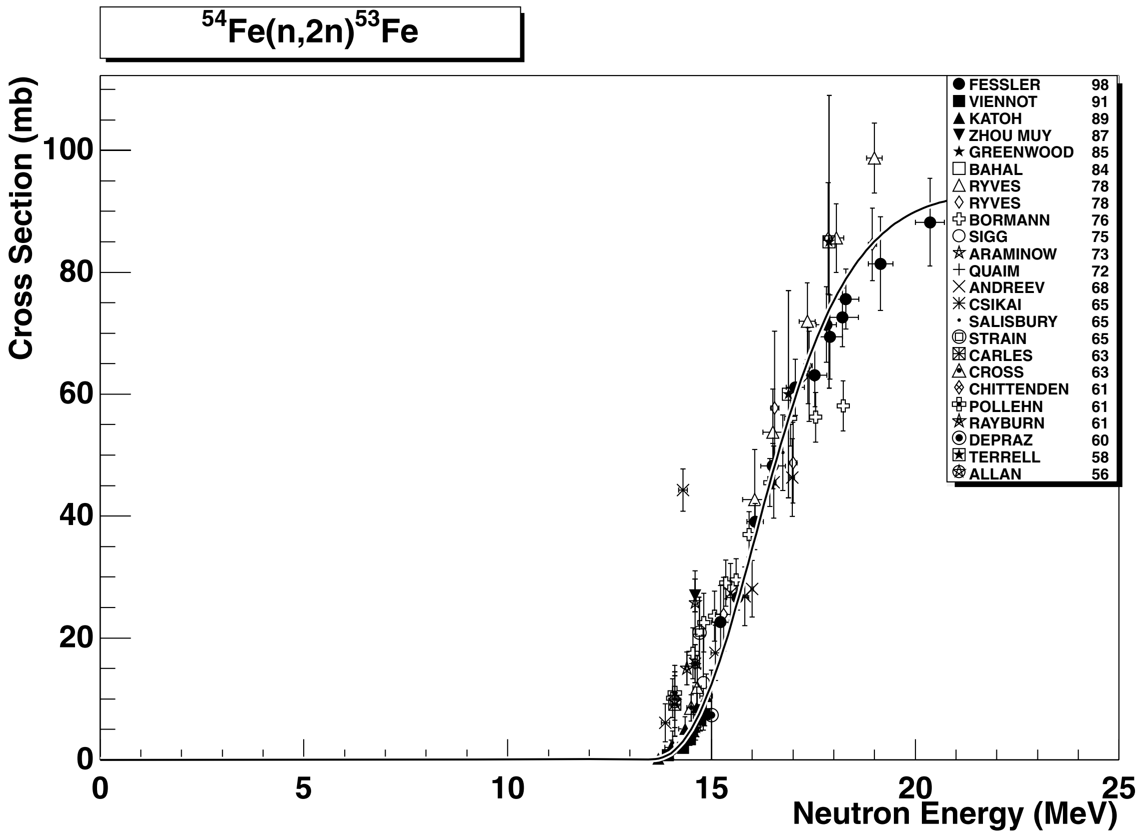

2.72. ^{54}Fe (n,2n) ^{53}Fe

final states: g.s., meta
source: RRDF-98

Experimental data plotted above were renormalized according to the new recommended standards and decay schemes which resulted in a very consistent set. The RRDF-98 evaluation reproduces this set very well.

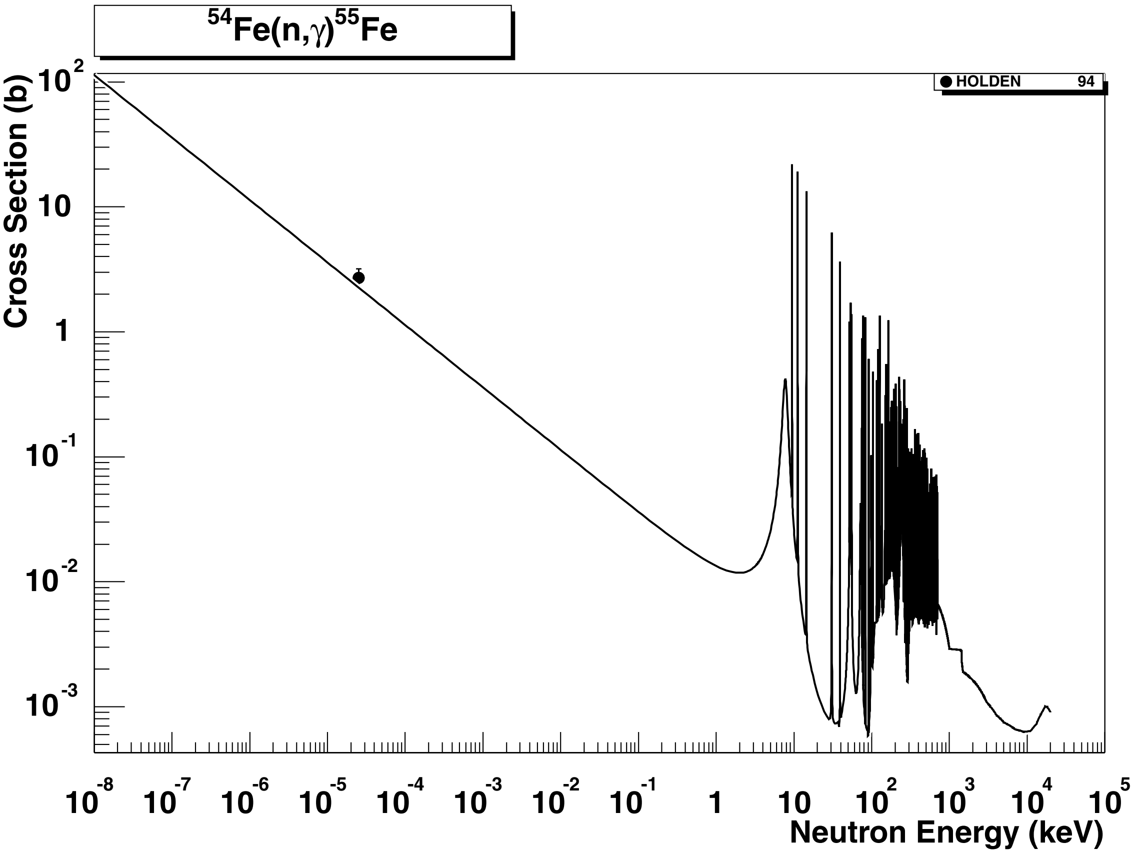

2.73. ^{54}Fe (n,γ) ^{55}Fe

final state: total
source: EAF-4.1 (ENDF/B-VI)

ENDF/B-VI evaluation includes the resolved resonance data. No EXFOR data are available outside the resonance region. The thermal cross-section of Holden94 [32] is reproduced with C/E=0.83.

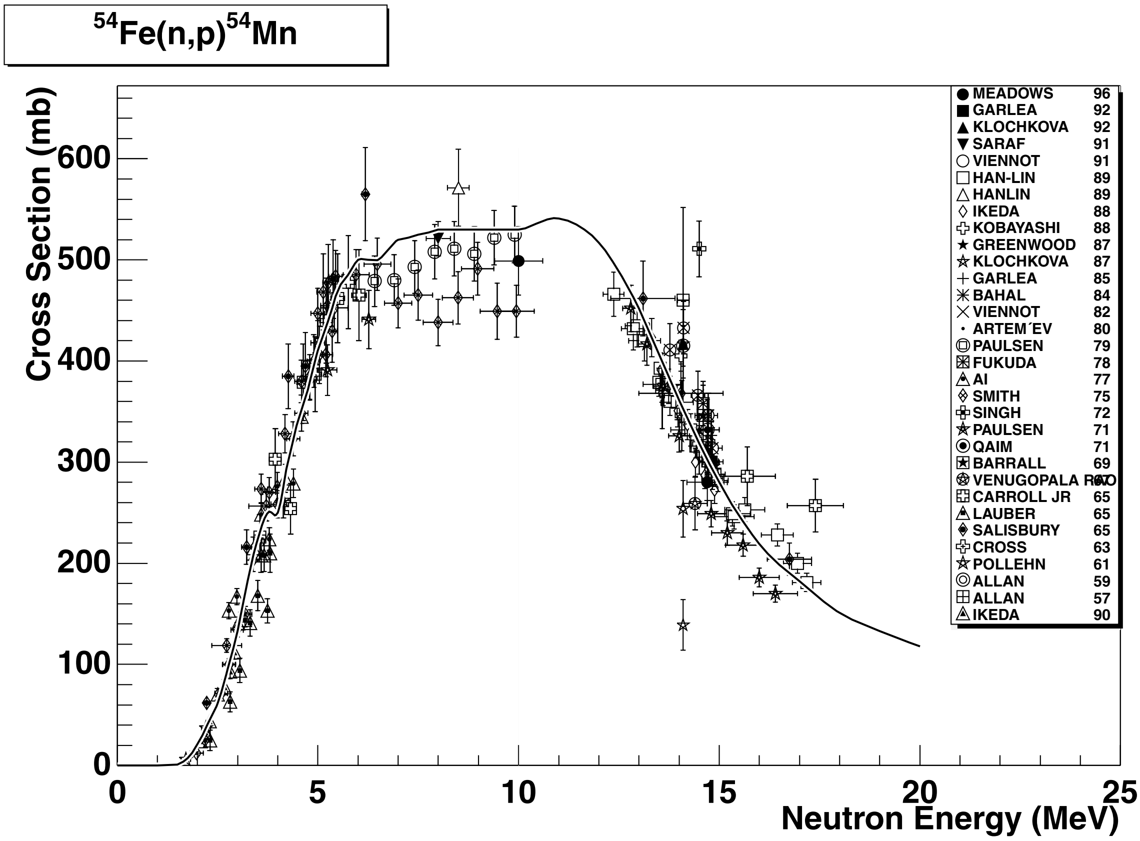

2.74. ^{54}Fe (n,p) ^{54}Mn

final state: total
source: JENDL-Act96

JENDL-Act96 evaluation reproduces the consistent data very well in the whole energy range.

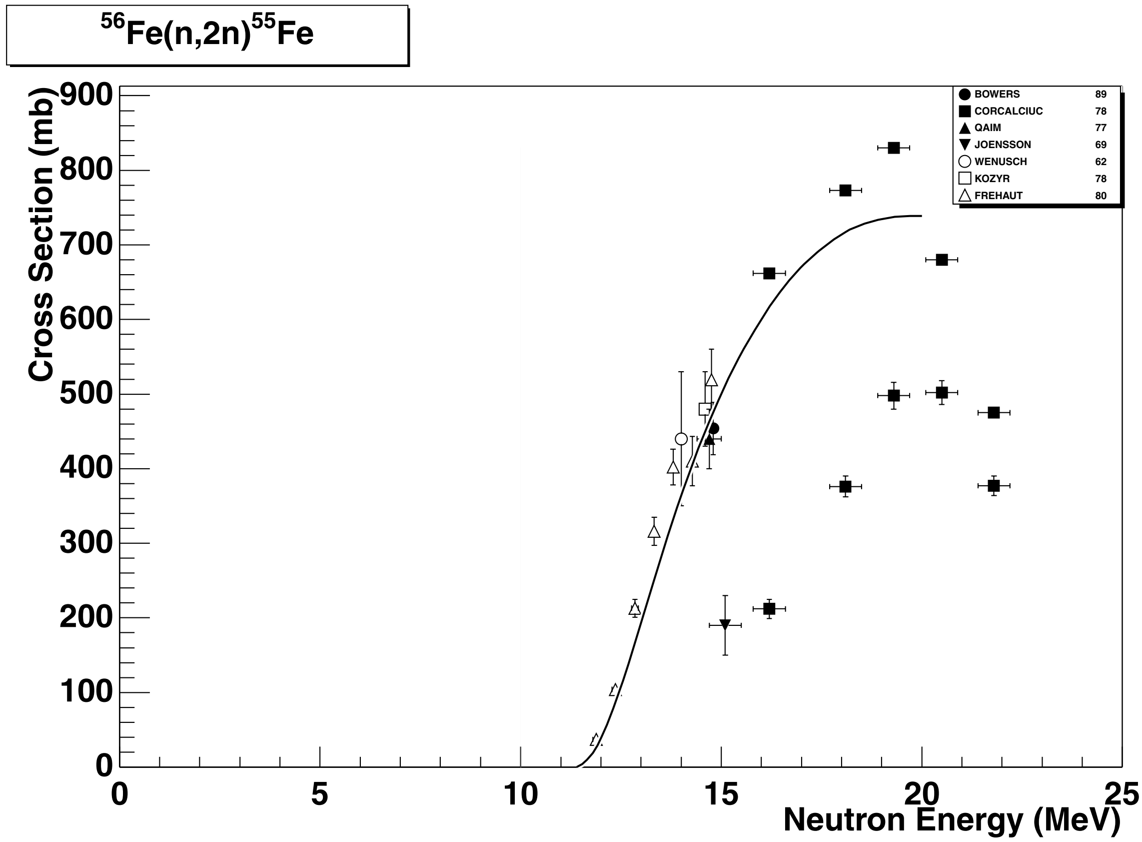

2.75. ^{56}Fe (n,2n) ^{55}Fe

final state: total
source: ADL-3

ADL-3 evaluation agrees reasonably with the data of Frehaut80 and Bowers89. The data of Corcalciuc78 above 15 MeV are a combination of calculations with partial data and may be disregarded.

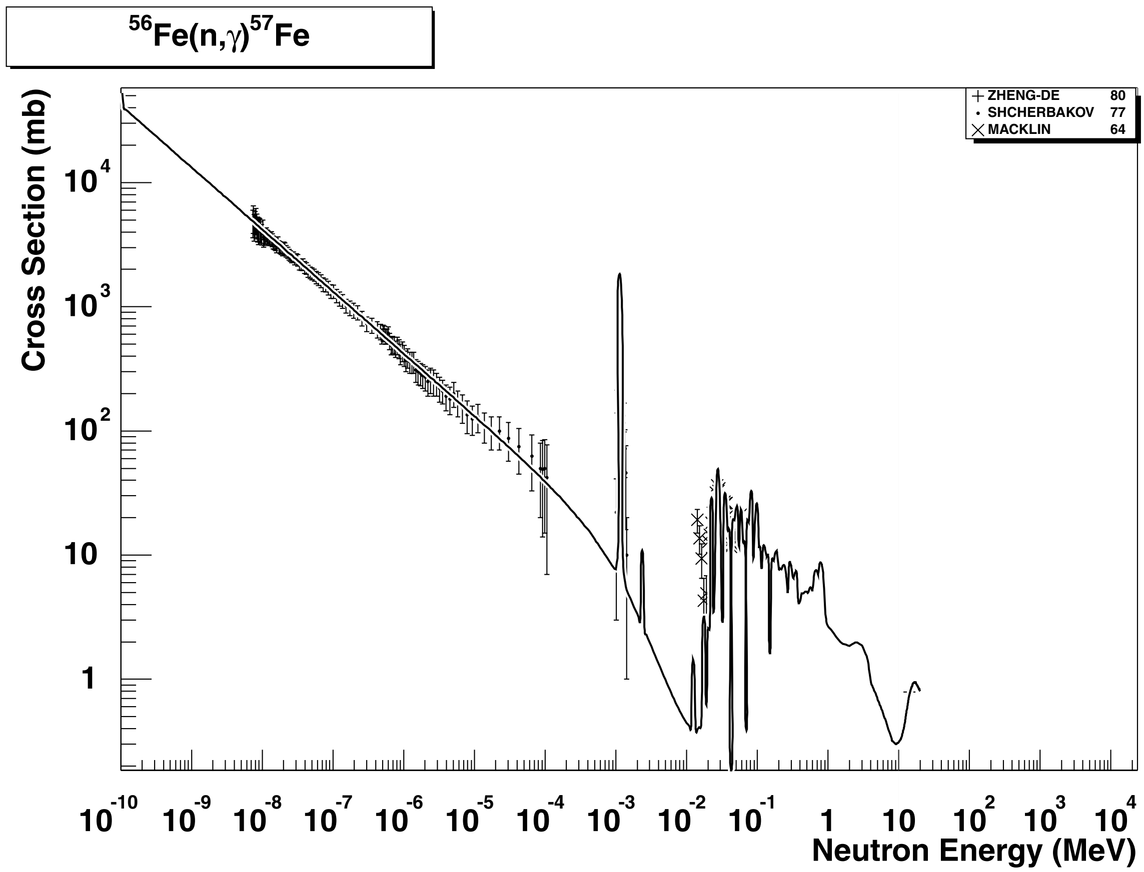

2.76. ^{56}Fe (n,γ) ^{57}Fe

final state: total
source: EAF-4.1 (ENDF/B-VI)

ENDF/B-VI evaluation reproduces well the experimental data in the whole energy range. Data are stored in SANDII group structure, the original ENDF/B-VI evaluation includes 41312 energy points.

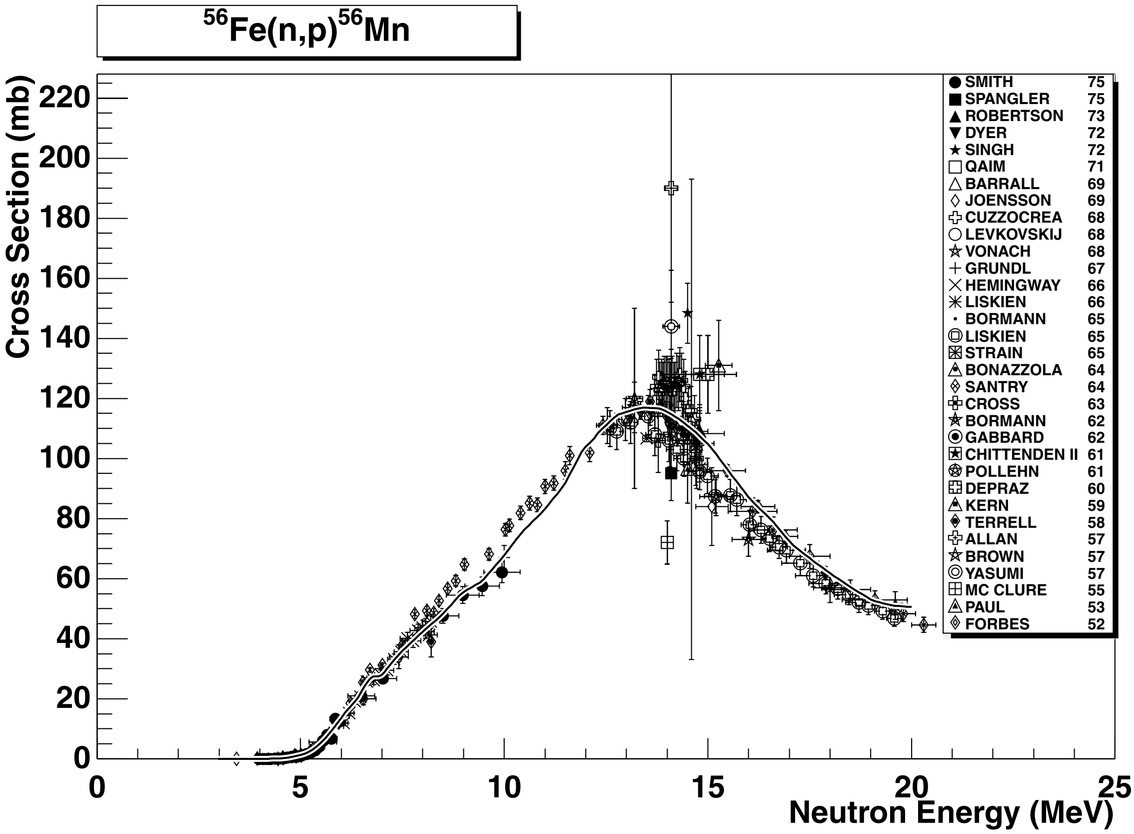

$^{56}Fe(n,p)^{56}Mn$
Cross Section (mb)
Neutron Energy (MeV)
0
20
40
60
80
100
120
140
160
180
200
220
0
5
10
15
20
25
SMITH 75
SPANGLER 75
ROBERTSON 73
DYER 72
SINGH 72
QAIM 71
BARRALL 69
JOENSSON 69
CUZZOCREA 68
LEVKOVSKIJ 68
VONACH 68
GRUNDL 67
HEMINGWAY 66
LISKIEN 66
BORMANN 65
LISKIEN 65
STRAIN 65
BONAZZOLA 64
SANTRY 64
CROSS 63
BORMANN 62
GABBARD 62
CHITTENDEN II 61
POLLEHN 61
DEPRAZ 60
KERN 59
TERRELL 58
ALLAN 57
BROWN 57
YASUMI 57
MC CLURE 55
PAUL 53
FORBES 52

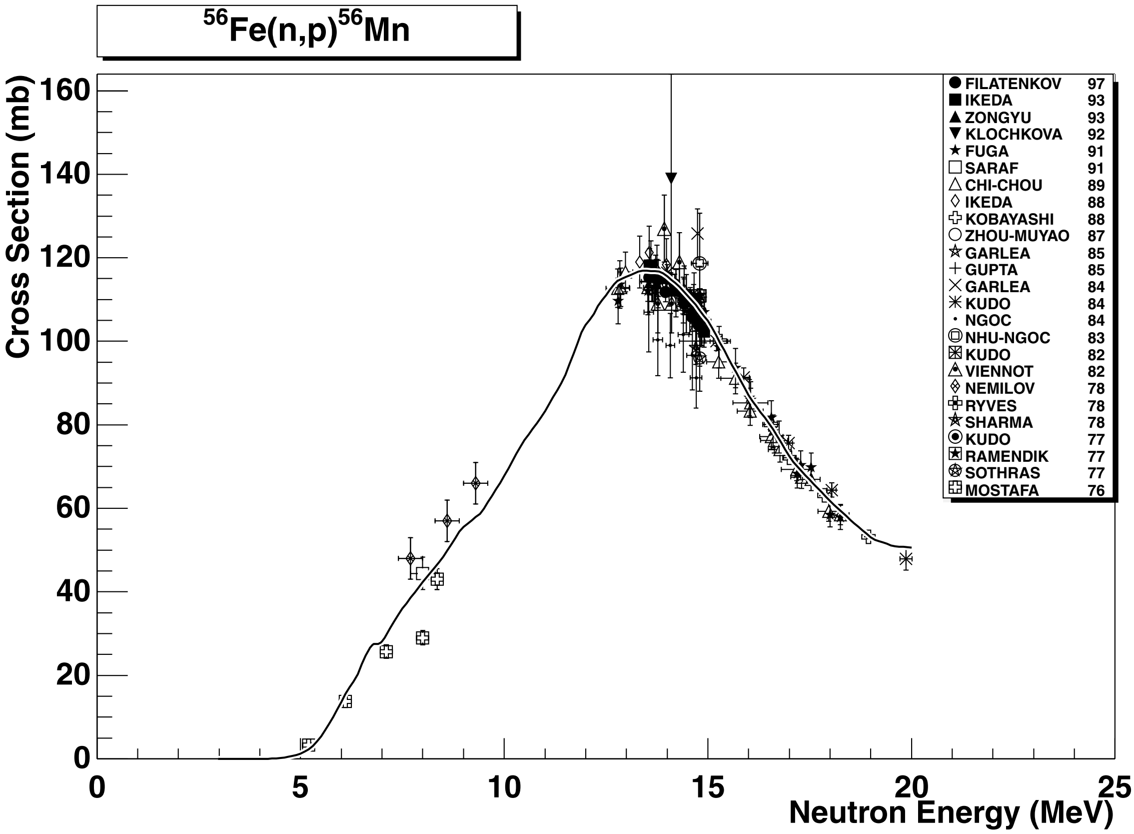

2.77. ^{56}Fe (n,p) ^{56}Mn

final state: total
source: EAF-4.1 (IRDF-90.2)

An excellent agreement of the IRDF-90.2 evaluation with all experimental data.

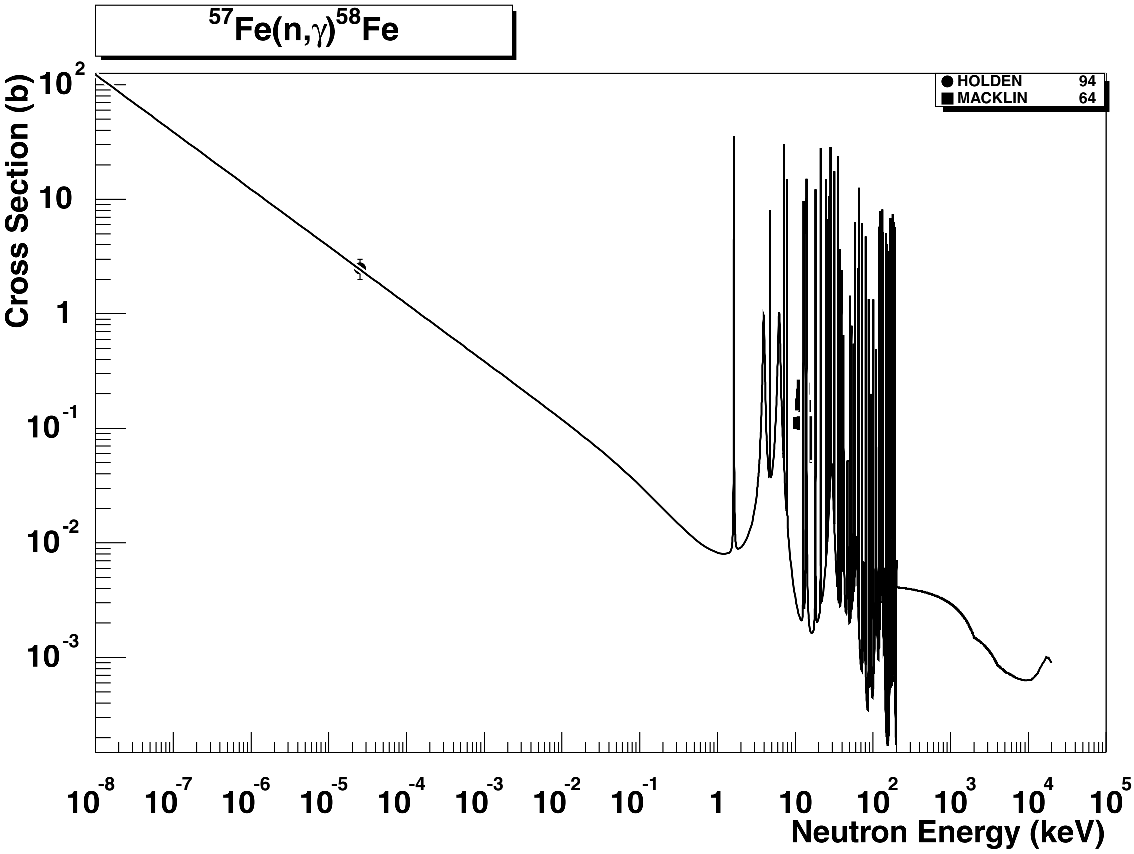

2.78. ^{57}Fe (n,γ) ^{58}Fe

final state: total
source: EAF-4.1 (ENDF/B-VI)

Experimental data are rather scarce, only a few points are available in the resolved resonance region. The thermal cross-section of Holden94 [32] is reproduced with C/E=0.98.

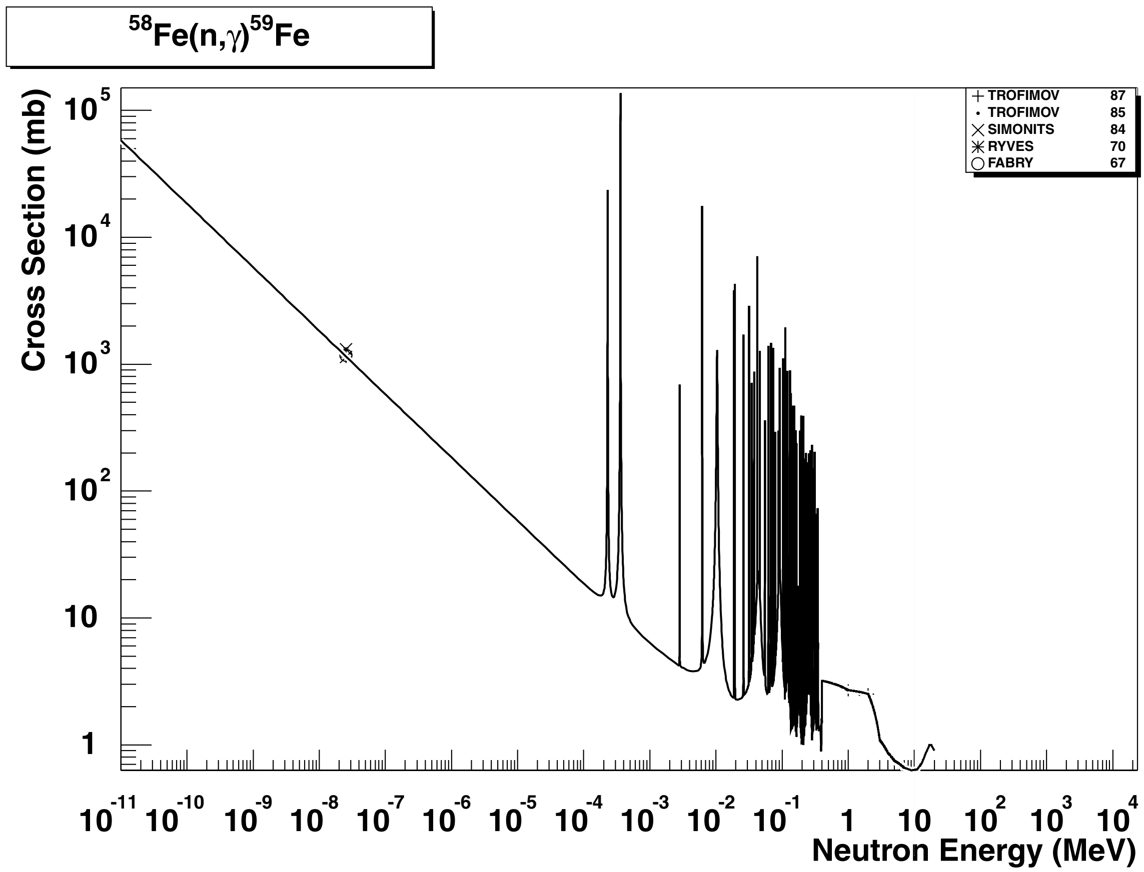

2.79. ^{58}Fe (n,γ) ^{59}Fe

final state: total
source: EAF-4.1 (ENDF/B-VI)

ENDF/B-VI is in good agreement with experimental data, both in the thermal region and in the smooth statistical region around 1 MeV (Trofimov85,87).

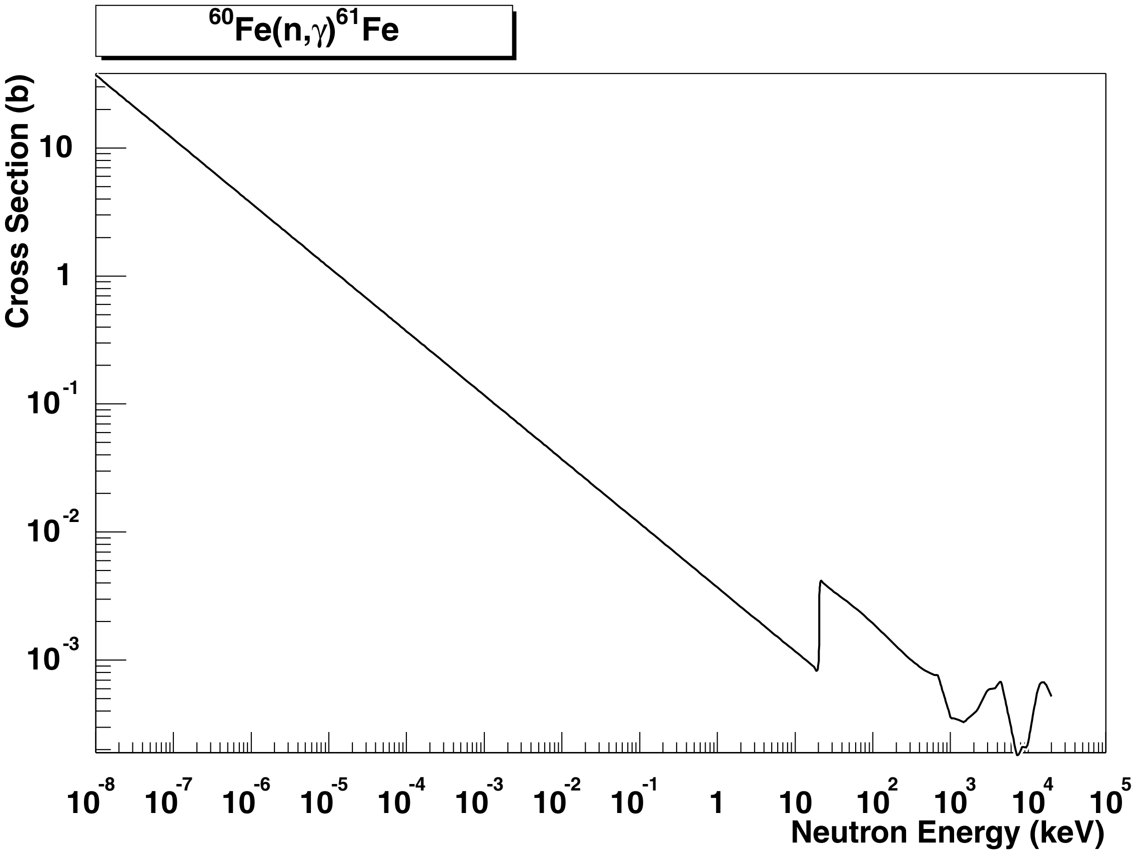

2.80. ^{60}Fe (n,γ) ^{61}Fe

final state: total
source: EAF-4.1

No experimental data are available. The evaluated data are based on the simplified model calculations with the code MASGAM with global parameters (Hauser-Feshbach and DSD model with no resonance region generation, E_H is based on a $D_0/2$ estimate; for details see Ref. [35]).

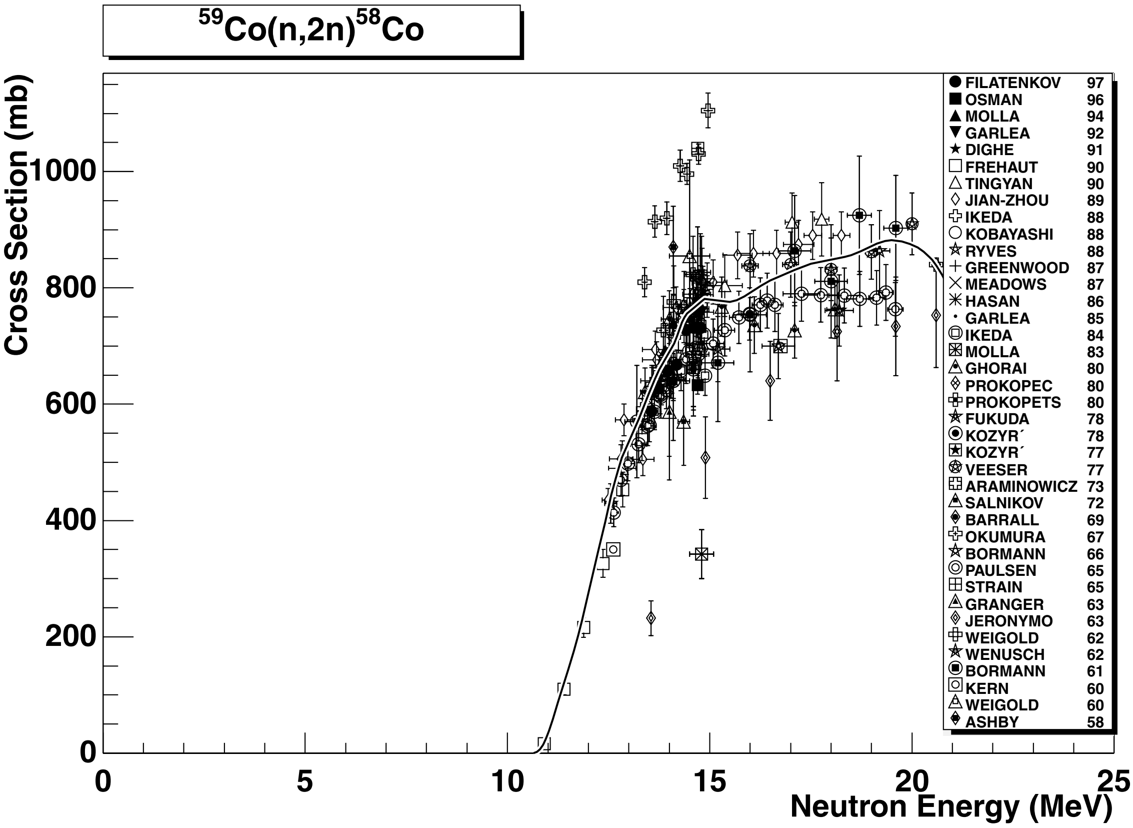

2.81. ^{59}Co (n,2n) ^{58}Co

final state: total
source: IRDF-90.2 (pointwise)

IRDF-90.2 agrees well with the experimental data below 15 MeV and runs through the data up to 20 MeV. Data set Ikeda88 is wrong and can be disregarded.

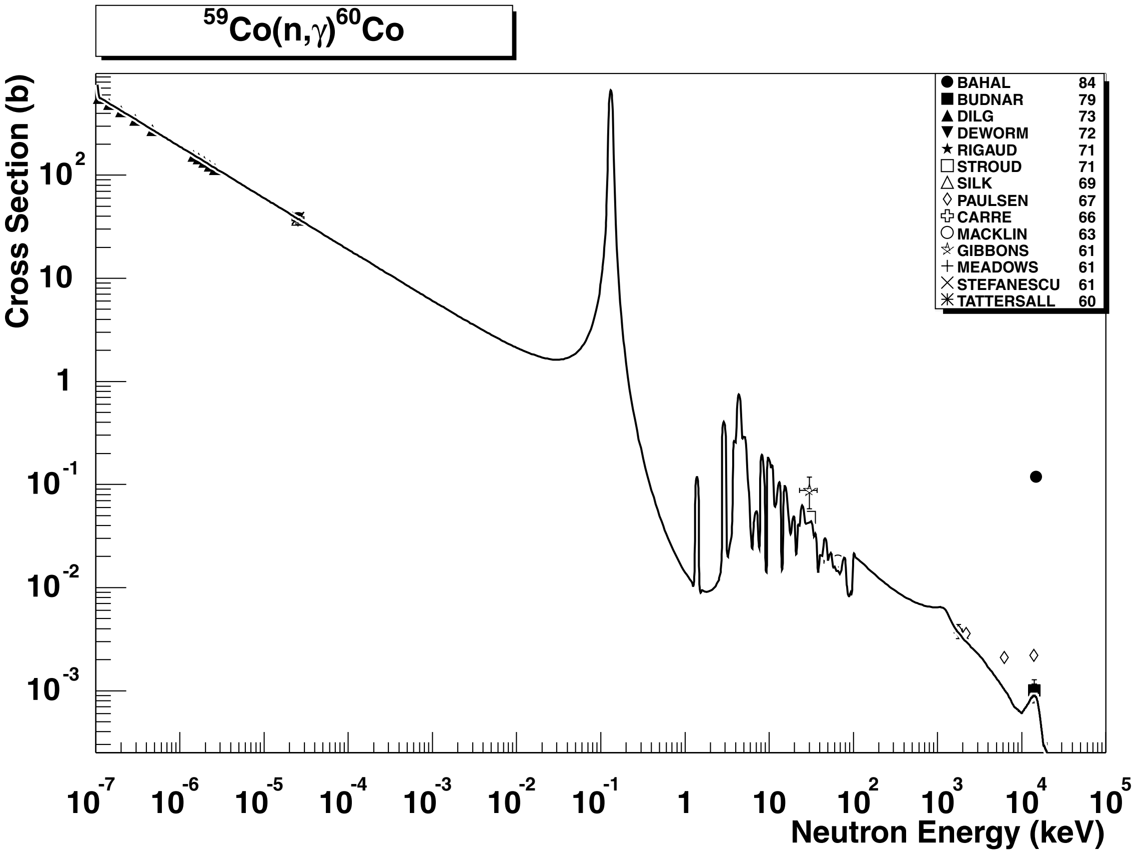

2.82. ^{59}Co (n,γ) ^{60}Co

final state: g.s., meta
source: EAF-4.1 (JEF-2.2)

ENDF/B-VI data are adopted in JEF-2.2. The evaluation agrees well with the data in the 1/v region and is in reasonable agreement to the a scattered data around 10 keV and above 1 MeV. The 14 MeV data point of Bahal84 is ignored.

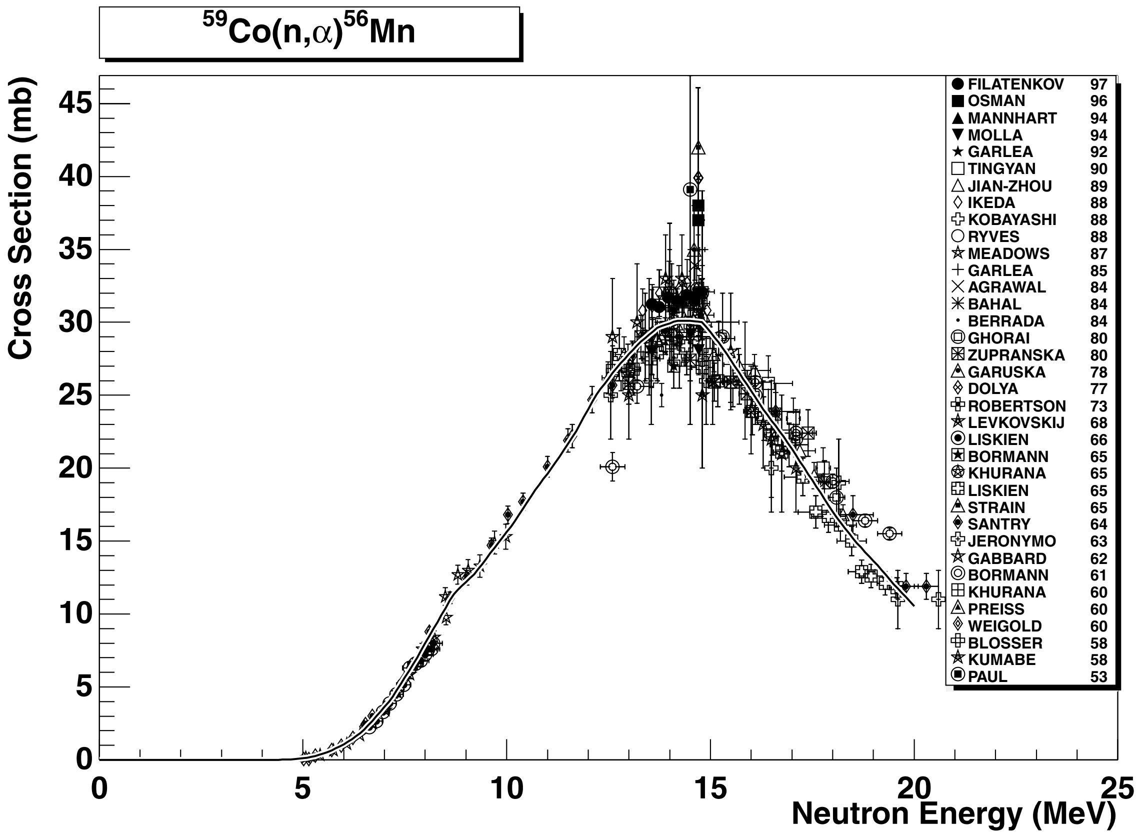

2.83. ^{59}Co (n,α) ^{56}Mn

final state: total
source: EAF-4.1 (IRDF-90.2)

IRDF-90.2 runs through a very consistent set of experimental data in an excellent way.

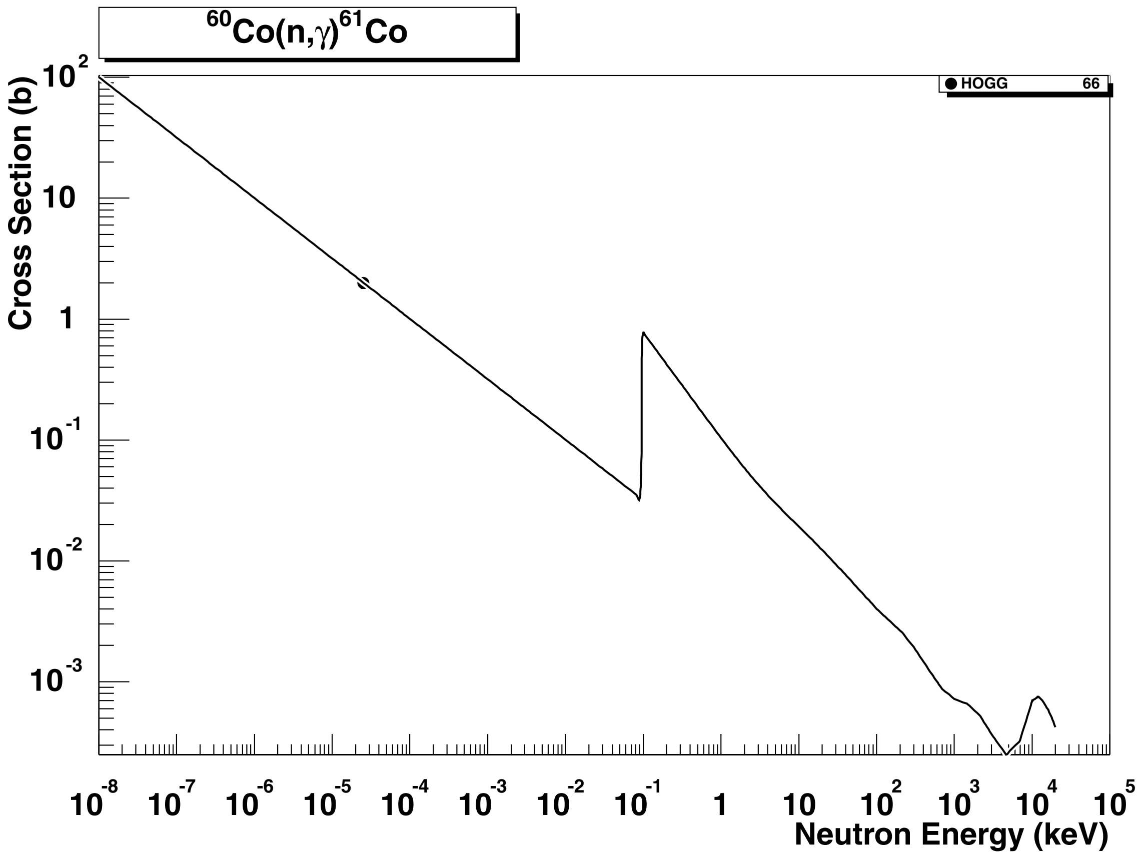

2.84. ^{60}Co (n,γ) ^{61}Co

final state: total
source: EAF-4.1

Data are based on the simplified model calculations with the code MASGAM (Hauser-Feshbach and DSD model with no resonance region generation, E_H is based on $D_0/2$ estimate; for details see Ref. [35]). The 1/v component is adjusted to the experimental value of (2.0 +- 0.2) b [32].

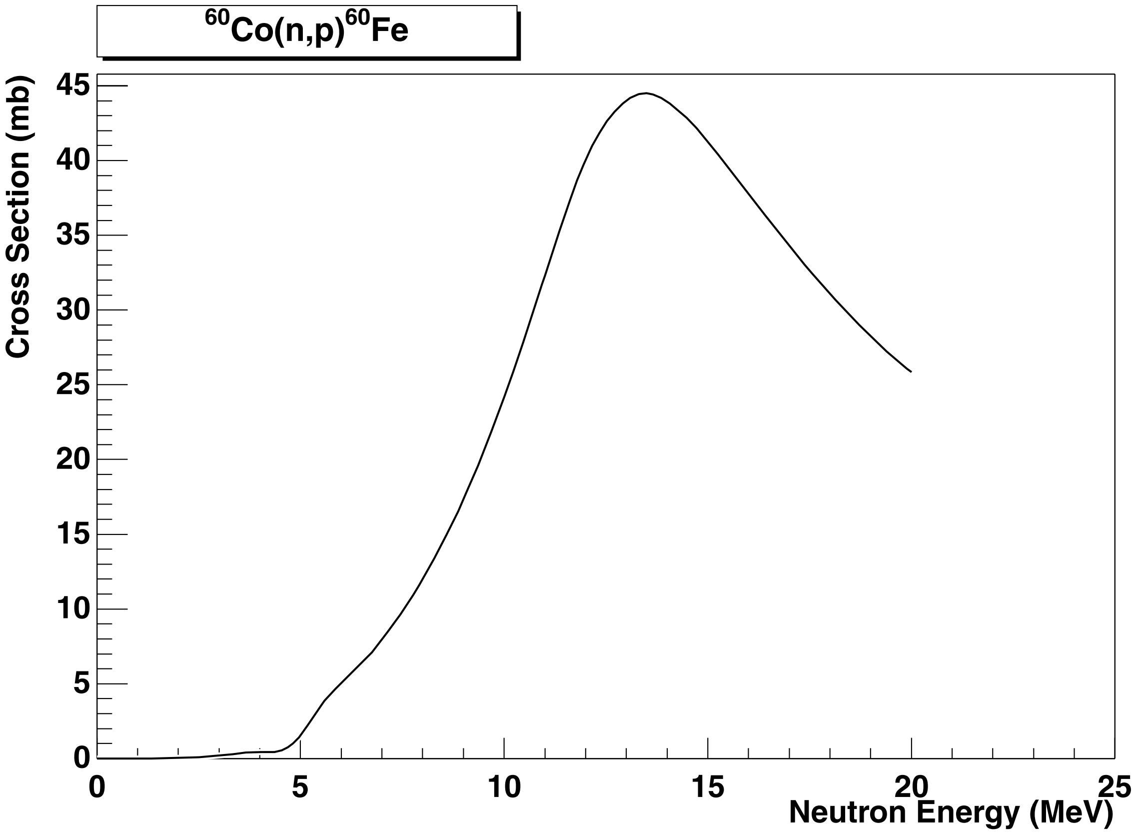

2.85. ^{60}Co (n,p) ^{60}Fe

final state: total
source: ADL-3

No experimental data in EXFOR, the ADL-3 evaluation adopted.

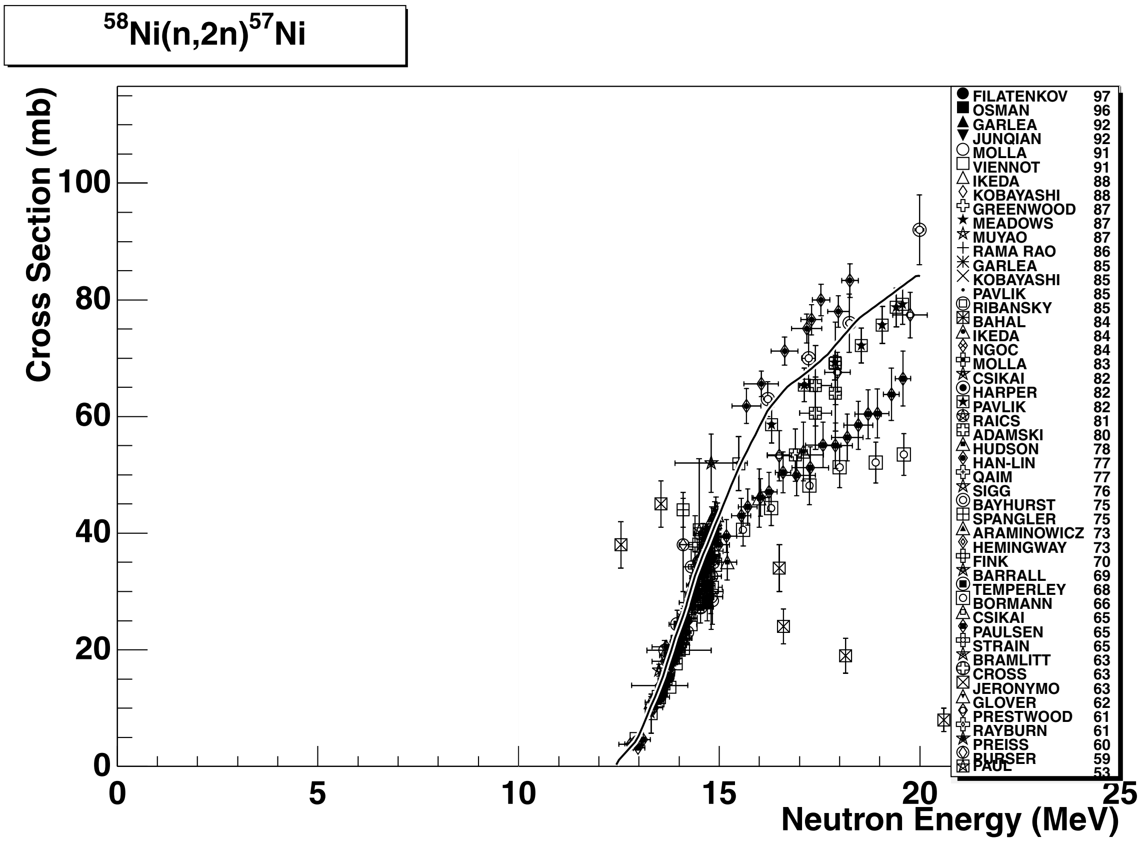

2.86. ^{58}Ni (n,2n) ^{57}Ni

final state: total
source: EAF-4.1 (IRDF-90.2)

IRDF-90.2 reproduces well the data below 15 MeV and slightly overestimates the data of Pavlik82 above 16 MeV.

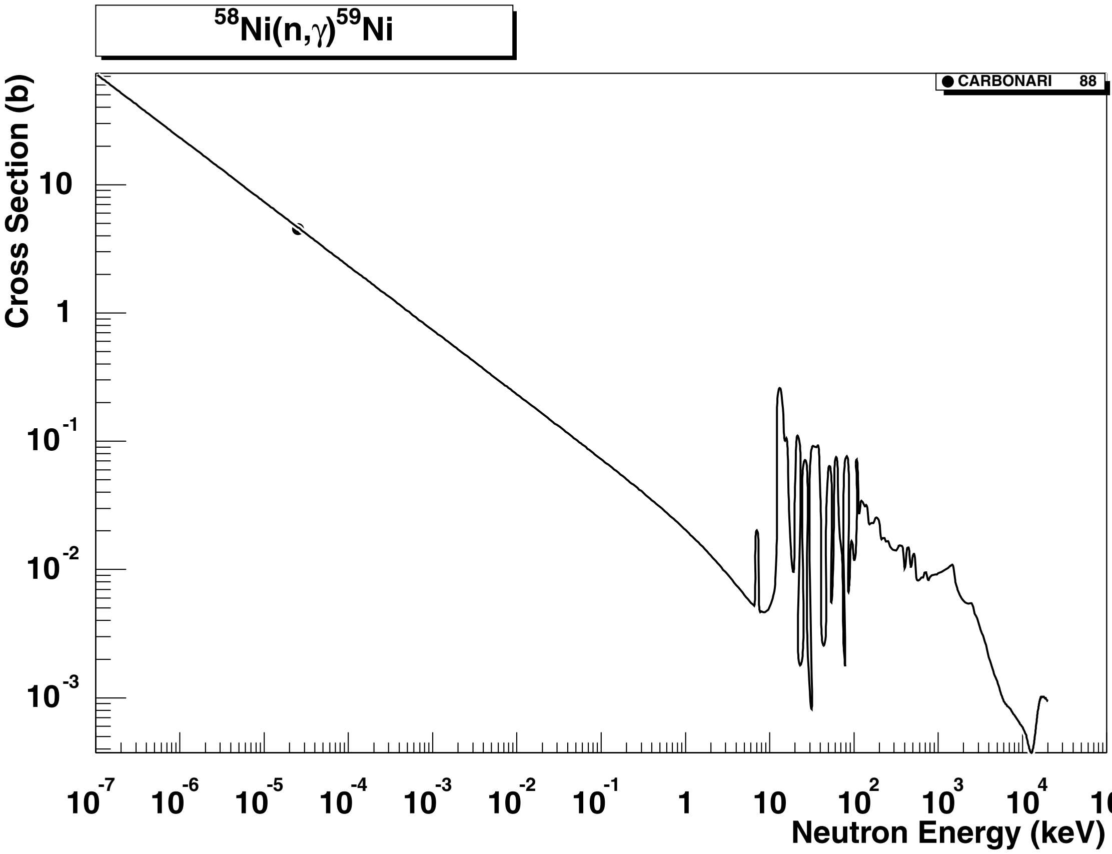

2.87. ^{58}Ni (n,γ) ^{59}Ni

final state: total
source: EAF-4.1 (EFF-2.4)

EFF-2.4 evaluation reproduces well the thermal cross-section of Carbonari88. No other EXFOR data are available outside the resonance region. Data are stored in SANDII group structure, the original evaluation includes 69138 energy points.

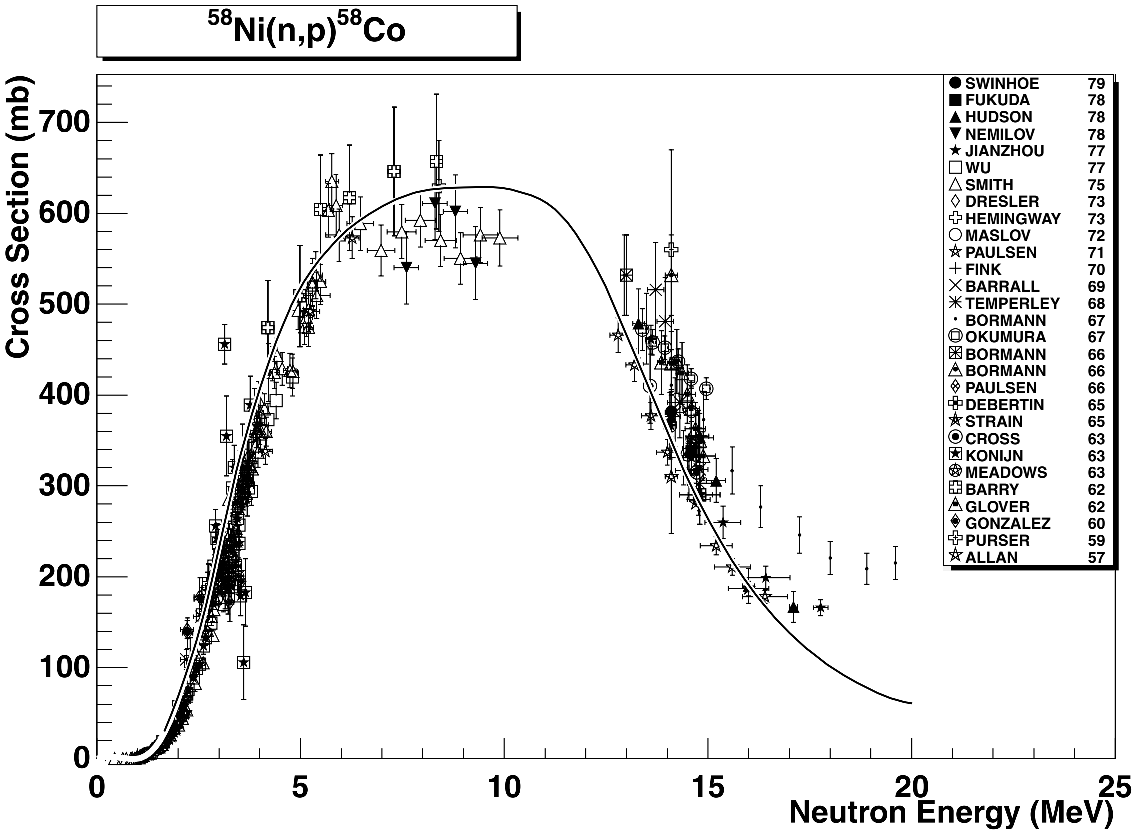

^{58}Ni(n,p)^{58}Co
Cross Section (mb)
Neutron Energy (MeV)
0
100
200
300
400
500
600
700
0
5
10
15
20
25
SWINHOE 79
FUKUDA 78
HUDSON 78
NEMILOV 78
JIANZHOU 77
WU 77
SMITH 75
DRESLER 73
HEMINGWAY 73
MASLOV 72
PAULSEN 71
FINK 70
BARRALL 69
TEMPERLEY 68
BORMANN 67
OKUMURA 67
BORMANN 66
BORMANN 66
PAULSEN 66
DEBERTIN 65
STRAIN 65
CROSS 63
KONIJN 63
MEADOWS 63
BARRY 62
GLOVER 62
GONZALEZ 60
PURSER 59
ALLAN 57

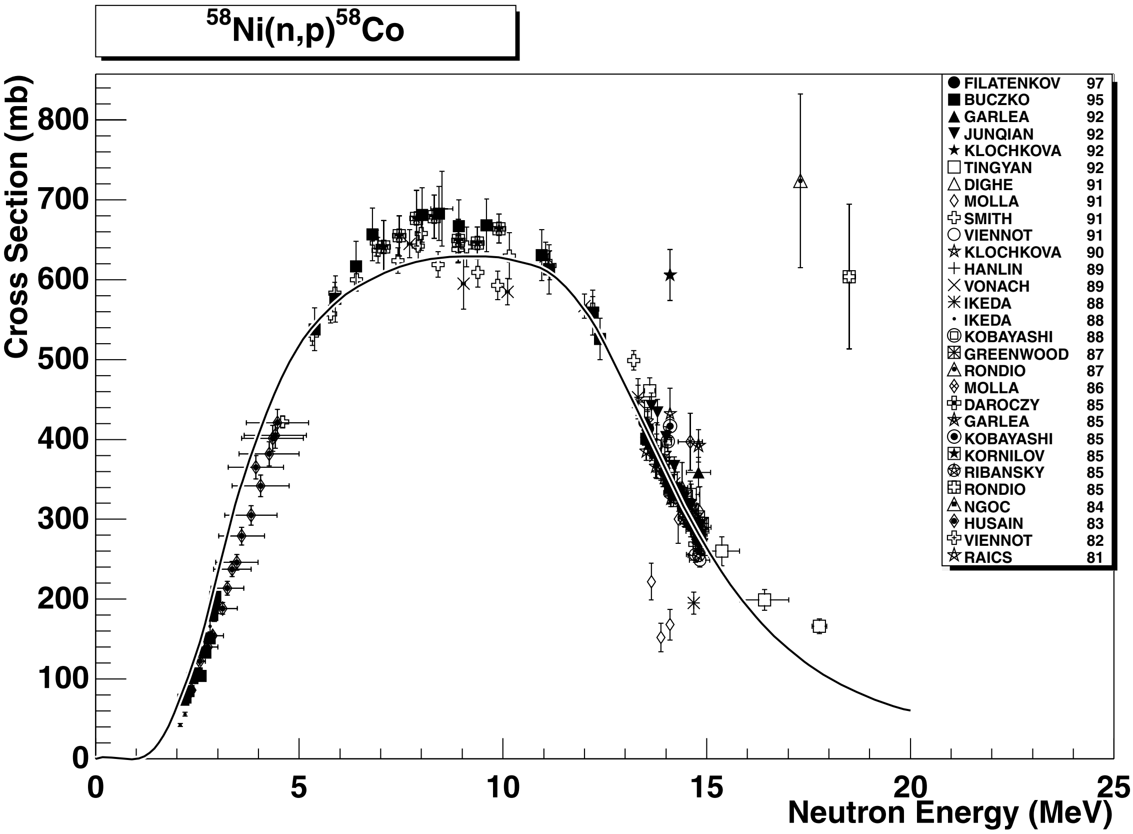

2.88. ^{58}Ni (n,p) ^{58}Co

final state: total
source: IPPE

The IPPE evaluation [12] reproduces very well all consistent experimental data. The remaining discrepant results can be disregarded.

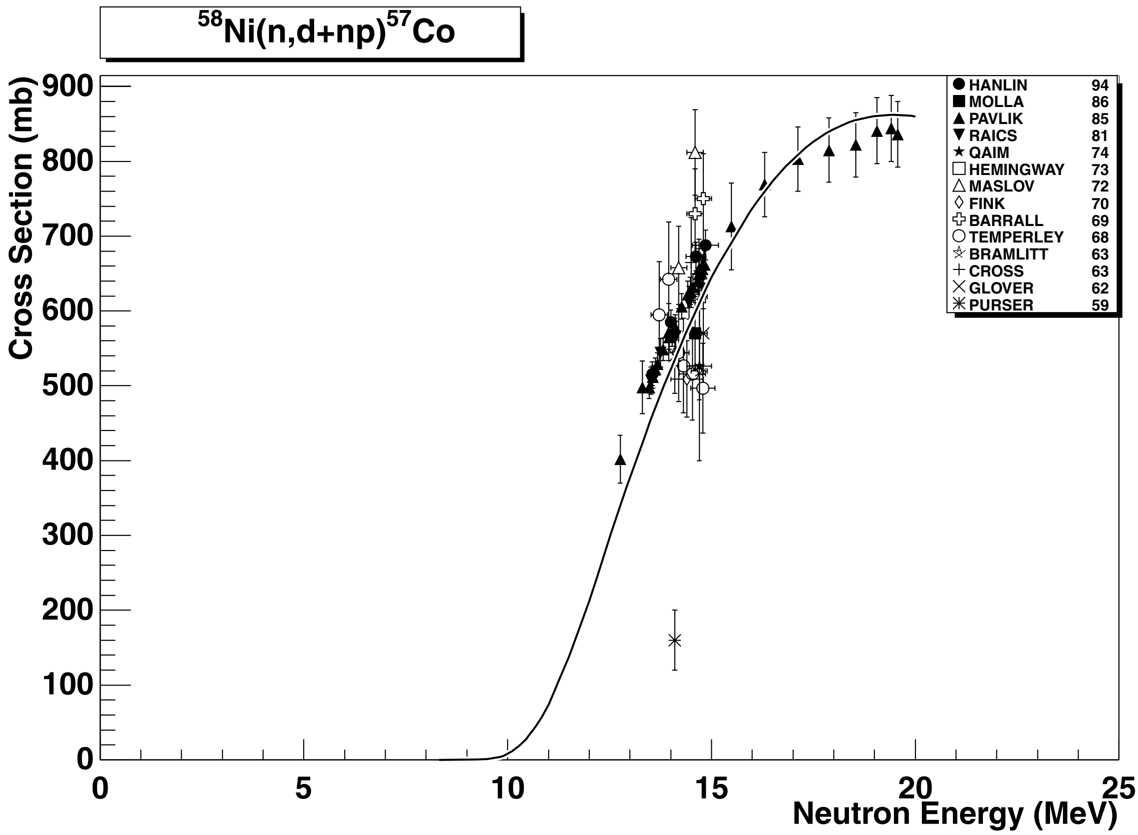

2.89. ^{58}Ni (n,d+np) ^{57}Co

final state: total
source: EAF-4.1 (JEF-2.2)

The combined JEF-2.2 and EFF-2.4 evaluation is plotted against (n,d+np) data. The agreement with the experimental data is very good. The data are stored separately as (n,d) and (n,np) reaction channels, adopted from JEF-2.2 and EFF-2.4, respectively.

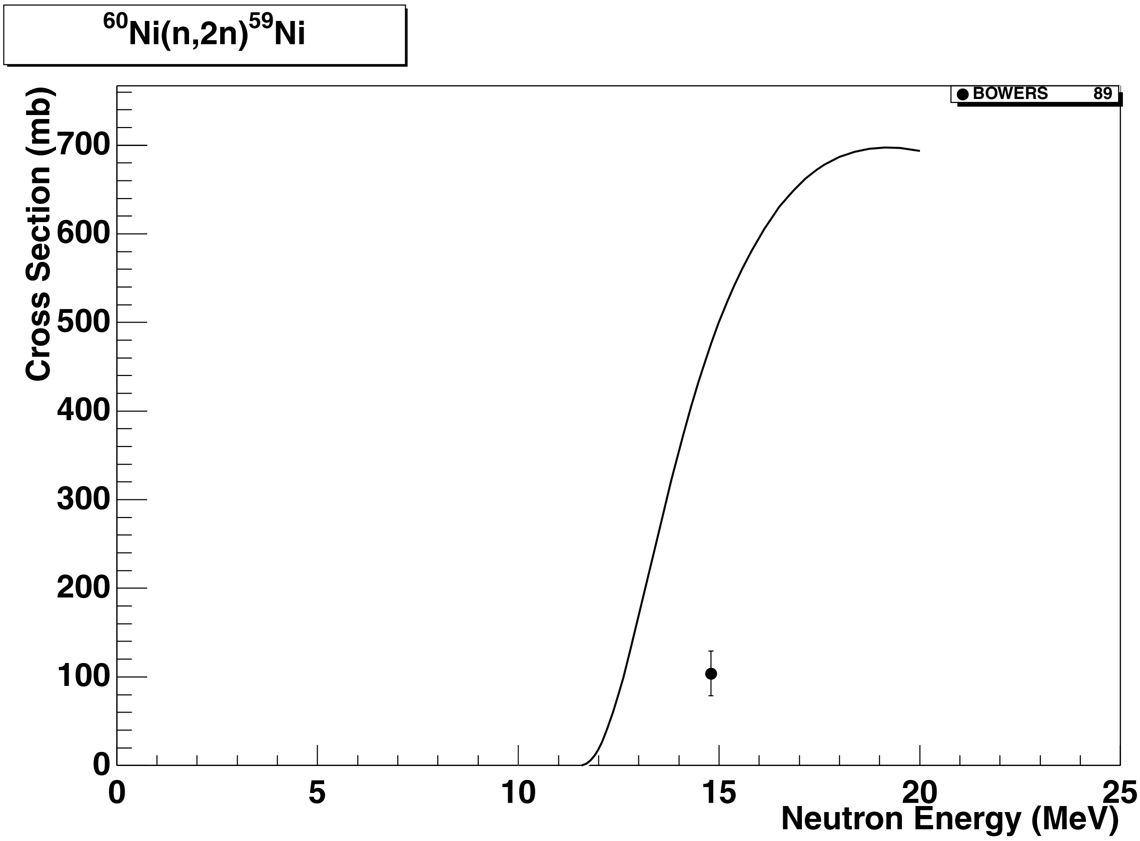

2.90. ^{60}Ni (n,2n) ^{59}Ni

final state: total
source: ADL-3

The single experimental point (at about 15 MeV) extracted from EXFOR is wrong. It is considerably smaller than values of (311 +- 55) mb and (309 +- 83) mb from references [37] and [38], respectively. These values are reasonably reproduced by the adopted ADL-3 evaluation.

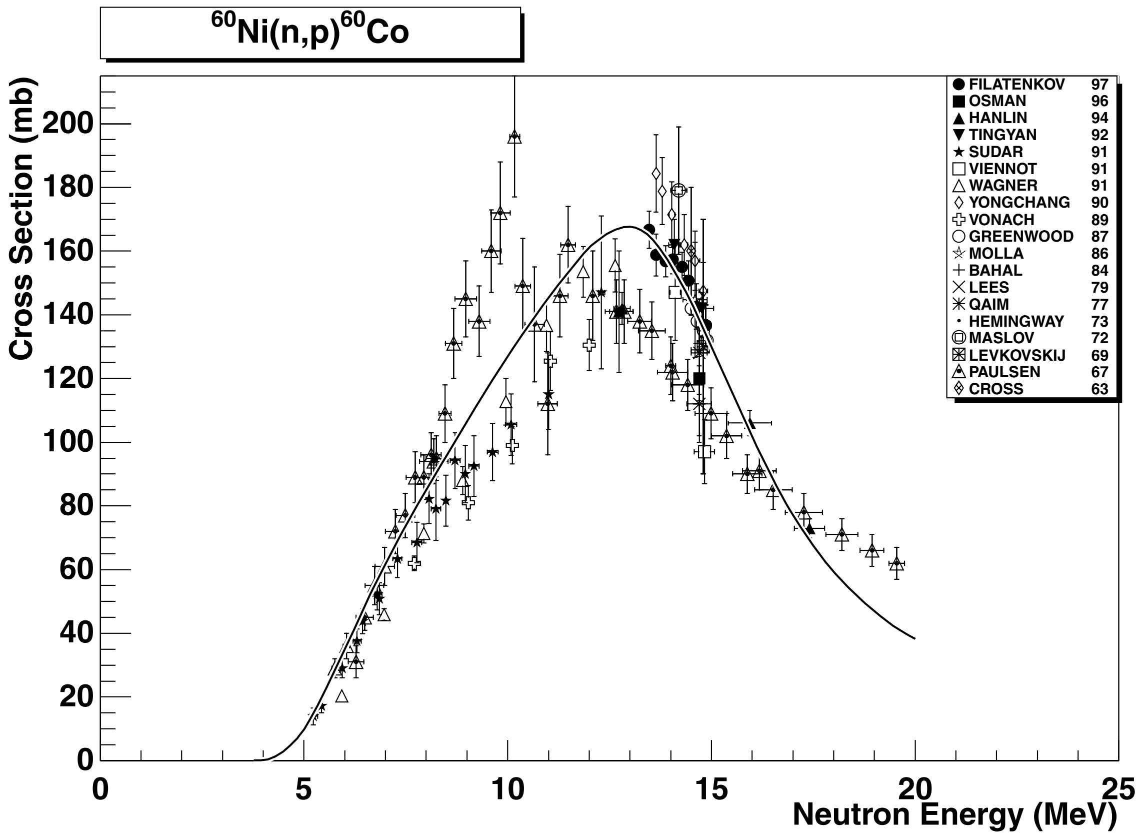

2.91. ^{60}Ni (n,p) ^{60}Co

final states: g.s., meta
source: ADL-3

ADL-3 runs in the middle of the experimental data, fitting well the very recent experiment of Filatenkov97 between in the 13-15 MeV range. The branching ratio between the g.s. and meta state is based on model calculations.

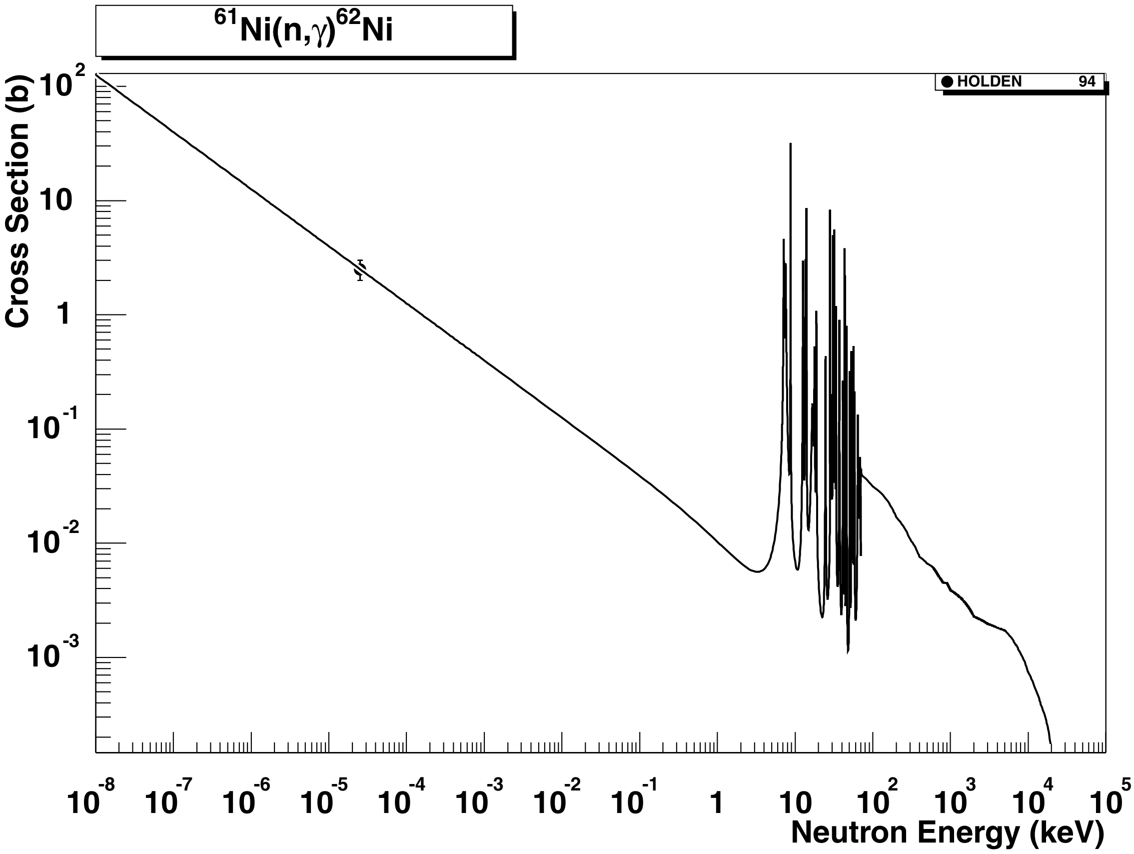

2.92. ^{61}Ni (n,γ) ^{62}Ni

final state: total
source: EAF-4.1 (EFF-2.4)

ENDF/B-VI was chosen for EFF-2.4. No EXFOR data are available outside the resonance region. The thermal cross-section of Holden94 [32] is reproduced with C/E=1.00.

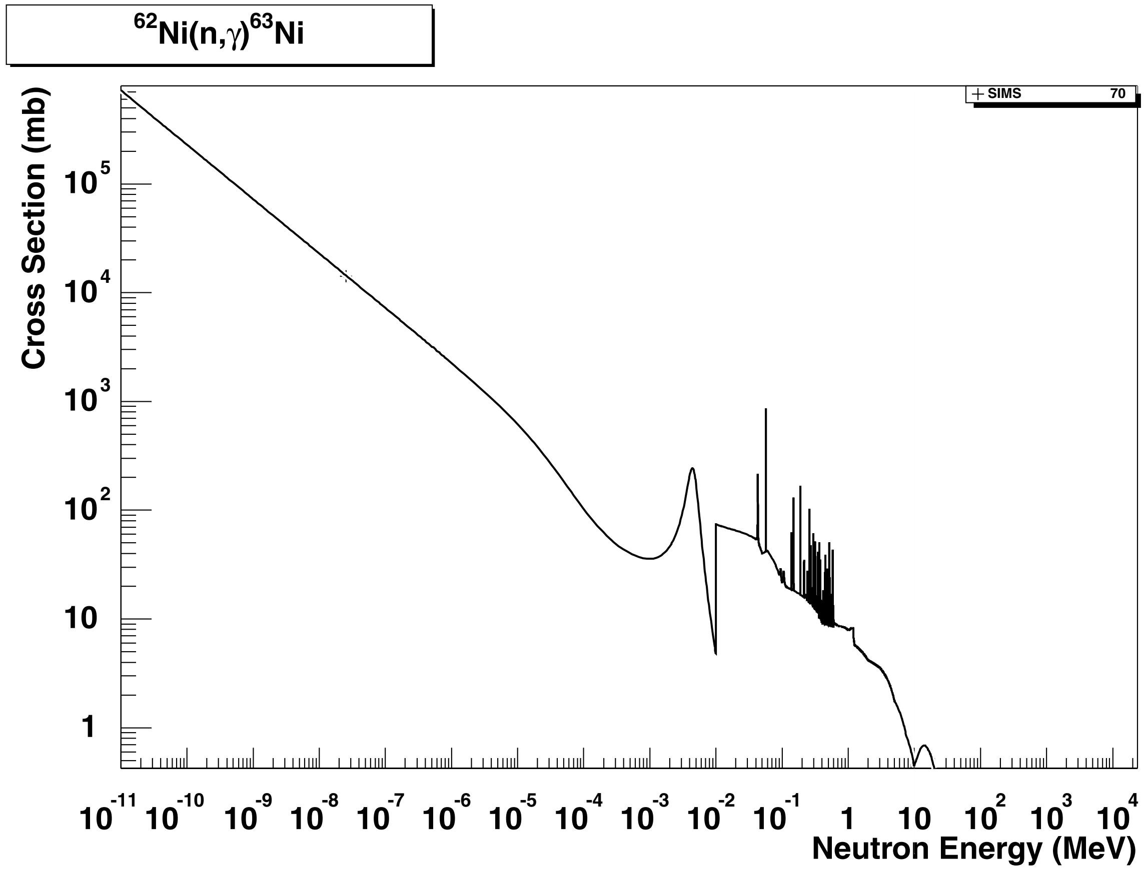

2.93. ^{62}Ni (n,γ) ^{63}Ni

final state: total
source: EAF-4.1 (EFF-2.4)

ENDF/B-VI was chosen for EFF-2.4. The only experimental point of Sims70 at 0.0253 eV is well reproduced.

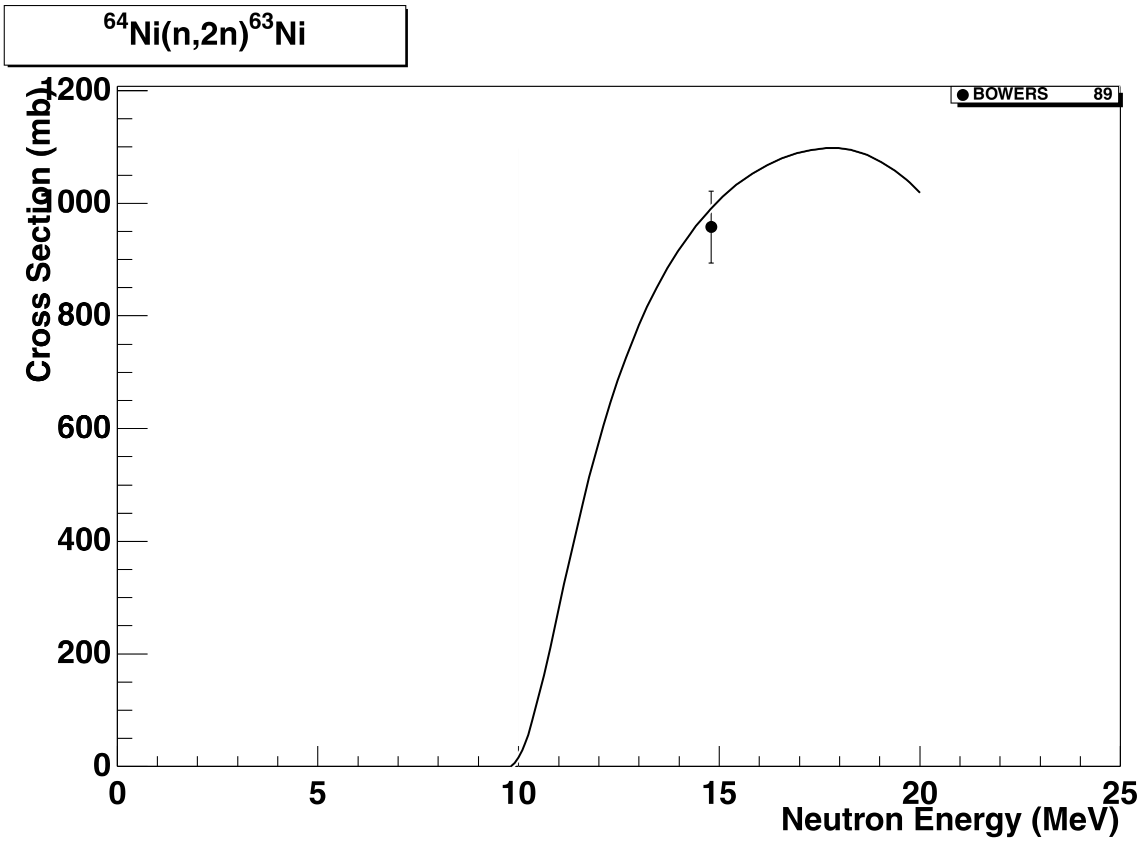

2.94. ^{64}Ni (n,2n) ^{63}Ni

final state: total
source: ADL-3

ADL-3 is close to the single experimental point of Bowers89 around 15 MeV.

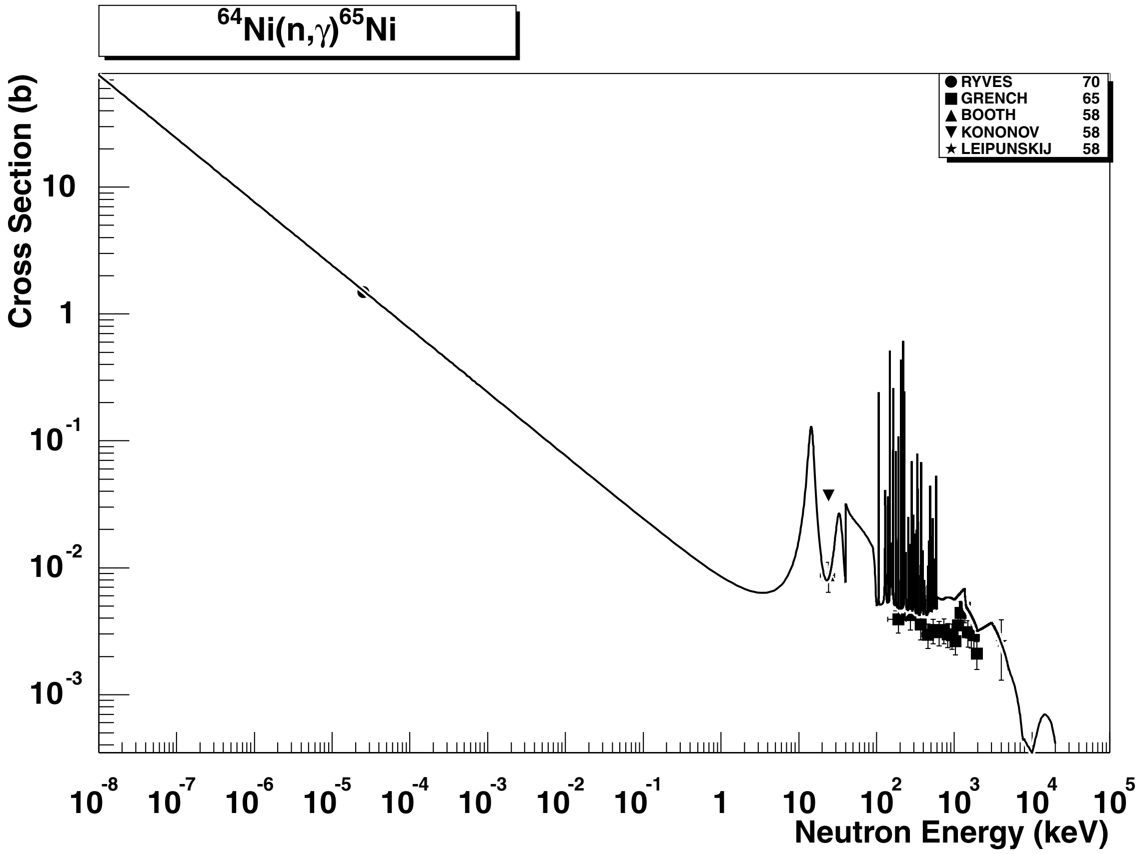

2.95. ^{64}Ni (n,γ) ^{65}Ni

final state: total
source: EAF-4.1 (EFF-2.4)

ENDF/B-VI was adopted for EFF-2.4. The experimental point of Ryves70 at 0.0253 eV is well reproduced. The smooth statistical component above 50 keV slightly overestimates the averaged data of Greench65.

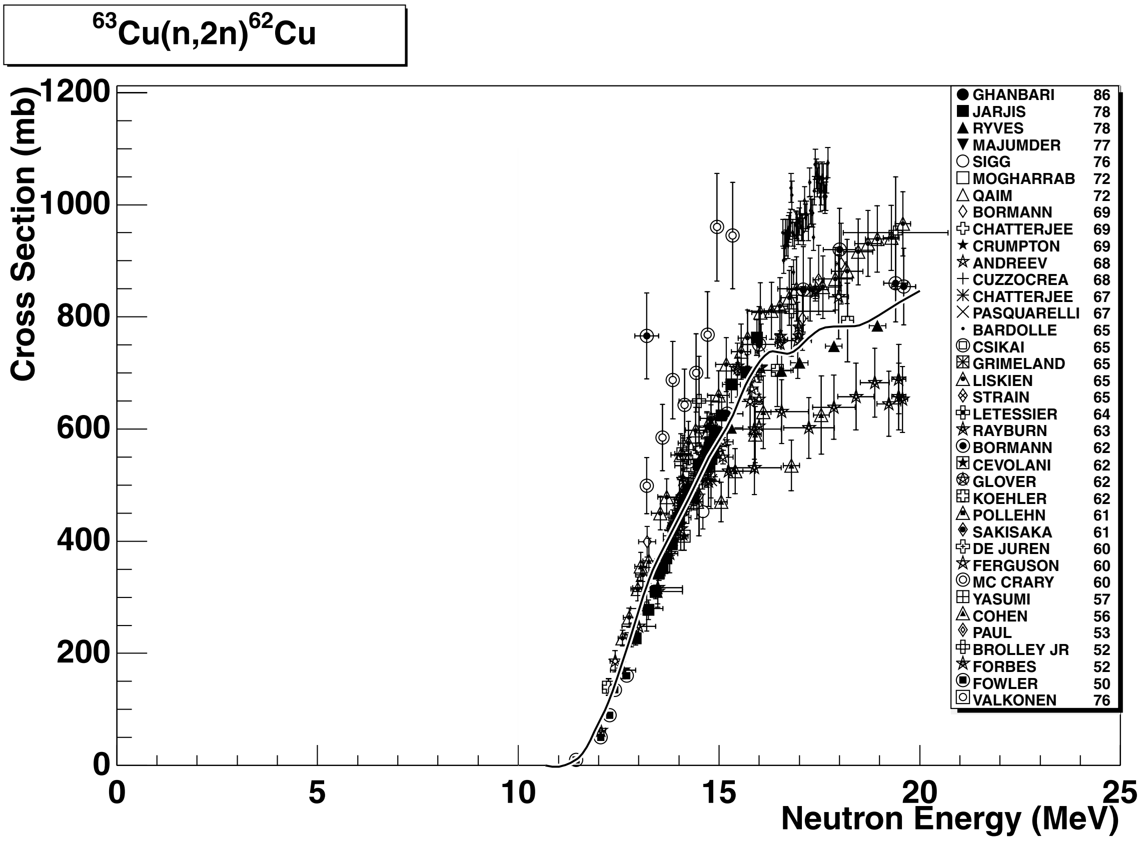

2.96. ^{63}Cu (n,2n) ^{62}Cu

final state: total
source: EAF-4.1 (IRDF-90.2)

IRDF-90.2 fits well the data below 15 MeV and runs in the middle of the data above 15 MeV (close to the data of Ryves78).

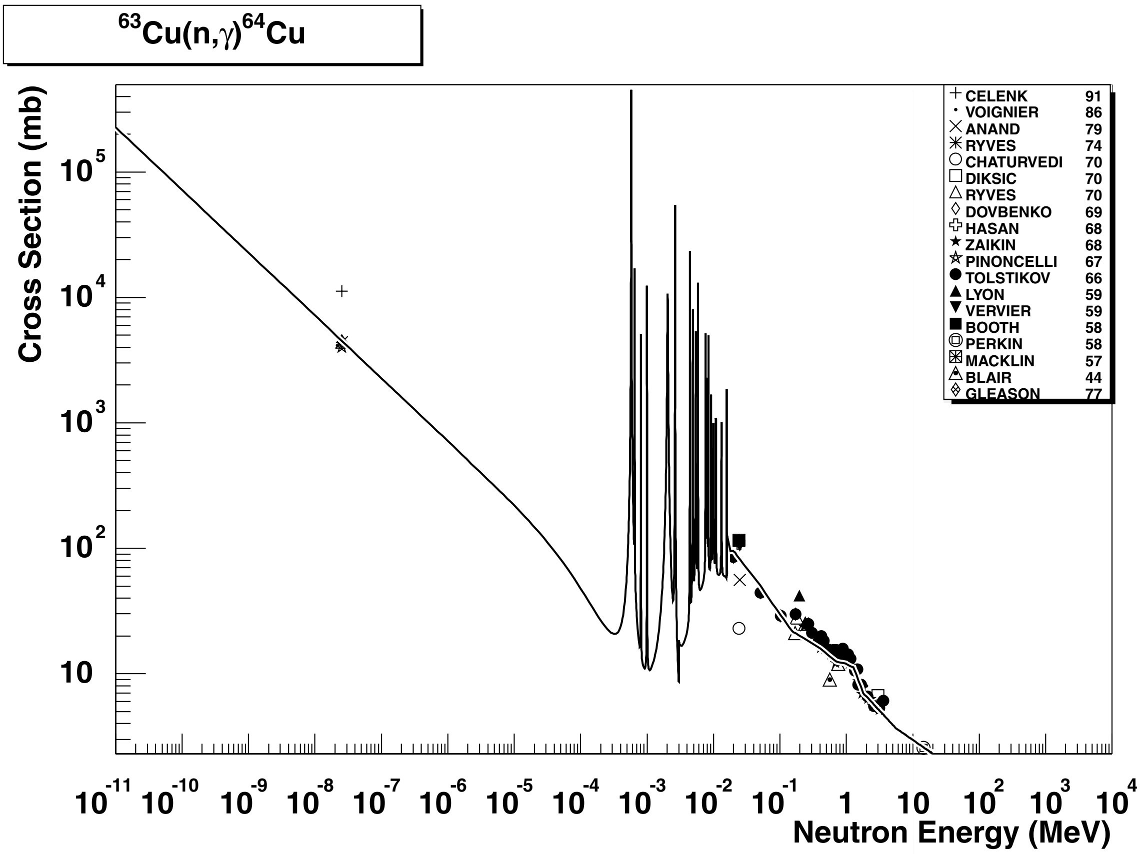

2.97. ^{63}Cu (n,γ) ^{64}Cu

final state: total
source: EAF-4.1 (ENDF/B-VI)

ENDF/B-VI evaluation is very close to all experimental data, both in the thermal range and the smooth statistical region above 20 keV. The thermal value of Celenk91 contradicts the other measurements and the value of 4.5 ± 0.02 b recommended in [26] by more than a factor of two. This point can be disregarded.

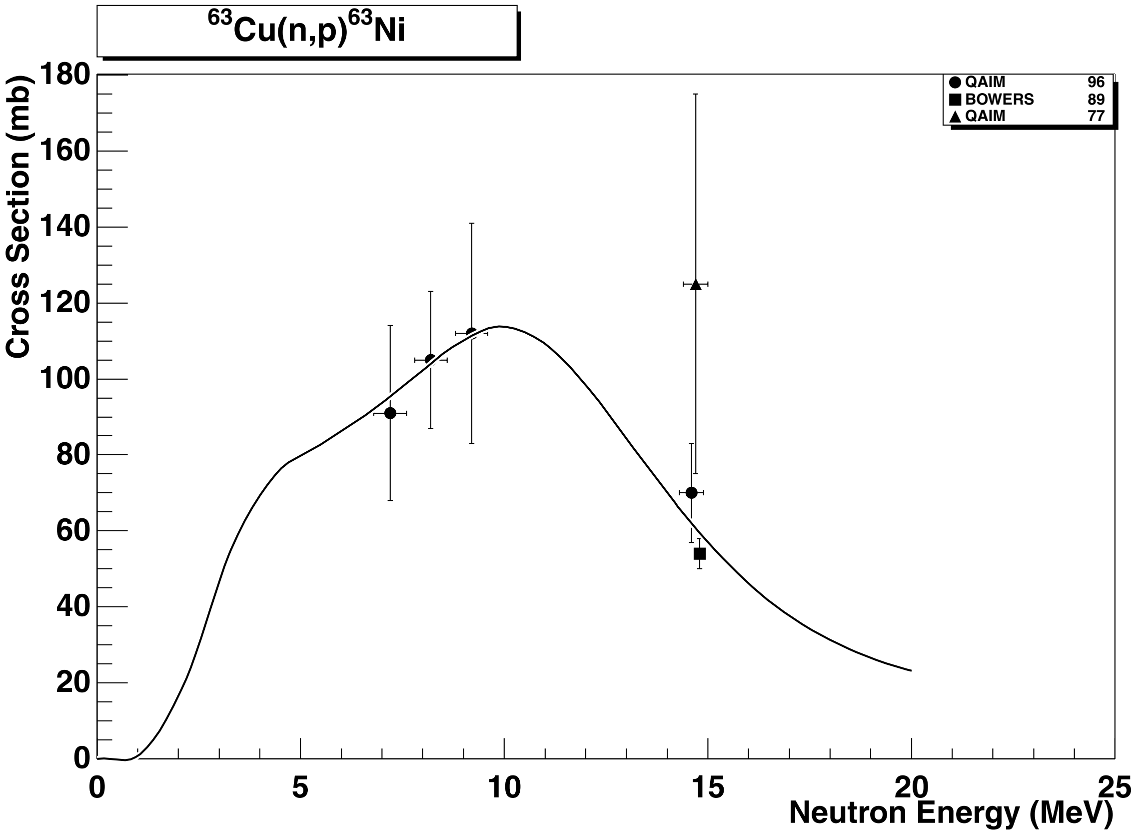

2.98. ^{63}Cu (n,p) ^{63}Ni

final state: total
source: ADL-3

ADL-3 agrees with all experimental data. The point by Qaim77 is consistent with the recommended evaluation considering its large error.

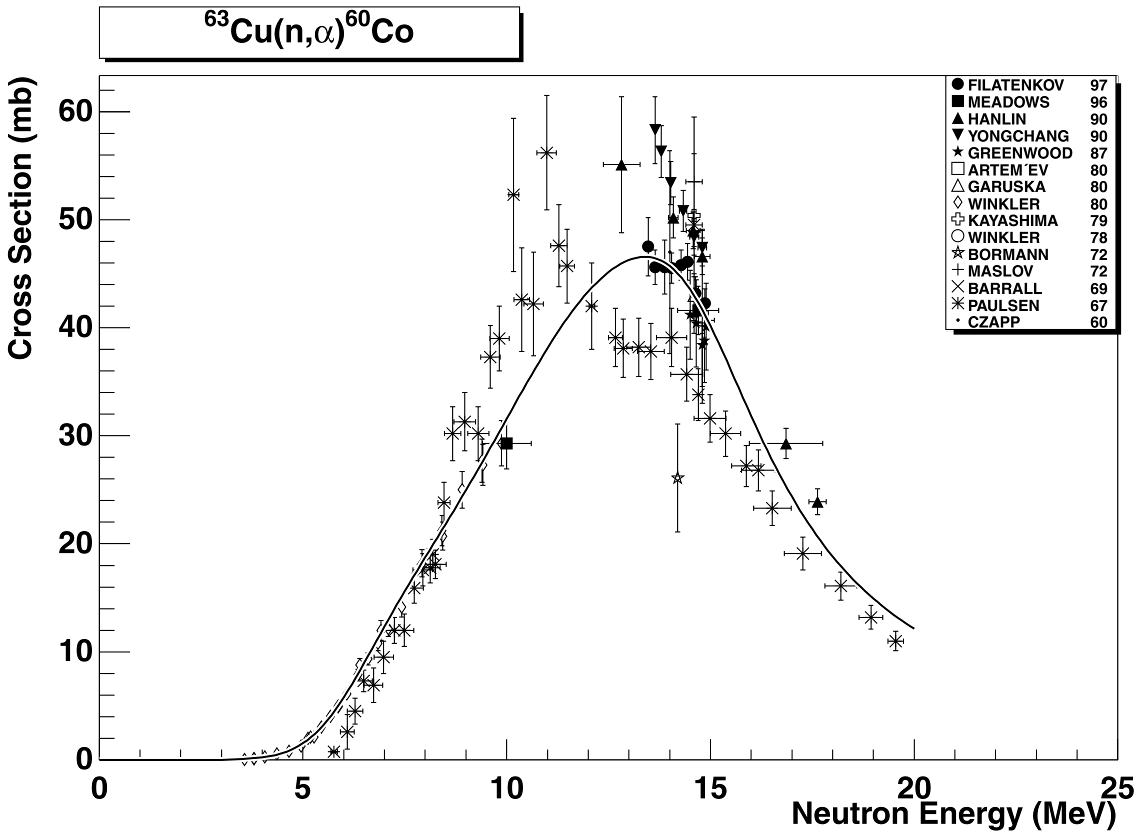

2.99. ^{63}Cu (n,α) ^{60}Co

final state: total
source: RRDF-98

RRDF-98 has been adopted. The total cross-section data are not very consistent. RRDF-98 is a reasonable representation. It runs in the middle of the data around 14 MeV and overestimates high energy data of Barrall69 to account for the more recent and reliable data by Hanlin90.

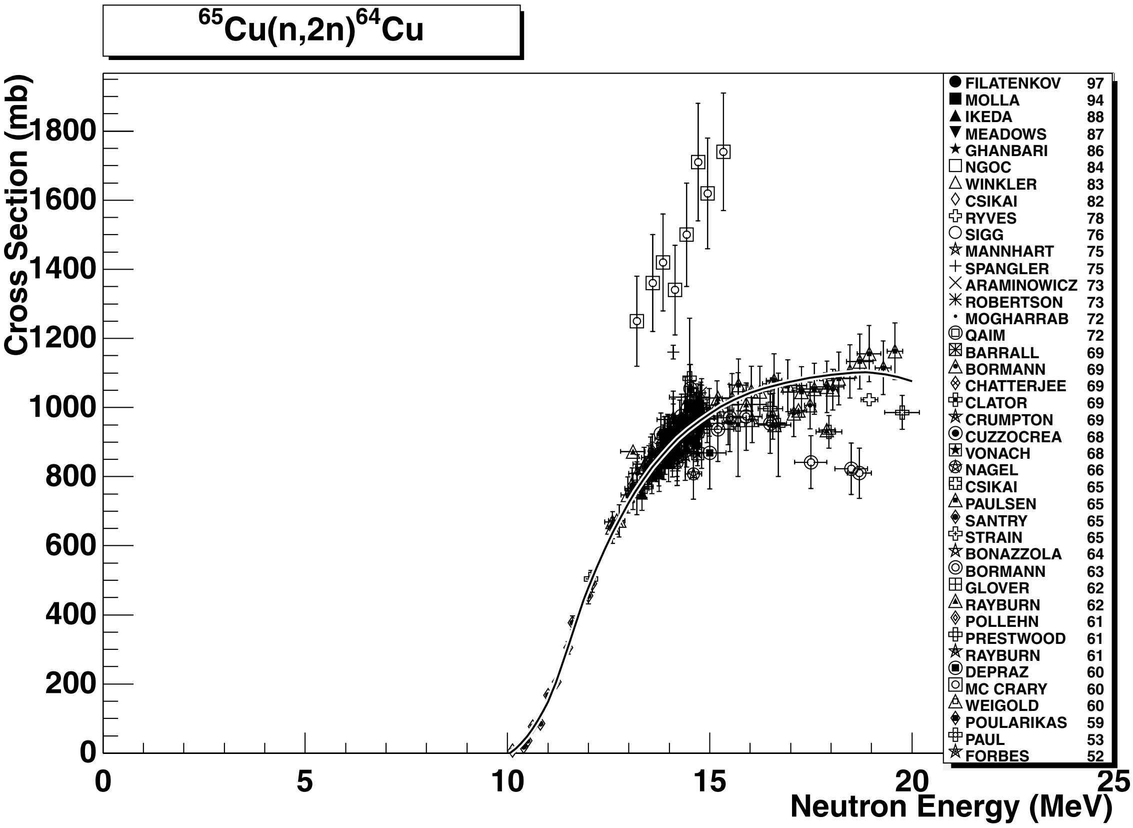

2.100. ^{65}Cu (n,2n) ^{64}Cu

final state: total
source: JENDL-Act96

JENDL-Act96 reproduces the relevant and recent data in the whole energy range very well. The data of Mc Crary60 are obviously wrong and can be disregarded.

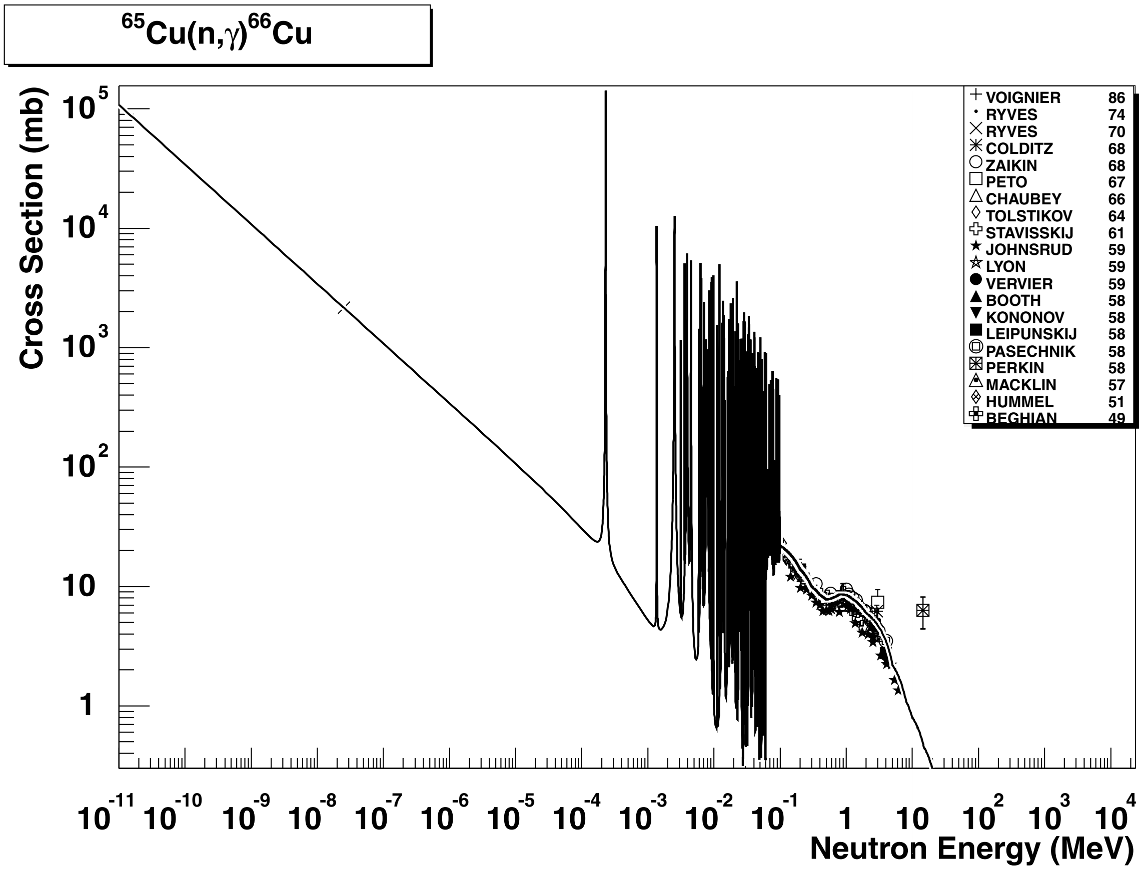

2.101. ^{65}Cu (n,γ) ^{66}Cu

final state: total
source: EAF-4.1 (ENDF/B-VI)

ENDF/B-VI evaluation is in good agreement with all experimental data, both in the thermal range and in the smooth statistical region above 100 keV. The single point at about 15 MeV of Perkin58 is about ten times higher than the value resulting from the 14.5 MeV systematics and can be disregarded.

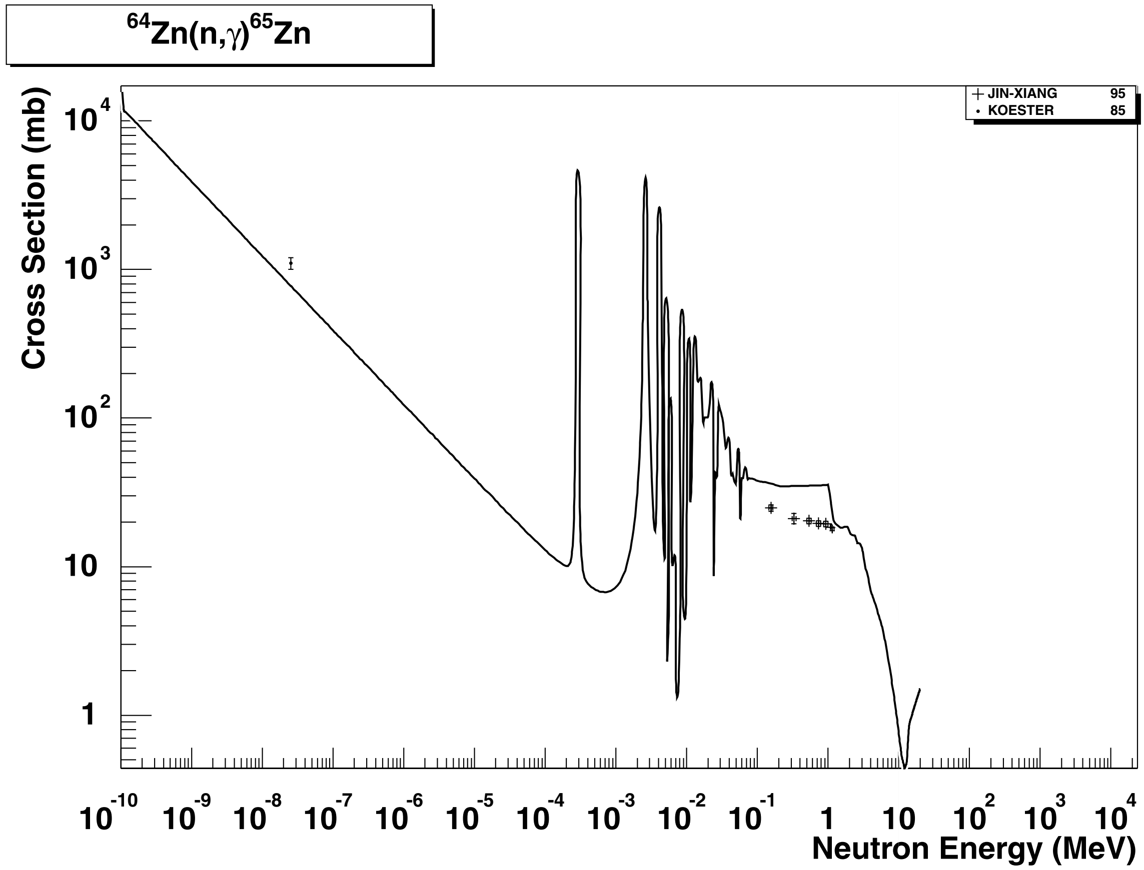

2.102. ^{64}Zn (n,γ) ^{65}Zn

final state: total
source: EAF-4.1 (JEF-2.2)

This is the original JEF-2.2 evaluation (from RCN fission products subfile) given in the multigroup structure. The thermal cross-section of Koester85 is slightly underestimated, however, the evaluation is in agreement with the recommended value of (740+-50) mb from Ref. [26] with C/E=1.02. The statistical component between 0.1 MeV and 1 MeV overestimates the recent data of Jin-Xian95 by about a factor of two. Re-evaluation of this component is recommended.

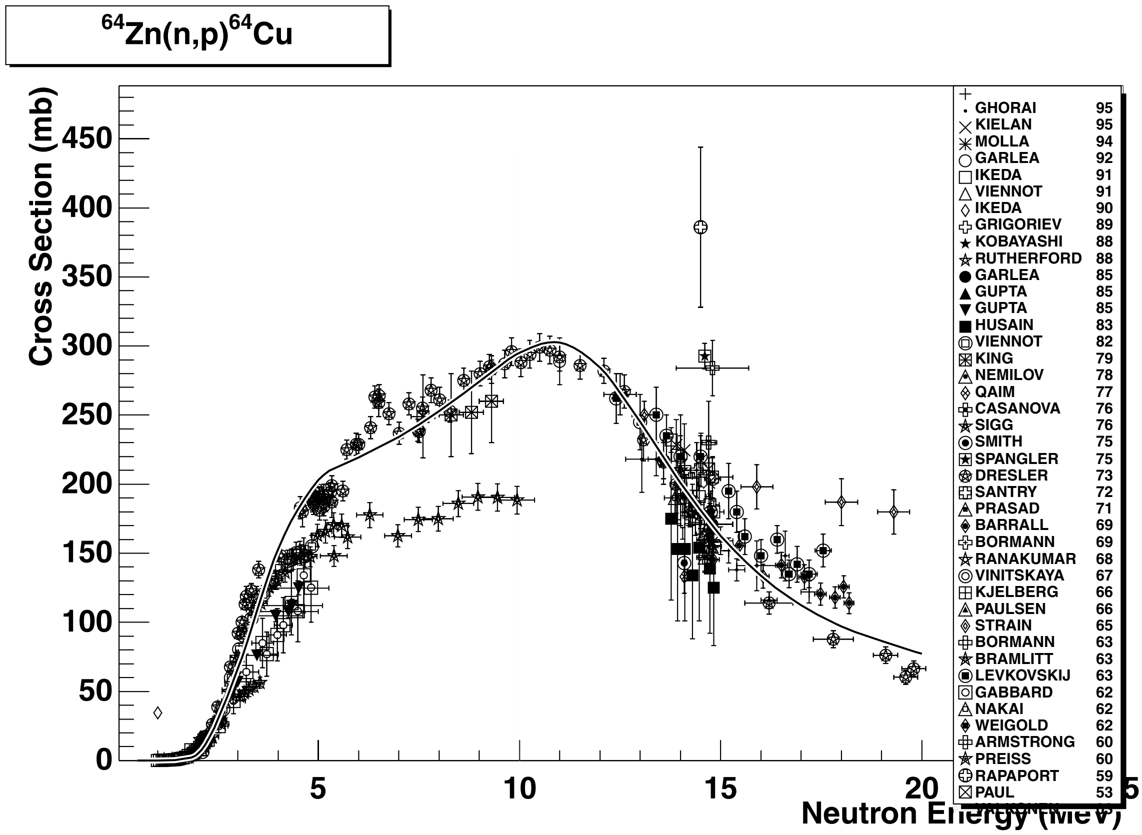

2.103. ^{64}Zn (n,p) ^{64}Cu

final state: total
source: JENDL-Act96

An very good agreement of JENDL-Act96 excitation curve with the relevant and recent experiments. Some of the data (deviating from the main experimental trend) may be disregarded, in particular Smith75 between 5-10 MeV and a few points above 300 mb around 15 MeV.

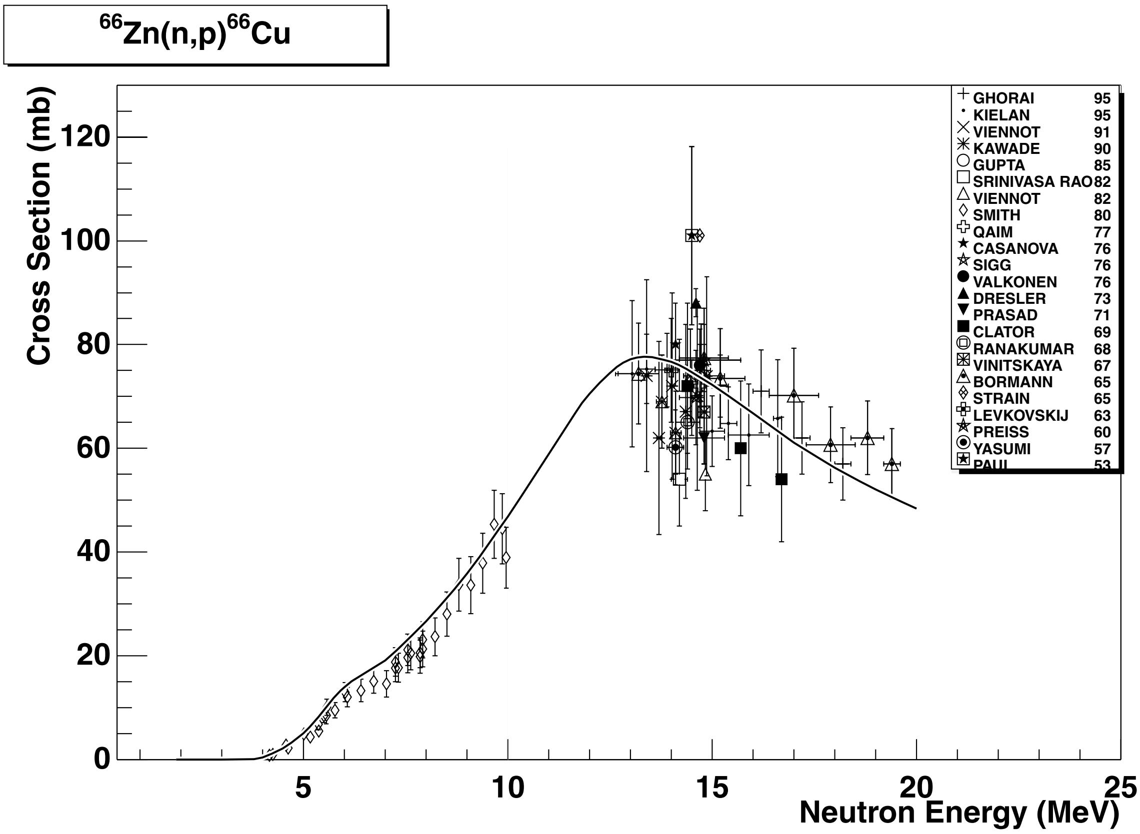

2.104. ^{66}Zn (n,p) ^{66}Cu

final state: total
source: JENDL-Act96

JENDL-Act96 reproduces very well almost all data, except two single, and highly uncertain, points at 15 MeV with values around 100 mb (Paul53 and Strain65).

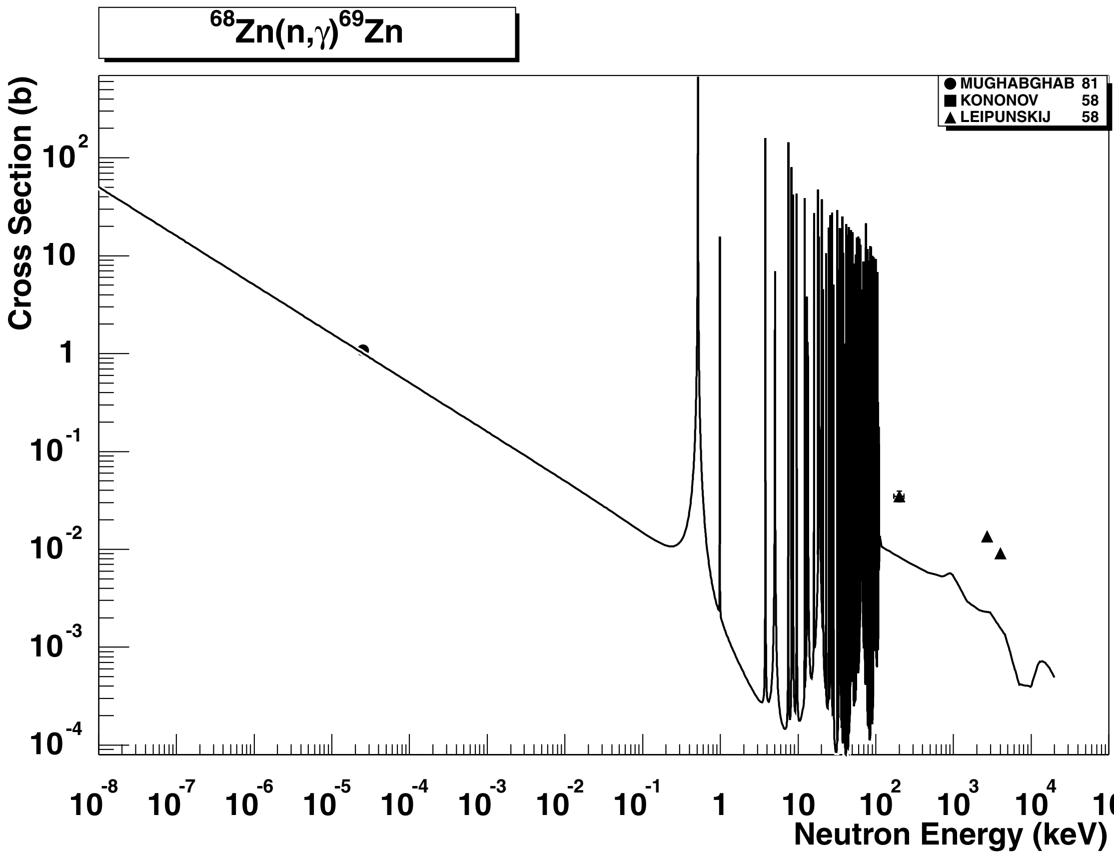

2.105. ^{68}Zn (n,γ) ^{69}Zn

final states: g.s., meta
source: EAF-4.1

This is the original EAF-4.1 evaluation calculated with the code SIGECN-MASGAM. Branching ratio between the g.s. and meta state is based on experimental data (thermal cross-sections) and applied up to the end of the resolved resonance region, and on the energy dependent branching ratio systematics [2] for the high energy region. Full MLBW resonance treatment is included and the total and partial thermal cross-sections [26] are reproduced with C/E=0.93. However, the smooth statistical component between 100 keV and 4 MeV severely underestimates three experimental data points of Leipunskij58. Since the statistical component is based on simplified calculations with the code MASGAM (using global parameters), it might be recommended to repeat these calculations in a more rigorous way. However, the pre-equilibrium part of the excitation curve looks reasonable.

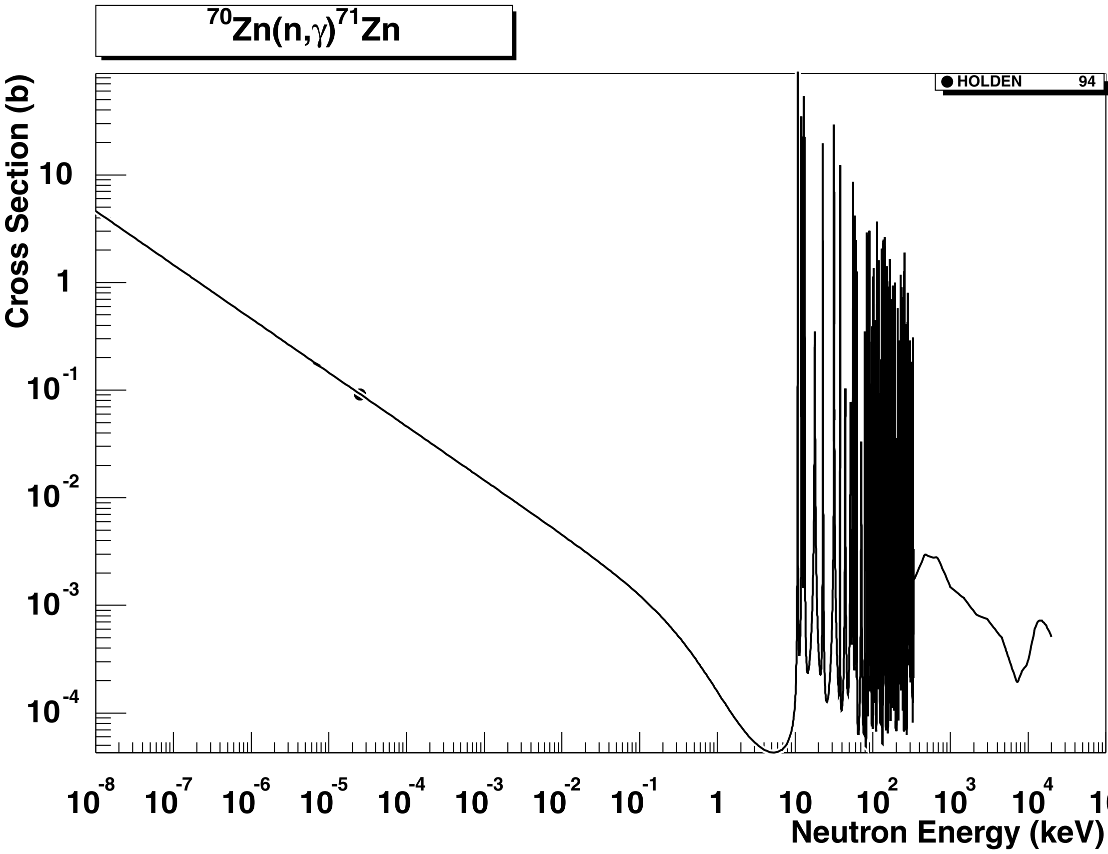

2.106. ^{70}Zn (n,γ) ^{71}Zn

final state: g.s., meta
source: EAF-4.1

This is the EAF-4.1 evaluation calculated with the code SIGECN-MASGAM. Branching ratio between the g.s. and meta state is based on the experimental data (thermal cross-sections) applied up to the end of the resolved resonance region, and on the energy dependent branching ratio systematics [2] for the high energy region. Full MLBW resonance treatment is included and the total and partial thermal cross-sections [26] are well reproduced (C/E=1.0). The statistical component is based on simplified calculations with the code MASGAM using global parameters.

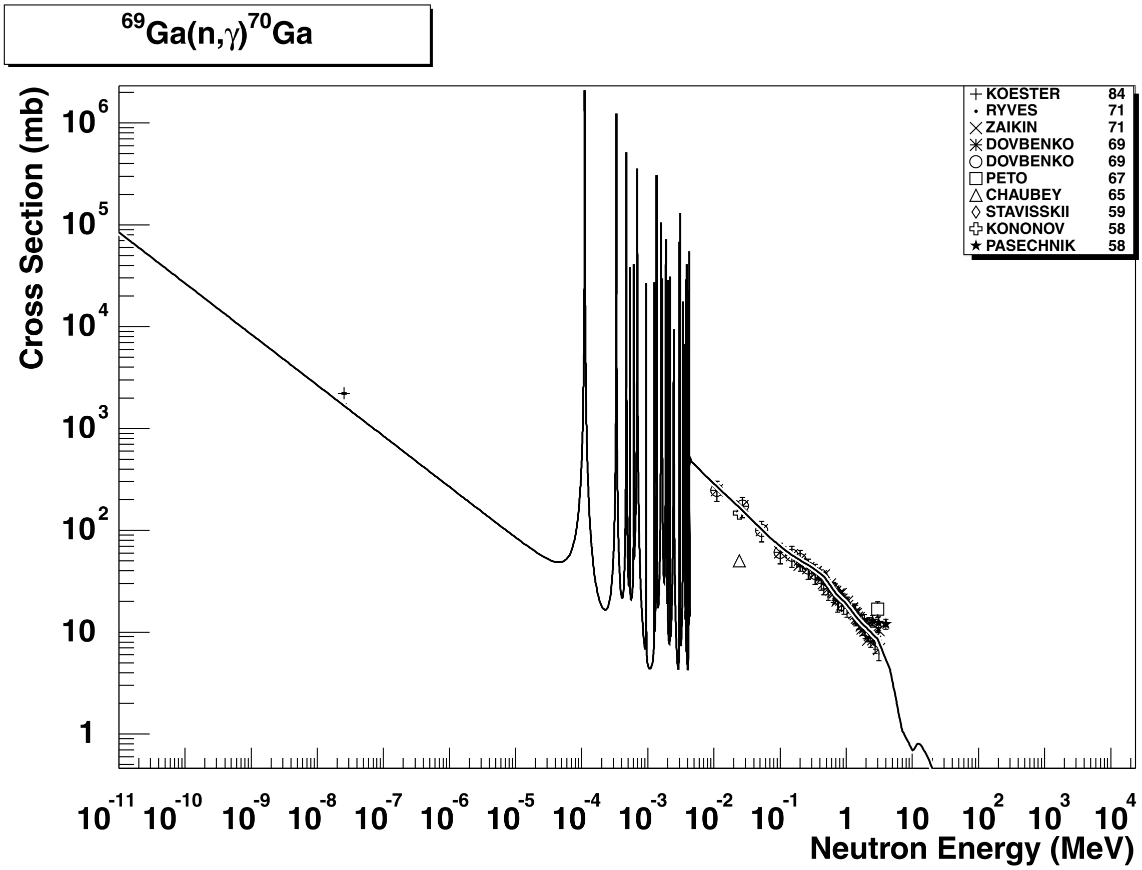

2.107. ^{69}Ga (n,γ) ^{70}Ga

final state: total
source: EAF-4.1

This is the EAF-4.1 evaluation calculated with the code SIGECN-MASGAM. Full MLBW resonance treatment is included and the total thermal cross-section [26] is well reproduced (C/E=1.0). The statistical component is based on simplified calculations with the code MASGAM (using global parameters) and agrees very well with experimental data between 10 keV and 4 MeV.

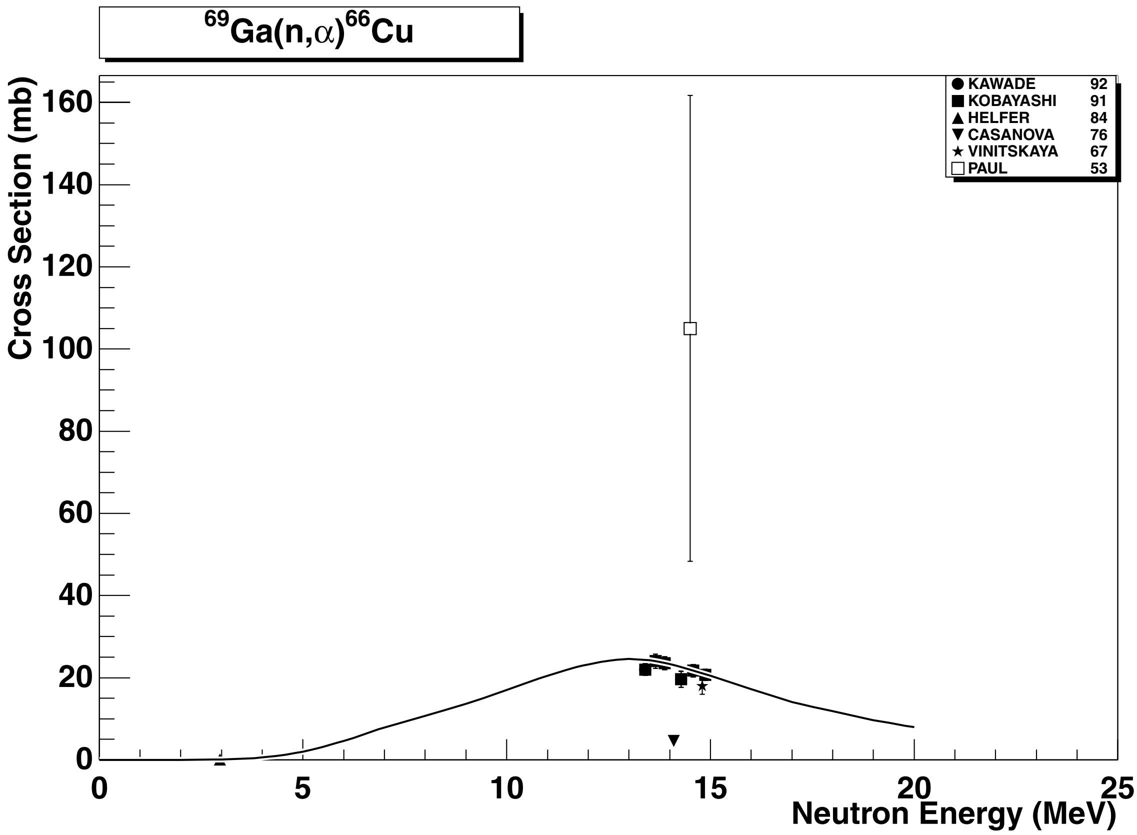

2.108. ^{69}Ga (n,α) ^{66}Cu

final state: total
source: JENDL-Act96

JENDL-Act96 agrees very well with the experimental data between 13-15 MeV, except Casanova76, which is obviously too low.

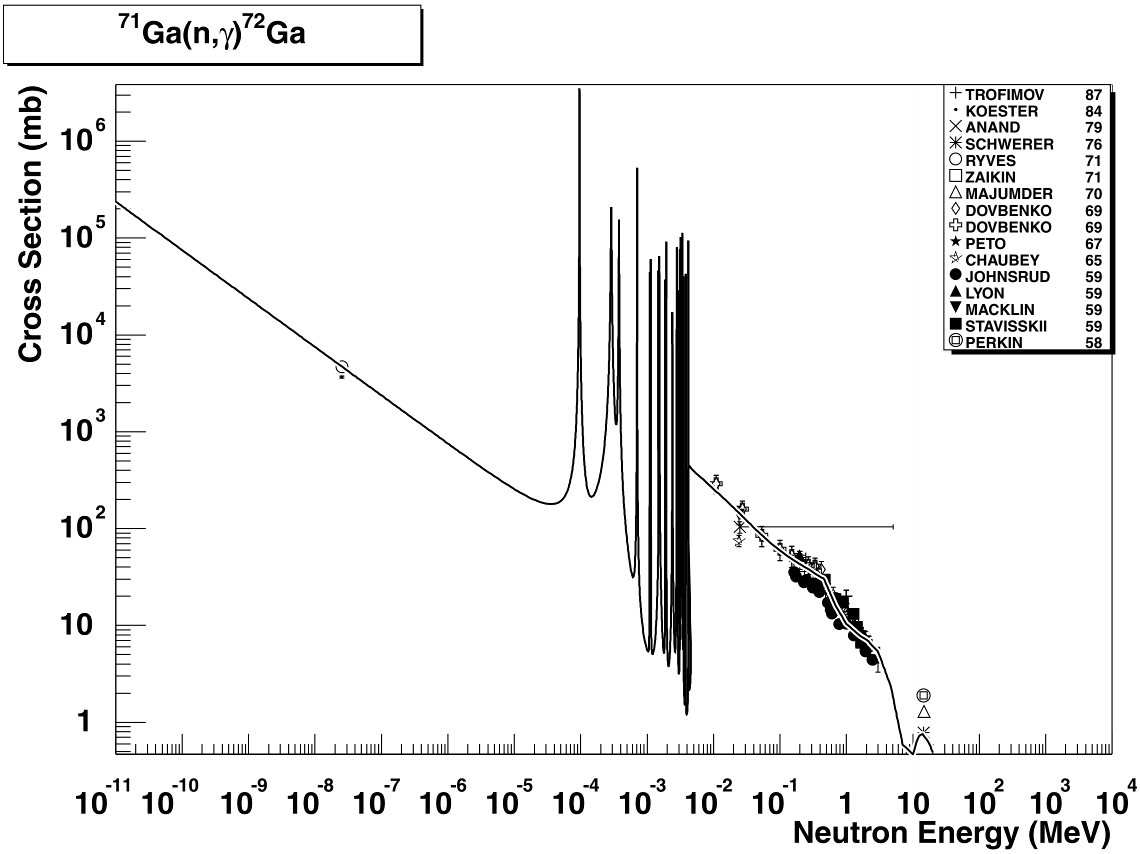

2.109. ^{71}Ga (n,γ) ^{72}Ga

final state: total
source: EAF-4.1

This is the EAF-4.1 evaluation calculated with the code SIGECN-MASGAM. Full MLBW resonance treatment is included and the total thermal cross-section [26] is well reproduced (C/E=1.0). The statistical component is based on simplified calculations with the code MASGAM using global parameters and agrees very well with experimental data between 10 keV and 3 MeV. The 14 MeV value agrees with Schwerer76, Majumder70 and the 14.5 MeV systematics. The value of Perkin58 is too large.

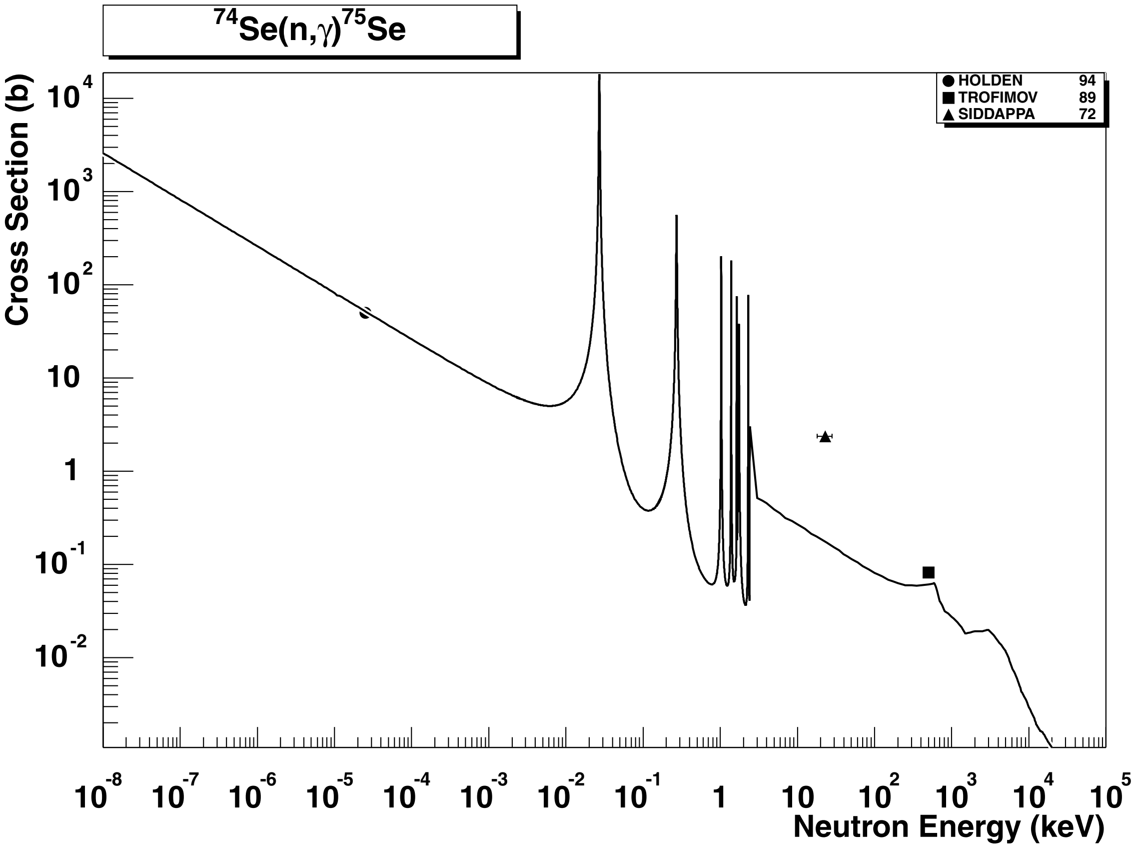

2.110. ^{74}Se (n,γ) ^{75}Se

final state: total
source: EAF-4.1 (JEF-2.2)

Data originate from the upgraded ENDF/B-V evaluation. The thermal cross-section of (50 ± 4) b from [32] is reproduced with C/E=1.12. The single experimental point of Siddappa72 seems to be too large and is also contradicted by the recommended 30 keV value of 0.24 b from [27]. The evaluation is close to Tromifov89 at about 500 keV.

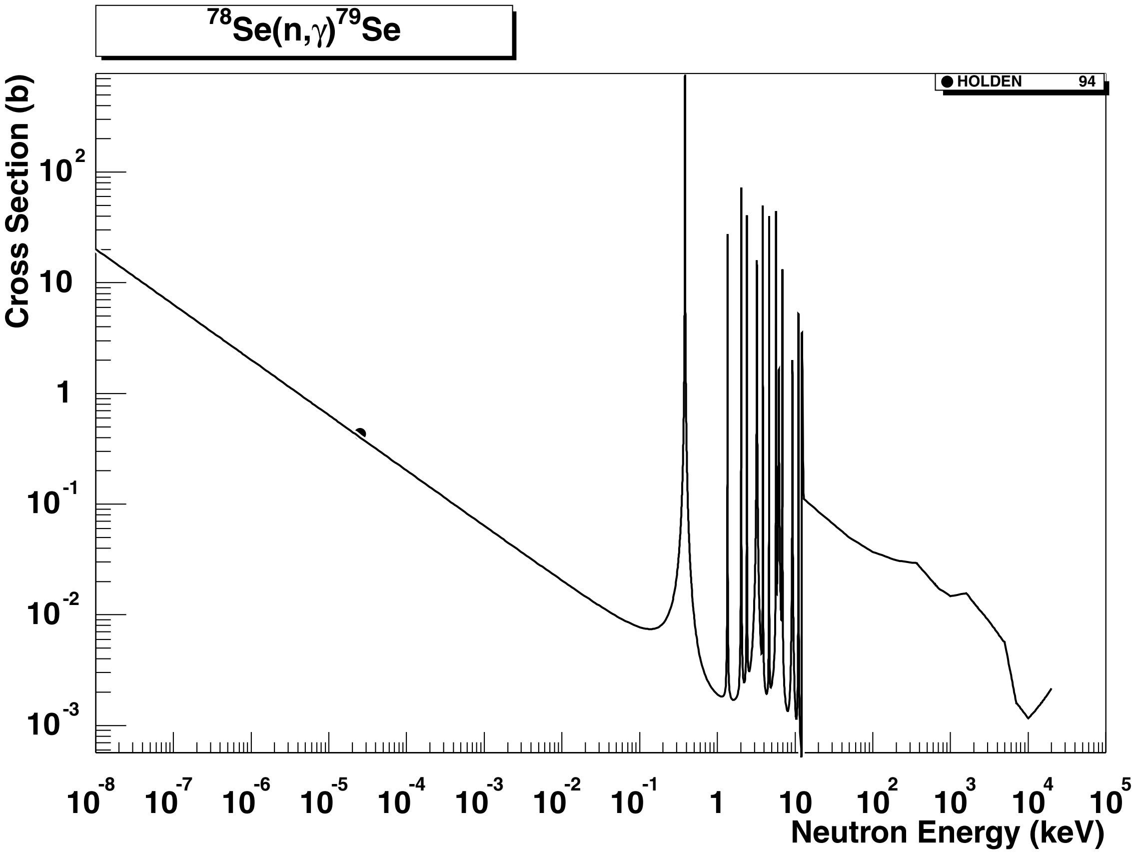

2.111. ^{78}Se (n,γ) ^{79}Se

final states: g.s., meta
source: EAF-4.1 (JEF-2.2)

This is the EAF-4.1 evaluation calculated with the code SIGECN-MASGAM. Branching ratio between the g.s. and meta state is based on experimental data (thermal cross-sections [31]) applied up to the end of the resolved resonance region, and on the energy dependent branching ratio systematics [2] for the high energy region. Full MLBW resonance treatment is included and the total and partial thermal cross-sections [26] are reproduced with C/E=0.93. The statistical component is based on simplified calculations with the code MASGAM using global parameters and is supported by the adopted 30 keV cross-section [26].

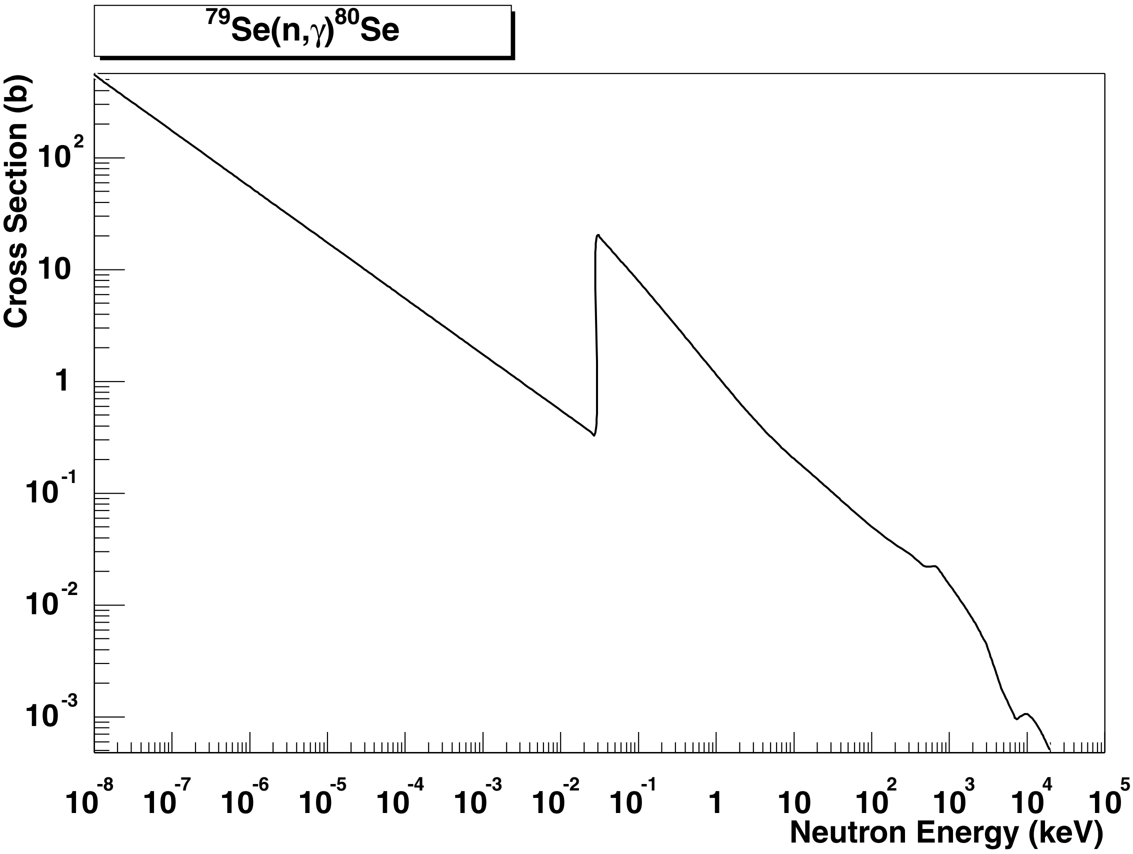

2.112. ^{79}Se (n,γ) ^{80}Se

final state: total
source: EAF-4.1

No experimental data is available. The evaluation is based on the simplified model calculations with the code MASGAM and the global parameters (Hauser-Feshbach and DSD model with no resonance region generation, E_H is based on a $D_0/2$ estimate; for details see Ref. [35]). The statistical component is supported by the adopted 30 keV cross-section [26].

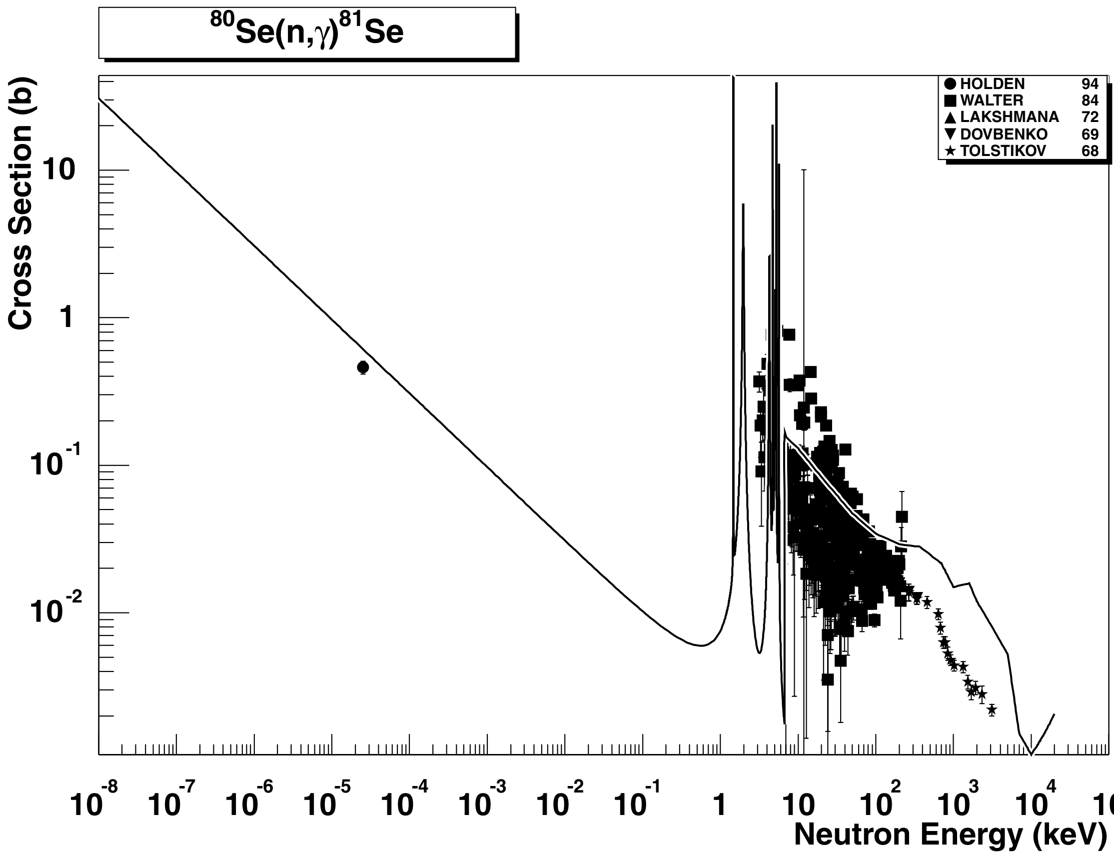

2.113. ^{80}Se (n,γ) ^{81}Se

final states: g.s., meta
source: EAF-4.1 (JEF-2.2)

Data originate from the upgraded ENDF/B-V evaluation. Branching ratio between the g.s. and meta state is based on experimental data (thermal cross-sections [26]) applied up to the end of the resolved resonance region, and on the energy dependent branching ratio systematics [2] for the high energy region. The total and partial thermal cross-sections [26] are well reproduced (C/E=1.0). The smooth statistical part severely overestimates the experimental data of Tolstikov68 above 100 keV. A revision of this component is recommended together with the check for the validity of Tolstikov68 data.

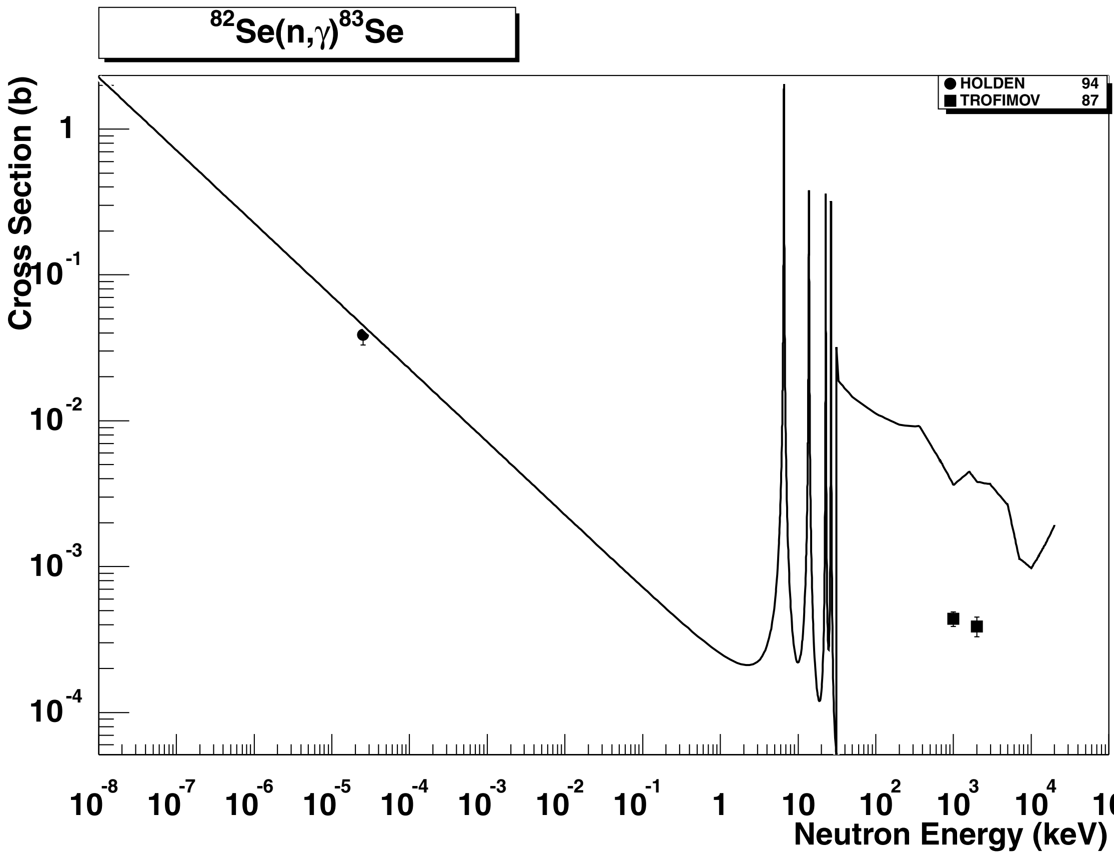

2.114. ^{82}Se (n,γ) ^{83}Se

final states: g.s., meta
source: EAF-4.1 (JEF-2.2)

Data originate from the upgraded ENDF/B-V evaluation. Branching ratio between the g.s. and meta state is based on experimental data (thermal cross-sections [26]) applied up to the end of the resolved resonance region, and on the energy dependent branching ratio systematics [2] for the high energy region. The total and partial thermal cross-sections [26] are well reproduced (C/E=1.2). Also, the averaged cross-section at 30 keV [27] supports the evaluation. The smooth statistical part overestimates two experimental data points of Trofimov87 at 1 and 2 MeV, which, however, seem to be too small. A revision of this component is recommended together with the check of the experimental information.

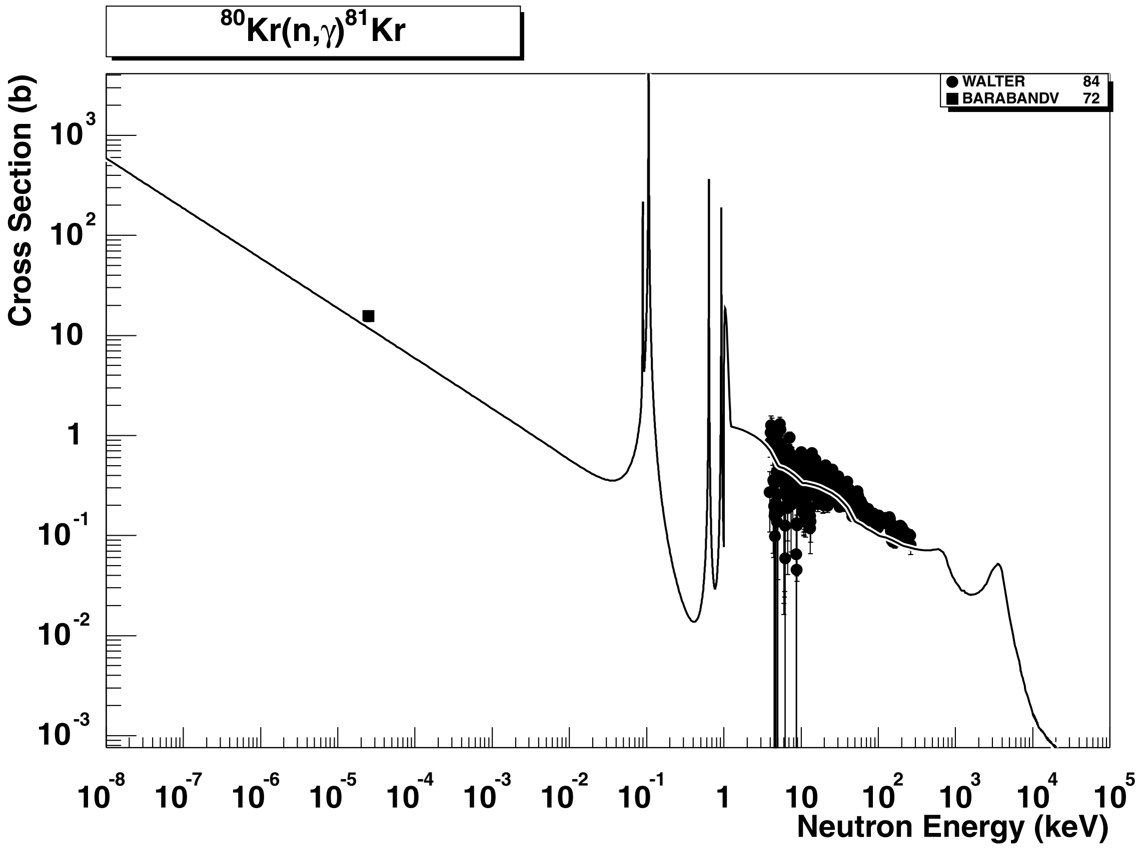

2.115. ^{80}Kr (n,γ) ^{81}Kr

final states: g.s., meta
source: EAF-4.1 (JEF-2.2)

Data originate from the upgraded ENDF/B-V evaluation. Branching ratio between the g.s. and meta state is based on experimental data (thermal cross-sections [26]) applied up to the end of the resolved resonance region, and on the energy dependent branching ratio systematics [2] for the high energy region. The total thermal cross-sections of Barabanov72 is slightly underestimated, the partial cross-sections (g.s. and meta state) are reproduced with C/E=0.94. The smooth statistical part runs reasonably through the experimental data between 4 and 300 keV.

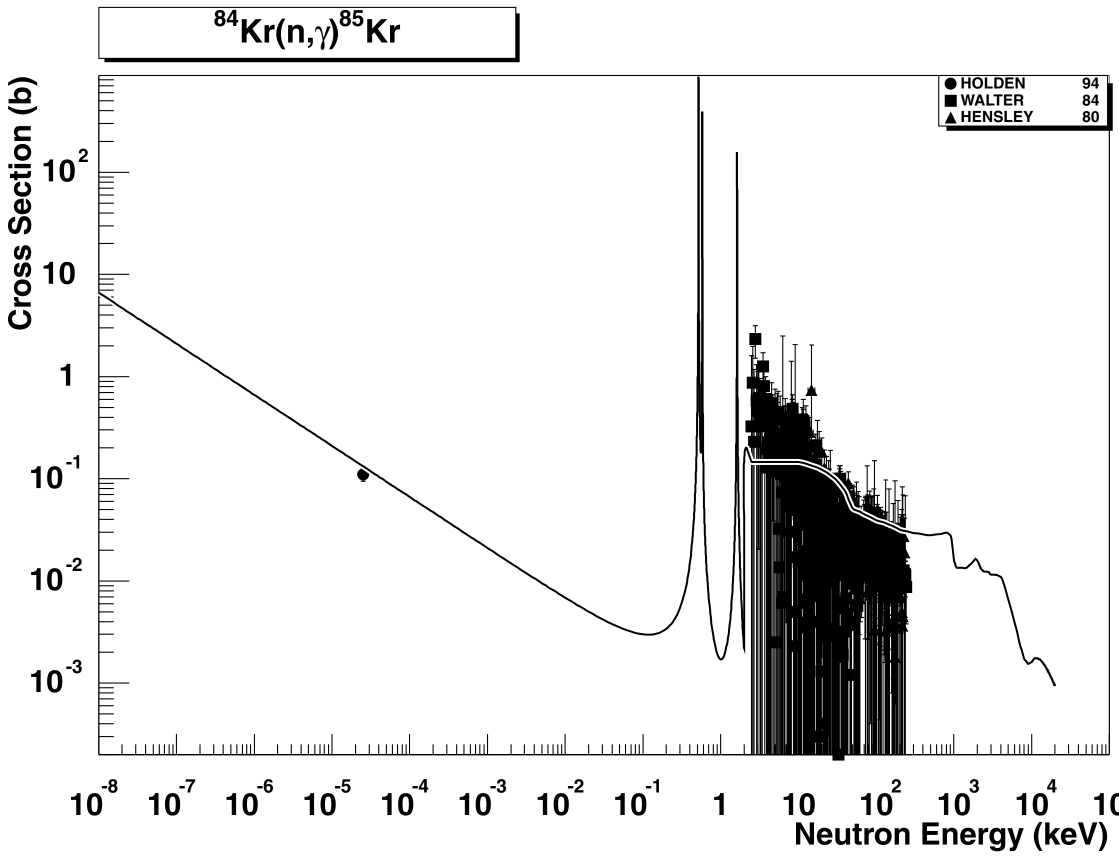

2.116. ^{84}Kr (n,γ) ^{85}Kr

final states: g.s., meta
source: EAF-4.1 (JEF-2.2)

Data originate from the upgraded ENDF/B-V evaluation. Branching ratio between the g.s. and meta state is based on experimental data (thermal cross-sections [26]) applied up to the end of the resolved resonance region, and on the energy dependent branching ratio systematics [2] for the high energy region. The total and partial thermal cross-sections [26] are well reproduced (C/E=1.0). The smooth statistical part runs within the scattered data between 2 and 200 keV, however, the shape of the excitation curve could be improved.

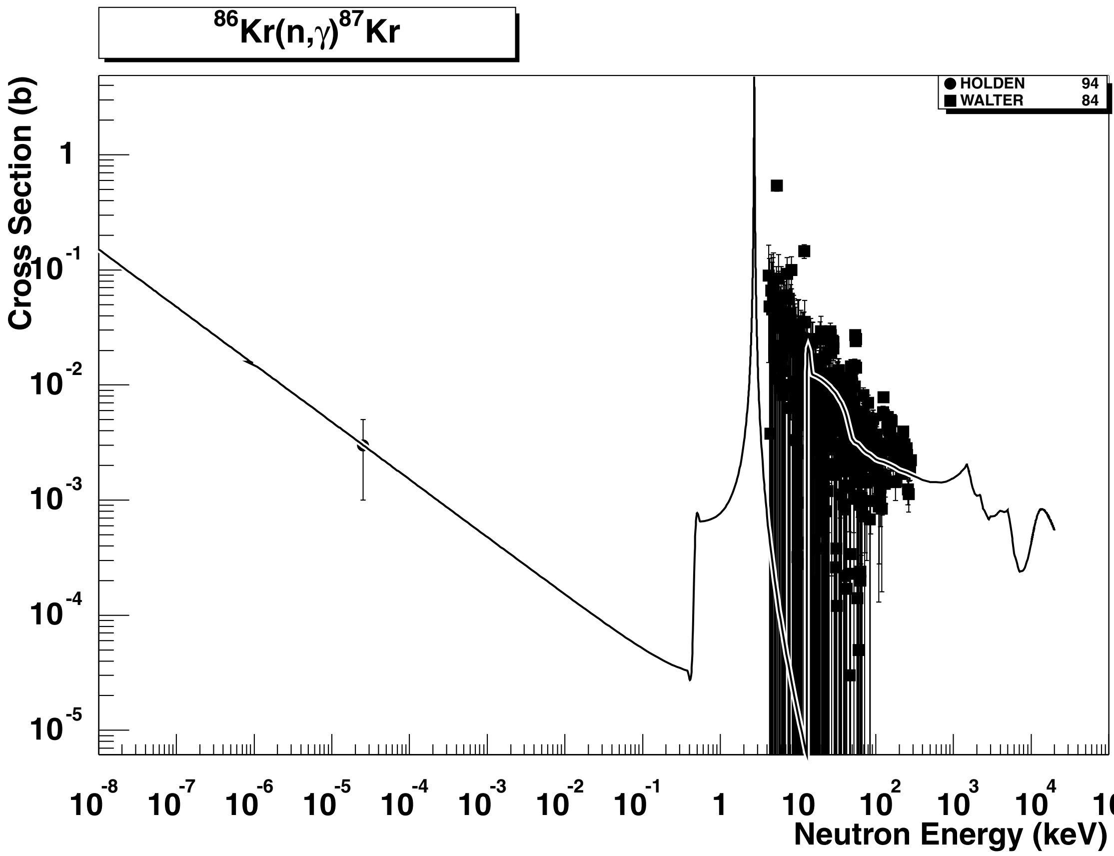

2.117. ^{86}Kr (n,γ) ^{87}Kr

final state: total
source: EAF-4.1 (JEF-2.2)

Data originate from the upgraded ENDF/B-V evaluation. The 1/v component has been adjusted to the thermal cross-section of 3 ± 2 mb [26], which resulted in a non-physical shape of the excitation curve between 0.1 and 1 keV (just below the only included resonance). The better treatment would call for a new adjustment of the 'averaged' resonance parameters or an introduction of a destructively interfering negative resonance. The statistical component reproduces reasonably the data of Walter84 up to 300 keV.

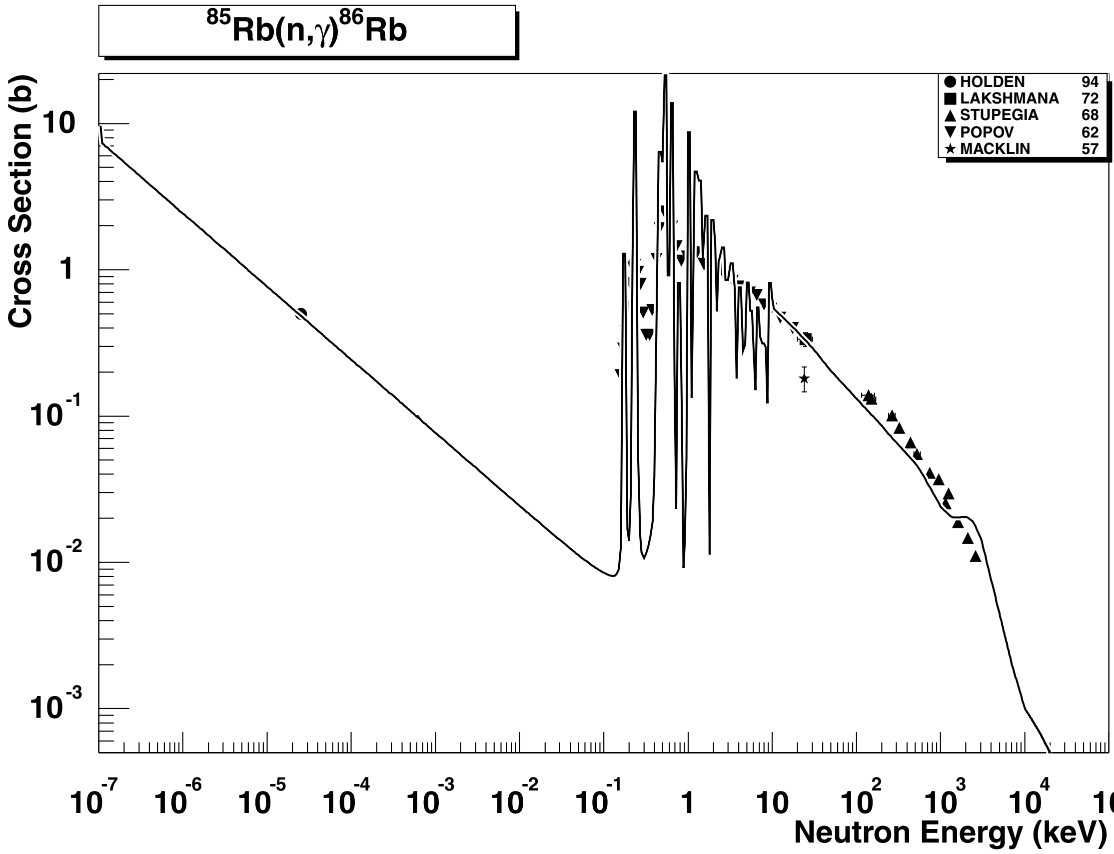

2.118. ^{85}Rb (n,γ) ^{86}Rb

final states: g.s., meta
source: EAF-4.1 (JEF-2.2)

Data originate from the upgraded ENDF/B-V evaluation. Branching between the g.s. and meta state is based on experimental data (thermal cross-sections [26]) applied up to the end of the resolved resonance region, and on the energy dependent branching ratio systematics [2] for the high energy region. The total and partial thermal cross-sections [26] are well reproduced (C/E=0.99). The smooth statistical part agrees very well with the data up to 2 MeV.

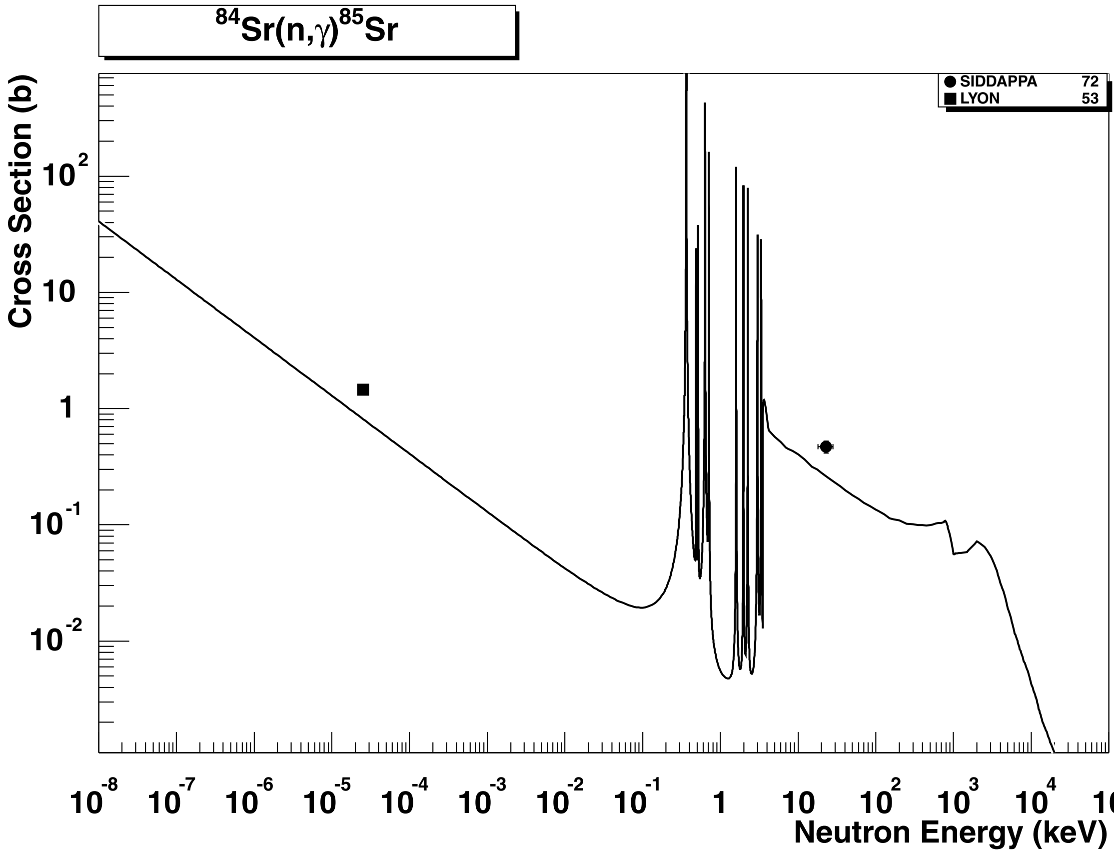

2.119. ^{84}Sr (n,γ) ^{85}Sr

final states: g.s., meta
source: EAF-4.1

Data originate from the upgraded ENDF/B-V evaluation. Branching ratio between the g.s. and meta state is based on experimental data (thermal cross-sections [26]) applied up to the end of the resolved resonance region, and on the energy dependent branching ratio systematics [2] for the high energy region. The total and partial thermal cross-sections [26] are reproduced with C/E=0.86, similar as the old measurement of Lyon53. The statistical component slightly underestimates the single experimental point of Siddapa72 at about 30 keV.

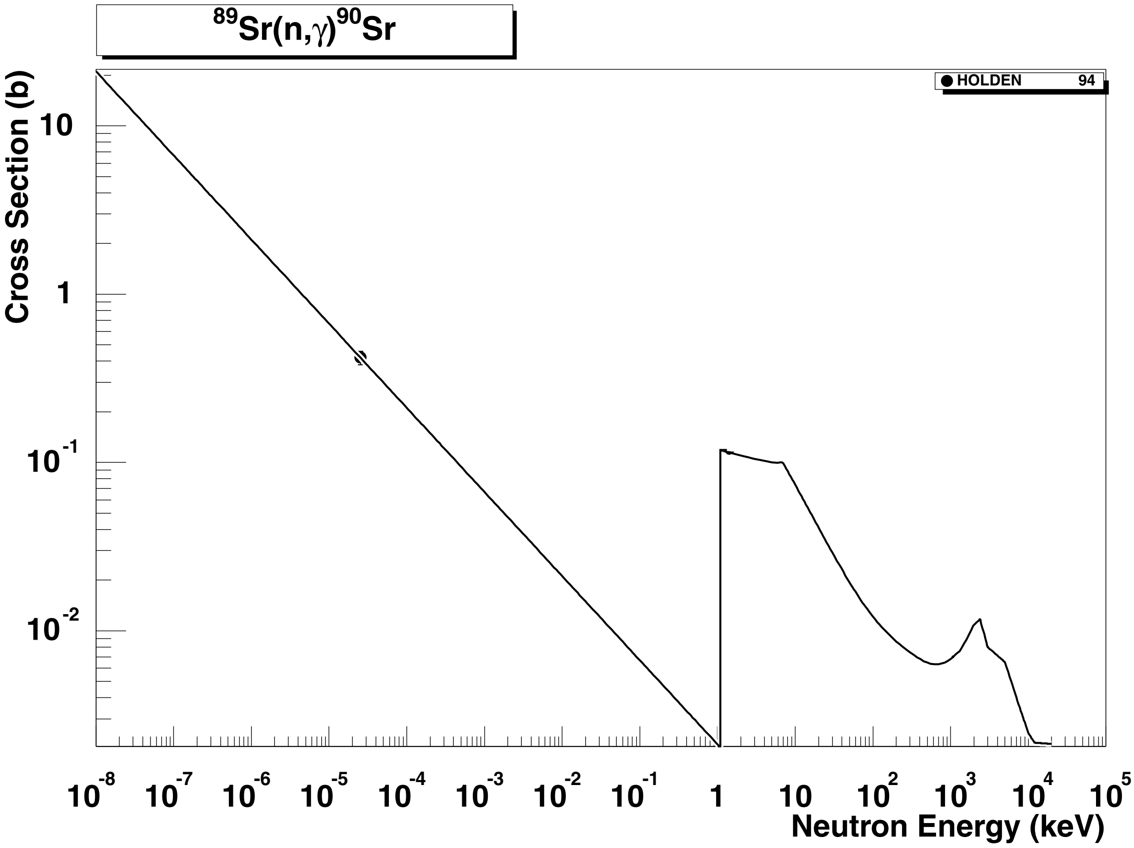

2.120. ^{89}Sr (n,γ) ^{90}Sr

final state: total
source: EAF-4.1 (JEF-2.2)

Data originate from the upgraded ENDF/B-V evaluation in a simplified approach. No data in the resolved resonance region are available. The thermal region is compares reasonably with the value of Holden94 [32] (C/E=0.83).

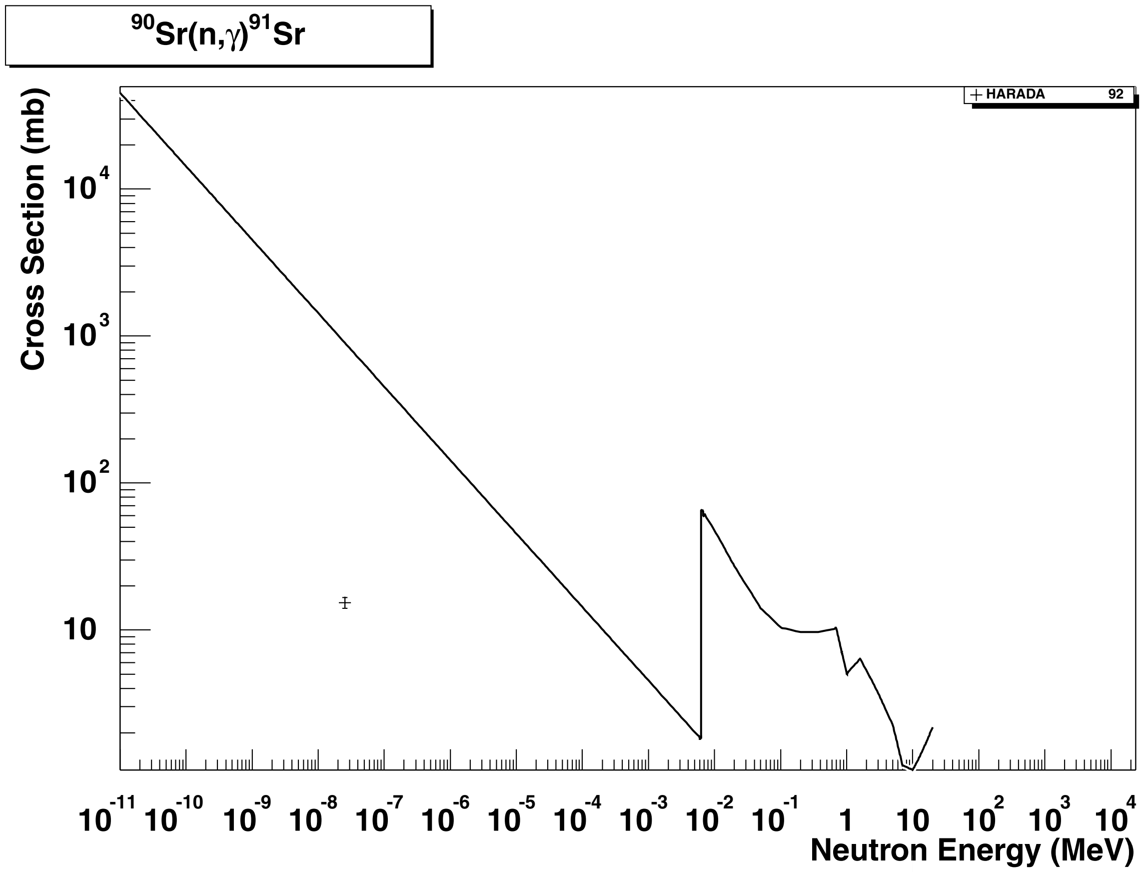

2.121. ^{90}Sr (n,γ) ^{91}Sr

final state: total
source: EAF-4.1 (JEF-2.2)

Data originate from the upgraded ENDF/B-V evaluation with no resolved resonance region (no data available). The thermal region severely overestimates the experiment of Harada92, which results in a value of C/E=92.4. The reason for this overestimation is that the ENDF/B-V evaluation was adjusted to the old value of (0.9 $\pm$ 0.5) b from the BNL cross-section compilation [31]. The discrepancy between these two experimental values is so big, that a new analysis of experimental data is needed in order to decide on their validity. For this reason there has been no renormalization of the 1/v component yet. However, Harada92 seems more reliable and reevaluation of this reaction is recommended.

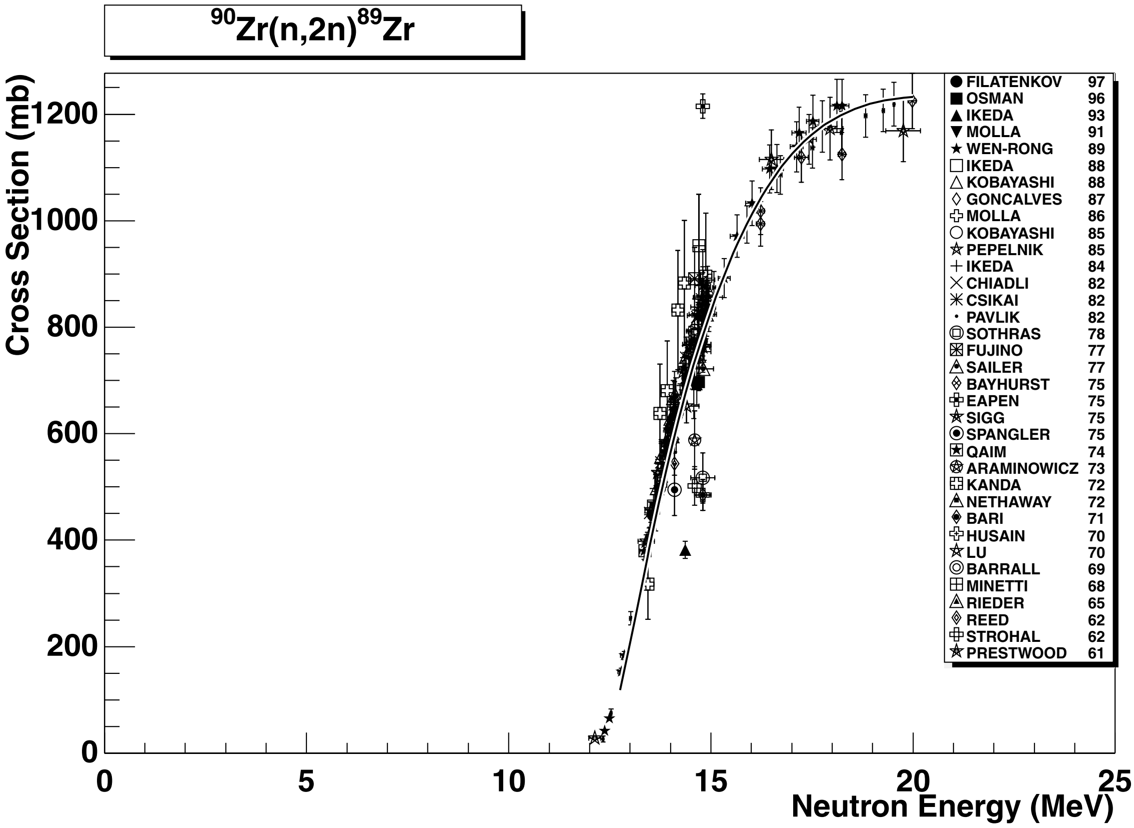

2.122. ^{90}Zr (n,2n) ^{89}Zr

final states: g.s., meta
source: ADL-3

An excellent agreement of ADL-3 evaluations with all experimental data. Splitting of the cross-section into the g.s. and meta state channels is based on the model calculations.

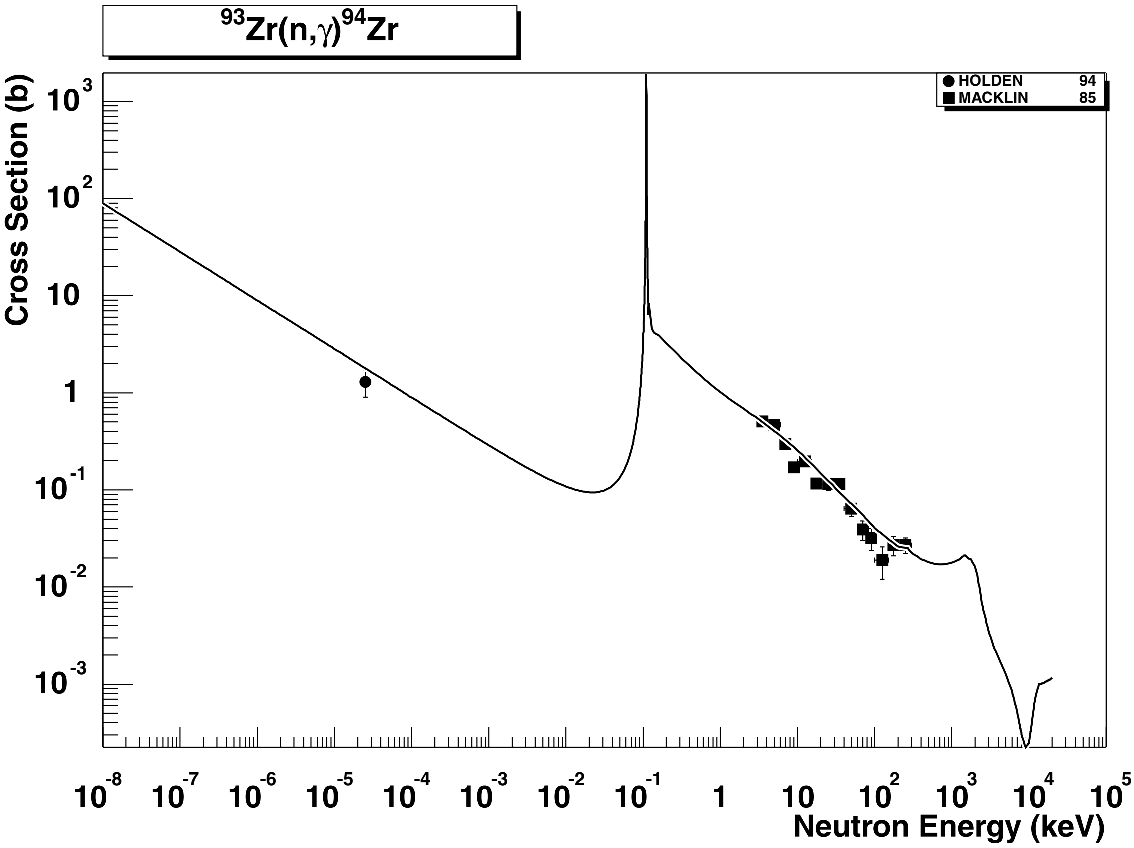

2.123. ^{93}Zr (n,γ) ^{94}Zr

final state: total
source: EAF-4.1 (JEF-2.2)

The JEF-2.2 evaluation with the single resonance at 110 eV with resonance parameters adjusted to reproduce the thermal scattering and capture cross-sections of Holden94 [32] has been adopted. The capture value is reproduced with C/E=1.24. The smooth statistical part is supported by the recommended 30 keV capture cross-section from Ref. [27] and experimental data of Macklin85.

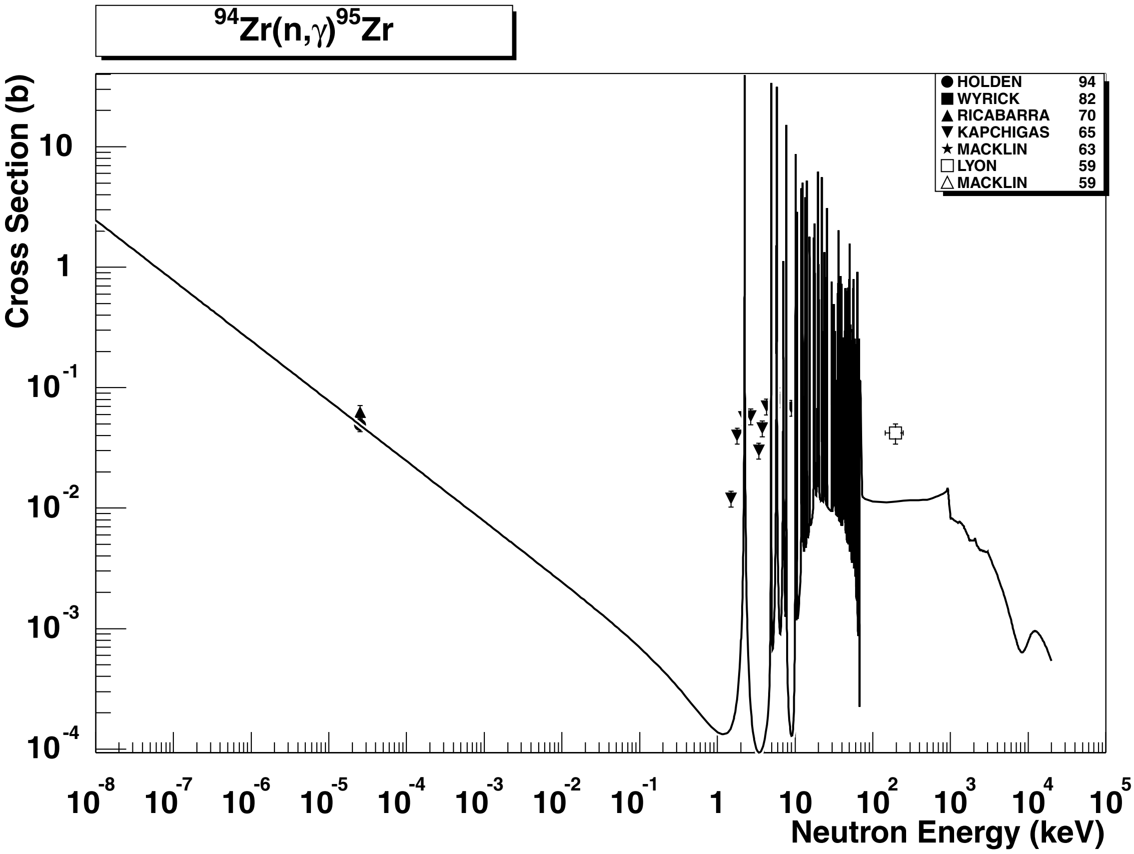

2.124. ^{94}Zr (n,γ) ^{95}Zr

final state: total
source: EAF-4.1 (JEF-2.2)

The JEF-2.2 evaluation agrees rather well with the recommended thermal cross-section of Holden94 [32] (C/E= 0.98) and with the experimental point of Ricabarra70. The statistical component is well below the single point of Lyon59, however, using a single experimental point to re-normalize the statistical calculations carried out with the local parameters is not advisable. The JEF-2.2 evaluations is still recommended, however, a revision of the statistical component may be considered.

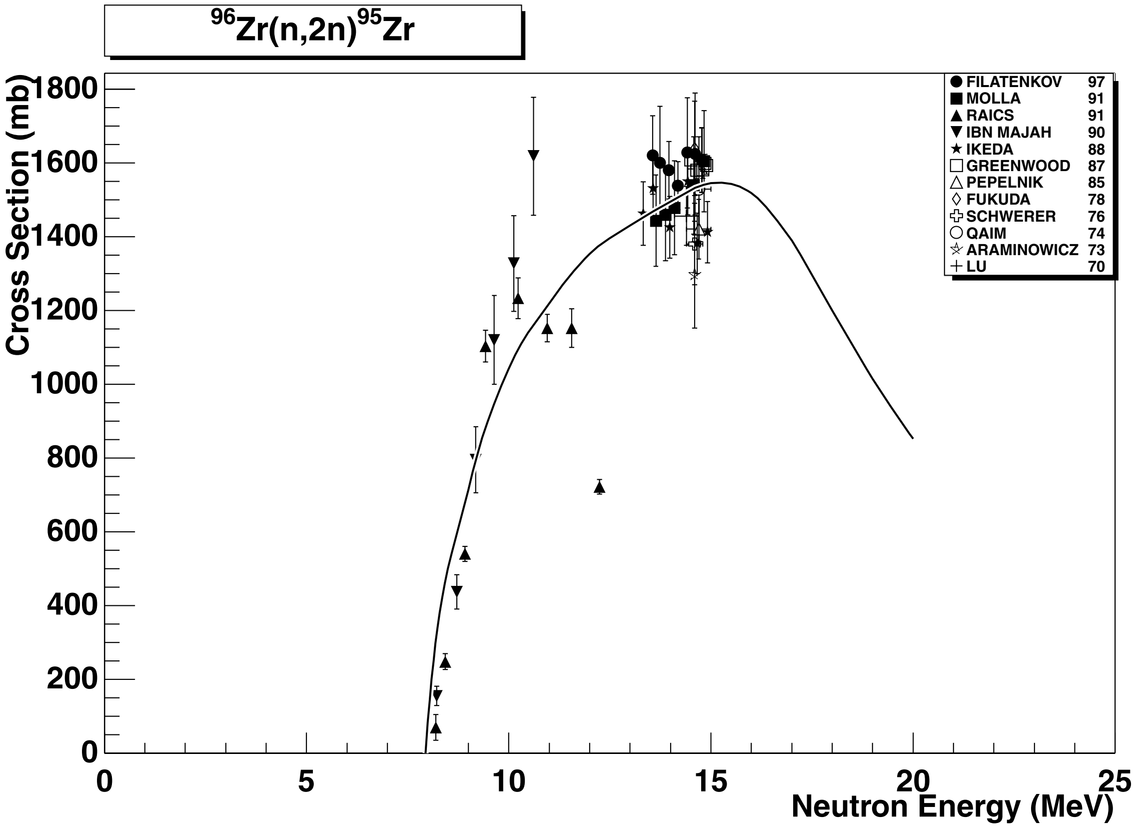

2.125. ^{96}Zr (n,2n) ^{95}Zr

final state: total
source: JENDL-Act96

JENDL-Act96 curve runs reasonably in the middle of the available experimental data points. The data point of Raics91 at about 12.5 MeV looks suspicious, it disagrees also with other data from the same measurement.

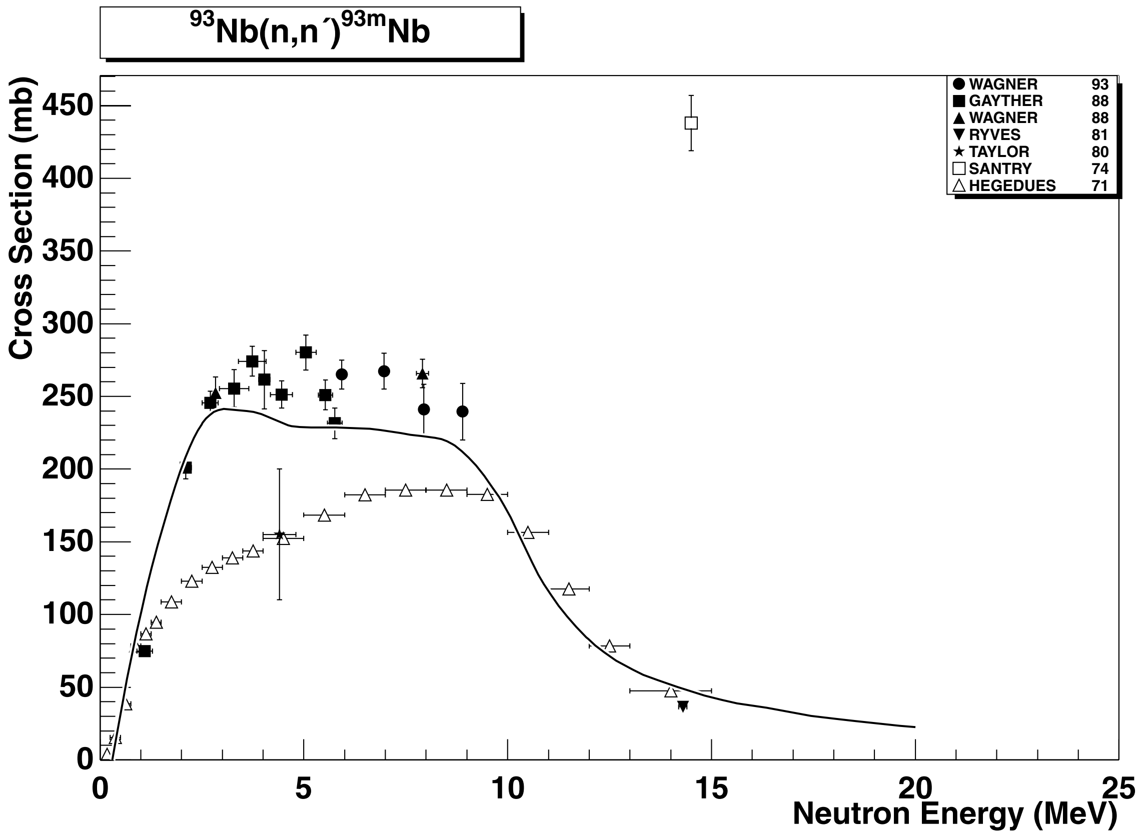

2.126. ^{93}Nb (n,n') ^{93m}Nb

final state: meta
source: RRDF-98

RRDF-98 evaluation underestimates by about 10% a flat part of the excitation curve between 3 and 9 MeV when compared with the data of Wagner88,93 and Gayther88. Strange results of Hegedues71 may be disregarded as well as the single point of Santry74.

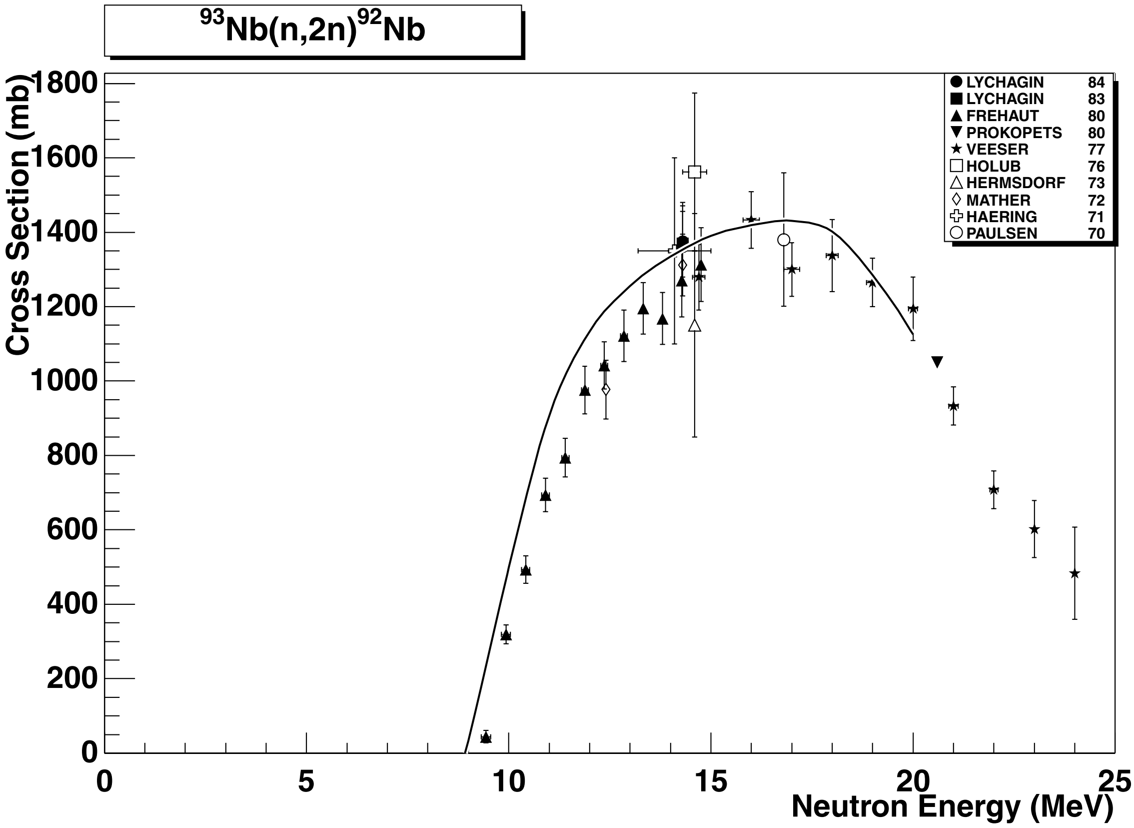

2.127. ^{93}Nb (n,2n) ^{92}Nb

final states: g.s., meta
source: JENDL-Act96

JENDL-Act96 evaluation slightly overestimates the experimental data (Frehaut80) between 9 and 15 MeV, although the two most recent data points at 14.5 MeV (Lychagin83,84) are close to the excitation curve. However, in general the evaluation can be considered satisfactory. Partial cross-sections to the g.s. and meta state are based on the model calculations.

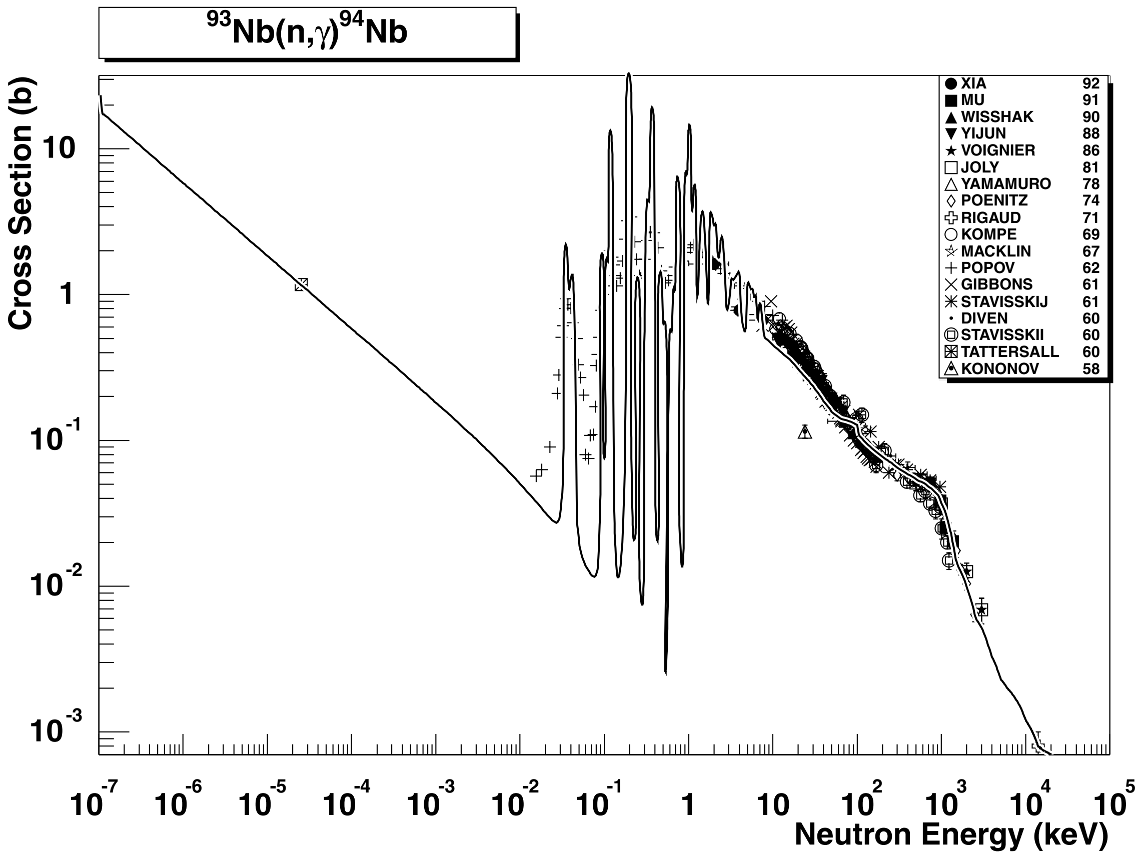

2.128. ^{93}Nb (n,γ) ^{94}Nb

final states: g.s., meta
source: EAF-4.1 (JEF-2.2)

ENDF/B-VI evaluation has been adopted in JEF-2.2. Branching ratio between the g.s. and meta state is based on the energy dependent systematics [2]. The excitation curve reproduces all EXFOR data rather well. Data are stored in SANDII group structure, the original ENDF/B-VI evaluation includes 29016 energy points.

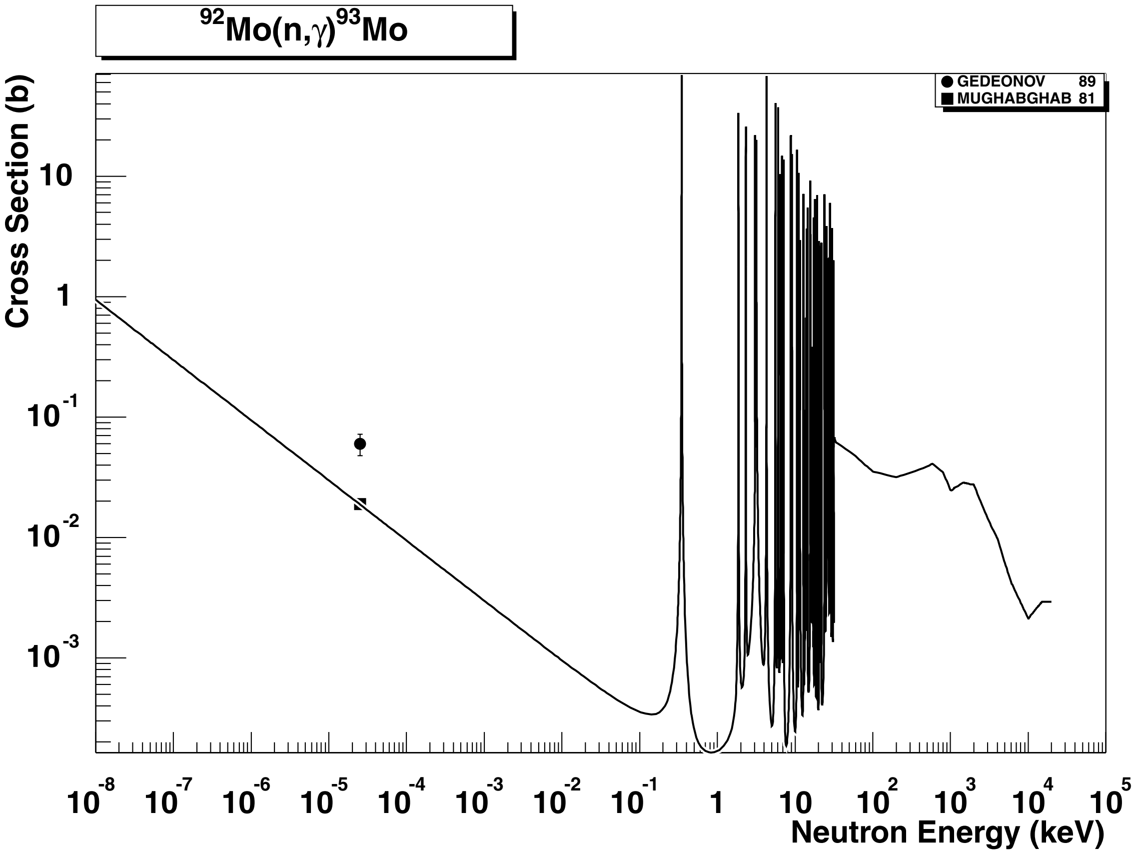

2.129. ^{92}Mo (n,γ) ^{93}Mo

final states: g.s., meta
source: EAF-4.1 (JEF-2.2)

ENDF/B-VI evaluation has been adopted in JEF-2.2. Branching ratio between the g.s. and meta state is based on the energy dependent systematics [2]. The recommended thermal cross-section (19 mb from Ref. [26]) is reproduced with C/E=0.99. The value of Gedeonov89 is about a factor of three larger. The recommendation of Ref. [26] has been adopted.

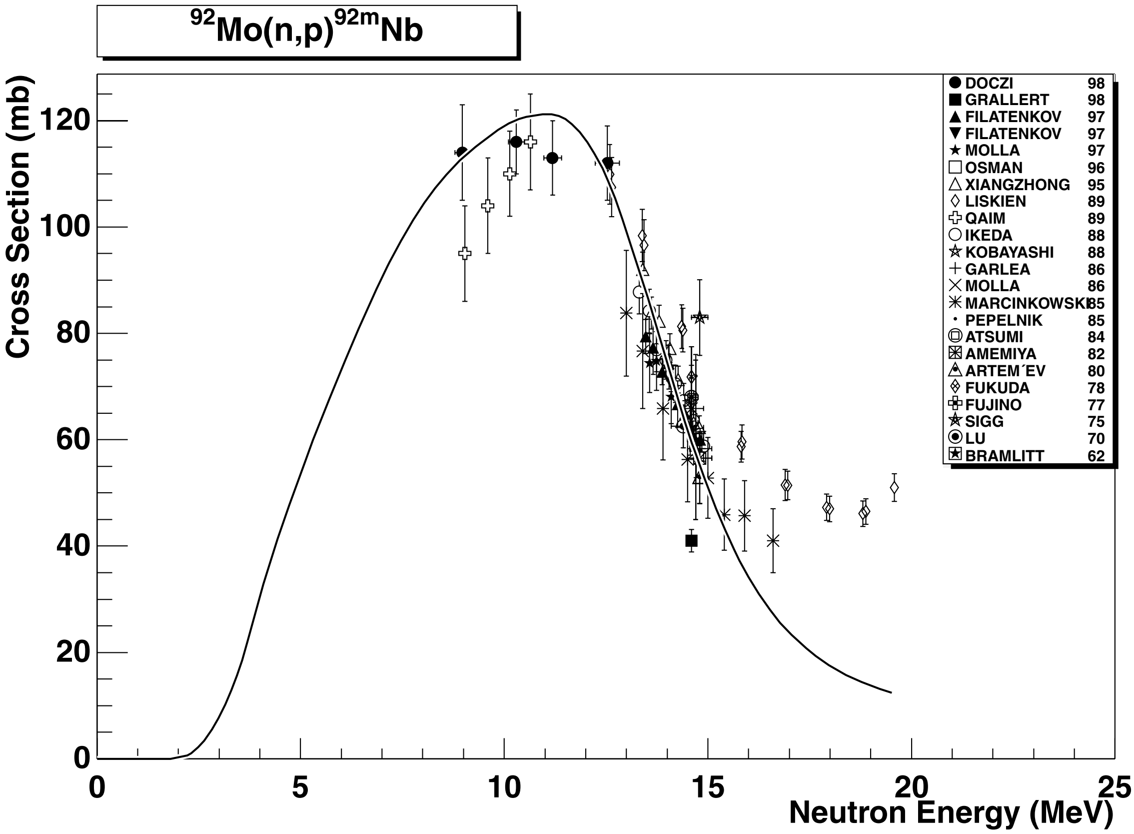

2.130. ^{92}Mo (n,p) ^{92m}Nb

final states: meta
source: ADL-3

Only cross-sections to the metastable state are included since g.s. life-time is 34 million years. ADL-3 evaluation agrees very well with all experimental data up to 15 MeV. Above this energy the evaluated cross-section follow data of Marcinkowski rather than those of Liskien, which, however, seem to be discrepant with the remaining sets. The evaluated data might be slightly too low above 15 MeV indicating underestimation of the preequilibrium contribution. cross-sections to the meta state are based on the model calculations.

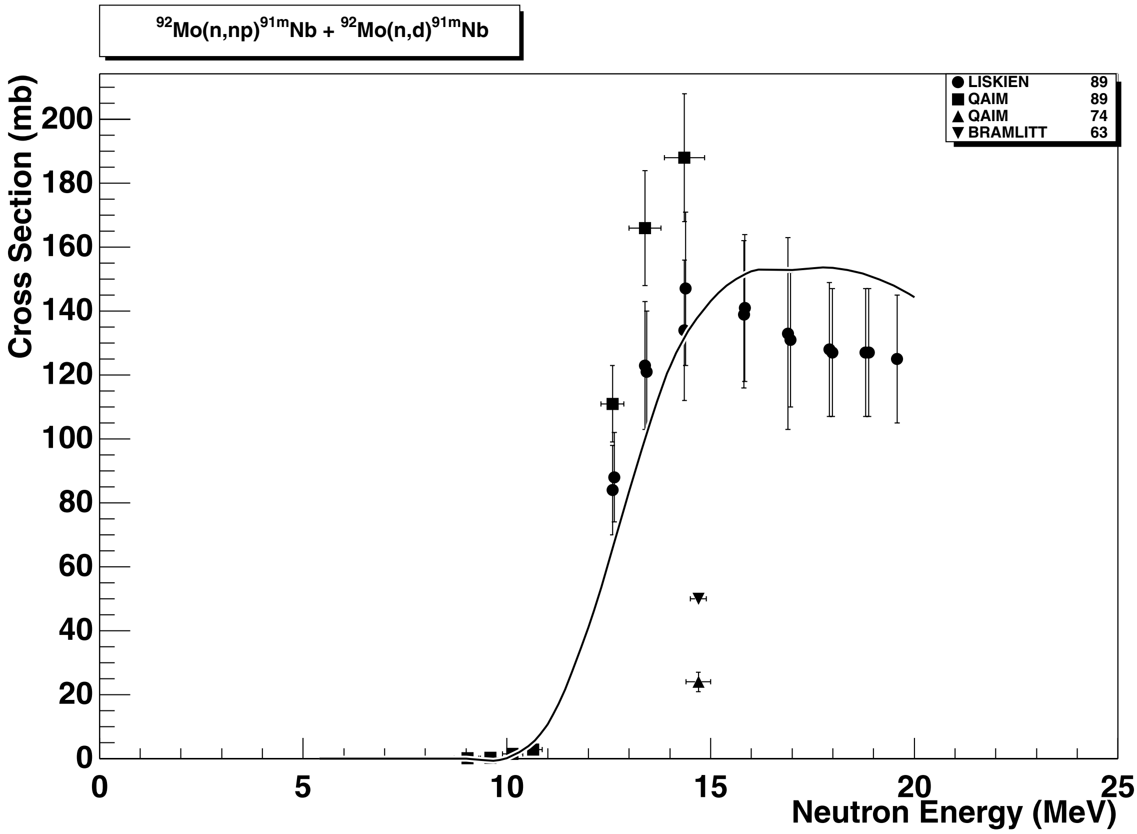

2.131. ^{92}Mo (n,d+np) ^{91}Nb

final states: meta
source: RNAL

The reaction leading to the first isomeric state is the reference reaction. Slightly adjusted calculations performed with the EMPIRE-2.13[36] code are fairly close to the most recent experimental data. The two old measurements (Qaim74 and Bramlitt63) are considered too low. The data are stored as a sum of the (n,d) and (n,np) reaction channels using threshold of the (n,d) reaction.

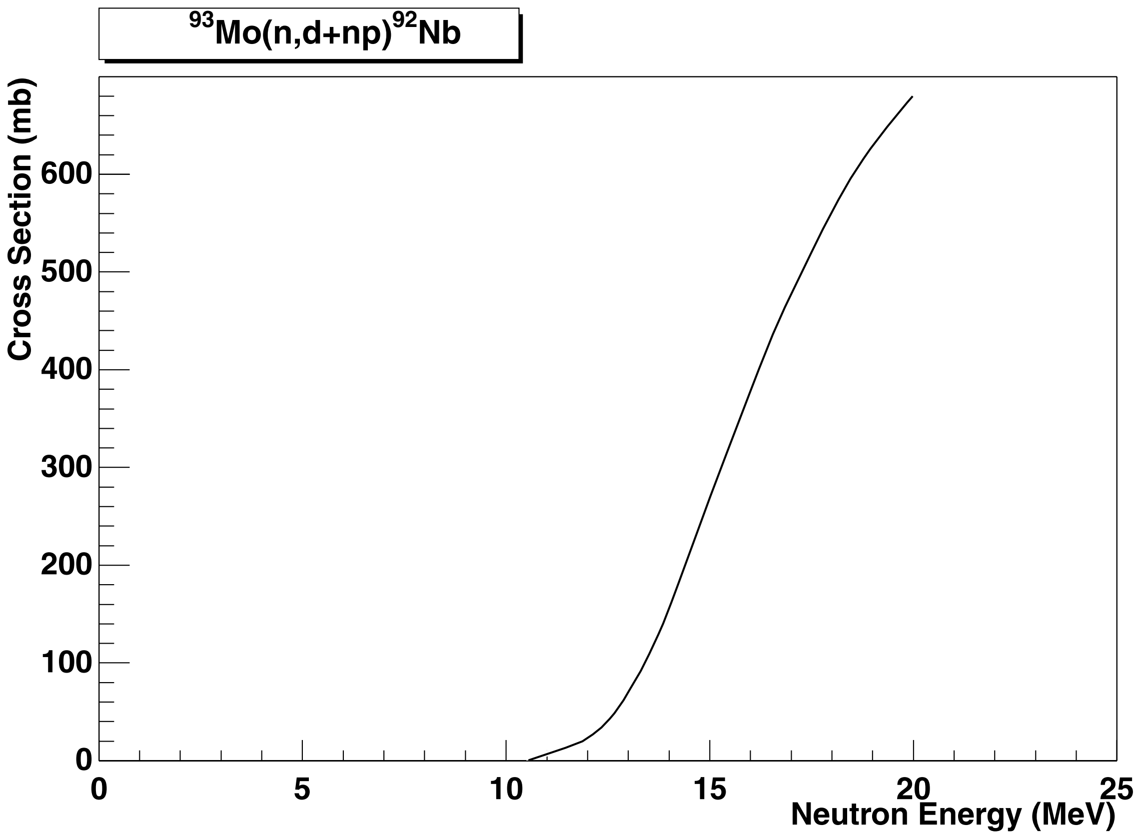

2.132. ^{93}Mo (n,d+np) ^{92}Nb

final states: g.s., meta
source: ADL-3

ADL-3 evaluation with no EXFOR data. Partial cross-sections to the g.s. and meta state are based on the model calculations. The data are stored separately as (n,d) and (n,np) reaction channels.

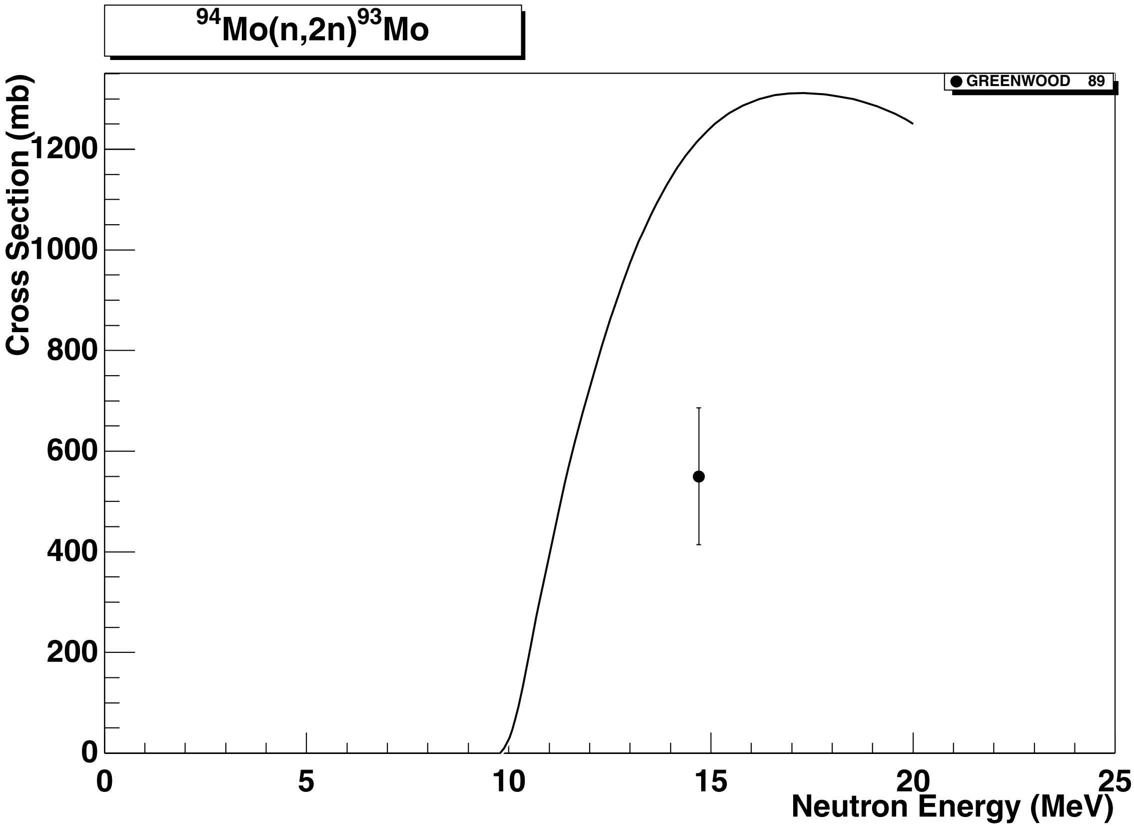

2.133. ^{94}Mo (n,2n) ^{93}Mo

final states: g.s., meta
source: ADL-3

ADL-3 evaluation is adopted. The only experimental value of the total cross section is the single point of Greenwood89, which underestimates the evaluation and the 14.5 MeV systematics by about a factor of two. Apparently, the value from the systematics was used to normalize the model calculation. All other experimental data of this reaction are the isomeric cross-sections, with values around 5 mb. A new measurement of the total cross-section is urgently needed to verify the value of Greenwood89 and to use it eventually for the renormalization. Partial cross-sections to the g.s. and meta state are based on the model calculations.

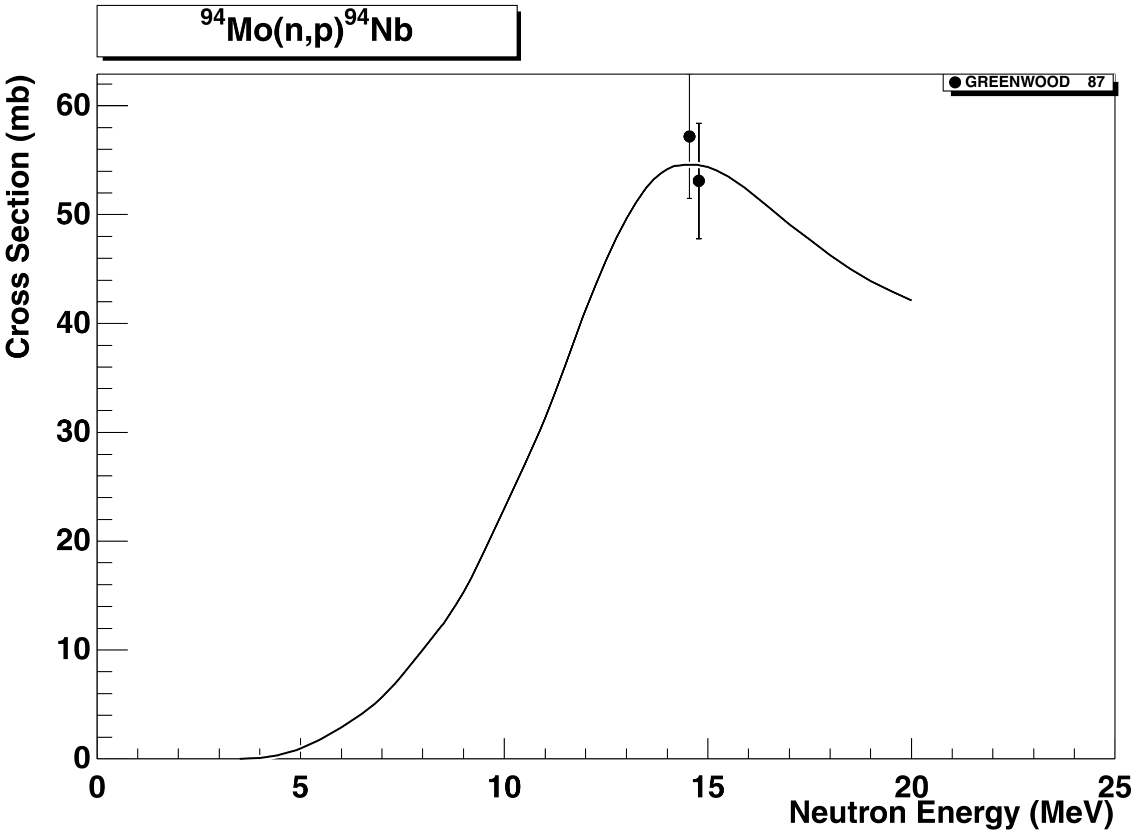

2.134. ^{94}**Mo (n,p)** ^{94}**Nb**

final states: g.s., meta
source: CRP

The evaluation originates from the IAEA CRP on long lived nuclides . Two experimental points of Greenwood87 at 15 MeV are well reproduced. Partial cross-sections to the g.s. and meta state based on the model calculations.

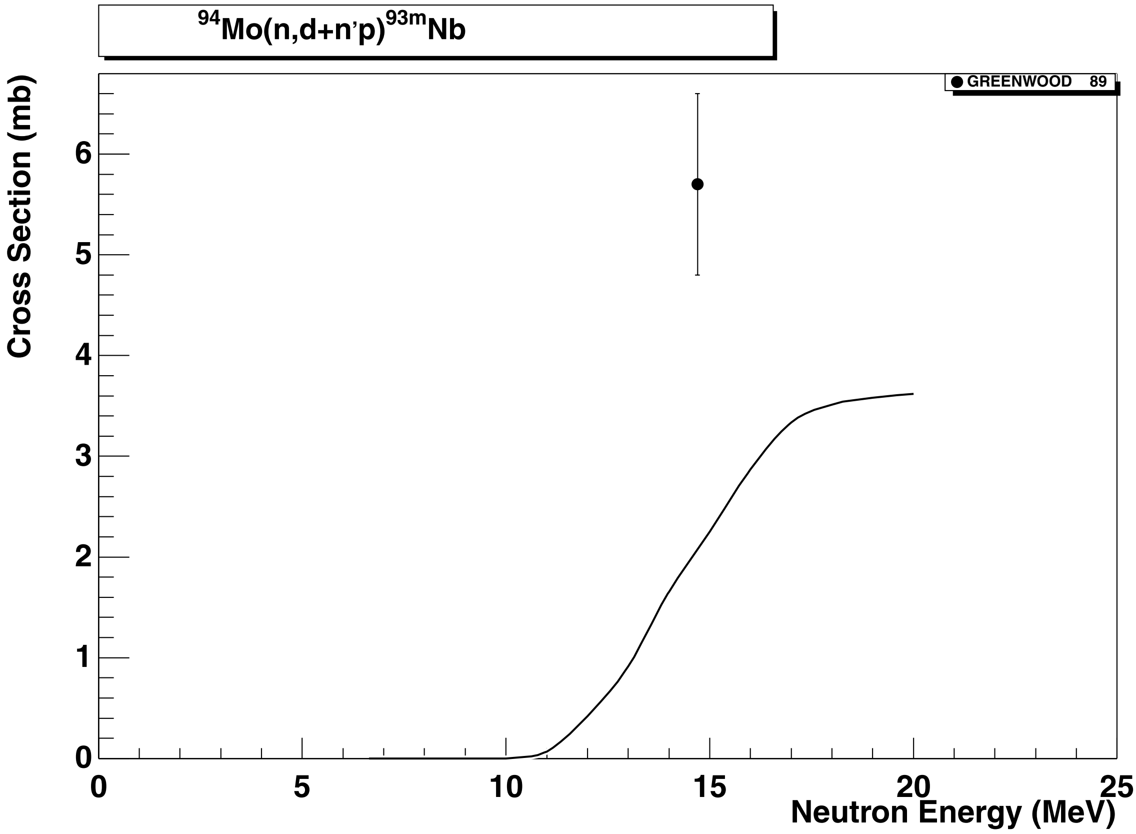

2.135. ^{94}Mo (n,d+np) ^{93m}Nb

final states: meta
source: ADL-3

The (n,d+np) reaction leading to the first isomeric state is the reference reaction. ADL-3 evaluation is adopted with partial cross-sections to the g.s. and meta state based on the model calculations. The calculated excitation function to the first isomeric state severely underestimates the single experimental point of Greenwood89, which is supported by the earlier value of (9 +- 3) mb from Ref. [39]. A renormalization of the branching ratio is recommended. The data are stored separately as (n,d) and (n,np) reaction channels.

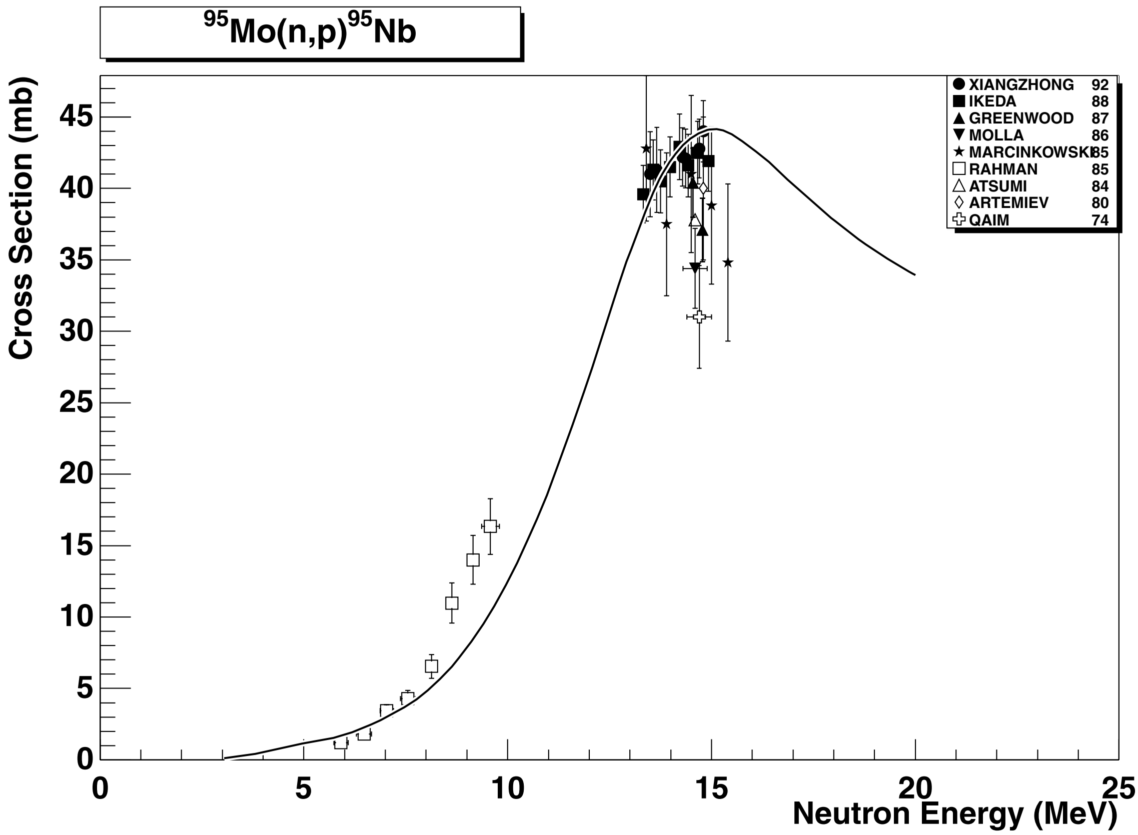

2.136. ^{95}Mo (n,p) ^{95}Nb

final states: g.s., meta
source: ADL-3

ADL-3 runs reasonably through the experimental points, in particular the latest data of Xiangzhong92 and Ikeda88 around 15 MeV. A small shape disagreement with three points of Rahman85 around 9 MeV is noted.

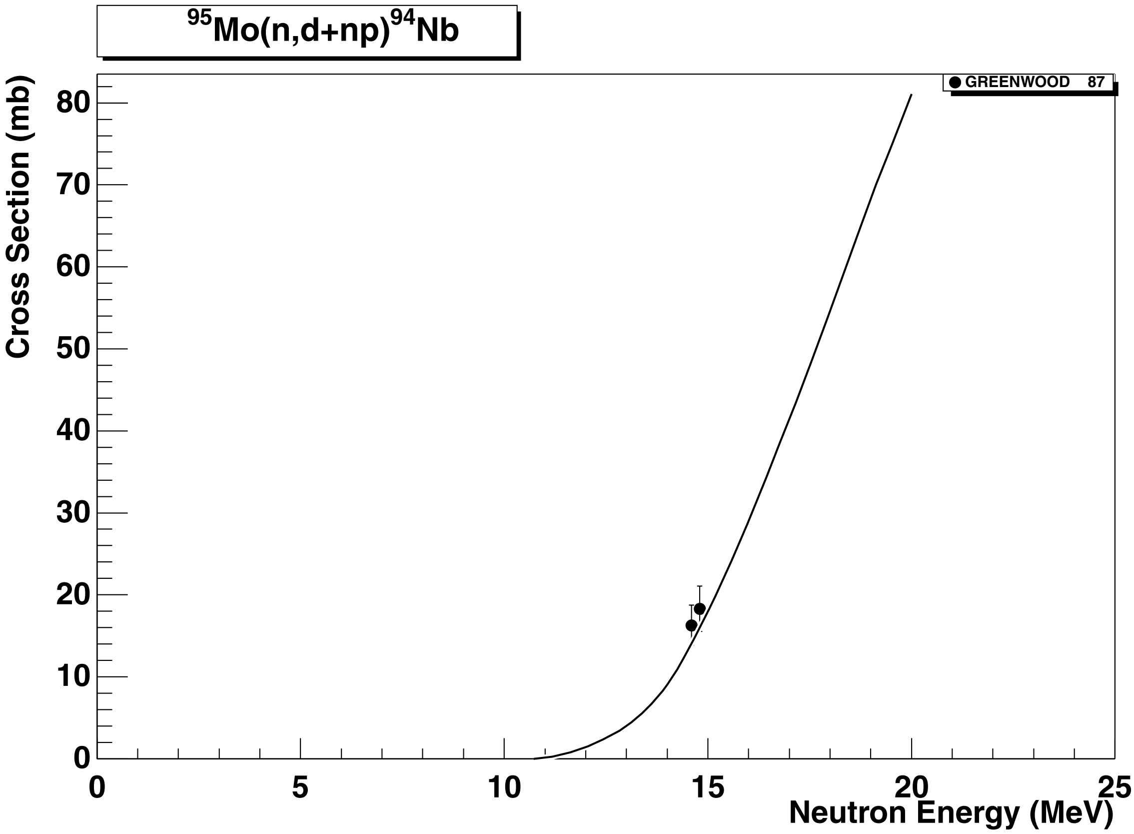

2.137. ^{95}Mo (n,d+np) ^{94}Nb

final states: g.s., meta
source: ADL-3

ADL-3 nicely agrees with two experimental points of Greenwood87 at 15 MeV. Partial cross-sections to the g.s. and meta state are based on the model calculations. The data are stored separately as (n,d) and (n,np) reaction channels.

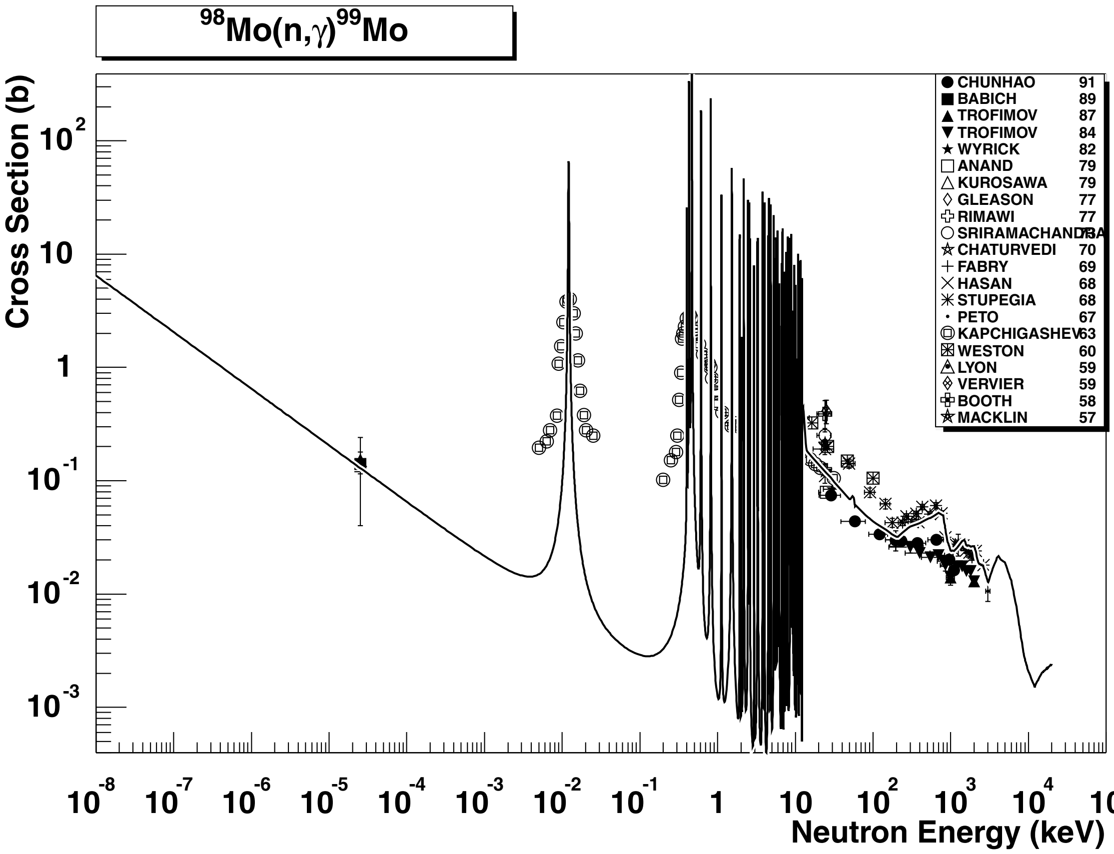

2.138. ^{98}Mo (n,γ) ^{99}Mo

final state: total
source: EAF-4.1 (JEF-2.2)

The JEF-2.2 evaluation reproduces well the thermal region and runs reasonably close to experimental data above 10 keV. However, it seems that this statistical component has been adjusted to the older data (e.g. Stupegia68), which between 200 keV and 1 MeV slightly overestimate more recent data of Chunhao91 and Trofimov84,87.

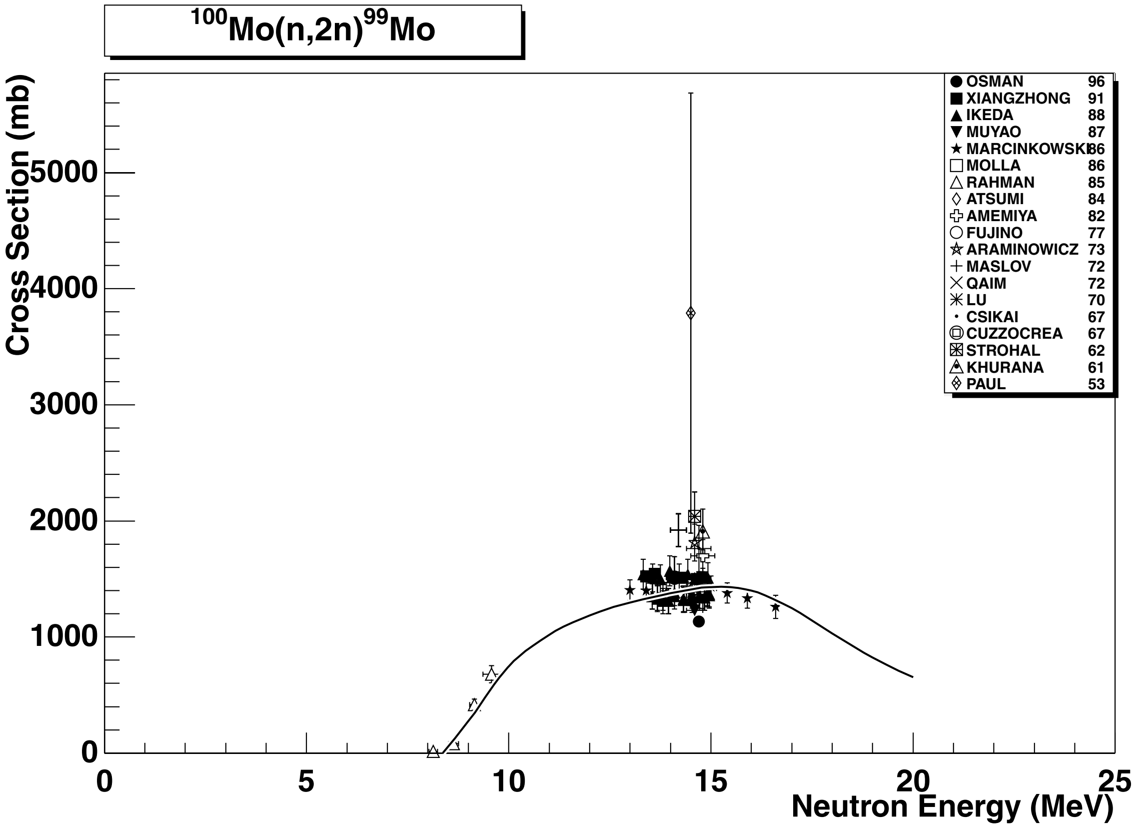

2.139. ^{100}Mo(n,2n) ^{99}Mo

final state: total
source: JENDL-Act96

JENDL-Act96 agrees well with all experimental data.

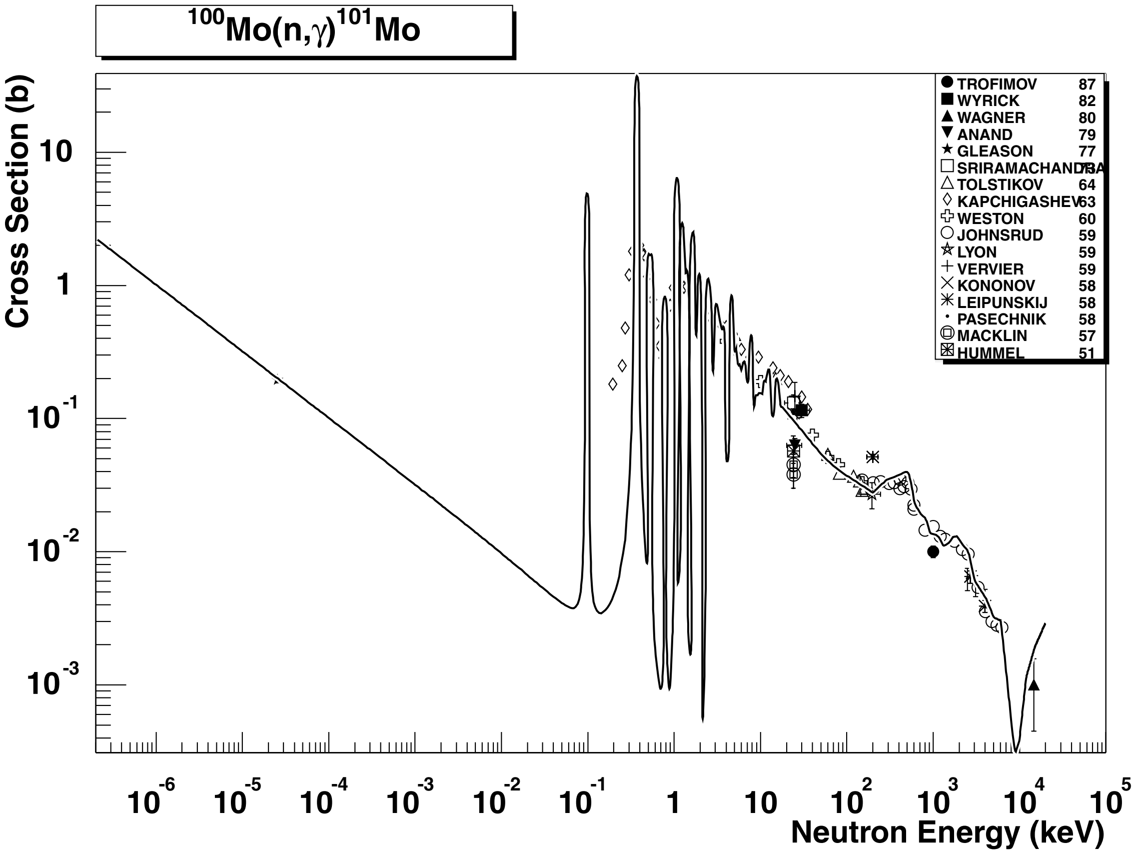

2.140. ^{100}Mo(n,γ) ^{101}Mo

final state: total
source: EAF-4.1 (JEF-2.2)

This is the JEF-2.2 evaluation, which is stored in the SANDII structure. The original evaluation includes 20361 data points. The thermal- as well as the smooth statistical regions are in a good agreement with all experimental data.

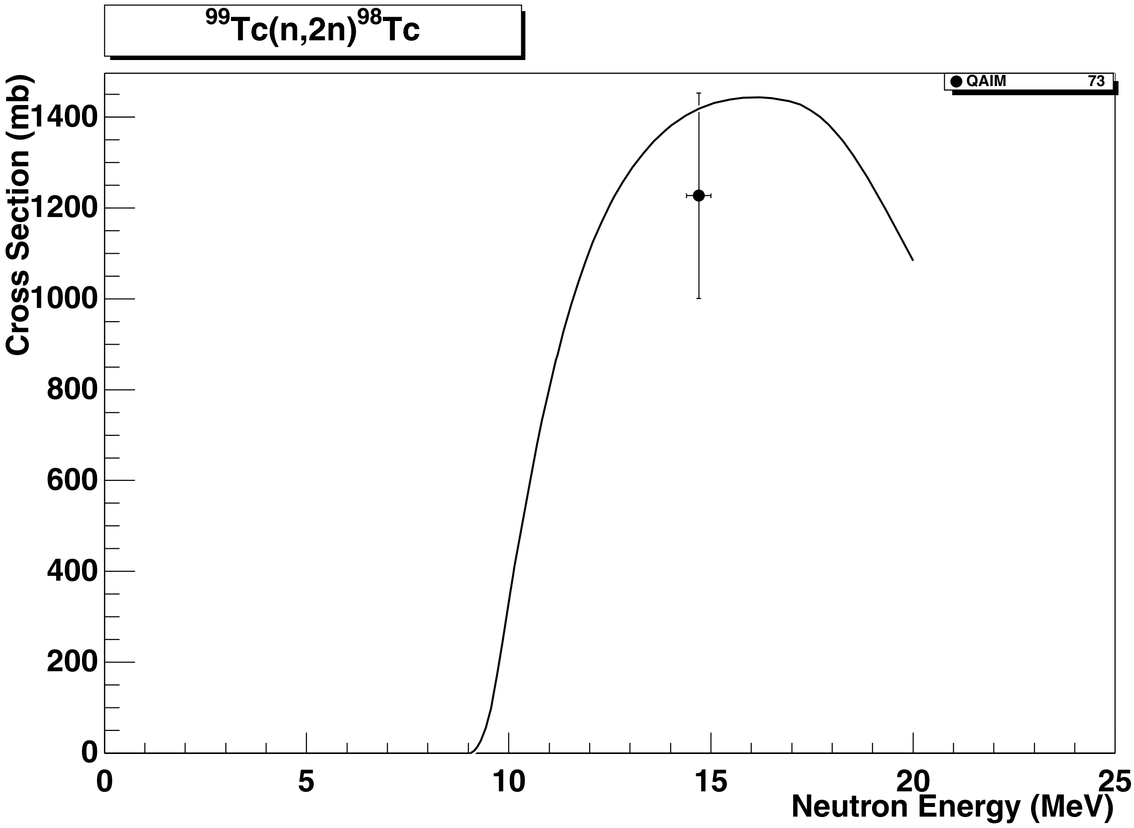

2.141. ^{99}Tc (n,2n) ^{98}Tc

final state: total
source: ADL-3

ADL-3 evaluation is supported by the single experimental point of Qaim73 at about 15 MeV.

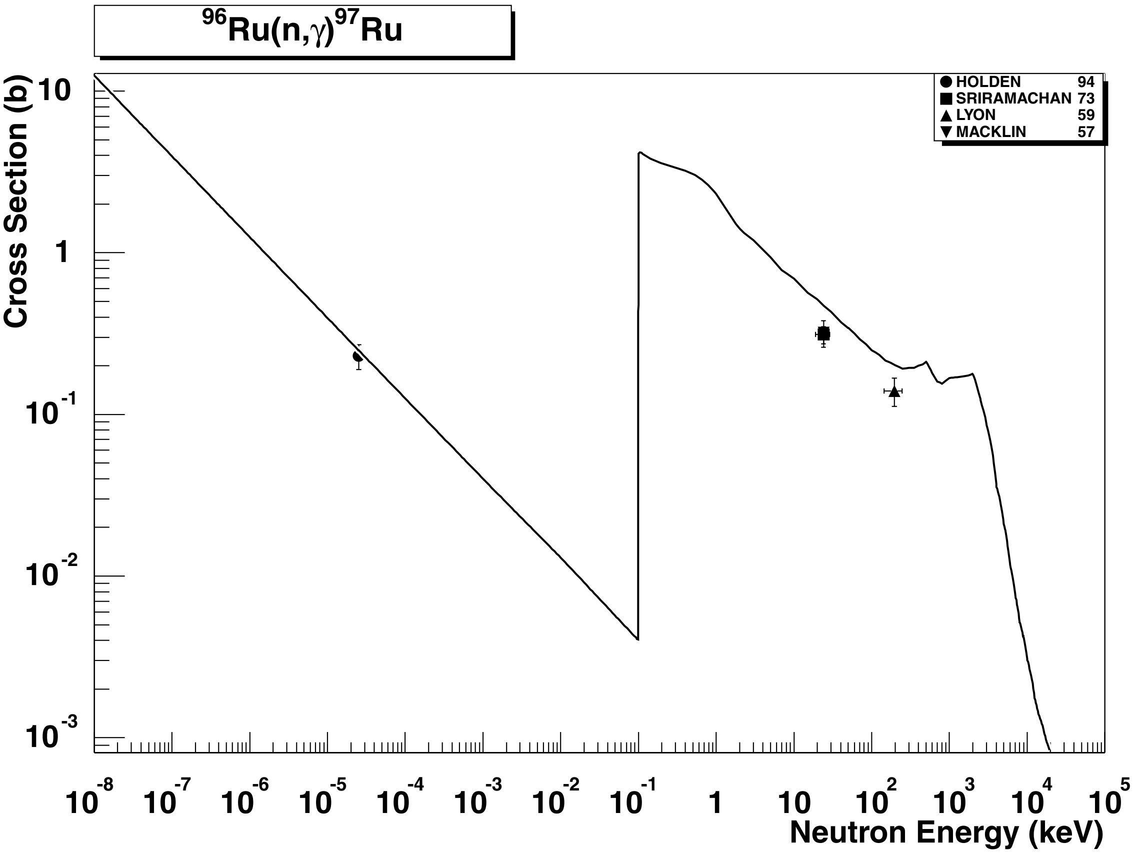

2.142. ^{96}Ru (n,γ) ^{97}Ru

final state: total
source: EAF-4.1 (JEF-2.2)

Data originate from the revised ENDF/B-V evaluation. A simplified evaluation, no resolved resonance are available. The thermal cross-section of Holden [32] is reproduced with C/E=0.99. The statistical component is reasonably close to three experimental data points at about 10 keV and 200 keV.

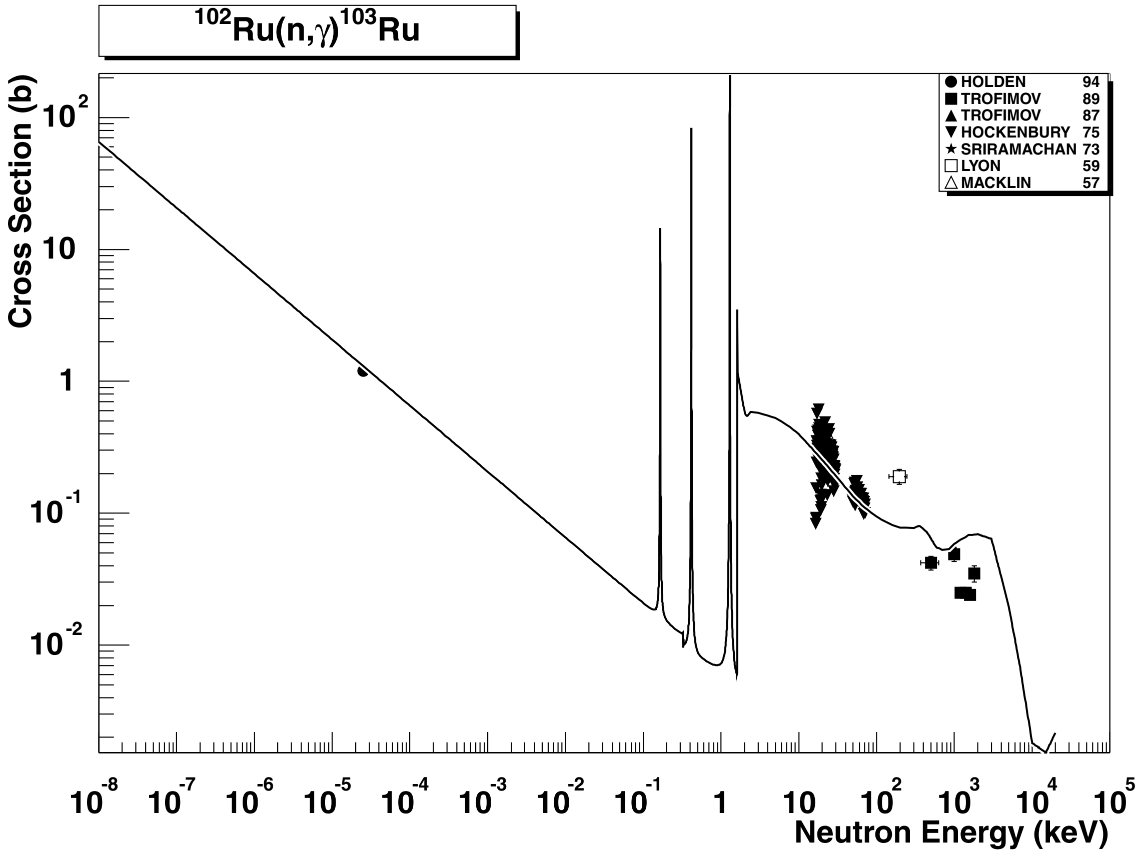

2.143. ^{102}Ru(n,γ) ^{103}Ru

final state: total
source: EAF-4.1 (JEF-2.2)

This is again a revised ENDF/B-V evaluation. The thermal cross-section of Holden94 from Ref. [32] is reproduced with C/E=1.07. The evaluation runs reasonably in the middle of experimental data between 10 keV and 1 MeV. The few last points of Trofimov89 (above 1 MeV) are slightly below the excitation curve.

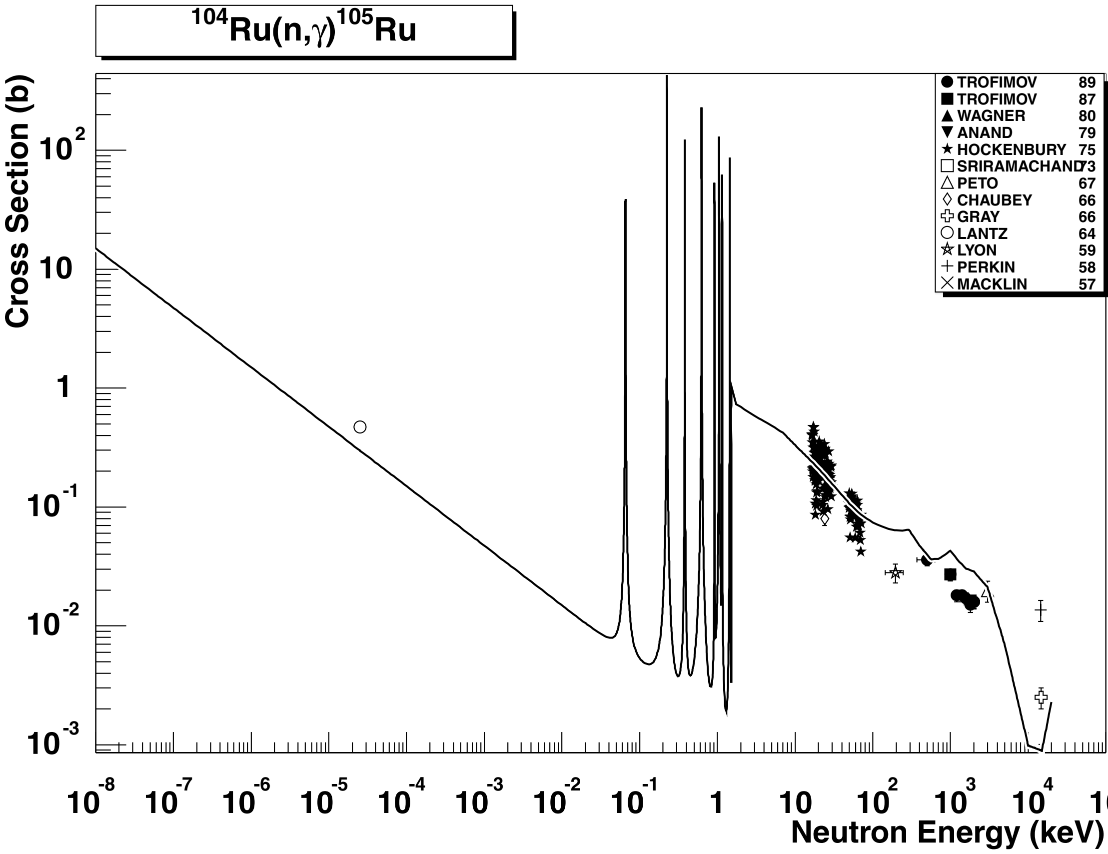

2.144. ^{104}Ru (n,γ) ^{105}Ru

final state: total
source: EAF-4.1 (JEF-2.2)

The JEF-2.2 evaluation reasonably reproduces the experimental data in the region between 10 keV and 3 MeV. The thermal cross-section of Lantz64 is about 30% underestimated. The 14 MeV experimental point of Perkin58 may be disregarded, it is larger than Gray66 by a factor of five and ten times larger than the 14.5 MeV systematics.

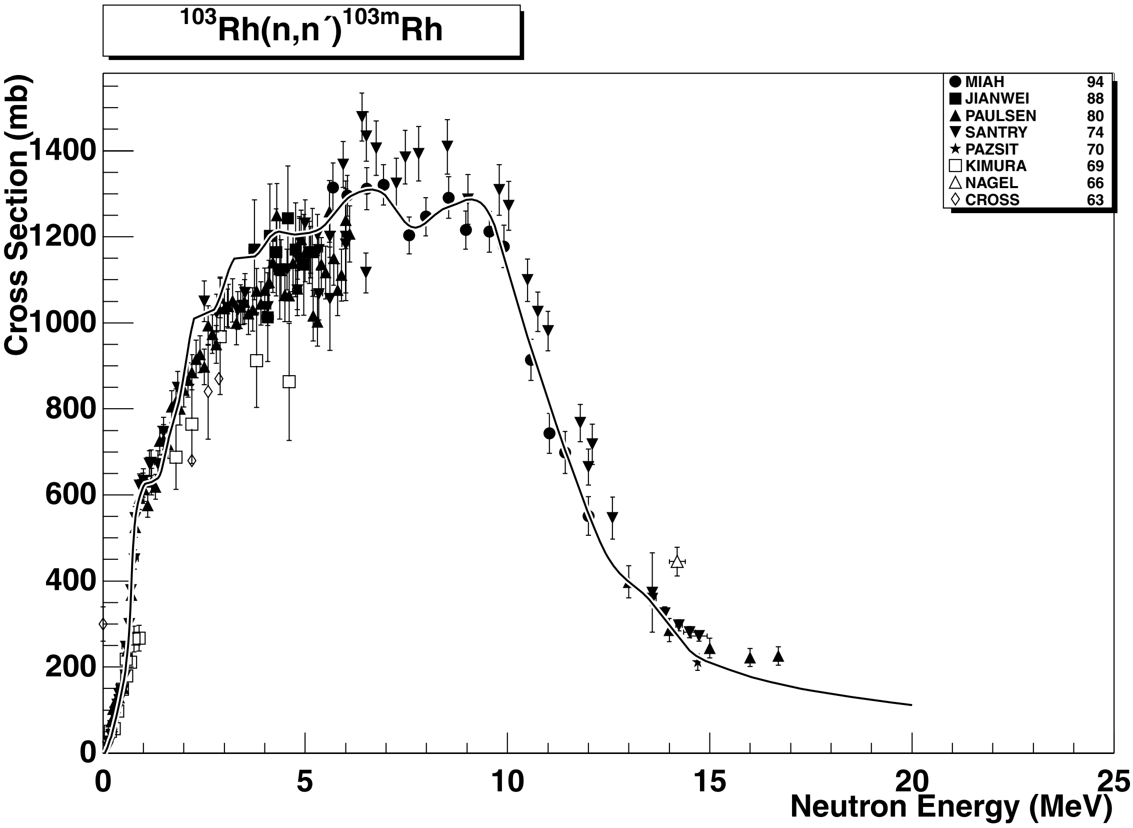

2.145. ^{103}Rh (n,n') ^{103m}Rh

final state: meta
source: IRK [40]

The new update [40] of this reaction data is available and has been adopted. The experimental data are well reproduced in the whole energy range.

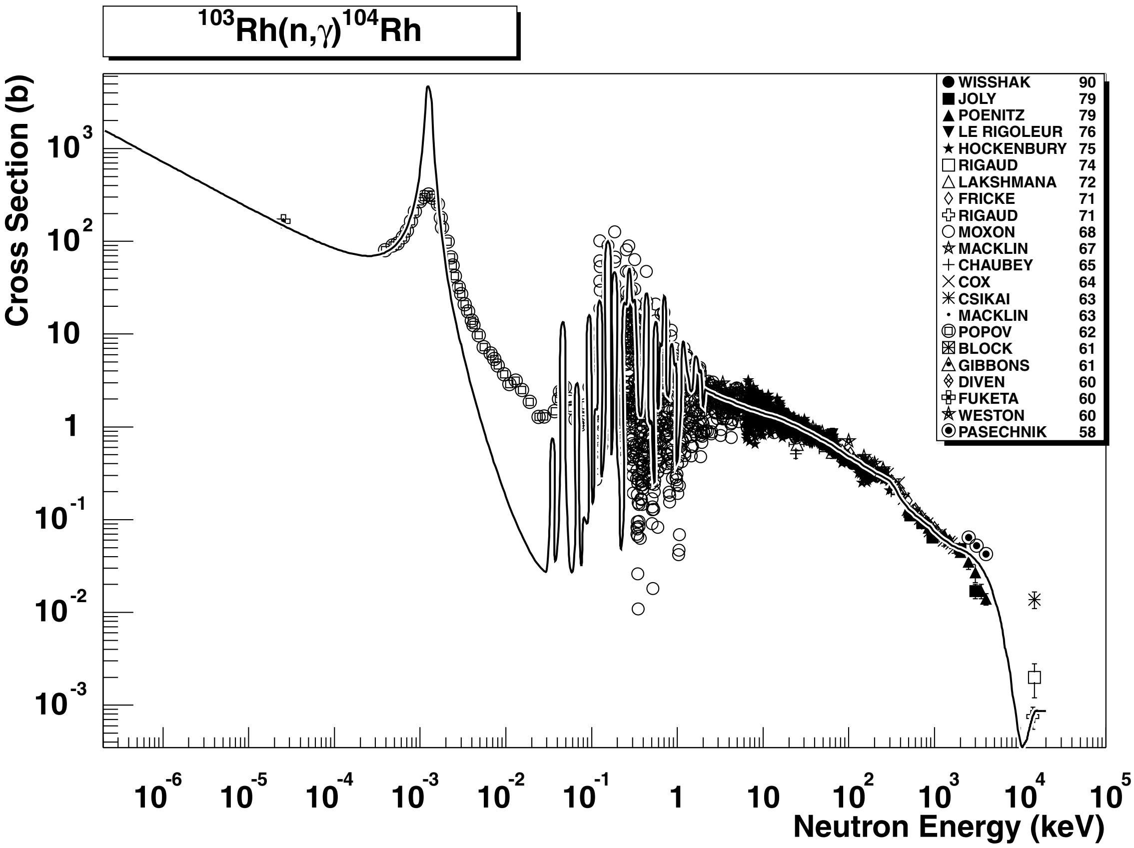

2.146. ^{103}Rh (n,γ) ^{104}Rh

final states: g.s., meta
source: EAF-4.1 (JEF-2.2)

The JEF-2.2 evaluation reasonably reproduces the experimental data in the whole energy region. The data around the first resonance are measured with finite resolution. The value of Csikai63 at 14 MeV may be disregarded, it is about ten times larger than the other values or the systematics. The data are stored in the SANDII structure. The original evaluation includes 21072 data points.

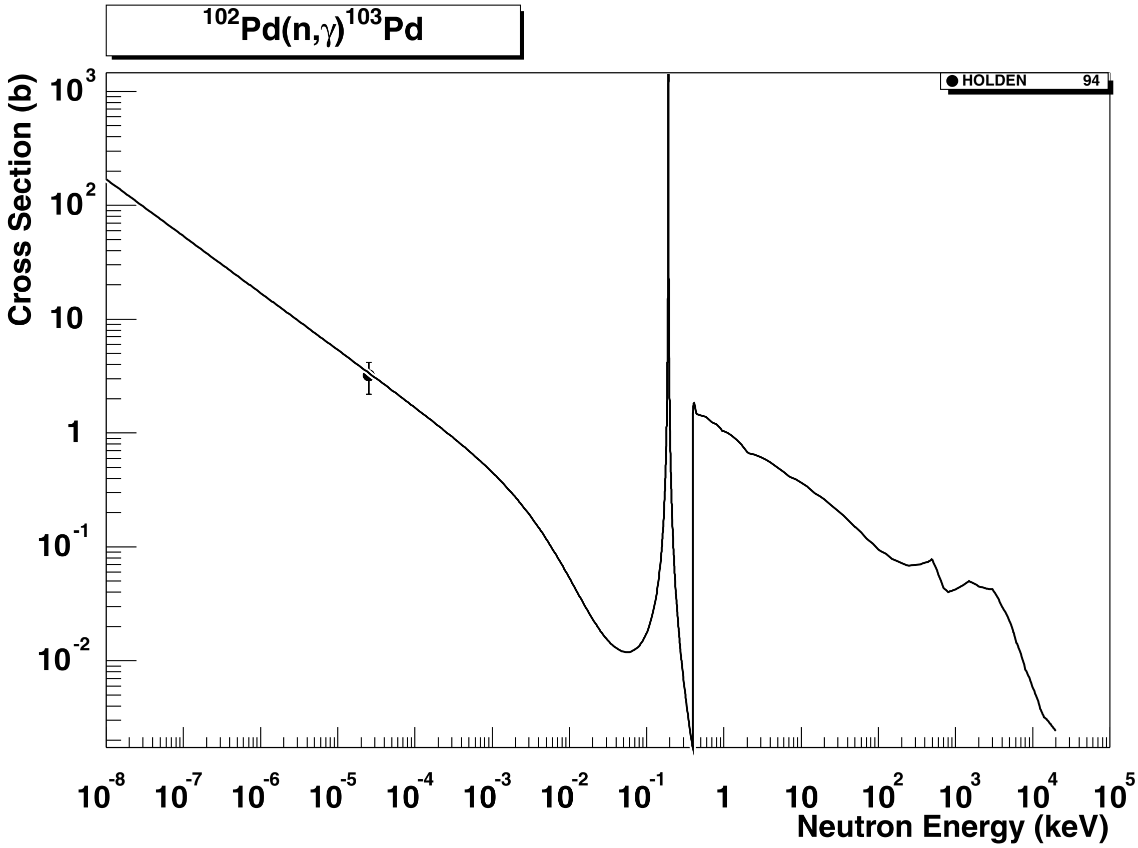

2.147. ^{102}Pd (n,γ) ^{103}Pd

final state: total
source: EAF-4.1 (JEF-2.2)

This is a simplified (a single resonance in the resolved resonance region) evaluation, which originates from ENDF/B-V. No EXFOR data are available. The thermal cross section of Holden94 [32] is reproduced with C/E=0.99. The smooth statistical component is supported by the recommended 30 keV cross-section from Ref. [27].

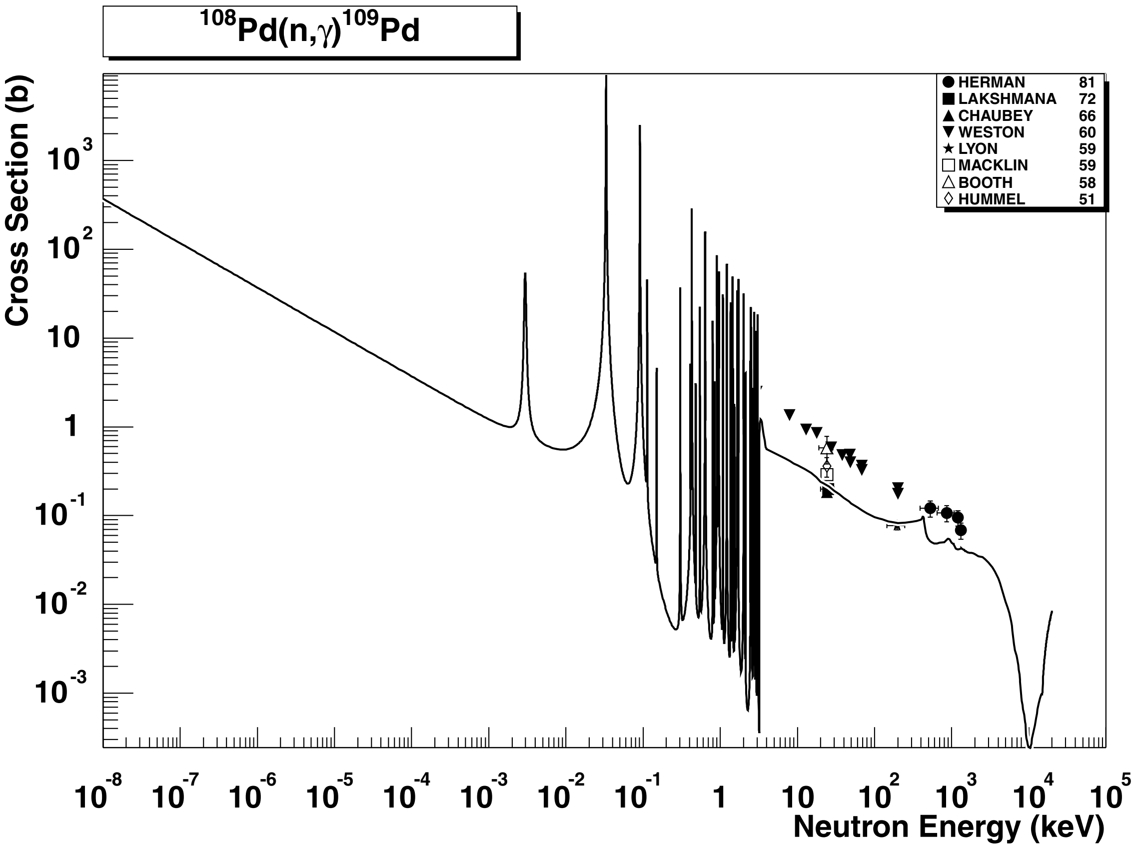

2.148. ^{108}Pd (n,γ) ^{109}Pd

final states: g.s., meta
source: EAF-4.1 (JEF-2.2)

The JEF-2.2 original evaluation. Branching ratio between the g.s. and meta state is based on experimental data (thermal cross-sections from [26]) applied up to the end of the resolved resonance region, and on the energy dependent branching ratio systematics [2] for the high energy region. The total and partial thermal cross-sections are reproduced with C/E=0.87. The statistical component agrees with the data of Lakshama72, Chaubey66 and Macklin59, but underestimates two consistent sets of data, Weston60 and Herman81. Probably an upwards renormalization of this component may be recommended.

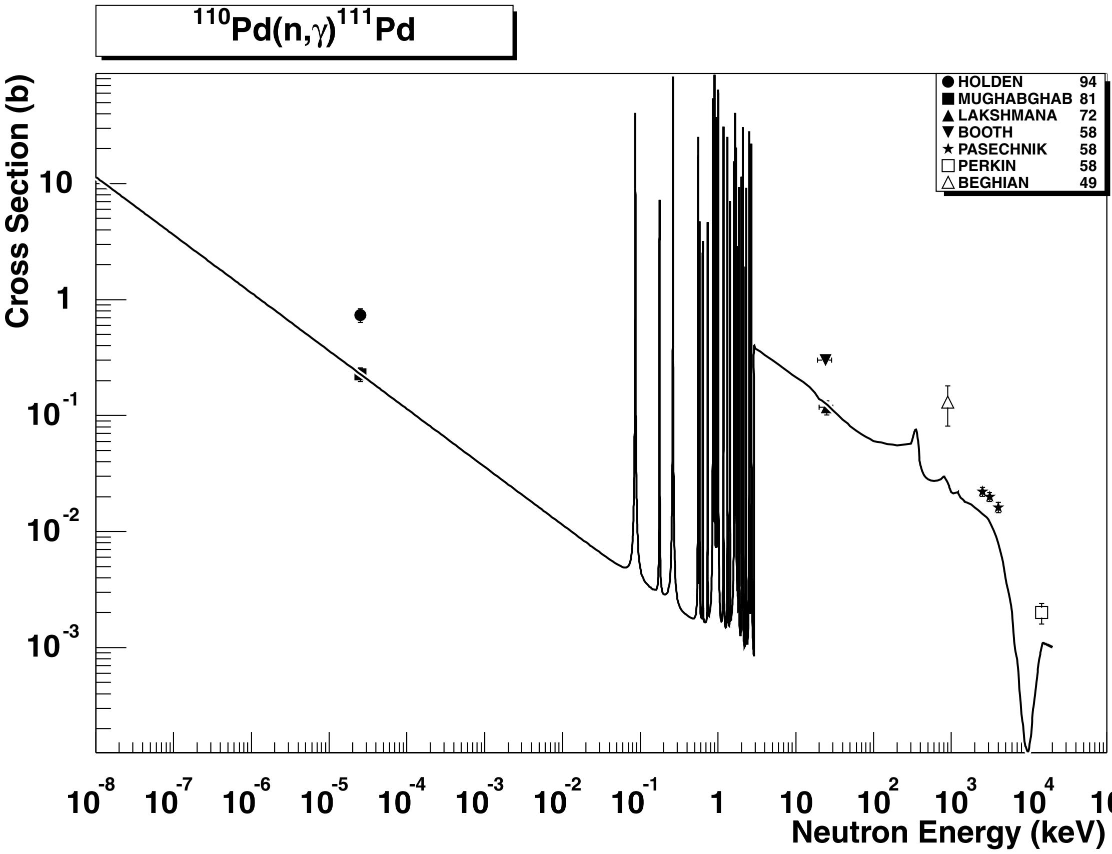

2.149. ^{110}Pd (n,γ) ^{111}Pd

final states: g.s., meta
source: EAF-4.1 (JEF-2.2)

This is the JEF-2.2 evaluation. Branching ratio between the g.s. and meta state is based on the energy dependent branching ratio systematics [2] for the whole energy region. The total thermal cross-sections of Mughabghab81 [31] is reproduced with C/E=1.00 but more reliable Holden94 point is 3 times higher. The evaluation is also below the few scattered high energy data above 20 keV. Therefore, reevaluation is recommended.

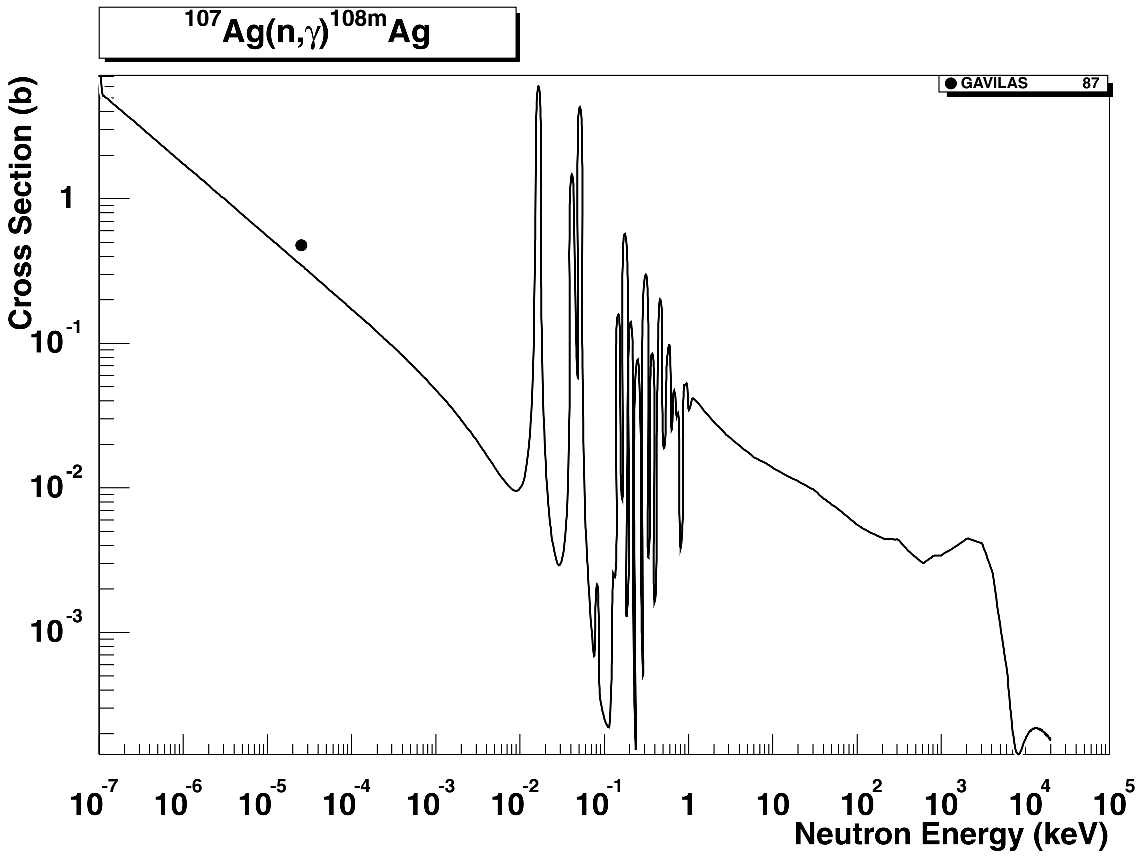

2.150. ^{107}Ag (n,γ) ^{108m}Ag

final state: meta
source: EAF-4.1 (JEF-2.2)

The reaction leading to the first isomeric state is the reference reaction. A revised ENDF/B-V evaluation is adopted with partial cross-sections to the g.s. and meta state based on experimental data (from [26]) and the deduced branching ratio applied up to the end of the resolved resonance region, and the energy dependent branching ratio systematics [2] for the high energy region. The total and partial thermal cross-sections are reproduced with C/E=1.05. The value of Gavilas87 is slightly above the recommended value of 370 $\pm$ 80 mb from [26], which is well reproduced by the evaluation. The 30 keV cross-section from [27] supports the magnitude of the statistical component at this energy for the total cross-section. The data are stored in the SANDII structure. The original evaluation includes 10551 data points.

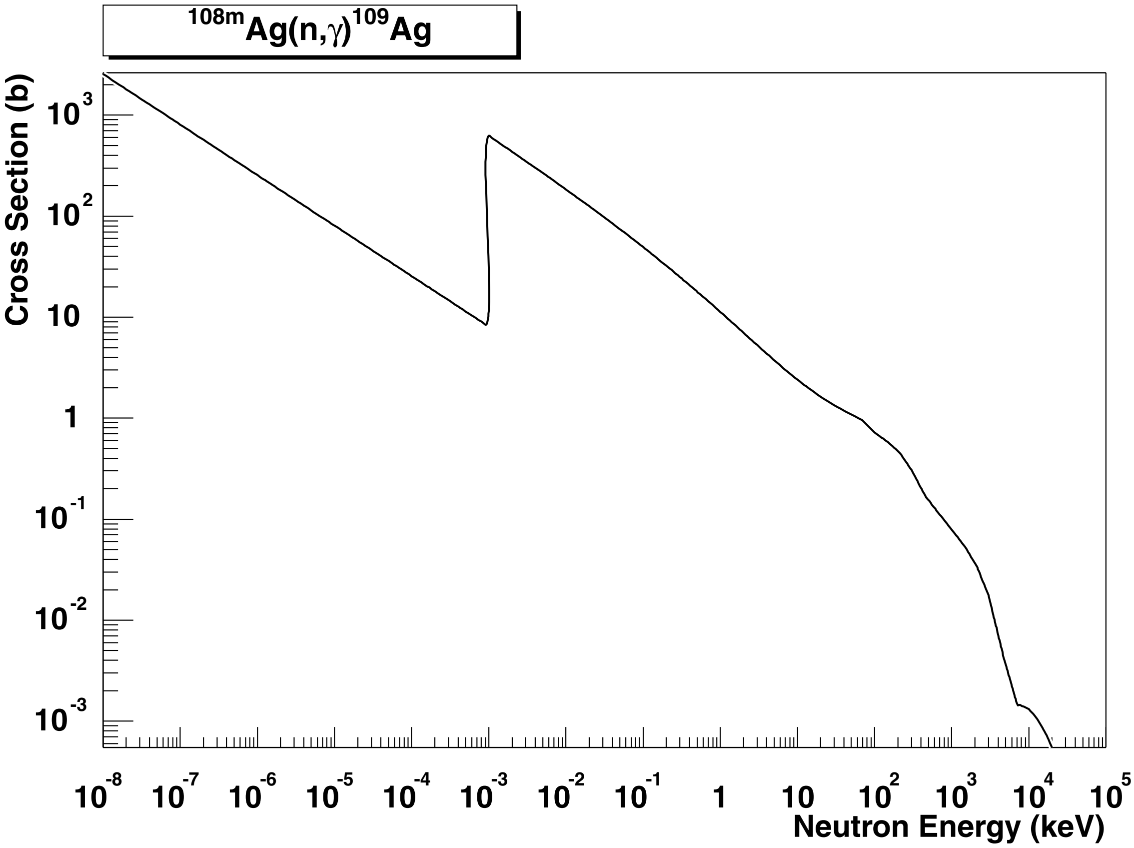

2.151. ^{108m}Ag (n,γ) ^{109}Ag

final states: g.s., meta
source: EAF-4.1

In this reaction it is the first isomeric state which is the target nucleus. No experimental data are available, also not for the thermal range. Evaluation is based on the simplified model calculations with the code MASGAM and the global parameters (Hauser-Feshbach and DSD model with no resonance region generation, E_H is based on a $D_0/2$ estimate; for details see [35]) assumed to be equal to those for the target ground state. The thermal cross-section is based on a very crude systematic [35] and is rather uncertain.

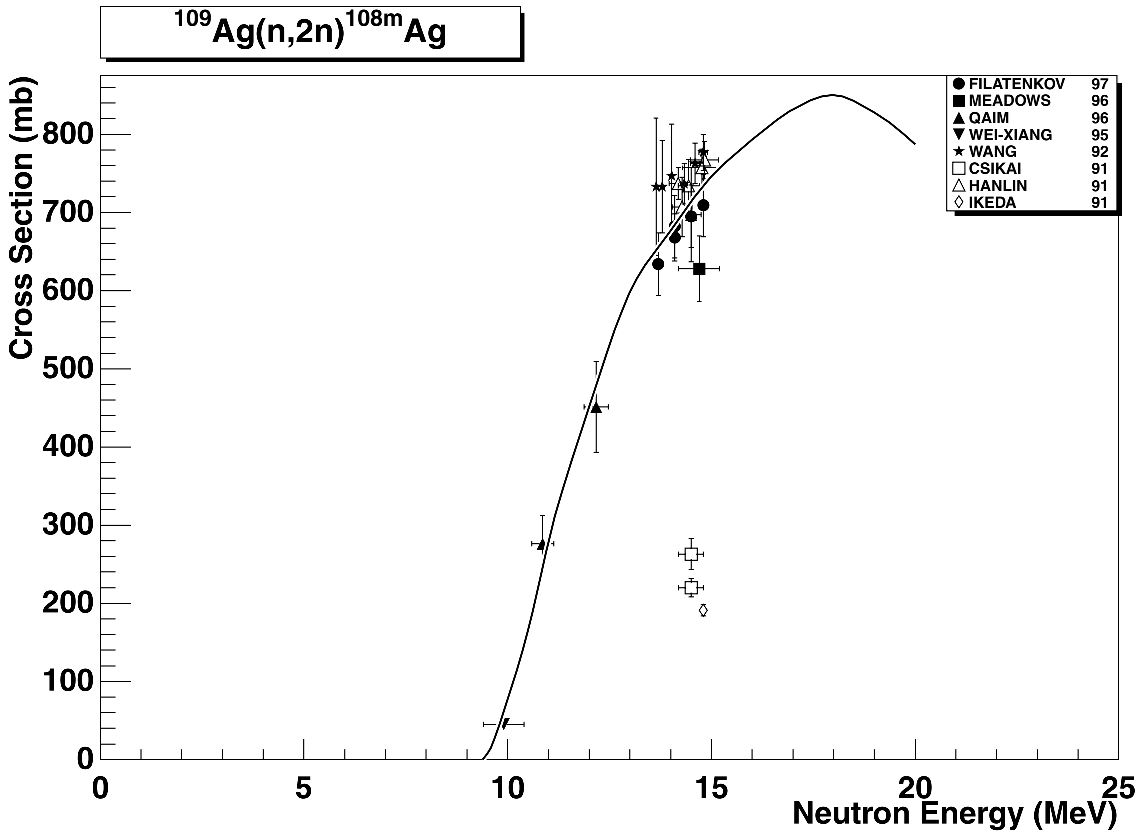

2.152. ^{109}Ag (n,2n) ^{108m}Ag

final state: meta
source: CRP

The reaction leading to the first isomeric state is the reference reaction. The adopted evaluation (resulting from the IAEA CRP on long lived nuclei) runs through the most recent data. Experimental data of Ikeda91 and Csikai91 shown on the plot were obtained using wrong lifetime for ^{108m}Ag. These results, when renormalized to the proper lifetime, agree with the remaining data and confirm the selected evaluation.

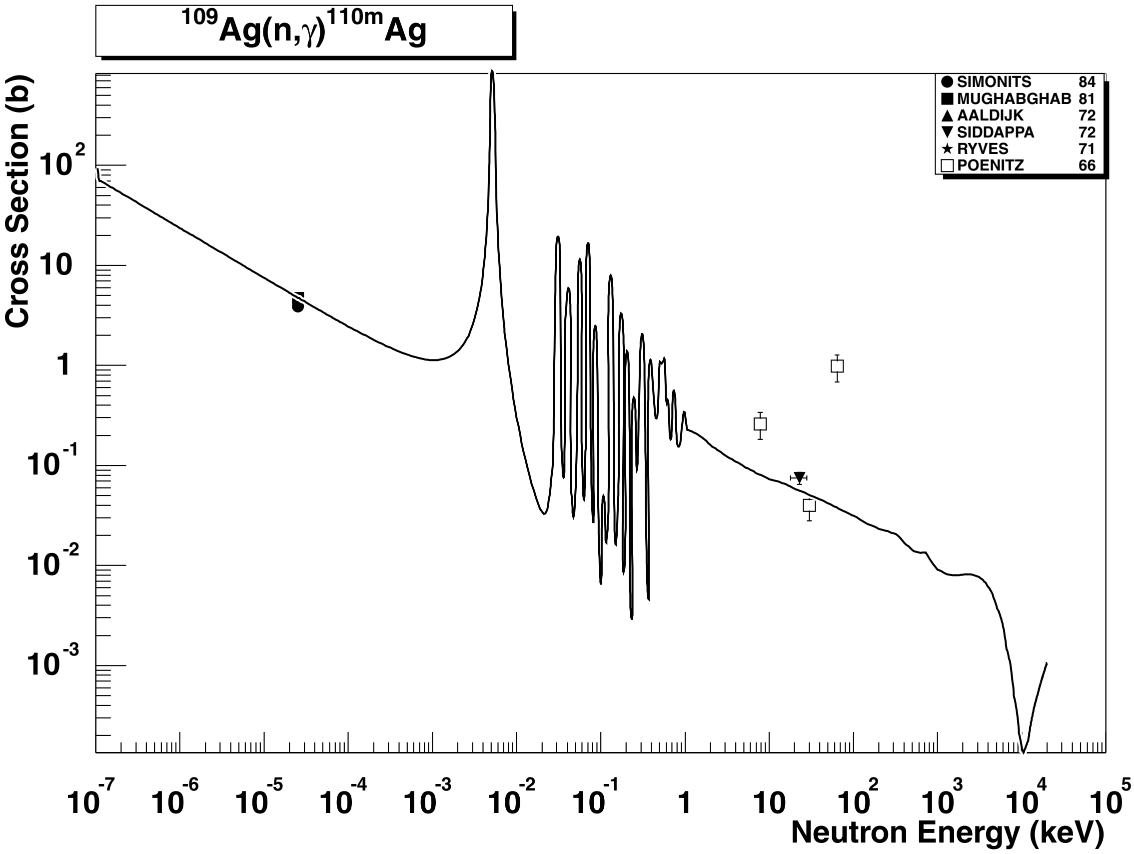

2.153. ^{109}Ag (n,γ) ^{110m}Ag

final state: meta
source: EAF-4.1 (JEF-2.2)

The reaction leading to the first isomeric state is the reference reaction. The original JEF-2.2 evaluation is adopted with partial cross-sections to the g.s. and meta state based on thermal data (from [26]) and the deduced branching ratio applied up to the end of the resolved resonance region, and the energy dependent branching ratio systematics [2] for the high energy region. The thermal cross-sections of Simonits84 and Mughabghab81 are well reproduced. In the smooth statistical region the evaluation runs close to the point of Siddappa72. The three points of Poenitz66 are unphysically scattered. The data are stored in the SANDII structure. The original evaluation includes 11304 data points.

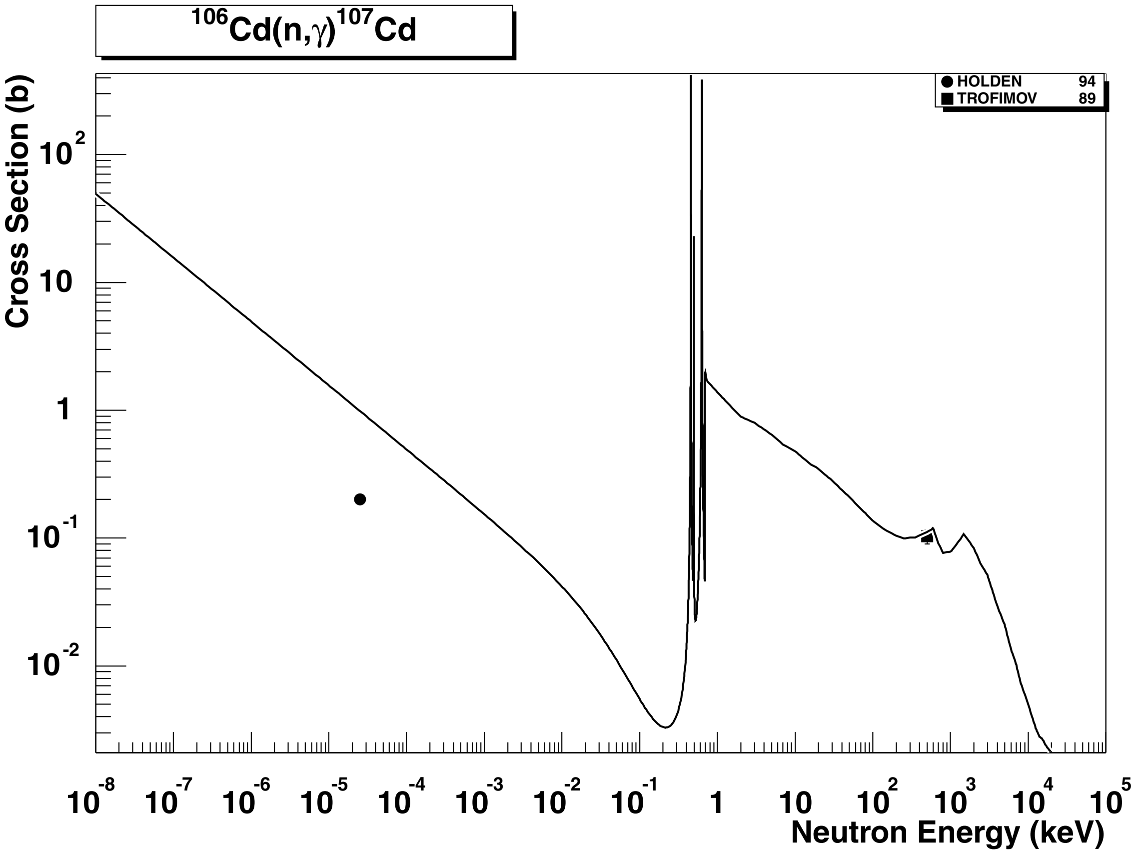

2.154. ^{106}Cd (n,γ) ^{107}Cd

final state: total
source: EAF-4.1 (JEF-2.2)

The ENDF/B-V evaluation has been adopted in JEF-2.2. The 1/v region overestimates the recommended thermal cross-section of Holden94 [32] by C/E=4.92. This is due to a postulated negative resonance, which was introduced in [31] to fit the old value of the thermal cross-section (of about 1 b) measured with reactor neutrons and the prompt method. The parameters of the negative resonance have to be revised. The single experimental point of Trofimov89 at about 500 keV is reproduced well.

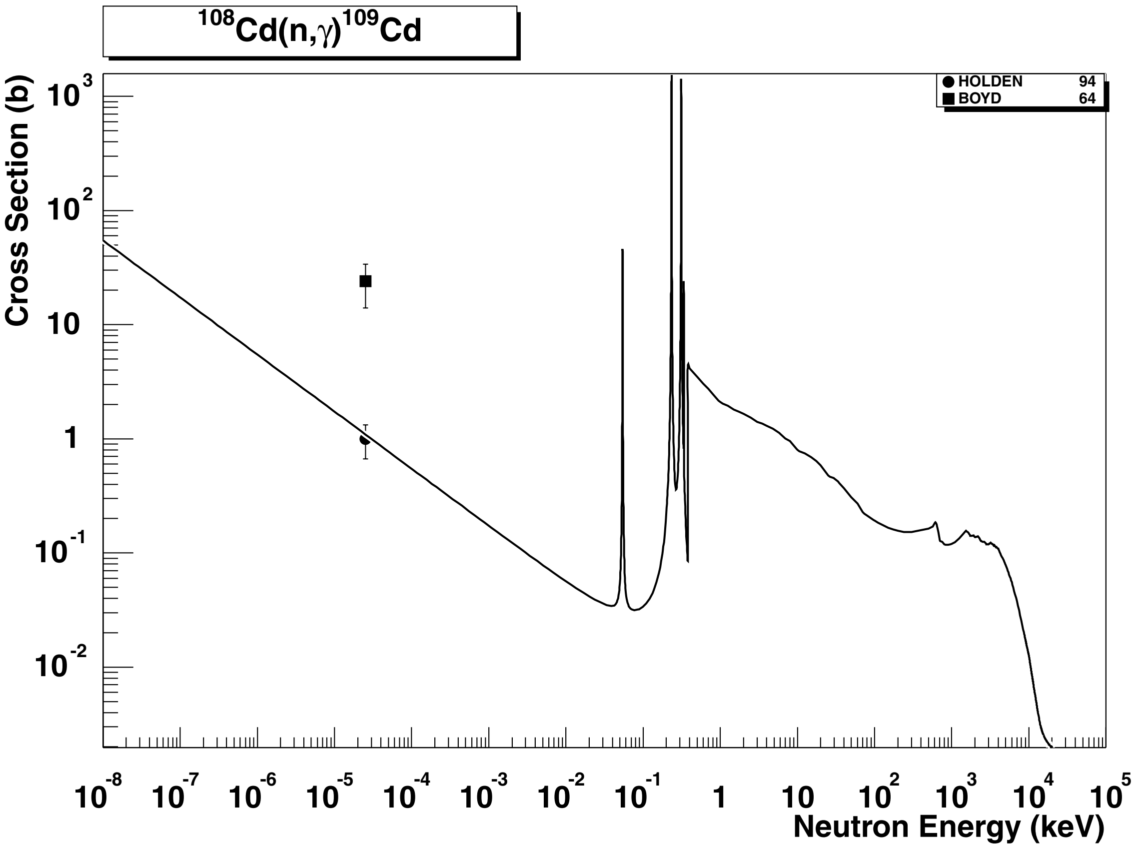

2.155. ^{108}Cd (n,γ) ^{109}Cd

final state: total
source: EAF-4.1 (JENDL-3.1)

The adopted ENDF/B-V evaluation fits the recommended thermal cross-section of Holden94 from [32] with C/E=0.99. The value of Boyd64 is about 20 times larger and can be disregarded. The 30 keV cross-section from [27] supports the statistical component of the excitation curve.

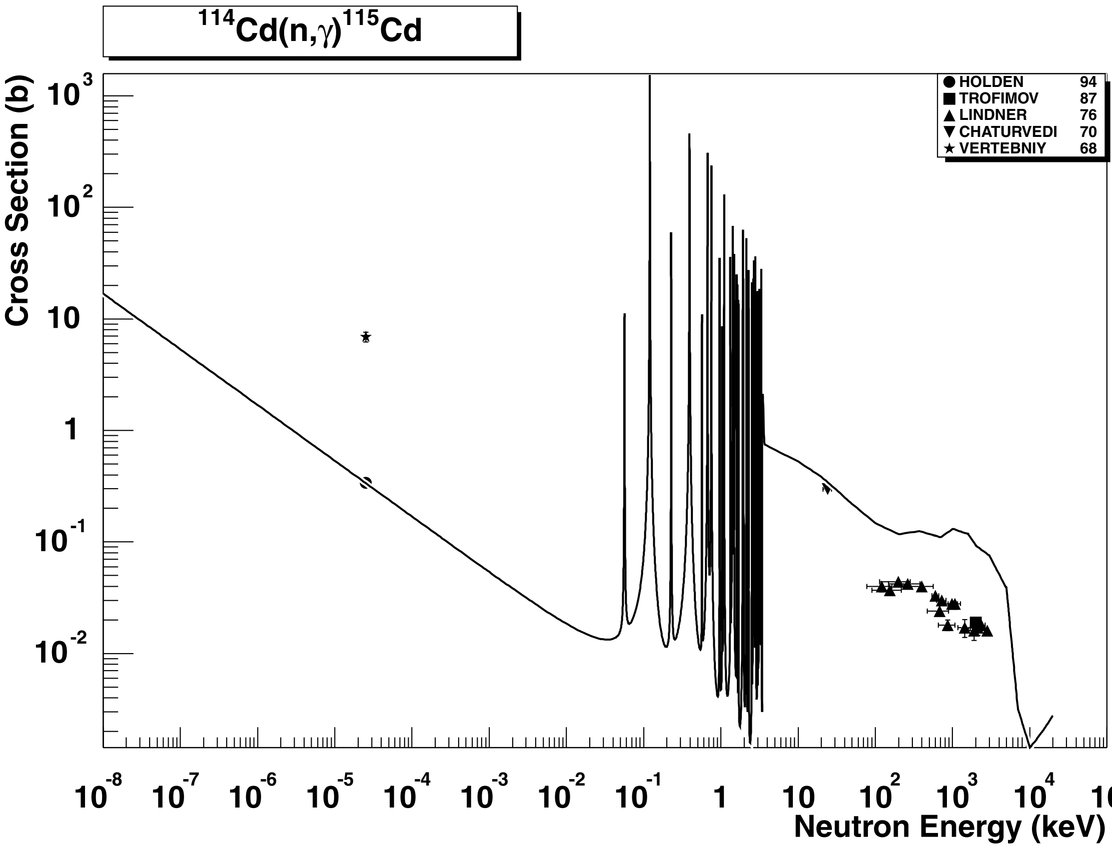

2.156. ^{114}Cd (n,γ) ^{115}Cd

final states: g.s., meta
source: EAF-4.1 (JEF-2.2)

The revised ENDF/B-V evaluation is adopted with partial cross-sections to the g.s. and meta state based on the experimental data (from [26]) and the deduced branching ratio applied up to the end of the resolved resonance region, and the energy dependent branching systematics [2] for the high energy region. The total and partial thermal cross-sections are reproduced with C/E=1.12. The thermal cross-section of Vertebny68 is much larger than the recommended value of σ_γ = 300 $\pm$ 20 mb from [26] and [32]. The smooth statistical component overestimates the data of Lindner76 and Trofimov87 between 100 keV and 3 MeV and most probably should be decreased. The re-evaluation of the data above the end of the resolved resonance region is recommended.

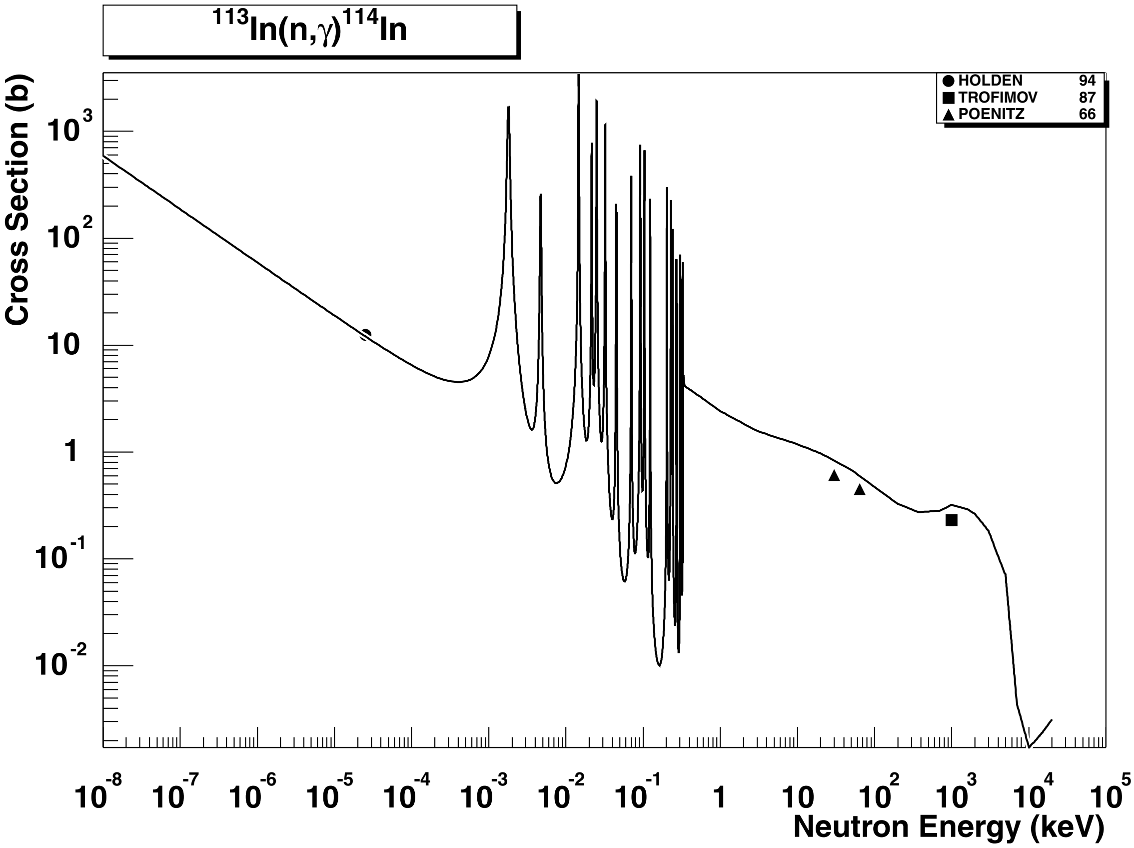

2.157. ^{113}In (n,γ) ^{114}In

final states: g.s., meta
source: EAF-4.1 (JEF-2.2)

The revised ENDF/B-V evaluation is adopted with partial cross-sections to the g.s. and meta state based on the experimental data (from [26]) and the deduced branching ratio applied up to the end of the resolved resonance region, and the energy dependent branching systematics [2] for the high energy region. The total and partial thermal cross-sections are reproduced with C/E=1.35. The data of Trofimov87 and Poenitz66 between 10 keV and 1 MeV are close to the evaluated curve.

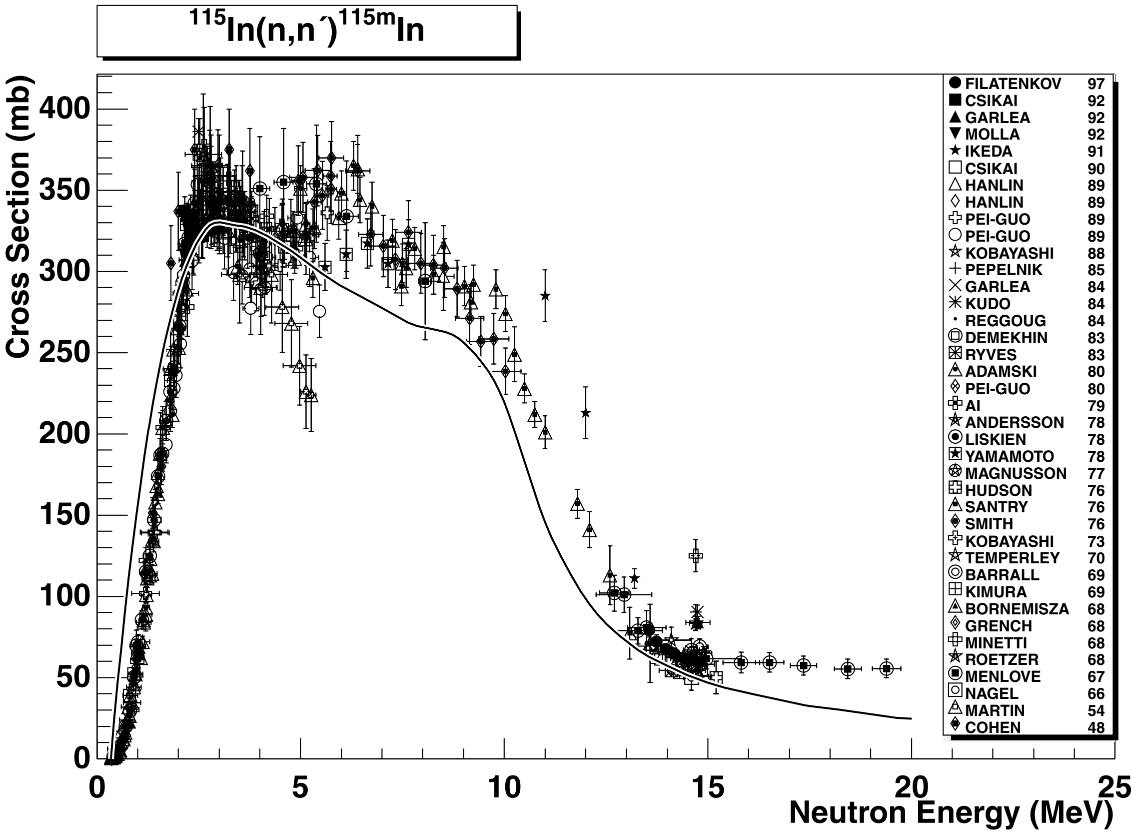

2.158. ^{115}In (n,n') ^{115m}In

final state: meta
source: ENDF/B-VI

The adopted ENDF/B-VI evaluation reproduces the general trend of data, however, small deviations are present. In particular, in the increasing part of the excitation curve (up to 2 MeV) and the decreasing part from 5 MeV it underestimates the data by about 10-15%. A revision of the evaluation may be needed.

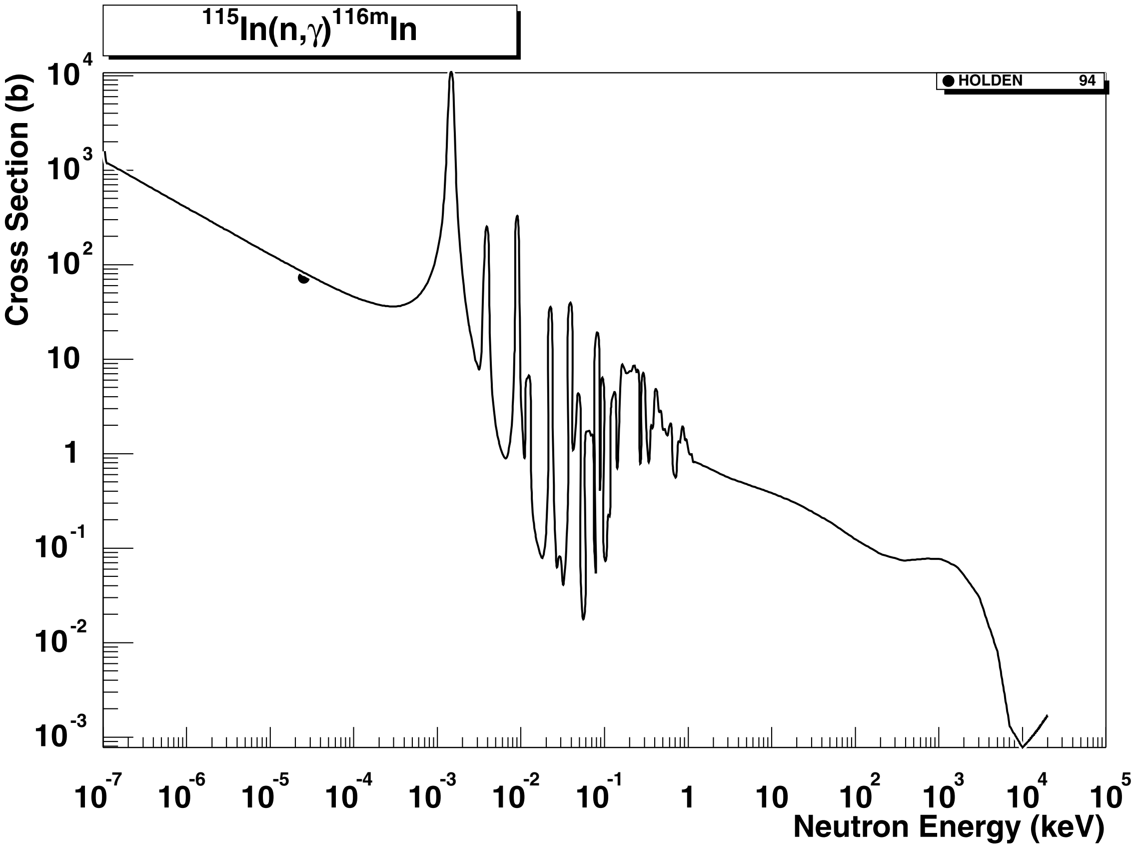

2.159. ^{115}In (n,γ) ^{116}In

final states: g.s., meta
source: ENDF/B-VI [g.s.], JEF-2.2 [meta]

The revised ENDF/B-V evaluation is adopted with partial cross-sections to the g.s. and meta state based on the experimental data (from [26]) and the deduced branching ratio applied up to the end of resolved resonance region, and the energy dependent branching systematics [2] for the high energy region. The total and partial thermal cross-sections of Holden94 are reproduced with C/E=1.01. No EXFOR data are available outside the resonance region, however, the 30 keV and 14.5 MeV cross-sections from [27] support the excitation curve in the high energy region.

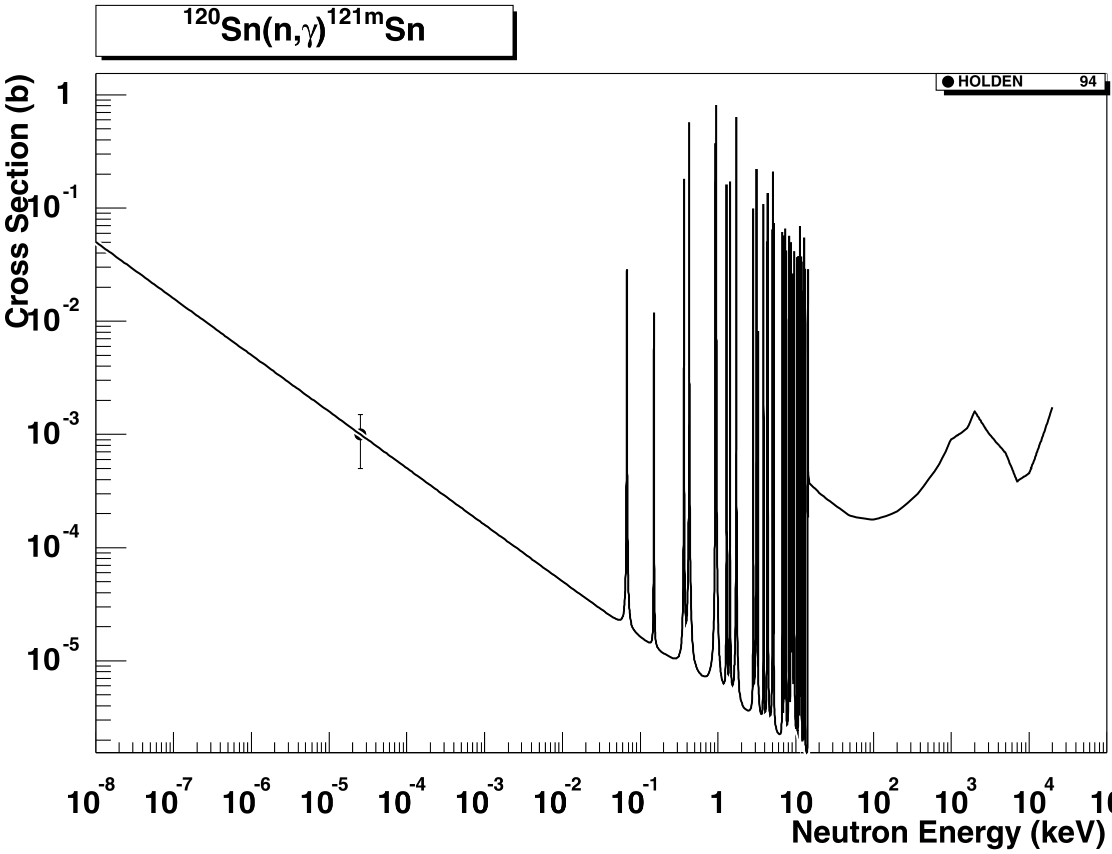

2.160. ^{120}Sn (n,γ) ^{121m}Sn

final state: meta
source: EAF-4.1 (JEF-2.2)

The reaction leading to the first isomeric state is the reference reaction. The revised ENDF/B-V evaluation is adopted with partial cross-sections to the g.s. and meta state based on the experimental data (from [26]) and the deduced branching ratio applied up to the end of the resolved resonance region, and the energy dependent branching systematics [2] for the high energy region. The total and partial thermal cross-sections of Holden94 are reproduced with C/E=1.0. No EXFOR data are available outside the resonance region, however, the 30 keV cross-section from [27] support the excitation curve in the high energy region.

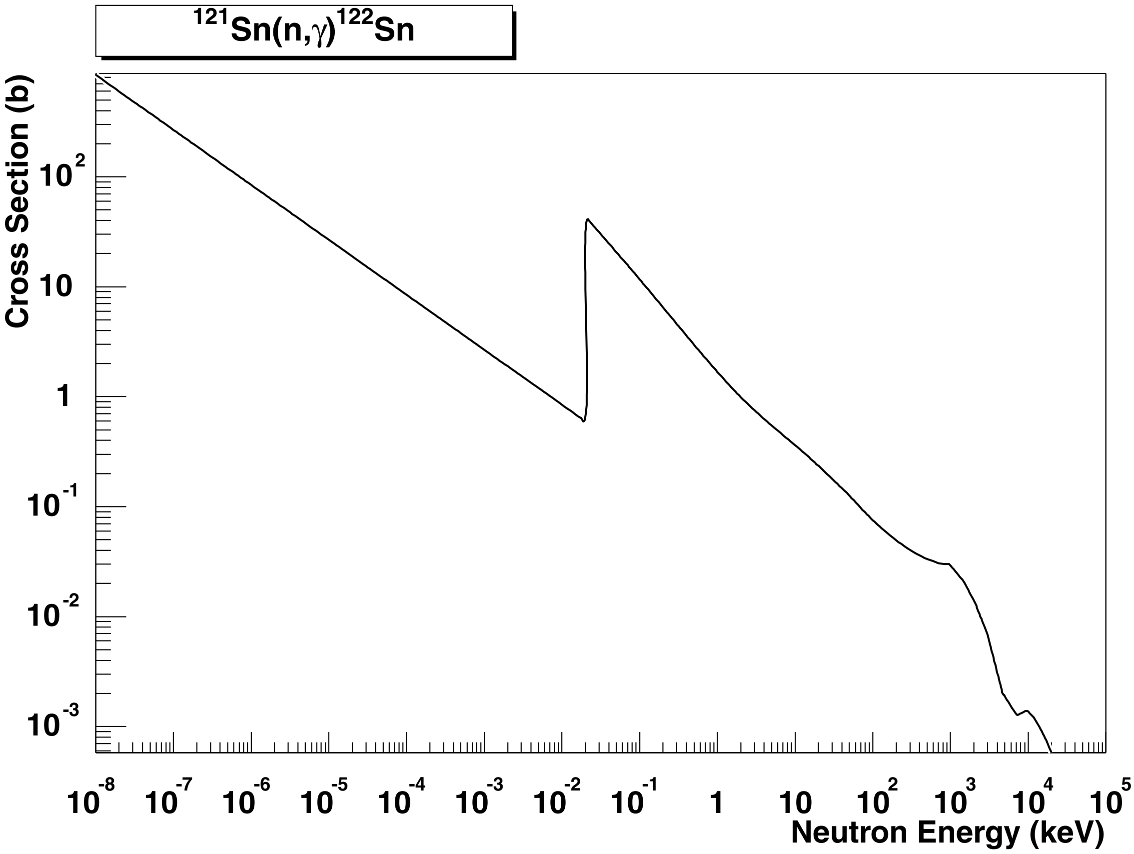

2.161. ^{121}Sn (n,γ) ^{122}Sn

final state: total
source: EAF-4.1

No experimental data are available, also not for the thermal range. Evaluation is based on the simplified model calculations with the code MASGAM and the global parameters (Hauser-Feshbach and DSD model with no resonance region generation, E_H is based on a $D_0/2$ estimate; for details see Ref. [35]). The thermal cross-section is based on a very crude systematic (see Ref. [35]) and is very uncertain.

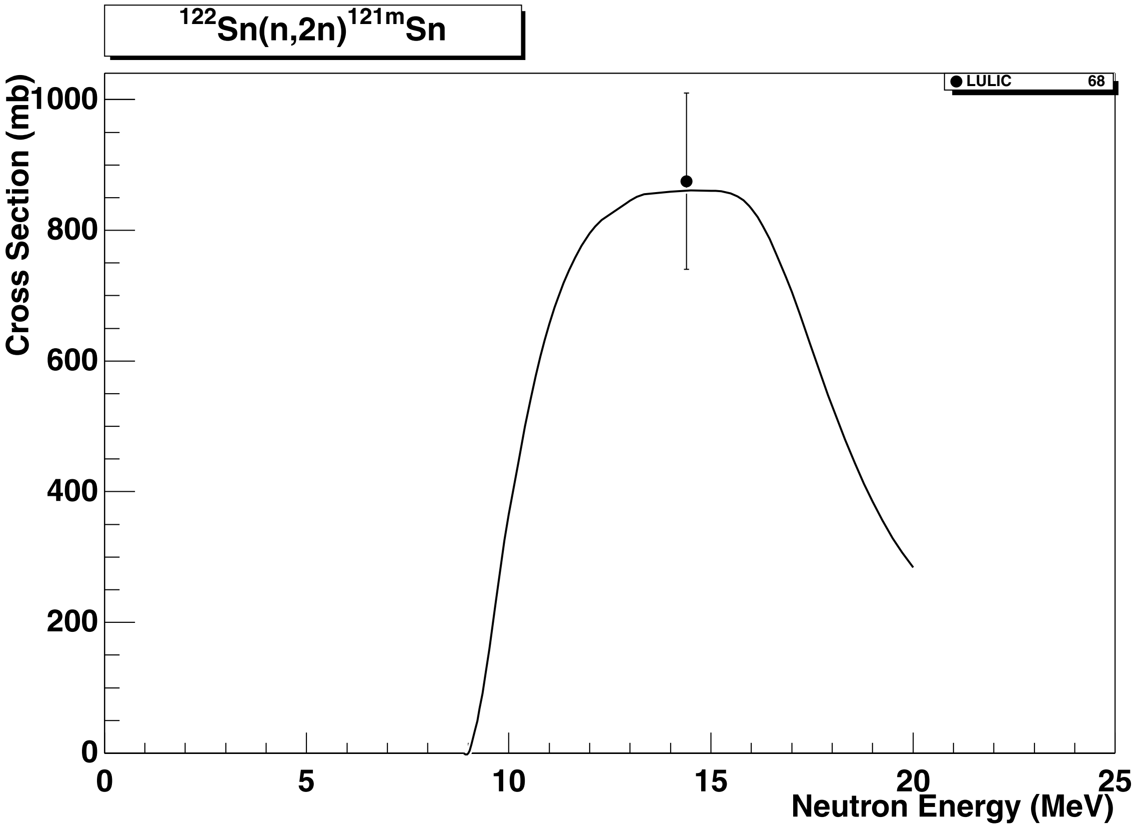

2.162. ^{122}Sn (n,2n) ^{121m}Sn

final state: meta
source: EAF-4.1 (JEF-2.2)

The reaction leading to the first isomeric state is the reference reaction. The ENDF/B-V evaluation was adopted in JEF-2.2. Partial cross-sections to the g.s. and meta state are based on the branching ratio systematics [2]. The single experimental point of Lulic68 for the meta state is reproduced well.

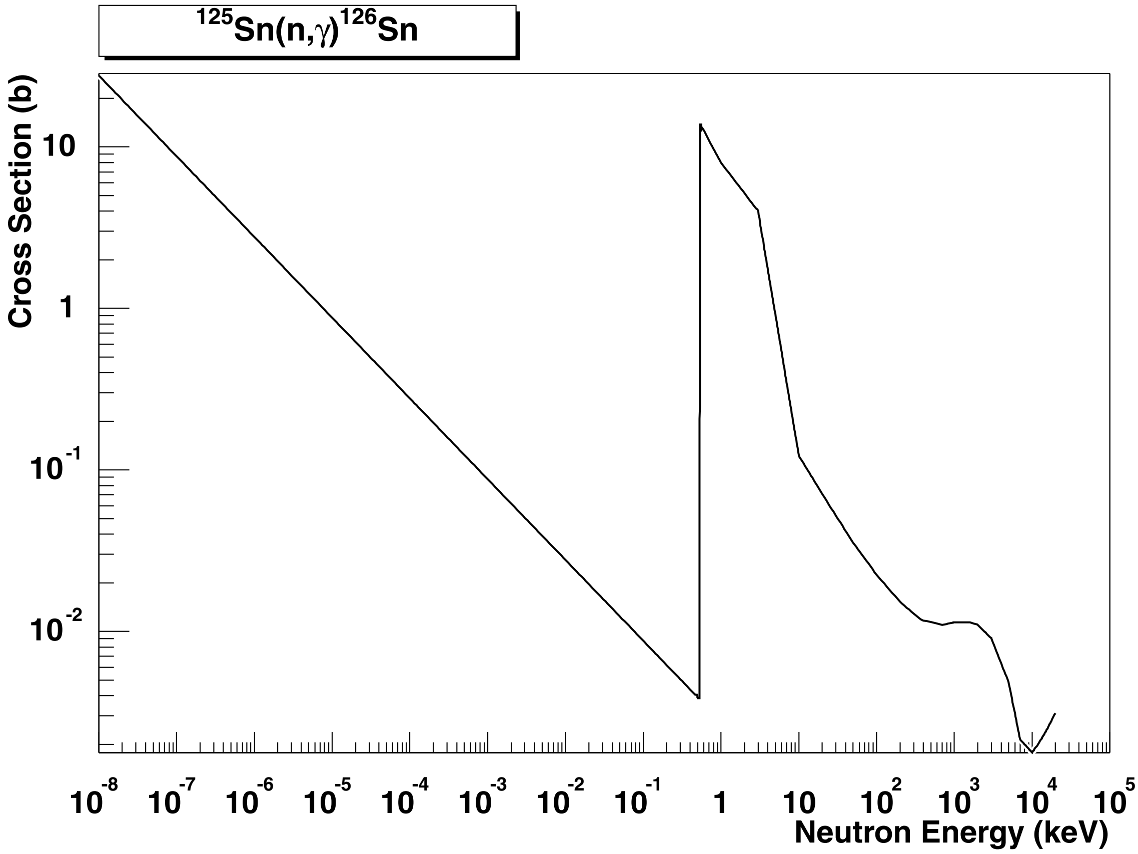

2.163. ^{125}Sn (n,γ) ^{126}Sn

final state: total
source: EAF-4.1 (JEF-2.2)

No experimental data are available, also not for the thermal range. Evaluation is based on the simplified model calculations with the code MASGAM and the global parameters (Hauser-Feshbach and DSD model with no resonance region generation, E_H is based on a $D_0/2$ estimate; for details see Ref. [35]). The thermal cross-section is based on a very crude systematic (see Ref. [35]) and is very uncertain.

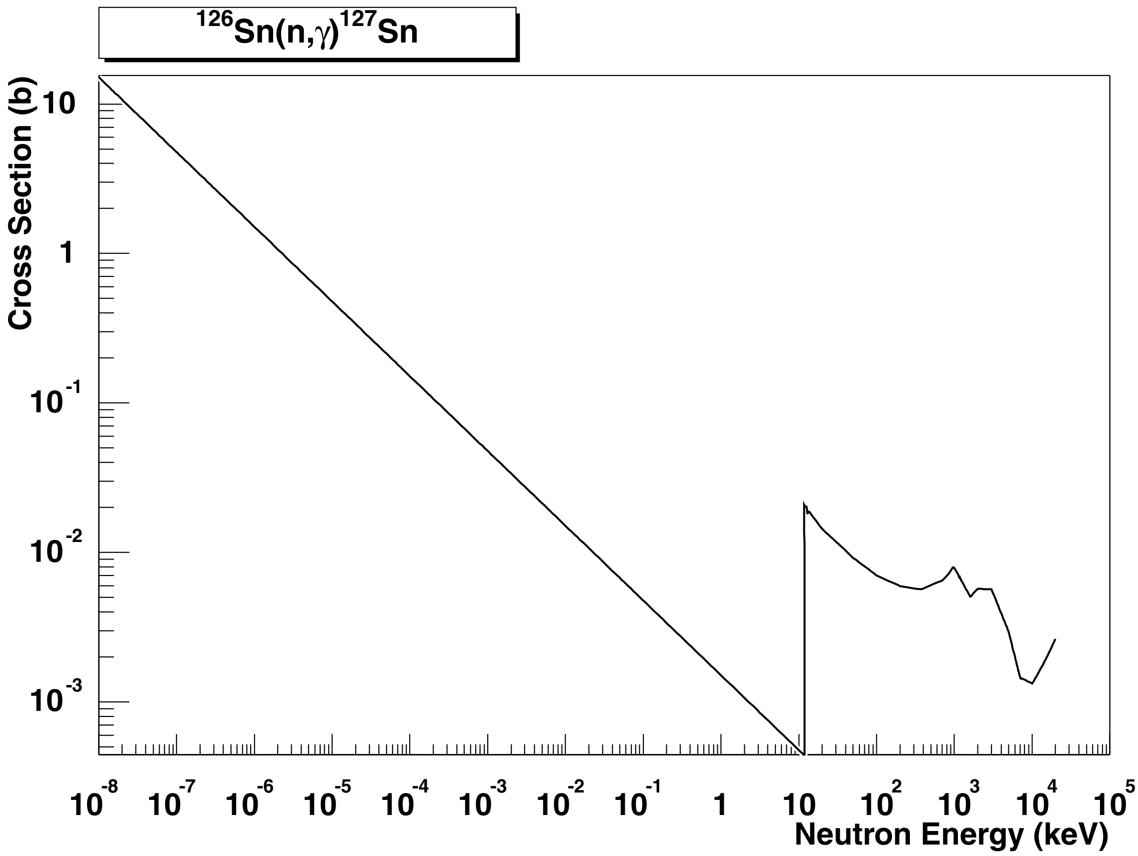

2.164. ^{126}Sn (n,γ) ^{127}Sn

final state: total
source: EAF-4.1 (JEF-2.2)

No experimental data are available, also not for the thermal range. Evaluation is based on the simplified model calculations with the code MASGAM and the global parameters (Hauser-Feshbach and DSD model with no resonance region generation, E_H is based on a $D_0/2$ estimate; for details see Ref. [35]). The branching between g.s. and meta state is based on the branching ratio systematics [2]. The thermal cross-section is based on a very crude systematic (see Ref. [35]) and is very uncertain.

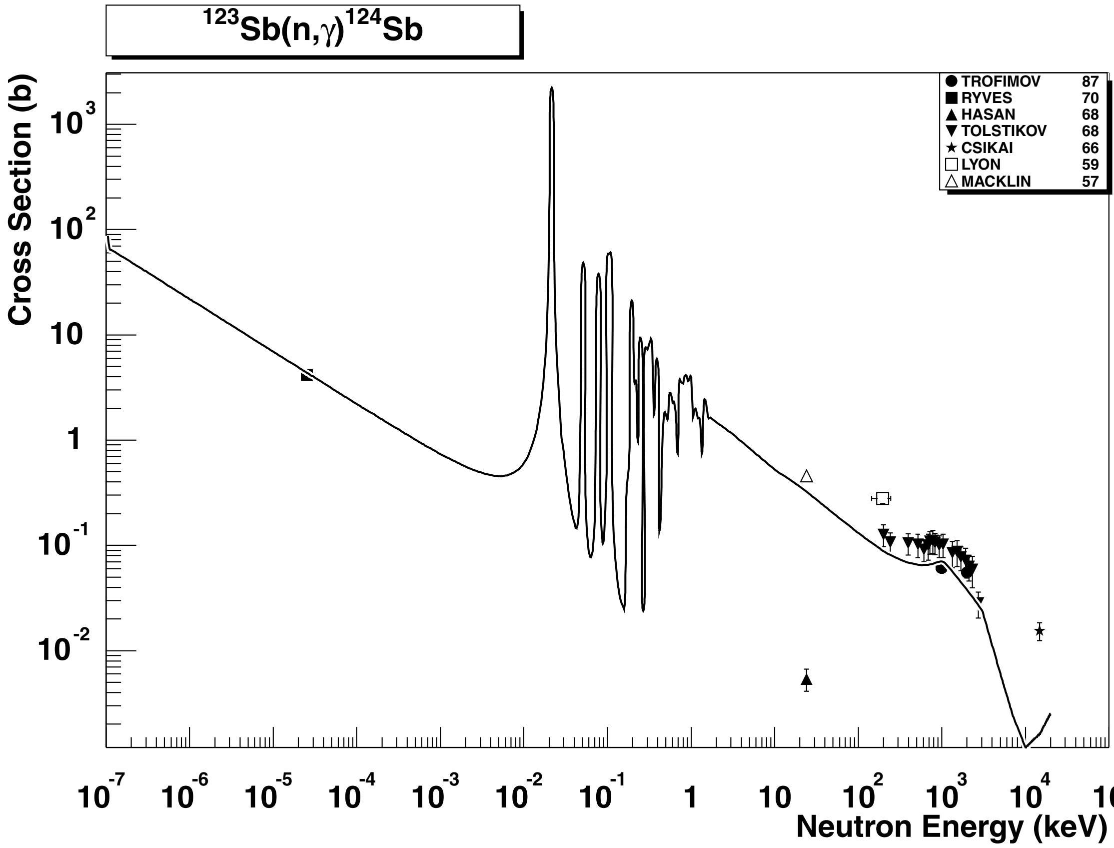

2.165. ^{123}Sb (n,γ) ^{124}Sb

final states: g.s., meta-1, meta-2
source: EAF-4.1 (JEF-2.2)

The revised ENDF/B-V evaluation is adopted with partial cross-sections to the g.s., meta-1 and meta-2 states based on the experimental data (from [26]) and the deduced branching ratio applied up to the end of the resolved resonance region, and the energy dependent branching systematics [2] for the high energy region. The total and partial thermal cross-sections are reproduced with C/E=1.05. The smooth high energy component is reasonably close to several data. Hasan68 and Csikai66 can be disregarded as both measurements give rather unrealistic values. The data are stored in the SANDII structure. The original evaluation includes 13407 data points.

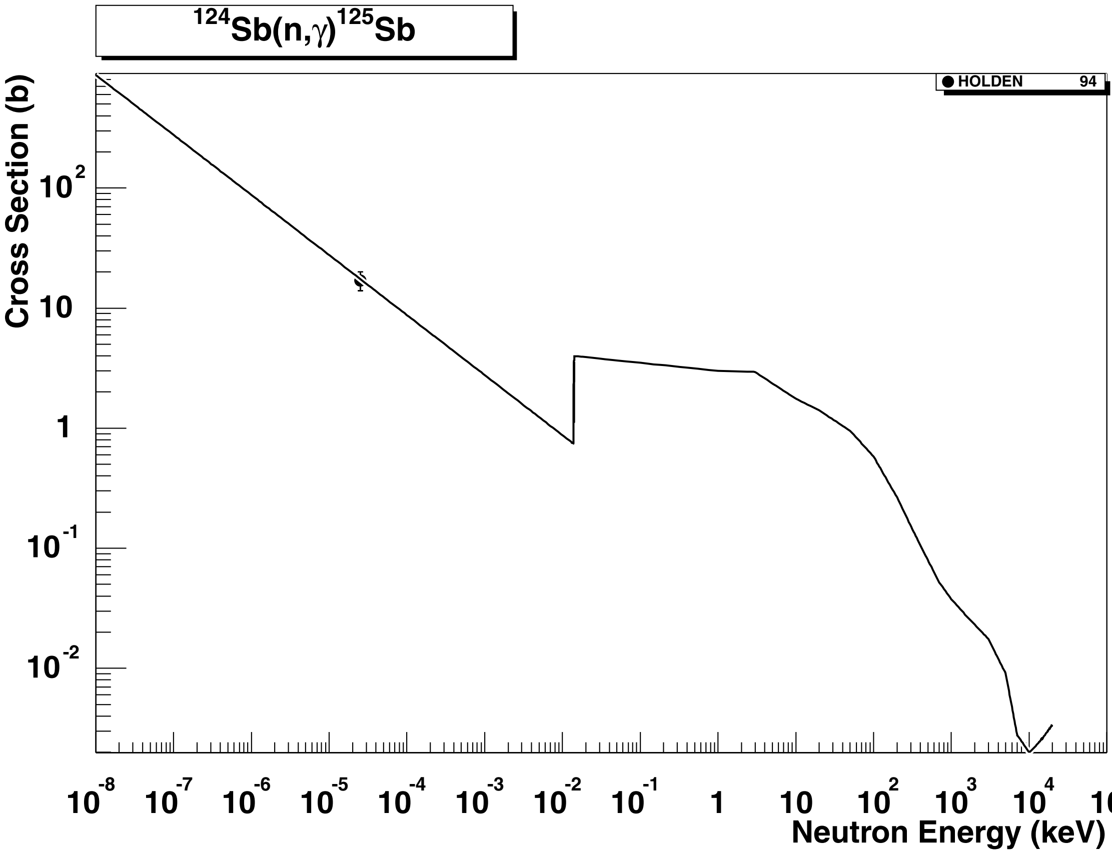

2.166. ^{124}Sb (n,γ) ^{125}Sb

final state: total
source: EAF-4.1 (JEF-2.2)

No EXFOR data are available. The evaluation fits the recommended thermal cross-section from [26] and [32] with C/E=1.0 . Data are based on the simplified model calculations with the code MASGAM and the global parameters (Hauser-Feshbach and DSD model with no resonance region generation, E_H is based on a $D_0/2$ estimate; for details see Ref. [35]).

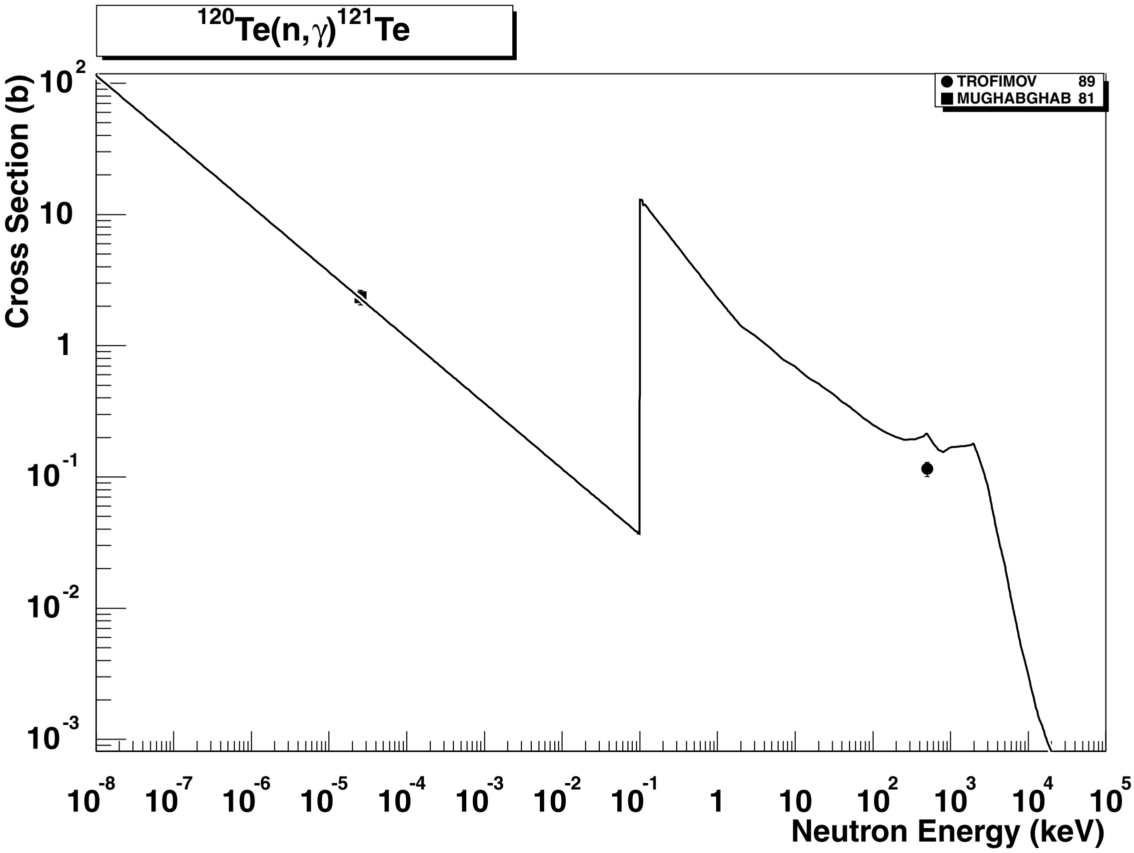

2.167. ^{120}Te (n,γ) ^{121}Te

final states: g.s., meta
source: EAF-4.1 (JEF-2.2)

The revised ENDF/B-V evaluation is adopted in a simplified form, no resolved resonance data are available. Partial cross-sections to the g.s. and meta state are based on the experimental data (from [26] and [31]) and the deduced branching ratio is applied up to the end of the resolved resonance region, and the energy dependent branching systematics [2] for the high energy region. The total and partial thermal cross-sections are reproduced with C/E=0.98. The single point of Trofimov89 at about 0.5 MeV is close to the evaluated smooth part of the excitation curve, which is also supported by the 30 keV cross-section from [26].

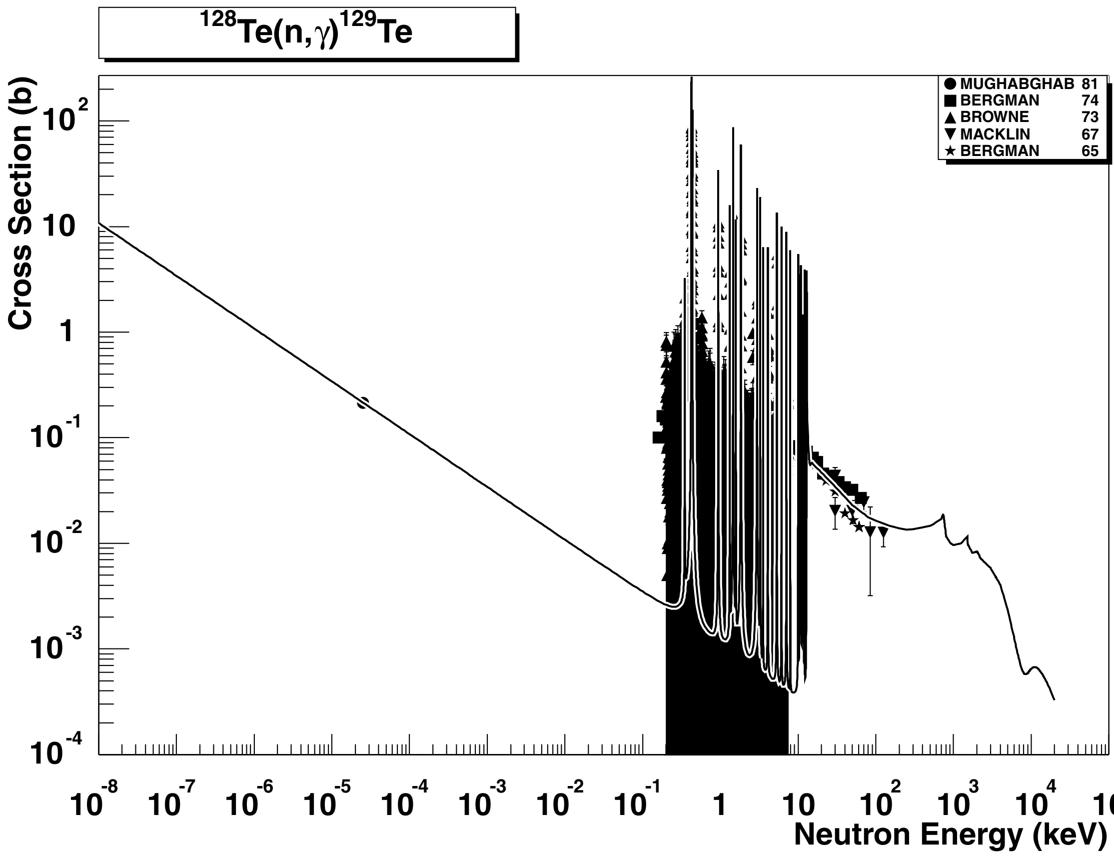

2.168. ^{128}Te (n,γ) ^{129}Te

final states: g.s., meta
source: EAF-4.1 (JEF-2.2)

The revised ENDF/B-V evaluation is adopted with partial cross-sections to the g.s. and meta state based on the experimental data (from [26] and [31]) and the deduced branching ratio applied up to the end of resolved resonance region, and the energy dependent branching systematics [2] for the high energy region. The total and partial thermal cross-sections are reproduced with C/E=1.00. The smooth high energy component is reasonably close to several data between 10 and 100 keV.

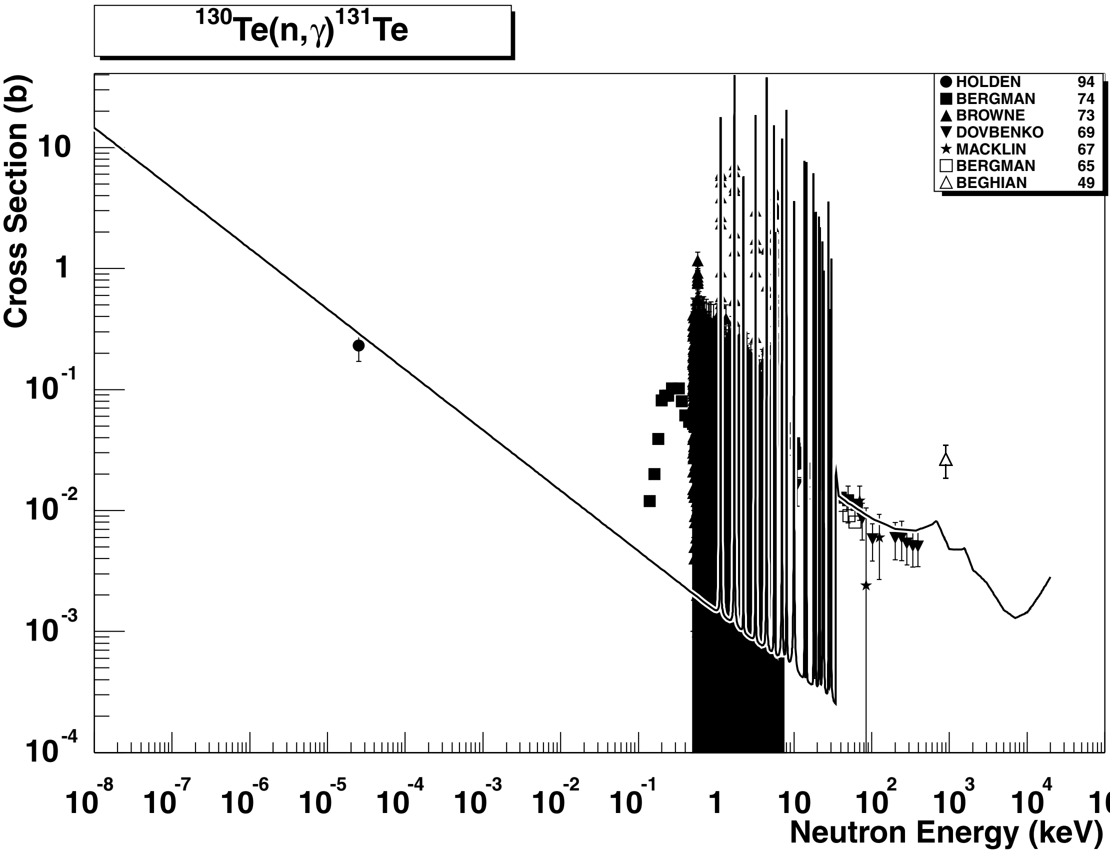

2.169. ^{130}Te (n,γ) ^{131}Te

final states: g.s., meta
source: EAF-4.1 (JEF-2.2)

The revised ENDF/B-V evaluation is adopted with partial cross-sections to the g.s. and meta state based on the experimental data (from [26]) and the deduced branching ratio applied up to the end of the resolved resonance region, and the energy dependent branching ratio systematics [2] for the high energy region. The total and partial thermal cross-sections are reproduced with C/E=1.45. Experimental data points below the first resonance are probably due to other isotopes or low resolution data. The position of the first resonance is certain. The smooth high energy component is reasonably close to several data below 300 keV. The single point of Beghian49 can be disregarded.

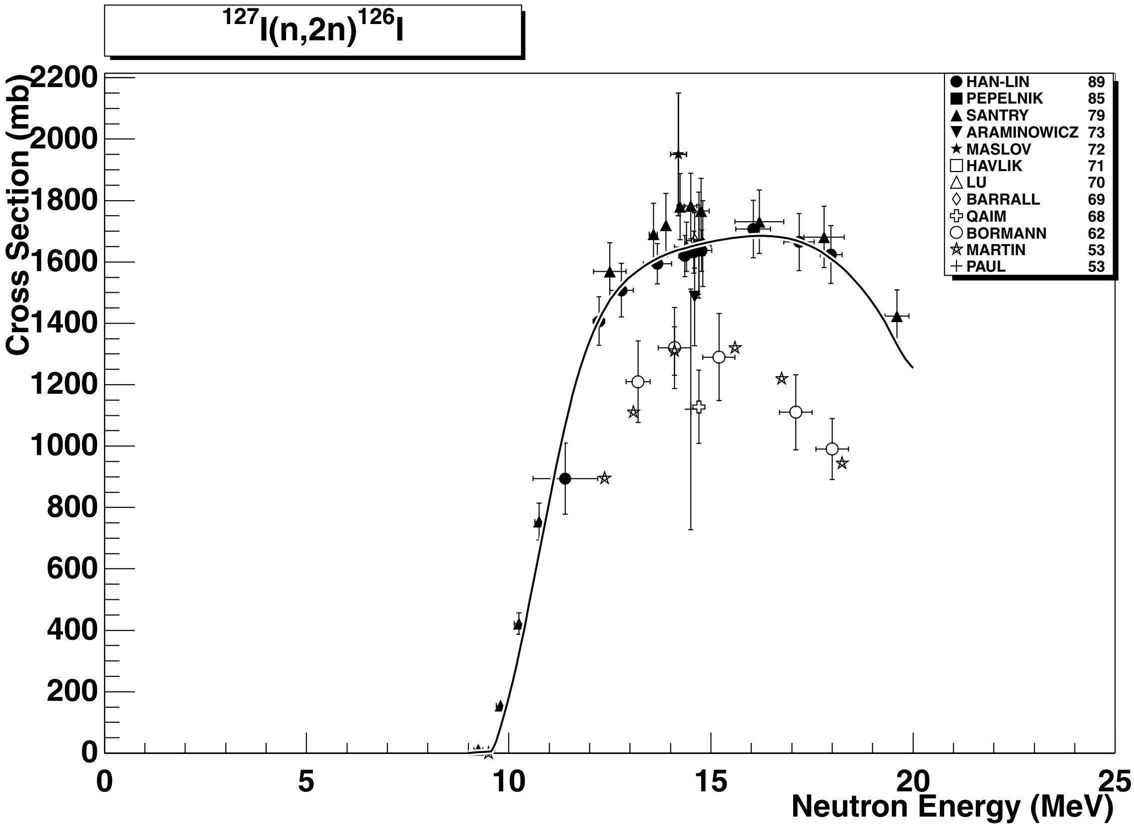

2.170. ^{127}I (n,2n) ^{126}I

final state: total
source: EAF-4.1 (IRDF-90.2)

IRDF-90.2 is in a very good agreement with the recent data of Santry79, Pepelink85 and Han-Lin89. Some of the older data (Borman62, Martin53 and Qaim68) can be disregarded.

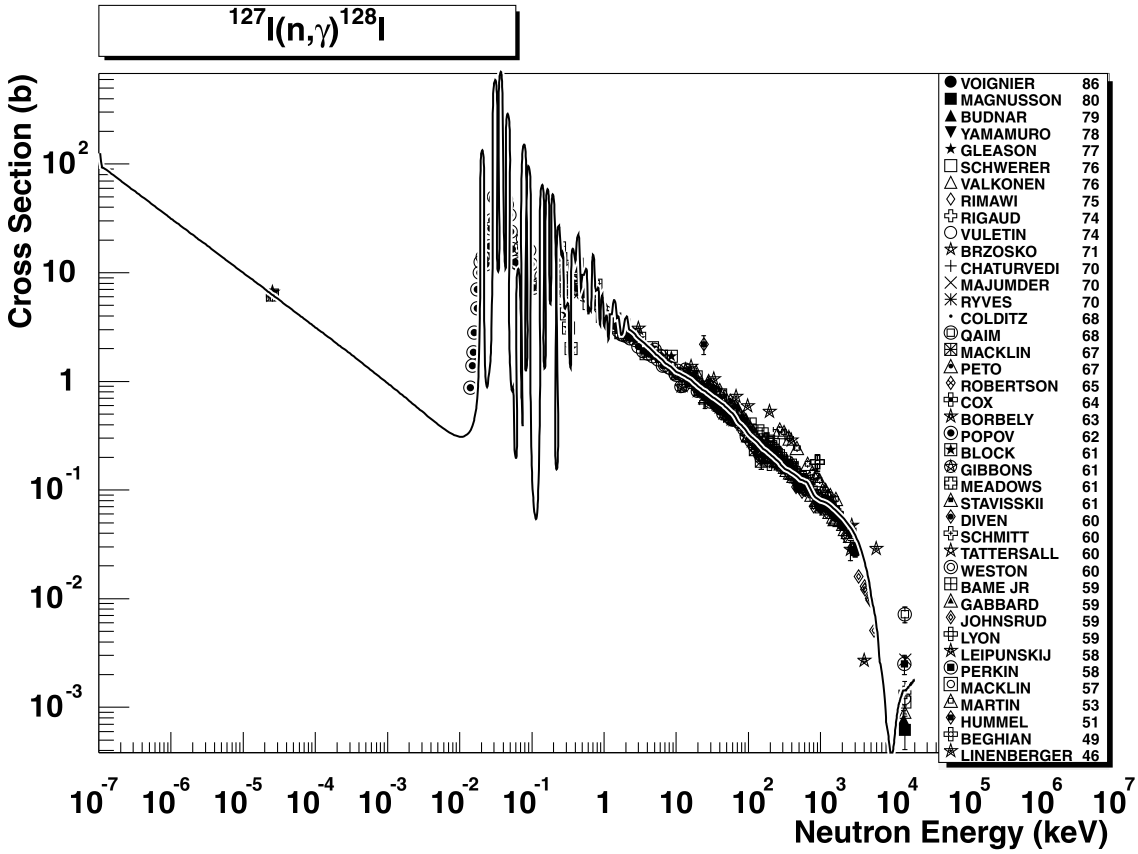

2.171. ^{127}I (n,γ) ^{128}I

final state: total
source: EAF-4.1 (JEF-2.2)

The JEF-2.2 evaluation is in a good agreement with all retrieved data starting from the thermal region up to 15 MeV.

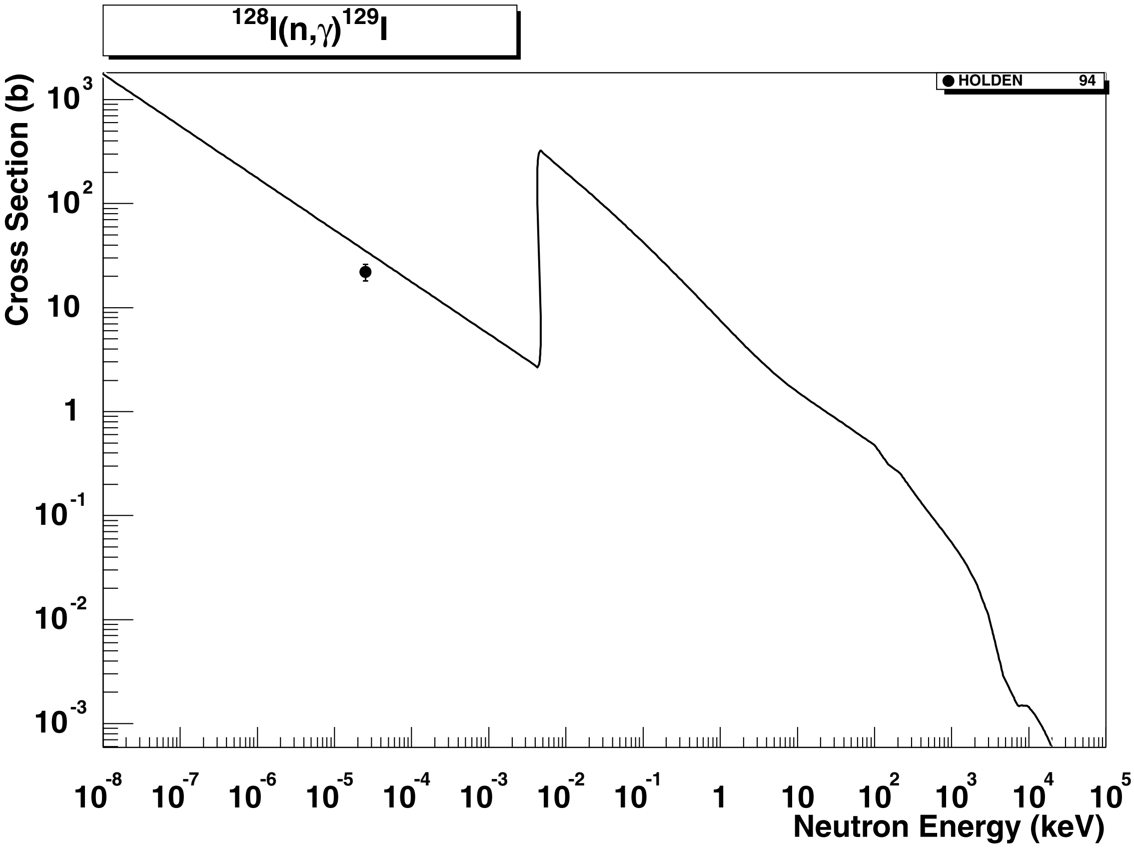

2.172. ^{128}I (n,γ) ^{129}I

final state: total
source: EAF-4.1

No EXFOR data are available. The evaluation fits the recommended thermal cross-section of Holden94 [32] with C/E=1.59. Data are based on the simplified model calculations with the code MASGAM and the global parameters (Hauser-Feshbach and DSD model with no resolved resonance region, E_H is based on a $D_0/2$ estimate; for details see Ref. [35]).

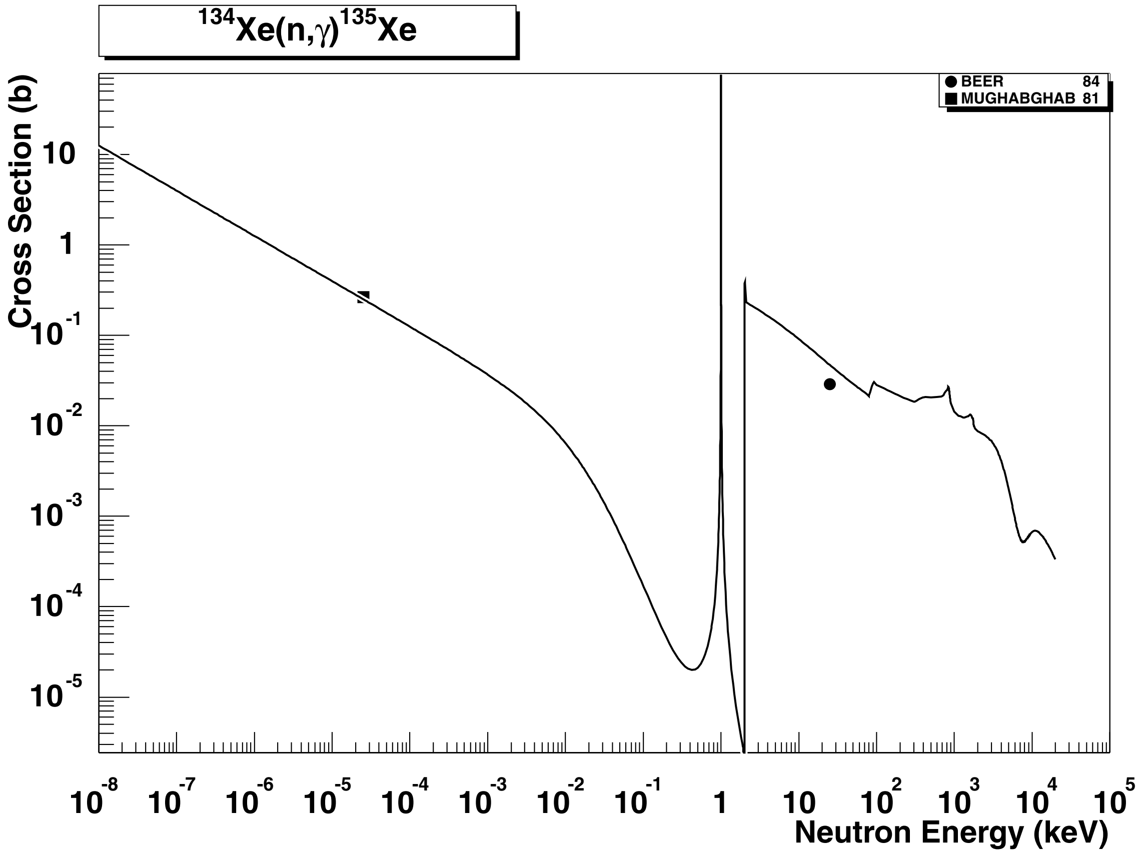

2.173. ^{134}Xe (n,γ) ^{135}Xe

final states: g.s., meta
source: EAF-4.1 (JEF-2.2)

The revised ENDF/B-V evaluation is adopted with partial cross-sections to the g.s. and meta state based on the experimental data (from [26] and [31]) and the deduced branching ratio applied up to the end of the resolved resonance region, and the energy dependent branching ratio systematics [2] for the high energy region. The total and partial thermal cross sections are reproduced with C/E=0.95. The smooth high energy component is reasonably close to the single point of Beer84.

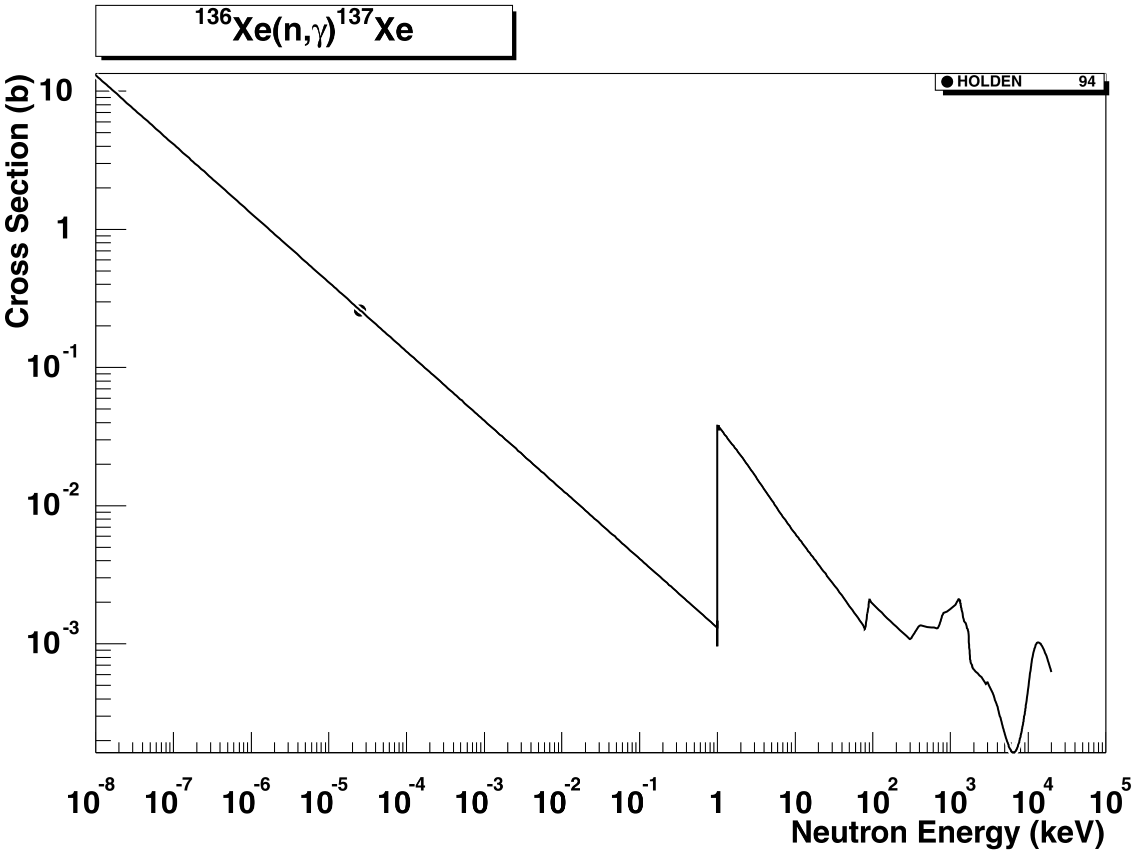

2.174. ^{136}Xe (n,γ) ^{137}Xe

final state: total
source: EAF-4.1 (JEF-2.2)

No EXFOR data are available. Adopted excitation curve is based on simplified model calculations taken from ENDF/B-V with no resolved resonance region generation. The 1/v component reproduces the thermal cross-section of Holden94 [32] with C/E=1.0. The 30 keV cross-section from [27] supports the smooth excitation curve in the high energy region.

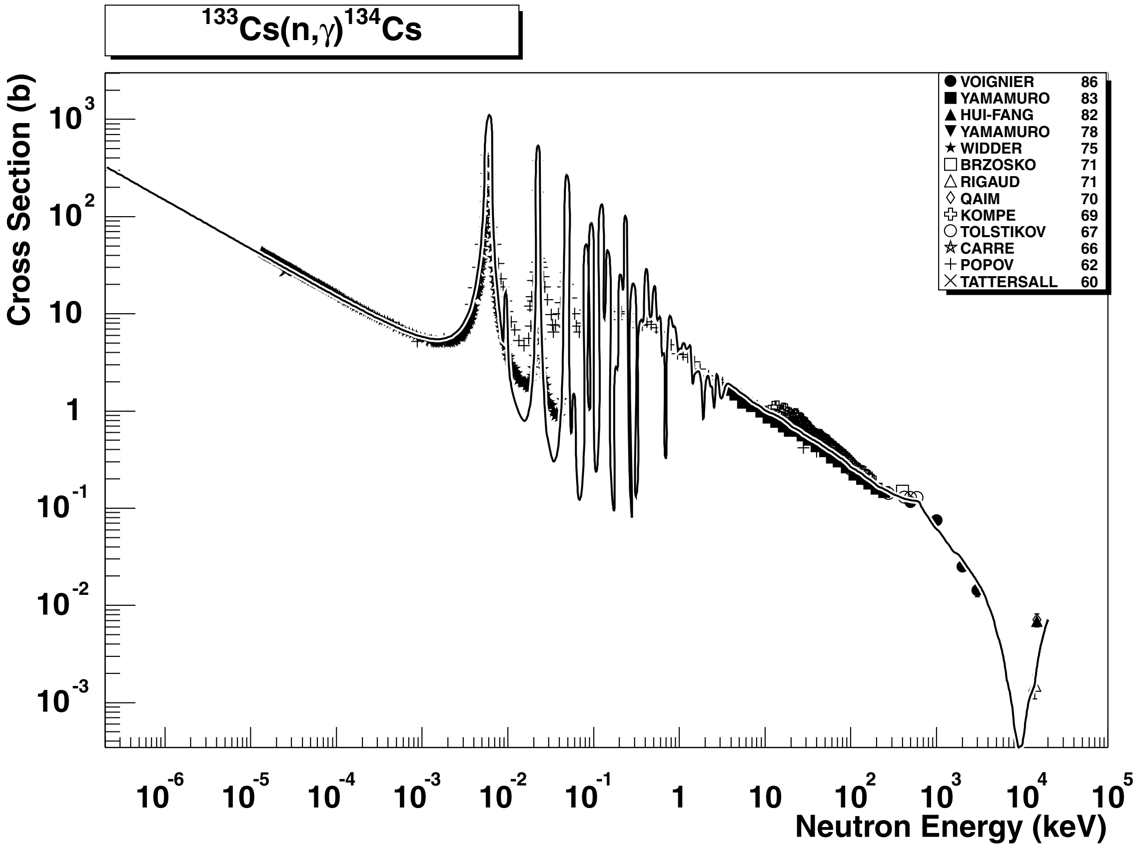

2.175. ^{133}Cs (n,γ) ^{134}Cs

final states: g.s., meta
source: EAF-4.1 (JEF-2.2)

The JEF-2.2 evaluation is in a perfect agreement with all retrieved data from the thermal region up to 15 MeV. Partial cross-sections to the g.s. and meta state are based on the experimental data (from [26]) and the deduced branching ratio applied up to the end of the resolved resonance region, and the energy dependent branching ratio systematics [2] for the high energy region. The data are stored in the SANDII structure. The original evaluation includes 29358 data points.

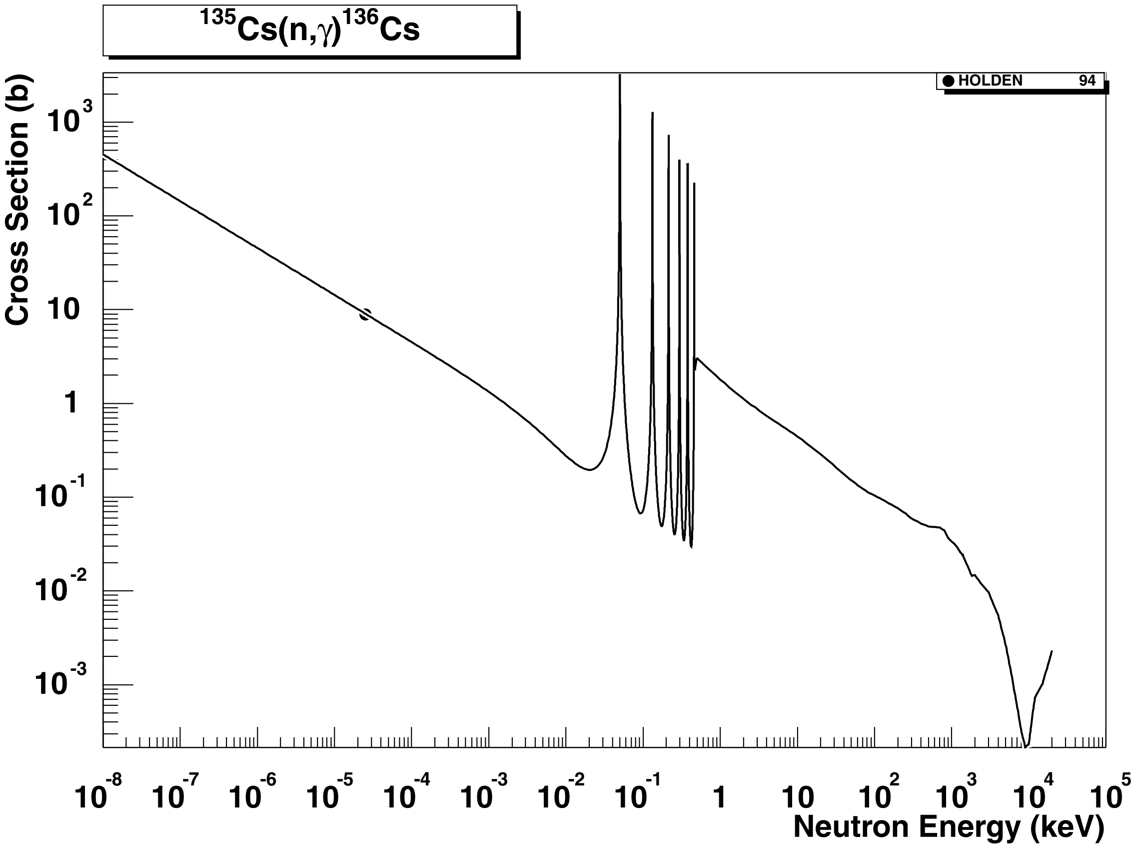

2.176. ^{135}Cs (n,γ) ^{136}Cs

final state: g.s., meta
source: EAF-4.1 (JEF-2.2)

This is the JEF-2.2 evaluation. Partial cross-sections to the g.s. and meta state are based on the energy dependent branching systematics [2]. The thermal cross-section of Holden94 [32] is reproduced with C/E=1.04. The 30 keV cross-section from [27] supports the smooth excitation curve in the high energy region.

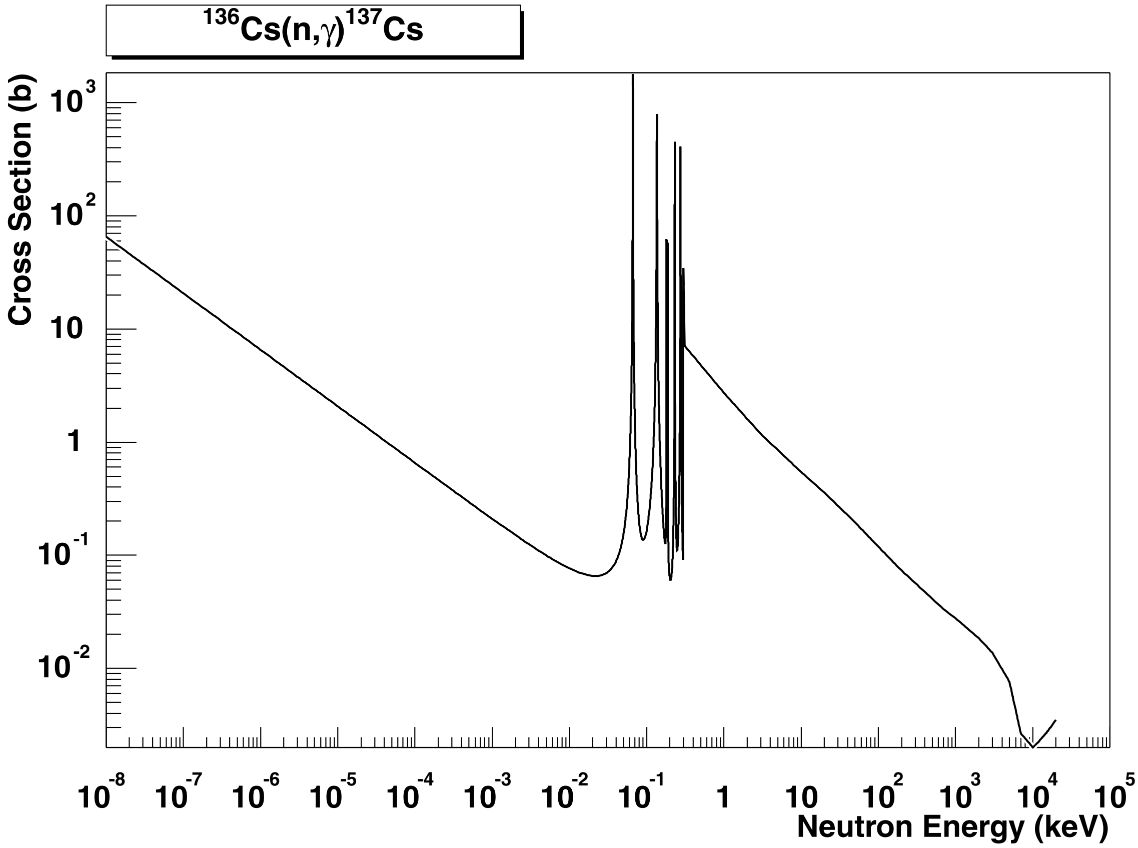

2.177. ^{136}Cs (n,γ) ^{137}Cs

final state: total
source: EAF-4.1 (JEF-2.2)

The revised ENDF/B-V evaluation has been adopted. No EXFOR experimental data are available outside the resonance region.

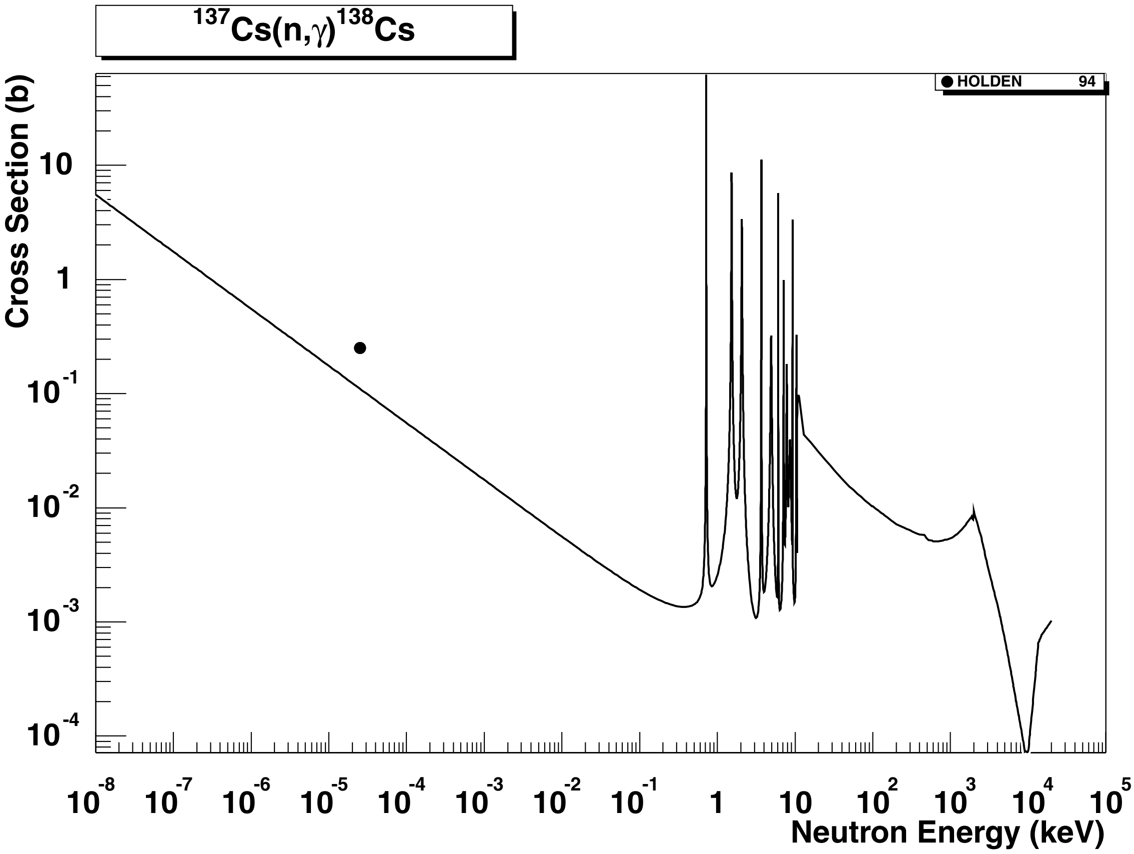

2.178. ^{137}Cs (n,γ) ^{138}Cs

final state: g.s., meta
source: EAF-4.1 (JEF-2.2)

The original JEF-2.2 evaluation. No EXFOR data are available outside the resonance region. Partial cross-sections to the g.s. and meta state are based on the energy dependent branching systematics [2]. The thermal cross-section [26] of 250 ± 10 mb is reproduced with C/E=0.44 only. Apparently parameters used to generate the resolved resonance region require a revision.

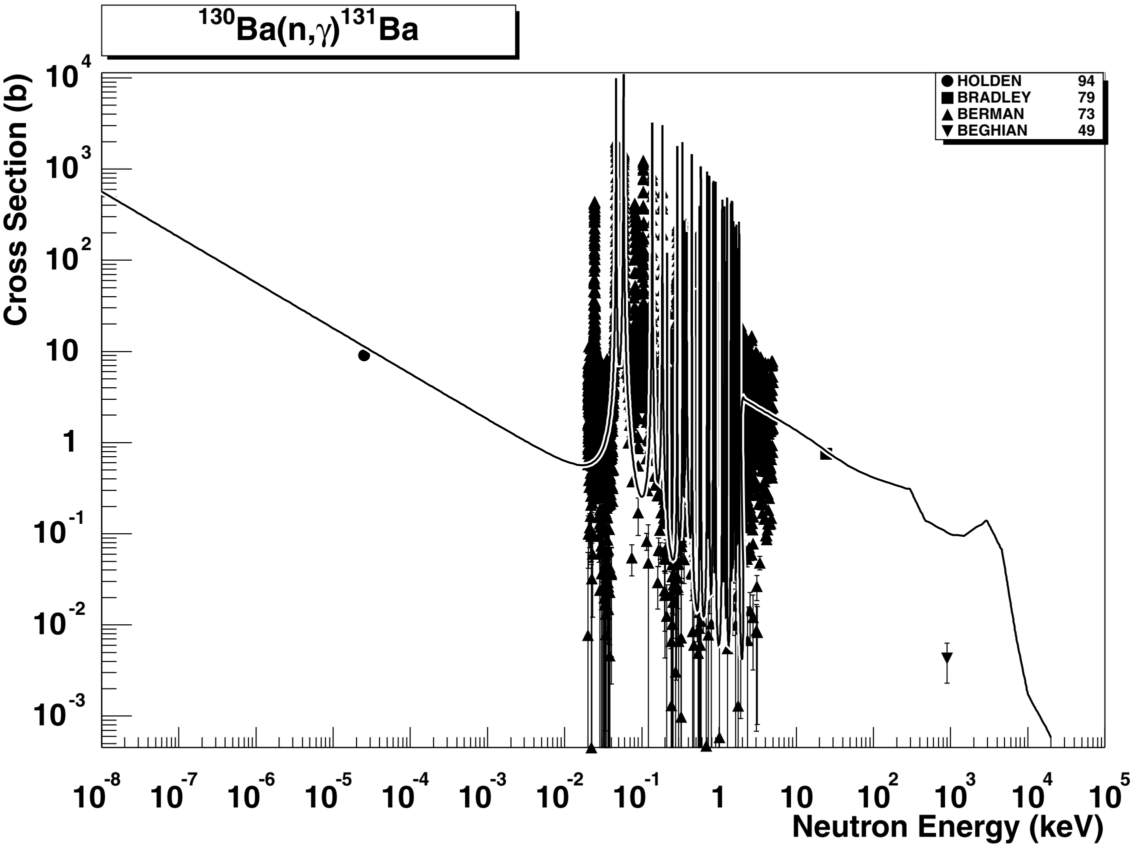

2.179. ^{130}Ba (n,γ) ^{131}Ba

final states: g.s., meta
source: EAF-4.1

This is the EAF-4.1 evaluation calculated with the code SIGECN-MASGAM. Branching ratio between the g.s. and meta state is based on experimental data (thermal cross-sections [26]) and applied up to the end of the resolved resonance region, and the energy dependent branching ratio systematics [2] for the high energy region. Full MLBW resonance treatment is included and the total and partial thermal cross-sections [26] are well reproduced with C/E=1.00. The statistical component is based on simplified calculations (with global parameters) with the code MASGAM and is supported by the recommended 30 keV cross-section [27] and by a single point of Bradley79. The value of Beghian49 at 1 MeV is probably wrong (too low).

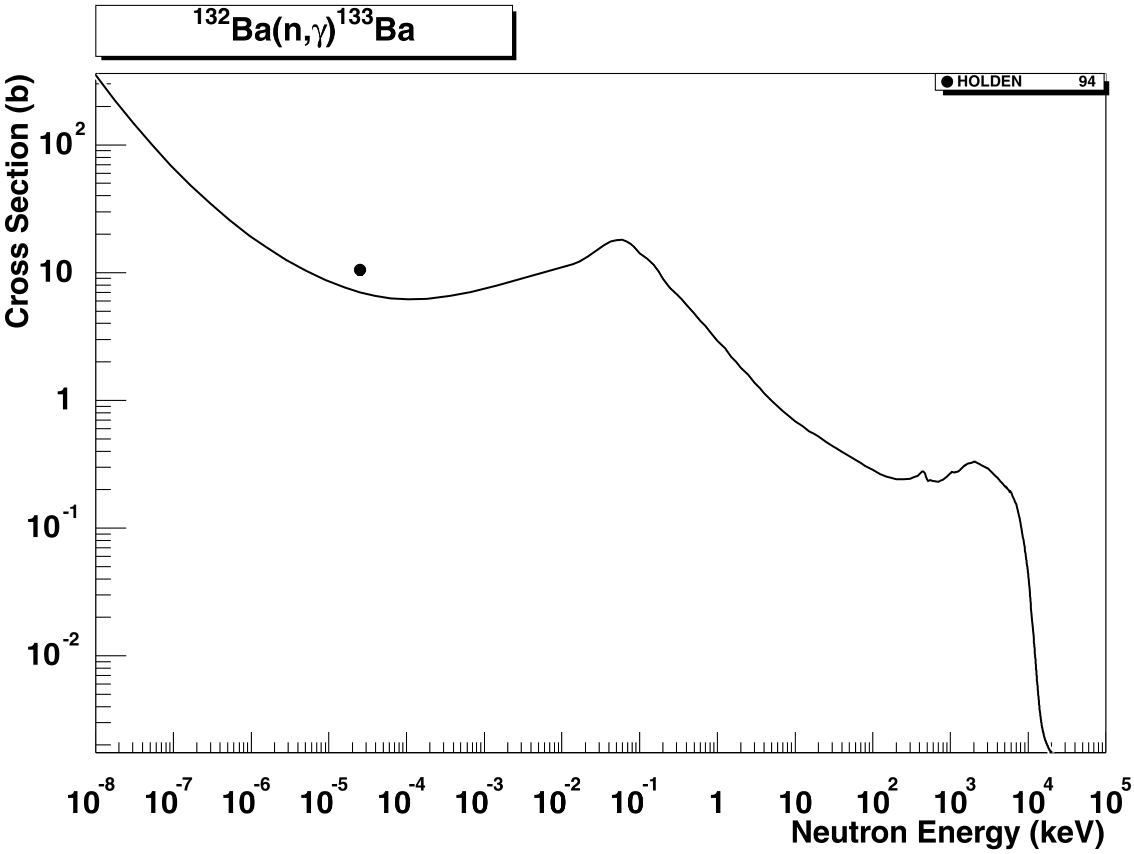

2.180. ^{132}Ba (n,γ) ^{133}Ba

final states: g.s., meta
source: EAF-4.1 (JENDL-3.1)

No EXFOR data are available. The data are adopted from JENDL-3.1 and fit the recommended thermal cross-section of Holden94 [32] with C/E=1.00. Data are based on simplified model calculations with no resolved resonance region generation. Branching ratio to the g.s. and meta state is based on the energy dependent systematics [2].

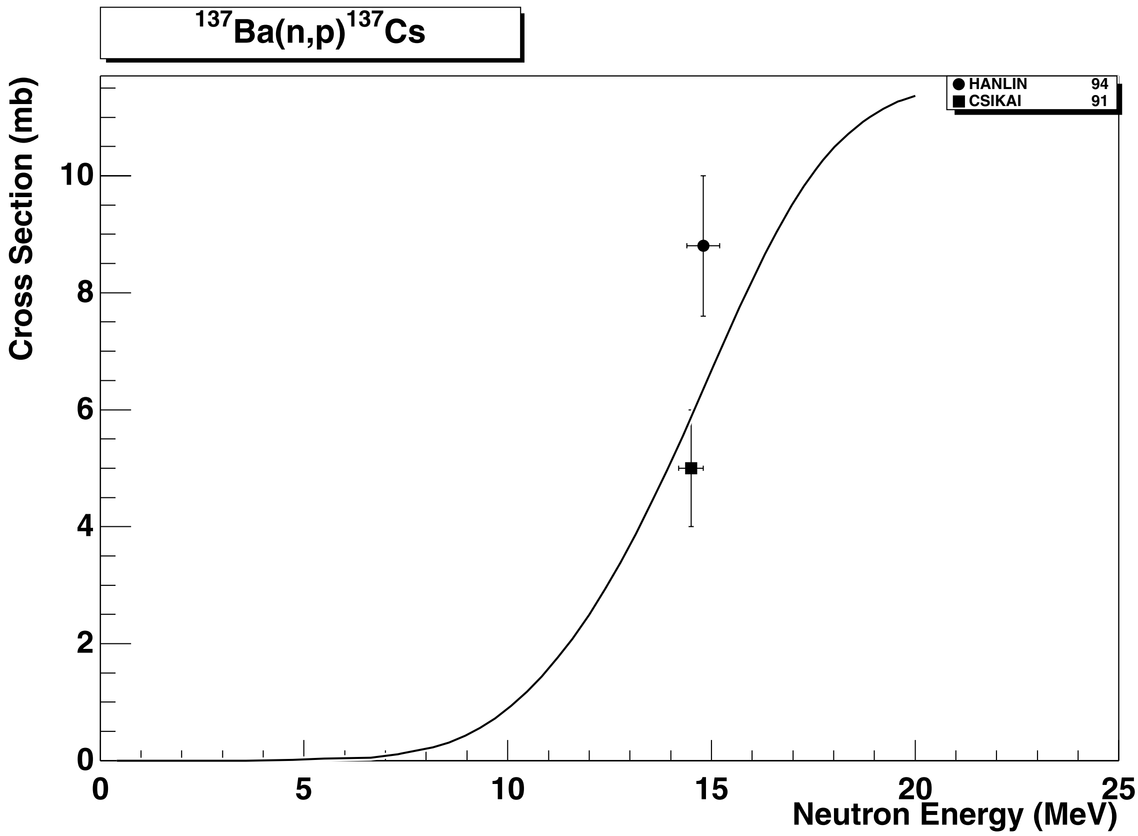

2.181. ^{137}Ba (n,p) ^{137}Cs

final state: total
source: ADL-3

ADL-3 evaluation runs between two experimental points around 15 MeV.

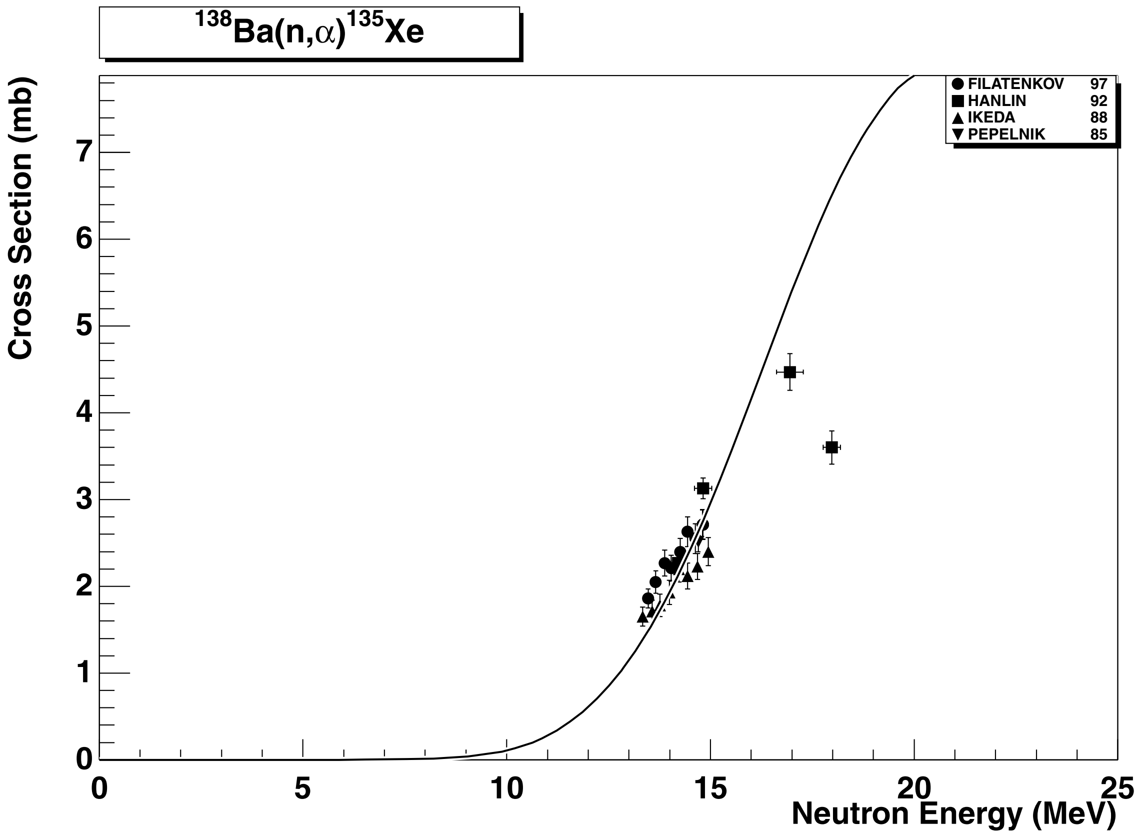

2.182. ^{138}Ba (n,α) ^{135}Xe

final states: g.s., meta
source: ADL-3

ADL-3 evaluation is in good agreement with the experimental data up to 17 MeV. The highest point of Hanlin92 at 18 MeV may suggest that the shape of the excitation curve close to 20 MeV might be different (lower).

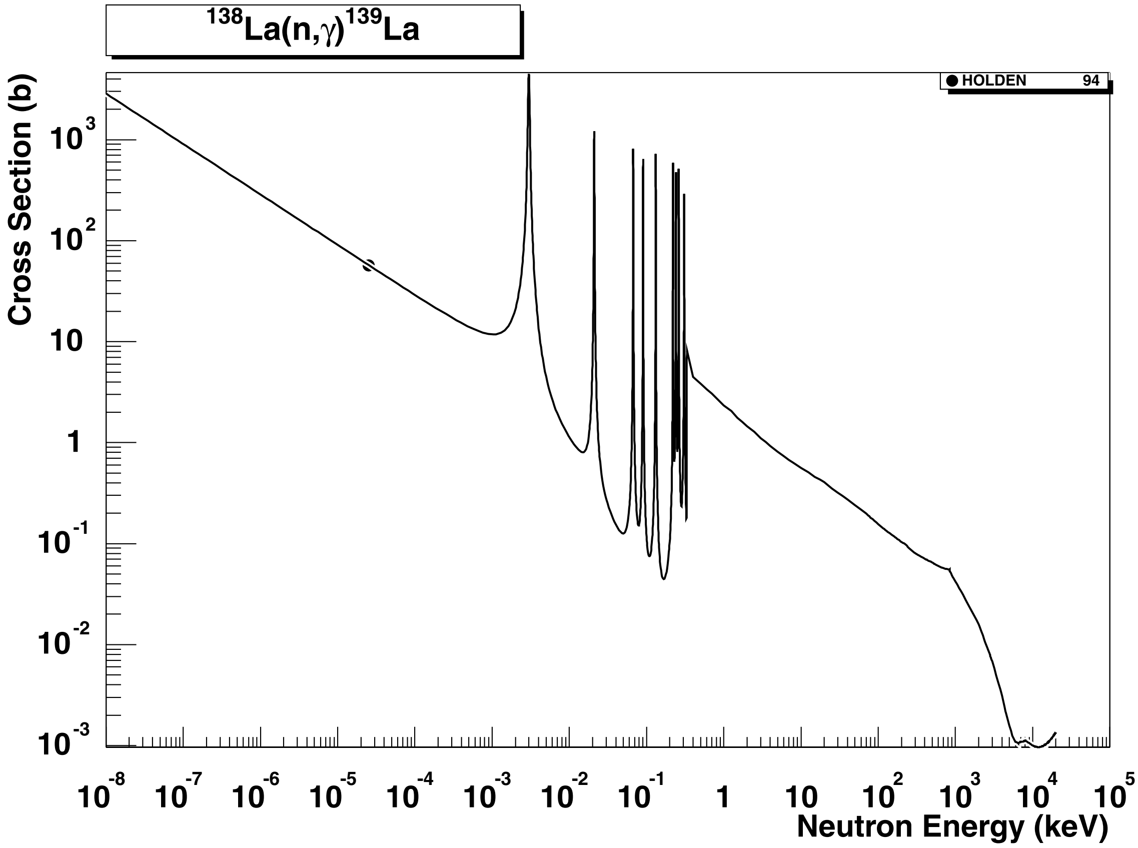

2.183. ^{138}La (n,γ) ^{139}La

final state: total
source: EAF-4.1 (JENDL-3.1)

The JENDL-3.1 evaluation has been adopted. No EXFOR data are available outside the resonance region. JENDL-3.1 fits the recommended thermal cross-section of Holden94 [32] with C/E=1.00.

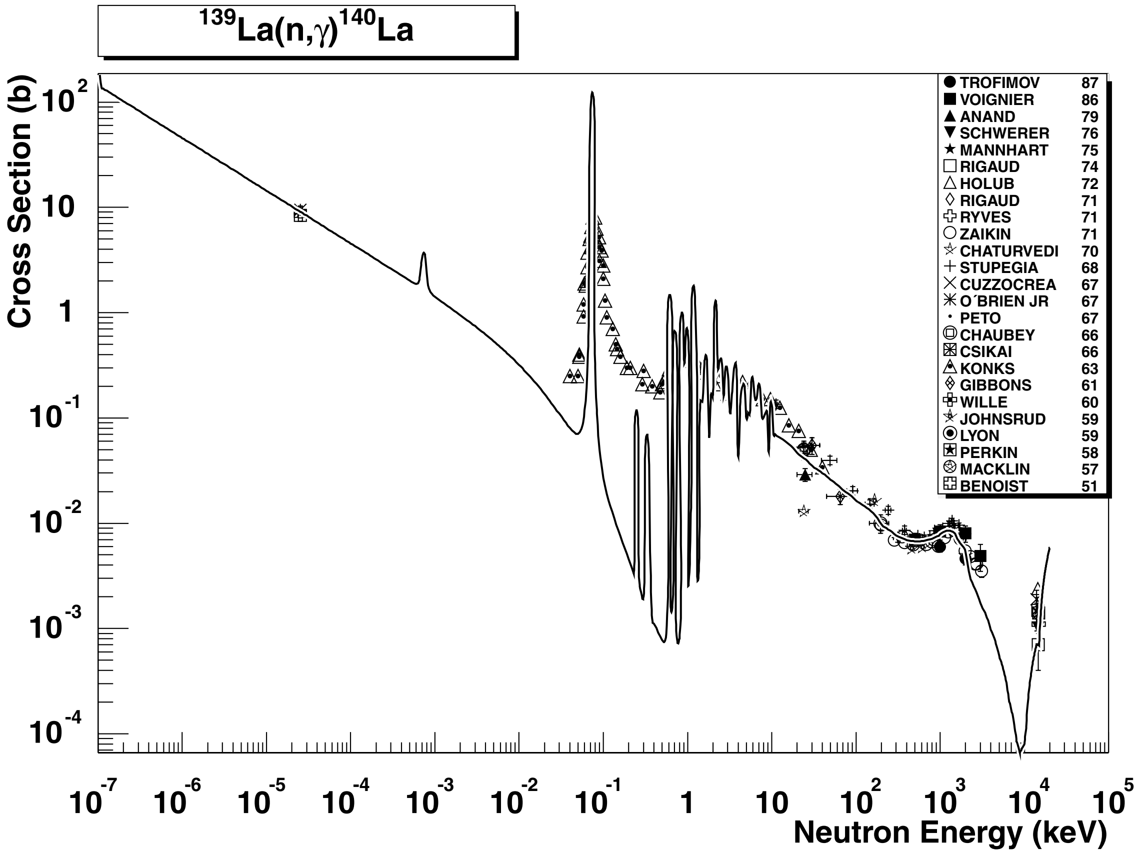

2.184. ^{139}La (n,γ) ^{140}La

final state: total
source: EAF-4.1 (JEF-2.2)

The original JEF-2.2 evaluation is in a perfect agreement with all retrieved data from the thermal region up to 15 MeV. The finite resolution of the data around the strong resonance should be taken into account. The data are stored in the SANDII structure. The original evaluation includes 21120 data points.

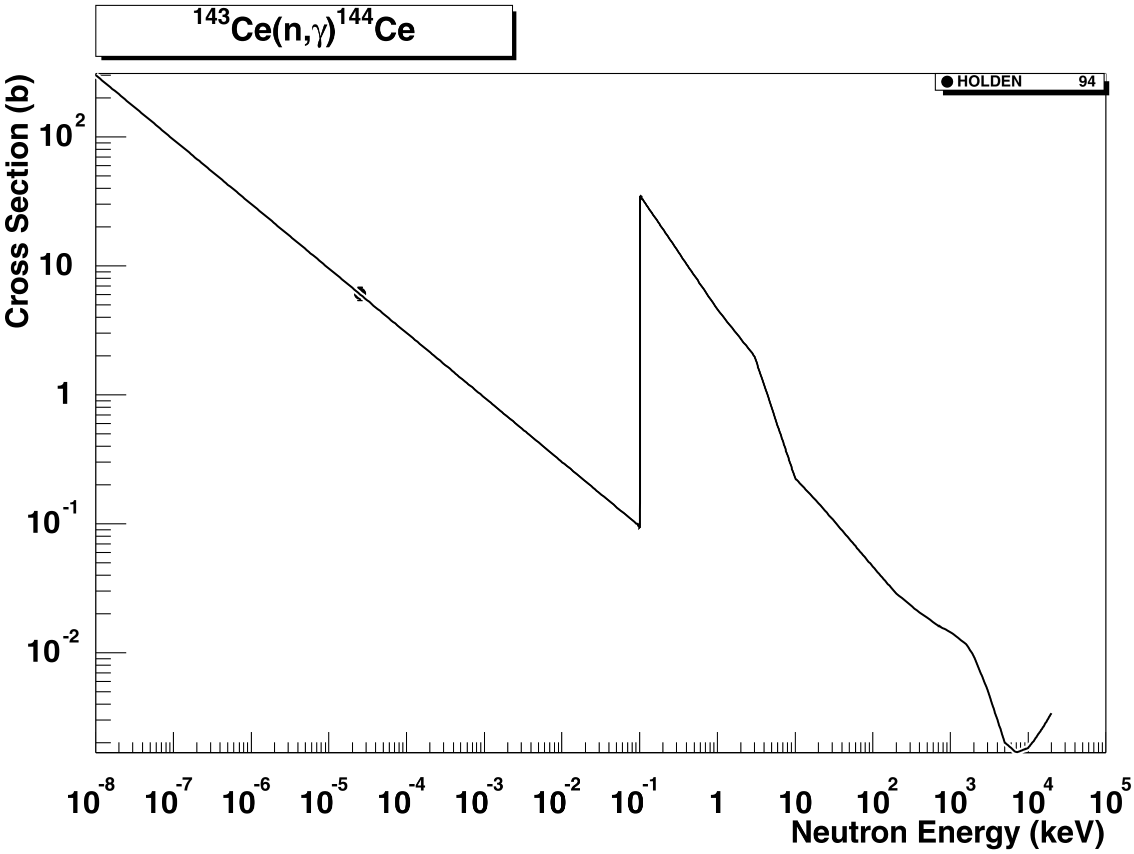

2.185. ^{143}Ce (n,γ) ^{144}Ce

final state: total
source: EAF-4.1 (JEF-2.2)

No EXFOR data are available. The data are adopted from the revised ENDF/B-V evaluation and fit the recommended thermal cross-section of Holden94 [32] with C/E=1.00. Data are based on simplified model calculations without resolved resonance region.

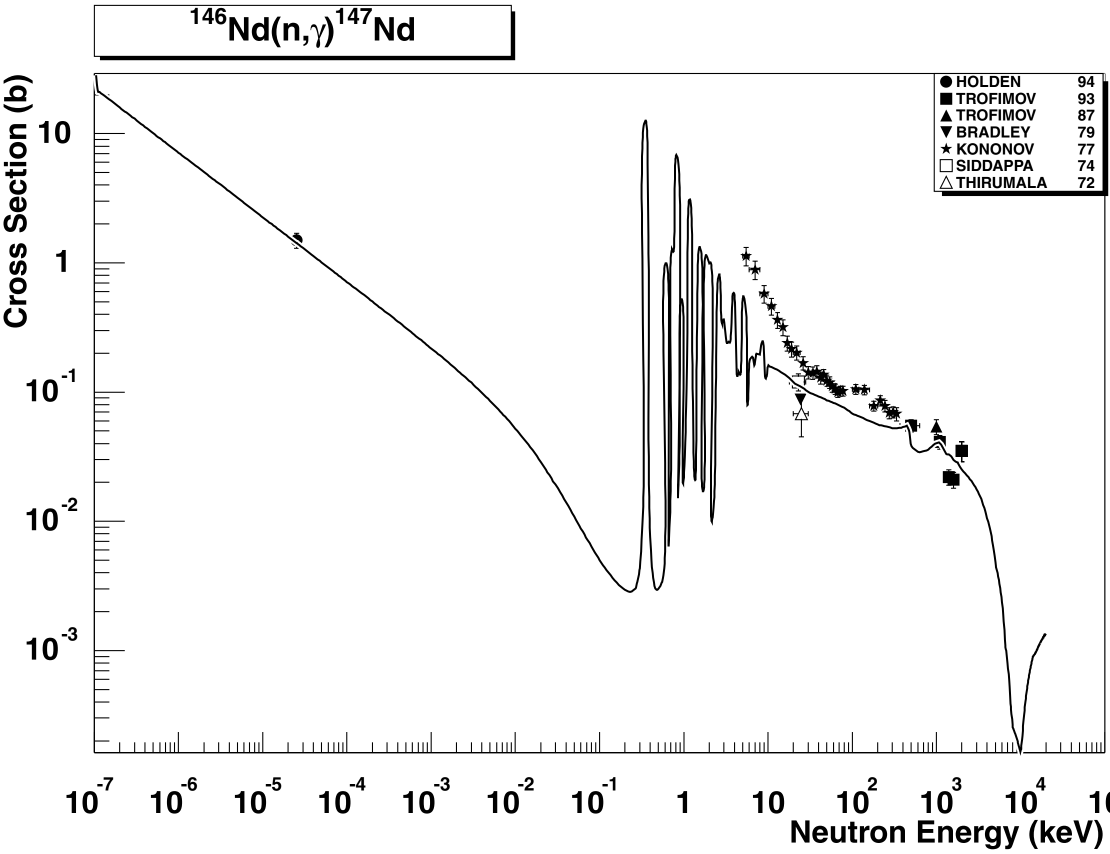

2.186. ^{146}Nd (n,γ) ^{147}Nd

final state: total
source: EAF-4.1 (JEF-2.2)

The JEF-2.2 evaluation is in a good agreement with thermal cross-section of Holden94 [32] reproducing this value with C/E=1.01. The smoothed overlapping data around 10 keV may be the reason of the disagreement with the evaluated statistical component. Several data around 30 keV support the evaluated curve, which is also close to the experimental data between 1-3 MeV. The data are stored in the SANDII structure. The original evaluation includes 17079 data points.

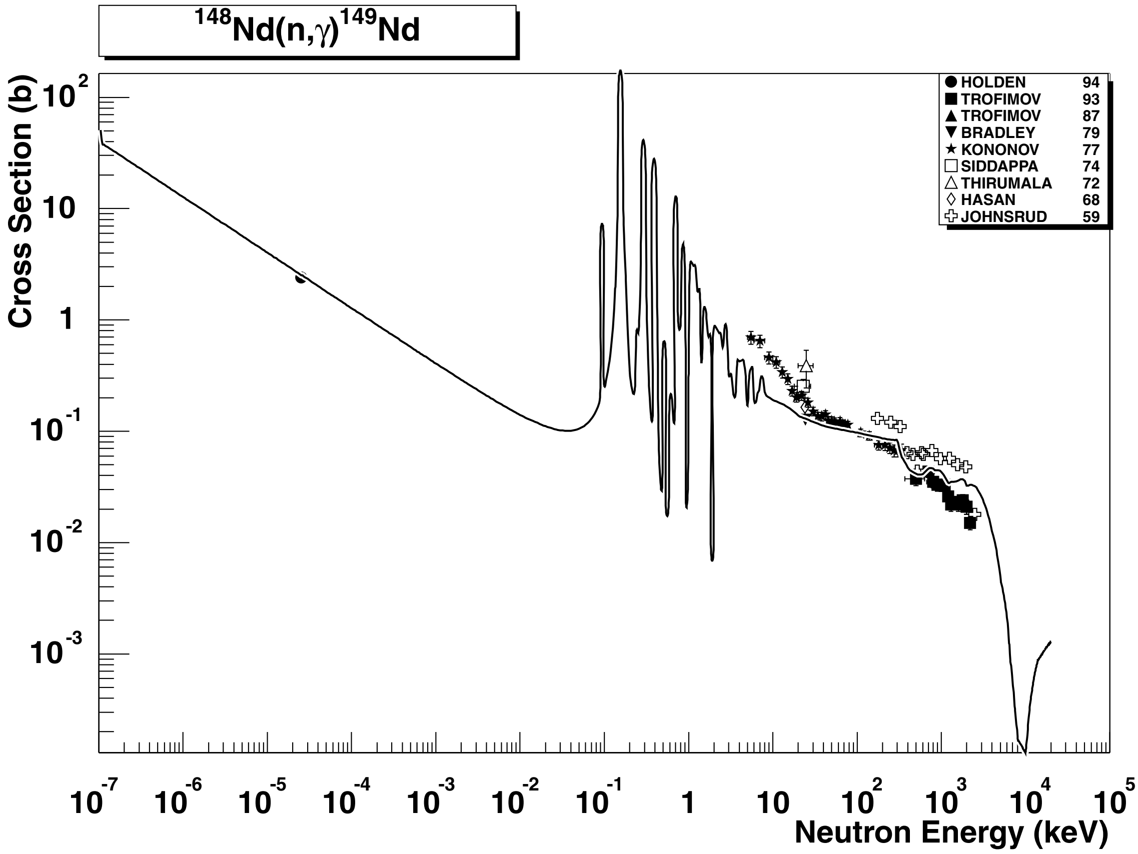

2.187. ^{148}Nd (n,γ) ^{149}Nd

final state: total
source: EAF-4.1 (JEF-2.2)

This is the original JEF-2.2 evaluation. The thermal cross-section of Holden94 [32] is well reproduced with C/E=1.01. The smooth statistical component runs reasonably between the experimental data between 5 keV and 3 MeV. The data are stored in the SANDII structure. The original evaluation includes 20 298 data points.

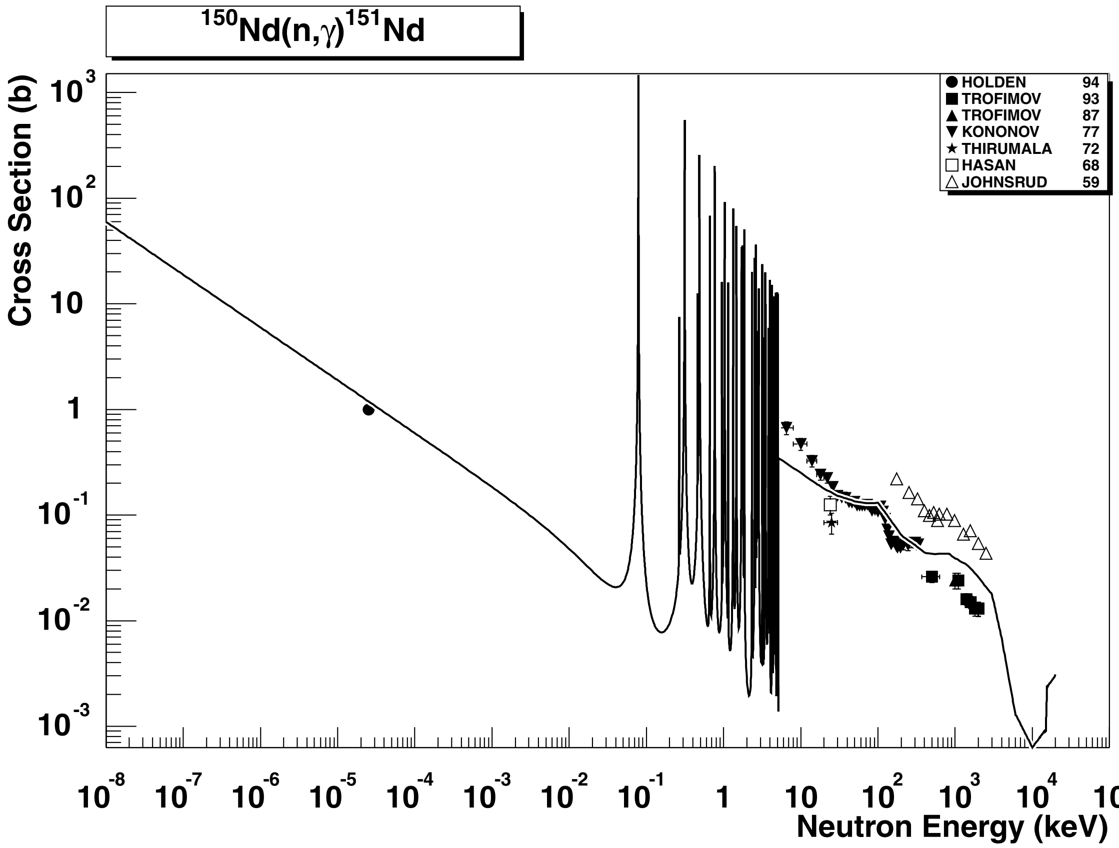

2.188. ^{150}Nd (n,γ) ^{151}Nd

final state: total
source: EAF-4.1 (JEF-2.2)

The revised ENDF/B-V evaluation has been adopted. The thermal cross-section of Holden94 [32] is reproduced with C/E=1.19. The smooth statistical component lies close to experimental data up to 3 MeV, except the data of Johnsrud59. This data set disagrees with the remaining data, which are consistent among themselves, and therefore Johnsrud59 can be disregarded.

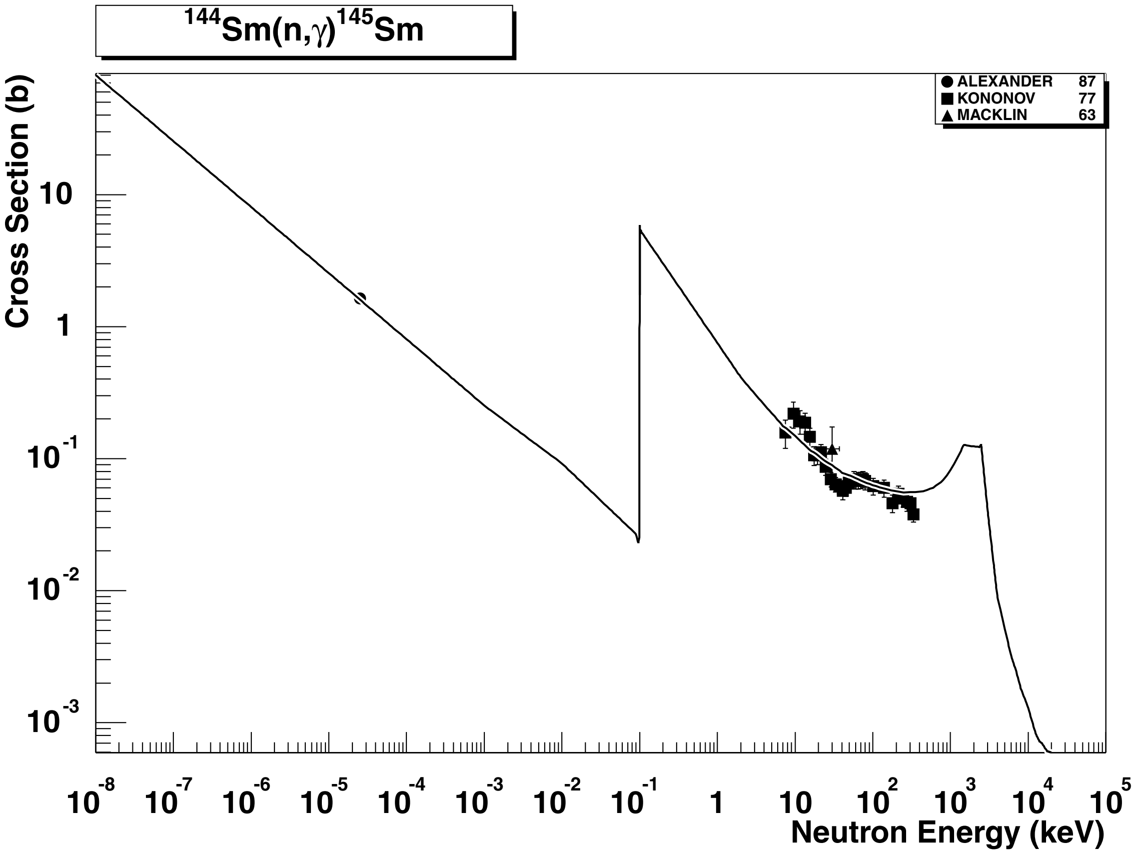

2.189. ^{144}Sm (n,γ) ^{145}Sm

final state: total
source: EAF-99

The revised ENDF/B-V simplified excitation curve (no resonance region) fits the thermal cross-section. The high energy component has been renormalized to the data of Macklin63 and Kononov77.

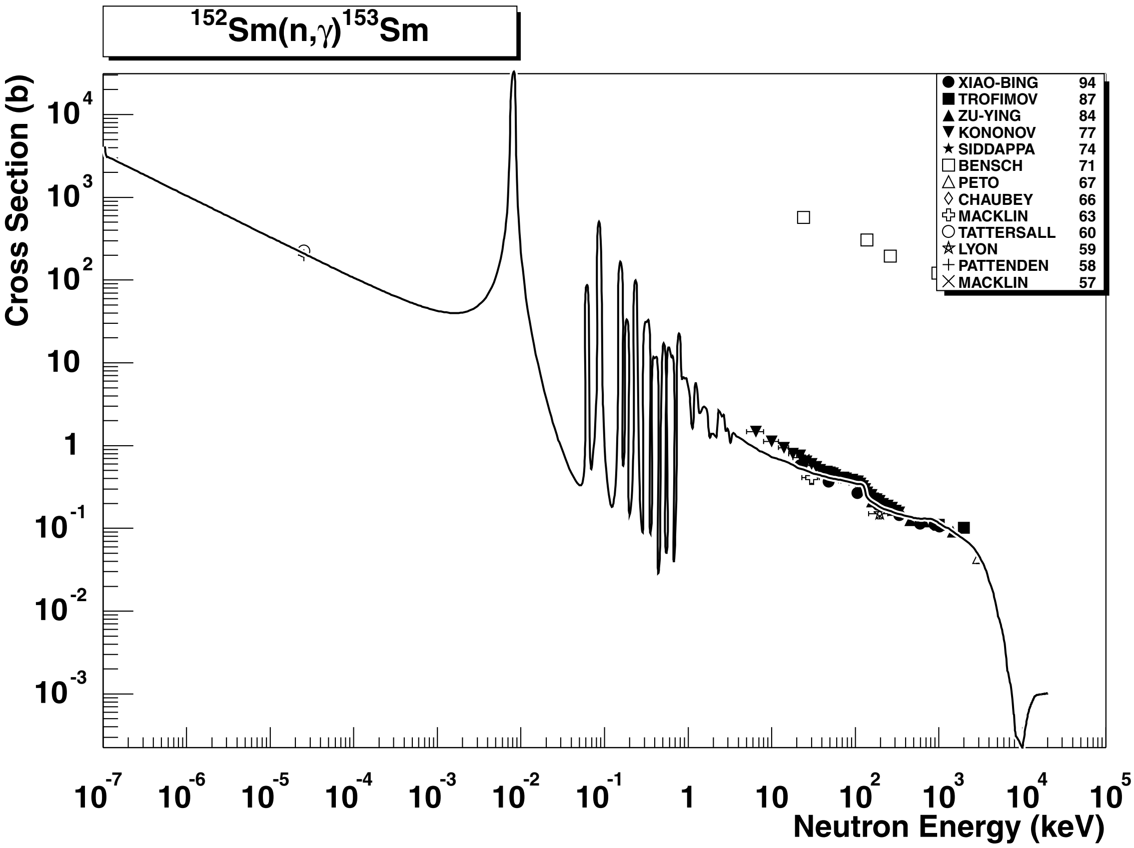

2.190. ^{152}Sm (n,γ) ^{153}Sm

final state: total
source: EAF-4.1 (JEF-2.2)

The JEF-2.2 evaluation is in a good agreement with all retrieved data from the thermal region up to 3 MeV, except the data of Bensch71 which are wrong. The data are stored in the SANDII structure. The original evaluation includes 16 572 data points.

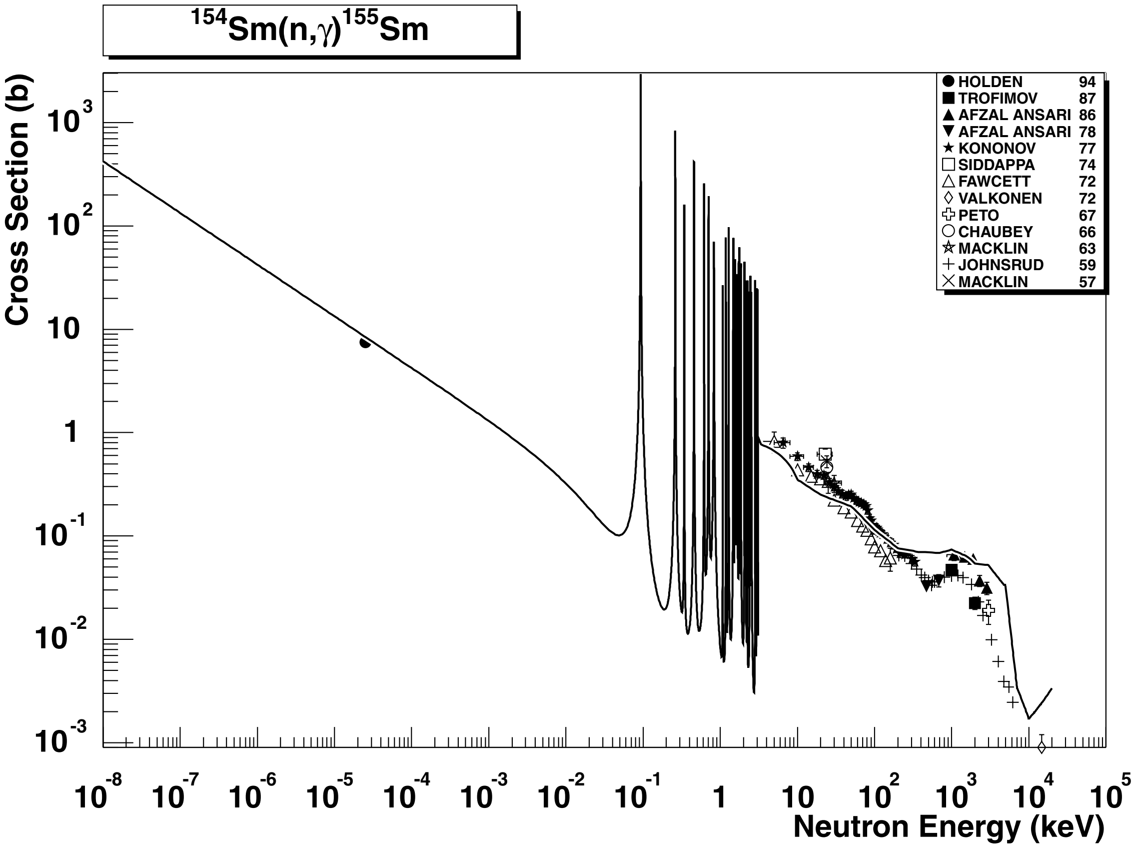

2.191. ^{154}Sm (n,γ) ^{155}Sm

final state: total
source: EAF-4.1 (JEF-2.2)

The revised ENDF/B-V evaluation has been adopted. The thermal cross-section of Holden94 [32] is reproduced with C/E=1.17. The smooth statistical component runs reasonably close to experimental data up to 6 MeV. The pre-equilibrium component is slightly too large, overestimating the experimental value of Valkonen76 and also the 14.5 MeV systematics. However, the overestimation is acceptable.

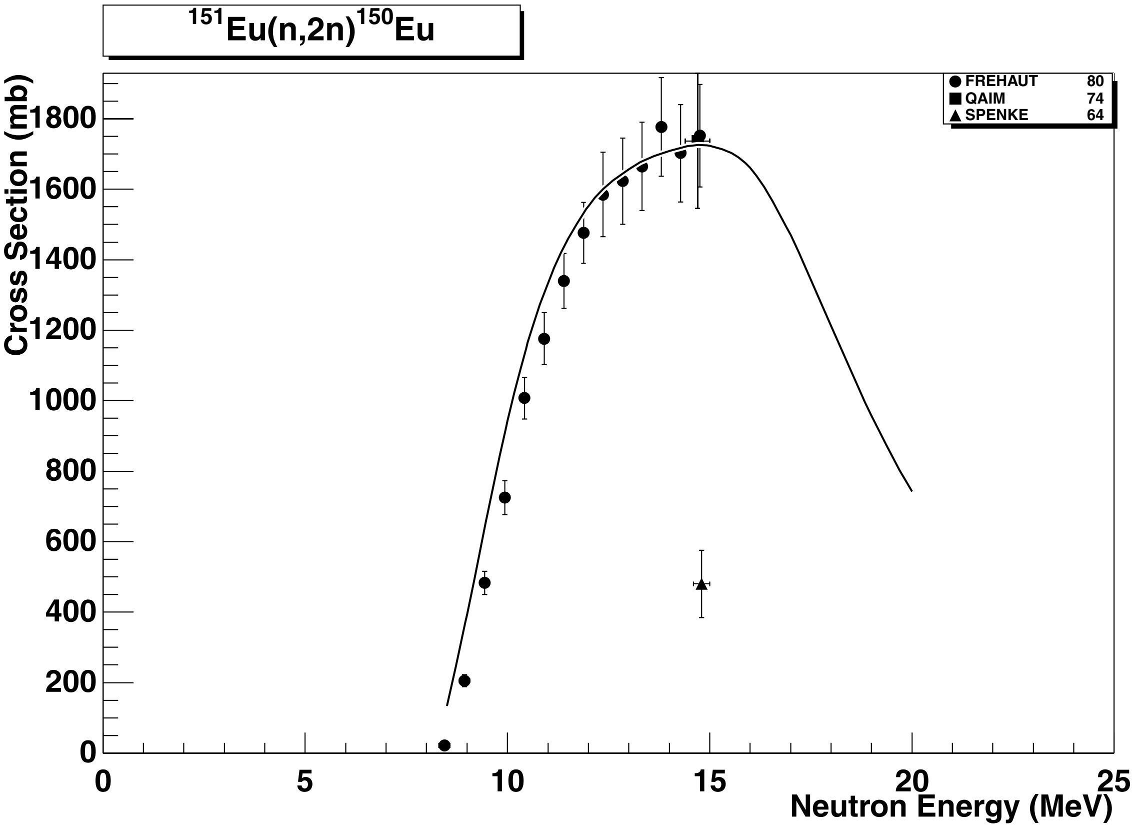

2.192. ^{151}Eu (n,2n) ^{150}Eu

final states: g.s., meta
source: CRP [g.s.], ADL-3 [meta]

The total cross-section is the reference reaction. The combined CRP and ADL-3 evaluations have been adopted for the g.s. and meta state, respectively. The evaluated total cross-section runs well through the data of Qaim74 and Frehaut80. Spenke64 looks wrong and can be disregarded.

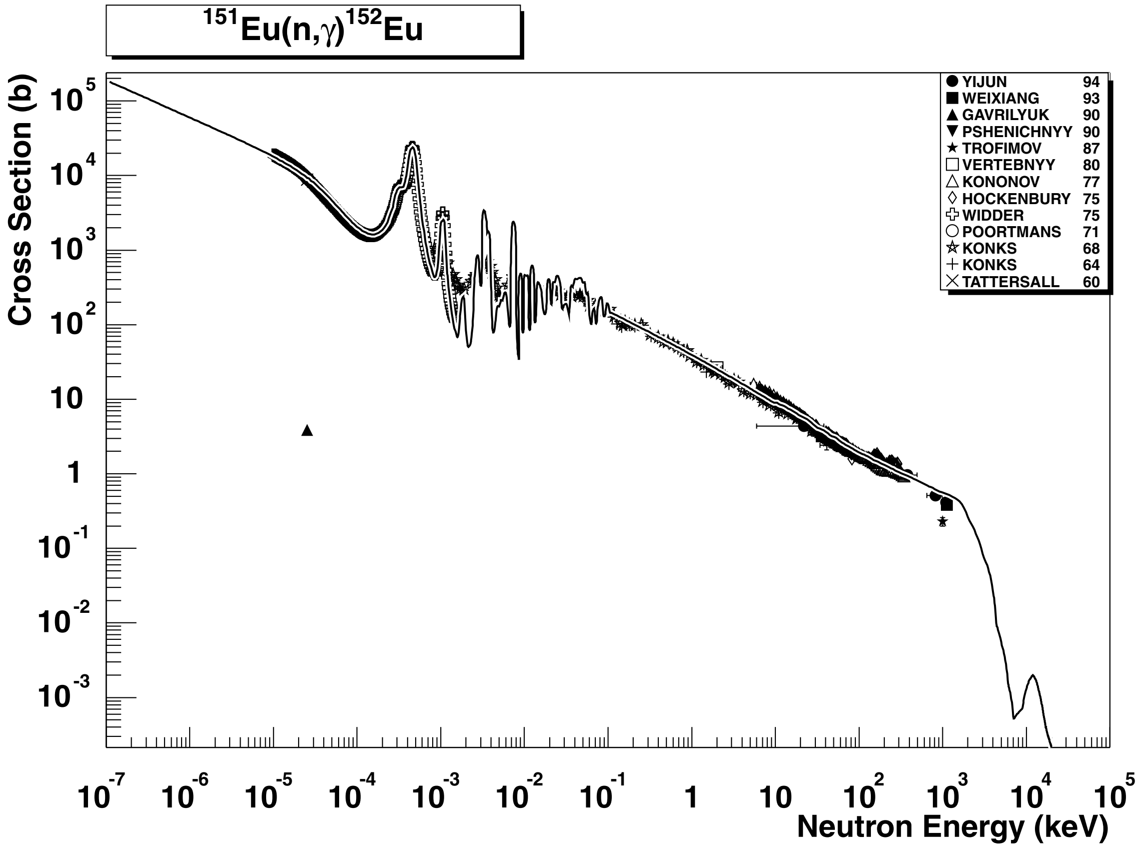

2.193. ^{151}Eu (n,γ) ^{152}Eu

final states: g.s., meta-1, meta-2
source: EAF-4.1 (JEF-2.2)

The evaluation, based on the revised ENDF/B-V data, is in a perfect agreement with all EXFOR retrieved data from the thermal region up to 1 MeV, except Gavrilyuk90, which can be disregarded. cross-sections to the g.s., meta1 and meta-2 states are based on the energy dependent branching ratio systematics [2].

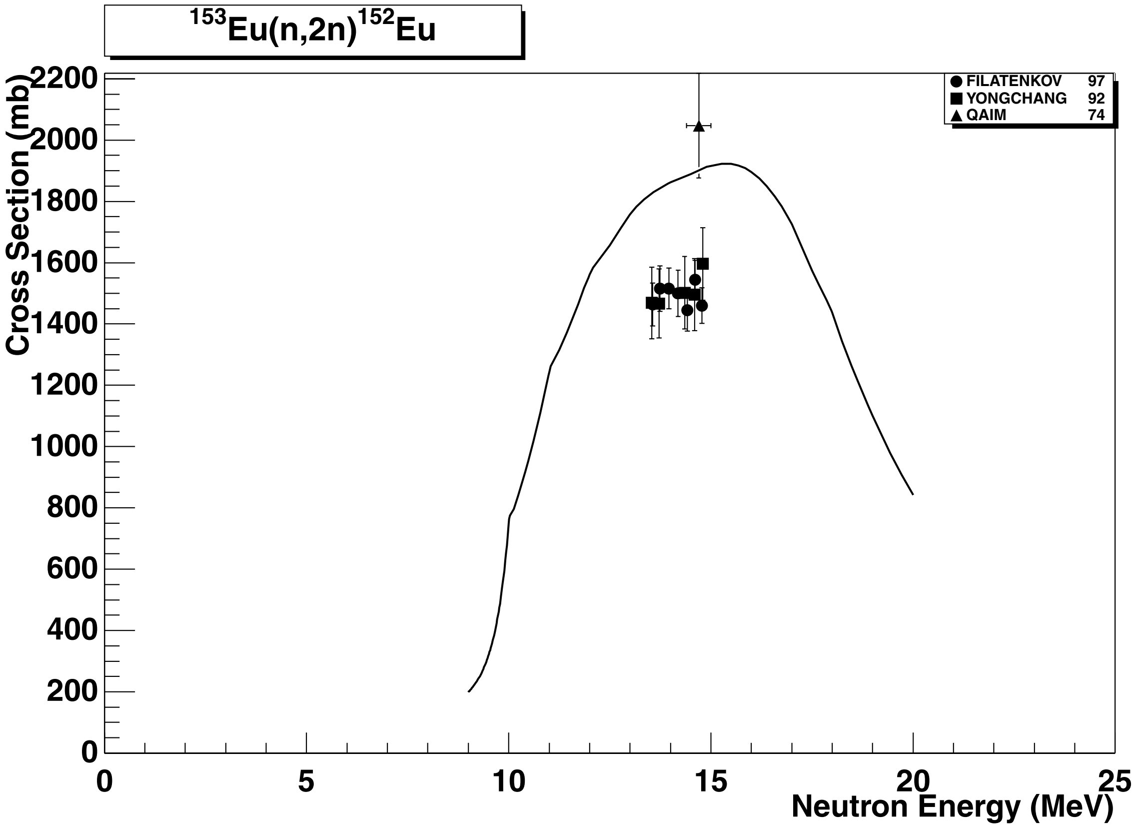

2.194. ^{153}Eu (n,2n) ^{152}Eu

final states: g.s., meta-1, meta-2
source: CRP [g.s.], EAF-4.1 [meta-1, meta-2]

The total cross-section is the reference reaction. The combined CRP and EAF-4.1 evaluations have been adopted for the g.s., meta-1 and meta-2 states, respectively. The total cross-section around 15 MeV is close to Qaim74 but overestimates (by about 15%) the recent data of Yongchang92. The data of Filatenkov97 are for g.s. + meta-2 only, without the meta-1 contribution. Their agreement with Yongchnag92 may suggest, that these may be the same quantities. Two very recent total cross-section measurements, with values of 1.722 ± 0.08 b [41] and 1.97 ± 0.095 b [42], support the value of Qaim74 and the evaluated curve.

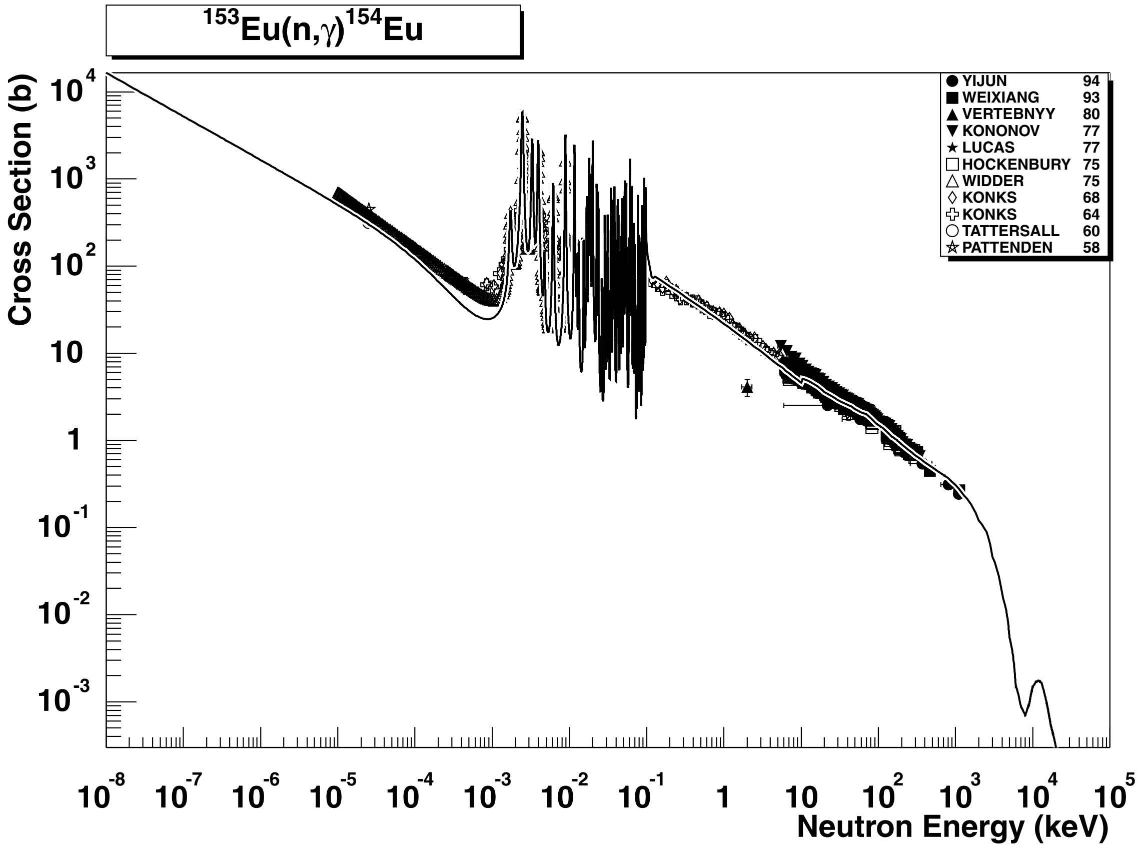

2.195. ^{153}Eu (n,γ) ^{154}Eu

final states: g.s., meta
source: EAF-4.1 (JEF-2.2)

The revised ENDF/B-V evaluation is in good agreement with all data, starting from the thermal region up to 1 MeV. cross-sections to g.s. and meta state are based on the energy dependent branching ration systematics [2].

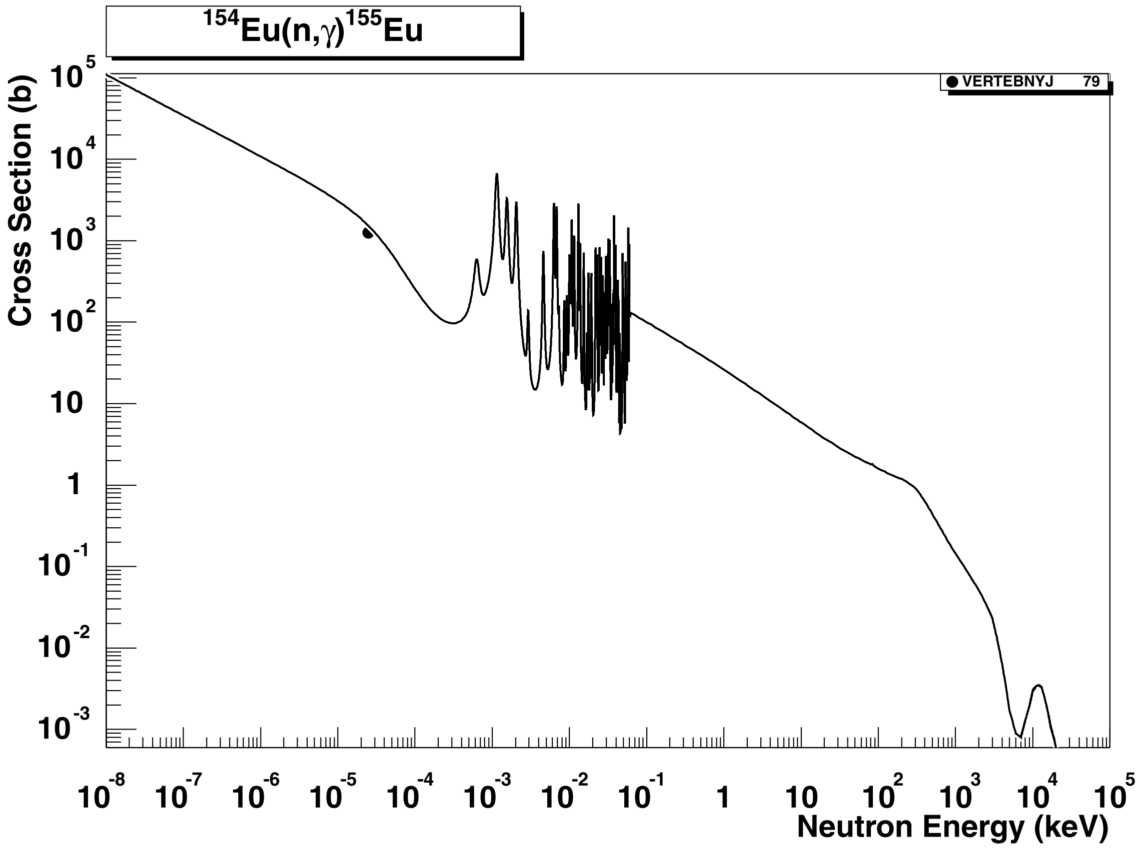

2.196. ^{154}Eu (n,γ) ^{155}Eu

final state: total
source: EAF-4.1 (JEF-2.2)

The revised ENDF/B-V evaluation agrees with the thermal cross-section experimental value of Vertebnyj79. The recommended 30 keV cross-section from [27] supports the smooth excitation curve above the resonance region.

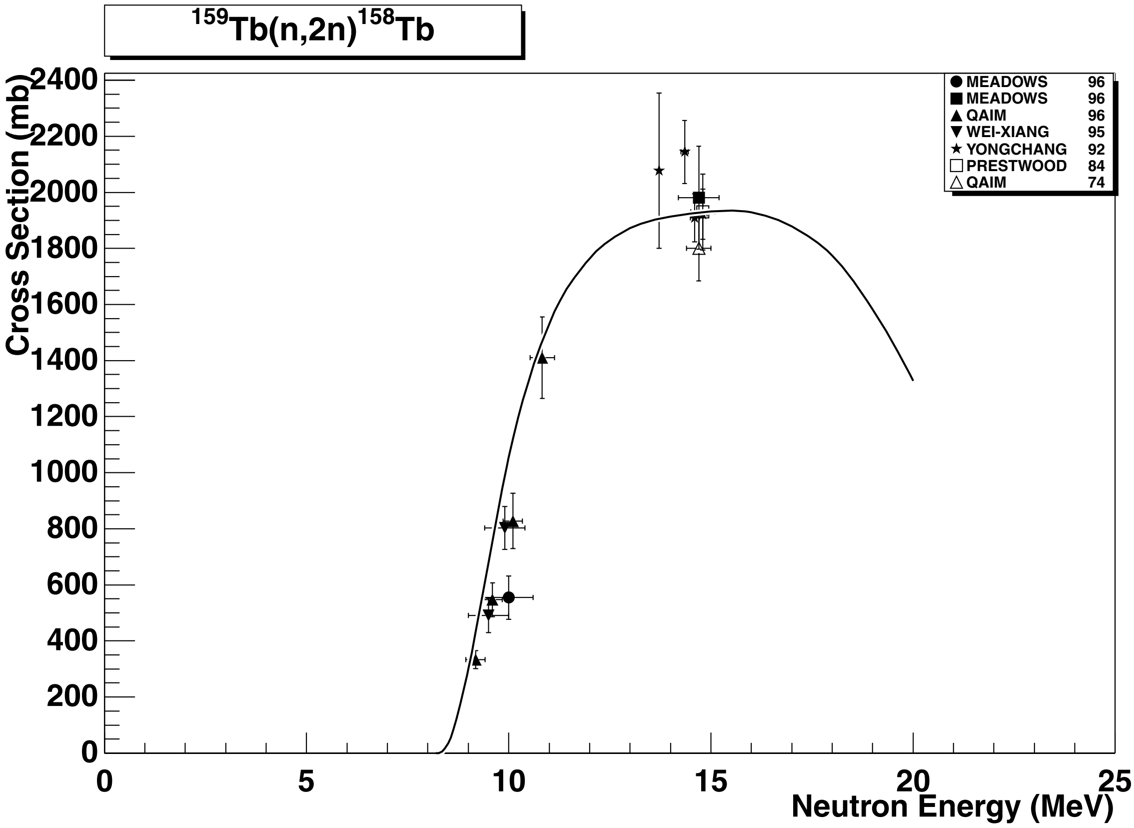

2.197. ^{159}Tb (n,2n) ^{158}Tb

final states: g.s., meta
source: CRP [g.s.], ADL-3 [meta]

The total cross-section is the reference reaction. The combined CRP and ADL-3 evaluations have been adopted for the g.s. and meta state, respectively. The total cross-section curve is reasonably close to the experimental data points.

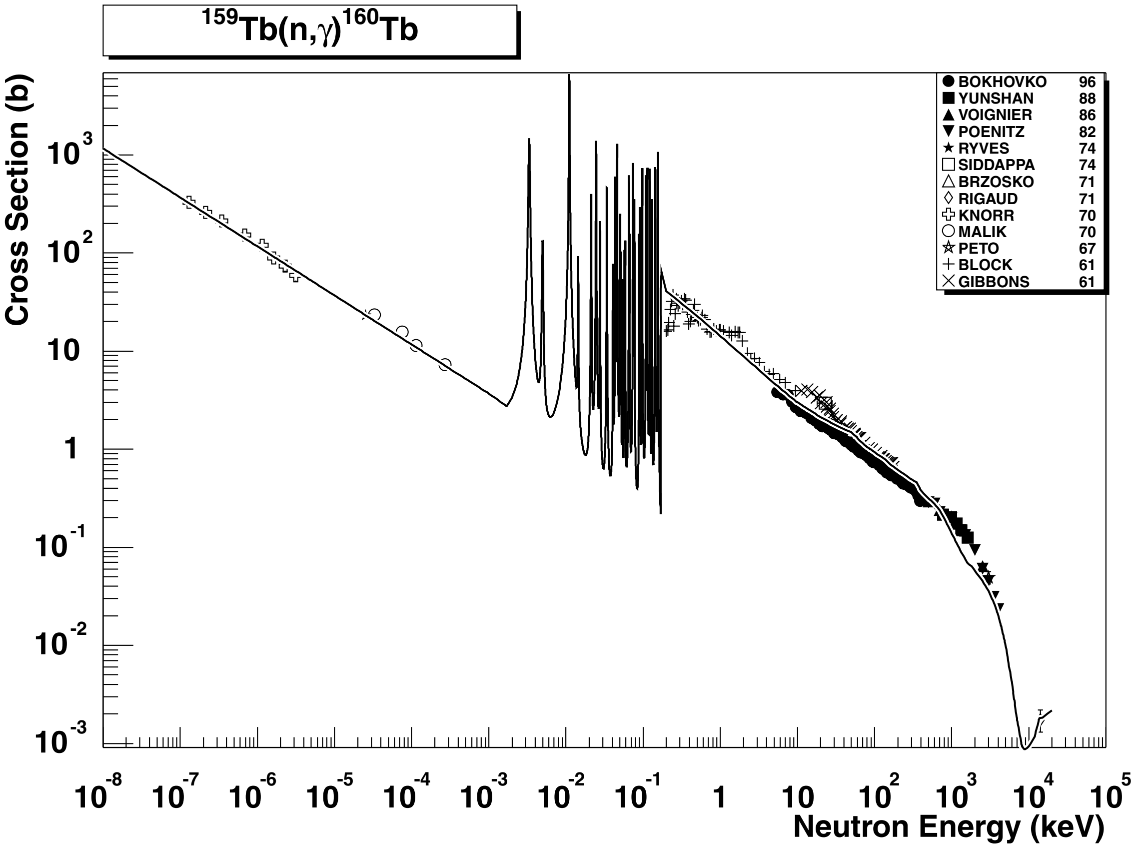

2.198. ^{159}Tb (n,γ) ^{160}Tb

final state: total
source: EAF-4.1 (JEF-2.2)

The JEF-2.2 evaluation is in a good agreement with all retrieved data starting from the thermal region up to 15 MeV.

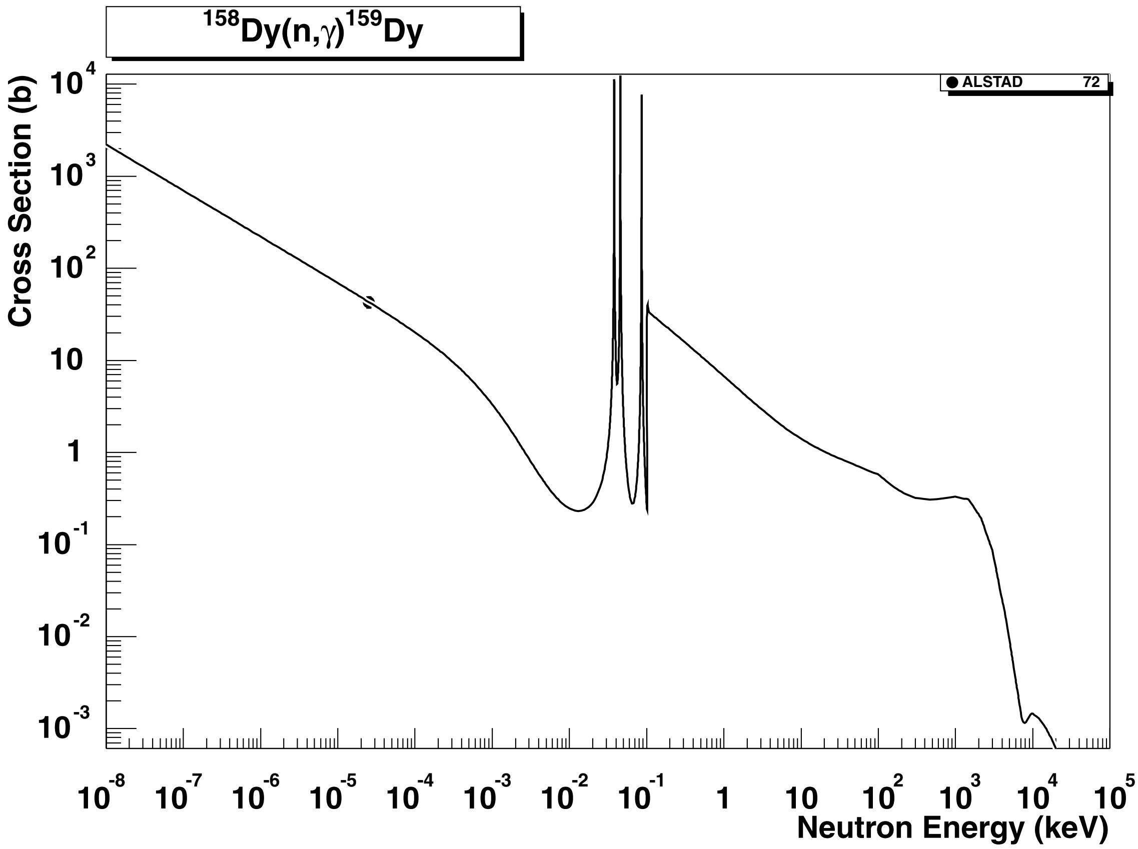

2.199. ^{158}Dy (n,γ) ^{159}Dy

final state: total
source: EAF-4.1

This is the EAF-4.1 evaluation calculated with the code SIGECN-MASGAM. The MLBW resonance treatment is included and the total thermal cross-section of Alstad72 is well reproduced. The statistical component is based on simplified calculations (with global parameters) with the code MASGAM and is supported by the recommended 30 keV cross-section [27].

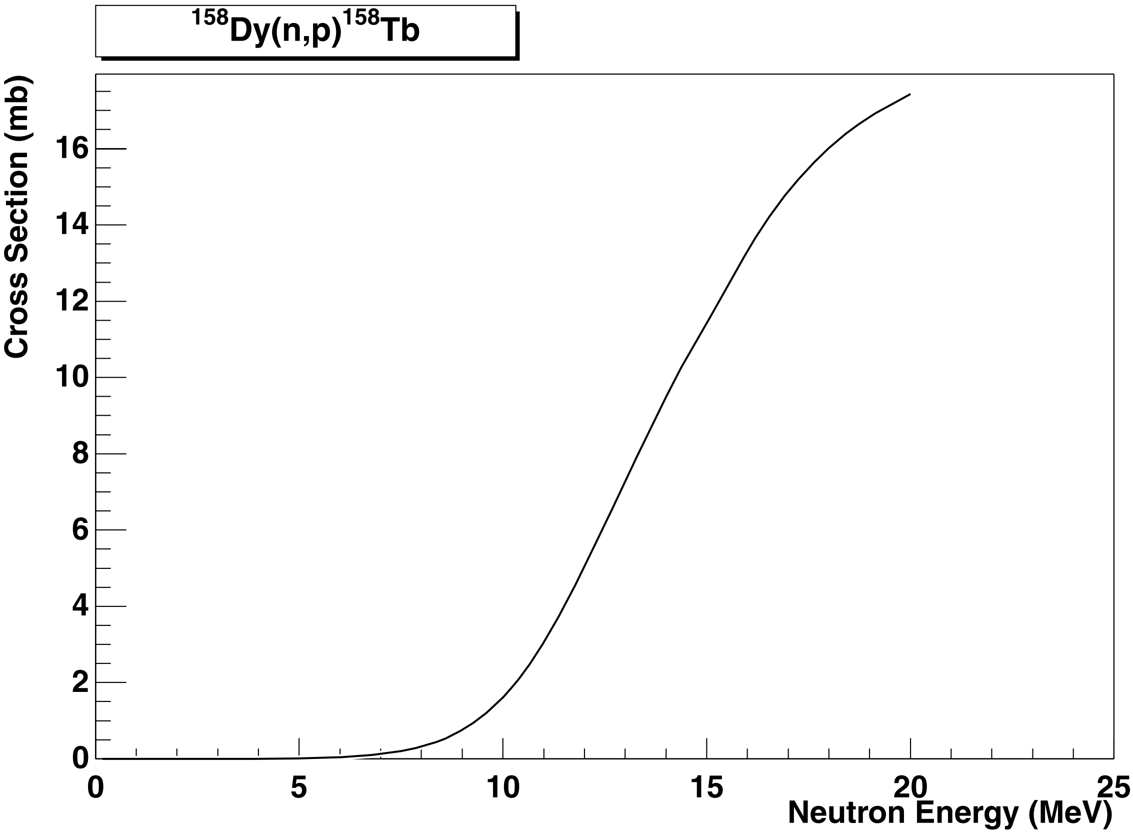

2.200. ^{158}Dy (n,p) ^{158}Tb

final state: g.s., meta
source: EAF-4.1 (ADL-3)

ADL-3 evaluation, with partial cross-sections to the g.s. and meta state based on model calculations, has been adopted. No EXFOR data are available.

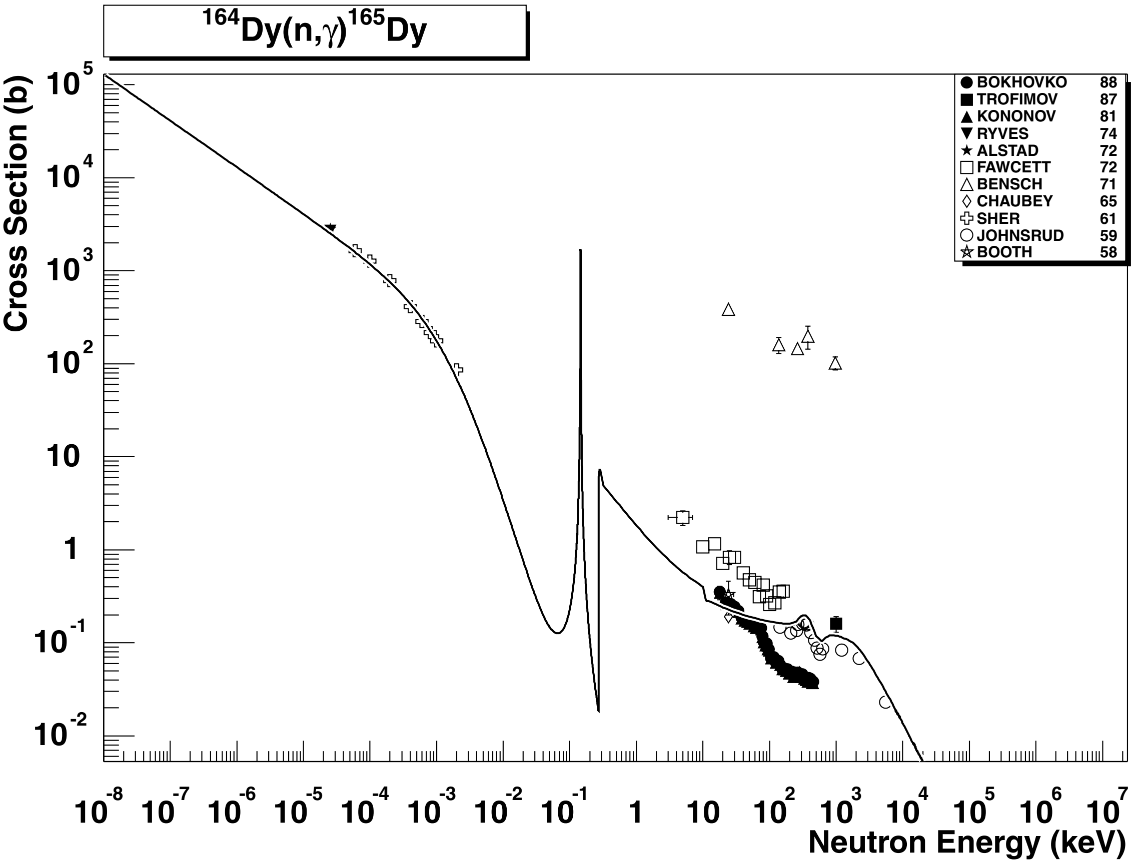

2.201. ^{164}Dy (n,γ) ^{165}Dy

final states: g.s., meta
source: EAF-4.1 (JEF-2.2)

The only available evaluation, originating from ENDF/B-III, has been adopted. cross-sections to the g.s. and meta state are based on experimental data (thermal cross-sections [26]) and applied up to the end of the resolved resonance region, while the energy dependent branching ratio systematics [2] is used for the high energy region. The resonance region is represented only by the first strong s-wave resonance. Other resonances (see [31]) have not been included. The evaluation agrees nicely in the thermal region with several experimental data points. Although the smooth statistical component runs intermediate to data between 10 keV and 6 MeV, the improvement is needed in particular by inclusion of more resonances. The data of Bensch71 are definitely wrong (too large).

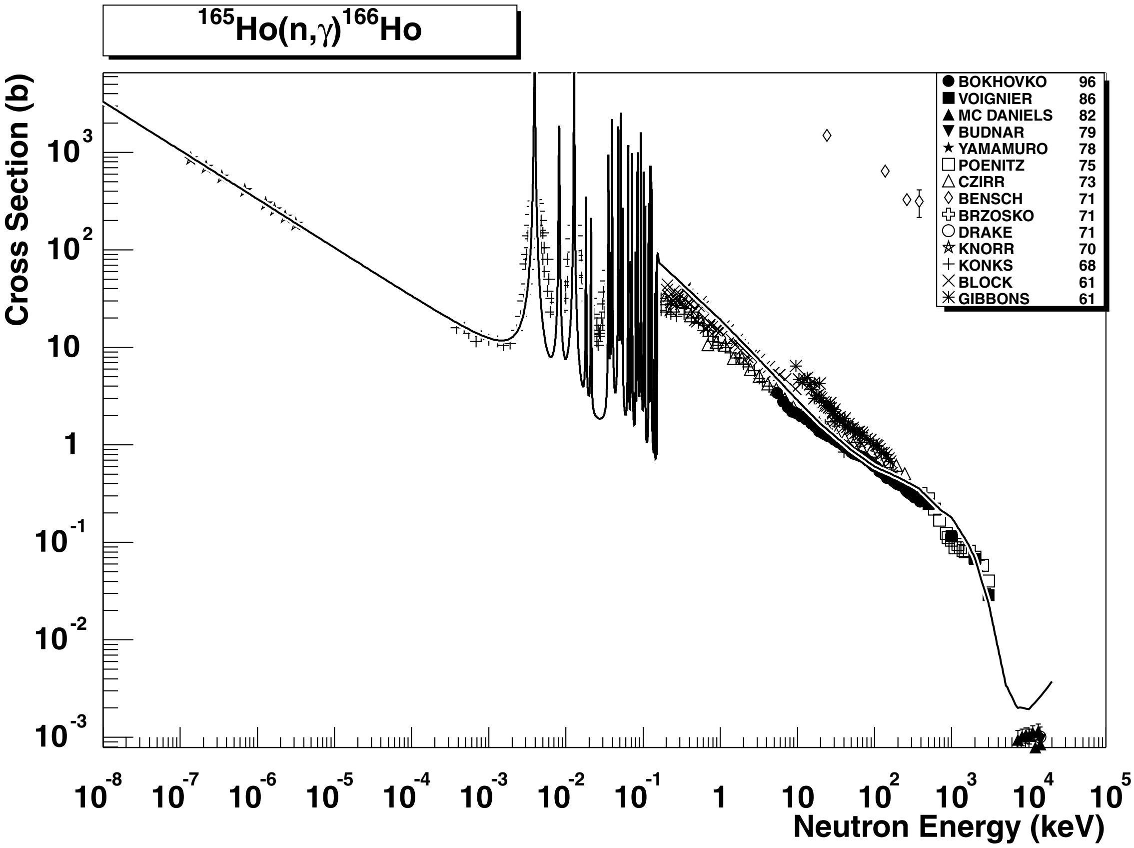

2.202. ^{165}Ho (n,γ) ^{166}Ho

final states: g.s., meta
source: EAF-4.1 (JEF-2.2)

The revised ENDF/B-V evaluation is in a good agreement with all EXFOR retrieved data from the thermal region up to 15 MeV. The data of Bensch71 are wrong, unrealistically large. cross-sections to the g.s. and meta state are based on experimental data (thermal cross-sections [26]) and applied up to the end of the resolved resonance region, while the energy dependent systematics [2] is used for the high energy region. The evaluated pre-equilibrium component is too large by about factor of two.

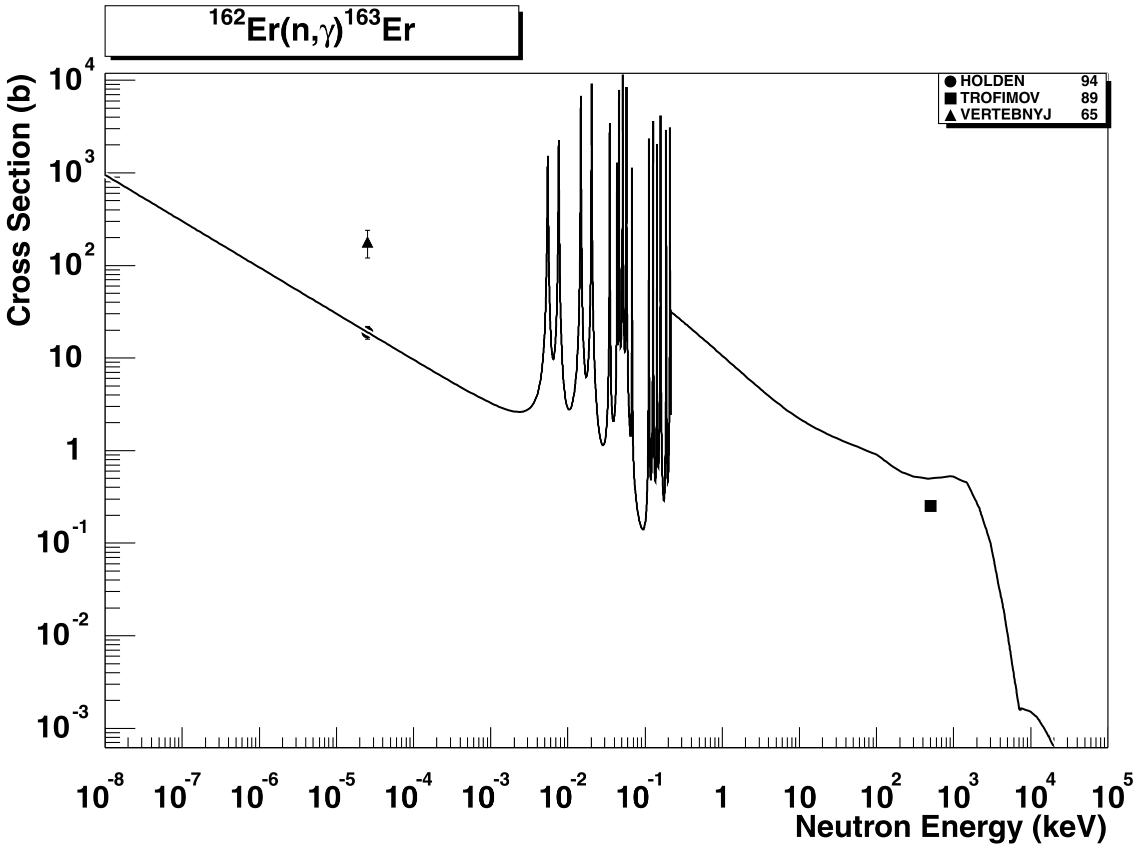

2.203. ^{162}Er (n,γ) ^{163}Er

final state: total
source: EAF-4.1

This is the original EAF evaluation calculated with the code SIGECN-MASGAM. The MLBW resonance treatment is included and the thermal cross-section of Holden94 from [32] is reproduced with C/E=1.00. The value of Vertebnyj65 is about ten times larger and can be disregarded. The statistical component is based on simplified calculations with the code MASGAM using global parameters. It is supported by the recommended 30 keV cross-section [27] and is reasonably close to the single point around 500 keV of Trofimov89.

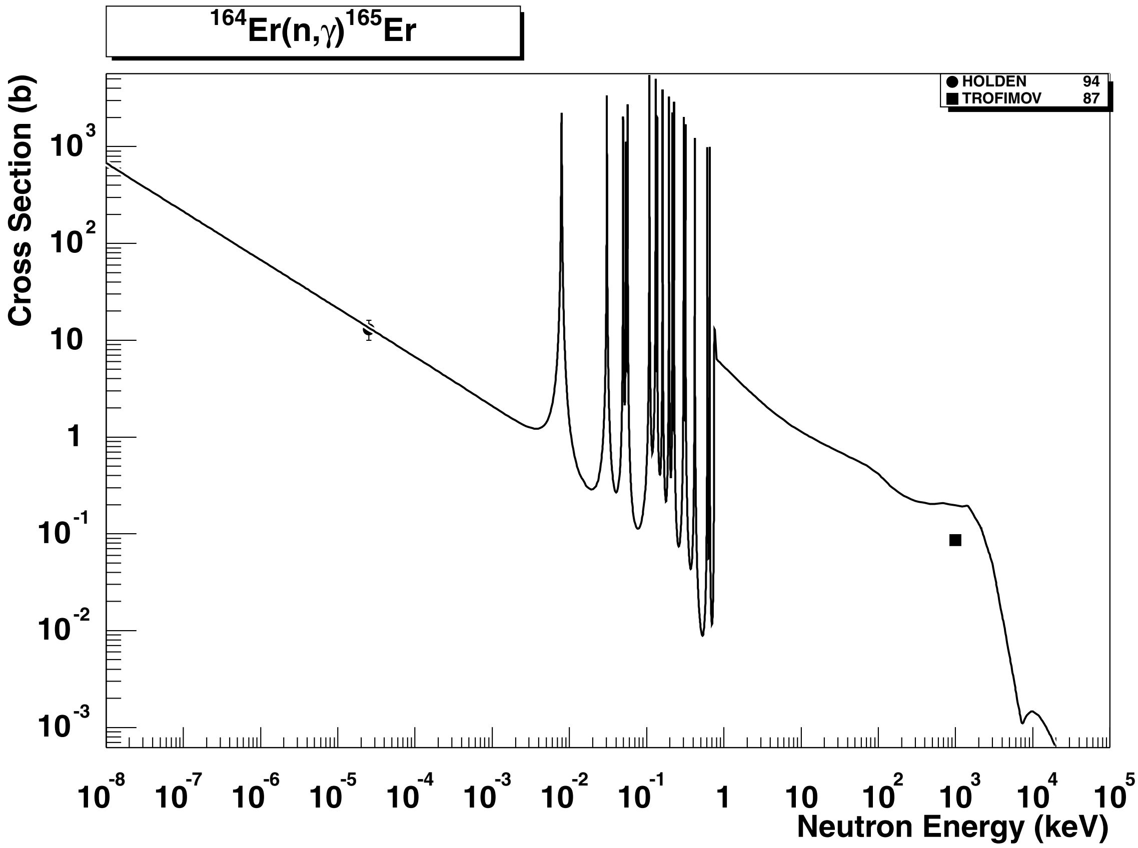

2.204. ^{164}Er (n,γ) ^{165}Er

final state: total
source: EAF-4.1

The EAF-4.1 evaluation with the SIGECN-MASGAM code fits the thermal cross section of Holden94 from [32] with C/E=1.03. The statistical component is based on simplified calculations with the code MASGAM using global parameters. It is supported by the recommended 30 keV cross-section [27] and is reasonably close to the single point of Trofimov89 at about 1 MeV.

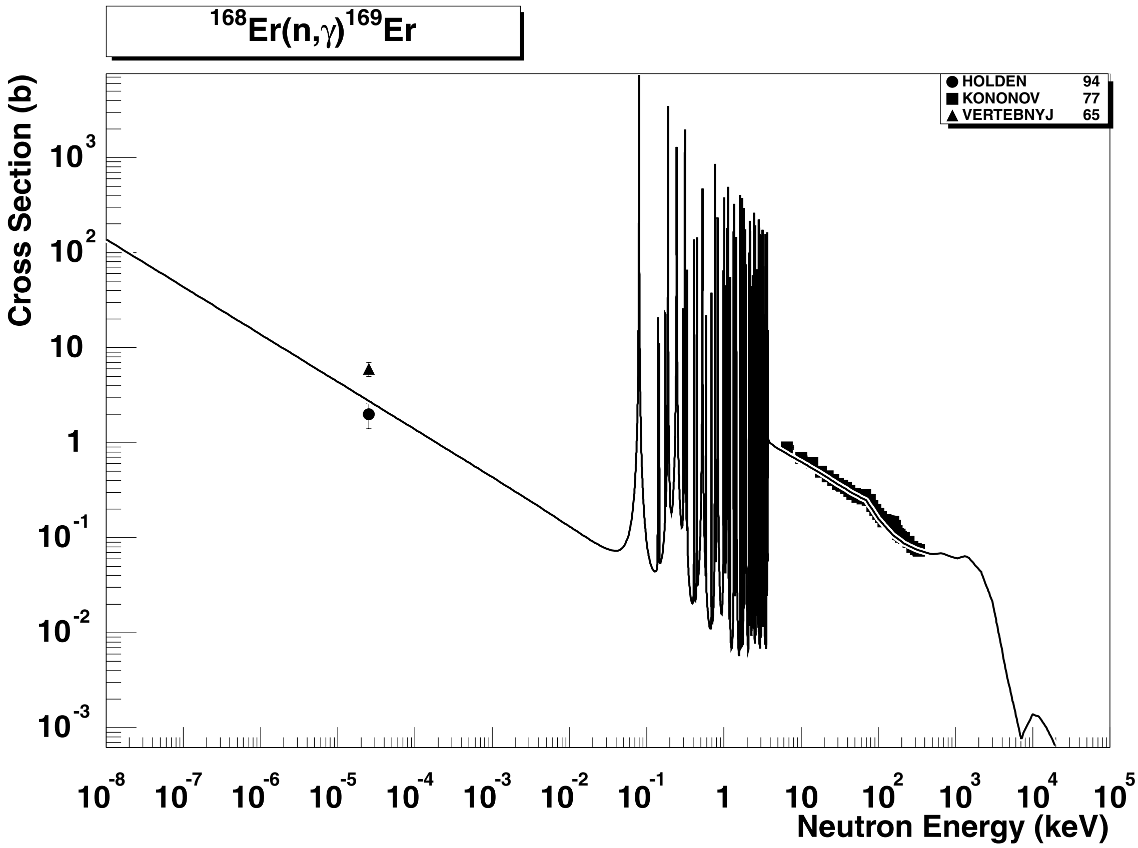

2.205. ^{168}Er (n,γ) ^{169}Er

final state: total
source: EAF-4.1

The EAF-4.1 evaluation with the SIGECN-MASGAM code fits the thermal cross section from [26] and Holden94 rather well. The less reliable point of Vertebnyj65 is about 2 times higher. The statistical component, based on simplified calculations with the code MASGAM using global parameters agrees very well with the data of Kononov77 below 400 keV.

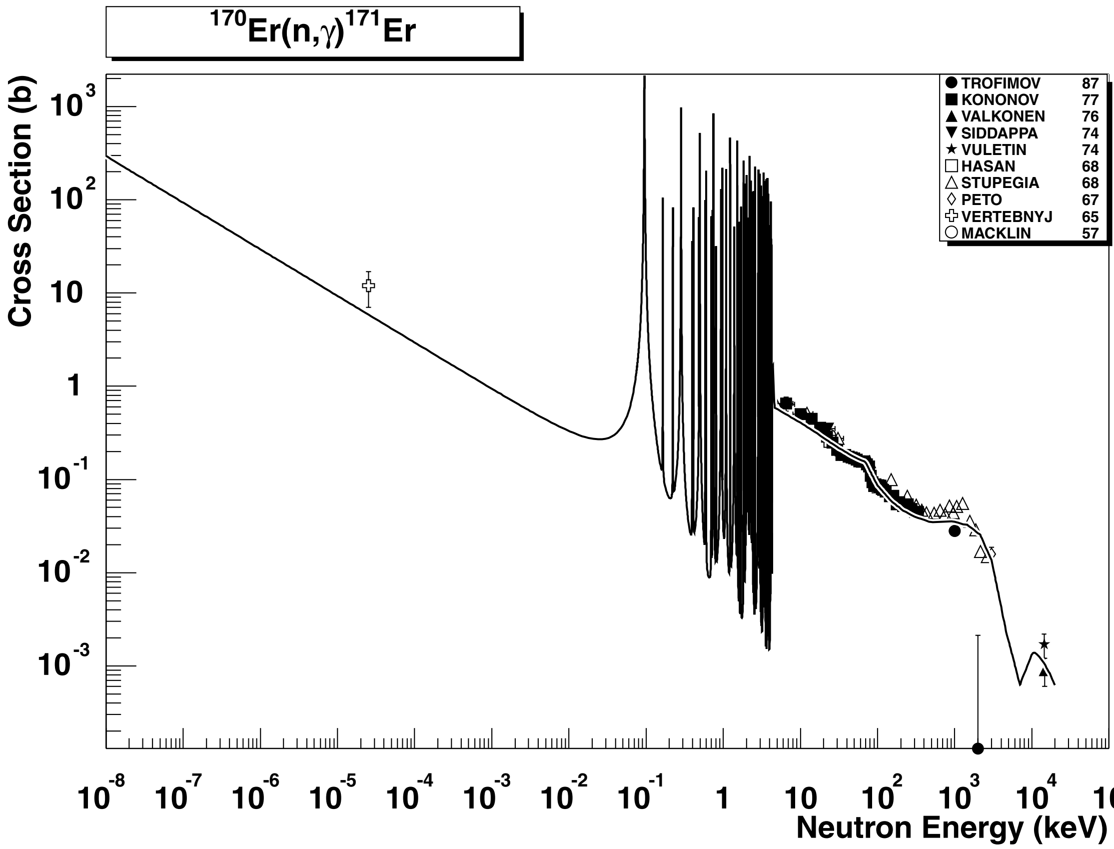

2.206. ^{170}Er (n,γ) ^{171}Er

final state: total
source: EAF-4.1

A very good agreement of the EAF-4.1 evaluation (with the code SIGECN-MASGAM) with the experimental data in the whole energy range. The thermal point of Vertebnyj65 is slightly underestimated but the more recent value of 6±2 b, adopted in Ref. [26] is well reproduced. The single point of Trofimov at 3 MeV is too low but the experimental error is large.

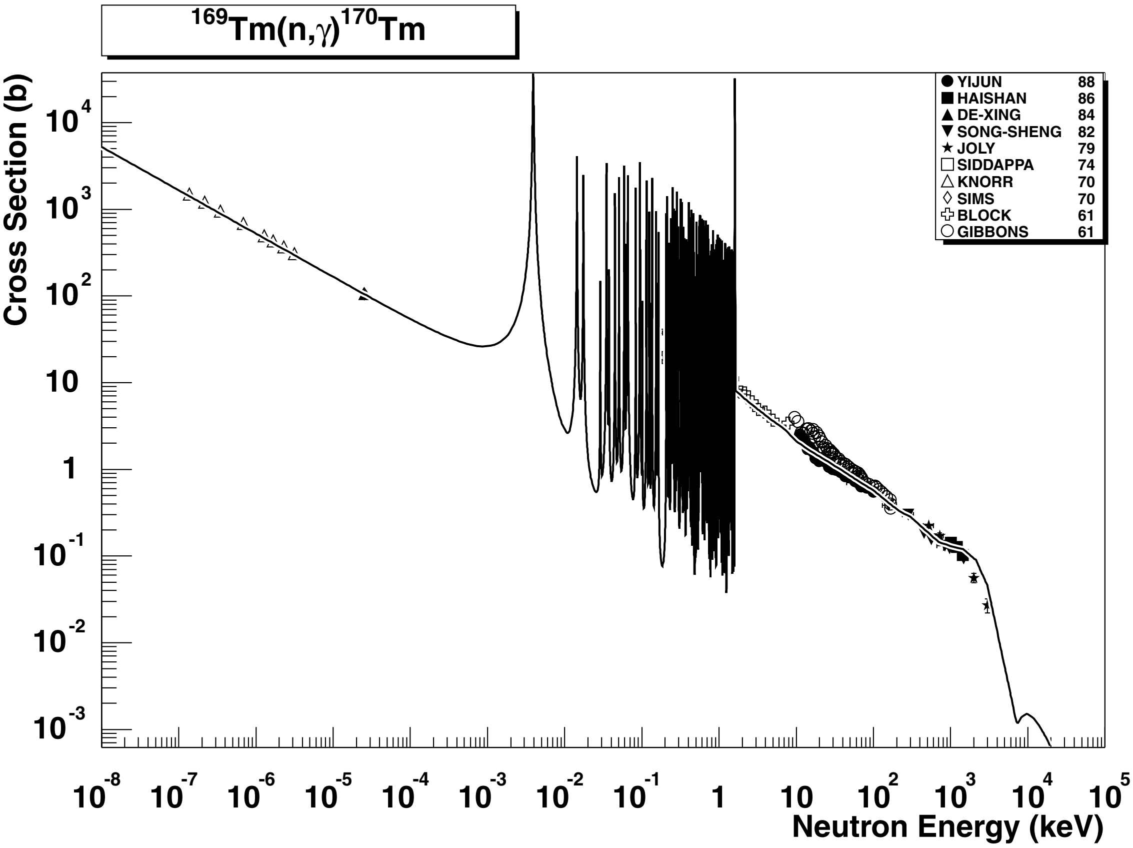

2.207. ^{169}Tm (n,γ) ^{170}Tm

final state: total
source: EAF-4.1

The EAF-4.1 evaluation (with the code SIGECN-MASGAM) is in an excellent agreement with the experimental data up to the energy of 3 MeV.

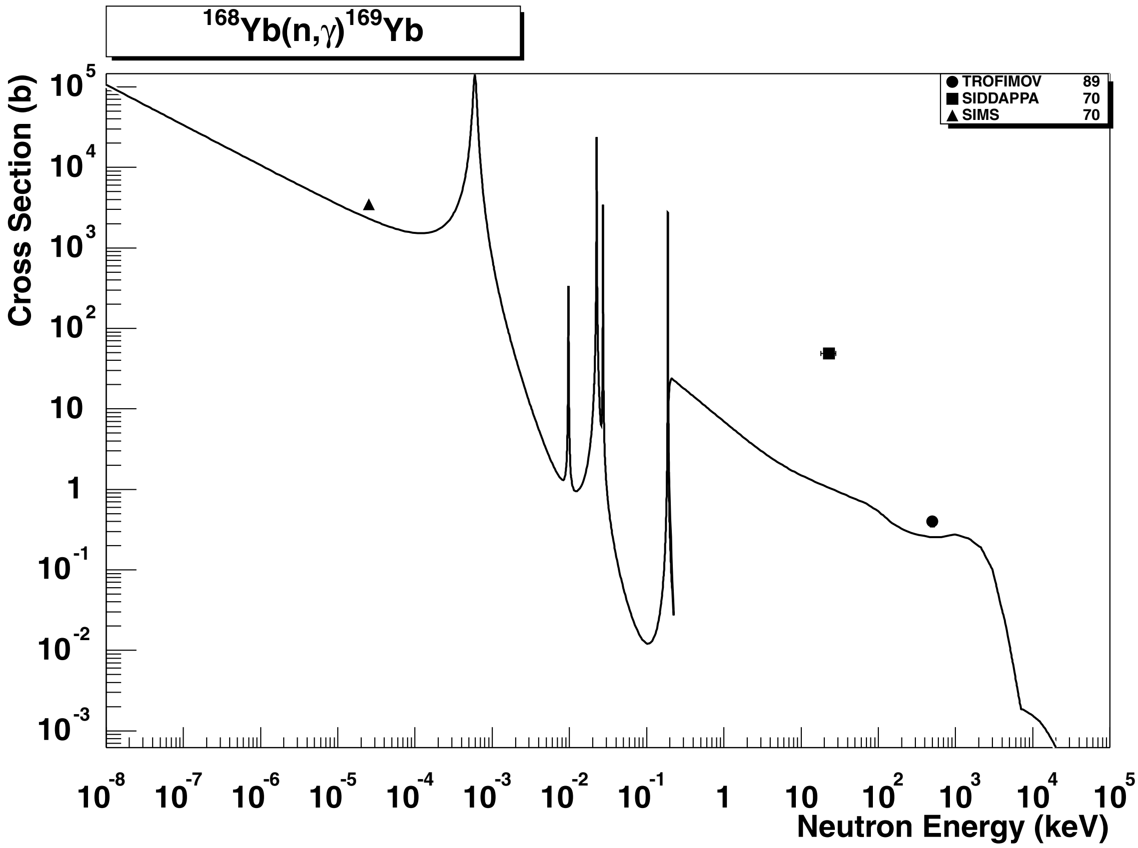

2.208. ^{168}Yb (n,γ) ^{169}Yb

final state: g.s., meta
source: EAF-4.1

This is the EAF-4.1 evaluation calculated with the code SIGECN-MASGAM. The MLBW resonance treatment is included and the thermal cross-section of Sims70 is reasonably reproduced, as well as the recommended value of Ref. [26] (C/E=1.00). Cross sections to the g.s. and meta state are based on the energy dependent branching ratio systematics [2]. The statistical component is based on simplified calculations with the code MASGAM using global parameters. It is supported by the recommended 30 keV cross-section [27] and is reasonably close to the single point around 500 keV of Trofimov89. The single point of Siddappa70 is wrong (too large) contradicting the 30 keV data in [27].

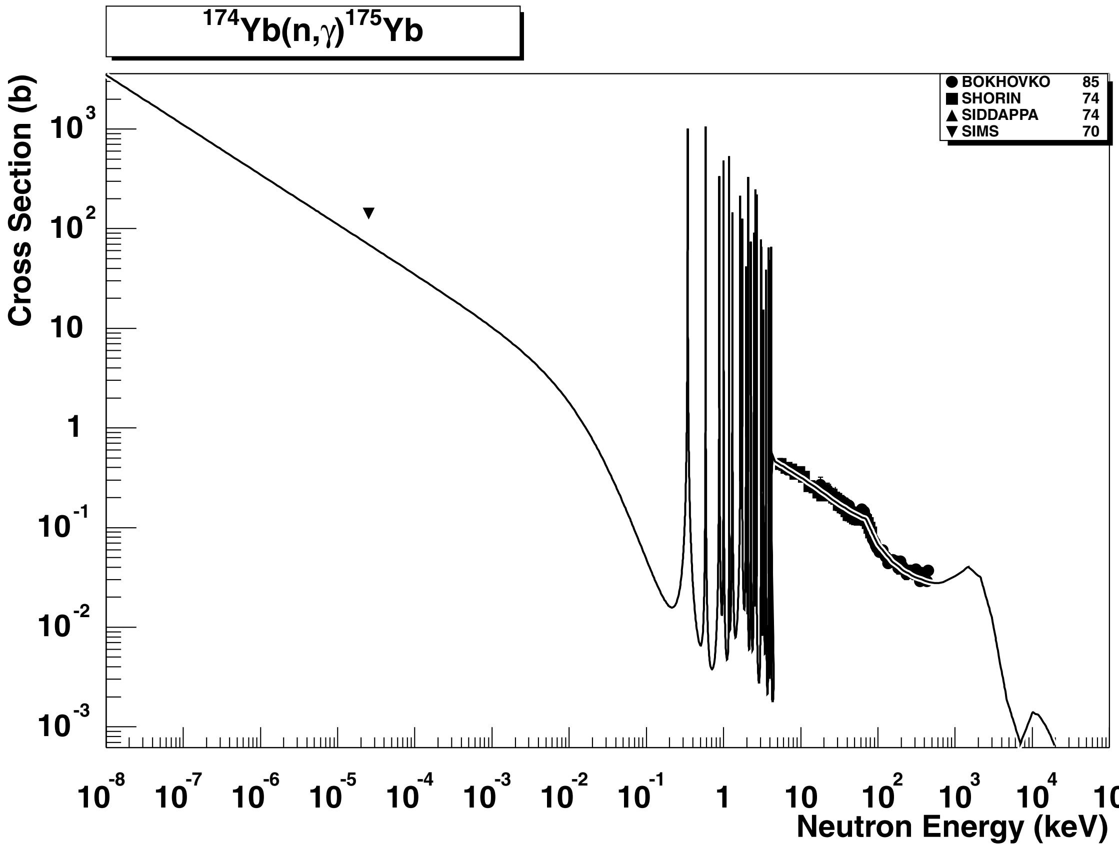

2.209. ^{174}Yb (n,γ) ^{175}Yb

final state: total
source: EAF-4.1

The EAF-4.1 evaluation with the SIGECN-MASGAM code (with MLBW resonance treatment) underestimates the thermal cross-section of Sims70 and the recommended value [26] by C/E=0.58. The statistical component, based on simplified calculations (code MASGAM with global parameters) is in a very good agreement with the experimental data between 5-400 keV.

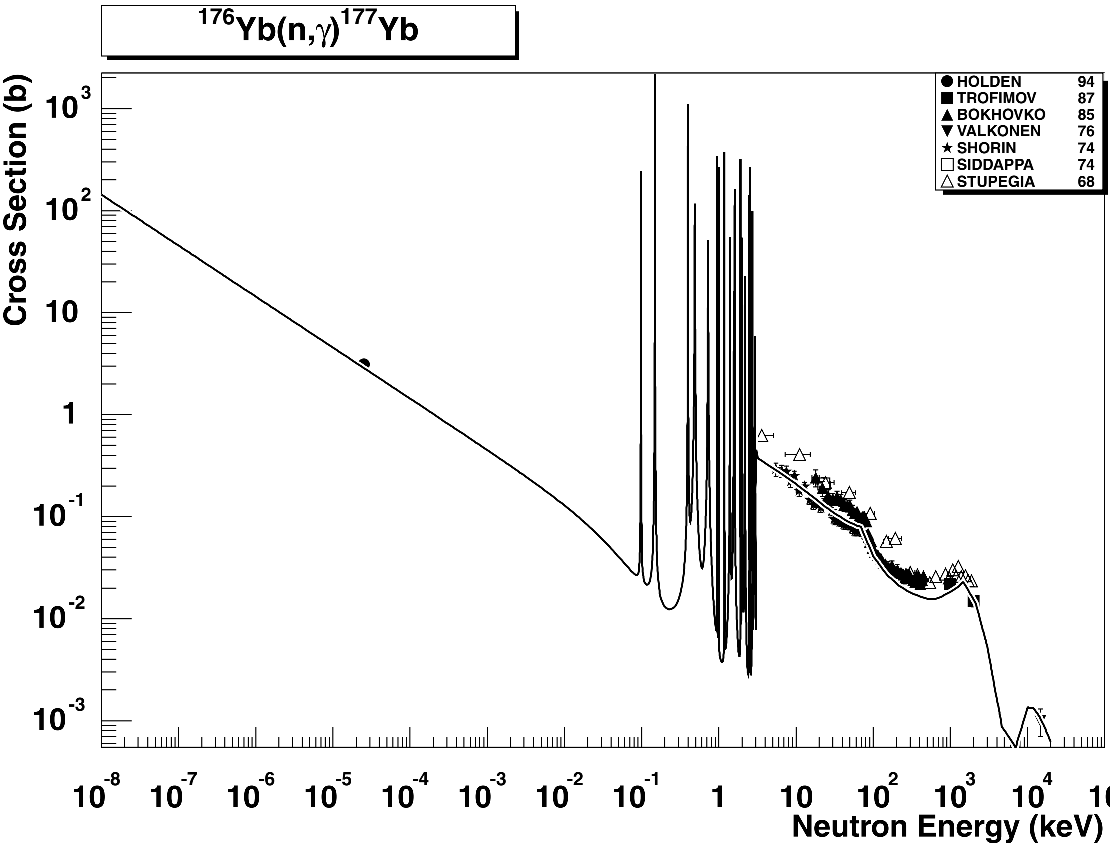

2.210. ^{176}Yb (n,γ) ^{177}Yb

final states: g.s., meta
source: EAF-4.1

The EAF-4.1 evaluation calculated with the code SIGECN-MASGAM. The MLBW resonance treatment is applied and the thermal cross-section of Holden94 [32] is reproduced with C/E=1.00. cross-sections to the g.s. and meta state are based on the energy dependent branching ratio systematics [2]. The statistical component is based on simplified calculations with the code MASGAM using global parameters and runs reasonably close to many experimental points up to 2 MeV.

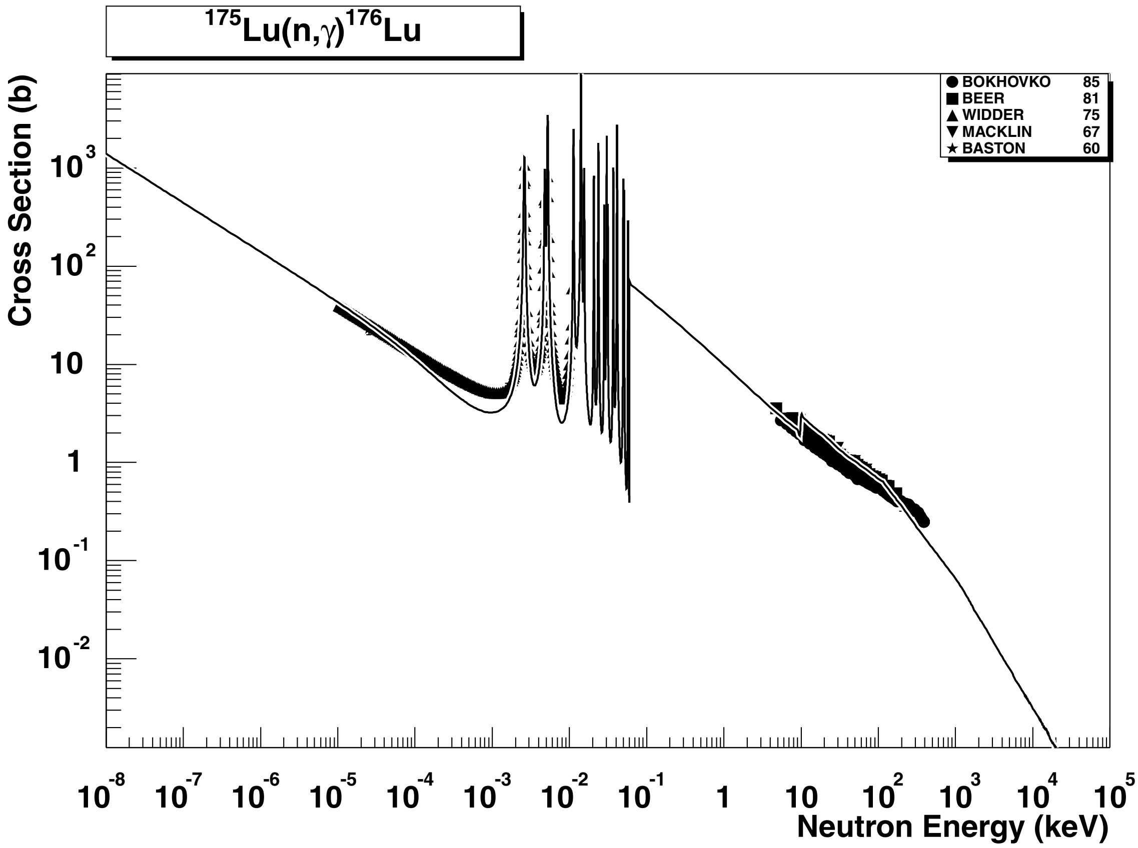

2.211. ^{175}Lu (n,γ) ^{176}Lu

final states: g.s., meta
source: EAF-4.1 (JEF-2.2)

The evaluation adopted in JEF-2.2 is based on the revised ENDF/B-IV data. It agrees well with experimental data both in the thermal- and high energy (5-50 keV) ranges. The cross-sections to the g.s. and meta state are based on experimental data (thermal cross-sections [26]) and applied up to the end of the resolved resonance region, while the energy dependent branching ratio systematics [2] is used for the high energy region.

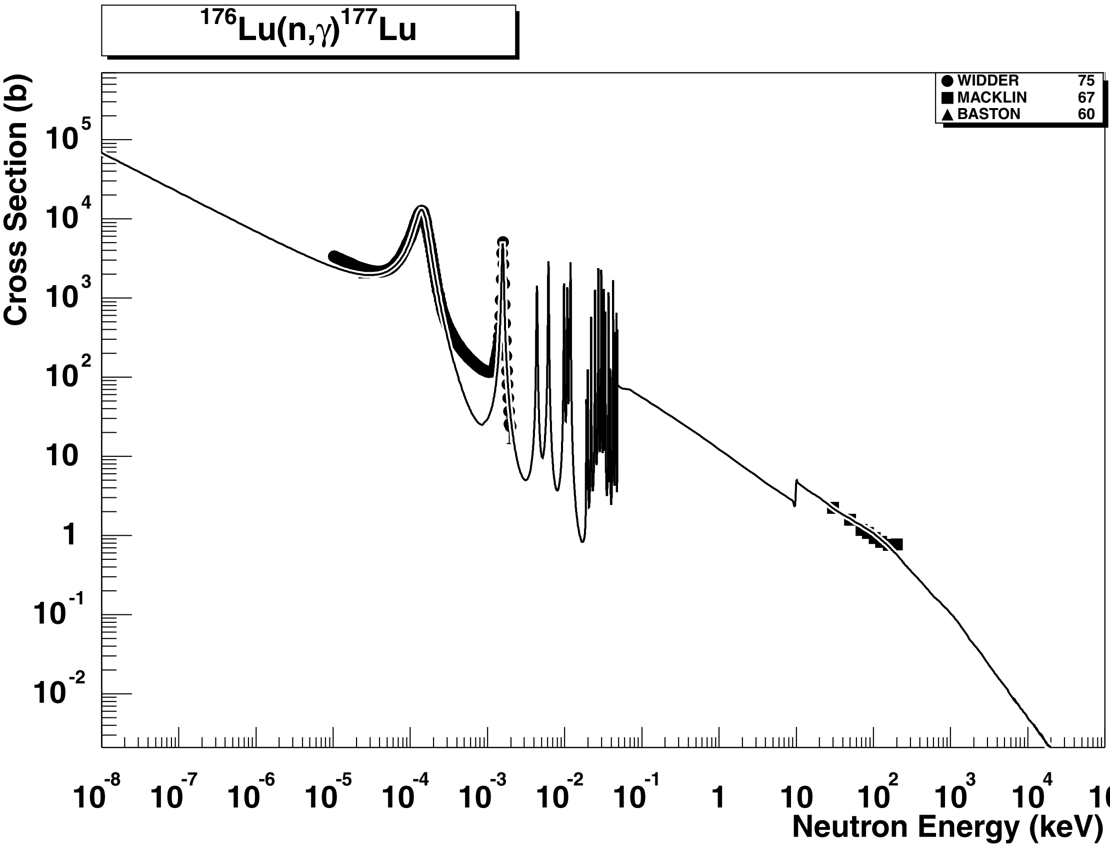

2.212. ^{176}Lu (n,γ) ^{177}Lu

final states: g.s., meta
source: EAF-4.1 (JEF-2.2)

The revised ENDF/B-IV evaluation has been adopted in JEF-2.2. It agrees well with experimental data both in the thermal- and high energy (20-200 keV) ranges. cross-sections to the g.s. and meta state are based on experimental data (thermal cross-sections [26]) and applied up to the end of resolved resonance region, while the energy dependent branching ratio systematics [2] is used for the high energy region.

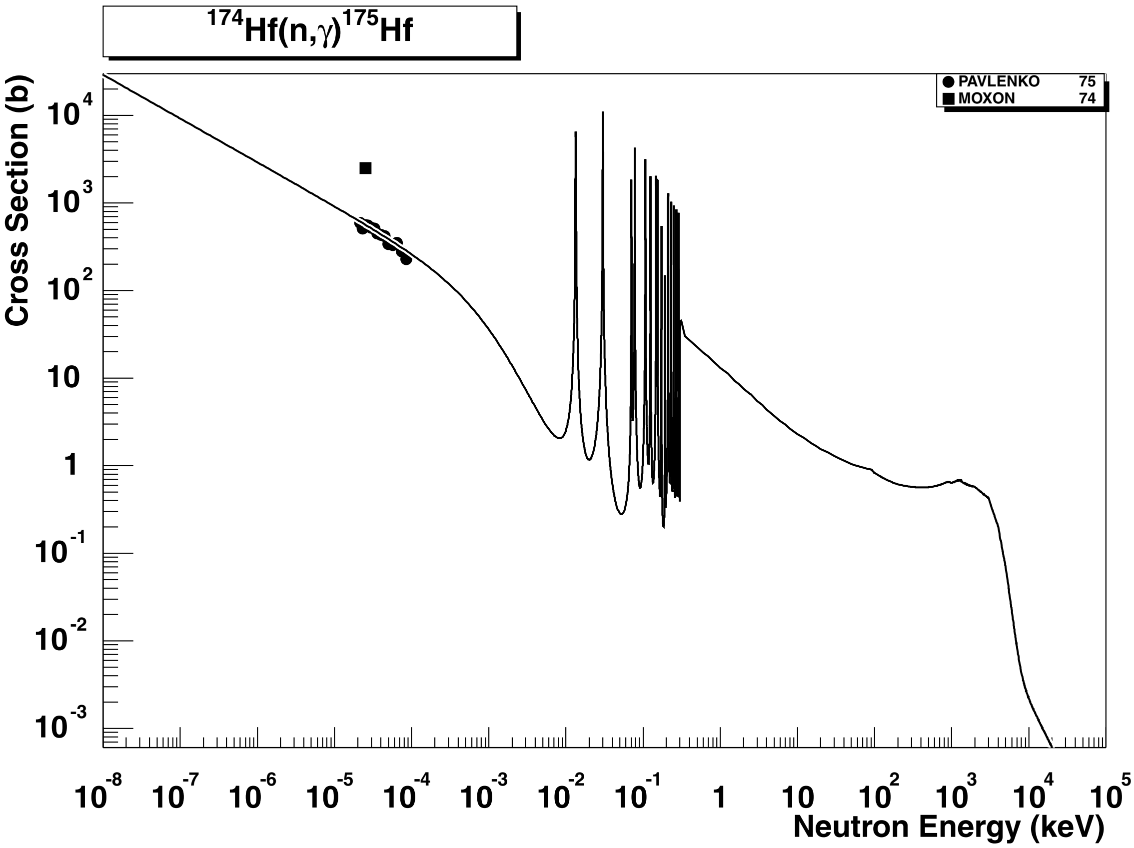

2.213. ^{174}Hf (n,γ) ^{175}Hf

final state: total
source: EAF-4.1 (JEF-2.2)

The JEF-2.2 evaluation agrees in the thermal range with data of Pavlenko75 and with the recommended value from [26]. The single point of Moxon74 deviates from these data by factor of three and can be disregarded. The statistical component is supported by the recommended 30 keV cross-section [27].

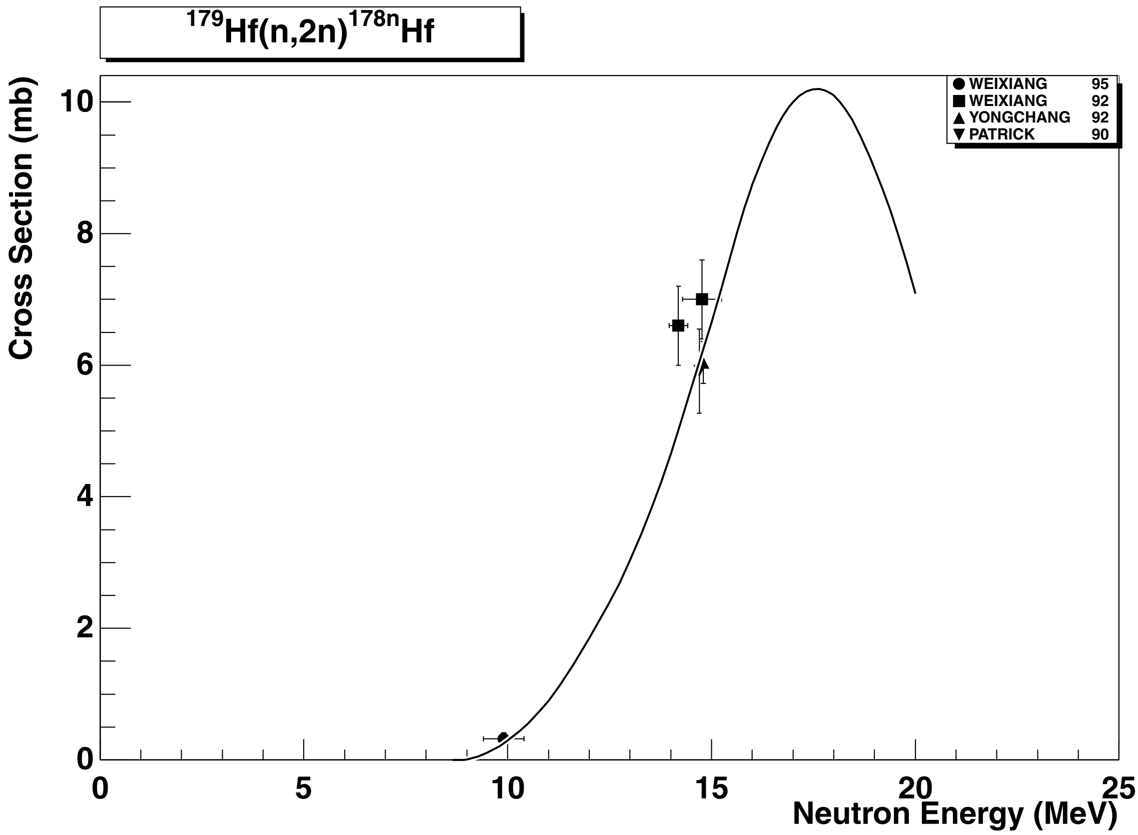

2.214. ^{179}Hf (n,2n) ^{178n}Hf

final state: meta-2
source: CRP

The reaction leading to the second isomeric state is the reference reaction. The CRP evaluation has been adopted for this reaction channel and fits well the reaction data.

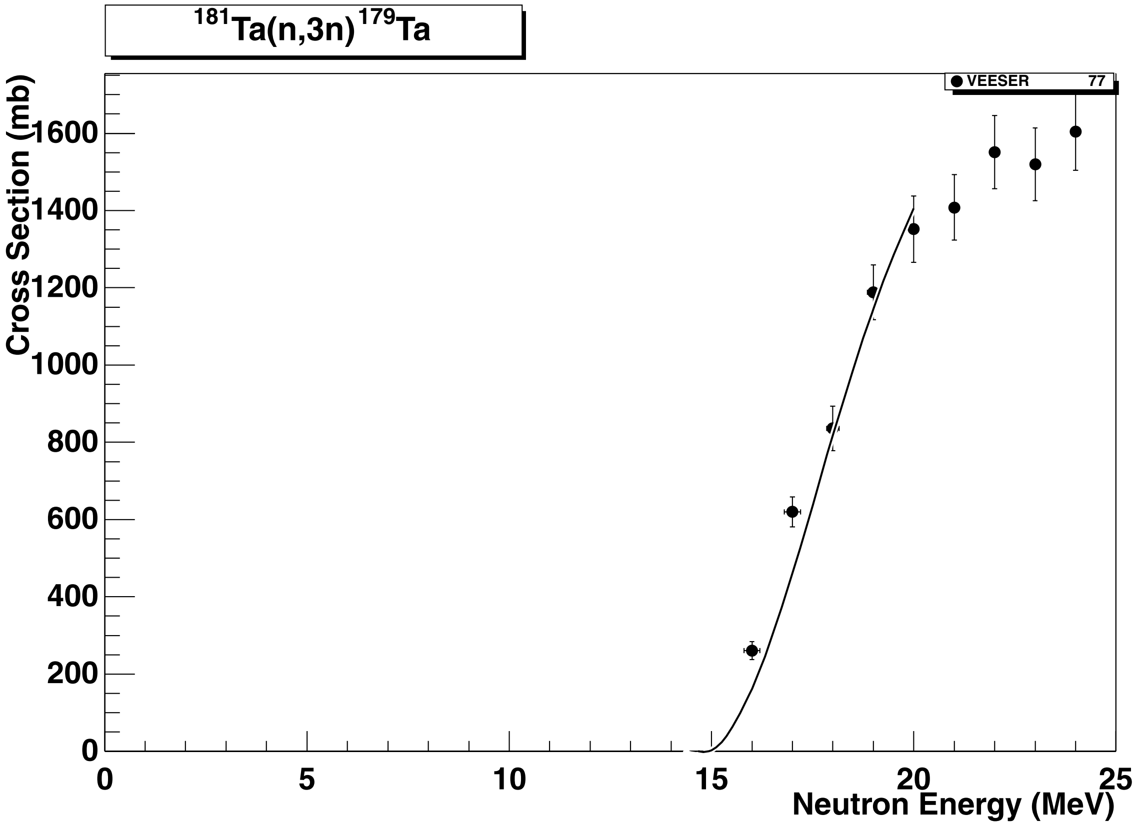

2.215. ^{181}Ta (n,3n) ^{179}Ta

final state: total
source: ADL-3

ADL-3 excitation curve runs close to the experimental data between 16-20 MeV.

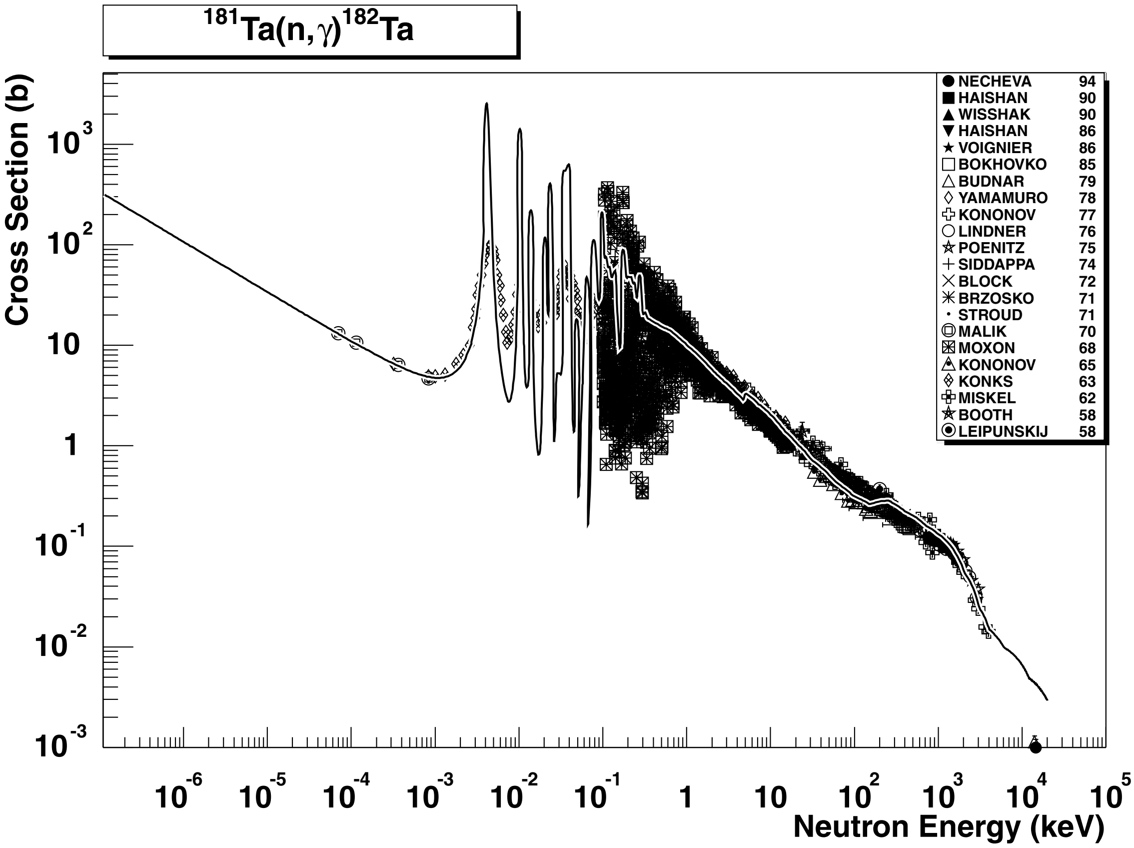

2.216. ^{181}Ta (n,γ) ^{182}Ta

final states: g.s., meta-1, meta-2
source: EAF-4.1 (JEF-2.2)

The evaluation adopted in JEF-2.2 is based on the revised ENDF/B-IV data. ENDF/B-IV agrees nicely with experimental data in the thermal region and runs reasonably in the middle of highly dispersed high energy data (in particular in the range up to few keV). cross-sections to the g.s., meta-1 and meta-2 states are based on experimental data (thermal cross-sections [26]) and applied up to the end of the resolved resonance region. The energy dependent branching ratio systematics [2] is used for the high energy region. The data are stored in the SANDII structure. The original evaluation includes 11 532 data points.

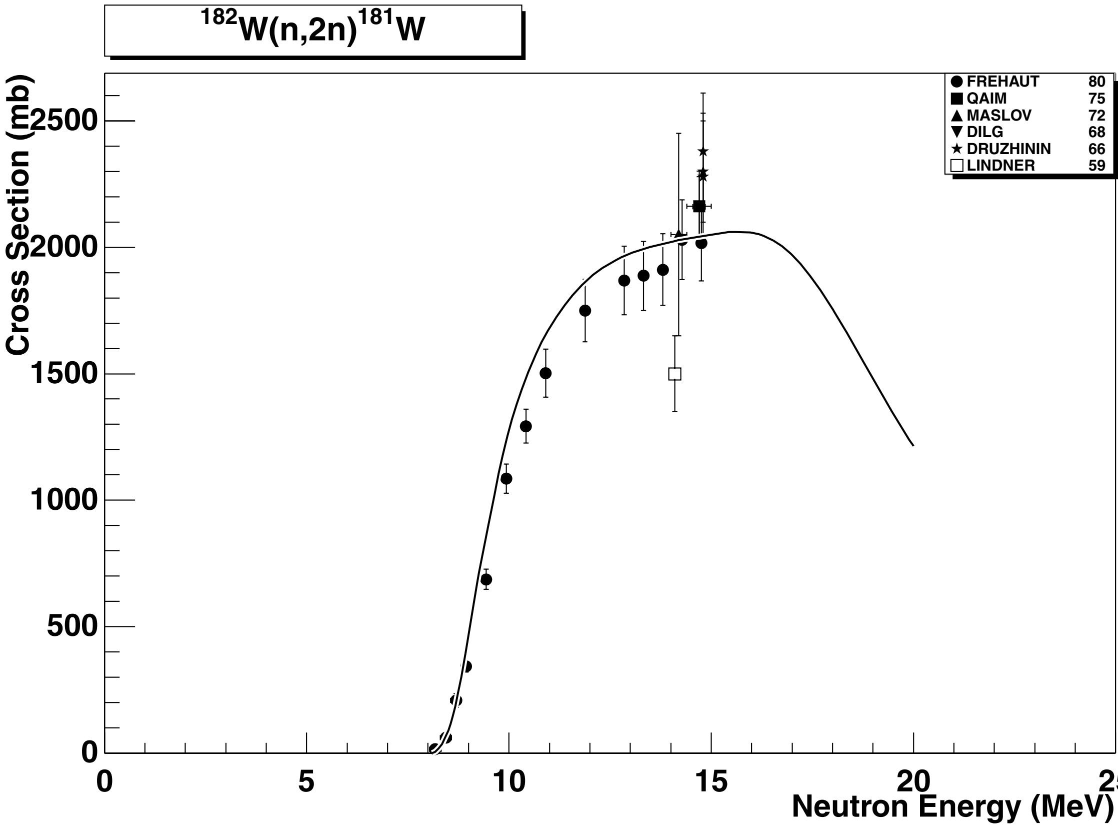

2.217. ^{182}W (n,2n) ^{181}W

final state: total
source: ADL-3

ADL-3 is in good agreement with all experimental data, except Lindner59, which is judged to be too low.

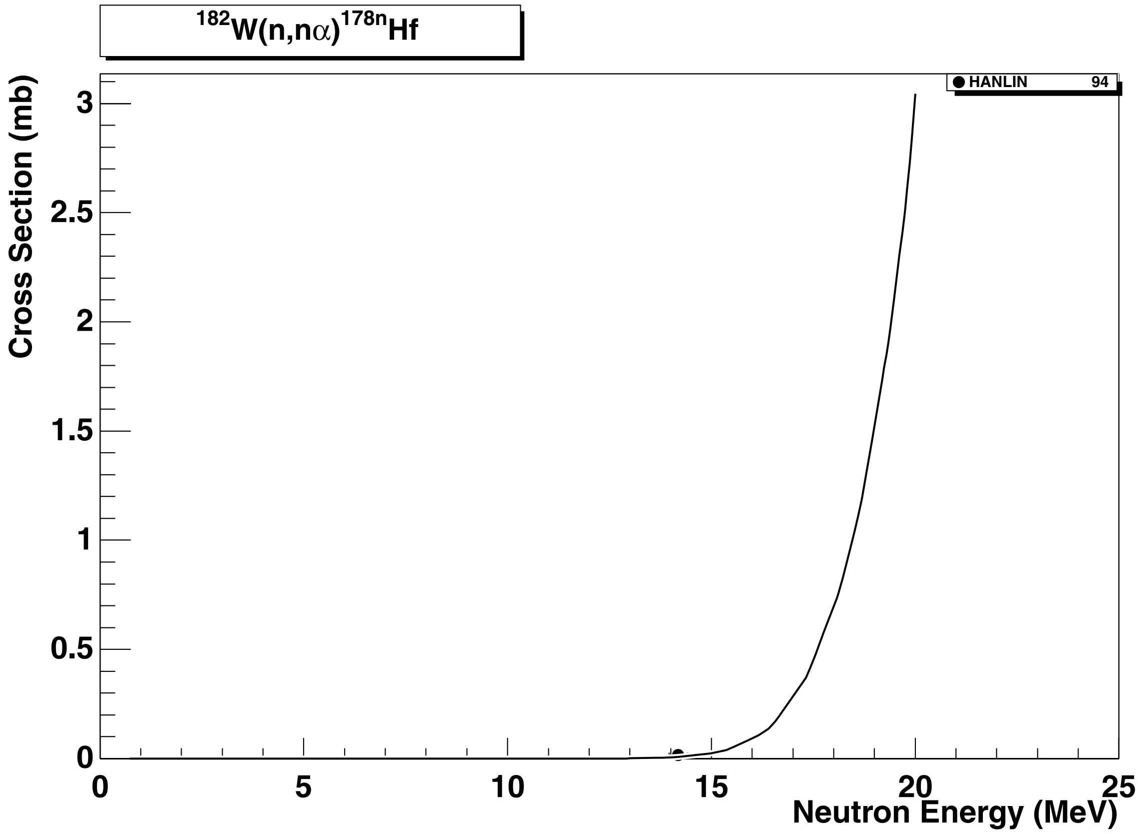

2.218. ^{182}W (n,nα) ^{178n}Hf

final states: meta-2
source: ADL-3

The reaction leading to the second isomeric state is the reference reaction. The ADL-3 evaluation, based on nuclear model calculations, has been adopted for this reaction channel and agrees with the single point of Hanlin94.

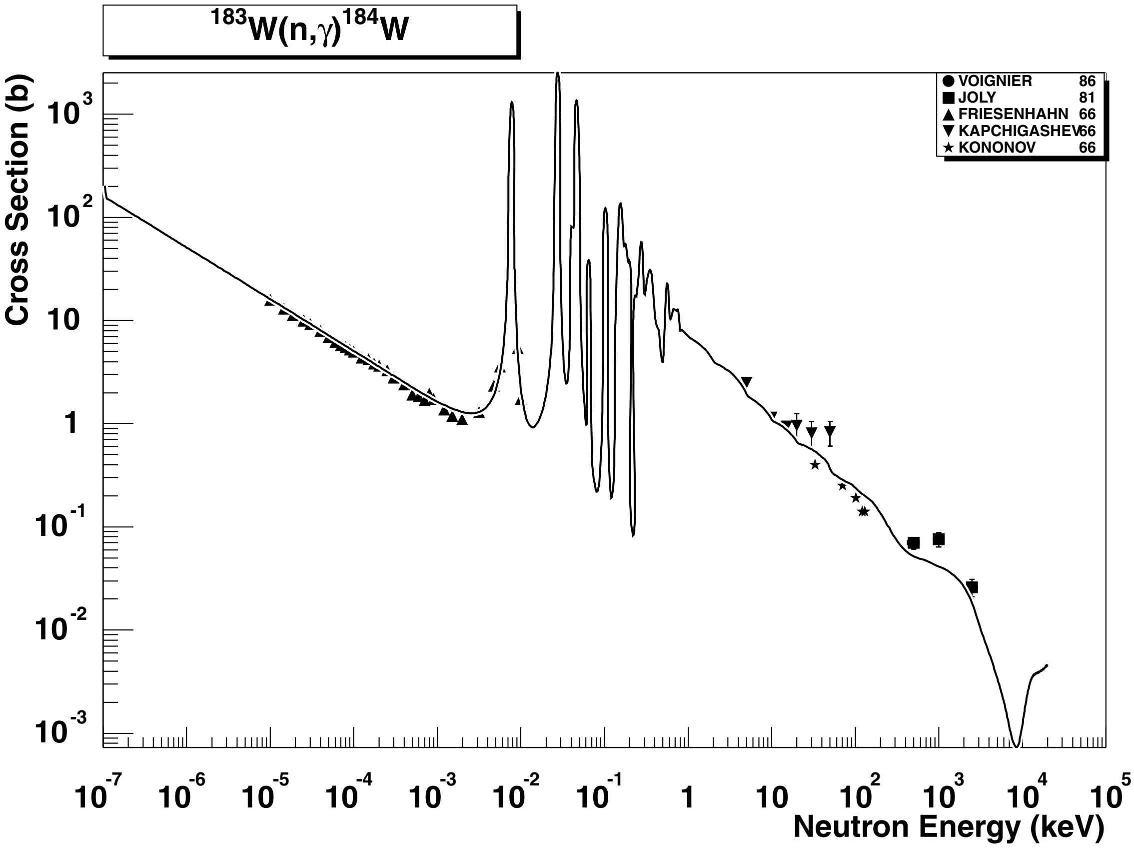

2.219. ^{183}W (n,γ) ^{184}W

final state: total
source: EAF-4.1 (JEF-2.2)

The revised ENDF/B-IV evaluation is in good agreement with all retrieved data from the thermal region up to 3 MeV. The data are stored in the SANDII structure. The original evaluation includes 10 137 data points.

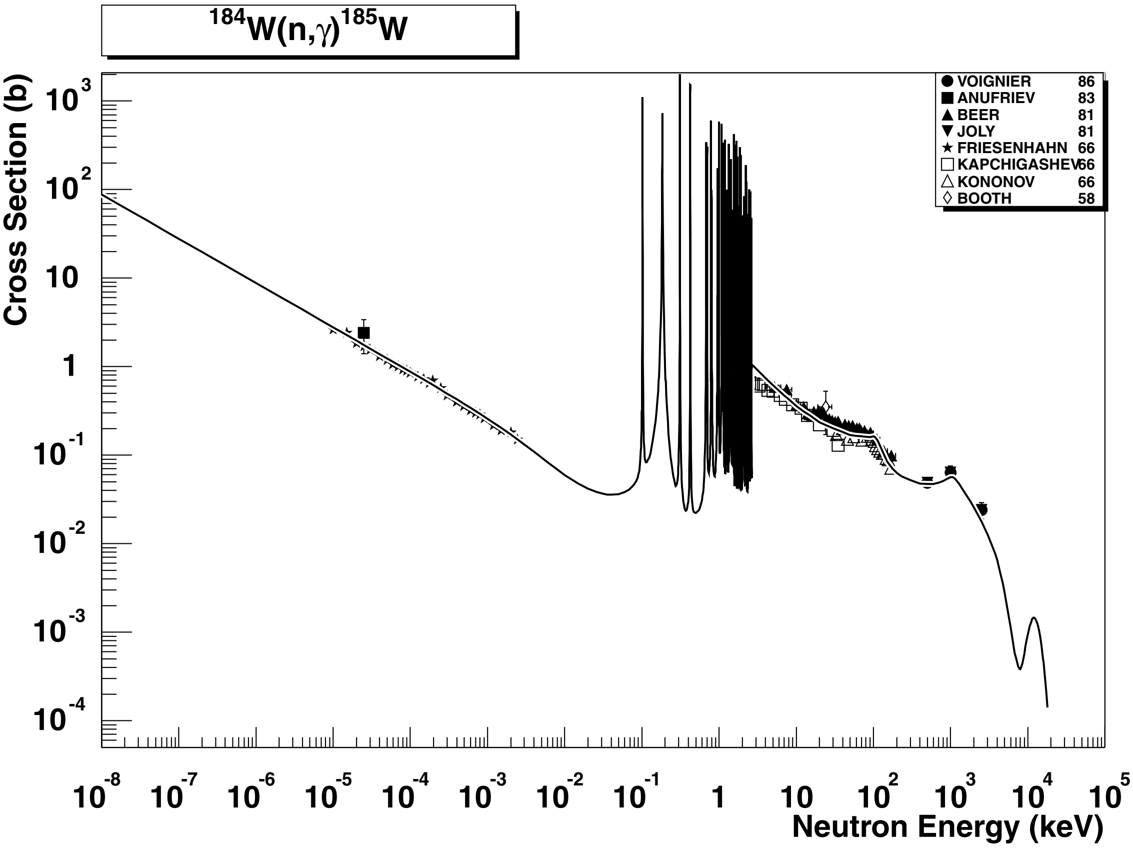

2.220. ^{184}W (n,γ) ^{185}W

final state: total
source: EAF-4.1 (LANL)

The adopted LANL evaluation originates from calculations with the code GNASH, which calculates cross-sections to the g.s. and meta state separately. The partial cross-sections fit the thermal cross-section with C/E=0.97. The total cross-section is in an excellent agreement with the experimental data in the whole energy range up to 3 MeV.

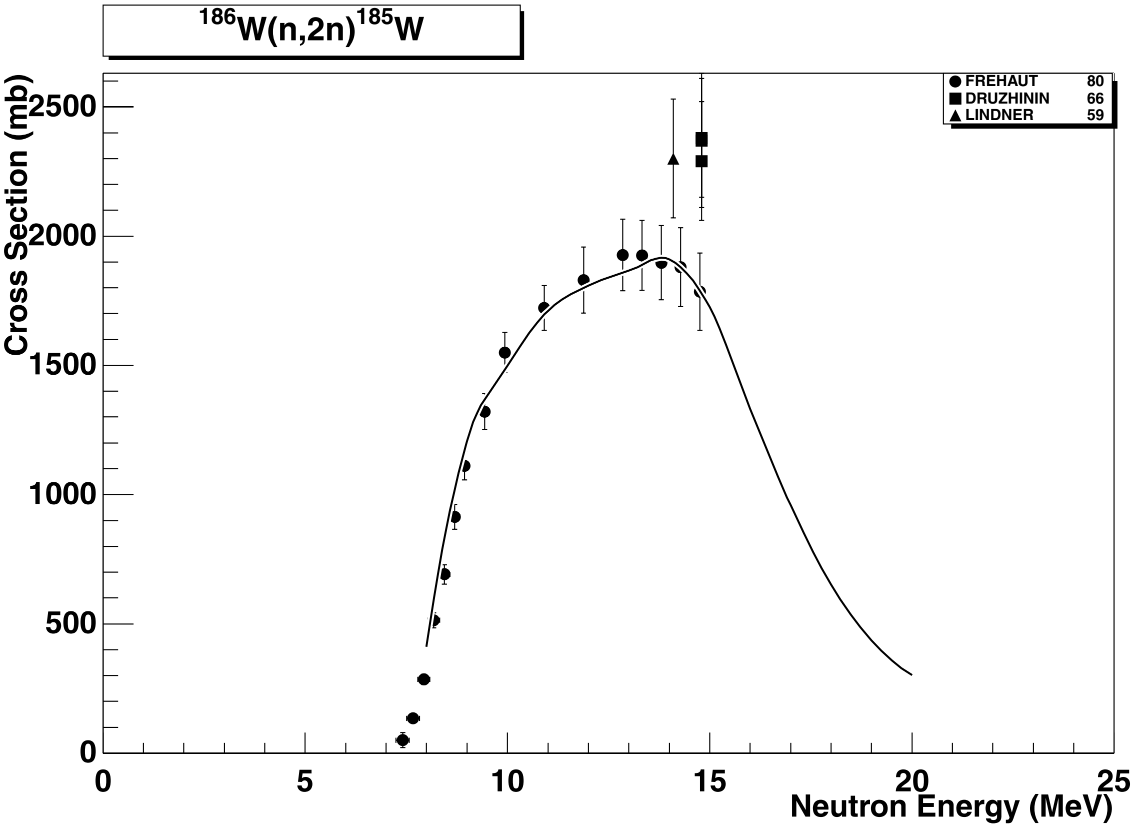

2.221. ^{186}W (n,2n) ^{185}W

final states: g.s., meta
source: JENDL-Act96

JENDL-Act96 is in very good agreement with the data of Frehaut80 in the whole energy range. The overestimating data of Druzhinin66 and Lindner59 may be neglected. The branching ratio between the g.s. and meta state is based on the model calculation.

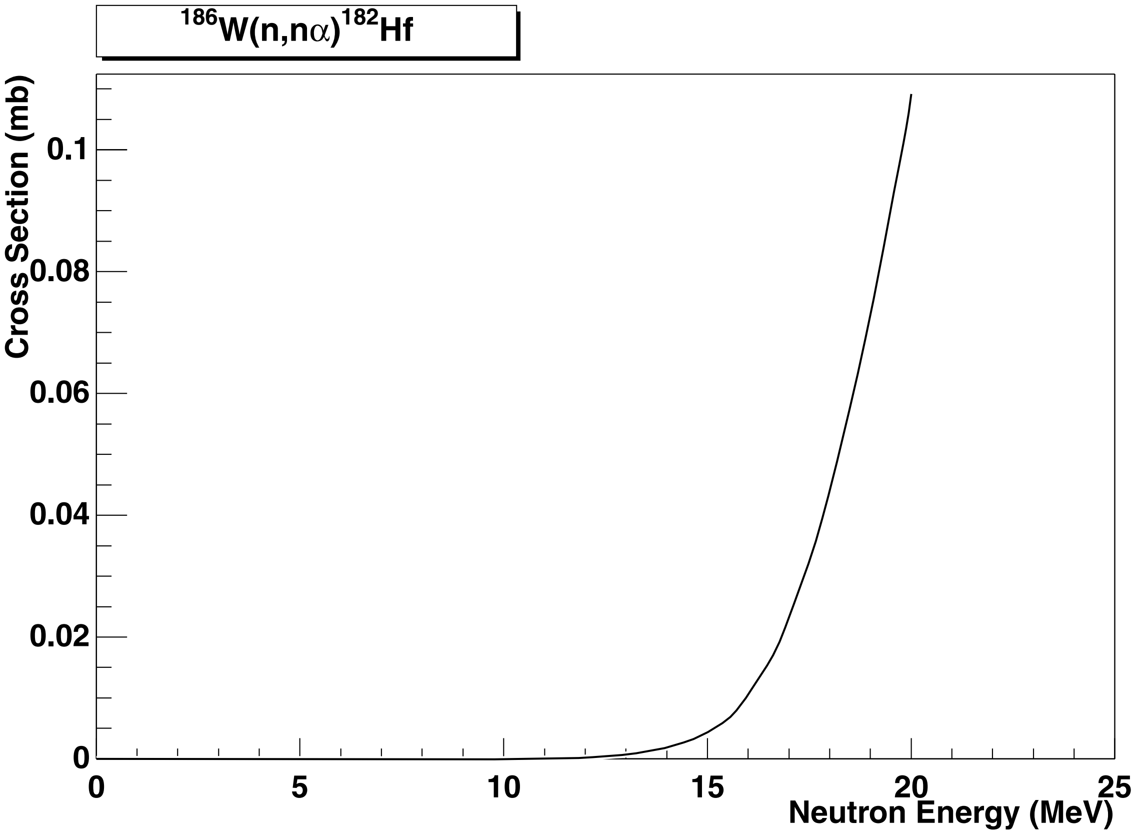

2.222. ^{186}W (n,nα) ^{182}Hf

final state: g.s., meta
source: ADL-3

ADL-3 evaluation has been chosen. Partial cross-sections to the g.s. and meta state result from nuclear model calculations. No EXFOR data are available.

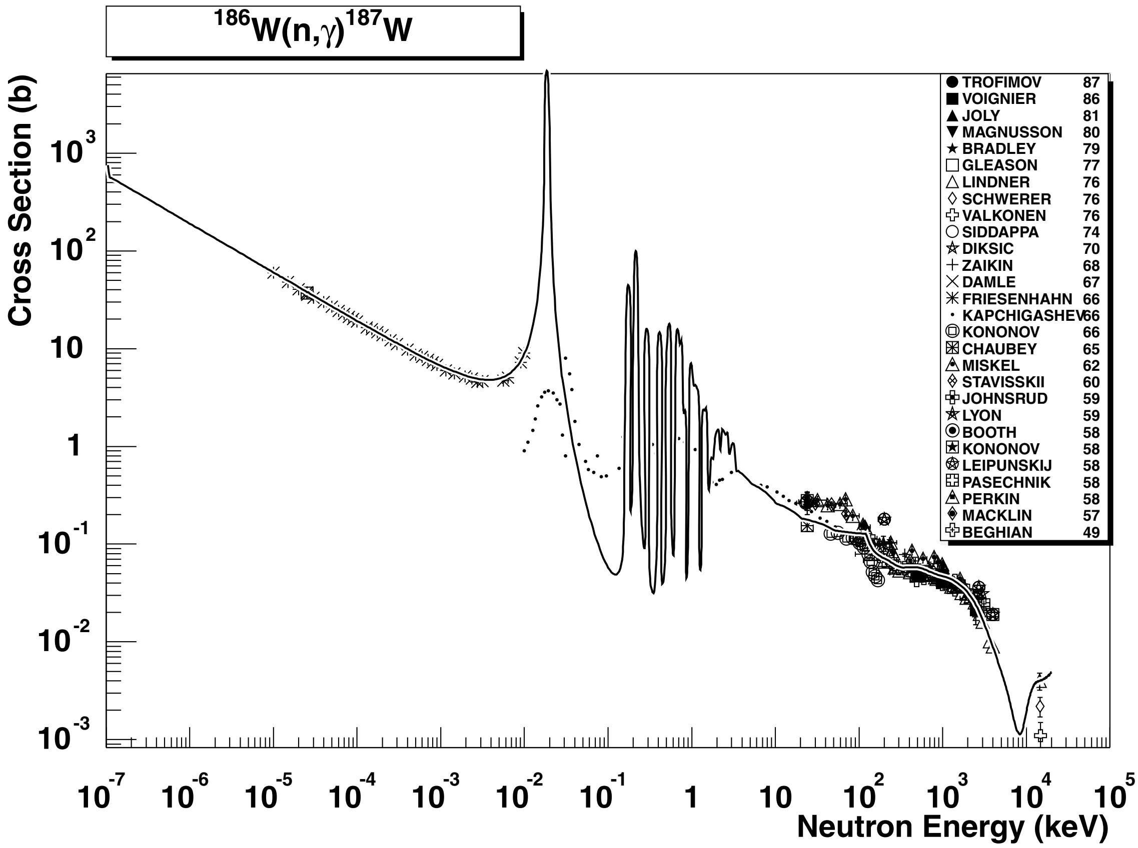

2.223. ^{186}W (n,γ) ^{187}W

final state: total
source: EAF-4.1 (JEF-2.2)

The revised ENDF/B-IV evaluation is in a very good agreement with all retrieved data from the thermal region up to 3 MeV. The data of Kapchigashev66 under the first resonance look strange and can be safely disregarded. The pre-equilibrium component at 14 MeV is too large, a value between 1-2 mb (as measured by Valkonen76 and Schwerer76) is more realistic. The data are stored in the SANDII structure. The original evaluation includes 9294 data points.

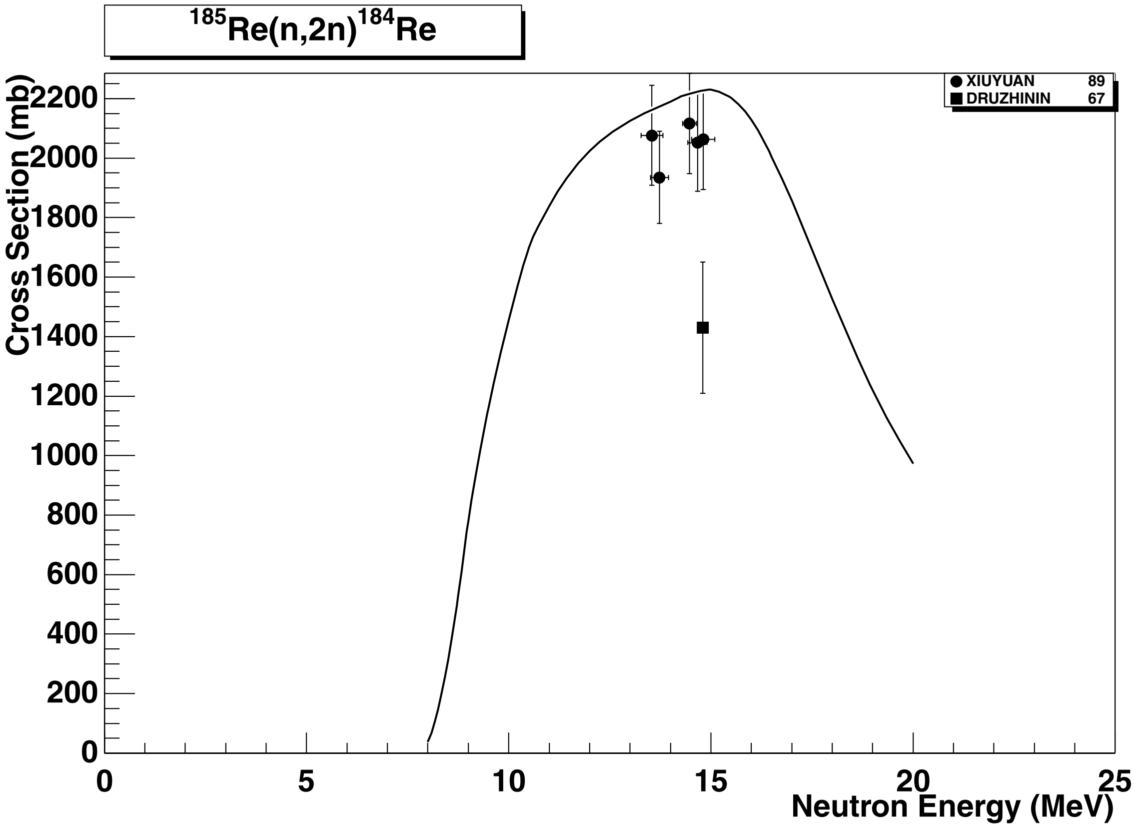

2.224. ^{185}Re(n,2n) ^{184}Re

final states: g.s., meta
source: EAF-4.1 (ENDF/B-VI)

The ENDF/B-VI evaluation has been adopted, with the g.s. to meta branching ratio based on the systematics [2]. The excitation curve slightly overestimates (by about 5%) the data of Xiuyuan89 between 13-15 MeV, however, the evaluated curve is within the error bars.

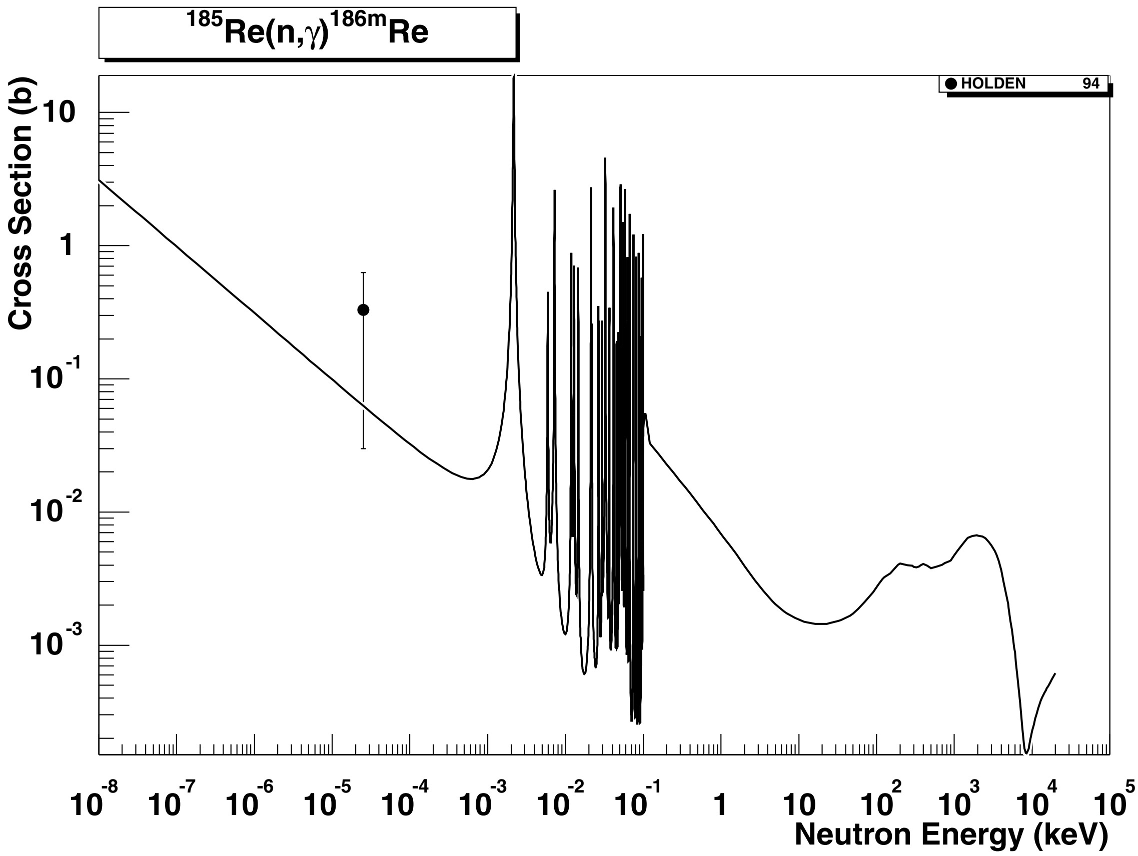

2.225. ^{185}Re (n,γ) ^{186m}Re

final state: meta
source: EAF-4.1 (LANL)

The reaction leading to the first excited state is the reference reaction. The adopted evaluation is based on calculated cross-sections to the g.s. and meta state, performed with the code GNASH at LANL. Partial thermal cross-sections fit the experimental values [26] with C/E=0.98. The total thermal cross-section is in agreement with the value of Holden94 [32]. The statistical component is supported by the recommended 30 keV cross-section [27].

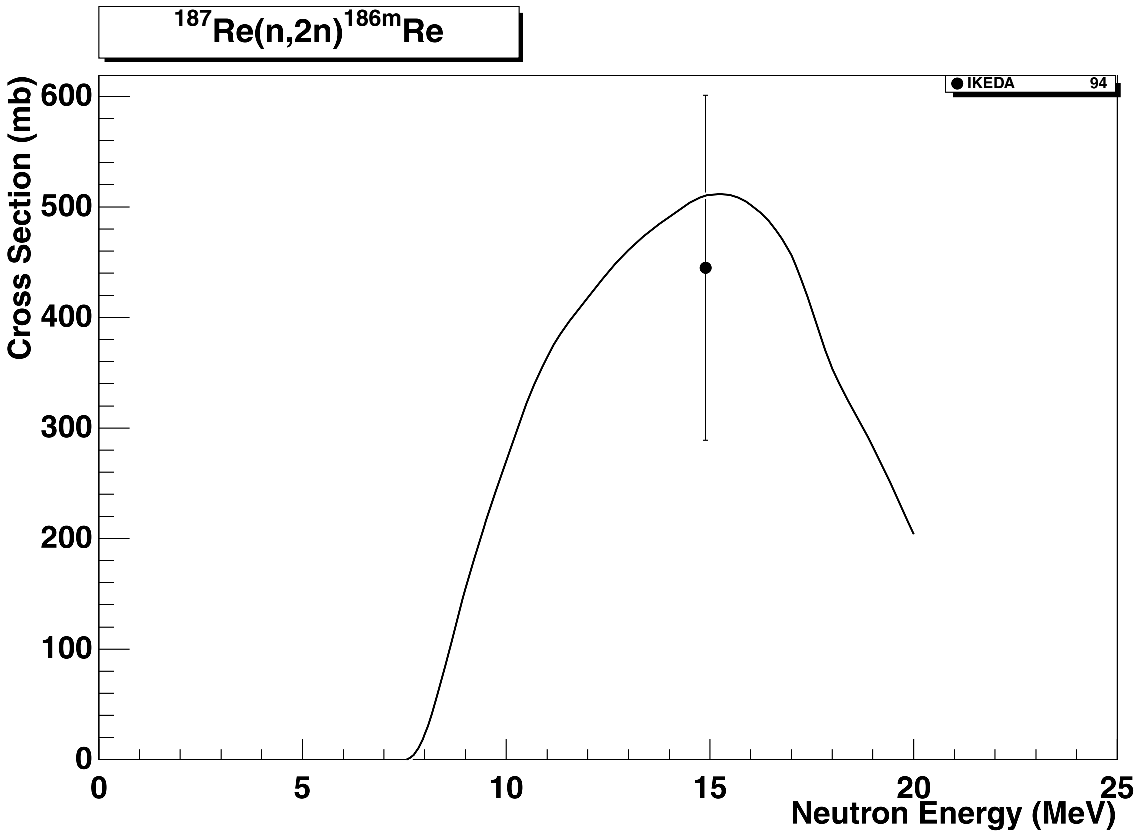

2.226. ^{187}Re (n,2n) ^{186m}Re

final state: meta
source: CRP

The reaction leading to the first isomeric state is the reference reaction. The CRP evaluation has been adopted for this reaction channel and agrees well with the single point of Ikeda94.

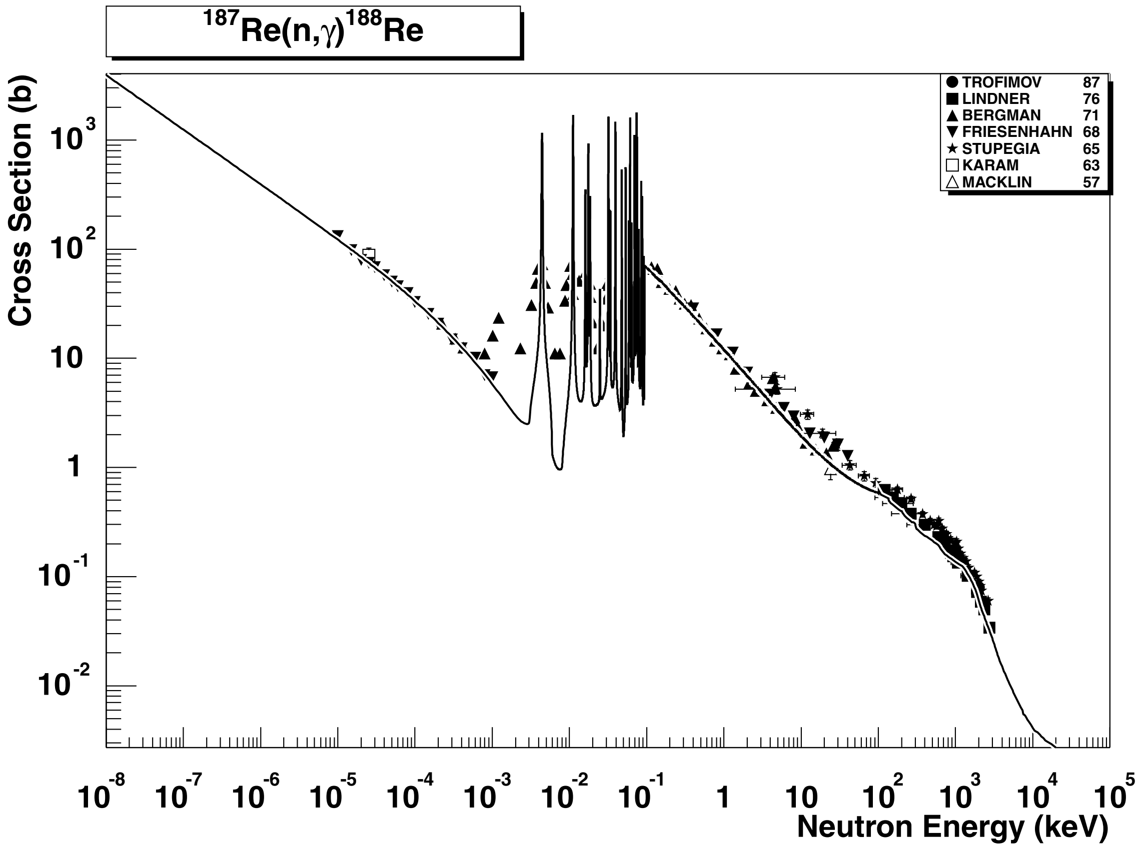

2.227. ^{187}Re (n,γ) ^{188}Re

final states: g.s., meta
source: EAF-4.1 (JEF-2.2)

The revised ENDF/B-IV evaluation is in very good agreement with all retrieved data from the thermal region up to 3 MeV. A few data points of Bergman71, just below the first resolved resonance, are probably wrong. There is no resonance at that energy in ^{187}Re. Thermal cross-sections to the g.s. and meta state are based on experimental data (reproduced with C/E=0.98) and the derived branching ratio is applied up to the end of the resolved resonance region, and the energy dependent branching ratio systematics [2] is used for the high energy region.

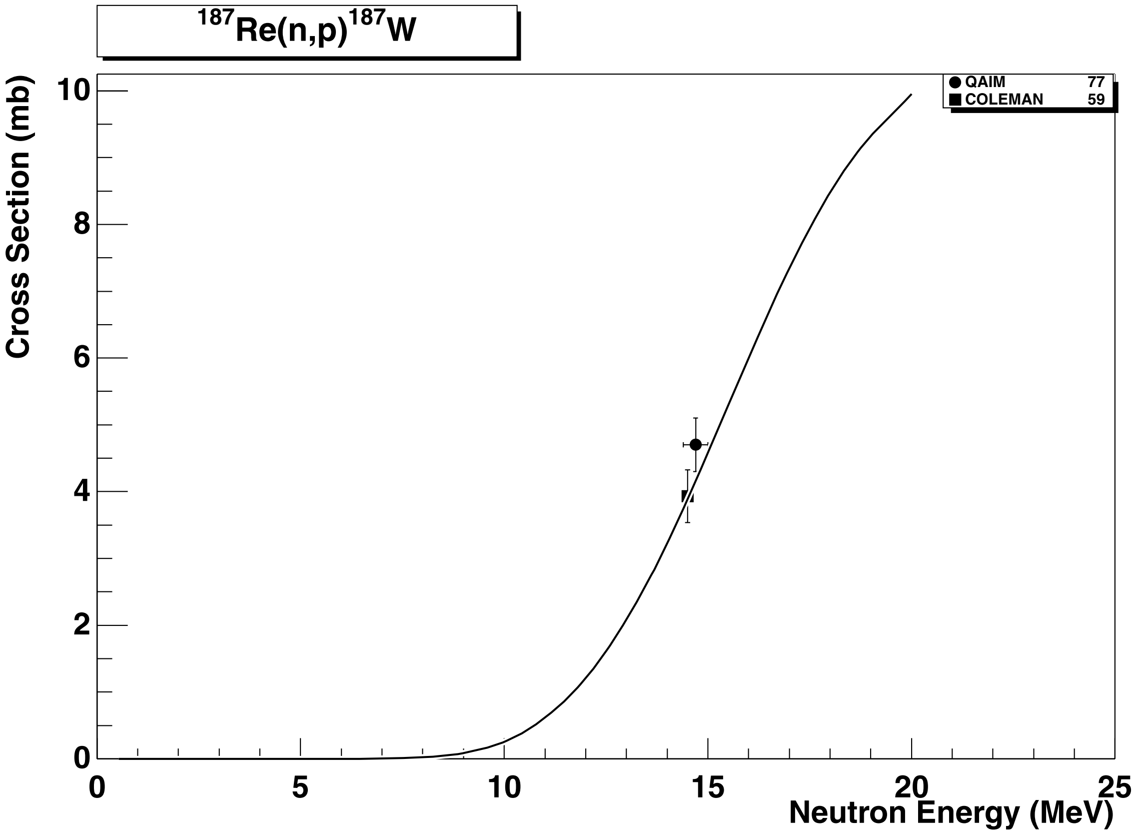

2.228. ^{187}Re (n,p) ^{187}W

final state: total
source: ADL-3

ADL-3 evaluation is close to the two experimental points at about 15 MeV.

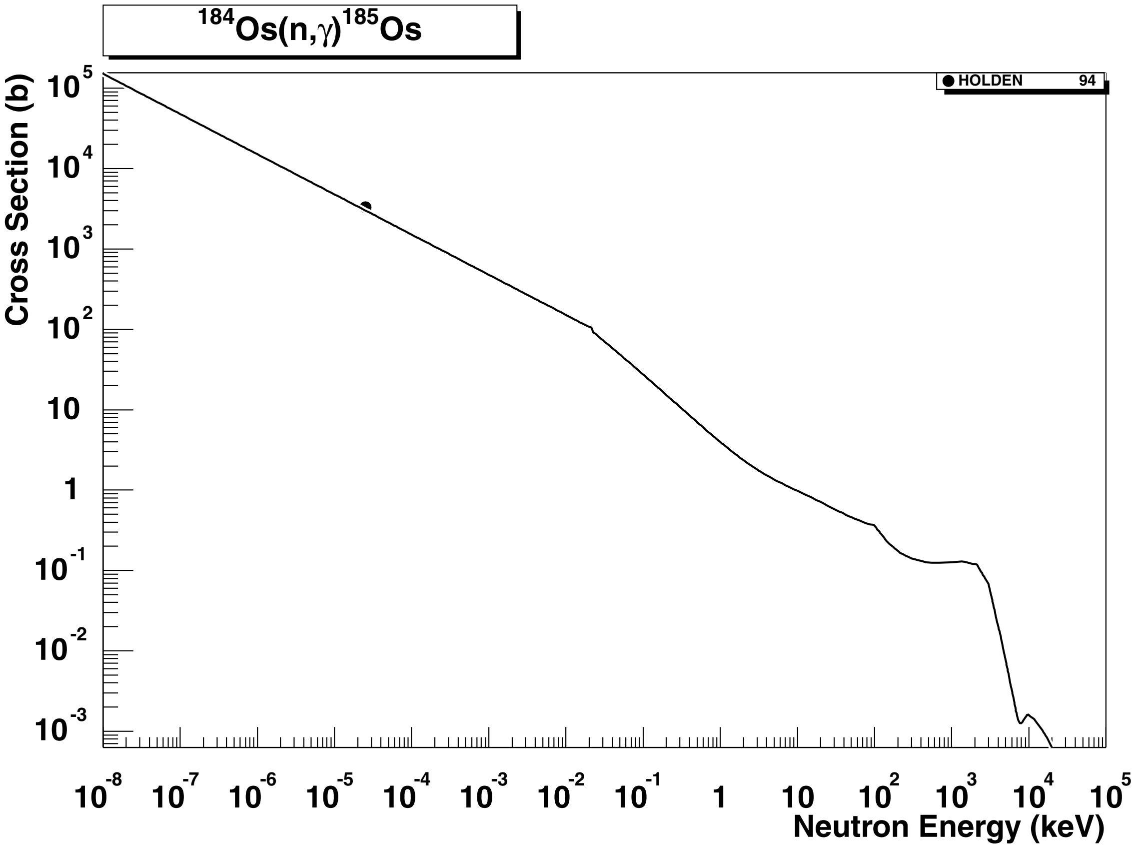

2.229. ^{184}Os (n,γ) ^{185}Os

final state: total
source: EAF-4.1

No EXFOR data are available. The original EAF-4.1 evaluation is based on the simplified model calculations with the code MASGAM and the global parameters (Hauser-Feshbach and DSD model with no resonance region generation, E_H is based on a $D_0/2$ estimate; for details see Ref. [35]). The MASGAM evaluation fits the recommended thermal cross-section of Holden94 from [32] with C/E=1.00 . The statistical component is supported by the recommended 30 keV cross-section [27].

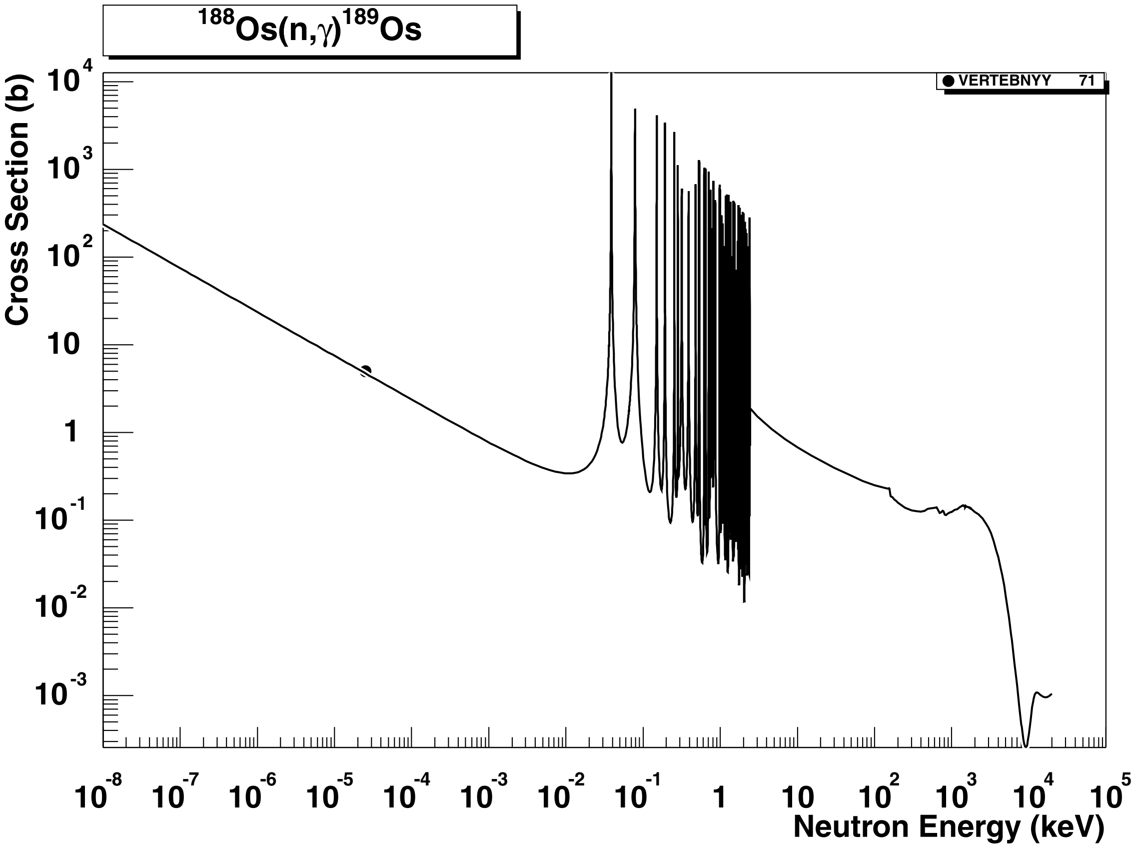

2.230. ^{188}Os (n,γ) ^{189}Os

final states: g.s., meta
source: EAF-4.1

The EAF-4.1 evaluation performed with the code FISPRO is in good agreement with the thermal cross-section of Vertebnyy71. cross-sections to the g.s. and meta state are based on experimental data (thermal cross-sections [26]) and applied up to the end of the resolved resonance region. The energy dependent branching ratio systematics [2] is used for the high energy region. The statistical component in the total cross-section is supported by the recommended 30 keV cross-section [27].

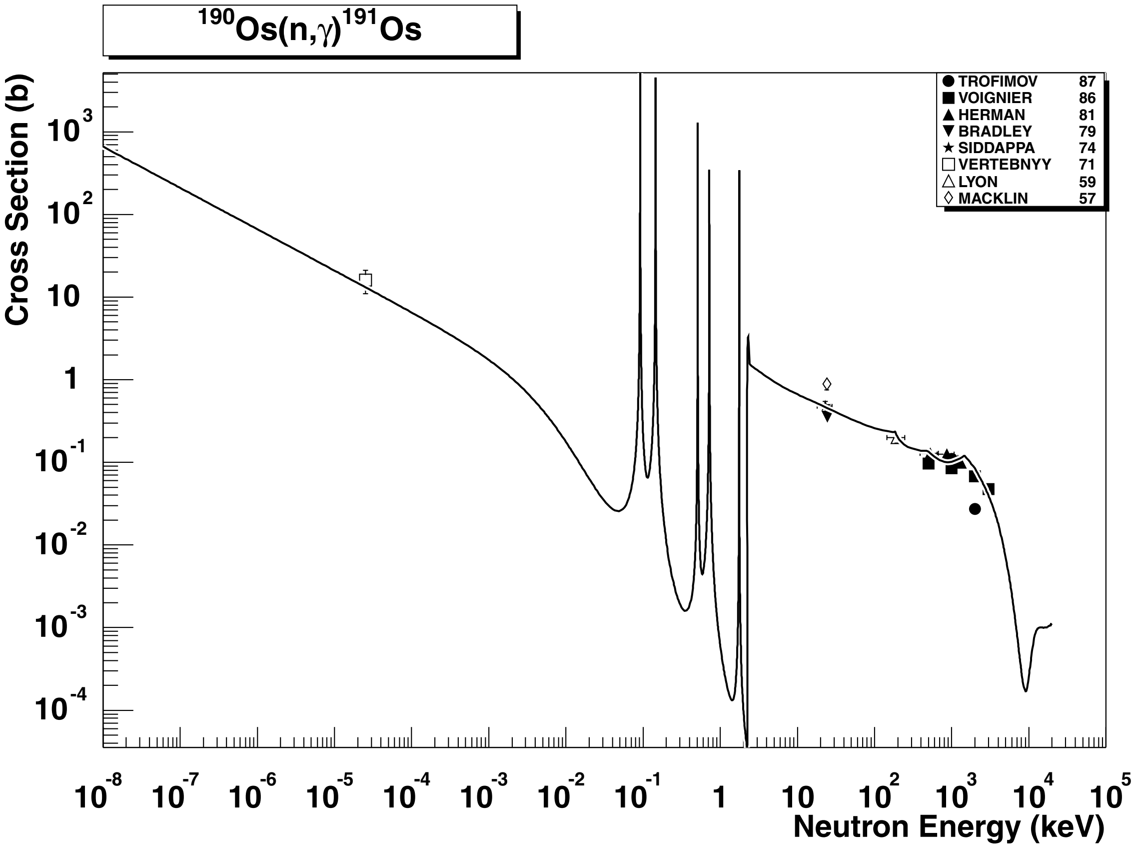

2.231. ^{190}Os (n,γ) ^{191}Os

final states: g.s., meta
source: EAF-4.1

The EAF-4.1 evaluation, based on the code FISPRO, is in good agreement with the thermal cross-section of Vetrebnyy71 and also with several experimental data in the high energy region (10 keV and 3 MeV). cross-sections to the g.s. and meta state are based on experimental data (thermal cross-sections [26]) applied up to the end of the resolved resonance region. The energy dependent branching ratio systematics [2] is used for the high energy region.

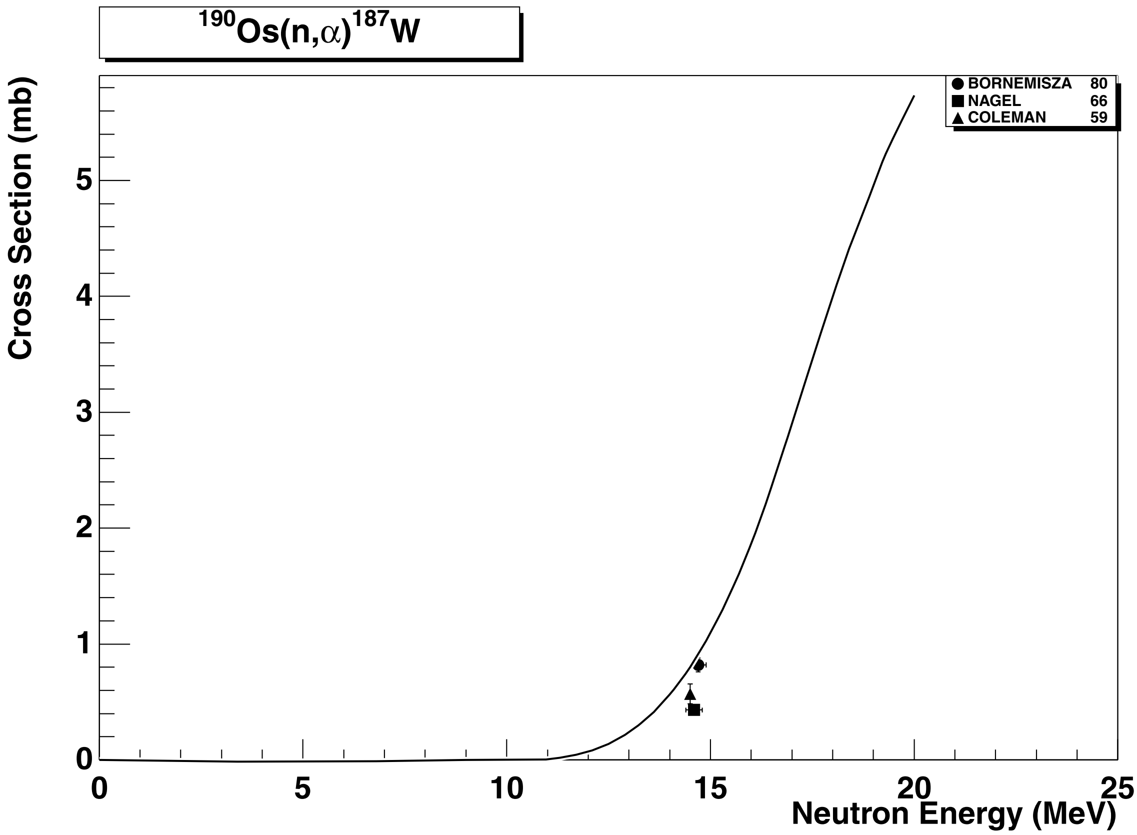

2.232. ^{190}Os (n,α) ^{187}W

final states: total
source: EAF-99

The adopted EAF-99 evaluation agrees with the three experimental data points between 14 and 15 MeV. The value from the 14.5 MeV systematics is reproduced with C/S=1.00.

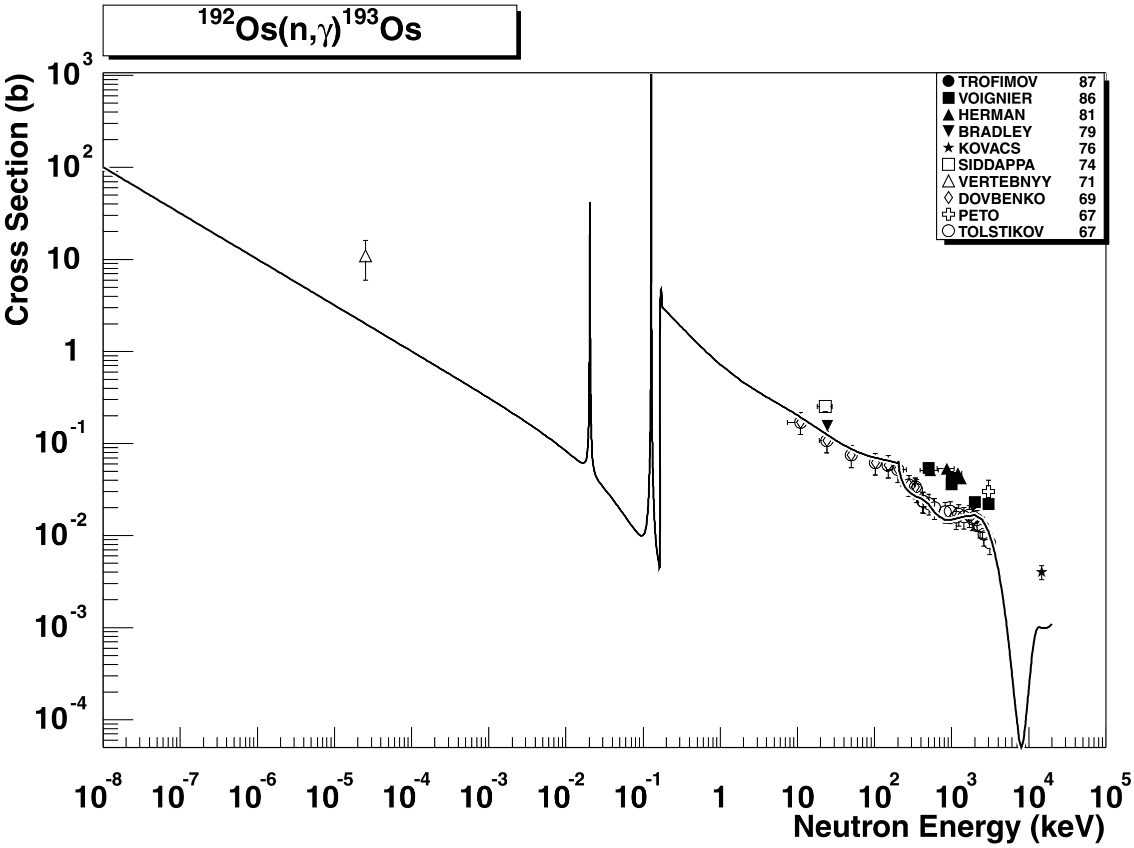

2.233. ^{192}Os (n,γ) ^{193}Os

final state: total
source: EAF-4.1

This is the EAF-4.1 evaluation with the code FISPRO. Thermal cross-section of Vertebnyy71 is underestimated as well as the recommended value of Ref. [26] with C/E=0.67. The smooth statistical component runs well through the older data (primarily Tolstikov67) but slightly underestimates few recent data points of Voignier86 and Herman81. Reevaluation is recommended.

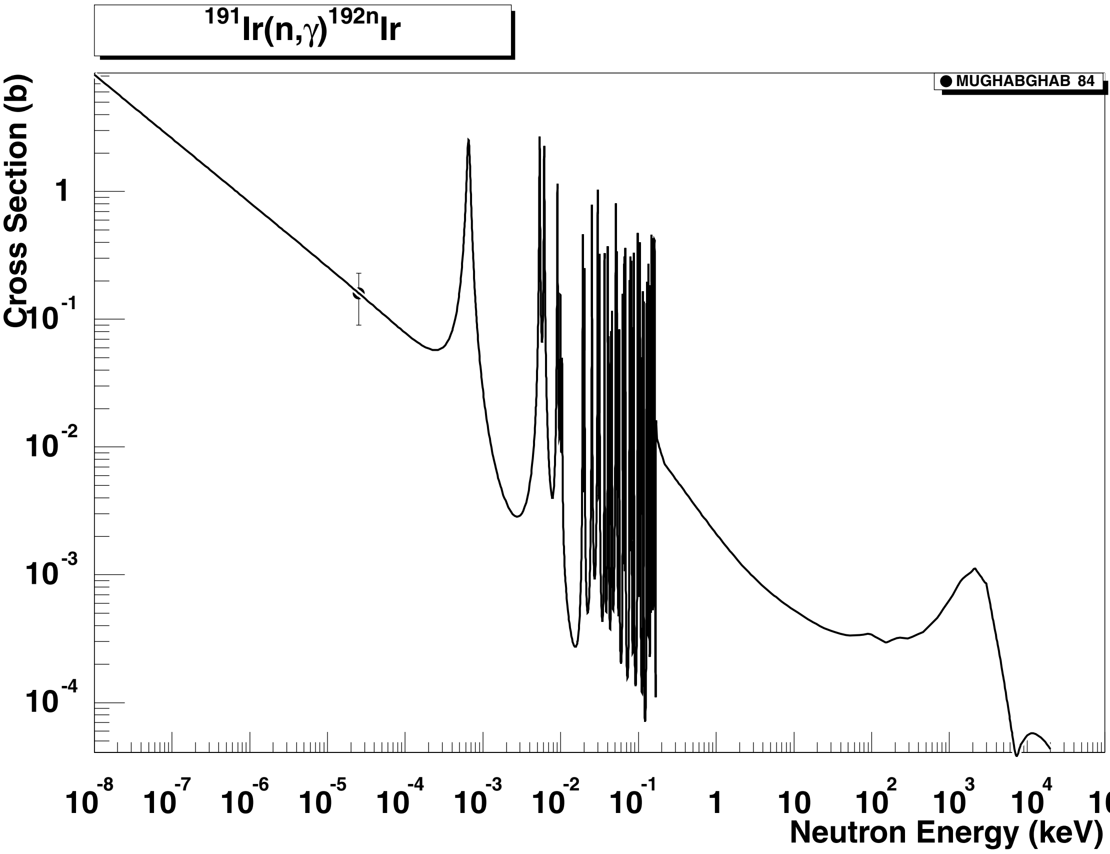

2.234. ^{191}Ir (n,γ) ^{192n}Ir

final state: meta-2
source: EAF-4.1

The reaction leading to the second isomeric state is the reference reaction. No EXFOR data are available outside the resonance region. The original EAF-4.1 evaluation with the code SIGECN-MASGAM has been adopted. cross-sections to the g.s., meta-1 and meta-2 states are based on experimental data (thermal cross-sections [26] and [31]) applied up to the end of the resolved resonance region. The energy dependent branching ratio systematics [2] is used for the high energy region. The partial thermal cross-section agrees with the experiment [31] with C/E=1.00. The smooth statistical component, based on a simplified calculation with the code MASGAM, is supported by the 30 keV cross-section [27].

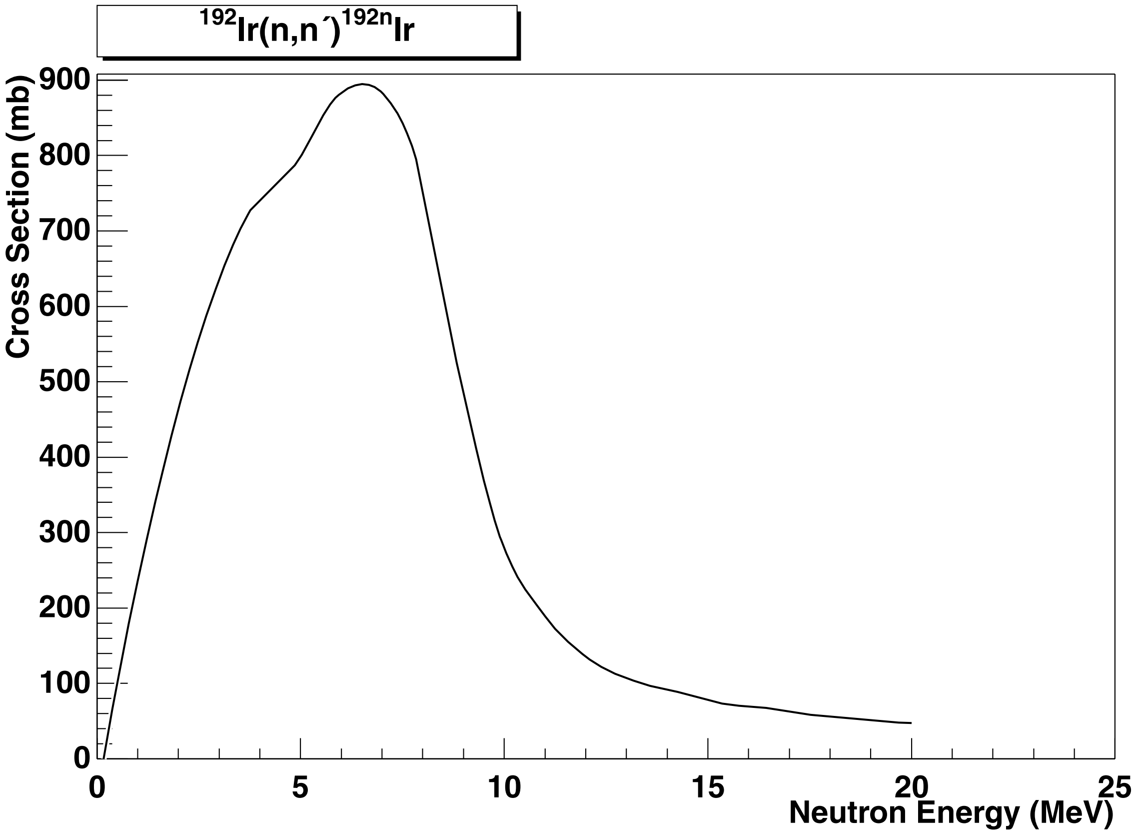

2.235. ^{192}Ir (n,n') ^{192n}Ir

final state: meta-2
source: EAF-4.1 (ADL-3)

The reaction leading to the second isomeric state is the reference reaction. No EXFOR data are available. The adopted data are based on model calculations from ADL-3.

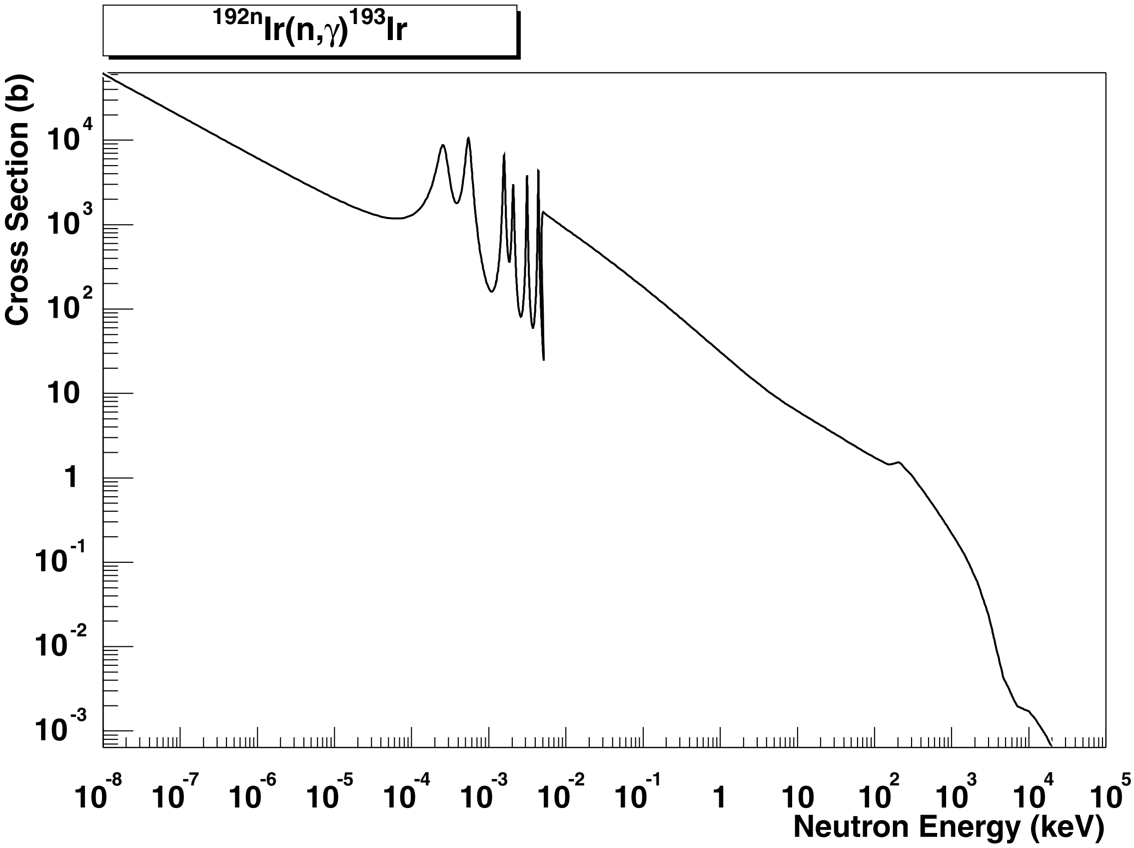

2.236. ^{192n}Ir (n,γ) ^{193}Ir

final states: g.s., meta
source: EAF-4.1

The reference reaction is based on the second isomeric state of Ir-192. There are no EXFOR data available and the evaluation is based on a SIGECN-MASGAM calculations for the Ir-192 ground state target, assuming the identical excitation curve. The branching ratio is based on the energy dependent systematics (see Ref. [2]).

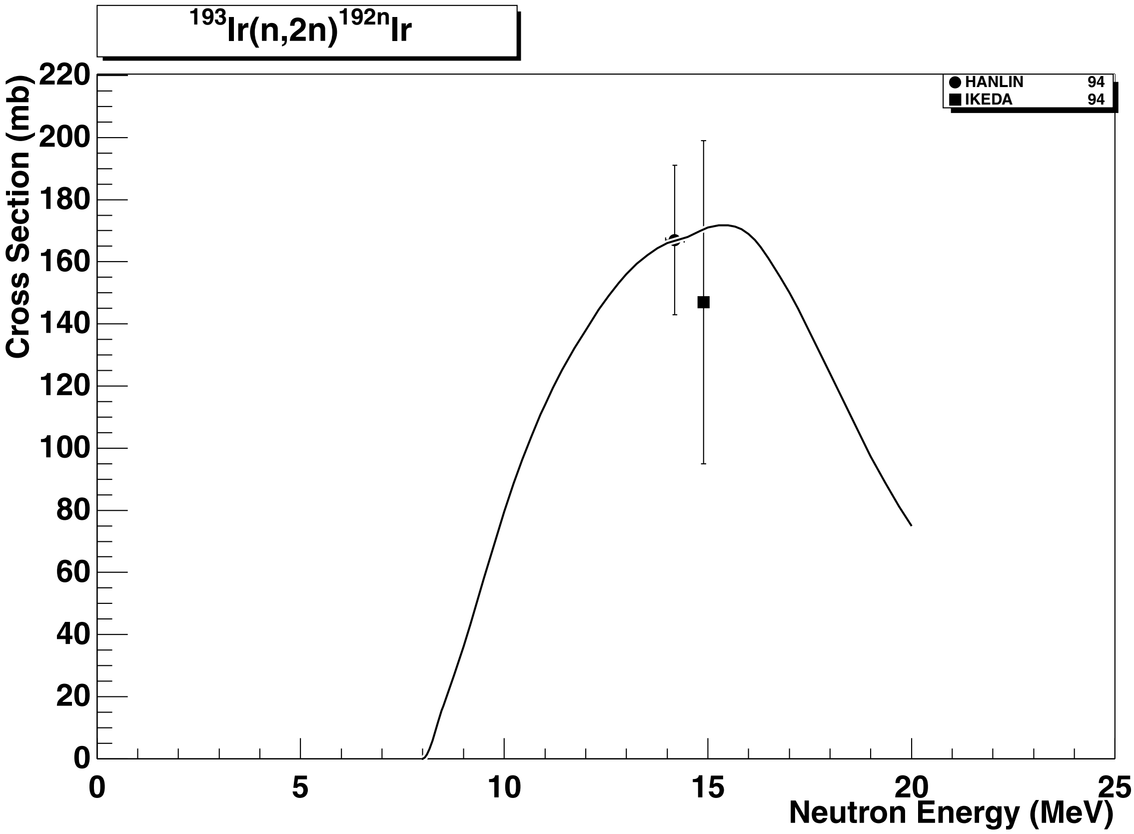

2.237. ^{193}Ir (n,2n) ^{192n}Ir

final state: meta-2
source: EAF-4.1 (ADL-3)

The reaction leading to the second isomeric state is the reference reaction. The adopted data are based on nuclear model calculations from ADL-3 and agree with the data of Hanlin94 and Ikeda95.

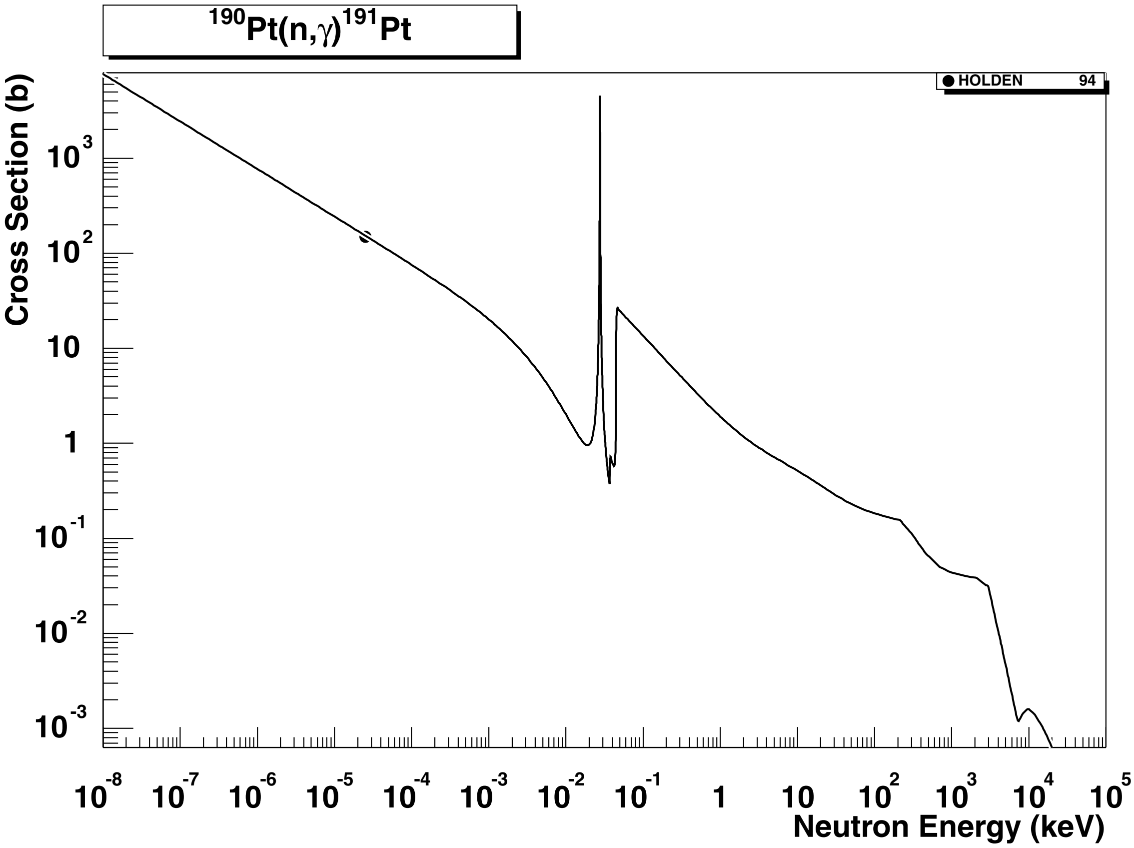

2.238. ^{190}Pt (n,γ) ^{191}Pt

final state: total
source: EAF-4.1

The EAF-4.1 evaluation with the code SIGECN-MASGAM. No EXFOR data are available. The thermal cross-section of Holden94 from Ref. [26] is reproduced with C/E=1.00. The smooth statistical component, based on a simplified calculation with the code MASGAM, is supported by the recommended 30 keV cross-section [27].

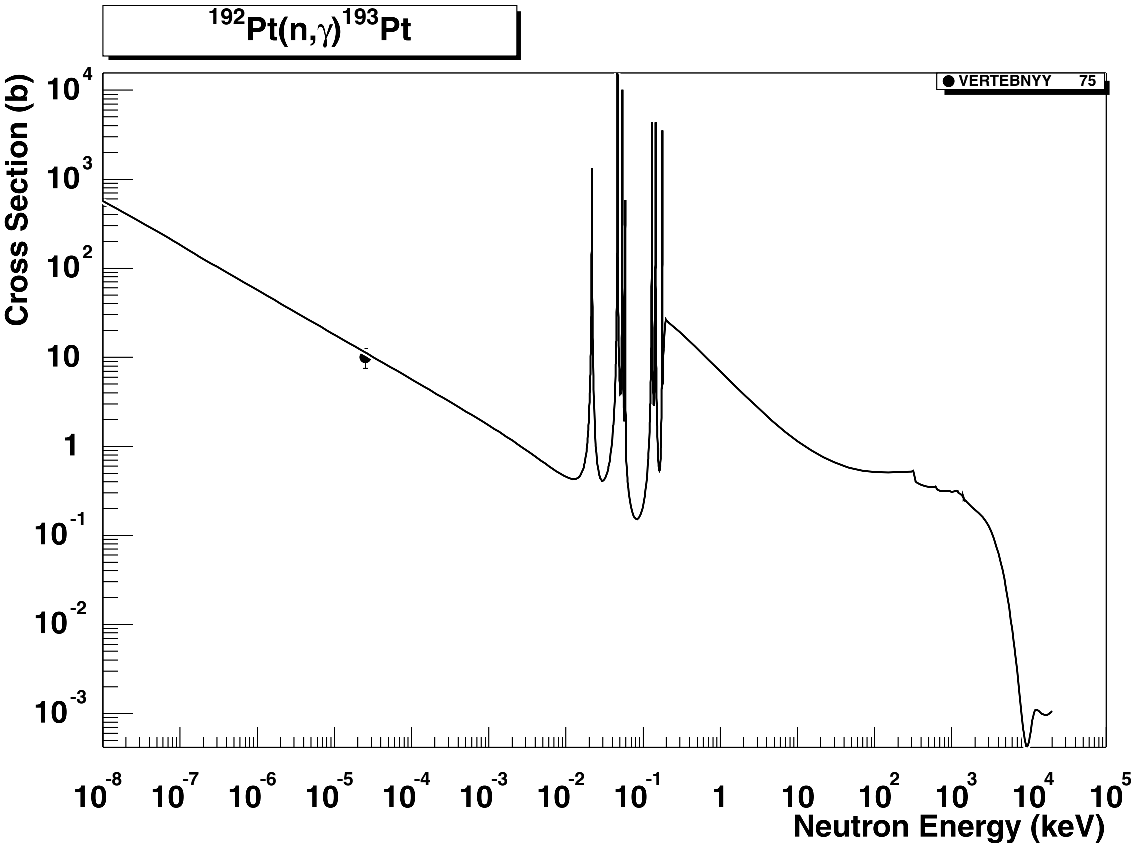

2.239. ^{192}Pt (n,γ) ^{193}Pt

final states: g.s., meta
source: EAF-4.1

The EAF-4.1 evaluation, with the code FISPRO, is in a good agreement with the thermal cross-section of Vetrebnyy75. No other experimental data outside resonance region are available in EXFOR. cross-sections to the g.s. and meta state are based on experimental data (thermal cross-sections [26]) applied up to the end of the resolved resonance region. The energy dependent branching ratio systematics [2] is used for the high energy region. The smooth statistical component is supported by the recommended 30 keV cross-section [27].

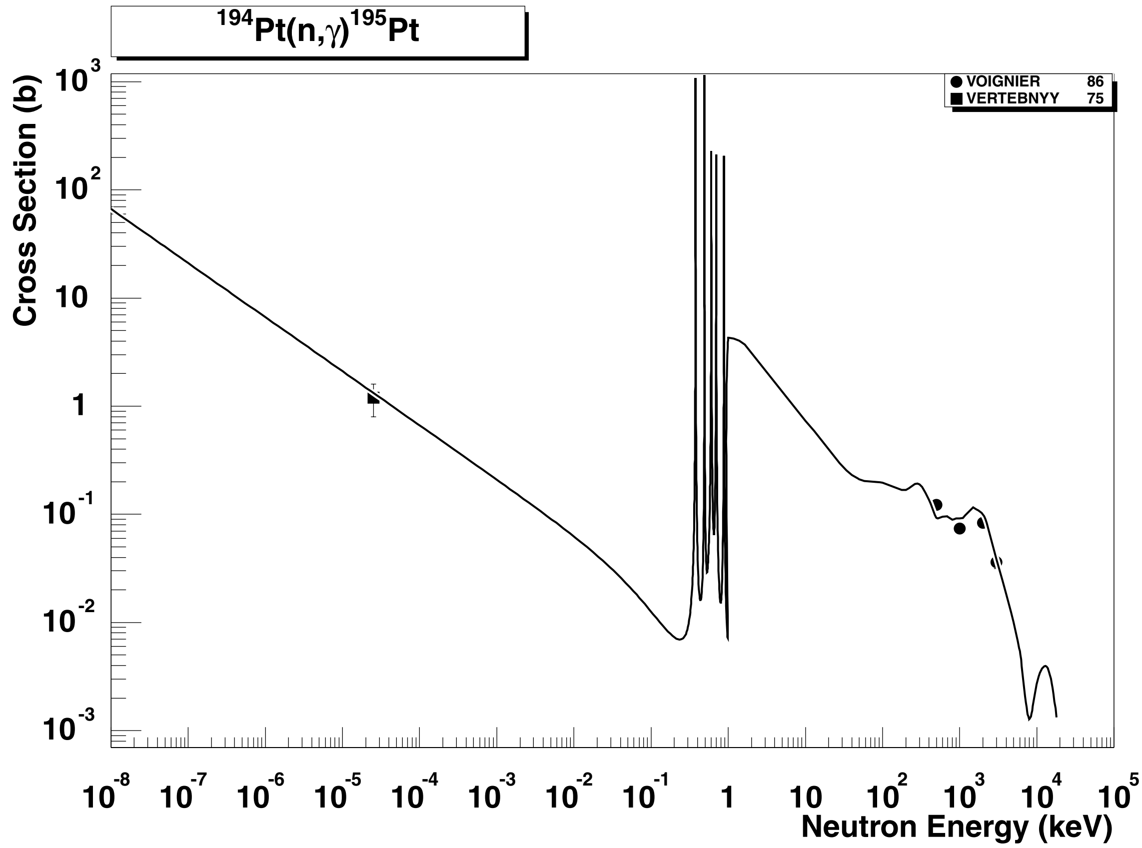

2.240. ^{194}Pt (n,γ) ^{195}Pt

final state: total
source: LANL-96

LANL-96 [22] evaluation runs through a few available experimental points. cross-sections above 1 keV were calculated with the code EMPIRE-2.8 using Hauser-Feshbach and Multi-step Compound theories. Below 1 keV EAF-4.1 was adopted.

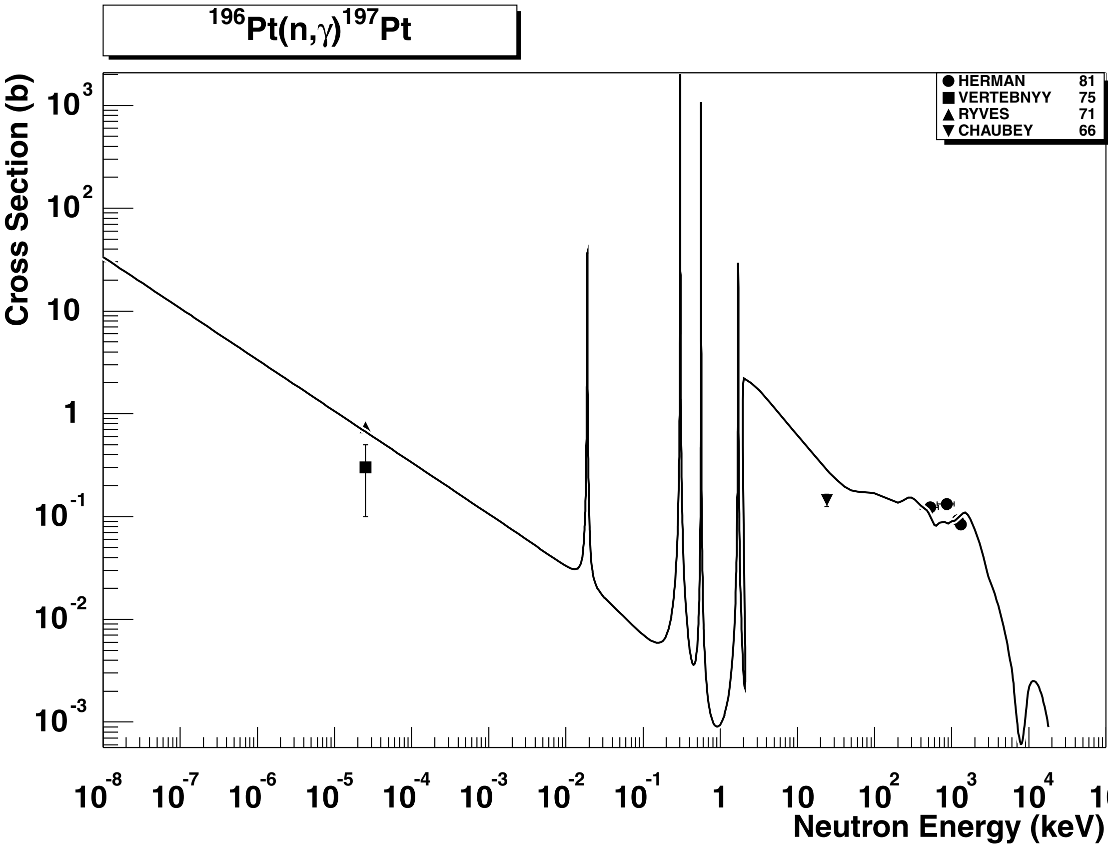

2.241. ^{196}Pt (n,γ) ^{197}Pt

final state: total
source: LANL-96

LANL-96 [22] evaluation adequately describes experimental points of Ryves71 and Herman81. cross-sections above the resonance region are based on calculations with the code EMPIRE-2.8 using Hauser-Feshbach and Multi-step Compound theories. In the low energy region EAF-4.1 is adopted.

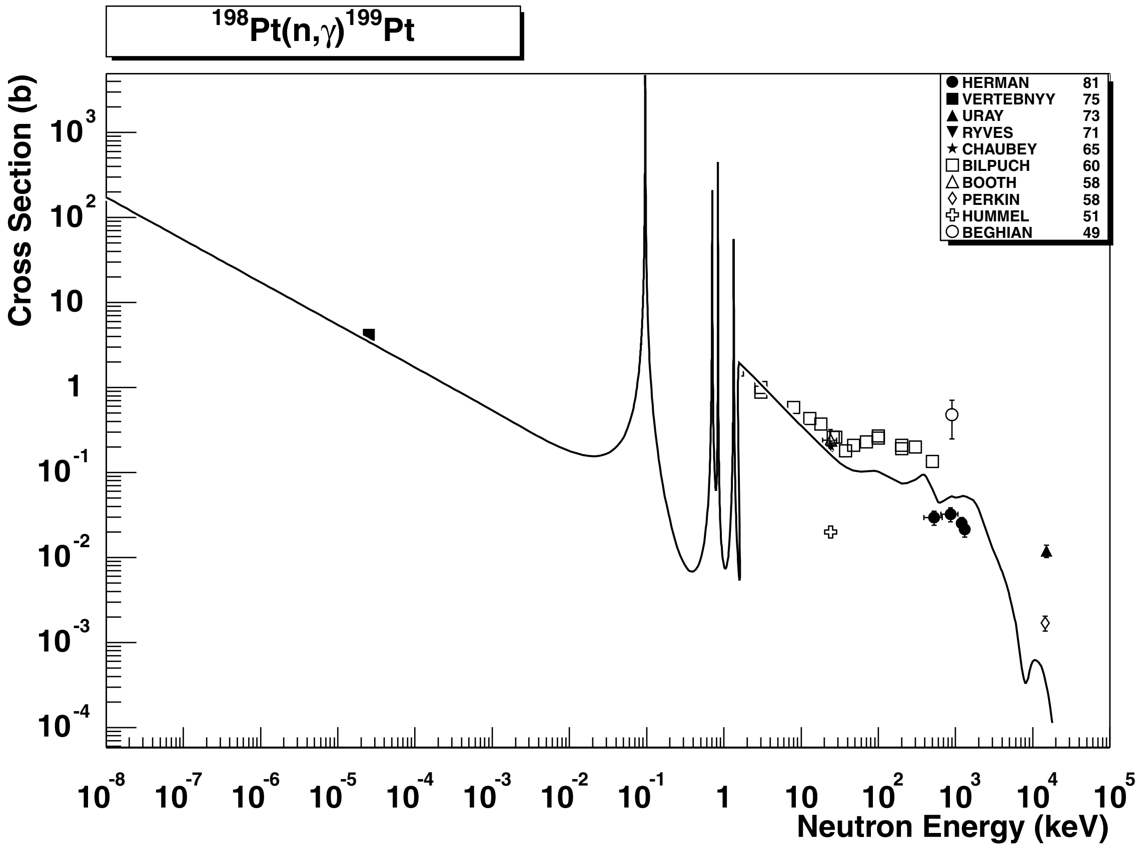

2.242. ^{198}Pt (n,γ) ^{199}Pt

final state: total
source: LANL-96

LANL-96 [22] evaluation is based on the EAF-4.1 data in the resonance region and below and on the EMPIRE-2.8 calculations above 2 keV. Thermal cross section is well reproduced. High energy data are strongly discrepant. Experimental points by Beghian49 and Hummel51 are clearly wrong. The more recent sets by Bilpuch60 and Herman81 differ nearly by an order of magnitude. Adopted EMPIRE-2.8 calculations with default parameters run in the middle of both but underestimate two (also discrepant) points above 10 MeV where Semi-Direct capture mechanism is expected to dominate.

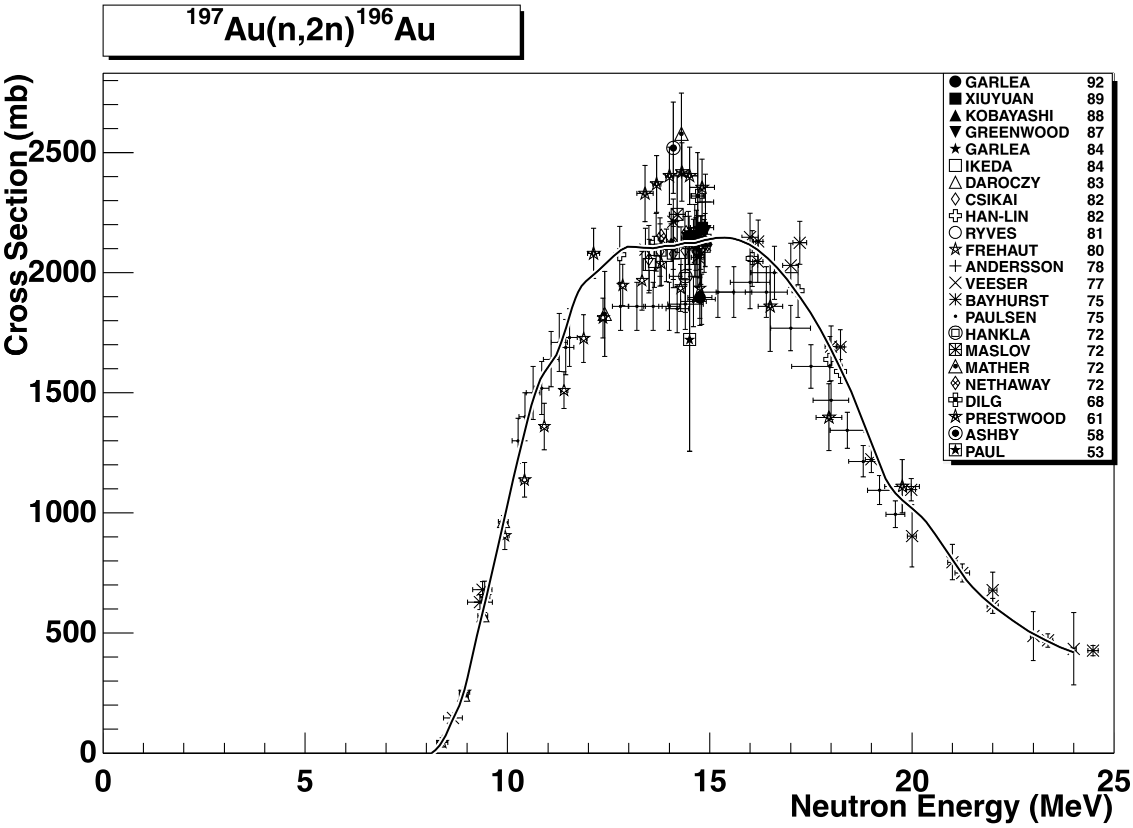

2.243. ^{197}Au (n,2n) ^{196}Au

final state: total
source: EAF-4.1 (IRDF-90.2 pointwise)

The IRDF-90.2 evaluation is in good agreement with the data in the increasing and decreasing parts of the excitation curve. In the maximum, around 15 MeV, runs through the middle of the data, agreeing well with the recent data of Garlea92 and Xiuyuan89.

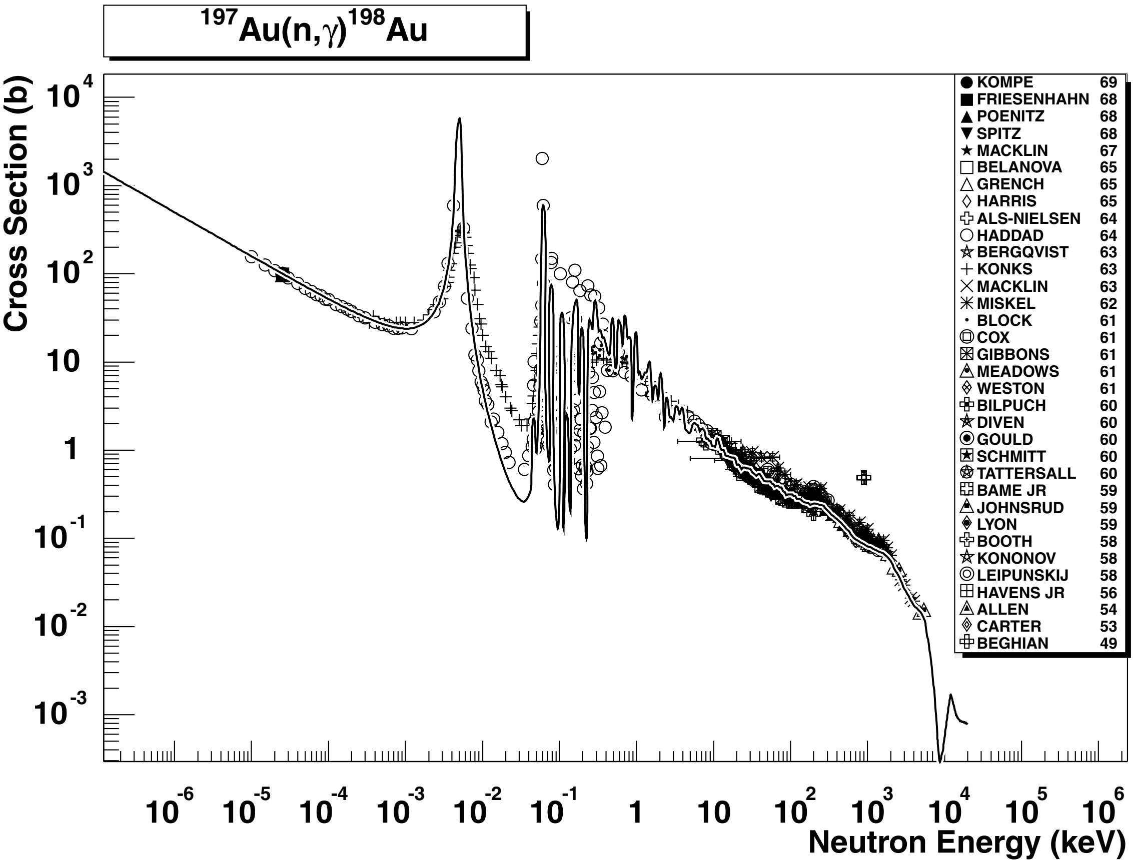

$^{197}Au(n,\gamma)^{198}Au$
Cross Section (b)
Neutron Energy (keV)
KOMPE 69
FRIESENHAHN 68
POENITZ 68
SPITZ 68
MACKLIN 67
BELANOVA 65
GRENCH 65
HARRIS 65
ALS-NIELSEN 64
HADDAD 64
BERGQVIST 63
KONKS 63
MACKLIN 63
MISKEL 62
BLOCK 61
COX 61
GIBBONS 61
MEADOWS 61
WESTON 61
BILPUCH 60
DIVEN 60
GOULD 60
SCHMITT 60
TATTERSALL 60
BAME JR 59
JOHNSRUD 59
LYON 59
BOOTH 58
KONONOV 58
LEIPUNSKIJ 58
HAVENS JR 56
ALLEN 54
CARTER 53
BEGHIAN 49

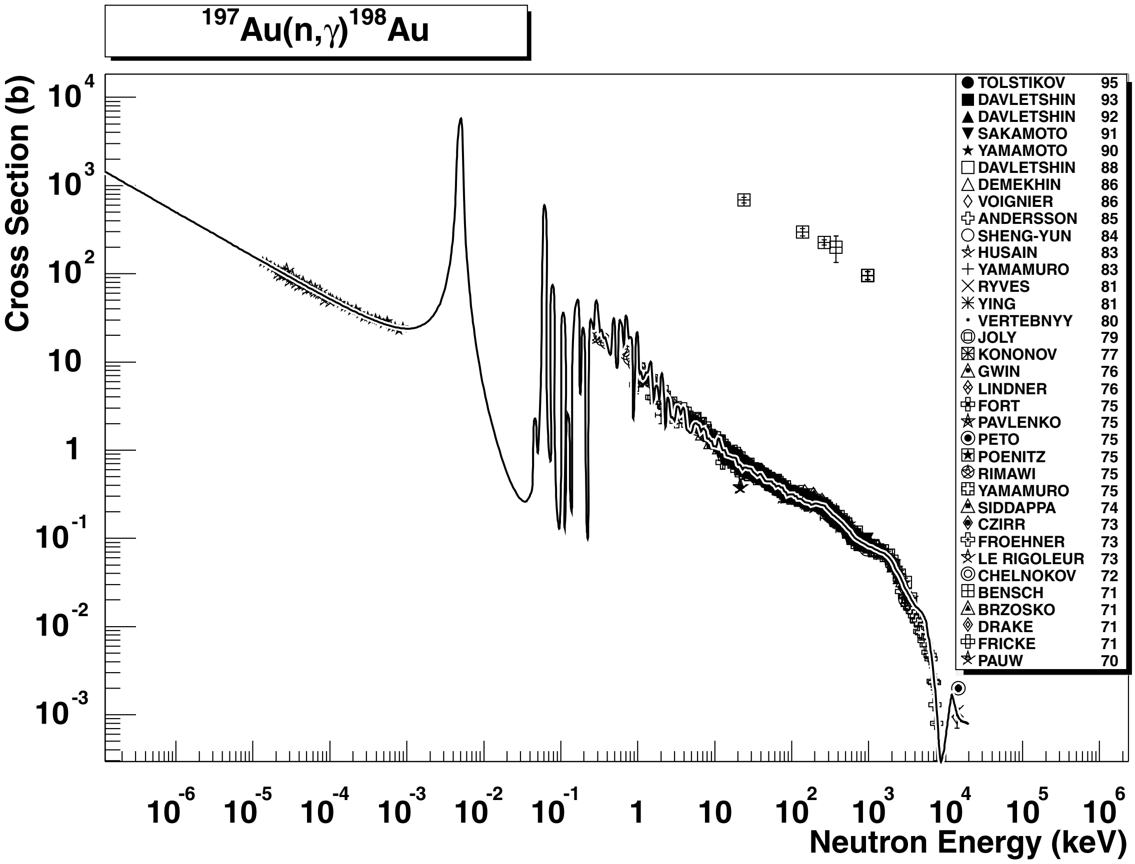

2.244. ^{197}Au (n,γ) ^{198}Au

final states: g.s., meta
source: EAF-4.1 (JEF-2.2)

The revised ENDF/B-V evaluation agrees very well with all experimental data from the thermal region up to 15 MeV. The data of Bensch71 are wrong and may be disregarded. The branching ratio between the g.s. and meta state is based on experimental values (thermal cross-sections [26]) and applied up to the end of the resolved resonance region. The energy dependent branching ratio systematics [2] is used for the high energy region.

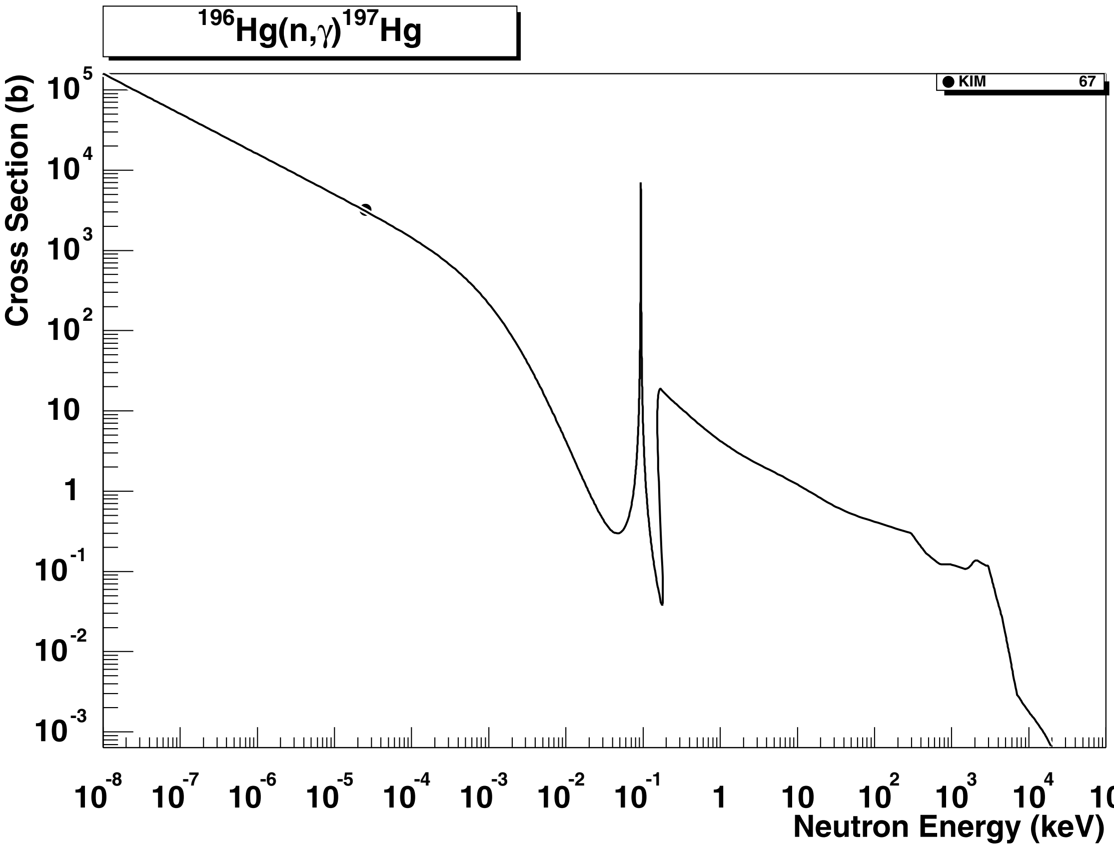

2.245. ^{196}Hg (n,γ) ^{197}Hg

final states: g.s., meta
source: EAF-4.1

The EAF-4.1 evaluation with the code SIGECN-MASGAM. cross-sections to the g.s. and meta state are based on experimental data (thermal cross-sections values from [26]) and applied up to the end of the resolved resonance region. The energy dependent branching ratio systematics [2] is used for the high energy region. Partial thermal cross-sections agree with the experiment with C/E=0.96. The total cross-section agrees in the thermal region with data of Kim67. The smooth statistical component, based on a simplified calculation with the code MASGAM, is supported by the recommended 30 keV cross-section [27].

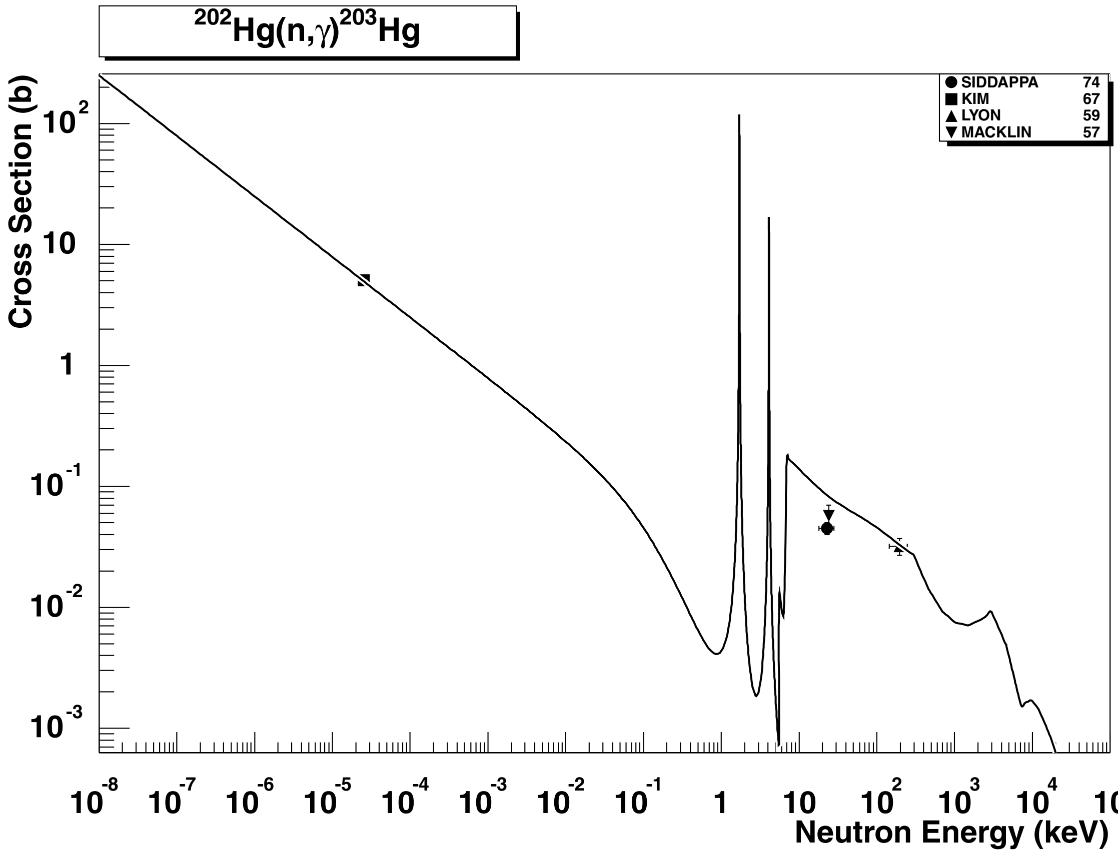

2.246. ^{202}Hg (n,γ) ^{203}Hg

final state: total
source: EAF-4.1

The EAF-4.1 evaluation with the code SIGECN-MASGAM agrees with the thermal cross section data of Kim67. The smooth statistical component, based on a simplified calculation with the code MASGAM, is reasonably close to the data of Macklin57, Lyon59 and Siddappa74.

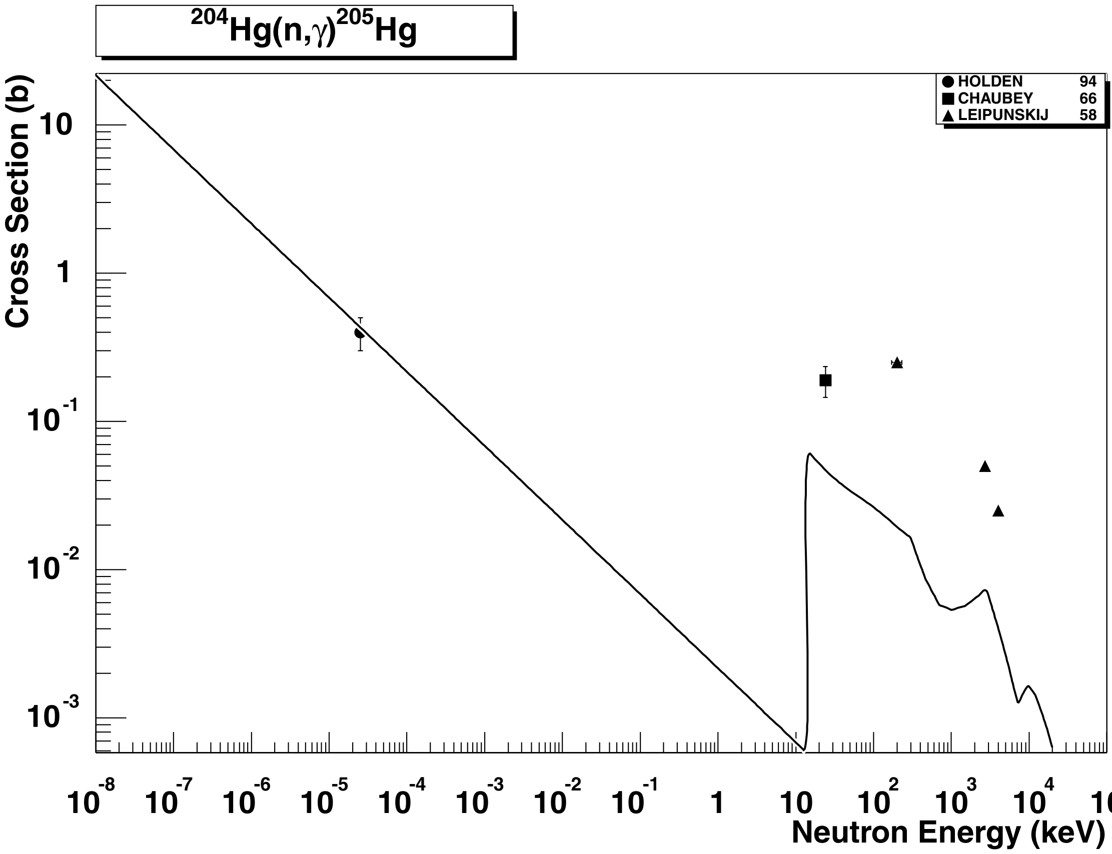

2.247. ^{204}Hg (n,γ) ^{205}Hg

final state: total
source: EAF-4.1

The EAF-4.1 evaluation is based on the simplified model calculations with the code MASGAM and the global parameters (Hauser-Feshbach and DSD model with no resonance region generation, E_H is based on a $D_0/2$ estimate; for details see Ref. [35]). The MASGAM evaluation fits the recommended thermal cross-section of Holden94 [32] with C/E=1.00. The statistical component is supported by the recommended 30 keV cross-section [27] of 42±4 mb. The data of Chaubey66 (around 25 keV) and Leipunskij58 (between 200 keV and 3 MeV) are clearly above this value and the evaluated curve. However, the recommended value of Ref. [27], based on the measurement of Beer and Macklin from 1985, is considered the most reliable.

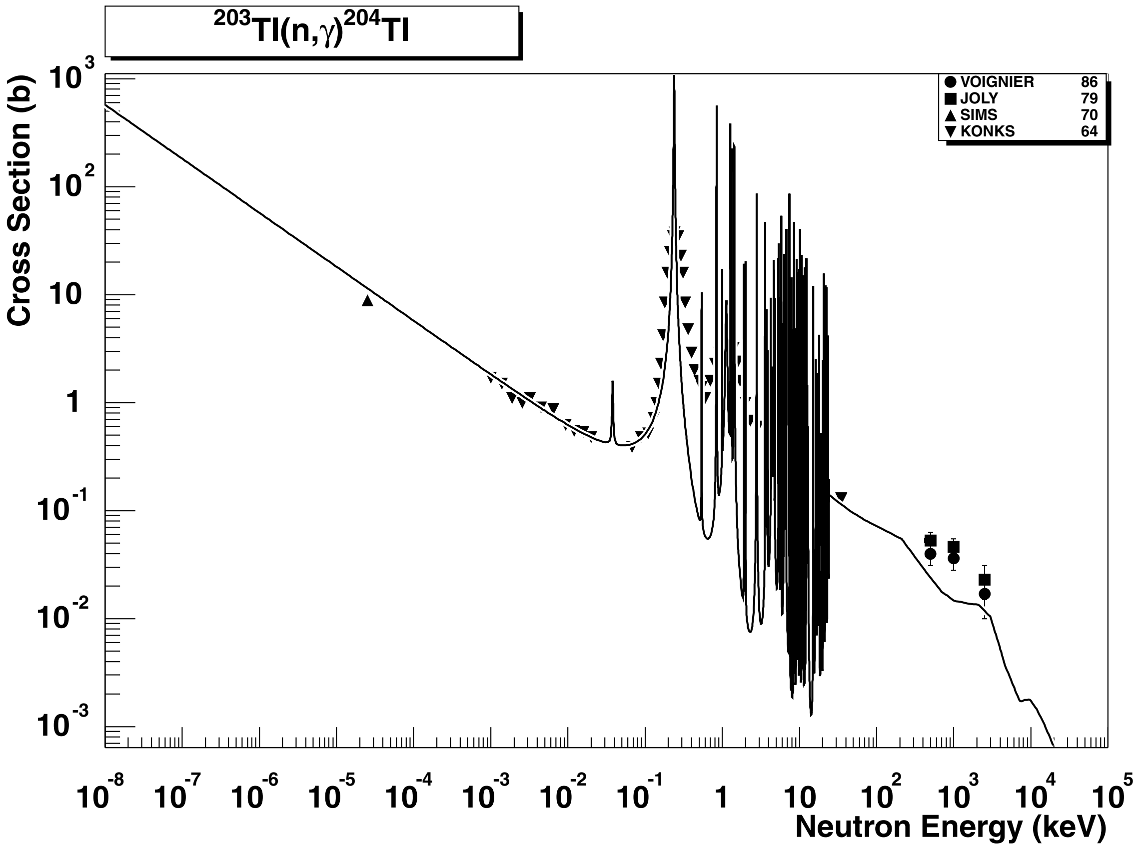

2.248. ^{203}Tl (n,γ) ^{204}Tl

final state: total
source: EAF-4.1

The EAF-4.1 evaluation with the code SIGECN-MASGAM is in a good agreement with many EXFOR data in particular in the low energy range. The smooth statistical component, based on a simplified calculation with the code MASGAM, is reasonably close to the data just above the end of the resolved resonance region. A small deviation from the data of Voignier86 and Joly79 may again be ascribed to the inaccuracy of the global parameters for the level densities. A renormalization of the recommended evaluation might be considered.

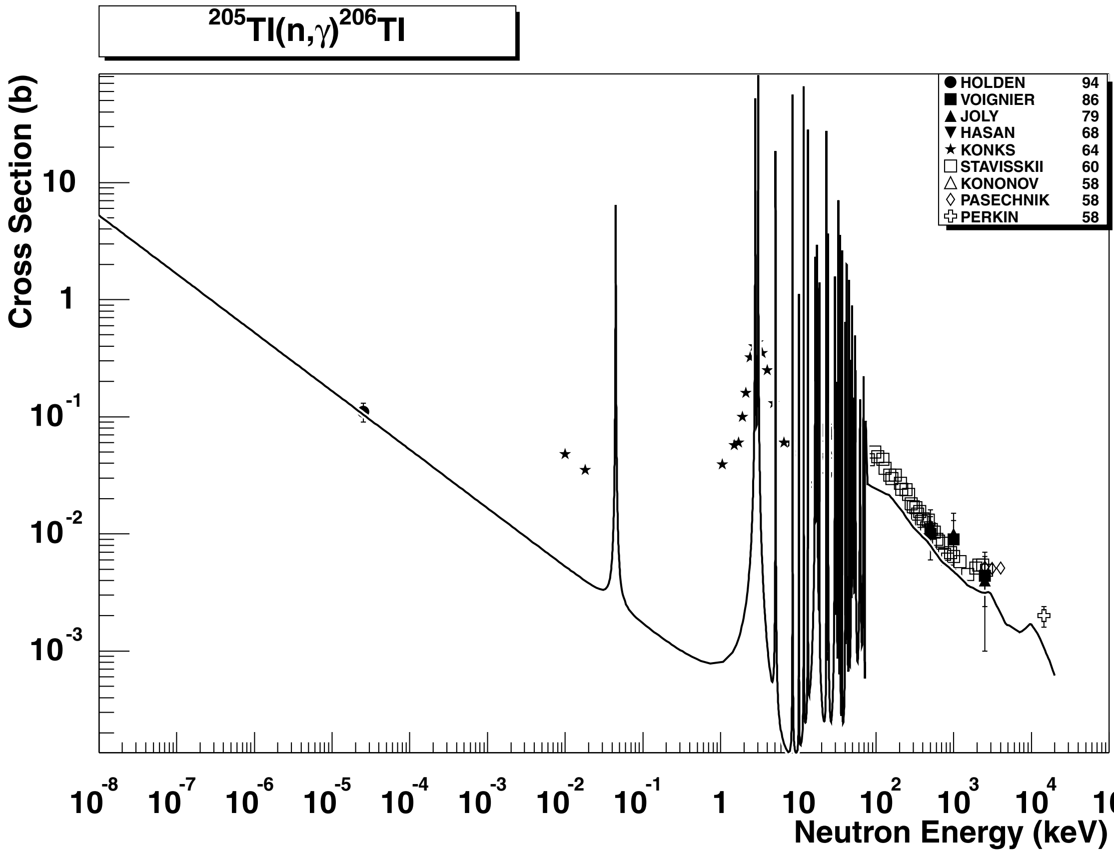

2.249. ^{205}Tl (n,γ) ^{206}Tl

final states: g.s., meta
source: EAF-4.1

The EAF-4.1 evaluation with the code SIGECN-MASGAM agrees with the thermal cross section data of Holden94 [32]. Two data points of Konks64 below the first resonance are doubtful. The smooth statistical component, based on a simplified calculation with the code MASGAM, slightly underestimates experimental data above 100 keV. A renormalization of the evaluation may be considered.

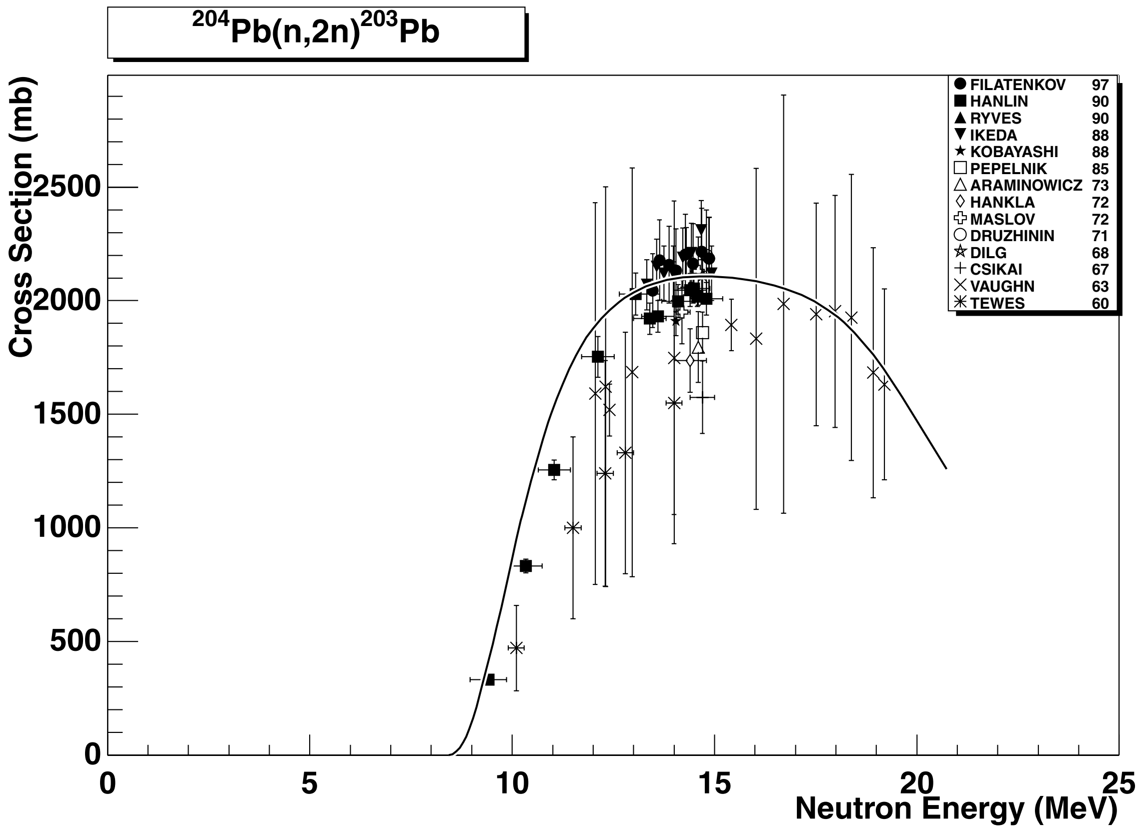

2.250. ^{204}Pb (n,2n) ^{203}Pb

final states: g.s., meta-1
source: ADL-3

The total cross-section data of ADL-3 are in a reasonable agreement with the experimental data. The branching between the g.s., meta-1 and meta-2 states is based on 14.5 MeV experimental data (see Ref. [26]).

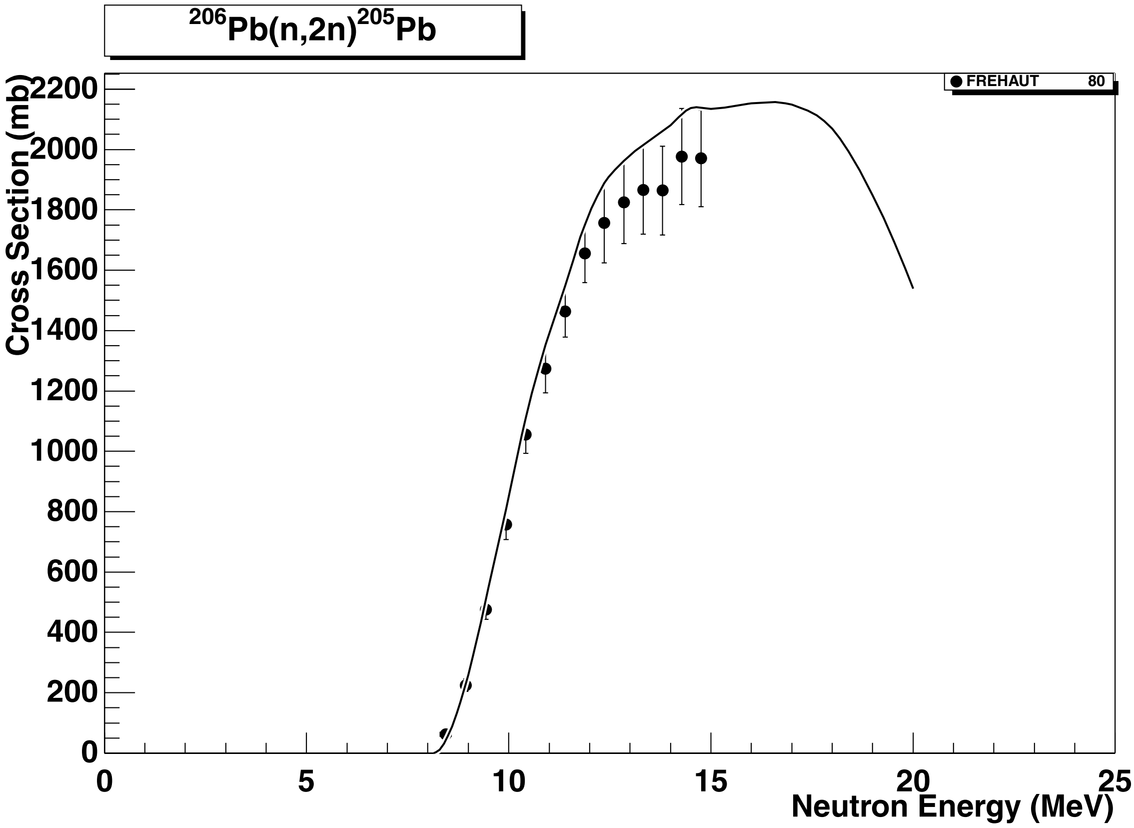

2.251. ^{206}Pb (n,2n) ^{205}Pb

final state: total
source: FENDL/A-1 (ENDF/B-VI)

The ENDF/B-VI excitation curve runs close to the data of Frehaut80, with a very small overestimation above 12 MeV, but still on the border of one standard deviation.

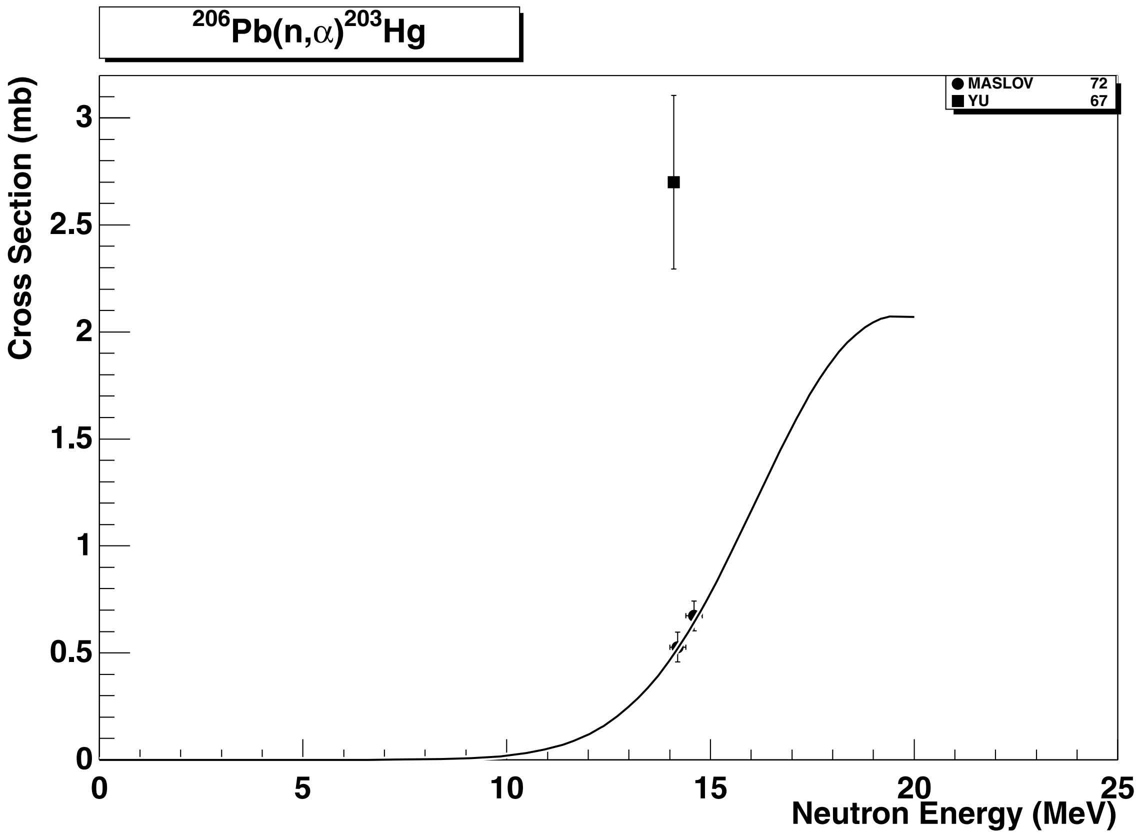

2.252. ^{206}Pb (n,α) ^{203}Hg

final state: total
source: ADL-3

ADL-3 evaluation agrees with the two data points of Maslov72. This measurement is also supported by the recommended value from the compilation of Csikai et al. (see in Ref. [26]). A discrepant result of Yu67 may be disregarded.

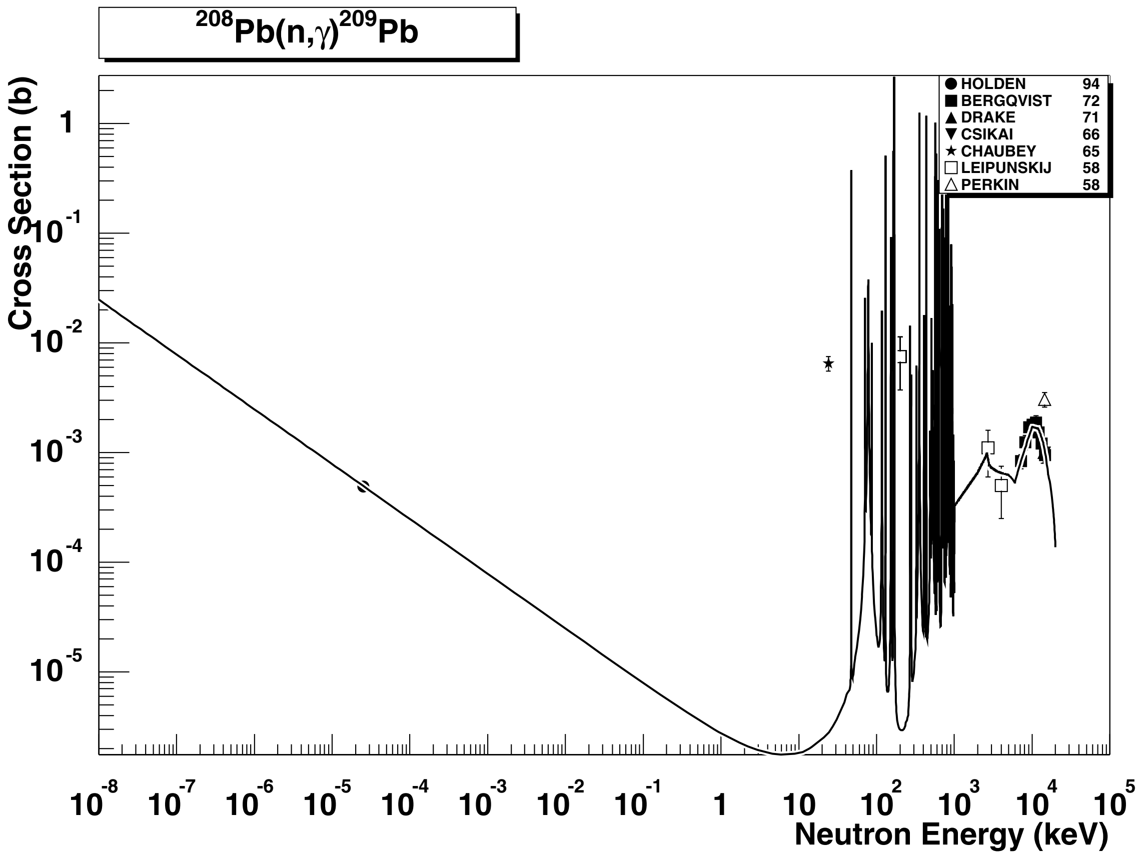

2.253. ^{208}Pb (n,γ) ^{209}Pb

final state: total
source: EAF-4.1 (ENDF/B-VI)

ENDF/B-VI evaluation agrees well with the experimental data in the high energy range. The thermal cross-section of Holden94 from [26] is reproduced with C/E=1.00.

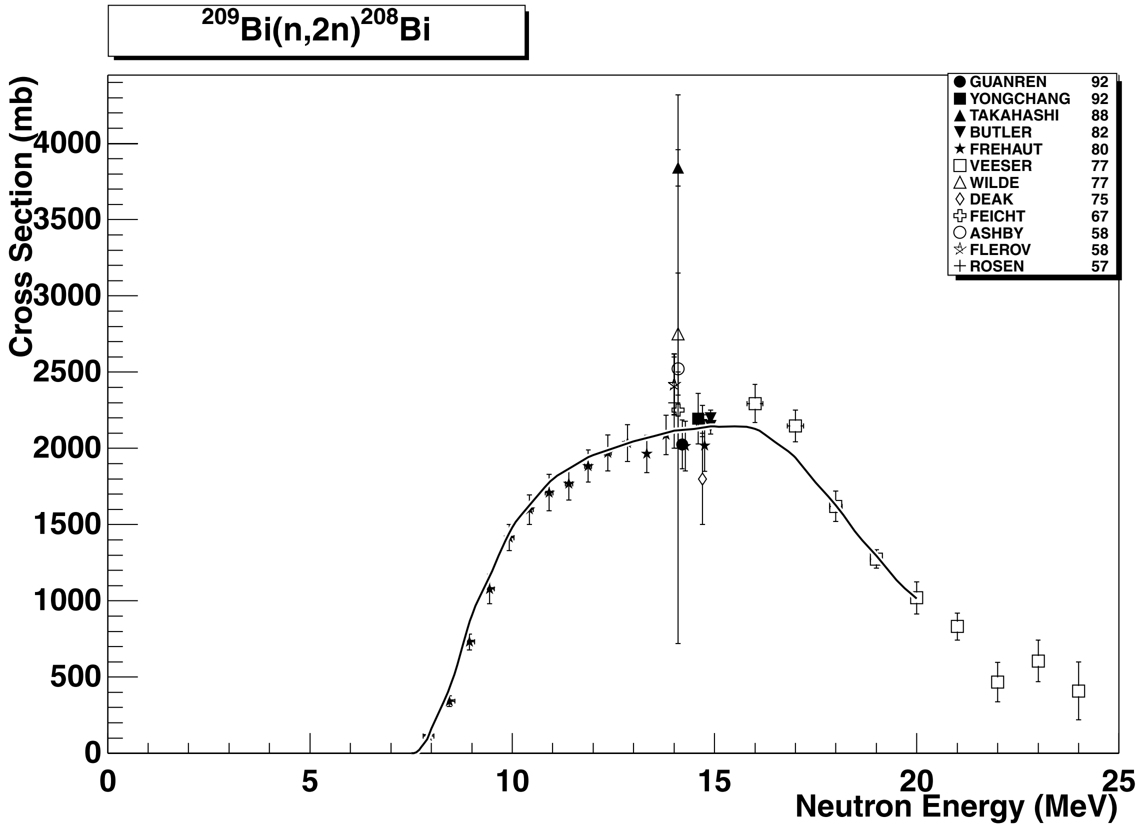

2.254. ^{209}Bi (n,2n) ^{208}Bi

final state: total
source: IPPE

IPPE evaluation [13] describes very well all experimental data from the threshold up to 20 MeV.

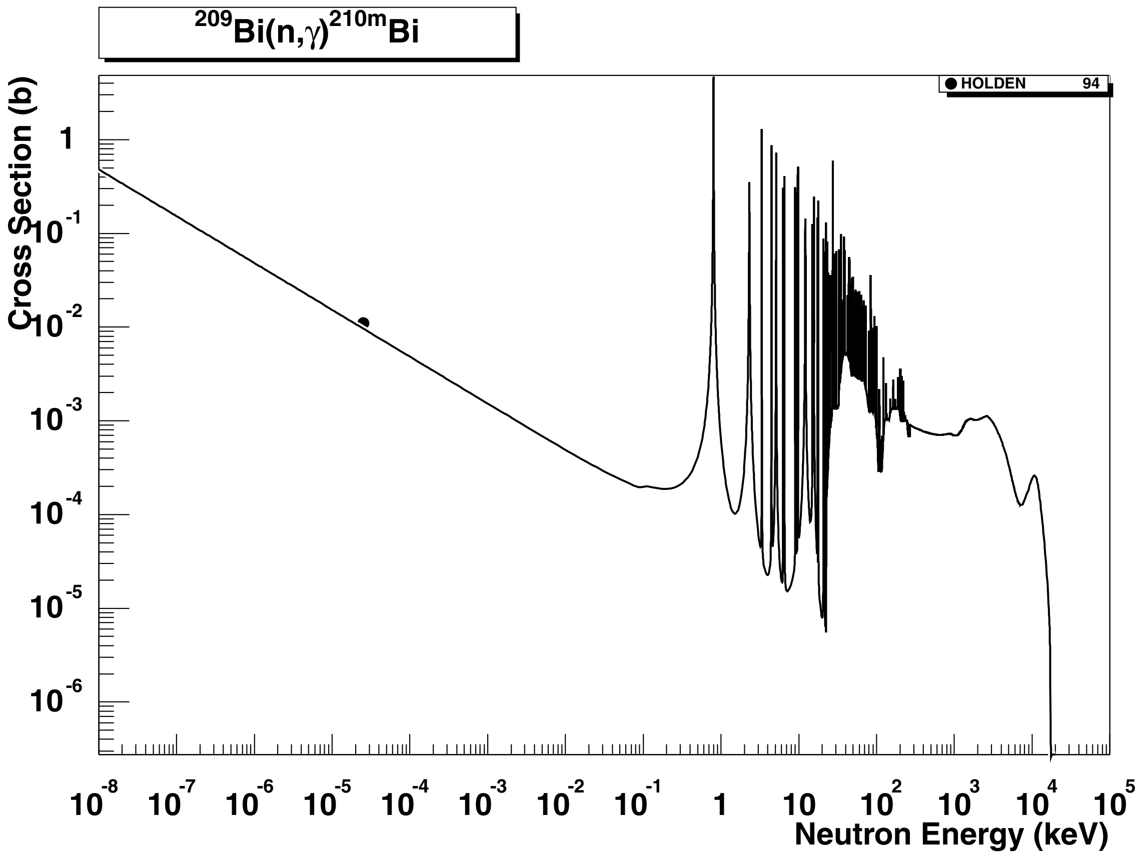

2.255. ^{209}Bi (n,γ) ^{210m}Bi

final state: meta
source: EAF-4.1 (JEF-2.2)

The reaction leading to the first isomeric state is the reference reaction. No EXFOR data are available outside the resonance region. The adopted curve is based on the JEF-2.2 evaluation. cross-sections to the g.s. and meta state are based on experimental data (thermal cross-sections [26] and [31]) and applied up to the end of the resolved resonance region. The energy dependent branching ratio systematics [3] is used for the high energy region. Partial thermal cross-sections of Holden94 agree with the experimental data with C/E=1.00.

REFERENCES

[1] Nakajima Y., 'Status of the JENDL Activation File', JAERI-Conf 96-008 (1996) 50.

[2] Grudzevich, O.T., Zelenetskij, A.V., Ignatyuk, A.V., Pashchenko, A.B., Catalogue of ADL-3 Library, Voprosy Atomnoi Nauki i Tekhniki **3–4** (1993).

[3] Kopecky, J., Nierop, D., The European Activation File EAF-4 — Summary Documentation, ECN-C-95-072 (1995).

[4] Pashchenko, A.B., McLaughlin, P.K., FENDL/A-1.1 — Neutron Activation Cross-Section Data Library for Fusion Applications, Rep. INDC(NDS)-148 (1995).

[5] Pashchenko, A.B., Wienke, H., Kopecky, J., Sublet, J-Ch., Forrest, R.A., FENDL/A-2.0 — Neutron Activation Cross-Section Data Library for Fusion Application, Rep. IAEA-NDS-173 (1997).

[6] Pashchenko, A.B., Establishment of an International Reference Data Library of Nuclear Activation Cross-Sections, Madrid, May 13–16, 1996, Rep. INDC(NDS)-361 (1997).

[7] Pashchenko, A.B., (Ed.), Activation Cross-Sections for the Generation of Long-Lived Radionuclides of Importance in Fusion Reactor Technology, Final CRP Report, INDC(NDC)-342 (1996).

[8] Sublet, J-Ch., Kopecky, J., Forrest, R.A., The European Activation File EAF-99 Cross-Section Library, Rep. UKAEA FUS 408 (1998).

[9] Kopecky, J., Gruppelaar, H., Hogenbirk, A., van der Kamp, H.A.J., Nierop, D., European Fusion File EFF-2.4 — Final report on basic data file, ECN Rep. ECN-C-94-016 (1994).

[10] Rose, P.F., (Ed.), ENDF/B-VI Summary Documentation, Rep. BNL-NCS-17541 (1991); McLane, V., et al., ENDF/B-VI Summary Documentation — Supplement I, Rep. BNL-NCS-17541 (1996).

[11] Zolotarev, K., Manokhin, V., Pashchenko, A., Scripova, M., Helium production cross-section data library, Voprosy Atomnoi Nauki i Tekhniki, Ser. YK, 1996, **2** 103–110.

[12] Zolotarev, K., et al., Status of Russian dosimetry file, Proceedings of the International Conference on Nuclear data for Science and Technology, Trieste, 19–24 May 1997 (Reffo, G., Ventura, A., Grandi, C., Eds), Editrice Compsitori, Bologna, Vol. 2, 1258–1261.

[13] Zolotarev, K., et al., Gamma-ray production cross-sections on ^{209}Bi(n,2n), Voprosy Atomnoi Nauki i Tekhniki, Ser. YK, 1998, **2** 52–57.

[14] The International Reactor Dosimetry File IRDF-90 Version 2, Rep. IAEA-NDS-141, Rev. 2 (1993).

[15] Vonach, H., private communication.

[16] JEF-2.2, Summary documentation, Rep. IAEA-NDS-120, Rev. 3 (1992).

[17] Shibata, K., et al., Japanese Evaluated Nuclear Data Library, Version-3 — JENDL-3, Rep. JAERI 1319 (1990).

[18] Nakagawa, T., et al., Japanese Evaluated Nuclear Data Library Version-3, Revision-2: JENDL-3.2, J. Nucl. Sci. Technol. **32** (1995) 1259.
[19] Chiba, S., Yu, B., Fukahori, T., Evaluation of JENDL Fusion File, Rep. JAERI-M 92-027 (1992) 35.
[20] Chiba, S., Fukahori, T., Yu, B., Kosako K., Evaluation of the double-differential cross-sections of medium-heavy nuclei for JENDL fusion file, Proc. 3rd Specialists Meeting on Nuclear Data for Fusion Reactors, 1995, Tokai, Japan, JAERI-Conf 96-005 (1996) 45.
[21] Chadwick, M.B., Young, P.G., Calculations of the production cross-sections of high spin isomeric states in Hf, Nucl. Sci. Eng. 108 (1991) 117; Chadwick, M.B., Young, P.G., Calculation of long-lived isomer production in neutron reactions, Rep. LA-UR-91-3454 (1991).
[22] Herman, M., LANL Update II of the ECNAF Neutron Activation Cross-Section Library, Rep. LANL, Los Alamos (1996).
[23] Zolotarev, K.I., Ignatyuk, A.I., Manokhin, V.N., Paschenko, A.B., RRDF-98, Russian Reactor Dosimetry File, Report IAEA-NDS-193, Rev. 0, Summary documentation by A.B. Paschenko, 1999; Zolotarev, K.I., Badikov, S.A., Ignatyuk, A.I., Manokhin, V.N., Proc. Int. Conf. on Nuclear Data for Science and Technology, Trieste, 1997, (Reffo, G., Ventura, A., Grandi, C., Eds), Editrice Compsitori, Bologna, Vol. II, 1258.
[24] Audi, G., Wapstra, A.H., The 1995 update to the atomic mass evaluation, Nucl. Phys. **A595** (1995) 409–480.
[25] http://www-nds.iaea.org/nudat/
[26] Kopecky, J., in Simpson, J.A., Sublet, J-Ch., Nierop, D., SYMPAL: User guide, Rep. UKAEA FUS 356 (1997). Recommended set of thermal cross-sections for the (n,γ) reactions based on [31], [32], [27], [33] and some recent private communications.
[27] Bao, Z.Y., Kappeler, F., Neutron Capture Cross Sections for s-Process Studies, Atomic Data and Nuclear Data Tables **36** (1987) 411.
[28] Sublet, J-Ch., Simpson, J.A., Forrest, R.A., Kopecky, J., Nierop, D., EAF-97: Cross-Section Library — (n,γ) Reactions, Rep. UKAEA FUS 352 (1997).
[29] Mengoni, A., Otsuka, T., Ishihara, M., Direct Radiative Capture of p-Wave Neutrons, Phys. Rev. **C 52** (1995) R2334.
[30] Ohsaki, T., Nagai, Y., Igashira, M., Shima, T., Takeda, K., Seino, S., Irie, T., New Measurement of the ^{12}C(n,γ)^{13}C Reaction Cross-Section, Astrophys. J. 422 (1994) 912.
[31] Mughabghab, S.F., Divadeenam, M., Holden, N.E., Neutron Cross-Sections, Vol. 1, Neutron Resonance Parameters and Thermal Cross-Sections, Part A, Z = 1–60, Academic Press, New York (1981); Mughabghab, S.F., Neutron Cross-Sections, Vol. 1, Neutron Resonance Parameters and Thermal Cross-Sections, Part B, Z=61–100, Academic Press, New York (1984).
[32] Holden, N.E., Review of Thermal Neutron Cross Sections, Rep. BNL-45255 (1991) and BNL-49710 (1994).
[33] Wagner, M., Warhanek, H., Activation measurements on neutron capture cross-sections at 14.6 MeV and a critical survey of such data in the litera-

ture, Acta Phys. Austriaca **52** (1980) 23.
[34] Wallner, A., Golser, R., Kutschera, W., 47th Annual Symposium of the Austrian Physical Society, Vienna, 1997.
[35] Kopecky, J., Delfini, M.G., van der Kamp, H.A.J., Nierop, D., Revisions and Extensions of Neutron Capture Cross-Sections in the European Activation File EAF-3, Rep. ECN-C–92-058 (1992).
[36] Herman, M., "EMPIRE-II statistical model code for nuclear reaction calculations (version: 2.13 Trieste)", Proc. Workshop on Nuclear Reaction Data and Nuclear Reactors: Physics, Design and Safety, ICTP Trieste, 2000, in press.
[37] Pavlik, A., et al., Physics Data, No - 13 - 6, Fachinformationszentrum Karlsruhe (1991).
[38] Vonach, H., Evaluated cross-sections for major structural materials, private communication.
[39] Haight, R.C., Grimes, S.M., Johnson, R.G., Charged-particle emission in reactions of 15-MeV neutrons with ^{89}Y, ^{90}Zr, and ^{92,94,95,96}Mo", Phys. Rev. **C23** (1981) 700.
[40] Pavlik, A., Miah, M.M.H., Strohmaier, B., Vonach, H., Update of the Evaluation of the Cross-Section of the Neutron Dosimetry Reaction ^{103}Rh(n,n')^{103m}Rh, Rep. INDC(AUS)-015 (1995).
[41] Filatenkov, A.A., Systematic measurement of Activation Cross-Sections at Neutron Energies from 13.4–14.9 MeV, Rep. INDC(CCP)-402 (1997).
[42] Ikeda, Y., Konno, C., Smith, D.L., Measurement of long-lived activation cross-sections at 14.7 MeV, Interlaboratory collaboration ANL/LANL/JAERI, in press.

CONTRIBUTORS TO DRAFTING AND REVIEW

Baosheng Yu	China Nuclear Data Center, China
Hlavac, S.	Slovak Academy of Sciences, Slovakia
Csikai J.	Kossuth Lajos University, Hungary
Forrest, R.A.	UK Atomic Energy Authority, United Kingdom
Grudzevich, O.T.	Institute of Nuclear Power Engineering, Russian Federation
Herman, M.	International Atomic Energy Agency, Austria
Ignatyuk, A.V.	Fiziko-Energeticheskij Institut, Russion Federation
Kopecky, J.	JUKO Research, Netherlands
Nakajima, Y.	Japan Atomic Energy Research Institute, Japan
Pashchenko, A.B.	Fiziko-Energeticheskij Institut, Russian Federation
Perlado, J.M.	Instituto de Fusion Nuclear, Spain
Sanz, J.	Insituto de Fusion Nuclear, Spain
Trkov, A.	International Atomic Energy Agency, Austria
Zolotarev, K.I.	Fiziko-Energeticheskij Institut, Russian Federation